

SSC-452

**ALUMINUM STRUCTURE DESIGN
AND FABRICATION GUIDE**



This document has been approved
For public release and sale; its
Distribution is unlimited

SHIP STRUCTURE COMMITTEE
2007

Ship Structure Committee

RADM Brian M. Salerno
U. S. Coast Guard Assistant Commandant,
Assistant Commandant for Marine Safety, Security and Stewardship
Chairman, Ship Structure Committee

{Name}
{Title}
Naval Sea Systems Command

Mr. Joseph Byrne
Director, Office of Ship Construction
Maritime Administration

Mr. Kevin Baetsen
Director of Engineering
Military Sealift Command

CONTRACTING OFFICER TECHNICAL REP.

Mr. Chao Lin / MARAD
Mr. Glenn Ashe / ABS
DRDC / USCG

Dr. Roger Basu
Senior Vice President
American Bureau of Shipping

Mr. William Nash
Director General, Marine Safety,
Safety & Security
Transport Canada

Dr. Neil Pegg
Group Leader - Structural Mechanics
Defence Research & Development Canada - Atlantic

EXECUTIVE DIRECTOR

Lieutenant Commander, Jason Smith
U. S. Coast Guard

SHIP STRUCTURE SUB-COMMITTEE

AMERICAN BUREAU OF SHIPPING

Mr. Glenn Ashe
Mr. Derek Novak
Mr. Phil Rynn
Mr. Balji Menon

MARITIME ADMINISTRATION

Mr. Chao Lin
Mr. Carl Setterstrom
Mr. Richard Sonnenschein

ONR / NAVY / NSWCCD

{Name}
{Name}
{Name}
{Name}

US COAST GUARD

CDR Charles Rawson
Mr. James Person
Mr. Rubin Sheinberg

DEFENCE RESEARCH & DEVELOPMENT CANADA ATLANTIC

Dr. David Stredulinsky
Mr. John Porter

MILITARY SEALIFT COMMAND

Mr. Michael W. Touma
Mr. Paul Handler

TRANSPORT CANADA

Paul Denis Vallee

SOCIETY OF NAVAL ARCHITECTS AND MARINE ENGINEERS

Mr. Jaideep Sirkar
Mr. Al Rowen
Mr. Norman Hammer

Member Agencies:

*American Bureau of Shipping
Defence Research Development Canada
Maritime Administration
Military Sealift Command
Naval Sea Systems Command
Society of Naval Architects & Marine Engineers
Transport Canada
United States Coast Guard*



Ship
Structure
Committee

Address Correspondence to:

Executive Director
Ship Structure Committee
U.S. Coast Guard (CG-5212/SSC)
2100 2nd Street, SW
Washington, D.C. 20593-0001
Web site: <http://www.shipstructure.org>

SSC – 452
SR – 1448

OCTOBER 3, 2008

ALUMINUM STRUCTURE DESIGN AND FABRICATION GUIDE

This guide is intended to serve as a reference to the shipbuilding industry to support their understanding of aluminum ship design and fabrication, and aid in the exploitation of aluminum as a building material.

Towards the close of WW II, some merchant ships built in the U.S. had aluminum incorporated into the construction of their deckhouses. This practice began to be adopted worldwide after the war, particularly in the fabrication of the superstructures of passenger ships.

Over the years, manufacturers have developed unique alloys and innovative fabrication procedures for use in ship and boat construction. The SSC has sponsored this project to address these recent changes in aluminum marine structure design.

The guide addresses the following subject areas in each chapter of the report: material characteristics, structural design, structural details, welding and fabrication, riveting, joining aluminum to steel structure, residual stresses and distortion, fatigue and fracture design and analysis procedures, fire protection, vibration, maintenance and repair, mitigating slam loads, emerging technologies, and research needs.

A handwritten signature in black ink, appearing to read 'B. Salerno', with a long, sweeping underline.

BRIAN M. SALERNO
Rear Admiral, U.S. Coast Guard
Chairman, Ship Structure Committee

Technical Report Documentation Page

1. Report No. SSC - 452	2. Government Accession No.	3. Recipient's Catalog No.	
4. Title and Subtitle Aluminum Structure Design and Fabrication Guide		5. Report Date May 11, 2007	6. Performing Organization Code
7. Author(s) R.A.Sielski,	8. Performing Organization Report No. SR-1448		
9. Performing Organization Name and Address Naval Architect – Structures 40391 Camino Montecito Indio, CA 92203		10. Work Unit No. (TRAIS)	11. Contract or Grant No.
12. Sponsoring Agency Name and Address Ship Structure Committee C/O Commandant (CG-3PSE/SSC) United States Coast Guard 2100 2 nd Street, SW Washington, DC 20593-0001		13. Type of Report Final Report	14. Sponsoring Agency Code CG - 5
15. Supplementary Notes Sponsored by the Ship Structure Committee and its member agencies			
16. Abstract <p>This guide is intended to bring together work by the interagency Ship Structure Committee and other extensive research in aluminum ship structures being conducted internationally and will provide the shipbuilding industry a reference to support their understanding of aluminum ship design and fabrication, and aid in the exploitation of aluminum as a building material. The SSC has sponsored this project to develop an aluminum marine structure design and fabrication guide. The guide addresses the following subject areas: material characteristics and properties, structural design, fatigue design and analysis procedures, typical structural details used for aluminum, welding and fabrication of aluminum, joining to steel structure, residual stresses and distortion of aluminum structure, fire protection, vibration, mitigating slam loads, maintenance and repair of aluminum structures, emerging technologies such as friction stir welding, and research needs.</p>			
17. Key Words Aluminum structure, marine structure, aluminum design, aluminum fabrication		18. Distribution Statement Distribution Available From: National Technical Information Service U.S. Department of Commerce Springfield, VA 22151 Ph. (703) 487-4650 / www.ntis.gov	
19. Security Classif. (of this report) Unclassified	20. Security Classif. (of this page) Unclassified	21. No. of Pages 794	22. Price

CONVERSION FACTORS
(Approximate conversions to metric measures)

To convert from	to	Function	Value
LENGTH			
inches	meters	divide	39.3701
inches	millimeters	multiply by	25.4000
feet	meters	divide by	3.2808
VOLUME			
cubic feet	cubic meters	divide by	35.3149
cubic inches	cubic meters	divide by	61,024
SECTION MODULUS			
inches ² feet ²	centimeters ² meters ²	multiply by	1.9665
inches ² feet ²	centimeters ³	multiply by	196.6448
inches ⁴	centimeters ³	multiply by	16.3871
MOMENT OF INERTIA			
inches ² feet ²	centimeters ² meters	divide by	1.6684
inches ² feet ²	centimeters ⁴	multiply by	5993.73
inches ⁴	centimeters ⁴	multiply by	41.623
FORCE OR MASS			
long tons	tonne	multiply by	1.0160
long tons	kilograms	multiply by	1016.047
pounds	tonnes	divide by	2204.62
pounds	kilograms	divide by	2.2046
pounds	Newtons	multiply by	4.4482
PRESSURE OR STRESS			
pounds/inch ²	Newtons/meter ² (Pascals)	multiply by	6894.757
kilo pounds/inch ²	mega Newtons/meter ² (mega Pascals)	multiply by	6.8947
BENDING OR TORQUE			
foot tons	meter tons	divide by	3.2291
foot pounds	kilogram meters	divide by	7.23285
foot pounds	Newton meters	multiply by	1.35582
ENERGY			
foot pounds	Joules	multiply by	1.355826
STRESS INTENSITY			
kilo pound/inch ² inch ^{1/2} (ksi√in)	mega Newton MNm ^{3/2}	multiply by	1.0998
J-INTEGRAL			
kilo pound/inch	Joules/mm ²	multiply by	0.1753
kilo pound/inch	kilo Joules/m ²	multiply by	175.3

Table of Contents

Section	Title	Page
1	Introduction	1-1
1.1	Background	1-1
1.2	Material Characteristics	1-3
1.3	Structural Design	1-4
1.4	Structural Details	1-4
1.5	Welding and Fabrication	1-4
1.6	Riveting	1-5
1.7	Joining Aluminum to Steel Structure	1-5
1.8	Residual Stresses and Distortion	1-6
1.9	Fatigue and Fracture Design and Analysis Procedures	1-6
1.10	Fire Protection	1-6
1.11	Vibration	1-7
1.12	Maintenance and Repair	1-7
1.13	Mitigating Slam Loads	1-7
1.14	Emerging Technologies	1-8
2	Material Characteristics	2-1
2.1	Properties of Aluminum	2-1
2.1.1	Chemical Composition	2-1
2.1.2	Alloy and Temper Designations	2-2
2.1.3	Mechanical Properties	2-3
2.1.4	Properties at Elevated Temperatures	2-4
2.1.5	Fracture Strength	2-6
2.1.6	Other Properties	2-7
2.2	Marine Alloys	2-8
2.2.1	5xxx Series	2-9
2.2.2	6xxx Series and Corrosion Resistance	2-13
2.2.3	7xxx-Series	2-16
2.2.4	Classification Society Requirements	2-17
2.3	Welded Properties	2-18
2.4	Corrosion	2-22
2.4.1	General Corrosion	2-23
2.4.2	Exfoliation	2-25
2.4.3	Intergranular Corrosion	2-26
2.4.4	Stress-Corrosion Cracking	2-26
2.4.5	Corrosion-Erosion, Impingement, and Cavitation	2-28
2.4.6	Galvanic Corrosion	2-29
2.4.7	Crevice Corrosion	2-30
2.5	Product Forms	2-31
2.6	The Extrusion Process	2-36
2.6.1	Process Description	2-36
2.6.2	Cost of Development	2-39

Aluminum Marine Structure Guide

2.6.3	Length of Extrusions	2-40
2.6.4	Limitations in Extrusion Thickness	2-40
2.6.5	Heat Treatment	2-42
2.6.6	Considerations for Extrusion Design	2-42
2.6.7	Dimensional Tolerances	2-47
2.7	Summary	2-49
3.	Structural Design	3-1
3.1	Introduction	3-1
3.2	Structural Loads	3-3
3.2.1	Hull Girder Bending	3-4
3.2.2	Slamming Pressures	3-10
3.2.3	Hydrostatic Pressures	3-13
3.3	Structural Analysis Procedures	3-14
3.3.1	Frames and Stiffeners	3-14
3.3.2	Effective Plating	3-15
3.3.3	Analysis of Plating under Lateral Load	3-18
3.4	Allowable Stress Levels	3-28
3.5	Buckling Strength	3-30
3.5.1	Buckling Strength of Plating	3-30
3.5.2	Buckling Strength of Stiffeners	3-32
3.5.3	Stiffener Tripping	3-35
3.5.4	Stability of Stiffener and Frame Flanges and Webs	3-40
3.5.5	Stability of Grillages	3-41
3.6	Finite Element Analysis	3-41
3.7	Summary of Design	3-42
4	Structural Details	4-1
4.1	Introduction	4-1
4.2	Detail Classification	4-2
4.2.1	Beam Brackets	4-3
4.2.2	Tripping Brackets	4-11
4.2.3	Nontight Collars	4-13
4.2.4	Tight Collars	4-16
4.2.5	Gunwale Connection Details	4-18
4.2.6	Miscellaneous Opening Details	4-19
4.2.7	Miscellaneous Cutout Details	4-23
4.2.8	Deck Cutouts	4-25
4.2.9	Stanchion Heads and Heels	4-26
4.2.10	Stiffener End Details	4-30
4.2.11	Panel Breakers	4-32
4.3	Details Specific to Aluminum Structure	4-34
4.3.1	Deck Panels	4-35
4.3.2	Tubular Stiffeners	4-37
4.3.3	Egg Crate Detailing	4-38
4.3.4	Special Extrusions at the Gunwale	4-39
4.4	Conclusions	4-39

5	Welding and Fabrication	5-1
5.1	Introduction	5-1
5.2	Cutting and Forming	5-1
5.3	Structural Assembly	5-5
5.4	Welding	5-6
5.4.1	Procedures	5-6
5.4.2	Joint preparation	5-7
5.5	Tolerances	5-8
5.6	Fabrication with Special Panels	5-10
5.7	Fabrication with Adhesives	5-12
5.8	Summary	5-13
6	Riveting	6-1
6.1	Selection of Rivet Material	6-1
6.2	Guidance for Riveted Design	6-2
6.2.1	U.S. Navy Requirements	6-2
6.2.2	Classification Society Requirements	6-3
6.2.3	Aluminum Design Manual	6-4
6.3	Fatigue of Riveted Joints	6-7
6.4	Summary	6-8
7	Joining Aluminum to Steel Structure	7-1
7.1	Introduction	7-1
7.2	Riveted Joints	7-1
7.3	Bimetallic Joints	7-3
7.4	Deckhouse-Hull Interaction	7-9
7.4.1	Expansion Joints	7-9
7.4.2	Calculation of Stress in a Deckhouse	7-11
7.5	Isolation of the Deckhouse from the Hull	7-16
7.6	Summary	7-18
8	Residual Stresses and Distortion	8-1
8.1	The Nature of Distortions	8-1
8.1.1	Distortion from other than Welding	8-1
8.1.2	Welding Distortion	8-2
8.1.3	Patterns of Welding Distortion	8-3
8.1.4	Analysis of a Weld Bead	8-6
8.1.5	Analysis of Aluminum Welding	8-9
8.2	Distortion in Panel Fabrication	8-15
8.2.1	Welded Panels	8-16
8.2.2	Extruded Panels	8-21
8.3	Tolerances in Welded Aluminum Structures	8-22
8.4	Summary	8-24
9	Fatigue and Fracture Design and Analysis Procedures	9-1
9.1	Introduction	9-1
9.2	Comparison of Aluminum and Steel	9-2
9.3	Fatigue Design Curves	9-3
9.4	Fatigue Data for Specific Ship Details	9-10

Aluminum Marine Structure Guide

9.5	Fatigue Analysis for Operation in a Seaway	9-12
9.6	Development of Fatigue Loading Spectra	9-14
9.7	Fatigue Analysis Procedure for Preliminary Design	9-18
9.8	Spectral Fatigue Analysis	9-19
9.9	Fatigue Crack Growth	9-20
9.10	Fracture	9-27
9.11	Summary	9-29
10	Fire Protection	10-1
10.1	Introduction	10-1
10.2	Regulatory Requirements	10-1
10.2.1	SOLAS Requirements	10-2
10.2.2	IMO HSC Code	10-4
10.2.3	U.S. Coast Guard Requirements	10-5
10.2.4	U.S. Navy Requirements	10-7
10.3	Fire Protection Insulation	10-8
10.3.1	Insulation Necessary to Protect Unexposed Surfaces	10-9
10.3.2	Insulation to Protect the Aluminum Structure	10-15
10.3.3	Aluminum Surrounded by Fire	10-16
10.3.4	Insulation to Meet U.S. Navy Requirements	10-17
10.4	Alternative Design Approach	10-17
10.5	Support of Insulation	10-20
10.6	Research in Fire Protection Materials	10-20
10.7	Summary	10-21
11	Vibration	11-1
11.1	Introduction	11-1
11.2	Computing Vibration Frequencies	11-1
11.2.1	Single Degree of Freedom System	11-1
11.2.2	Beam Vibrations	11-2
11.2.3	Uniform Beams with a Lumped Mass	11-4
11.2.4	Uniform Plate with Simply Supported Edges	11-4
11.2.5	Continuous Structural Systems	11-5
11.3	Determining the Forcing Function	11-6
11.4	Hull Girder Whipping	11-7
11.5	Energy and Damping	11-8
11.6	Comparison of Aluminum and Steel	11-10
11.6.1	Plates	11-10
11.6.2	Stiffeners	11-11
11.7	Summary	11-13
12	Maintenance and Repair	12-1
12.1	Painting and Preservation	12-1
12.1.1	Preparation for Painting	12-1
12.1.2	Painting	12-2
12.2	Corrosion Problems	12-4
12.3	Repair of Cracking	12-6
12.3.1	Safe-ending Cracks	12-7

12.3.2	Welding a Doubler Plate	12-7
12.3.3	Grinding out the Crack and Welding	12-9
12.4	Repairs of Overstressed or Improperly Designed Details	12-12
12.5	Repairs for Corrosion or Stress Corrosion	12-14
12.6	Summary	12-17
13	Mitigating Slam Loads	13-1
13.1	Structural Design	13-1
13.2	Preferred Course and Speed	13-2
13.3	Weather Routing	13-3
13.4	Hull Instrumentation	13-3
13.5	Summary	13-7
14	Emerging Technologies	14-1
14.1	Stir Welding	14-1
14.1.1	Friction Stir Welding	14-1
14.1.2	Laser Stir Welding	14-10
14.1.3	Thermal Stir Welding	14-17
14.1.4	Electrospark Fusion	14-18
14.2	Laser Welding	14-19
14.3	Electron Beam Welding	14-22
14.4	Summary	14-24
15	Research Needs	15-1
15.1	Design Strength of Welded Aluminum	15-1
15.2	Fatigue of Aluminum Structural Details	15-2
15.3	Corrosion Properties of Marine Alloys	15-3
15.4	Structural Loads on High Performance Aluminum Marine Vehicles	15-3
15.5	Fatigue Loading Spectrum for High Performance Aluminum Marine Vehicles	15-4
15.6	Fatigue Strength Under Multi-Axial Loading	15-5
15.7	Elevated-Temperature Resistance Aluminum Alloys	15-5
15.8	Reliability of Aluminum High Speed Vessels	15-6
15.9	Fire Protection of Aluminum Structure	15-7
15.10	Friction Stir Welded Bimetallic Strip	15-7
15.11	Mitigation of Loads on High-Speed Vessels	15-8
15.12	Line-heating of Aluminum Plates	15-9
15.13	Development of Improved Welding Processes	15-9
16	Summary	16-1
17	References	17-1
A	Appendix A: Design Studies	A-1
B	Appendix B: Course Notes	B-1

List of Figures

Figure	Title	Page
2-1	Stress-strain curve of 5083 aluminum compared to steel and FRP	2-4
2-2	Reduction of yield strength with temperature	2-6
2-3	Example of exfoliation on the edge of a waterway bar	2-10
2-4	An example of intergranular corrosion	2-11
2-5	Grain structure of 5xxx-series aluminum	2-12
2-6	A transverse tensile specimen from a weld joint	2-19
2-7	Analysis of welded plate in tension	2-21
2-8	Strain in heat affected zone of welds in a panel	2-22
2-9	Accelerated corrosion tests of friction stir weld and GMAW	2-28
2-10	Rounded tee profile	2-34
2-11	Comparison of section moduli of rounded tees with conventional tees	2-35
2-12	Bulb flat	2-36
2-13	Typical extrusion press	2-37
2-14	Solid die	2-38
2-15	Semihollow die	2-38
2-16	Hollow die	2-39
2-17	Drift expansion test	2-39
2-18	The extrusion process	2-41
2-19	An extrusion plant	2-41
2-20	Dimensional control of extrusions	2-44
2-21	Effect of sharp transitions on extrusions	2-45
2-22	Use of webs in extrusion design	2-46
2-23	Use of ribs in extrusion design	2-46
2-24	Rounded corners in extrusion design	2-47
2-25	Index marks in extrusion design	2-47
3-1	The structural design triangle	3-2
3-2	Comparison of ABS and DNV slam pressure reduction factors	3-12
3-3	Effective breadth of plating based on shear lag	3-16
3-4	Comparison of computations of permanent set of plating as calculated using Jones and Walters	3-26
3-5	Nondimensional stress in a stiffened panel subject to impact loads	3-28
3-6	Geometrical tripping parameters for tee stiffeners	3-37
3-7	Buckling of a panel from shear in the stiffeners	3-41
4-1	Recess in deck transverse in way of lightweight deck extrusion	4-35
4-2	Lightweight deck extrusion on deck beam	4-35
4-3	Lightweight deck extrusion at a bulkhead	4-36
4-4	Alternate design for lightweight deck extrusions	4-36
4-5	Corrugated deck extrusion	4-37
4-6	Framing with tubular members	4-38
4-7	Egg crate intersection of tee with transverse	4-39
4-8	Special extrusions for gunwale	4-39

5-1	Hull with stick construction of framing	5-6
5-2	Stiffened panel extrusion	5-11
5-3	Recess in deck to accommodate stiffened panel extrusion	5-12
6-1	Swaged fastener	6-3
6-2	Strap in tension	6-6
6-3	Angle in tension	6-6
6-4	Fatigue classification of riveted joint	6-8
7-1	Typical mild steel frame with aluminum plate in US Navy DD 693 Class destroyers	7-1
7-2	Riveted connection of an aluminum deckhouse to a steel deck at an expansion joint	7-2
7-3	Riveted connection with corrosion in the aluminum	7-3
7-4	Bimetallic connection of aluminum deckhouse to a steel deck	7-3
7-5	Bimetallic joints exposed to seawater spray at Wrightsville Beach, North Carolina	7-4
7-6	Photomicrographs illustrating corrosion penetration into uncoated bimetallic joint	7-5
7-7	Fixture and test specimen for tensile test of bimetallic joint	7-6
7-8	Fatigue test specimen geometry for bimetallic joint required by MIL-J 24445	7-7
7-9	Fatigue strength of bimetallic joint	7-8
7-10	Typical fashion plate at ends of a deckhouse	7-9
7-11	Cracking at the base of expansion joints	7-10
7-12	Suggested detail at the base of an expansion joint	7-10
7-13	Indent at the base of an expansion joint	7-11
7-14	Factor B vs. effective length for single level deckhouse	7-12
7-15	Stress ratio for a single level deckhouse, height above hull neutral axis 15 feet	7-13
7-16	Correction factor for height of strength deck above hull neutral axis for single level deckhouse	7-13
7-17	Factor B vs. effective length for 2-level deckhouse	7-14
7-18	Stress ratio for a 2-level deckhouse, height above hull neutral axis 15 feet	7-14
7-19	Correction factor for height of strength deck above hull neutral axis for a 2-level deckhouse	7-15
7-20	Shear lag correction factor K_4 for determining the effective area of the deckhouse	7-15
7-21	Shock mount supporting a corner of a deckhouse	7-17
7-22	Close-up of deckhouse shock mount	7-17
7-23	Catamaran with independent deckhouse raised for maintenance	7-18
8-1	Comparison of distortion at a fillet weld	8-3
8-2	Six types of distortion identified by Masubuchi	8-4
8-3	Use of heating and cooling to pretension plate	8-5
8-4	Patterns of distortion for fabricated shapes	8-6
8-5	Simplified model of welding process	8-7
8-6	Cross section through a weld bead defining the inherent strain region	8-7
8-7	Comparison of experimental determination of residual stress with analysis with a calibration factor applied	8-10

Aluminum Marine Structure Guide

8-8	Comparison of experiment and analysis of a fillet weld of 5454-H34 aluminum	8-10
8-9	Panel analyzed for distortion	8-11
8-10	Definition of joint rigidity	8-11
8-11	Experimental welding sequence for panels	8-12
8-12	Comparison of experiment and analysis of sequence 4 of panels	8-13
8-13	Best welding sequence determined through the joint rigidity method	8-14
8-14	Recommended welding sequence for butt welds	8-15
8-15	Angular distortion at a fillet weld	8-16
8-16	In-line preheating prior to fillet welding	8-17
8-17	Cross-section of fillet welded stiffeners with and without in-line preheating	8-17
8-18	Effect of the position of the preheating torch	8-18
8-19	Effect of longitudinal stretching on the longitudinal distortion of welded panels	8-19
8-20	Apparatus for stretching welded panels	8-19
8-21	Reduction of deflection of stretched panel when welding transverse frames	8-20
8-22	Comparison of panels with and without stretching after welding of transverse frames	8-20
8-23	Distortion of extruded panels during welding together	8-21
8-24	Jig used to restrain rotation of extruded panels during longitudinal welding	8-21
8-25	Use of strongbacks to reduce distortion when welding extruded panels	8-22
8-26	Flatness tolerances for aluminum plate in critical areas	8-23
8-27	Flatness tolerances for aluminum plate in secondary structure	8-24
9-1	Comparison of aluminum and steel fatigue strength	9-3
9-2	Comparison of 5086-H116 aluminum and ordinary strength steel fatigue strength normalized by yield strength	9-3
9-3	Box stiffener lap joints	9-10
9-4	Fatigue of lapped joints of box girders	9-10
9-5	Intersection of a vertical bulkhead stiffener with a bottom longitudinal stiffener	9-11
9-6	Fatigue data for stiffener intersection compared to Eurocode 9	9-11
9-7	Non-load carrying chock	9-12
9-8	Typical fatigue loading spectrum for a 100-meter ship	9-13
9-9	Comparison of fatigue spectrum computed by SPECTRA 8.2 with a Weibull distribution	9-16
9-10	Weibull coefficient for fatigue spectra versus ship length	9-17
9-11	Total fatigue loading cycles for operation 80 percent over 20 years versus ship length	9-17
9-12	Average encounter period versus ship length	9-18
9-13	Fatigue crack growth da/dN curve for 5083 aluminum	9-23
9-14	Predicted crack growth for a 43.9-m 32-knot craft	9-25
9-15	Fatigue crack growth da/dN curve for ABS Grade CH 36 steel	9-26
9-16	Fracture Toughness R-curves for several aluminum alloys	9-28
9-17	Fracture toughness R-curve for 9.5-mm ABS Grade EH 36 steel in the L-T orientation	9-29

10-1	Result of fire aboard cruise ship <i>Star Princess</i> March 2006	10-1
10-2	Air spaces with insulating value of 0.0 S	10-13
10-3	Air spaces with insulating value of 0.05 S	10-14
10-4	Air spaces with insulating value of 0.10 S	10-14
10-5	Air spaces with insulating value of 0.15 S	10-15
10-6	Example of fire protection insulation	10-16
11-1	Single degree of freedom system	11-2
11-2	Simply supported plate vibrating	11-5
11-3	Simply supported beam vibrating in its second mode	11-9
12-1	Corrosion of aluminum where lead or iron oxide primer spilled over from priming a steel door frame	12-5
12-2	Corrosion of aluminum primed with iron oxide	12-5
12-3	Corrosion where standing water at an internal stiffener permitted buildup of salt concentrations	12-6
12-4	Doubler plate welded over a crack	12-8
12-5	Improving weld profiles in fillet welds	12-8
12-6	Inserting a backing strip in a tubular member	12-9
12-7	Improving the profile of a butt weld	12-10
12-8	Comparison of Eurocode 9 and NSWCCD fatigue S-N curves for butt welds	12-11
12-9	Recracking of one-sided repair weld where the original crack was not removed	12-11
12-10	Reinforcement of a hatch opening	12-13
12-11	Exfoliation of 5454-H321 plate at a deck drain	12-14
12-12	Exfoliation at a joint between a 5456-H321 deckhouse and a steel coaming	12-15
12-13	Intergranular corrosion with plate beginning to pop out	12-16
12-14	Pitting corrosion on a plate susceptible to intergranular corrosion	12-16
12-15	Stress corrosion cracking and pitting on shell plating	12-17
13-1	Polar plot of pitch angle for a patrol vessel in Sea State 3	13-2
13-2	Example of the bridge display from a hull monitoring system for a tanker	13-5
13-3	Display of monitoring system of super liner Ogasawara	13-7
14-1	Schematic illustration of friction stir welding	14-2
14-2	Tip of the friction stir welding tool	14-2
14-3	Section through friction stir weld	14-3
14-4	Completed friction stir welds	14-3
14-5	Friction stir welding panels together	14-4
14-6	Friction stir welding facilities at the Tamano works of Mitsui Engineering and Shipbuilding Company	14-4
14-7	Panels fabricated using friction stir welding at the Tamano works of Mitsui Engineering and Shipbuilding Company	14-4
14-8	Friction stir welding aluminum to steel	14-6
14-9	Scanning electron microscope image and EDS line analysis of friction stir welding joint between aluminum and steel	14-7
14-10	Cross-sectional view aluminum to steel friction stir welded joint after tension test	14-7
14-11	Friction stir weld joint geometries	14-8

Aluminum Marine Structure Guide

14-12	Transverse friction stir welds on aluminum alloys 6013 and 6082 compared with EC-9 curves	14-9
14-13	Laser beam welding process	14-10
14-14	Laser beam welding of a lap-penetration joint with the conduction mode	14-11
14-15	Concept for simultaneously welding with the laser beam process in the keyhole and conduction modes	14-12
14-16	Experimental apparatus for laser stir welding	14-12
14-17	Laser stir lap weld	14-13
14-18	Laser beam lap weld	14-14
14-19	Laser stir lap fillet weld	14-14
14-20	Laser beam lap fillet weld	14-15
14-21	Laser stir fillet weld	14-15
14-22	Laser beam fillet weld	14-15
14-23	Fatigue testing of laser stir welded and laser welded lap penetration joints	14-16
14-24	Possible applications of laser stir welding	14-17
14-25	Electrospark welding apparatus	14-19
14-26	Laser welding schematic	14-21
14-27	Section through laser welds in of 5182 and 5754 alloys	14-22
14-28	Electron beam welding of panels	14-23

List of Tables

Table	Title	Page
2-1	Chemical Composition of Aluminum Alloys	2-2
2-2	Mechanical Properties Marine Aluminum Alloys	2-5
2-3	True Stress-Strain Properties of Aluminum Alloys	2-5
2-4	Yield Strength of Some Aluminum Alloys at Elevated Temperatures	2-6
2-5	Dynamic Tear Energy of Aluminum Alloys	2-7
2-6	J-Integral Fracture Toughness of Aluminum Alloys	2-7
2-7	Corrosion Testing of Aluminum	2-14
2-8	Yield Strength of Welded Aluminum Alloys	2-20
2-9	Corrosion-Erosion Resistance of Different Alloys	2-29
2-10	Seawater Galvanic Series	2-31
2-11	SNAME Tee Sections	2-33
2-12	SNAME Angle Sections	2-33
2-13	Properties of Rounded Tees	2-34
2-14	Properties of Bulb Flats	2-36
2-15	Exit and Quench Temperature Data For Selected 6xxx-Series Alloys	2-42
2-16	Standard Tolerances for Extruded Wire, Rod, Bar and Profiles	2-48
3-1	Comparison of Requirements of ABS HSC and DNV High Speed Light Craft	3-10
3-2	Allowable Stress Levels for Bottom Plating	3-12
3-3	Effective Width of Plate based on Buckling Strength	3-17
3-4	Values of Coefficient C to be used in U.S. Navy Equation for Plating	3-22
3-5	Comparison of Requirements for the Bottom Plating of a 61-meter, 50-Knot	3-25

	Craft	
3-6	Coefficients for Paik-Duran Stiffener Buckling Formula	3-35
4-1	Steel Structural Detail Classifications	4-3
5-1	Minimum Bend Radii for Cold Bends in Aluminum Alloys as a Multiple of Plate Thickness, t	5-2
5-2	Reduction of Mechanical Properties of 5456-H116 with Increased Thickness	5-4
5-3	Permissible Alignment of Butt Welds	5-7
5-4	Comparison of Distortion of Plate Panels Reported by Paik et al. (2006b) with ABS and MIL-STD 1689 Tolerances	5-9
6-1	Materials for Mechanical Fasteners	6-3
6-2	Ultimate Shear Strength for Rivets	6-5
6-3	Fatigue Classification of Riveted Joints	6-7
9-1	Fatigue Classification of Aluminum Structural Details under Eurocode 9, Butt Welds	9-5
9-2	Fatigue Classification of Aluminum Structural Details under Eurocode 9, Cruciform Joints	9-6
9-3	Fatigue Classification of Aluminum Structural Details under Eurocode 9, Lap Joints	9-6
9-4	Fatigue Classification of Aluminum Structural Details under Eurocode 9, Welded Attachments, Transverse Weld Toe	9-7
9-5	Fatigue Classification of Aluminum Structural Details under Eurocode 9, Welded Attachments, Longitudinal Welds	9-8
9-6	Fatigue Classification of Aluminum Structural Details under Eurocode 9, Welded Attachments to Built-up Beam	9-9
9-7	Fatigue Classification of Aluminum Structural Details not Covered under Eurocode 9	9-9
9-8	Example of Cumulative Linear Fatigue Calculation	9-14
9-9	Stress Intensity Factors for a Few Geometries	9-21
9-10	Fatigue Crack Growth Calculation for a 42.7-meter Aluminum Vessel	9-24
10-1	Vessel Types Under U.S. Code of Federal Regulations 46	10-5
10-2	U.S. Coast Guard Approved Fire Protection	10-11
10-3	Minimum F_T Values Required to Limit the Temperature Rise on the Unexposed Face	10-12
10-4	F_E Values to Limit Temperature Rise of Aluminum Structure to 200 °C (360 °F)	10-15
10-5	F_C Values to Limit Temperature Rise of Aluminum Structure Surrounded by Fire to 200 °C (360 °F)	10-17
10-6	Typical Fire Loading of Various Spaces	10-19
10-7	Equivalent of Fire Loading to Duration of the Standard Fire Test	10-20
10-8	F_C Values Required for Structure	10-20
11-1	Coefficients for Natural Frequencies of Beams	11-3
11-2	Comparison of Vibration Frequencies of Equivalent Aluminum and Steel Panels	11-13
12-1	Improvement in Fatigue Life of Structural Detail by Adding Brackets	12-12
14-1	Typical Mechanical Properties of Friction Stir Welded Aluminum Specimens	14-9

Acknowledgements

This work was sponsored by the interagency Ship Structure Committee. I would like to thank the members of the SSC Project Technical Committee, which had technical oversight for this project, especially committee chair Derek S. Novak of the American Bureau of Shipping, Sergei Petinov of St. Petersburg Polytechnic University, Matthew Collette of SAIC, Jeom Kee Paik of Pusan National University, and Paul Hess of the Office of Naval Research, all of whom made many helpful suggestions and provided much reference material.

I received help from many shipyard personnel, especially Grant Pecoraro of Gulfcraft, Al Dodson of Swiftships, Jim Towers of Kvichak Marine Industries, Michael Duquesnoy of Austal USA, Paul Kotzebue of Swath Ocean Systems, W. Philip Nuss of Trinity Yachts, and George Lundgren of Workskiff. I visited Textron Marine and Land systems, and met with Dan Mirelez, Don Thomas, David Levy, Angel Brignac, C. Booty Cancienne, and Jan Baudoin.

Many producers and suppliers of aluminum were helpful, including Michael Skillingberg of The Aluminum Association, Stan Guess of Tower Extrusions, Larry Moffett of Taber Extrusions, Joseph B. Wolf and Rob Menard of Aluminum and Stainless, Inc., Douglas J Waldron of Advanced Joining Technologies, Harold Bushfield of Alcoa, Inc., and Mike Farrell of G. James Australia Pty. Ltd. I was kindly received at the Alcoa Technical Center, and received helpful information from Robert Evert, Nathaniel Beavers, Francine Bovard, Israel Stol, Michael Brandt, James Burg, Roger Kaufold, James Marinelli, Jean Ann Skiles, and Rebecca Wyss. David Williams, Alcoa Defense Director of Naval Programs, supported the Alcoa effort. Manny Tesfaye of IPS Structural Adhesives supplied information on the use of adhesives.

Catherine Wong of NSWCCD provided much useful advice and information on corrosion, Edward Devine of NSWCCD reviewed the chapter on design, and Raymond H. Kramer of Raytheon provided information on the INCAT design. Steve Slaughter of MCA Consultants also provided comments on the draft report. Usman Sorathia of NSWCCD reviewed the material on fire protection.

Chapter 1

Introduction

1.1 Background

In the 1890s, aluminum had become popular for lightweight applications, and was used for household cookery, among other applications. Experimental small craft were constructed of aluminum, and further use seemed promising. The first sizable craft constructed of aluminum was the sloop-rigged yacht *Vendenesse*, which was built at St. Denis in France in 1892. Aluminum plate was used for the shell plating, decks and bulkheads, although the frames, keel and stringers were steel. The aluminum used was a six-percent copper alloy, and the construction was riveted. Within four months after launch, corrosion was observed over 20 square meters (200 square feet) of her bottom, where the paint had failed. Afterwards, corrosion continued, although a special paint was developed to ease the problem (Hobson, 1897).

The first use of aluminum in this country for a sizable craft occurred in 1895 when Herrshoff designed and built the America's Cup yacht *Defender*, which was to be the pride of American technology. The side shell plating and some of the frames of *Defender* were of a nickel aluminum alloy. This alloy, called "Pittsburgh Reduction Co.'s Nickel Aluminum" contained four percent nickel and had a yield strength of about 205 MPa (30 ksi). The portion of the hull plating below the waterline was bronze, as were the rivets for the aluminum. This combination of aluminum with bronze led to rapid corrosion of the aluminum, but not before the Cup was won by *Defender* (Hobson, 1897) (McGuire, 1895).

At the same time, Yarrows in England was using aluminum for torpedo boats being built for the French Navy. In this case, a six-percent copper alloy was used, with iron rivets and a mild steel frame. Evidently, the French were pleased with that design, as they began a series of their own design. The lead ship of that class, *Foudre*, was completed in 1895. This 18-meter (60-foot) second class torpedo boat spent the winter of 1895 moored at Cherbourg. When inspected in the spring of 1896, she was found to be extensively corroded, especially between the riveted seams of the plates. The boat would have had to be taken apart to clean these seams and repair them, so instead she was scrapped, and the five sister ships were ordered of steel.

Aluminum was first used in the U.S. Navy for some topside fittings for the torpedo boats intended for the battleship USS *Maine*. These stanchions, sockets and decklight frames quickly corroded and were replaced with steel. A similar experiment with the same results was made with the torpedo boats *Foote*, *Rodgers*, and *Winslow*, which were built in Baltimore between 1895 and 1898.

The first aluminum deckhouses for U.S. Navy ships were for the torpedo boats *Dahlgren* and *Craven*, which were designed and built by Bath Iron Works in 1898. To design these, General Thomas W. Hyde, the founder of Bath Iron Works, bought the plans for torpedo boats from the French Normand shipyard. He also hired naval architect Charles P. Wetherbee, who had worked summers in the Normand yard while a student at Ecole d' Applications du Genie

Aluminum Marine Structure Guide

Maritime. Possibly, the use of aluminum for the hulls by other French yards interested Wetherbee, who used this new technology (Friedman, 1982). However, the aluminum in these boats evidently fared no better than it had in other applications, for aluminum was not used again in structural applications for forty years.

In the 1930s, lightweight topside structure was becoming important for destroyers. A welded corrosion resisting steel panel, consisting of face sheets of 0.5-mm (0.02-inch) plate, spot welded to stiffeners separated 51 mm (2 inches) and 25 mm (1 inch) thick, was riveted to frames which were originally corrosion resistant steel, but in later ships changed to mild steel (C&R, 1934). These CRES panels were used for DD-364 through DD-396.

In 1935, aluminum was reintroduced to deckhouse design as a replacement for brass in the portion of the pilot house near the magnetic compass (C&R, 1935). Aluminum was used extensively at that time for many other nonstructural purposes, including furniture and joiner bulkheads. With the DD-409 class, designed in 1936, came the greatest use of aluminum for exposed deckhouse structure. Plating was mixed, some of aluminum, some of mild steel, with the framing of mild steel (C&R, 1936). This application of aluminum plate was apparently successful, because the next class designed, the DD-423, used aluminum for plating throughout the entire deckhouse, except where thick steel was used for fragment protection (C&R, 1938).

Insight as to the reasoning behind this change is documented in the newsletter of the Bureau of Construction and Repair (C&R, 1936A). Aluminum was accepted, even though it weighed more than the corrosion-resisting steel panels, because of lower cost, less likelihood of local damage, easier repair, and better corrosion resistance. The effect of fire was considered, but “the steel framing would ... support such weights as needed to be supported until repairs could be made.”

The first technical bulletin of the newly formed Bureau of Ships is a summary of U.S. Navy experience up to 1940 with riveted aluminum. Troubles were found with the early applications that could be “traced to improper methods of design, fabrication, or upkeep” (Pyne et al., 1940). Design problems were caused by improper alloy selection, insufficient rigidity, use of welding, use of tap bolts, improper riveting and overheating. Severe corrosion resulted when gasketing materials on faying surfaces were not impregnated with a suitable paint. The early years of aluminum use evidently were not trouble-free.

Design of deckhouse structure became rather standardized with mild steel transverse frames spaced 21 inches supporting aluminum plating that was 4.8 mm (3/16 inches) thick everywhere except in way of gun blast, where it was 6.3 mm (1/4 inches) thick. The next major design, the Fletcher (DD-445) class destroyers, used this configuration from the beginning of the class in 1940. However, with the onset of World War II, all uses of aluminum except for aircraft came under careful scrutiny because of shortages, and the use of aluminum in Navy ships was temporarily discontinued. The DD-445 class was thus a mixture of steel and aluminum.

With the USS Gearing (DD-692) and USS Sommer (DD-710) class destroyers, riveted aluminum came back, being used for about half of the deckhouse sides and decks, although the transversely framed stiffeners were welded steel. Following the war, the development of

aluminum welding had an effect, and in 1948 the new destroyer leaders, the USS Mitcher (DL-2) class had aluminum deckhouses that were entirely welded, including the transversely oriented frames. Although the Dealy (DE-1008) class started with steel deck houses, weight growth led to an aluminum deckhouse on USS Courtney (DE 1021) when contracted in 1953 and on subsequent ships of the class. From then on, all new U.S. Navy combatants (destroyers, destroyer escorts, frigates and cruisers) had aluminum for the majority of their deckhouses. In addition, aluminum is used for the deckhouse in landing ships, and for the islands of aircraft carriers and amphibious assault ships.

Towards the close of World War II, some merchant ships built in the US has aluminum in their deckhouses, and this practice continued after the war, primarily in the superstructures of passenger ships. Aluminum began to be adopted worldwide for fabrication of the superstructure of passenger ships, a practice that continues today. Aluminum began to be used in the 1940s for pleasure craft and for workboats, the size of which has increase greatly over the years. The use of aluminum for the hulls of high-speed merchant vessels began in the 1990s with increased construction of high-speed ferries. These vessels have become so technologically advanced that they have surpassed the capabilities of many naval vessels; many navies today are adapting derivatives of these high speed vessels to combatant craft.

1.2 Material Characteristics

In addition to standard aluminum alloys that have seen many years of satisfactory service in a marine environment, manufacturers have developed new alloys for use in ship and boat construction. The U.S. Aluminum Association maintains the international standards for aluminum alloys, including temper designation, chemical composition and material properties. Recent problems with corrosion of aluminum from a particular producer led to a revision of the standards of the American Society of Testing and Materials, and those standards are being adopted internationally, including by the International Association of Classification Societies.

The marine-grade aluminum alloys used today have generally good corrosion resistance. Until recently, there were no standards for evaluating corrosion resistance in actual seawater environments, and developers of new alloys relied on accelerated lab tests that had not been rigorously correlated with field-testing to verify suitability of their products for use in marine environments. Consequently, such alloys should be used with caution.

The American Society of Testing and Materials (ASTM) formed the ASTM B07.03 Task Group on Marine Alloys, and the Aluminum Association formed a similar group in an effort to establish a correlation between accelerated corrosion lab tests (ASTM G66 and G67) and long-term exposure to seawater and seacoast atmospheric environments and ultimately create a standard by which new alloys could be evaluated to determine acceptability. The Task Group developed a new specification for marine aluminum alloys, ASTM B 928-04, High Magnesium Aluminum-Alloy Sheet & Plate for Marine Service.

Aluminum for hull construction is used in two basic product forms, plate and extrusions. Aluminum structural shapes are produced by the extrusion process, where hot metal is pressed through a die to form the structural profile. This process is rather versatile, and a new shape can

be easily designed and extruded. For this reason, there are a variety of different extrusions used in marine construction, but few to any standard cross-section.

1.3 Structural Design

The basic principles for structural design with aluminum are similar to those for design with steel. Consideration needs to be made for the reduced elastic modulus of aluminum, which means reduced buckling strength and stiffness. In aluminum the strength of welds and the adjacent heat-affected-zone are significantly less than in the base metal, and the designer needs to be aware of this. Design codes generally address the issue of weaker welded properties by designing all of the structure for this reduced strength, although there are instances when the properties of the base metal are used.

Naval authorities and classification societies document methods for design of aluminum hull structures. These methods have historical backing, but new materials, emerging technologies, different hull forms, and high-speed operation mean that application of these methods will require interpretation. The designer must be aware of the basic principles, and not try to apply blindly a method to a use for which it was not intended.

For the smaller, high-speed craft that are being fabricated with aluminum, the design loads are different from those of larger vessels in that the loads are reduced if the craft is to operate in a more benign environment. Furthermore, even though equations are given for determining the design loads, for most of these craft model testing or hydrodynamic analysis is necessary and required for determining the design loads actually used. Likewise, even though equations are given by the classification societies to compute the structural response to the loads, in most situations detailed finite element analysis is required to determine the scantlings.

1.4 Structural Details

Many of the same structural problems are posed in aluminum structure as in steel structure for details such as intersections of structural members or avoidance of discontinuities. In many cases the solution to the problem, the structural detail selected, will be the same in aluminum as in steel. However, considerations of fatigue, which is a far greater concern in aluminum, will dictate the use of details that have lower stress concentrations.

Opportunities in aluminum, particularly for the ease with which unique structural shapes can be extruded, leads to structural details that are unique to aluminum structure. The result is generally lighter structure at a reduced total cost. However, such details often have discontinuities for which detailed stress analysis, including fatigue analysis should be performed, and fatigue testing of such details is needed.

1.5 Welding and Fabrication

Aluminum welding is generally performed with gas-metal arc welding (MIG), similar to the use of the process with steel. The only other process used with aluminum is gas-tungsten arc welding (TIG), which is used for thinner material. Although the processes in aluminum are

similar to those in steel, the welding parameters and techniques are sufficiently different that retraining of welders is required for aluminum, and most shipyards do not have the same welders work with both metals. Friction stir welding is also becoming popular for some areas of the structure. A greater amount of cleanliness is generally required for aluminum, and more care is required to reduce welding distortion because the low elastic modulus of aluminum means greater distortion and a greater chance of buckling from residual stresses.

Cutting aluminum is easier than steel, and modified forms of woodworking tools are used for cutting aluminum. However, much of the cutting of aluminum done today is with numerically controlled plasma-arc cutting or fluid jet cutting, both of which result in very accurate dimensions. Aluminum plate is easily bent, although cracking can occur if the bend radii are too small. Because the alloys used obtain their strength from either work hardening or from heat treatment, aluminum generally cannot be heated for forming. Likewise, flame straightening is limited for fabricated structure that does not meet required distortion tolerances. Although aluminum plate can be easily rolled to form curved shapes, the difficulties associated with heating generally preclude forming plates with any degree of compound curvature, which places a limitation on the lines of aluminum vessels.

Aluminum subassemblies can be fabricated in panel lines similar to steel structure, but most shipyards prefer to use stick construction where the bulkheads, frames, and stiffeners are laid up and welded together before plate is welded to them. Some shipyards are moving towards prefabricating subassemblies, but this practice is limited today, especially in smaller yards producing one-off designs.

1.6 Riveting

Riveting is seldom used today for fabricating marine structures. When the process is used, care must be taken to minimize corrosion. The alloys being joined and the fasteners joining them should be of the same alloy or of alloys with the same electrochemical potential in seawater. The faying surfaces should be treated with preservatives prior to joining, although working of the structure over time will tend to break down this preservation with the possibility of crevice corrosion occurring.

When mechanical fastening is used, it is generally done with swaged fasteners instead of actual rivets. These fasteners have more consistent tension after installation than rivets, require less labor, and do not require as high a skill level as with riveting.

1.7 Joining Aluminum to Steel Structure

When steel and aluminum are used on the same vessel, such as the aluminum superstructure of a naval combatant or a passenger ship, the bimetallic strip is welded to the steel on one side and aluminum on the other. This joint has good fatigue resistance and good corrosion resistance as long as it is not used underwater or exposed to standing water.

When aluminum is used as a superstructure on a steel hull, the stresses in the aluminum are generally lower than in the steel hull because of the lower elastic modulus of aluminum. However, the reduced fatigue strength of aluminum means that care must still be taken in design

1.8 Residual Stresses and Distortion

The lower elastic modulus of aluminum compared to steel has benefits and drawbacks. Residual stress from welding is lower, but the stress that does occur causes greater distortion and buckling of thin structure. The ability to predict distortion in steel structure is still limited today, even with very involved finite element analysis. The prediction models rely to an extent on experimental data, and there is far less data for aluminum, so that the state-of-the-art in prediction of distortion in aluminum has not advanced. Rules of thumb for such things as weld sequencing are available, but experience with fabricating similar structure is the best guide today.

Because of the greater distortion that generally occurs in aluminum structure, fabrication tolerances are greater than for similar steel structure. However, the impact of these increased tolerances on strength has not been well addressed.

1.9 Fatigue and Fracture Design and Analysis Procedures

The low fatigue resistance of aluminum is primarily due to the faster fatigue crack growth rates in aluminum, which are about 30 times faster for the same stress level with the same size crack. The primary method of reducing the risk of failure from fatigue cracking is to prevent crack initiation. This is done by using fatigue analysis during design and ensuring that the stress levels and structural details used will not result in cracks initiating during the service life of the vessel.

Fatigue analysis requires knowledge of the loading history that will occur during the lifetime of the vessel. Analytical methods exist for doing this, but the high speeds and unusual hull forms associated with many aluminum vessels sometimes exceed the capabilities of all but the most advanced methods, which are expensive and time-consuming to use.

Aluminum has good tolerance to resist fracture from single overloads, such as unexpected events or weapons effects. However, the fracture resistance is not as great as for marine-grade steel. The greatest risk of hull girder fracture comes from fatigue crack propagation, but means to arrest a growing crack have not been developed.

1.10 Fire Protection

Aluminum has a relatively low melting point, and must be insulated to protect the structure from softening or melting in a shipboard fire. Requirements for fire zone boundaries on commercial vessels are established by international convention and by the regulations of the U.S. Coast Guard. The procedures for designing the insulation to meet these requirements for aluminum structure were established in the 1970s by the Society of Naval Architects and Marine Engineers, and have not significantly advanced since that time.

The need for fire protection insulation in aluminum structure slightly reduces the weight advantage of aluminum over steel, and adds to the price, which is generally higher than for steel. Less expensive and lighter means of insulating aluminum are being sought, such as spray-on insulation, but these materials are not generally accepted today.

1.11 Vibration

Although aluminum has one-third the elastic modulus of steel, it also has one-third the density, so similar structures in aluminum and steel will have the same natural frequency of vibration if there is no other mass associated with the mode of vibration. Indeed, because of the reduced strength of aluminum, the structure designed for the same conditions will have greater stiffness, and the frequency of vibration will actually be higher. This increased frequency will be offset if the structure has a large mass associated with it, and aluminum structure in such situations may have to be made stiffer to prevent vibration problems from occurring.

Aluminum may be less tolerant of vibration if there are stress concentrations in the vibrating structure that could become points of fatigue crack initiation. Concern for hull girder vibration and local vibration of structural members has led to some classification societies imposing minimum inertia requirements for the hull girder and for structural members.

1.12 Maintenance and Repair

Because of the generally excellent corrosion resistance of aluminum, no painting is required for many alloys, which have seen many years of service without problems. However, other alloys are more prone to corrosion and must be coated to protect them. Painting of topside structure is also done for cosmetic reasons, and once painted, the coating will have to be maintained. Painting is also required below the waterline to prevent fouling, and in some tanks, such as sewage and gray water tanks because of the corrosive nature of the fluids in these tanks. It is more difficult to paint aluminum than steel because the preparation and atmospheric control requirements are more stringent.

Because of the low fatigue resistance of aluminum, structural cracking can become a maintenance headache for an improperly designed structure. Generally, areas that crack will have to be redesigned with improved structural details to prevent recurrence of the cracks in the same place.

1.13 Mitigating Slam Loads

High-speed craft are subject to large loads on the bottom structure from slamming into waves, and these loads can cause local structural damage or damage to the hull girder. The best way to reduce these loads is to operate at reduced speeds or at more favorable headings when experiencing high loads. However, the ship's force often will not be able to perceive the occurrence of these damaging slams, and hull instrumentation is required to alert the operators when the loads are becoming too severe. Classification societies provide special classification for vessels so equipped, but the usage is not well accepted.

1.14 Emerging Technologies

Friction stir welding has advanced rapidly since its development in the early 1990s, and is used extensively today, primarily for joining light-weight extruded panels. The size of extrusion dies limits the size of the panels produced, but many have found it more economical with improved fabrication tolerances to have extrusions shipped to a friction stir welding facility and joined into panels that are not so large to prevent shipping over the road to the shipyard.

Inspection standards have been developed for friction stir welding, but testing is required to confirm some of the properties of the joints, including fatigue and corrosion resistance. The process still lacks versatility today, and its use is confined to materials that can be brought to the welding machines.

Chapter 2

Material Characteristics

2.1 Properties of Aluminum

Aluminum is an elemental material with the atomic number 13 and atomic weight of 26.98. Although spelled “aluminum” in the United States, the spelling by international convention is “aluminium” as adopted by the International Union of Pure and Applied Chemists in order to conform to the "ium" ending of most elements. It is one of the most abundant minerals in the earth's crust, occurring as aluminum oxide, or bauxite. In 1808 Sir Humphry Davy in Britain, also known for the invention of a mine safety lamp, established the existence of aluminum and named it alumium. In 1827 Friedrich Wöhler in Germany described a process for producing aluminum as a powder by reacting potassium with anhydrous aluminum chloride. In 1854 Henri Sainte-Claire Deville France improved Wöhler's method to create the first commercial process, and the metal's price, initially higher than that of gold and platinum, dropped by 90 percent over the following 10 years. In 1886 two unknown young scientists, Paul Louis Toussaint Héroult in France and Charles Martin Hall in the United States, working separately and unaware of each other's work, simultaneously invented a new electrolytic process, the Hall-Héroult process, which is the basis for all aluminum production today. They discovered that if they dissolved aluminum oxide (alumina) in a bath of molten cryolite and passed a powerful electric current through it, then molten aluminum would be deposited at the bottom of the bath. (IAI, 2006).

This chapter provides a brief review of the characteristics of aluminum alloys, including chemical composition, physical and mechanical properties, welding, corrosion, product forms and the extrusion process. More detailed information, particularly on welding, should be sought from the documents that are referenced.

2.1.1 Chemical Composition

In its pure form, aluminum does not have very great strength, with a yield strength of about 28 MPa (4.0 ksi). However, when alloyed and work or precipitation hardened, the yield strength can be 621 MPa (90 ksi) or higher. A variety of elements are used in alloying aluminum. In the late 19th century, copper was the predominant element used to improve the strength of aluminum, and it was used for several marine applications, including racing yachts and torpedo boats. The unsuitability of these copper-based aluminum alloys for marine use became readily apparent when these craft almost dissolved at their piers within a few years because of corrosion. It may be that some persons at that time were in sympathy with the Roman Emperor Tiberius, who, according to the historian Pliny the Elder, had beheaded a goldsmith who showed him a very light plate that was almost as bright as silver, and according to the goldsmith, had been made from plain clay! Corrosion problems generally do not occur with the aluminum alloys used today for marine service, which are alloyed with the predominant alloying element of either magnesium or magnesium and silicon. By international agreement all wrought aluminum alloys except for experimental alloys not produced in the United States are registered with The Aluminum Association. The chemical composition of some aluminum alloys is given in Table 2-1, as provided by The Aluminum Association (2006).

Table 2-1 Chemical Composition of Aluminum Alloys (Percentage by weight)

Alloy	Si	Fe	Cu	Mn	Mg	Cr	Zn	Ti	Zr
5052	0.25	0.40	0.10	0.10	2.2-2.8	0.15-0.35	0.10	-	xx
5059	0.45	0.50	0.25	0.60-1.2	5.0-6.0	0.25	0.40-0.90	0.20	xx
5083	0.40	0.40	0.10	0.40-1.0	4.0-4.9	0.05-0.25	0.25	0.15	xx
5086	0.40	0.50	0.10	0.20-0.70	3.5-4.5	0.05-0.25	0.25	0.15	xx
5383	0.25	0.25	0.20	0.7-1.0	4.0-5.2	0.25	0.40	0.15	xx
5454	0.25	0.40	0.10	0.50-1.00	2.4-3.0	0.05-0.20	0.25	0.20	xx
5456	0.25	0.40	0.10	0.50-1.00	4.7-5.5	0.05-0.20	0.25	0.20	xx
6005A	.50-.90	0.35	0.3	0.5	.40-.70	0.3	0.2	0.1	xx
6061	.40-.80	0.7	.15-.40	0.15	.80-1.20	0.04-0.35	0.25	0.15	xx
6063	0.20-0.60	0.35	0.10	0.10	0.45-0.90	0.10	0.10	0.10	xx
6082	0.7-1.3	0.50	0.1	0.40-1.0	0.6-1.2	0.25	0.20	0.10	xx

2.1.2 Alloy and Temper Designations

The Aluminum Association has a numbering system for aluminum wrought products that consists of 4-digit number followed by a letter and then additional numbers. The first four numbers refer to the chemical composition of the alloy, and the letter and following number indicates the temper. Properties are defined by the alloy and its temper. An alloy can be processed to a variety of tempers, which can have varied properties. This designation system is now internationally accepted and has largely replaced the former numbering schemes that varied from country to country (Aluminum Association, 2005A).

The alloys that have 5 as the first digit of their alloy designation, (i.e. the 5xxx-series) have magnesium as the principal alloying agent, and many also may have a significant amount of manganese. The 5xxx-series are not heat-treatable, but obtain additional strengthening by work hardening. The alloys with a 6 as the first digit, the 6xxx series, have magnesium and silicon as principal alloying agents. These form magnesium silicide, which makes the alloys heat-treatable. The remaining three digits represent the specific alloy composition.

In an aluminum alloy, the 4-digit alloy designation is followed by a letter and several numbers to indicate the temper of the alloy. The letter H indicates strain hardening, and T indicates heat treatment. For strain-hardened alloys, such as those in the 5xxx series, a 1 following the H indicates that the alloy is only strain hardened. If the digit is 2, the alloy is strain hardened and then slightly annealed, and if the first digit is a 3, the alloy is strain hardened and then has the properties stabilized by either low-temperature treatment, or by heat introduced during fabrication.

The second digit in the H-tempers relates to the degree of strain hardening above the annealed temper, with 8 typically indicating the greatest hardening normally produced. The third digit indicates a variant of the 2-digit temper. A formal system for indicating the degree of hardening by which the ultimate strength of an alloy can be estimated was introduced by the Aluminum Association in 1992. However, alloys developed before 1992 do not have to comply with that system.

For heat-treatable alloys such as those in the 6xxx series, the letter T following the alloy designation is followed by one or more digits, which indicate the type of heat treatment and additional process variables that might impact the product characteristics. For marine alloys, the most common is T6, which indicates that the alloy is solution heat-treated and then artificially aged. This is often achieved during the extrusion process by quenching the shape at a rate rapid enough to hold constituents in solution. Generally, stretching of the marine-grade extrusions to achieve straightness after cooling does not affect the mechanical properties.

2.1.3 Mechanical Properties

The elastic modulus of aluminum is about one-third that of steel, as is the density. As these properties vary slightly between alloys, and are necessary for structural design, the values for some marine alloys are listed in Table 2-2. The table also lists the ultimate and yield strength and the density of these alloys. The strength values are given for the base metal, and are not the welded properties, which will be provided in Table 2-8.

Unlike many steel alloys, aluminum alloys do not have a defined yield point. Rather, there is a gradual increase in strain rate with added stress. The yield strength, or proof stress, is defined by a 0.2 percent offset of the engineering stress-strain curve from testing of a tensile specimen. The specimen is placed under increasing load and the stress and strain determined with load increments, and a curve of stress versus strain is plotted. Then a line parallel to the initial stress-strain curve is drawn with 0.2 percent greater strain. The point where this line crosses the initial stress-strain curve is defined as the yield strength, and is also called the proof stress.

A typical aluminum engineering stress-strain curve for aluminum is shown in Figure 2-1 for 5083 aluminum in the base metal and welded conditions. The curves for ship-grade mild steel and for typical FRP are also shown. Both the base metal and the welded aluminum show continued work hardening as strain is increased and considerable energy under the stress-strain curve. However, that total energy is much less than that of the steel, which ruptures at about 20 percent elongation, compared with 12 percent for the aluminum. By comparison, the FRP shows no plasticity and fails in a brittle manner.

The strength properties in Table 2-2 represent engineering stress strain curves, where the stress is determined by dividing the load by the original cross-sectional area of the specimen. Although this is the commonly accepted method of determining strength, it is inaccurate because the cross-section initially decreases because of the Poisson effect, and then even more as the specimen begins to yield and the elongation principally occurs in a small area of the specimen that “necks down” more than the other regions. A true stress-strain curve is more difficult to obtain, but the results from such tests should be used when modeling detailed material behavior, especially plastic flow at high stress levels. Gross (1963) provides the values in Table 2-3 where the true stress $\bar{\sigma}$ is related to the true strain $\bar{\epsilon}$ by the equation:

$$\bar{\sigma} = K \bar{\epsilon}^n$$

and the true fracture ductility ϵ_f is the true fracture strain at failure.

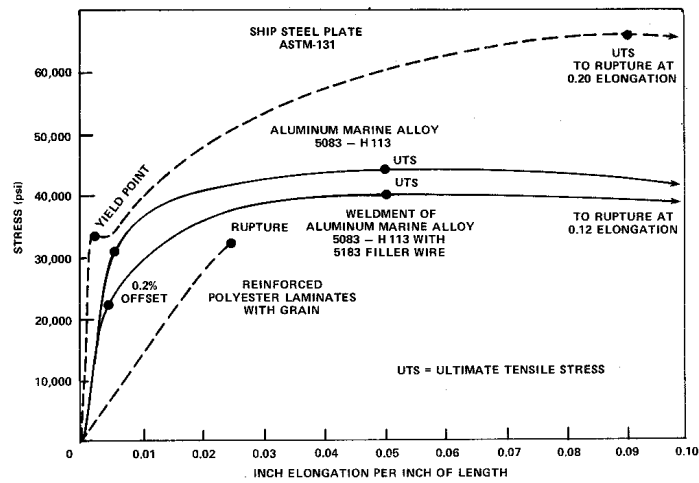


Figure 2-1 Stress-strain curve of 5083 aluminum compared to steel and FRP (Beach et al., 1984).

2.1.4 Properties at Elevated Temperatures

Some aluminum alloys retain their strength, and even increase in strength, at very low temperatures with little loss in ductility. For this reason, they are well suited for cryogenic applications. However, aluminum alloys soften at higher temperatures, and therefore have poor resistance to heating, especially in a shipboard fire. There is a common misconception that aluminum will burn in a shipboard fire. However, because it will melt at about 1,100 °F (600 °C) structure involved in a fire will apparently disappear (reappearing in puddles of melted and resolidified metal) giving the appearance of having burned.

The properties of some alloys at elevated temperature are given in Table 2-4 as provided in the Aluminum Design Manual of The Aluminum Association (Aluminum Association, 2005). The data is plotted in Figure 2-2. The Aluminum Association cautions that these data represent averages for various sizes, product forms, and methods of manufacture, and are intended only as a basis of comparing various alloys, and should not be used for design. Data is represented for common alloys used in marine construction but not necessarily for the particular tempers of the alloys that are used. However, the strength achieved by heat treatment or work hardening is lost at higher temperatures, so all tempers of the same alloy approach the same strength properties with increasing temperatures. Additional information on other alloys and tempers is available in the Aluminum Design Manual.

Table 2-2 Mechanical Properties Marine Aluminum Alloys

Alloy and Temper	Thickness Range		Ultimate Strength ⁵		Yield Strength ⁵ (0.2% Offset)		Elastic Modulus		Density	
	in	mm	ksi	MPa	ksi	MPa	ksi x10 ³	MPa x 10 ³	lbs/ in ³	g/ cm ³
5052-H32 (S&P)	All	All	31	215	23	160	10.2	70.3	0.097	2.68
5052-H34 (S&P)	All	All	34	235	26	180	10.2	70.3	0.097	2.68
5059-H111 (E) ¹	0.114-1.968	3.0-50	47.7	329	23.2	160			0.096	2.66
5059-H116 (S&P) ¹	0.114-0.787	3.0-20	53.5	438	39.1	270			0.096	2.66
5059-H116 (P) ¹	0.788-1.968	20.1-50	52.1	359	37.6	259				
5059-H321 (P) ¹	0.114-0.787	3.0-20	53.5	369	39.1	270				
5059-H321 (S&P) ¹	0.788-1.968	20.1-50	52.1	359	37.6	259				
5083-H111 (E)	<=5.0	<=130	40.0	275	24.0	165	10.3	71.0	0.096	2.66
5083-H116 (S&P)	0.188-1.5	4.0-40	44.0	305	31.0	215	10.3	71.0	0.096	2.66
5083-H116 (P)	1.5-3.0	40-80	41.0	285	29.0	200	10.3	71.0	0.096	2.66
5083-H321 (S&P) ¹	0.063-1.5	1.6-38	44.0	303	31.0	214			0.096	2.66
5083-H321 (P) ¹	1.501-3.0	38.1-76.5	41.0	283	29.0	200			0.096	2.66
5086-H111 (E)	<=5.0	<=130	36.0	250	21.0	145	10.3	71.0	0.096	2.66
5086-H116 (S&P)	All	All	40.0	275	28.0	195	10.3	71.0	0.096	2.66
5383-H-112 (E) ²			45.0	310	27.6	190	10.2	70.0	0.096	2.66
5383-H116 (P) ²	<0.79	<20	44.2	305	31.2	215	10.2	70.0	0.096	2.66
5454-H111 (E)	<=5.0	<=130	33.0	230	19.0	130	10.3	71.0	0.097	2.69
5454-H32 (S&P)	0.02-2.0	0.5-50	36.0	250	26.0	180	10.3	71.0	0.097	2.69
5456-H116 (S&P)	0.188-1.25	4.0-12.5	46.0	315	33.0	230	10.3	71.0	0.096	2.66
5456-H116 (P)	1.251-1.5	12.51-0.0	44.0	305	31.0	215	10.3	71.0	0.096	2.66
5456-H116 (P)	1.501-3.0	40.01-80	41.0	285	29.0	200	10.3	71.0	0.096	2.66
5456-H321 (S&P) ¹	0.188-0.499		46.0 59.0		33.0 46.0				0.096	2.66
6005A-T61 (E) ³			38.0	260	35.0	240	10.0	68.9	0.098	2.70
6061-T6 (E)	All	All	38.0	260	35.0	240	10.0	68.9	0.098	2.70
6063-T6 (E)	All	All	30.0	205	25.0	170	10.0	68.9	0.097	2.70
6082-T6 (E) ¹	All	All	45.0	310	38.0	262			0.098	2.70

(E) Extrusions, (S&P) Sheet and Plate, (P) Plate
Notes

1. ABS, Rules for Materials and Welding, 2006

2. ALCAN, 2004.

3. Data supplied by Tower Extrusions, Olney, Texas.

4. Aluminum Standards & Data – 2006

5. Where two values are given, the first is the minimum allowable, and the second is the maximum allowable.

Table 2-3 True Stress-Strain Properties of Aluminum Alloys (Gross, 1963).

Alloy	Yield Strength (0.2% offset)		Strength Coefficient K		Strain Hardening Exponent n	True Fracture Ductility ϵ_f
	(MPa)	(ksi)	(MPa)	(ksi)		
5086-H32	200	29.0	283	70.0	0.167	0.50
5456-H321	214	31.0	579	84.0	0.225	0.4
6061-T6	283	41.0	421	61.0	0.092	0.40

Table 2-4 Yield Strength of Some Aluminum Alloys at Elevated Temperatures (Aluminum Association, 2005)

Temperature		Yield Strength (ksi/MPa)									
⁰ F	⁰ C	5083-0		5086-0		5454-H32		5456-0		6061-T6	
75	24	21	145	17	115	30	205	23	160	40	275
212	100	21	145	17	115	29	200	22	150	38	260
300	149	19	130	16	110	26	180	20	140	31	215
400	204	17	115	15	105	19	130	17	115	15	105
500	260	11	75	11	75	11	75	11	75	5	34
600	316	7.5	50	7.5	50	7.5	50	7.5	50	2.7	19
700	371	4.2	29	4.2	29	4.2	29	4.2	29	1.8	12

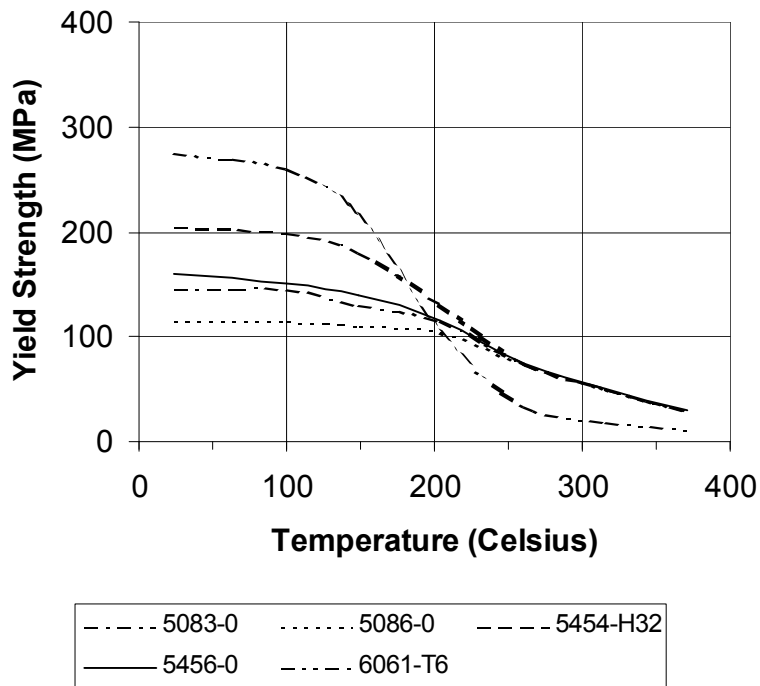


Figure 2-2 Reduction of yield strength with temperature (Aluminum Association, 2005).

2.1.5 Fracture Strength

One quantitative measure of fracture toughness is the dynamic tear test, which is similar to the Charpy V-notch test, except that the specimen is larger. Czyryca and Vassilaros (1972) provide the values in Table 2-5, which were tested at -1°C (30°F).

**Table 2-5 Dynamic Tear Energy of Aluminum Alloys
(Czyryca and Vassilaros, 1972).**

Alloy	Longitudinal		Transverse	
	Joules	ft-lbs	Joules	ft-lbs
5086-H112	2,996	2,210	2,006	1,480
5083-0	2,495	1,840	2,074	1,530
5456-H321	1,898	1,400	984	726
6061-T651	1,169	862	788	581

The J-Integral is a quantitative measure of elastic-plastic fracture toughness that can be used in calculations to determine fracture initiation loads. Czyryca and Vassilaros (1981) provide the values in Table 2-6. Further data will be provided in Chapter 9.

**Table 2-6 J-Integral Fracture Toughness of Aluminum Alloys
(Czyryca and Vassilaros, 1981).**

Alloy	J _{IC}	
	Kilo Joules/m ²	(in-lbs/in ²)
5086-H116	27	153
5456-H117	31	177

2.1.6 Other Properties

Aluminum has good electrical conductivity, with resistivity for the purer alloys being about 0.028 Ohm-mm²/m (17 Ohm-Circular mil/foot), approximately 60 percent greater than copper. Structural alloys have higher resistivity, 0.056 Ohm-mm²/m (33 Ohm-Circular mil/foot) for 5086, and 0.040 Ohm-mm²/m (24 Ohm-Circular mil/foot) for 6061-T6 (Aluminum Association, 2005). Again, the association cautions that these data represent averages for various sizes, product forms, and methods of manufacture, and are intended only as a basis of comparing various alloys, and should not be used for design. By contrast, alloy steels have electrical resistivity ranging between 0.21 and 1.25 Ohm-mm²/m, which means that aluminum can conduct electricity anywhere from 3.7 to 45 times better than steel.

Aluminum also has good thermal conductivity, and is often used in electrical applications as a heat sink. The purer alloys have thermal conductivities of about 234 W/m⁻⁰K (1,625 BTU-in/ft² hr⁻⁰F), 5086 has 126 W/m⁻⁰K (870 BTU-in/ft² hr⁻⁰F), and 6061-T6 has 167 W/m⁻⁰K (1,160 BTU-in/ft² hr⁻⁰F). Again, these values from The Aluminum Association are not to be used for design. For alloy steel, the thermal conductivity ranges from 26 to 48 W/m⁻⁰K, so aluminum conducts heat anywhere from 2.5 to 9 times faster than steel.

The coefficient of thermal expansion of aluminum is about twice that of steel. The coefficients for purer alloys, 5086, and 6061-T6 are 23.6, 23.8, and 23.6 x 10⁻⁶ per degree Celsius (13.1, 13.2, and 13.1 x 10⁻⁶ per degree Fahrenheit). (Aluminum Association, 2005, not to be used for design.) By comparison, the coefficient of thermal expansion for structural steel is about 11.7 x 10⁻⁶ per degree Celsius.

The specific heat of aluminum alloy 5083-0 is 900 joules per kilogram-degree Celsius, or 215 calories per kilogram-degree Celsius (ALCAN, 2004). By contrast, mild steel has a specific heat of 418 joules per kilogram-degree Celsius, or 100 calories per kilogram-degree Celsius (Seo and Jang, 1999).

2.2 Marine Alloys

Of the many different aluminum alloys available, the only alloys recommended for use in applications exposed to salt water are the 5xxx-series and the 6xxx-series. Other alloys have been used, such as the 2xxx-series and 7xxx-series alloys, which aircraft manufacturers used in the 1960s and 1970 for the construction of high-performance naval craft. These used coatings such as Alclad for protection from the marine environment. However, even with these coatings, the craft were found to be highly susceptible to stress corrosion and to have low fatigue strength in a saltwater environment (Beach et al., 1984). This experience and others clearly shows the importance of alloy selection.

Most of the alloys used today were selected after years of experimentation with various alloys, some of which performed poorly in service. In addition, corrosion testing was performed on some early alloys. Mears (1944) reported the results of the exposure of several alloys to a variety of marine environments, including the beach at Wilmington, North Carolina, which was the most severe. Tensile specimens from 1.6-mm (0.065 in) sheet were exposed for up to 4 years in the most severe environments, and the reduction in tensile strength noted. The alloy 52S, now designated as AA5052, had 2.5 percent Mg with 0.25 percent Cr, and the alloy 53S had 1.3 percent Mg, 0.7 percent Si, and 0.25 percent Cr. Alloy 52S is now designated as 5052, and 53S is designated 6063 (Aluminum Association, 1954). A third alloy tested, 61S (now designated 6061) had 0.25 percent Cu, 0.6 percent Si, 1.0 percent Mg, and 0.25 percent Cr, a composition within the range of 6061 alloy except for the lack of Mn, Zn, and Ti, which is today's 6061. (Mn, Zn, and Ti have maximum limits but are not listed as intentional alloy additions for 6061). The yield strengths of the alloys were 200 MPa, 230 MPa, and 270 MPa (29 ksi, 33 ksi, and 39 ksi) for 52S, 53S, and 61S, respectively. After four years of exposure, the tensile strength of the 52S alloy was reduced by only 3 percent, and the other two were reduced by 9 percent. By comparison, other alloys tested had 4.0 to 4.5 percent copper experienced a 20 percent reduction in strength. The original studies did not report the specific tempers of the alloys that were tested, and the behavior of the alloy could vary with temper. The above information should be used only to understand some of the historical testing that led to the alloys and tempers in use today.

Forrest (1947) reviewed the aluminum in use and described some testing that had been performed in addition to the corrosion testing described by Mears. Riveted panels of 53S with 61S angle stiffeners were tested in compression. Those two alloys were described as being those in use for construction at that time. Boykin and Sellers (1953) reviewed fabrication practices for the aluminum superstructures of naval and merchant ships, noting that the principle alloy used was 61S.

Muckle (1948) reviewed the use of aluminum for shipbuilding in the United Kingdom in 1948. Two alloys were principally used; alloy A.W.5, which had 3.5 percent magnesium and

alloy A.W.6, which had 5 percent magnesium. Both of these were tested for corrosion by exposure to tidal water for two years. Both alloys showed little evidence of corrosion, with the 3.5 magnesium alloy performing best, and still exhibiting a shiny appearance at the conclusion of the test.

2.2.1 5xxx Series

The magnesium-strengthened 5xxx-series was found to be best suited for marine use in the 1950s. The U.S. Navy in the 1960s standardized on alloys 5086 and 5456, and for higher temperature applications, 5454. However, many commercial builders used 5083 because it cost only a little more than 5086 and has greater strength. The 5456 alloy has even greater strength than 5083 but with a greater cost differential.

During the late 1960s, corrosion problems began to develop with aluminum plate, particularly with the 5456-H321 plate used for the deckhouses of U.S. Navy ships and in the hulls of the Swift Ships being used in the Vietnam conflict. The most prevalent problem was exfoliation corrosion that initiated at the edges of the plate. Exfoliation results from excess magnesium precipitating into the grain boundaries of the metal, causing separation along those boundaries. Exfoliation is defined as “Corrosion that proceeds laterally from the sites of initiation, along planes parallel to the surface, generally at grain boundaries, forming corrosion products that force metal away from the body of the material, giving rise to a layered appearance.” (ASTM G15-93). In 5xxx-series aluminum alloys, exfoliation results from excess magnesium precipitating as a secondary phase, Mg_2Al_3 or β -phase, in the grain boundaries of the metal. The β -phase is an electrochemically active phase. When the β -phase forms as a continuous and complete network on the grain boundaries, the material becomes “sensitized” or susceptible to intergranular forms of corrosion. This type of only occurs in 5xxx-series plate with a magnesium content greater than 3 percent, and does not seem to effect extrusions. An example of exfoliation is shown in Figure 2-3, showing the characteristic swelling, flaking, and white aluminum oxide accumulation.

Other forms of intergranular corrosion also were observed on vessels in service in the 1970s, including intergranular stress corrosion cracking (Fujii et al., 1972). To address the problem of exfoliation and intergranular stress corrosion cracking, the aluminum industry developed the H116 and H117 tempers for 5086, 5456, and 5083 alloys. The ASTM G 66 (ASSET) test was used to provide visual assessment of exfoliation corrosion susceptibility.

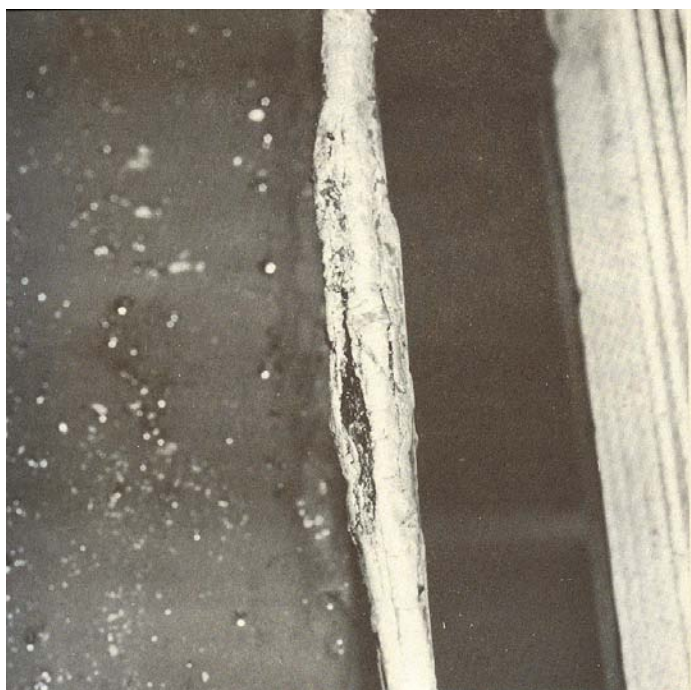


Figure 2-3 Example of exfoliation on the edge of a waterway bar (Dye and Dawson, 1974).

No further corrosion problems were noted for many years with aluminum ships and craft when constructed and maintained to avoid corrosion problems. (See Chapter 12 for problems associated with maintenance and repair.) There have been recent problems, however. In 2001, one producer of aluminum plate made a slight change to the processing of 5083-H321 plate. The resulting plate was susceptible to intergranular corrosion and intergranular stress corrosion cracking. Consequently, numerous vessels required either extensive replacement of plate, or in many cases, complete scrapping of the hull structure. The corrosion was especially noted at welds, and intermittent welds showed more of this type of corrosion and associated stress corrosion cracking than did continuous welds below the waterline.

Intergranular corrosion of 5xxx-series aluminum alloys is caused by β -phase precipitating into the grain boundaries of the metal. Intergranular corrosion is defined as “Preferential corrosion at or adjacent to the grain boundaries of a metal or alloy.” (ASTM G15-93). Figure 2-4 is an example of intergranular stress corrosion cracking, showing a typical semi-circular crack at an intermittent weld, what investigators called “smiley face cracks.” The cracks initiated at localized stress concentrations such as the ends of intermittent welds and at other details that had higher stress concentrations.

Resistance to intergranular, exfoliation, and stress corrosion also is influenced by the grain structure of the product, which is determined by the fabrication process. Some fabrication paths result in a fibrous elongated grain structure that is unrecrystallized, while others result in a recrystallized equiaxed grain structure. If continuous grain boundary precipitate networks are avoided, either microstructure will be resistant to intergranular forms of corrosion. However, if a

nearly continuous network of grain boundary precipitate develops in an elongated, unrecrystallized structure, it will become susceptible to exfoliation and short transverse stress corrosion cracking, but will remain remarkably resistant to longitudinal stress corrosion cracking. On the other hand, if a nearly continuous network of grain boundary precipitate develops in a material with an equiaxed, recrystallized grain structure, it will become susceptible to intergranular corrosion and stress corrosion cracking (all orientations) but remain remarkably resistant to exfoliation corrosion. Some fabrication paths also may result in a dual structure that is partially recrystallized near the surface but unrecrystallized in the center. If a nearly continuous network of grain boundary precipitate develops in material with a dual microstructure, it will exhibit intergranular corrosion, not exfoliation corrosion, on the surface. It also will be susceptible to stress corrosion cracking, particularly under mixed mode loading conditions with a significant short transverse component.



Figure 2-4 An example of intergranular corrosion (Bushfield et al., 2003).

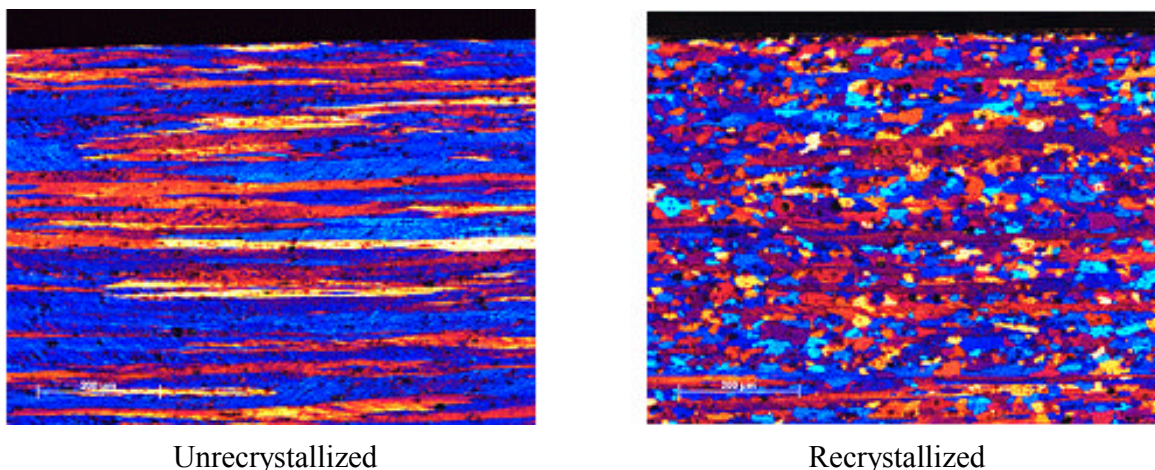


Figure 2- 5 Grain structure of 5xxx-series aluminum (Courtesy of Alcoa).

To address the problem of intergranular corrosion, the American Society of Testing and Materials (ASTM) formed the ASTM B07.03 Task Group on Marine Alloys, and The Aluminum Association formed a similar group. The task group developed a new specification for marine aluminum alloys, ASTM B 928-04, High Magnesium Aluminum-Alloy Sheet & Plate for Marine Service. This specification replaces specification ASTM B 209 for all high magnesium ($\geq 3\%$) alloys and tempers intended specifically for marine application service. Specification B 928-04 includes the ASTM G 67 (NAMLT) test to determine an alloy's susceptibility to intergranular corrosion in addition to the ASTM G66 (ASSET) test to determine susceptibility to exfoliation corrosion. The new ASTM standard and the Aluminum Association have reserved the H116 and H321 tempers for wrought products in the 5xxx-series having a nominal magnesium content of 3 percent or greater. In addition, the definitions of both the H116 and H321 tempers have been modified to require testing for both inter-granular and exfoliation corrosion resistance. Previously the H116 temper required only exfoliation corrosion testing, and the H321 temper had no defined requirement for corrosion testing.

The new definitions have been approved by American National Standards Committee H35 and are published in ANSI H35.1 / H35.1(M)-2006. The task group has brought about similar changes to document W25 of the International Association of Classification Societies, the organization by which classification societies such as ABS establish common standards. The task group is also working to eliminate the relevant subsections of the U.S. government material standard for aluminum sheet and plate, QQ-A-250 to avoid conflicts with the new ASTM specifications (Skillingberg, 2006).

The new definitions in ANSI H35.1 / H35.1(M)-2006 are as follows:

“H116 - Applies to products manufactured from alloys in the 5xxx series, for which the magnesium content is 3% nominal or more. Products are strain hardened at the last operation to specified stable tensile property limits and meet specified levels of corrosion resistance in accelerated type corrosion tests. They are suitable for continuous service at temperatures no greater than 150°F (66°C). Corrosion tests include inter-granular and exfoliation;”

“H321 - Applies to products from alloys in the 5xxx series, for which the magnesium content is 3% nominal or more. Products are thermally stabilized at the last operation to specified stable tensile property limits and meet specified levels of corrosion resistance in accelerated type corrosion tests. They are suitable for continuous service at temperatures no greater than 150°F (66°C). Corrosion tests include inter-granular and exfoliation.”

The marine service alloys and tempers listed in ASTM B 928-04 are the following:

- 5059-H116
- 5059-H321
- 5083-H116
- 5083-H321
- 5086-H116
- 5383-H116
- 5383-H321
- 5456-H116
- 5456-H321

Only these listed alloys and tempers should be used for sheet or plate in marine service where exposure to seawater will occur. The exceptions are the 5xxx alloys containing less than 3 percent Mg or in tempers that are not susceptible to sensitization, such as the annealed or –0 temper. An example is alloy 5454-H32, which has a specified magnesium range of 2.4 to 3.0 percent, or alloy 5454-H34, which has mechanical properties similar to 5083-H116 or 5083-H321. These alloy / temper products can be used in applications where the operating temperature is in excess of 65 °C (150 °F) to avoid problems of stress corrosion cracking. This limitation on service temperature would seem to affect all alloys in locations such as decks, where heat from the sun routinely increases temperatures above these limits. Some in-service problems of sensitization of the high-magnesium alloys have been experienced in recent years, including of cracking of decks and secondary bulkheads that is likely from solar exposure. In one instance sensitization was noted in plate from the engine room bulkheads in a commercial craft, although no cracking was observed. The 5454 alloy is used primarily in applications such as stack enclosures, but some builders use it for the upper decks that are exposed to strong sunlight.

2.2.2 6xxx Series and Corrosion Resistance

The 6xxx-series alloys are generally considered to have poorer corrosion resistance than the 5xxx-series. The principal strengthening mechanism of the 6xxx-series is precipitates of magnesium silicide (Mg_2Si), which are formed within the aluminum matrix during the heat treatment and aging process. These precipitates have approximately the same galvanic electrical potential as the aluminum matrix and therefore do not contribute to galvanic corrosion.

However, some 6xxx-series alloys contain copper, which can cause corrosion problems at the microstructural level, which results in local pitting. Most of the 5xxx-series alloys listed in Table 2-1 have maximum copper contents of 0.10 percent, except for the 5059 alloy. The 6xxx-series alloys listed have copper contents ranging from 0.10 to 0.40 percent. As the copper precipitates are cathodic to the aluminum matrix, they cause localized corrosion of the

aluminum. If the copper-rich precipitates form preferentially on the grain boundaries, the 6xxx alloys also can be susceptible to intergranular corrosion. As the aluminum is corroded, the copper remains, and the local concentration of copper increases above the average level in the alloy, intensifying the local percentage of copper, further increasing the local corrosion rate.

The 6xxx-series alloys also have higher silicon content than the 5xxx-series. If the silicon is proportioned with the magnesium so that all of the silicon is bound in the magnesium silicide, there is no corrosion problem. Alloy 6061-T4 is susceptible to stress corrosion cracking if a high heat-treating temperature is followed by a slow quench. Alloy 6061-T6, which is more commonly used, is highly resistant to stress corrosion cracking.

A difficulty in determining the relative corrosion resistance of aluminum alloys comes when the corrosion rate is measured by weight loss. In the 6xxx-series, seawater corrosion usually takes the form of pitting, which results in little weight loss, even when pits are deep. Any evaluation of corrosion resistance should therefore include the extent and depth of pitting. It is interesting to note that the International Association of Classification Societies in their Requirements Concerning Materials and Welding specify that “the alloy grades 6005A, 6061 of the 6000 series should not be used in direct contact with sea water unless protected by anodes and/or paint system.” Alloy 6061 has 0.15 to 0.40 percent copper, 6005A has 0.30 percent copper, but the 6082 alloy has only 0.10 percent copper, and has no such restriction on its use.

A test of the corrosion resistance of several aluminum alloys was reported in 1965 (Leveau, 1965). Seven different alloys were exposed to seawater for eight years with the results shown in Table 2-7. As is typical for pitting, there is little correlation between the depth of pitting and the reduction in strength of the test specimens. Unlike general corrosion, which causes a decrease in thickness, pitting is very localized and results in little change in thickness, and consequently there is little change in tensile strength of samples.

Table 2-7 Corrosion Testing of Aluminum (Leveau, 1965)

Alloy	Maximum measured pit depth (mm/ in.)	Change in tensile strength (%)
3003-H14	0.18 / 0.0070	-1
Alclad 3004-H18	0.064 / 0.0025	0
5050-H34	0.30 / 0.0120	-3
5052-H34	0.27 / 0.0105	-2
5052-H36	0.58 / 0.0230	-2
5086-H34	0.86 / 0.0340	0
6061-T6	0.36 / 0.0140	-8

In comparative testing of 6005A-T61 extrusions and 6061-T6 extrusions in accordance with ASTM G85 Annex 3, (Tower, 2006) the 6005A showed maximum pit depth of 0.03 inches (0.8 mm) and 632 pits per square foot (6,800/m²) and the 6061 showed maximum pit depth of 0.06 inches (1.5 mm) and 743 pits per square foot (8,000/m²). The ASTM test used is a cyclic spray test in acidified seawater. A 5 percent solution of synthetic seawater is acidified with acetic acid to a pH between 2.8 and 3.0 and atomized as a fog into a heated cabinet maintained at

120° F (49° C) in a cycle consisting of a 30-min. spray followed by a 90-min. soak period at above 98% relative humidity. This test is used to determine time to perforation primarily on aluminum alloy brazing sheet used to manufacture heat exchangers, and is presumably harsher than the ASTM B117 test, which is 120-day test in a continuous saltwater mist. Therefore, the results of the testing have comparative value only, and are not necessarily an indication of performance in a marine environment.

Little other data has been found to evaluate the general corrosion resistance of marine alloys. However, there are several references that indicate that the 6xxx-series alloys have less corrosion resistance than the 5xxx-series. Beach et al. (1984) in reviewing U.S. Navy experience with aluminum in service state “the 6061 alloy was found to be more susceptible to corrosion in the welded condition than the 5083, 5086, or 5456 alloys.” Like many negative statements concerning the 6xxx-series alloys, no further qualification was provided as to the type and extent of corrosion experienced.

Engh et al. (1985) compared the fatigue strength of aluminum in the welded and unwelded condition in air and in seawater. They examined three alloys, the first two being similar to 5xxx-series, one with a low (2.5 percent) magnesium content and the second with 4.5 percent magnesium. The third alloy was similar to a 6xxx-series alloy. The low-magnesium alloy had similar fatigue resistance in air and in seawater, with the test data representing loading with as many as 4×10^6 cycles. The 4.5 percent magnesium alloy had significantly less resistance to fatigue when in seawater, especially when it was tested with an R value of 0.5, meaning the minimum tensile stress was half of the maximum tensile stress, a condition in which the crack tip was constantly exposed to seawater and was constantly in tension. The 6xxx-series alloy, which was tested only at an R-value of 0.5, had significantly decreased fatigue resistance when tested in seawater and in a marine atmosphere compared to testing in air.

From the testing of Engh et al., it can be concluded that aluminum alloys have reduced fatigue resistance in seawater and in a marine atmosphere, which indicates a corrosive mechanism is present. This effect will be discussed further in Chapter 9. However, in this testing, the performance of a 6xxx alloy was similar to that of a high magnesium 5xxx series alloy.

In fatigue crack growth studies for the ongoing Ship Structure Committee project SR-1447, Fracture Mechanics Characterization of Aluminum Alloys for Marine Structural Applications, alloys 5083-H321, 5086-H32, and 5383-H116 were tested, and the preliminary results showed that none of the alloys had a significant difference in fatigue crack growth rates between testing in air and in seawater. The only noticeable difference was at the very low levels of applied stress intensity, where there was a slight increase in crack growth rate. The above results are preliminary and await the issuance of the final report before any definite conclusions can be drawn.

In the Aluminum Design Manual (Aluminum Association, 2005), alloys are ranked on a scale from A to D, with A the highest, for general corrosion and for stress corrosion cracking. On the basis of general resistance to corrosion, all 5xxx-series alloys rate an A unless held for a long time at elevated temperatures.

For stress corrosion cracking, Aluminum Standards and Data-2006 (Aluminum Association, 2006A) gives an A rating to 5083-H116, 5083-H321, 5086-H111, 5086-H116, and all tempers of 5454. However, a B rating is given to 5083-H111 and to all tempers of 5456. For the 6xxx-series, the general corrosion of all tempers of 6063 are given an A rating while all tempers of 6061, 6082, and 6005A are given a B rating. For stress corrosion cracking resistance, all tempers of 6063 and the T6 tempers of 6061, 6082, and 6005A are given an A rating. This information comes from data supplied to the association by its member companies. Much of the data is proprietary. Note that the H111 tempers refer to extrusions, while the H116 and H321 tempers refer to plate.

This limited data seems to indicate that alloy 6061 is not as suitable for marine use as some alloys of the 5xxx-series, yet it is ranked similar to 5456, which has seen many years of satisfactory marine service, although generally used for naval vessels in topside applications where it is coated. The most successful marine service experience is for the 5086 alloys, which have been used for the uncoated hulls of workboats and supply boats that have seen more than 30 years of service with little evidence of corrosion.

More data is needed for evaluation of the relative corrosion resistance of aluminum alloys intended for marine use. Compliance with the new ASTM B928 specification provides assurance of corrosion resistance for 5xxx-series alloys, but that specification does not apply to 6xxx-series alloys because they have low magnesium content and thus are not prone to the same sensitization phenomena. Caution is needed in the use of integrally stiffened extrusions that are being used as deck plating. Extension of that use to areas of the hull that receive continuous sea water exposure, including wet decks of multi-hulled vessels and side and bottom plating should not be made until conclusive corrosion testing has been accomplished.

2.2.3 7xxx-Series

The 7xxx-series alloys have zinc as their primary alloying agent, with a small amount of magnesium added. Some alloys also contain copper or chromium. These alloys are heat-treatable and can acquire very high strengths, with yield strengths as much as 540 MPa (78 ksi) for alloy 7178-T6. If the alloys do not contain copper, they are weldable, although with a significantly reduced yield strength, such as alloy 7005-T53, which has a welded yield strength of 165 MPa (24 ksi). 7xxx-series alloys are used in aerospace applications and for other service such as automobile bumpers.

One producer developed a variant alloy, designated RA7108.50-T79, which has a welded yield strength on a 50-mm gage length of 140 MPa (20.3 ksi). Initial testing indicated that the alloy had good corrosion resistance. (Hval and Sande, 1997). DNV accepted the use of this alloy in a few high-speed light craft in the period 1996 to 1998, but did not approve its use in larger vessels before service experience was obtained. The alloy was originally accepted for use in "dry spaces" internally in ships. In areas where contact with water was expected such as bilge areas, coating was to be applied. The alloy was not accepted in ballast tanks and other locations continuously exposed to seawater.

In the beginning of 1998 corrosion attacks were detected in one of the vessels using alloy 7108. Welded profiles in 7108 showed a tendency to localized corrosion attacks (pitting and “knife-line” attacks) in the heat-affected zone (HAZ) and in particular in the transition zone between base material (BM) and HAZ. The corrosion attacks were mainly located at a distance from the fusion line of about 20 – 30 mm. The extent of corrosion varied, probably depending on the amount of water, time of exposure and salt content. In some locations only a black line was seen with no visible corrosion attack, in other locations a narrow groove had started to develop and in some areas the corrosion had penetrated the web of the longitudinals and transverse stiffeners. The corrosion was particularly found in areas of the vessels where water had collected due to limited drainage. Base material of alloy 7108 not affected by welding showed no signs of corrosion attacks, even if it was submerged. The service experience has also shown that coating systems successfully applied for conventional aluminium alloys does not give the same degree of protection for this alloy in welded condition.

Based on the above experience DNV decided not to accept welded 7108 in DNV-classed vessels unless in areas that are truly dry, i.e. in areas where it can be guaranteed that no condense water or moisture will be present. (Private correspondence from John-Inge Marthinussen, DNV) This experience is an indicator of how caution must be exhibited in accepting new alloys or alloys not previously used in marine service. It also demonstrates a need for a standard test method for evaluating the corrosion resistance of aluminum alloys in marine service.

2.2.4 Classification Society Requirements

The International Association of Classification Societies (IACS, 2005) has set out requirements for aluminum alloys (W25) and for aluminum welding consumables (W26). The requirements cover rolled alloys 5083, 5086, 5383, 5059, and 5754, and 5456 in tempers 0, H111, H112, H116, and H321. Extruded products are covered in alloys 5083, 5383, 5059, and 5086 in tempers 0, H111, and H112. Extruded products in alloys 6005A, 6061, and 6082 in tempers T5 and T6 are also covered. However, these 6xxx-series alloys may not be used in direct contact with seawater unless they are protected by either a paint system or anodes, or both. Note that 6xxx-series plate is not covered.

The rolled 5xxx-series alloys in the H116 and H321 tempers are subject to testing for exfoliation in accordance with ASTM G 66 (ASSET), and to testing for intergranular corrosion in accordance with ASTM G 67 (NAMLT). The manufacturer may produce reference microphotographs taken at 500X that allow acceptance based on microstructural examination. Thereafter, this examination of the microstructure may be substituted for the ASTM testing for lot release purposes. If the microstructure appears unsatisfactory for a batch, the ASTM ASSET and NAMLT testing may be used. The producer is also required to run the test periodically on a surveillance basis.

The IACS requirements include chemical composition of alloys and required tensile properties. Their compositions are similar to but not identical to those listed in Table 2-1 and Table 2-2. Hollow extrusions that are formed by the heated metal flowing around a portion of a die are to be either examined with macrophotographs or by a drift expansion test as described more fully below. Thickness requirements for rolled plate are also given.

The requirements for welding consumables do not specify the chemical composition of the filler metal. Rather, a filler material is deposited using the welding process for which it is intended. The chemical composition is then to be in accordance with the manufacturer's specifications. Butt welds are made on plate 10 to 12 mm thick and 350 mm wide and of a length greater than 350 mm using the same welding process. The welded plate is then sectioned for transverse tensile tests and bend tests. A minimum tensile (but not yield) strength must be achieved and a 180-degree bend test passed.

All classification societies that are members of IACS incorporate these requirements in their rules, and in some cases amplify upon them. Therefore, the specific requirements of the classification society being used should be consulted.

2.3 Welded Properties

Marine aluminum alloys receive their strength through either work hardening or heat treatment. Exposure to temperatures of around 150 °C (300 °F) can begin the annealing process, significantly reducing material properties. Welding will produce this reduction in properties, particularly in the heat-affected zone of the weld. The O-tempers of the alloys are in the annealed condition, so welding does not reduce their strength. The 5xxx-series alloys in the H tempers are strengthened through work hardening, and the 6xxx-series alloys in the T tempers are heat treated, so all of these alloys lose strength when welded, with the 6xxx-series having the greatest reduction in strength. The effect of the annealing on the properties of the HAZ is obvious when small tensile specimens are taken of weld metal or HAZ metal alone. However, the effect on overall strength is less obvious.

The standard method of testing is to perform a butt weld to join two plates together, and then cut tensile specimens that include the weld. The "dog bone" tensile specimen is cut transverse to the weld, as shown in Figure 2-6. Standards call for the transverse specimens to be either 50 mm (2 inches) or 250 mm (10 inches) in length. Much data on the strength of welded aluminum was collected in the past using the 250-mm specimens. Because the weld metal and HAZ constitutes a smaller percentage of the material in these specimens, the measured properties are higher than when testing using 50-mm tensile specimens. Properties of the weld metal and the HAZ are obtained by taking sections parallel to the direction of the weld, sections b and c in Figure 2-6.

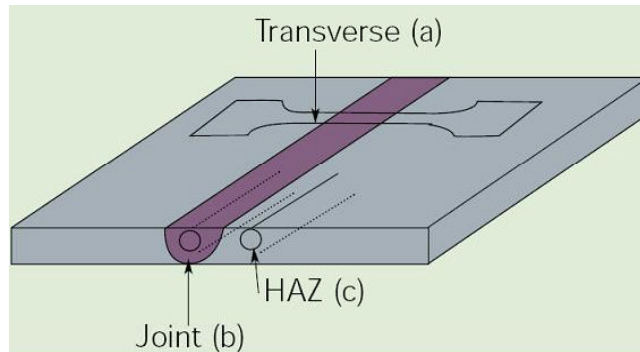


Figure 2-6 A transverse tensile specimen from a weld joint (ALCAN, 2004).

The data from the 250-mm specimens was published widely, including U.S. Navy specifications and design guides, the American Welding Society (AWS, 2004), and in previous editions of the Aluminum Association's Aluminum Design Manual. That manual did caution that the strength values from the 10-inch (250 mm) specimens should be reduced by 25 percent for design use, but that policy was not adapted in forming marine design documentation. The latest edition (2005) of the Aluminum Design Manual provides strength data based on 50-mm gauge length tensile specimens. However, the values from 250-mm specimens are generally used in the U.S. in the design guidance of the U.S. Navy and ABS.

However, use of 50-mm specimens is more common internationally and is the basis for the design guidance of many classification societies. This has led to some confusion in material properties, especially when comparing different alloys. When the tensile properties of one alloy based on a 50-mm specimen are compared to the properties of another alloy determined in 250-mm testing, the first alloy may show reduced strength. However, it may show the same or even greater strength when they are tested with the same sized specimens.

This apparent anomaly does not present a problem when properties are used in design guidance in a consistent manner to determine allowable stress levels. Allowable stress levels in design guides are only one leg of the triangle of standardized design loads, standardized analysis methods, and standardized allowable stresses. As long as all three are addressed in a consistent manner that has been tempered by experience, satisfactory designs should result. The difficulty comes with new and unusual vessels, which must be designed on a "first principles" basis. For these vessels, loads must be determined analytically or experimentally, which are statistical in nature, and require judgment of appropriate load values to be used in design, particularly when allowable stress levels have been based on past experience.

A comparison of the published yield strength values from various sources for some alloys is made in Table 2-8. The gauge length of the tensile specimens used to determine the properties is not always given in those sources. Lacking a consistent database, the designer is advised to use the strength values provided by the design guidance document being used for a particular vessel. If there are no specific design codes required, then the values based on 250-mm gauge length may be used with confidence because of the years of satisfactory use that these data have seen. However, if only strength data based on 50-mm gauge length is available, those values should not be proportioned up to reflect what they may be if data from 250-mm gauge length

were available. Additional data, including welded ultimate strength, on other alloys is available in the references for Table 2-8.

Table 2-8 Yield Strength of Welded Aluminum Alloys (MPa, ksi)

Alloy	Type ¹	Source					
		ABS ²	DnV ³	Aluminum Association ⁴	AWS Hull Welding ⁵	ALCAN ⁶	US Navy ⁷
5052-H32, H34				65 (9.5)	90 (13)		
5086-O	E		92 (13)	95 (14)			97 (14)
5086-H32	P	131 (19)	92	95 (14)	131 (19)		152 (22)
5086-H111	E	124 (18)	92	95 (14)	124 (18)		110 (16)
5086-H116	P	131 (19)	92	95 (14)	131 (19)		152 (22)
5083-H111	E	145 (21)		110 (16)	145 (21)		
5083-H116	P	165 (24)	116 ⁸ (17)	115 (18)	165 (24) ⁹	125 (18)	
5383-H111	E	145 (21)				145 (21)	
5383-H116	P	145 (21)	140 (20)			145 (21)	
5059-H111	E						
5059-H116	P						
5454-H111	E	110 (16)	76 (11)	85 (12)	110 (16)		110 (16)
5454-H34	P	110 (16)	76 (11)	85 (12)	110 (16)		110 (16)
5454-H32	P	110 (16)	76 (11)	85 (12)	110 (16)		
5456-H111	E	165 (24)			165 (24)		145 (21)
5456-H116	P	179 (26)		125 (19)	179 (26)		179 (26)
6061-T6 ¹⁰	E, P	138 (20)	105 (15)	105 (15)	138 (20)		
6061-T6	E, P	103 (15)	105 (15)	80 (11)	103 (15)		

1. E = Extrusion, P = Plate
2. Rules for Materials and Welding, Part 2, Aluminum and Fiber Reinforced Plastics, Chapter 5, Appendix 1, Table 2, American Bureau of Shipping
3. Det Norske Veritas, Rules for Classification of High Speed, Light Craft and Naval Surface Craft, Part 3, Chapter 3, Section 2, Table B4. Yield strength determined from the values of f_1 published by the equation $\sigma_1 = f_1 \times 240 / 1.1$.
4. Aluminum Design Manual, Table 3.3-2, The Aluminum Association, Arlington, Virginia. Based on 50 mm (2 in.) gauge length
5. Guide for Aluminum Hull Welding, AWS D3.7, American Welding Society, 2004. Based on 250 mm (10 in.) gauge length
6. Aluminium and the Sea, ALCAN, Paris, 2004.
7. A Guide for the Use of Aluminum Alloys in Naval Ship Construction and Design, Volume II, Table 4.1, David W. Taylor Naval Ship Research and Development Center, DTNSRDC 84/015, 1984.
8. Thickness ≤ 9.5 mm (0.275 in.)
9. 5083-H321 Plate, thickness ≤ 38 mm (1.5 in.)
10. Welded with 5356 filler.

Collette (2005) made an analysis of the tensile strength of the strength of welded aluminum. He analyzed panels of 5083-H116 and 6082-T6 considering the stress-strain curves of the base metals and of the heat-affected zone (HAZ) of the welds. Each panel was 1 meter long and 0.3 meters wide, and the HAZ was estimated as being either 12.5 mm or 25 mm wide. The results from analysis of the model are shown in Figure 2-7, where the initial stress-strain curve has been offset by 0.2 percent to suit the definition of yield strength.

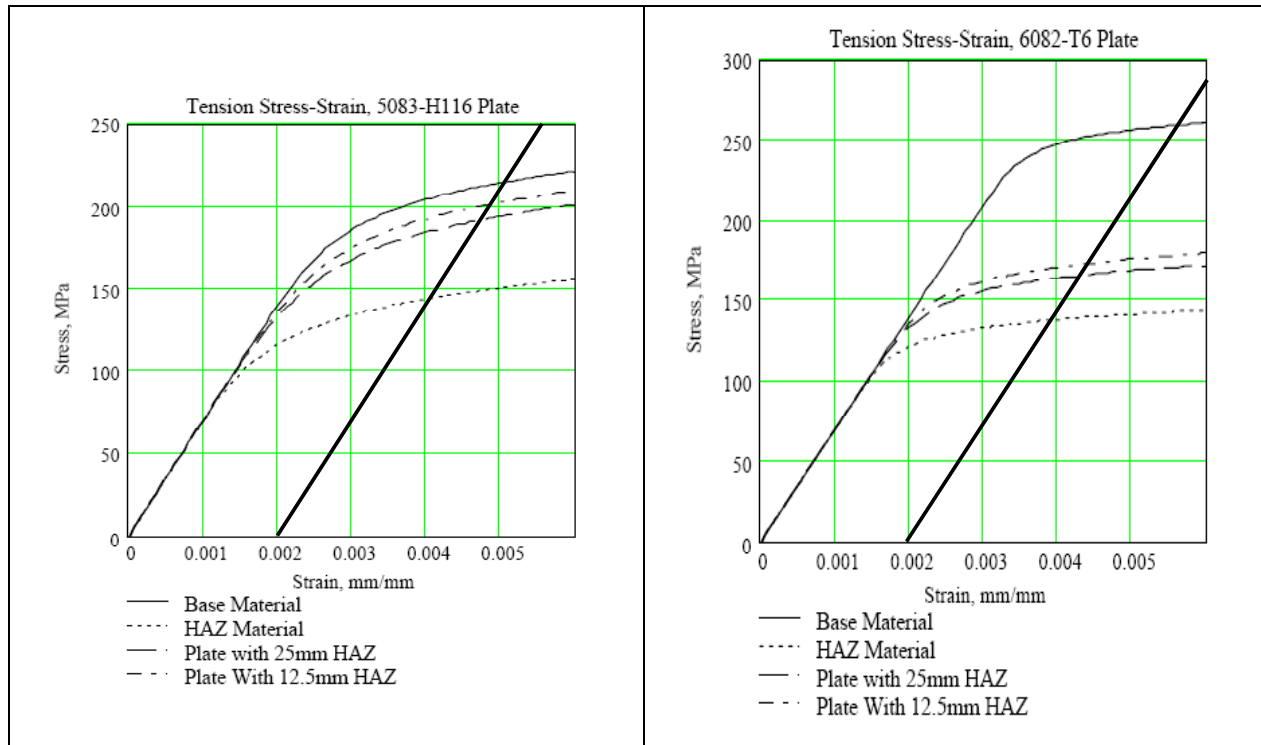


Figure 2-7 Analysis of welded plate in tension (Collette, 2005).

Collette assumed that the yield strengths of 5083-H116 in the base metal and welded condition are 215 MPa and 144 MPa, respectively. In the analysis of Collette, the panel with the 12.5-mm HAZ has an effective yield strength of 200 MPa, and the 25-mm HAZ plate has an effective yield strength of 193 MPa. For the study, Collette assumed a yield strength of 138 MPa for the 6082-T6 HAZ and 260 MPa for the base metal, and the calculated effective yield strength is 175 MPa for the 12.5-mm HAZ and 170 MPa for the 25-mm HAZ.

Paik and Duran (2004) have proposed another approach to developing an effective yield strength using a weighted average of yield strengths based on the volume of base metal and HAZ. For the geometry analyzed by Collette, the area-weighted yield strength in the 5083-H116 is 207 MPa for the 12.5-mm HAZ, and 200 MPa for the 25-mm HAZ, values only slightly greater than those from Collette. In the 6082-T6, the effective yield strength is 247 MPa for the 12.5-mm HAZ and 235 MPa for the 25-mm HAZ; values significantly higher than determined by the analysis of Collette.

The greater work-hardening coefficient of the 5083 HAZ compared to the 6082 HAZ was attributed by Collette to the fact that the effective yield strength of the 6082 was closer to the property of the HAZ than for the 5083. With plastic strain, the stress does not rise as rapidly in the 6082 HAZ compared to the 5083 HAZ.

If the analysis of Collette is correct, then the method proposed by Paik will over-predict the tensile strength of a welded panel. More detailed analysis validated by experiment is needed to determine an appropriate methodology. However, these analyses show that the effective yield strength in tension is greater than that of the HAZ alone.

Collette also examined the ultimate strength considering that the limiting strain for 5083-H116 HAZ as 12 percent and 8 percent in 6082 HAZ. The results are shown in Figure 2-8, with the strain concentration in the 6082 HAZ limiting the strain to produce failure of the overall plate significantly. This analysis may be overly conservative because the constraint imposed by the base metal may permit higher strains with the HAZ. However, the analysis clearly indicates the need for further analysis and experimentation to determine the tensile strength of welded structures.

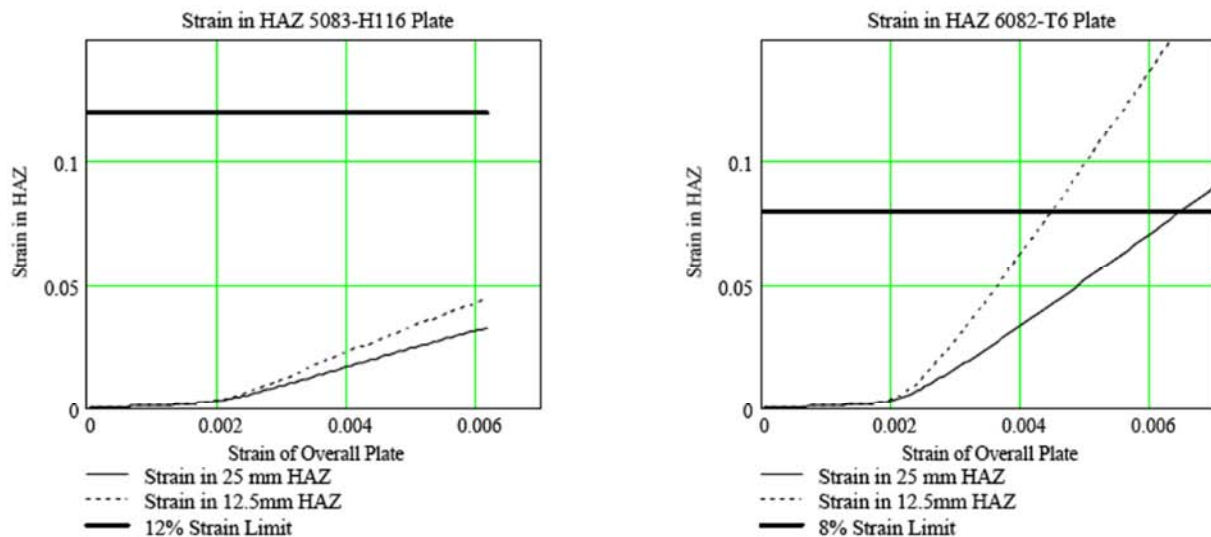


Figure 2-8 Strain in heat-affected zone of welds in a panel (Collette, 2005)

2.4 Corrosion

Compared to steel, aluminum has very good resistance to corrosion, and many vessels that are unpainted have operated for 30 years or more in seawater. Nevertheless, there are conditions in which corrosion can occur, and these conditions can sometimes lead to rapid deterioration of the structure. In general, there are seven types of corrosion that can occur (Czyryca and Vassilaros, 1972):

1. General corrosion and pitting
2. Exfoliation
3. Intergranular corrosion
4. Stress-corrosion cracking
5. Corrosion-erosion, impingement, and cavitation
6. Galvanic corrosion
7. Crevice corrosion

2.4.1 General Corrosion

General corrosion is the wastage of material that generally occurs over a broad area. It is typified by a gray oxide film forming over an unpainted surface. This oxide film is essential to the corrosion resistance of the alloy, as it can prevent further corrosion as long as it remains stable and unbroken.

Associated with general corrosion is pitting, where small holes appear scattered over the surface. The 5xxx-series alloys are noted for good resistance to general corrosion. Although the 6xxx-series are not considered to be as good, the data that is available on corrosion of those alloys do not completely support that assertion not does data support prohibitions on the use of 6xxx-series alloys.

A number of studies have concluded that 5xxx-series alloys are better than 6xxx-series, but since corrosion is affected by differences in the temper, salinity, pH, and the details of details of exposure, the scatter is large and it is not cut and dried. The number of studies where 5xxx and 6xxx go head-to-head is small. (Private correspondence from Catherine Wong, January 2007)

The general corrosion resistance of the 5xxx-series aluminum alloys has been established through testing by immersion in quiet and flowing seawater and exposure to a marine atmosphere. The results of the tests are not consistent; perhaps due to the variety of tempers evaluated. Many tests indicate minor corrosion, while the results from others are more severe. Ailor (1969) reported the results of general corrosion testing of 5xxx-series alloys by immersion in seawater for one, two, and five years. The maximum corrosion rate, determined by loss in thickness, was about 0.0056, 0.0043, 0.0038 mm (0.22, 0.17, and 0.15 mils) per year after 1, 2, and 5 years, respectively. Czyryca and Hack (1974) reported typical rates of thickness reduction from corrosion of 0.022, 0.013, and 0.010 mm (0.85, 0.50, and 0.40 mils) per year for samples tested in flowing seawater for 6 months, 1 year, and 2 years, respectively. In comparing test results, it is important to note that the greatest general corrosion occurs during the first 6 months of exposure, after that the corrosion film retards the corrosion rate.

The 5xxx-series alloys can be prone to reduced corrosion resistance from a condition known as aging or sensitization. Those alloys with a magnesium content greater than 3 percent are particularly susceptible to sensitization. During the process of rolling plate, the temperatures and degree of deformation during various stages is controlled so that the magnesium remains dispersed throughout the alloy. However, under some conditions, the magnesium in the form of Mg_2Al_3 will precipitate at the grain boundaries. The Mg_2Al_3 is highly anodic to the remainder of the alloy, and localized corrosion can occur. This type of corrosion is known as intergranular corrosion, because it proceeds along the grain boundaries of the metal.

The study by Czyryca and Hack included alloys that were in the sensitized condition. In this case, greater corrosion rates occurred. For sensitized 5456-H116, the corrosion rates of thickness reduction were 0.047, 0.026, and 0.029 mm (1.85, 1.02, and 1.15 mils) per year for samples tested in flowing seawater after six months, one year, and two years, respectively, of

Aluminum Marine Structure Guide

exposure. Because of the magnitudes of the corrosion rates reported by Ailor above, it is possible that those samples were in a sensitized condition.

The general corrosion rate of 6xxx-series is not as well established, despite anecdotal evidence that it is not as good in seawater as the 5xxx-series. One source of information comes from testing 6061-T6 in flowing seawater for one year (Rausch, 1958) who reported a corrosion penetration rate of 0.037 mm (1.2 mils) per year, which is comparable to 5xxx-series alloys. In another study (Wacker and Chu, 1970) the measured depth of corrosion was 0.025 mm (1 mil) per year for 6061-T652 forgings after 6 months in flowing seawater.

The difference in corrosion resistance of 6xxx-series alloys compared to 5xxx-series is exhibited more in the extent and depth of pitting that occurs after exposure. Goddard et al. (1967) report that the maximum pit depth in three 5xxx-series alloys (5052, 5056, and 5083) was 0.18 and 0.86 mm (7 mils and 34 mils) after five and ten years of immersion in seawater, respectively. In the same tests, 6061-T6 had 1.65 and 1.30 mm (65 and 51 mils) of pit depth when samples were removed after 5 and 10 years of immersion.

The maximum pit depth of the 5xxx-series alloys studied by Ailor (1967) were in the 5456-H321 alloy, which had maximum pit depth of 0.74, 1.14, 0.96 mm (29, 45, and 38 mils) after 1, 2, and 5 years of exposure. Leveau (1965) reported a maximum pit depth in several 5xxx-series alloys of 0.86 mm (34 mils) after 8 years of exposure to seawater, and 0.36 mm (14 mils) maximum pit depth in 6061-T6 after 8 years. Taylor et al. (1984) had samples of 6061-T6 immersed in quiet seawater for 120 days, after which the measured depth of the deepest pit was 0.034 mm (1.3 mils). Basil (1957) reported pits in 6061-T6 that was exposed for one year in quiet seawater that were mostly 0.076 mm (3 mils) deep, but one pit was 0.64 mm (25 mils) deep.

In comparative testing of 6005A-T61 extrusions and 6061-T6 extrusions in accordance with ASTM G85 Annex 3, (Tower, 2006) the 6005A showed maximum pit depth of 0.8 mm (0.03 inches) and 6,800 pits per square meter (632/ft²) and the 6061 showed maximum pit depth of 1.5 mm (0.06 inches) and 8,000 pits per square meter (743/ft²). The ASTM G85, Annex 3 test is a cyclic spray test in acidified seawater. A 5 percent solution of synthetic seawater is acidified with acetic acid to a pH between 2.8 and 3.0 and atomized as a fog into a heated cabinet maintained at 120° F (49° C) in a cycle consisting of a 30-min. spray followed by a 90-min. soak period at above 98% relative humidity. This test is used to determine time to perforation primarily on aluminum alloy brazing sheet used to manufacture heat exchangers and is presumably harsher than the ASTM B117 test, which is 120-day test in a continuous saltwater mist. This comparative test of two 6xxx-series alloys points up the need for a standardized test. An aluminum extruder, anxious to promote his product, used what seemed to be a good standardized test. Unfortunately, it has no basis for comparison in a marine context, so the results, while of some value on a comparative basis should not be relied upon for material selection.

The data on general corrosion or pitting do not support limiting the use of 6xxx-series alloys. Lacking a standard for acceptable corrosion rates or extent of pitting, it is difficult to

make a judgment as whether 6xxx-series alloys should be used for the same applications as 5xxx-series alloys.

Considerable testing of 5xxx-series aluminum alloys for general corrosion properties has occurred in the laboratory and in field tests. Less testing has been conducted on the 6xxx-series alloys. This testing suffers from a lack of a standard on which to base the acceptability of an alloy for use in high-speed craft. The only standard is the common marine grade alloys that have seen many years of service with no reported corrosion problems. However, even that standard may not be sufficient as thinner sections are being used in high-speed craft today. Corrosion of 0.05 mm is only 0.8 percent of 6.4 mm plate, but is 1.7 percent of 3 mm plate, and the greater percentage may make a difference.

Until recently, there were a number of standardized, accelerated corrosion tests, but they had not been calibrated against long-term exposure testing. The American Society of Testing and Materials (ASTM) formed the ASTM B07.03 Task Group on Marine Alloys, and the Aluminum Association formed a similar group in an effort to establish a correlation between accelerated corrosion lab tests (ASTM G66 and G67) and long-term exposure to seawater and seacoast atmospheric environments and ultimately create a standard by which new alloys could be evaluated to determine acceptability. The Task Group developed a new specification for marine aluminum alloys, ASTM B 928-04, High Magnesium Aluminum-Alloy Sheet & Plate for Marine Service. This group intends to calibrate the results of the accelerated testing against long-term exposure testing. If this were done, then a standard could be established against which new alloys could be evaluated to determine acceptability, especially if 6xxx-series alloys and low-magnesium 5xxx-series alloys were included in the long term testing program.

2.4.2 Exfoliation

The process of exfoliation was mentioned above in conjunction with the selection of alloys for marine service. It was found to occur in many vessels in the late 1960s, particularly in various patrol craft used by the U S. Navy, which initiated extensive investigations by the Annapolis Laboratory of the U.S. Naval Research and Development Center. Investigators from the laboratory inspected twelve aluminum alloy hulls constructed of 5456-H321 and 5086-H32 (MATLAB, September, 1968). Only one of the two 5086-H32 hulls had any service experience, and that was only two years. However, no corrosion was observed. Exfoliation was observed on two of the 5456-H321 craft, which had two and six years of service. This included exfoliation on “the flange of a T section” but the report did not identify if the section was built-up from plate or was an extrusion. None of the seven 5456-H321 PCF patrol craft, which had two to three years of service showed any corrosion.

The laboratory also inspected other vessels, including three craft constructed of 5086-H32, one of which showed pitting up to 1.5 mm (0.06 in) deep after only 8 months of service (MATLAB, October 1968). Two of three craft constructed of 5456-H321 showed no sign of corrosion, but they had only 2 months service. The other 5456-H321 craft had 18 months service, and some small areas of exfoliation were observed on the exterior hull plating where the edge extended beyond the transom.

Vreeland and Ferrara (1969) made an inspection of 72 aluminum-hulled vessels and the maintenance records of 88 Vietnam-based PCF patrol craft. On the PCF's, significant corrosion of the 5456-H321 plate in the interior bilge areas was observed after 3 to 30 months of service, with the average being 14 months. The corrosion consisted of exfoliation of the plate, with no exfoliation or other corrosion observed on either extrusions or weld zones in the same areas. Ten hulls of vessels constructed of 5086 alloy were also examined, with some pitting but no exfoliation observed. However, these vessels all had service times of two years or less.

As mentioned above, the H116 temper of exfoliation-prone alloys was developed to eliminate the exfoliation problem. As was discussed in section 2.2.1, it is important that an alloy with a magnesium content greater than 3 percent be tested through the ASTM G 66 test to ensure that it has no exfoliation corrosion susceptibility. However, the ASTM B 928 covers the H116 and H321 tempers, and the IACS requirements discussed above cover the 0, H111, H112, H116 and H321 tempers. All of these requirements are for rolled plate only, not extrusions. Also, because the 6xxx-series are not prone to exfoliation, there are no testing requirements for these alloys.

2.2.3 Intergranular Corrosion

As mentioned above, precipitation of magnesium to grain boundaries will increase the susceptibility to intergranular corrosion. It is important that an alloy with a magnesium content greater than 3 percent be tested through the ASTM G 67 (NAMLT) test to determine the material's susceptibility to intergranular corrosion.

Susceptibility to intergranular corrosion can result from sensitization of the alloy over time in service or through improper treatment during production. In testing programs, the method generally used to evaluate the propensity of a 5xxx-series alloy to sensitize is to heat it to 100 °C (212 °F) and hold at that temperature for one week. This thermal exposure is used to simulate precipitation that would occur in long-term service at ambient temperatures.

2.4.4 Stress-Corrosion Cracking

Czyryca and Vassilaros (1972) provide a description of stress-corrosion cracking. When alloys of certain susceptible metallurgical structures are subjected to a sustained tensile surface stress (external or residual) in a corrosive environment, failure by stress-corrosion cracking can occur with time. The mechanism of stress corrosion involves both electrochemical and mechanical processes. Local cell action creates a sharp pit, which may induce mechanical tearing at the root, thus exposing a fresh metal surface to accelerated corrosion. Further corrosion deepens the crack and continues the process. Stress corrosion in aluminum alloys is characterized by intergranular cracks normal to the metal surface and stress direction. The electrochemical processes involved in stress-corrosion cracking of the alloys are the same as those in intergranular corrosion; i.e., selective attack of grain boundaries sensitized by precipitates or of areas adjacent to grain boundaries which are highly anodic due to depletion of certain elements. However, not all alloys subject to intergranular corrosion will undergo stress corrosion. Stress corrosion causes a brittle-type failure in an otherwise ductile material.

Both the 5xxx-series and 6xxx-series alloys are considered to be resistant to stress-corrosion cracking. However, when the higher magnesium 5xxx-series alloys become sensitized, stress-corrosion cracking can result.

Niederberger et al. (1964) reported the results of stress corrosion tests on a number of 5xxx-series alloys that were welded and sensitized to stress-corrosion by holding for one week at 100 °C. The specimens were stressed to 75 percent of the annealed yield strength and held for five years in flowing seawater. The only failure was in the alloy 5456-H24, a temper not commonly used for marine structure. Wacker (1967) reported no failures when samples of 5456-H321 were held in flowing seawater for one year when stressed to 90 percent of the yield strength. Sutton (June 1961) and (September 1961) reported no failure in samples of 5xxx-series alloys that were welded, sensitized, and stressed to 75 percent of their yield strength for three to five years in flowing seawater.

Fujii et al. (1971) found that stress corrosion cracking was the cause of cracking in the 3.2-mm (0.125-in) 5456-H321 deck plate of a hydrofoil that had been in service for about 5 years. The cracks surfaces were characterized by the “mud-crack” pattern of the fracture surface that is seen in stress corrosion cracking of aluminum. In laboratory experiments, 3.2-mm plate taken from the deck and from the side shell of the hydrofoil, as well as 6.4 mm (0.25-inch) 5456-H321 plate taken from the deckhouse of a landing ship were tested for stress corrosion cracking by having a wedge driven into a slit in the plate, and then having the specimens exposed intermittently to saltwater. The plate from the deck of the hydrofoil and from the landing ship developed stress corrosion cracks within an hour, but no such cracking occurred in the plates from the side of the hydrofoil as well as some 6.4-m 5456-H321 plate obtained at the time of the testing. This experiment indicated that the plate was becoming sensitized in service from the higher temperatures seen in service.

Wacker and Chu (1970) studied the stress-corrosion cracking of 6061-T652 forgings, and found no indication of cracking when samples were held in seawater at 90 percent of their yield strength for 168 days. They also reported a value of K_{ISSC} for this alloy of 26.4 to 28.6 $\text{MN}\cdot\text{m}^{3/2}$ (24 to 26 $\text{ksi}\sqrt{\text{in}}$). Other data on stress-corrosion cracking of 6xxx is not contained in the reports reviewed.

The friction stir welding process has seen a great increase in recent years in the fabrication of aluminum for high-speed vessels and will be discussed in Chapter 13. The primary use has been for joining integrally stiffened extrusions to form deck panels. Many of the corrosion problems seen in high-magnesium 5xxx-series alloys, including stress-corrosion cracking, haven't been perceived as a problem in extruded tempers. However, the friction-stir welding process may cause the Mg_2Al_3 that is dispersed through the alloy to precipitate to the grain boundaries and increase the potential for corrosion problems.

Stress-corrosion cracking was a serious problem for a method explored in the late 1970s and early 1980s for joining integrally-stiffened aluminum 5456 extrusions to form structural panels in 5456 (Palko, 1981) and (Shumaker, 1979). The process used, called Alforge, subjected the panels to slightly higher temperatures than used in friction stir welding, but the potential for sensitization of the material exists and should be investigated.

The friction stir welding process is currently being used to join both plates and extrusions. Some builders are joining narrow plates using the process because this is less expensive than purchasing wide rolled plates. Therefore, even if sensitization of extrusions isn't a problem (and there is no data to date on this for friction stir welding), it definitely could be a problem for 5456 plate, which has shown susceptibility to stress-corrosion cracking after years of service in hot climates. Preliminary accelerated corrosion testing of friction stir welds has been performed at NSWCCD, and microphotographs of these welds compared to welds performed with conventional GMAW are shown in Figure 2-9. The friction stir weld has less general corrosion, but more testing is required, especially for stress corrosion cracking.

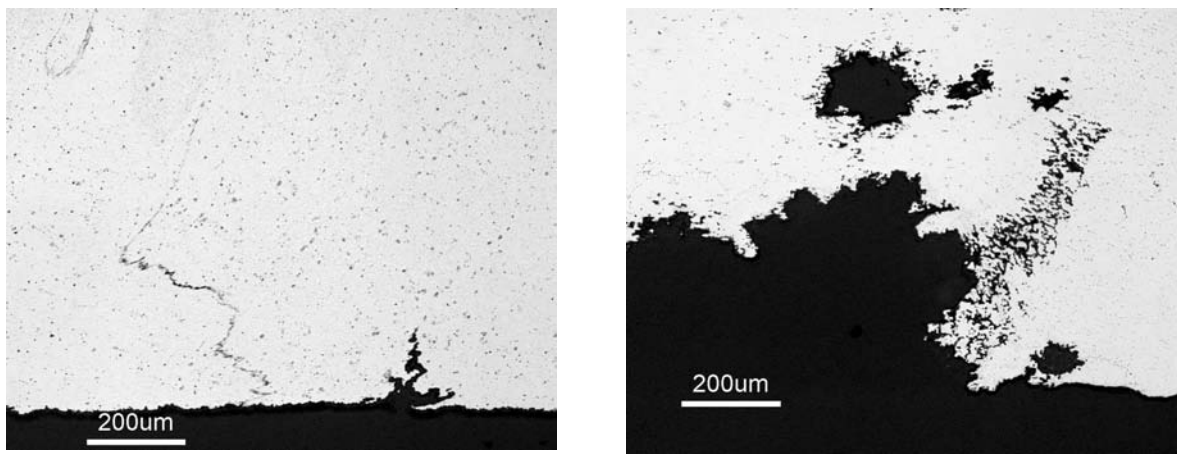


Figure 2-9 Accelerated corrosion tests of friction stir weld (left) and GMAW (Courtesy of Catherine Wong, NSWCCD).

2.4.5. Corrosion-Erosion, Impingement, and Cavitation

The corrosion resistance of aluminum comes from the oxide film that forms on the surface and protects the underlying metal from further oxidation. If some process such as high velocity fluid flow continuously disrupts that film, corrosion will continue to occur.

Corrosion-erosion resistance is sensitive to differences in seawater velocity and temperature. Tests to measure corrosion-erosion resistance consist of rotating disks or bars of metal in seawater. The results are qualitative only, showing the comparative resistance of different alloys. Basil (1952 and 1954) reported the results of such testing over a 60-day period as shown in Table 2-9.

Impingement attack occurs from a stream of liquid striking a surface, and it is accelerated by the presence of air bubbles in the liquid. Basil (1954) reported the results of testing using a stream of seawater containing 2 to 4 percent air impinging on an aluminum surface at 15 fps for 30 days. The alloys tested included 5052, 5056, 5154, 6061, and 3003, and the depth of attack was only 2 to 3 mils deep.

Table 2-9 Corrosion-Erosion Resistance of Different Alloys (Basil, 1952, 1954)

Tip Velocity, fps	5	10	13.5	15	15	30	30
Temperature (°F)	58	58	75	64	80	64	80
Order of Corrosion-Erosion Resistance (Best First)	5056	5056	5052	5056	5154	5056	4Mg-1Mn
	5052	5052	3004	5052	5056	5052	5154
	5154	5154	6063-T5	6061-T6	4Mg-1Mn	6061-T6	5056
	6061-T6	6061-T6	6061-T6	5154	Alclad 4.5 Mg	5154	Alclad 4.5Mg
	Alclad 3003	Alclad 3003	Alclad 3003	Alclad 3003	7072	Alclad 3003	3003
	3003	3003	7072-0	3003	3003	3003	7072
					Alclad 3003		Alclad 3003

Cavitation erosion is caused by the collapse of voids at high speed, and is the most severe form of combined mechanical and corrosion action. Resistance to cavitation is proportional to the hardness of the material, so the higher strength alloys generally have higher cavitation erosion resistance (Czyryca and Vassilaros, 1972). However, aluminum alloys have very poor cavitation erosion resistance compared to most other metals and should not be used where cavitation is anticipated, such as high-speed propellers.

2.4.6. Galvanic Corrosion

When two dissimilar metals are coupled in an electrolyte, galvanic corrosion results, with the metal that has the more positive electrical potential being the cathode that attacks the metal with the lower electrical potential, the anode. On the other hand, the anode can protect and prevent the corrosion of the cathodic material. The relative electrical potential of various metals in seawater are listed in Table 2-10 (Czyryca and Vassilaros, 1972), with more anodic (lower potential) metals listed first. Therefore, magnesium or zinc, if in electrical contact with aluminum in seawater will prevent the corrosion of the aluminum. However, most metals, including steel, lead, tin, brass, copper, stainless steel, Monel, Inconel, and nickel are cathodic towards aluminum. However, the extent to which a particular metal will cause accelerated corrosion of aluminum cannot be readily determined based on electrochemical potential alone. The more passive metals, such as stainless steel and super alloys can be quite polarizable and even though they are thermodynamically cathodic to aluminum, the kinetics of the interaction can be significantly less than would be predicted based on electrochemical potentials

The lower a metal in Table 2-10, the more cathodic they are, and the more deleterious they will be toward aluminum. Therefore, a metal such as Monel, which has great corrosion resistance by itself, will cause more corrosion to aluminum than steel. However, the use of steel in any form in contact with aluminum should be avoided unless the steel is coated to prevent its contact with seawater.

In addition to the difference in electrical potential influencing the degree of galvanic corrosion, the relative areas of the two metals influences the corrosion rate. For example, if a small amount of steel, such as a single bolt, is fastened to an unpainted aluminum hull, little corrosion will result. However, if the hull is painted, and a small scratch occurs in the paint, then the corrosion will be very intense at this small area.

Note that in Table 2-10, the various aluminum alloys have different electrical potentials. Therefore, the same alloy should be used in all applications that will result in immersion in seawater. This especially applies to mechanical fasteners, which will either corrode or cause corrosion of the aluminum to which they are fastened if they are dissimilar.

Because of galvanic corrosion, an aluminum hull must be protected from cathodic metals used in the propulsion train, such as brass, bronze and Monel used for shafting and propellers. This is done by installing either a passive or an active protection system. A passive system consists of zinc anodes that are attached to studs on the hull in the stern or near any other dissimilar metal that would be a source of current. An active impressed current system consists of titanium anodes that are either surface mounted or mounted in a recess in the hull. A reference electrode that is either zinc, silver or silver chloride is also mounted underwater. A small DC current is developed to protect the aluminum hull. Passive systems are less expensive to install, but have to be replaced every few years as the zinc is corroded away. Active systems cost more, but the anodes can last for 20 or more years, and the system weighs less. There is a danger that if an impressed current system is improperly designed or maintained, it can cause damage to the aluminum hull by imposing excessive current.

2.4.7. Crevice Corrosion

Crevice corrosion is similar to galvanic corrosion in that it is caused by a difference in electrical potential. However, in this case, the difference in potential is caused by a greater concentration of the electrolytes in different areas of the solution in which the metal is immersed. A difference in oxygen content can occur in locations such as lapped joints in riveted construction, and crevice corrosion can result. Therefore, faying surfaces should be primed before assembly, or a caulking compound can protect the metals.

The 5xxx-series alloys are generally resistant to crevice corrosion, as are the 6xxx-series. However, the presence of dissimilar metals can accelerate the tendency for crevice corrosion. Bieberich and Wong (1998) reported crevice corrosion under 5083-H3 plate that had 16 stainless steel bolts and Grade 8 steel bolts, a situation combining aspects of both crevice corrosion and galvanic corrosion, after exposure to a marine atmosphere environment for 30 months.

Table 2-10 Seawater Galvanic Series (Czyryca and Vassilaros, 1972)

Material	Galvanic Potential (Volts)
Magnesium	-1.73
Magnesium Alloys	
Zinc	-1.10
Alclad 7079-T6	-0.95
7072, Alclad 3003, Alclad 6061, Alclad 7075	-0.96
7005-T6, 7005-T63, 7039-T6, 7039-T63	-0.93 to -0.96
5086-0	-0.85
220-T4	-0.92
7079-T6	-0.91
1199, 5083-0, 5457-H34	-0.83 to -0.89
5154-H38, 5454-H32, 5456-H321, 5086-H32	-0.84 to -0.88
5056, 214, 218	-0.87
5050-H34, 7002-T6, 5257-H25, 5086-H112	-0.85 to -0.90
7178-T6	-0.83
1100-H14, 3003-H14, 5052-H34	-0.85
3004, 1060, 7075-T7, 7075-T4	-0.84
6151, 653, 6061-T6, 6063, Alclad 2014, Alclad 2024	-0.83
356-T6, 360	-0.81
2014-T6	-0.81
2219-T87	-0.79
333-T6	-0.79
6061-T4	-0.76
2014-T4, 2017-T4, 204-3, 2024-T4	-0.68 to -0.70
2219-T3, 2219-T4	-0.63 to -0.65
Mild Steel	-0.58
Lead-tin solders	
Lead	
Tin	-0.49
Brasses	
Copper	-0.20
Stainless Steel (403) (active)	-0.09
Monel, Inconel	
Nickel	-0.07
Stainless Steels (passive)	

Note: Potential is in reference to 0.1 N calomel electrode in aqueous solution of 1N NaCl + 0.3% hydrogen peroxide at 30 °C.

2.5 Product Forms

Aluminum for construction of marine vessels comes in three basic forms, sheet, flat plate, and extruded shapes. In some instances, forgings or castings may also be used. In the aluminum industry, product less than 0.25 inches (6 mm) thick is called sheet; otherwise it is called plate.

Aluminum Marine Structure Guide

Sheet and plate can be obtained in widths up to 5.33m (210 in) and lengths of 15 meters (49 feet). However, because wider sheets and plates are more expensive per pound than narrower products, some fabricators find it more economical to order narrow product and join them into wider sections, especially through use of friction stir welding.

Aluminum structural profiles are called extrusions because of the manner in which they are formed. The aluminum extrusion process involves the use of a hydraulic press to force heated (still-solid, but malleable) aluminum alloy through a steel die. The resulting aluminum profile (in cross section) assumes the shape of the die opening. The extrusion process follows a few simple steps but can yield a multitude of shapes and forms.

Like steel shapes, extrusions can be ordered in a variety of standard structural shapes, such as tees, angles, flat bars, bulb flats and bulb tees. However, the cost of producing a new die for making a special extrusion is very small compared to the cost of a new set of rollers for making a new steel shape. Therefore, designers often find it worthwhile to design their own extrusions to better meet the overall design requirements than would standard shape. Many extruders have continued to produce these special extrusions and make them available to all customers. In other cases, the shipyard developing an extrusion design has kept it proprietary, so that anyone wanting a similar extrusion must pay for its development.

In the 1960s, a series of tee-sections were developed for marine applications to suit the aluminum deckhouses of combatant ships, and they remain a standard today. These shapes were published in SNAME T&R Bulletin No. 207 and are offered by some extruders, although many do not include them in their catalogue of standard shapes. These tee sections vary from 3 to 12 inches in depth and are more efficient than standard tee sections because their webs are thinner than the flanges, whereas standard tee sections have the same web and flange thickness. The proportions of these SNAME tees are given in Table 2-11.

The SNAME tees should not be confused with what are called Army-Navy Tees, which are different profiles. Note that some extruders will offer what are called Car and Shipbuilding Channels. These are of the same proportions as steel sections of the same name, which are used in shipbuilding by cutting off one flange of the channel to form an L section. This is inappropriate and an unnecessary expense for aluminum construction; it is far easier to order the desired angle.

Table 2-11 SNAME Tee Sections

Shape Designation	Total depth (in)	t_{web} (in)	Flange width (in)	t_{flange} (in)	Fillet radius (in)	Weight (lbs/ft)	Properties with 8.75" 0.25" plate		
							I (in ⁴)	SM _r (in ³)	r (in)
3 x 1.5 T	3.0	0.188	3.0	0.257	0.282	1.5	5.7	2.54	1.28
4 x 2.0 T	4.0	0.188	4.0	0.254	0.282	2.0	12.4	4.57	1.78
5 x 2.5 T	5.0	0.188	4.5	0.282	0.282	2.5	22.0	6.99	2.25
6 x 3.0 T	6.0	0.219	4.5	0.291	0.329	3.0	33.8	9.23	2.65
7 x 3.5 T	7.0	0.255	4.75	0.312	0.338	3.5	49.7	12.17	3.08
8 x 4.0 T	8.0	0.258	4.75	0.300	0.387	4.0	66.8	14.43	3.32
8 x 4.5 T	8.0	0.258	4.75	0.397	0.387	4.5	74.0	17.10	3.49
8 x 5.0 T	8.0	0.277	4.75	0.459	0.416	5.0	79.0	18.98	3.48
10 x 5.75 T	10.0	0.324	5.0	0.352	0.486	5.75	124.0	23.00	4.16
10 x 6.5 T	10.0	0.324	5.0	0.492	0.486	6.5	138.5	26.28	4.21
10 x 7.25 T	10.0	0.349	5.0	0.578	0.524	7.25	148.0	27.01	4.18
12 x 8.0 T	12.0	0.391	5.0	0.457	0.587	8.0	213.7	34.42	4.83
12 x 9.0 T	12.0	0.391	5.0	0.645	0.587	9.0	237.0	35.48	4.87
12 x 10.0 T	12.0	0.430	5.0	0.732	0.645	10.0	250.8	36.72	4.81

A series of angle shapes varying in depth from 3 inches to 9 inches was also developed by SNAME. These angles have thicker flanges than webs and are generally more efficient than standard angle shapes, in which the web and flange are the same thickness. The proportions of these angles are given in Table 2-12.

Table 2-12 SNAME Angle Sections

Shape Designation	Total depth (in)	t_{web} (in)	Flange width (in)	t_{flange} (in)	Fillet radius (in)	Weight (lbs/ft)	Properties with 8.75" 0.25" plate		
							I (in ⁴)	SM _r (in ³)	r (in)
3 x 1.58 L	3.0	0.188	3.0	0.281	0.282	1.58	6.0	2.73	1.30
4 x 1.90 L	4.0	0.188	3.0	0.313	0.282	1.90	11.6	4.16	1.74
5 x 2.41 L	5.0	0.188	3.5	0.344	0.282	2.41	21.1	6.57	2.22
6 x 2.97 L	6.0	0.188	4.0	0.375	0.282	2.97	34.5	9.65	2.70
7 x 3.95 L	7.0	0.218	4.5	0.438	0.327	3.95	54.9	14.42	3.12
8 x 5.07 L	8.0	0.250	5.0	0.500	0.375	5.07	81.6	19.21	3.51
9 x 6.15 L	9.0	0.281	5.5	0.531	0.422	6.15	113.7	22.82	3.88

There are a number of special extrusions designed for marine structures that are available from extruders and suppliers of aluminum. One such is the rounded Tee profile shown in Figure 2-10. This shape has a narrower flange width than a conventional Tee. The narrower flange makes it easier to weld between stiffeners when they are closely spaced, and the rounded

underside makes it easier to paint when a coating is required. The geometric properties of the shapes are given in Table 2-13. However, there is a definite weight disadvantage to these shapes. Figure 2-11 compares the section moduli of the rounded tees with the SNAME tees with the weight per meter of the shapes. Properties are computed on 6.35 mm x 222 mm (0.25 in x 8.75 in) of effective plate. For the same section modulus, the SNAME tee has about one-third to one-fourth the weight.

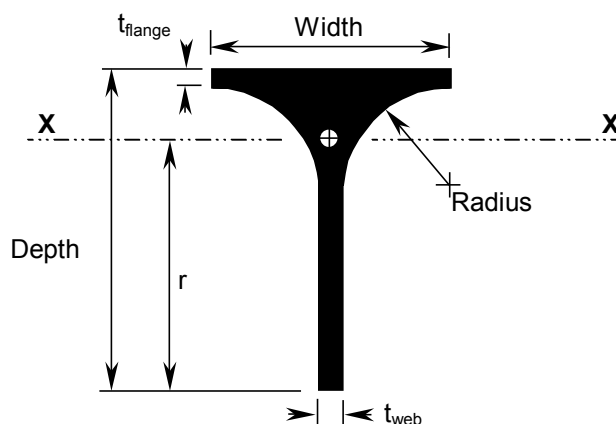


Figure 2-10 Rounded tee profile.

Table 2-13 Properties of Rounded Tees

Depth (mm)/ (in)	Width (mm)/ (in)	t_{flange} (mm)/ (in)	t_{web} (mm)/ (in)	Radius (mm)/ (in)	Area (mm ²)/ (in ²)	Weight (kg/m)/ (lb/ft)	Centroid height (mm)/ (in)	Ixx about centroid (mm ⁴)/ (in ⁴)	Iyy (mm ⁴)/ (in ⁴)
60 2.362	40 1.575	3 0.118	3.5 0.138	18.25 0.719	462 0.716	1.249 0.839	43.83 1.726	140,309 0.337	22,647 0.054
70 2.756	40 1.575	3 0.118	4 0.157	18 0.709	527 0.817	1.423 0.956	49.25 1.939	239,089 0.574	22,899 0.055
80 3.150	40 1.575	3 0.118	4.5 0.177	17.75 0.699	602 0.933	1.625 1.092	54.24 2.135	377,028 0.906	23,222 0.056
90 3.543	90 3.543	6 0.236	8 0.315	27 1.063	1,525 2.364	4.117 2.767	65.32 2.572	1,074,098 2.581	507,579 1.219
100 3.937	50 1.969	3 0.118	5.5 0.217	22.25 0.876	896 1.389	2.419 1.625	67.19 2.645	886,635 2.130	48,825 0.117
120 4.724	50 1.969	3 0.118	6.5 0.256	21.75 0.856	1,114 1.727	3.007 2.021	76.36 3.006	1,639,940 3.940	50,523 0.121
140 5.512	50 1.969	4 0.157	7.5 0.295	21.25 0.837	1,414 2.192	3.817 2.565	86.57 3.408	2,843,222 6.831	63,386 0.152
180 7.087	60 2.362	4 0.157	8 0.315	28 1.102	1,984 3.075	5.358 3.600	112.75 4.439	6,621,525 15.908	6,476,987 15.561
181.1 7.130	70.6 2.780	10.2 0.402	7.2 0.283	30 1.181	2,337 3.622	6.31 4.240	126.37 4.975	7,400,243 17.779	7,397,998 17.774

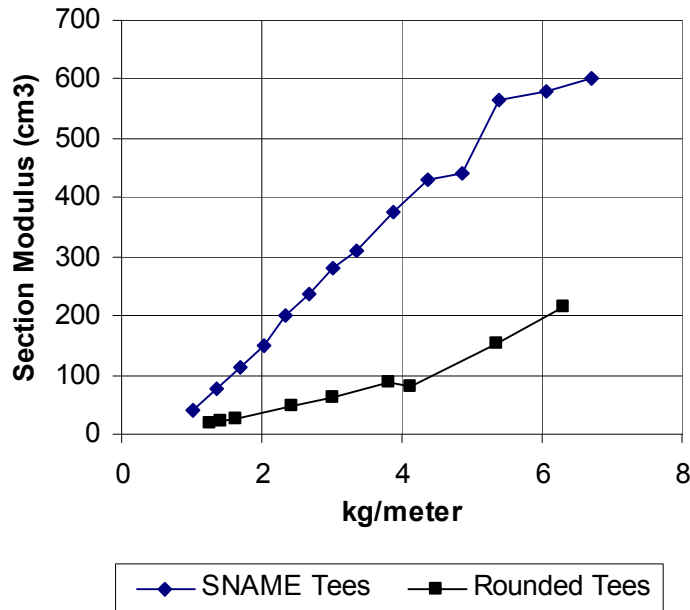


Figure 2-11 Comparison of section moduli of rounded tees with conventional tees.

Other profiles are also commonly used as stiffeners. The simplest of these is the flat bar, which is generally more economical to order as an extruded shape than is cutting plate into flat bars, as is common in steel fabrication. For structural columns or stanchions, extruded tube is used, either square, rectangular, or round, all of which can be procured in a variety of cross-sections. Square or rectangular tube is frequently used as stiffeners, particularly in topside structure and other exposed locations where it provides neater appearance. Other shapes that are used include bulb tees, which have a small flange on the bottom to which thin plate is fillet welded. Other shapes have the web thickened where it is welded to the plate to prevent burn-through when larger fillet sizes are used.

Some builders, particularly those building smaller craft that require smaller amounts of material on a short time schedule have difficulty obtaining the range of shapes that a builder of larger vessels can obtain, especially if there is time for special ordering. The 5xxx-series extrusions are more difficult to obtain, and builders desiring to use a 5xxx-series alloy sometimes cut plate into flat bars or bend plates to form angles.

Structural tube is different from seamless pipe and should not be used for applications requiring internal pressure. As will be explained below, structural tube is formed by extruding through a hollow die, which has several areas around the circumference that hold the center of the die in place. During the extrusion process, the hot metal flows around these areas of the die and then join to form a tube. Because the aluminum is not at a molten temperature, the joint where the metal flows together does not have a solid metallurgical bond. There is a drift expansion test, mentioned below, for testing the strength of that bond. However, structural tube that has passed that test should still not be considered the same as seamless pipe. To produce

seamless pipe, the aluminum is pressed over a mandrel that serves as the inside of the die. The process is slower, and therefore more expensive than producing structural tubing.

The bulb flat, shown in Figure 2-12, is more weight efficient than a flat bar. As with the rounded tee sections, some extruders offer several different profiles, although there are no standard aluminum bulb flats. The properties of a few sections that are commercially available are given in Table 2-14. Note that these profiles are not the same as standard steel bulb flats



Figure 2-12 Bulb flat.

Table 2-14 Properties of Bulb Flats

Depth (mm)/ (in)	Width (mm)/ (in)	d _{flange} (mm)/ (in)	t _{web} (mm)/ (in)	Tip radius (mm)/ (in)	Area (mm ²)/ (in ²)	Weight (kg/m)/ (lb/ft)	Centroid height (mm)/ (in)	I _{xx} about centroid (mm ⁴)/ (in ⁴)	I _{yy} (mm ⁴)/ (in ⁴)
50.0 1.969	14.0 0.551	8.0	4.5	2.5	280 0.435	0.757 0.508	29.31 1.15	68,243 0.1640	2,544 0.0061
50.0 1.969	15.0 0.591	6.2	5.0	2.0	297 0.461	0.802 0.539	28.56 1.12	72,227 0.1737	2,783 0.0067
76.2 3.00	19.05 0.75	10.72	5.38	3.18	515 0.799	1.392 0.935	45.04 1.77	295,531 0.7100	8,672 0.0208
76.2 3.00	21.0 0.827	10.9	5.0	3.0	505 0.783	1.363 0.916	46.43 1.83	292,736 0.7034	11,460 0.0275
98.7 3.866	19.05 0.75	10.72	5.35	3.18	634 0.978	1.711 1.144	56.88 2.23	609,035 1.4424	9,272 0.0223

2.6 The Extrusion Process

A designer may determine that the needs of a design may be best met with special extrusions, rather than the use of standard extrusions found in supplier's catalogues. To aid in determining the decisions that go into developing a new extrusion shape, the following material is provided. Most of the following information and figures are taken from the Aluminum Extrusion Manual produced by the Aluminum Extruders Council (AEC, 2002).

2.6.1 Process Description

The process of extrusion can be likened to squeezing a tube of toothpaste or a child producing shapes from a Playdough press. The heated billet of metal is forced through a die to form a cylinder with the cross-section in the desired shape. An aluminum extrusion press is comprised of many different parts that function together. Figure 2-13 is a diagram of a typical extrusion press.

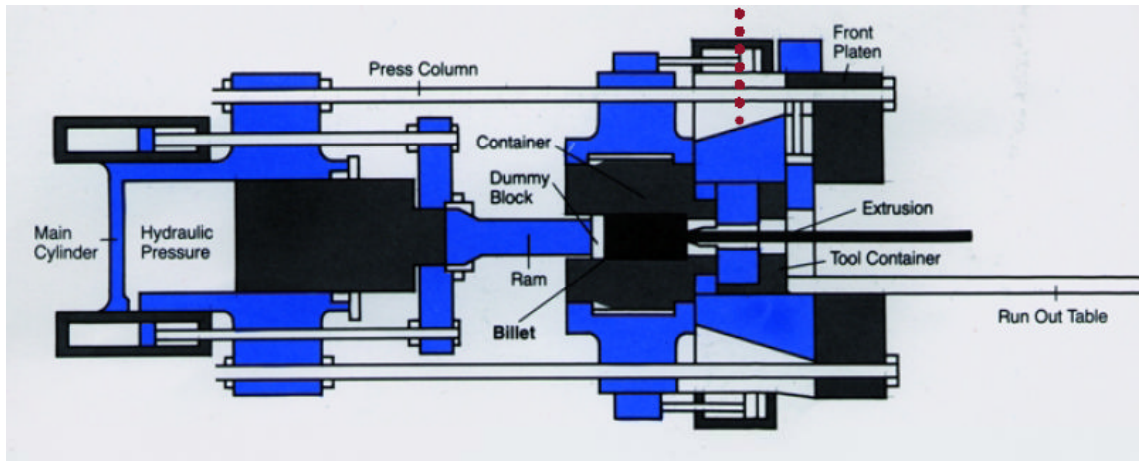


Figure 2-13 Typical extrusion press (AEC, 2002).

The aluminum alloy to be extruded is first cast into a cylindrical billet, which has the same diameter as the part of the extrusion press known as the container. The die is heated to the required temperature, generally ranging from 750 to 900 degrees Fahrenheit (approximately 400 to 480 degrees Celsius), where the material is malleable, but not molten. The heated die is then placed into the container, and is pressed against the die. The die is a steel disk at the end of the container, and the aluminum in the billet is forced through the opening in the die to create the extruded product. The pressure in an extrusion press is applied by a hydraulic ram, which uses from 100 tons to 15,000 tons or more of force to push heated aluminum through the container and out the die. The amount of force an extrusion press is able to exert dictates the size of the profiles it is capable of producing. The higher the tonnage of the press, the larger the possible extrusion.

Aluminum extrusion dies are available in three basic categories: solid, semihollow, and hollow. The names describe the shape of the extruded profiles, and each category has specific applications and advantages.

Solid dies have one or more openings, and produce extrusions without any enclosed internal voids. The opening in a solid die has the same cross sectional profile as the extruded shape. Solid dies are used primarily in the production of bars, channels and angles, as well as many custom shapes. A solid die is shown in Figure 2-14.

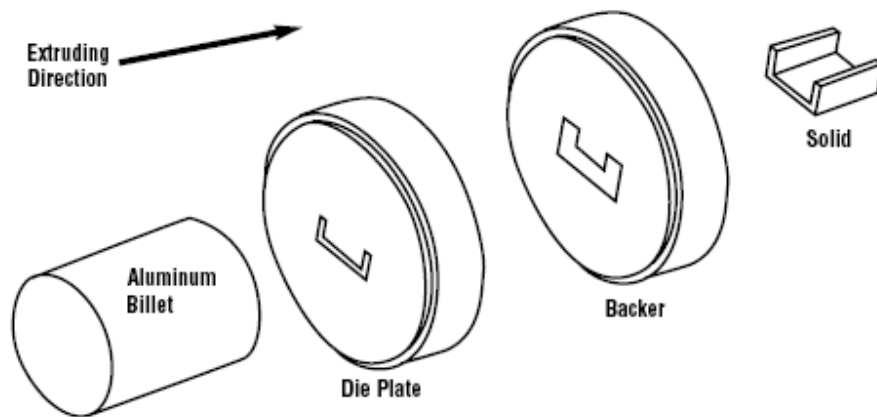


Figure 2-14 Solid die (AEC, 2002).

Semihollow dies produce shapes that include partially enclosed voids with "open" profiles. A semihollow profile partially encloses a void; however, a solid shape also may partially enclose a void, and the distinction may not be obvious. The void has an area that is generally in a ratio of three-to-one larger than the tongue of the die. Semihollow dies are used most often in the production of atypical channels and other custom shapes. A semihollow die is shown in Figure 2-15.

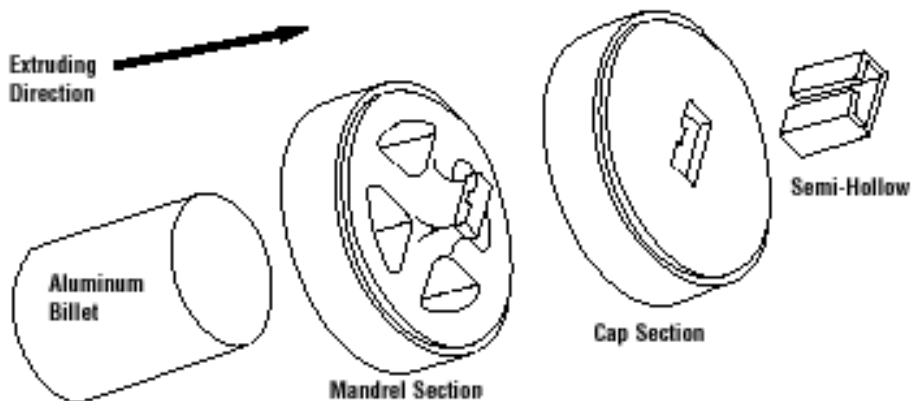


Figure 2-15 Semihollow die (AEC, 2002).

Hollow dies produce shapes that include an entirely enclosed internal void and have closed profiles. Hollow dies require two components, a die cap and a mandrel section, in order to produce required shapes. Hollow dies produce tubes and many custom hollow shapes. A hollow die is shown in Figure 2-16. Note that the mandrel has several solid areas about which the aluminum must flow to rejoin and form the final hollow shape. Because the aluminum is not in a molten state, the areas where the metal rejoins are not complete metallurgical bonds, and have reduced strength across these joints. This weakness is not important for most structural purposes but must be considered if the application will place high transverse stress on the section, if high shear stresses will be placed on the joint, or if the section is to be subjected to

high internal pressure. The International Association of Classification Societies has a requirement that these bonds be tested by using a wedge that is driven into the hollow as shown in Figure 2-17. However, some shapes may not be amenable to such testing, such as hollow deck panels.

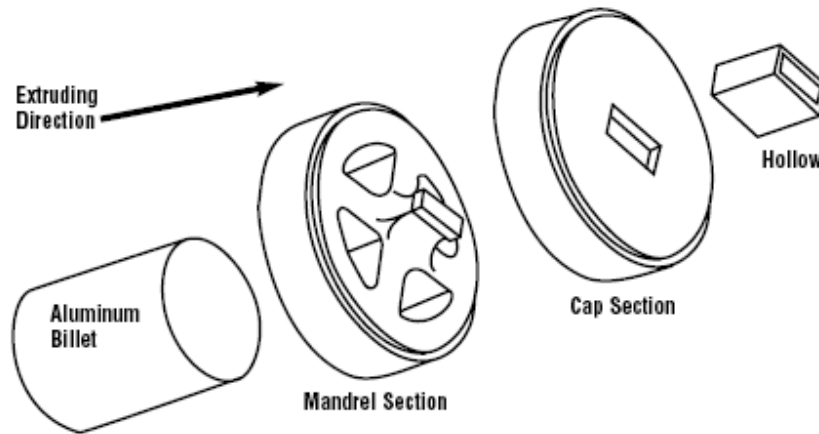


Figure 2-16 Hollow die (AEC, 2002).

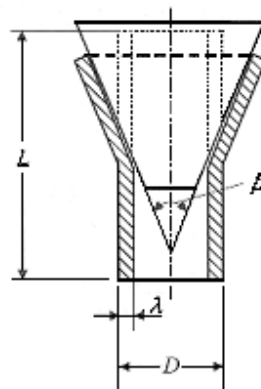


Figure 2-17 Drift expansion test (ABS, 2005).

2.6.2 Cost of Development

Depending on the size and complexity of the die, the cost of producing a new die can vary from \$800 for an easily made small die to \$30,000 for a large complex die (March 2006 prices). The minimum mill order for a special extrusion is generally 1,000 to 2,000 pounds, although an economic analysis is required to determine the cost-effectiveness of a new extrusion design. Current price (March 2006) for 5086 extrusions is about \$2.80 to 3.00 per pound, depending on the shape. Because 5083 is almost as easy to extrude as 5086, it is only \$0.03 more per pound. Compared to 5086, 5454 alloy is about \$0.05 more per pound, but 5456, which is much more difficult to extrude, is about \$1.00 per pound more than 5086. Current price for

ordinary 6xxx-series extrusions are about \$1.70 to 1.80 per pound. More difficult extrusions such as hollow truss-section deck sections are about \$2.00 per pound.

Using this cost data, the cost of a mill order of 1,000 pounds of 5086 would be about \$2,800, and having it made to a special design could be as little as 30 percent greater, a cost that could be offset by the reduced weight and reduced labor cost that a special extrusion could affect. Of course, with a larger mill order, the percentage in cost increase would be less. Alternately, some boat builders have found it advantageous to work with a supplier that would bear the price of the new die, purchase a mill order of minimum or greater size, and then provide the extrusions to the shipyard in small quantities as needed. This increases the cost per pound, but reduces inventory cost for the shipbuilder. Such an arrangement with the supplier can be either on an exclusive basis or the profile can be made available to other users to reduce cost.

2.6.3 Length of Extrusions

Extrusion presses operate in cycles, with a cycle defined as one thrust of the hydraulic ram. The length of time it takes a press to go through one cycle is related to alloy, billet size, number of holes in the die, and the shape of the extrusion. Depending on the alloy, a complex shape may emerge from the press as slowly as one or two feet per minute, while a simple shape may be extruded at a rate of more than 200 feet per minute. Taking various factors into consideration, a continuous extrusion as long as 300 feet may be produced with each stroke of the press. Pullers are commonly used to facilitate handling the hot and fragile profiles as they emerge from the die.

As the extrusion emerges from the press, it is cut into desired length by a “flying saw”, which moves along with the extrusion. When one billet has been pressed through the die, another billet is placed in the cylinder behind it, and the extrusion process continues, producing an extrusion of indefinite length. However, the area where the billets are extruded together lacks the desired properties, and must be cut out and discarded.

2.6.4 Limitations in Extrusion Thickness

The 5086 alloy generally cannot be extruded any thinner than about 3.3 mm (0.128 inches) thick, although the limit may depend on how intricate the shape is. For 5083, the limit is closer to 4.6 mm (0.18 inches). Hollow extrusions cannot be made in the 5xxx-series unless the wall thickness is very great. This limitation is mostly a function of the strength of the steel die. Some extrusion presses have the capacity for producing greater pressure than others and can therefore produce thinner extrusions at a faster pace, and the limitation depends on the shape of the extrusion. A designer of a new shape should therefore consult a variety of extruders if a shape close to those limitations is contemplated.

By contrast, 6xxx-series alloys are more malleable and can be extruded much thinner. Complex shapes such as hollow deck panels with 2-mm (0.08-inch) thick sections are common. This capability of 6xxx-series alloys to be extruded makes them the alloys of choice for very lightweight structure.

Heated aluminum flowing through the container and out the die is represented in Figure 2-18, with the direction of extrusion from left to right. Note that the center of the billet advances more rapidly than the periphery, causing the surface segregation oxide to cling to the container wall, collecting in back-end residue. (The dark lines are copper bands, placed as markers to illustrate the flow of metal.)



Figure 2-18 The extrusion process. (AEC, 2002).

Although the extrusion press is the main focus of the extrusion process, many other pieces of equipment are required to make an aluminum extrusion. In addition to the press, Figure 2-19 depicts a billet furnace; quenching systems, log shear, puller, age/anneal oven, handling equipment, saw and gauging system, stretcher, and stacking system.

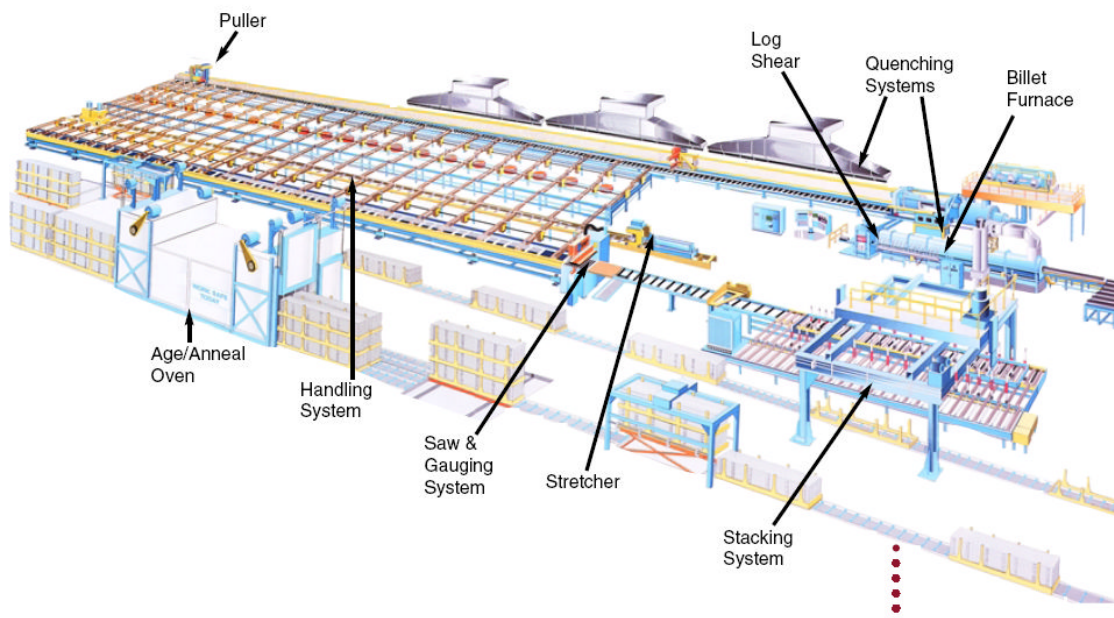


Figure 2-19 An extrusion plant. (AEC, 2002).

2.6.5 Heat Treatment

For some alloys, including those of the 6xxx series, the extrusion must be quenched to achieve the desired properties. Depending on the specific alloy, the thickness, and the shape of the extrusion, the quenching is performed by processes including blown air, water spray, water mist, or water bath. The die exit and quench temperatures for some 6xxx-series alloys are given in Table 2-15.

Table 2-15 Exit and Quench Temperature Data For Selected 6xxx-Series Alloys

Alloy	Die Exit Temp (deg-F)	Cooling Rate (deg-F/sec)	Cooling Range (deg-F)	Cooling Time (sec) at Minimum Cooling Rate	Cooling Time (sec) at Maximum Cooling Rate
6063	930	2-3	840-480	180 (at 2 deg/sec)	120 (at 3 deg/sec)
6463	930	5	840-480	72 (at 5 deg/sec)	72 (at 5 deg/sec)
6063A	930	3-5	840-480	120 (at 3 deg/sec)	72 (at 5 deg/sec)
6101	930	3-5	840-480	120 (at 3 deg/sec)	72 (at 5 deg/sec)
6005A	950	5-15	860-480	76 (at 5 deg/sec)	25 (at 15 deg/sec)
6061	950	10-20	860-480	38 (at 10 deg/sec)	19 (at 20 deg/sec)
6351	950	10-20	860-480	38 (at 10 deg/sec)	19 (at 20 deg/sec)

2.6.6 Considerations for Extrusion Design

Designers are encouraged to explore the vast opportunities available through the use of aluminum extrusions and to set high expectations for the performance of extruded aluminum components and end products. Of course, it is then the designer's challenge to figure out what it takes to meet these key criteria. From a functional perspective, it is important to ask what it is you want the part to do, not what the part should look like. In considering function, prepare a list of the following:

- What are the parts' essential functions?
- What essential shapes and dimensions do these functions require?
- How do these essential elements relate to each other?
- What secondary functional elements are necessary to connect, support, or strengthen the overall component?
- What other critical elements exist that may affect the final product?

In the detailed development of an aluminum extrusion design, the following five factors should be considered:

1. Shape (Profile) Configuration. Extruded profiles are described in three general categories: solid, semihollow, and hollow. A solid profile is the least complex, and a hollow profile is generally the most complex.
2. Dimensional Tolerances. Departure from standard dimensional tolerances and geometric tolerancing may be of value but will influence cost and producibility. For many

applications, in which the extrusion will be part of an assembly of components, dimensional tolerances are critical. A designer should be aware of the standard dimensional tolerances to which extrusions are commercially produced. These dimensional tolerances generally cover such characteristics as straightness, flatness, and twist, and such cross-sectional dimensions as thickness, angles, contours, and corner or fillet radii. The published standard dimensional tolerances may be very easy to achieve or very difficult, depending on the profile. The complexity of profile possibilities makes it impossible to publish standard dimensional tolerances that meet all situations. If desired, extrusions can be produced to closer-than-standard dimensional tolerances, generating cost savings in secondary operations; such savings may range from modest to very significant, depending on circumstances. The designer should carefully consider the requirements of the application and specify special tolerances only where they are really needed.

3. **Surface Finish.** Surfaces can be finished in a variety of ways, which may be useful for exposed shapes. One advantage of aluminum extrusions is the variety of ways the surface can be finished, and this offers another range of choices to the designer. As-extruded, or mill finish can range from structural, on which minor surface imperfections are acceptable, to architectural, presenting uniformly good appearance. Finishes other than mill finish include scratch finishing, satin finishing, and buffing. Aluminum can also be finished by clear or colored anodizing, or by painting, enameling, or other coatings.
4. **Alloy.** There are a number of aluminum extrusion alloys, each with distinct characteristics and properties. Some alloys are more easily extruded than others. 5xxx-series alloys are more difficult to extrude than 6xxx-series alloys.
5. **Circumscribing Circle Size.** Sometimes referred to as the circumscribing circle diameter (CCD), this is the most common industry measurement of a profile's diameter. The larger the diameter, the fewer extruders available to produce the profile. There are few extrusion presses worldwide capable of a 32-inch (810-mm) CDD, but there are many with a size of 18 inches (460 mm) or less. One common measurement of the size of an extrusion is the diameter of the smallest circle that will entirely enclose its cross-section, called its circumscribing circle. This dimension is one factor in the economics of an extrusion. In general, extrusions are most economical when they fit within a medium-sized circumscribing circle: that is, one with a diameter between one and ten inches. Most common profiles are less than 18 inches in diameter, but a few extruders are capable of producing extrusions with a much larger circumscribing circle diameter, some as large as 32 inches.

To develop a good extrusion design, the following key characteristics should be addressed:

- Specify the appropriate metal thickness. Specify metal thicknesses that are just heavy enough to meet your structural requirements. Even in low stress areas, however, keep sufficient thickness to avoid risking distortion or damage. Some shapes tend to invite distortion during the extrusion process (such as an asymmetric profile or thin details at

the end of a long flange); such tendencies exert more influence on thin-walled shapes than on those with typical metal thickness.

- Keep metal thickness as uniform as possible. Extrusion allows you to put extra metal where it is needed such as high stress areas and still save material by using normal dimensions elsewhere in the same piece. Adjacent-wall thickness ratios of less than two-to-one are extruded without difficulty, but large differences between thick and thin areas may create dimensional control problems during extrusion. It is best to maintain near uniform metal thickness throughout a shape if possible. When a design combines thick and thin dimensions, streamline the transitions with a radius (a curve, rather than a sharp angle) at junctions where the thickness changes sharply.
- Use metal dimensions for tolerances. Dimensions measured across solid metal are easier to produce to close tolerances than those measured across a gap or angle. So rely on so called metal dimensions as much as possible when designing close-fitted mating parts or other shapes requiring closer tolerances. Standard industry dimensional tolerances are entirely adequate for many applications, but special tolerances can be specified if necessary.

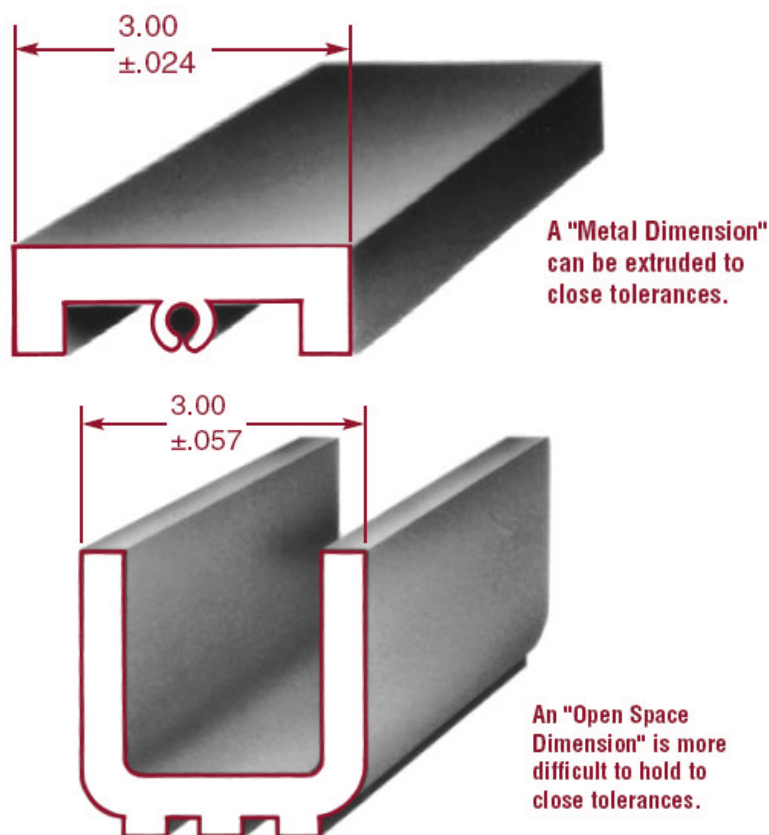


Figure 2-20 Dimensional control of extrusions (AEC, 2002).

- Design with surface finish in mind. Always indicate "exposed surfaces" on your design drawing so the extruder can give them special attention and protect their finish during both extrusion and post-extrusion handling. As a general rule, the narrower the exposed surface, the more uniform its finish. Webs, flanges, and abrupt changes in metal thickness may show up as marks on the opposite surface of an extrusion, particularly on thin sections. The marking of exposed surfaces can be minimized by thoughtful design.

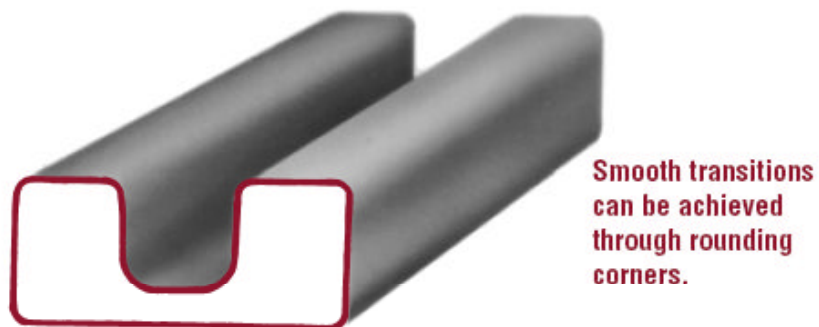
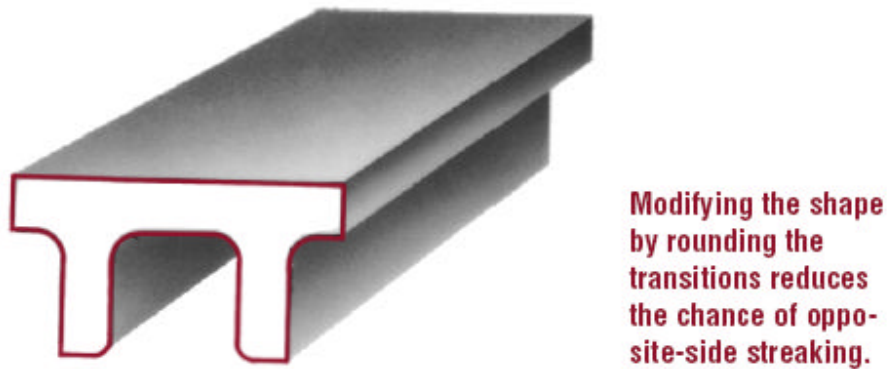
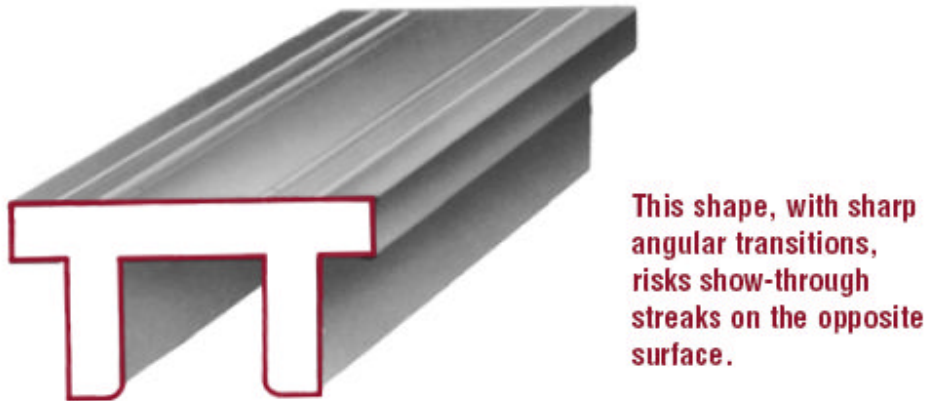


Figure 2-21 Effect of sharp transitions on extrusions (AEC, 2002).

- Smooth transitions. Transitions should be streamlined by a generous radius at any thick-thin junction.
- Use webs where possible to give better dimensional control. Metal dimensions are more easily held than gap or angle dimensions. The web also allows thinner wall sections in this example.

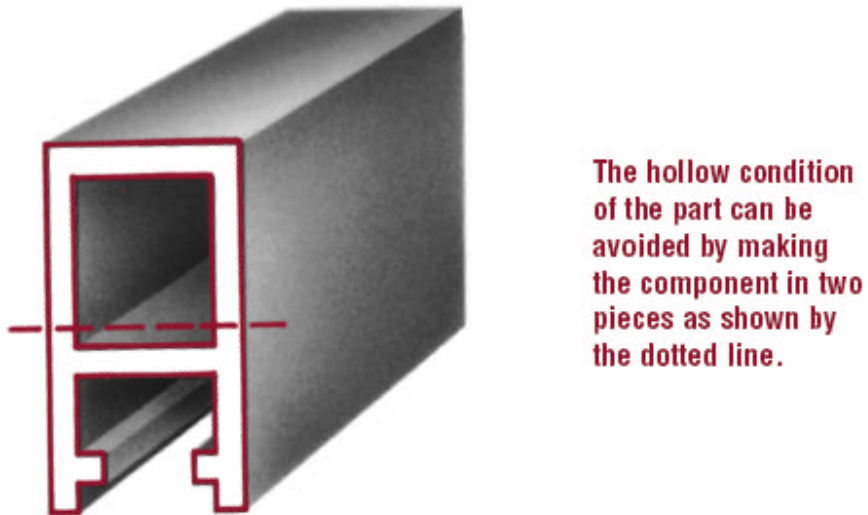


Figure 2-22 Use of webs in extrusion design (AEC, 2002).

- Use ribs to straighten. Wide, thin sections can be hard to straighten after extrusion. Ribs help to reduce twisting, and to improve flatness.

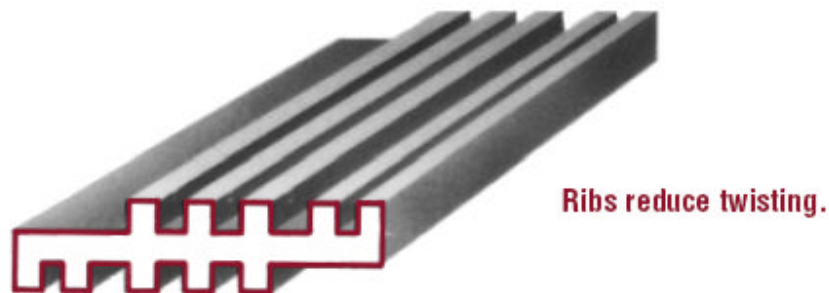


Figure 2-23 Use of ribs in extrusion design (AEC, 2002).

Round corners wherever possible, avoiding sharp edges. The die tongue is less likely to snap off when the corners of the profile are rounded at the narrowest area of the void.

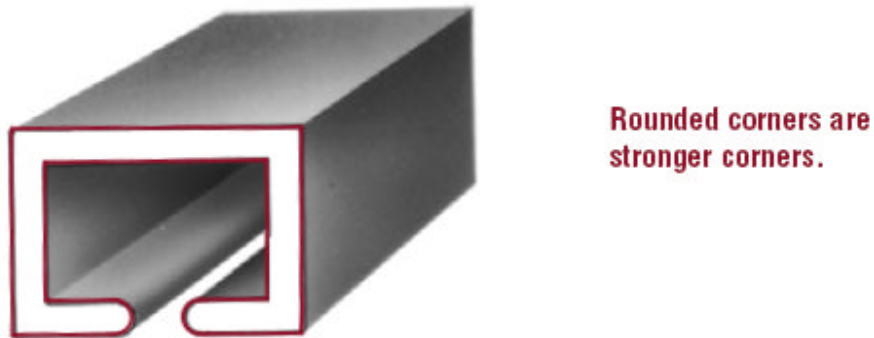


Figure 2- 24 Rounded corners in extrusion design (AEC, 2002).

- Incorporate indexing marks. Shallow extruded grooves make drilling, punching, and assembly easier by eliminating the need for center punching. An index groove can also be used to help identify pieces that are similar in appearance, or to distinguish an inside (rather than an outside) surface.

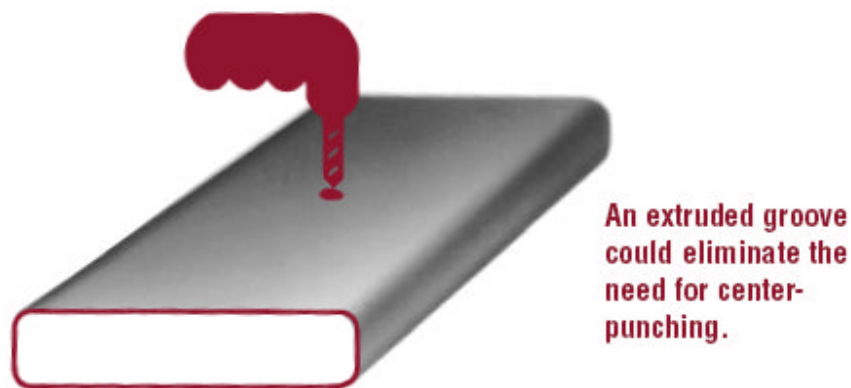


Figure 2-25 Index marks in extrusion design (AEC, 2002).

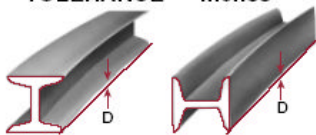
2.6.7 Dimensional Tolerances

Some of the standard dimensional tolerances for extrusions are given in Table 2-16 below. ANSI H35.2 or ANSI H35.2(M) provide a more complete listing. Tighter tolerances may be achieved, although for a higher cost. An example of a use of tighter tolerances is having extrusions cut to length. Some builders have found it profitable to have the extruder supply profiles cut to the finished length, and thus reduce the cost of scrap as well as reducing in-house cutting operations.

Table 2-16 Standard Tolerances for Extruded Wire, Rod, Bar and Profiles (AEC, 2002)

SPECIFIED DIAMETER (WIRE AND ROD): SPECIFIED WIDTH (BAR): CIRCUMSCRIBING CIRCLE DIAMETER ⁽¹⁾ (PROFILES): inches	TOLERANCE—inches plus			
	ALLOWABLE DEVIATION FROM SPECIFIED LENGTH			
	SPECIFIED LENGTH—feet			
	Up through 12	Over 12 through 30	Over 30 through 50	Over 50
Up through 2.999	1/8	1/4	3/8	1
3.000-7.999	3/16	5/16	7/16	1
8.000 and over	1/4	3/8	1/4	1

Table 8-3 Straightness⁽¹⁾—Rod, Bar and Profiles (Shapes)

PRODUCT	TEMPER	SPECIFIED DIAMETER (ROD): SPECIFIED WIDTH (BAR): CIRCUMSCRIBING CIRCLE DIAMETER ⁽¹⁾ (PROFILES): (inches)	SPECIFIED THICKNESS (RECTANGLES): MINIMUM THICKNESS (PROFILES): (inches)	TOLERANCE ⁽²⁾ —inches
				 IN TOTAL LENGTH OR IN ANY MEASURED SEGMENT OF ONE FOOT OR MORE OF TOTAL LENGTH
Rod and Square, Hexagonal and Octagonal Bar	All except O TX510 ⁽²⁾ TX511 ⁽²⁾	All	..	.0125 x Measured length, ft.
	O	0.500 and over	..	.050 x Measured length, ft.
	TX510 ⁽²⁾	0.500 and over	..	.050 x Measured length, ft.
	TX511 ⁽²⁾	0.500 and over	..	.0125 x Measured length, ft.
Rectangular Bar	All except O TX510 ⁽²⁾ TX511 ⁽²⁾	Up through 1.499	Up through 0.094 ⁽³⁾ 0.095 and over	.050 x Measured length, ft. .0125 x Measured length, ft.
		1.500 and over	All	.0125 x Measured length, ft.
	O	Over 0.500	0.500 and over	.050 x Measured length, ft.
	TX510 ⁽²⁾	Over 0.500	0.500 and over	.050 x Measured length, ft.
	TX511 ⁽²⁾	Over 0.500	0.500 and over	.0125 x Measured length, ft.
Profiles (Shapes)	All except O TX510 ⁽²⁾ TX511 ⁽²⁾	Up through 1.499	Up through 0.094 ⁽³⁾ 0.095 and over	.050 x Measured length, ft. .0125 x Measured length, ft.
		1.500 and over	All	.0125 x Measured length, ft.
	O	0.500 and over	Up through 0.094 ⁽³⁾ 0.095	.200 x Measured length, ft. .050 x Measured length, ft.
	TX511 ⁽²⁾	0.500 and over	Up through 0.094 ⁽³⁾ 0.095 and over	.050 x Measured length, ft. .0125 x Measured length, ft.

Footnotes for Tables 8-2 through 8-5

⁽¹⁾ These Standard Tolerances are applied to the average profile (shape); wider tolerances may be required for some profiles, and closer tolerances may be possible for others.

⁽²⁾ TX510 and TX511 are general designations for the following stress-relieved tempers: T3510, T4510, T61510, T6510, T8510, T73510, T76510, and T3511, T4511, T61511, T6511, T8511, T73511, T76511, respectively.

⁽³⁾ When weight of piece on the flat surface minimizes deviation.

⁽⁴⁾ The circumscribing circle diameter is the diameter of the smallest circle that will completely enclose the cross-section of the extruded product.

⁽⁵⁾ Tolerances for T3510, T4510, T6510, T73510, T76510, and T8510 tempers shall be as agreed upon between purchaser and vendor at the time the contract or order is entered.

⁽⁶⁾ See ASD, Standards Section (6), for Application of Twist Limits; for additional information, see Aluminum Association publication "Understanding Aluminum Extrusion Tolerances."

⁽⁷⁾ Applies only if the thickness along at least one-third of the total perimeter is 0.094 or less. Otherwise use the tolerance shown for 0.095 and over.

⁽⁸⁾ Tolerance for "O" temper material is four times the standard tolerances shown.

Excerpted from *Aluminum Standards and Data* (ASD), 1997, Tables 11.5 and 11.6.



2.7 Summary

Aluminum is versatile in the many product forms in which it can be obtained. There are a variety of alloys that are produced for the marine market, and the designer must determine the particular alloy or combinations of alloys best suited for a particular design. Often, that decision will be tempered by other considerations, such as the availability from suppliers as well as familiarity of shipyard fabricators and customers with the different alloys.

The relative ease with which new extrusion dies can be designed and manufactured presents both an opportunity and a challenge to the designer. The advantages of generally quicker procurement time and reduced cost for standard extrusions must be compared to the possible advantages of reduced weight, reduced total fabrication cost, and special functionality that a custom-designed extrusion can provide.

Long-term corrosion tests are needed for all of the alloys currently being used or considered for use in the structure of high-speed aluminum vessels, including 6xxx-series alloys. Testing should include partial immersion in seawater, immersion in flowing seawater, and exposure to a marine environment near the surf. The specimens should be in the base metal and welded condition, and should have one-half sensitized by holding for four weeks at 100 °C. The same alloys should be tested using standardized accelerated corrosion tests, and the results compared with the long-term testing to develop standards for accelerated corrosion tests.

The service temperature of deck structures for aluminum ships operating in very hot climates should be determined and the degree of sensitization that occurs under those conditions to 5xxx-series alloys determined. A process for rapid sensitization of these alloys should be developed and applied to a series of alloys that will then be tested for stress-corrosion testing in the welded and unwelded condition, both sensitized and unsensitized. For comparison, 6xxx-series alloys should be included in the stress-corrosion testing. Friction stir welds in 5xxx-series alloys and 6xxx-series alloys should also be tested.

Aluminum Marine Structure Guide

Chapter 3

Structural Design

3.1 Introduction

Structural design is the synthesis of all of the material contained in this design and fabrication guide. The designer must be aware of the properties of aluminum, including fatigue characteristics and fatigue analysis procedures to ensure the design takes advantage of the benefits of aluminum and minimizes the disadvantages. The structural design is dependent on the structural details that will be used, such as the type of stiffening and framing that will be used and the type of end connections for members. The fabrication scheme affects structural design in many ways from the type of structural details selected, minimum scantlings, use of special extrusions, and accessibility to joints for welding. The welding procedures affect structural design because reduced strength welds such as intermittent welding affects design parameters. Residual stresses and distortion, although limited by design codes, do not directly factor into present structural design equations, but the designer must be aware that the structural arrangement and scantlings selected can be fabricated to minimize them. Because aluminum alone cannot form an effective fire barrier, most fire protection is applied in a manner that is parasitic to the structure, increasing weight without increasing strength. However, some structural designers find it simpler to incorporate steel bulkheads into the aluminum structure to form fire barriers.

With lighter weight and lower stiffness, aluminum, if not properly designed, can present a problem in vibration, a subject that will be discussed in Chapter 11. Aluminum is favored as a structural material because it generally has less maintenance and repair over the life of the vessel, but the designer must be certain that the structure is sufficiently rugged to stand up to all service conditions that will be encountered, including abuse from cargo handling and slam loads. Access for inspection and repair should also be a design consideration. Finally, because the field of aluminum hull structures is changing rapidly, the designer must be aware of emerging technologies. New aluminum alloys are being marketed that may have benefits, and new fabrication techniques such as friction stir welding offer benefits and flexibility to the designer.

There are a number of different methods for analyzing and designing structure. Some of these are contained in the requirements of different classification societies. In the work that follows, the following terms will be used for simplicity:

- ABS HSC Guide: Guide for Building and Classing High-Speed Craft, American Bureau of Shipping, October 2001.
- ABS HSNC: Guide for Building and Classing High Speed Naval Craft, American Bureau of Shipping, 2003.
- DNV: Rules for Classification of High Speed, Light Craft and Naval Surface Craft, Det Norske Veritas, July, 2000.

The design procedures of the U.S. Navy are documented in the Structural Design Manual for Surface Ships, (NAVSEA, 1976) a document that is 30 years old. However, it still represents many aspects of U.S. Navy design practice today. U.S. Navy methods are also documented in the General Specifications for Design and Construction of U.S. Navy Ships, several Design Data

Sheets, and in the specifications for specific ships. All of these will be referred to as U.S. Navy design procedures.

The structural designer must consider the structural design triangle of loads, analysis methods, and allowable stress levels, which are all connected by the fabrication procedures and fabrication tolerances with which the structure will be fabricated. This relationship is illustrated in Figure 3-1. Mr. Malcolm Dick of Gibbs & Cox, Inc. first suggested the structural design triangle in the mid-1960s. Structural loads are often specified as nominal loads that are less than the maximum loads that a ship will see in its service life. Experience has shown that the use of these nominal loads will result in satisfactory structure if they are used with the assumed materials, fabrication procedures, analysis methods, and allowable stress levels for which they were developed. Even the use of loads defined through some probability level, such as 10^{-8} probability of exceedance must consider the manner in which they are to be used in design.

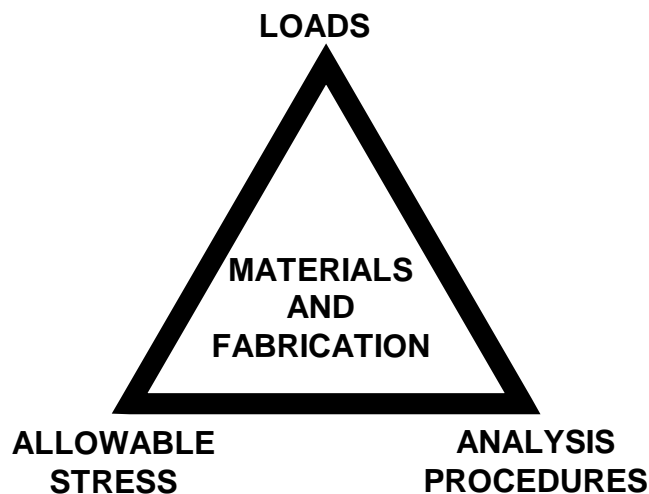


Figure 3-1 The structural design triangle.

An emerging technology for dealing with these interrelated areas is reliability-based structural design. Mansour et al. (1996) gave a review of the subject, although there has been no success to date in the development of any formal procedures to implement direct reliability principles in design. Rather, the emphasis has been on partial safety factor design, also called load and resistance factor design (LRFD), such as the effort by ABS to develop such rules for steel ships (Spencer et al., 2003). Such efforts in design of aluminum structures have been made by the Aluminum Association, which has both conventional allowable stress design and load and resistance factor design specifications for civil aluminum structures in their Aluminum Design Manual (Aluminum Association, 2005). Such procedures for design of aluminum marine structures would be of value, but development is a lengthy process that has not begun. Until reliability-based design procedures are formally developed, the designer must exercise caution in using so-called first-principles design methods, recognizing that factors of safety are present, even if not implicitly specified in the design criteria. This subject will be discussed later as specific design criteria are reviewed. Reliability analysis methods provide a tool for ensuring consistency between different design criteria, such as ensuring that equal reliability exists for similar steel and aluminum vessels.

The design triangle is an important consideration in the design of aluminum ship structure. Most of the design loads and analysis methods used have been developed for steel structures and have been adapted for design of aluminum structures. More consideration must be made of the change in material characteristics than to simply factor allowable stress levels for the change in yield strength. In many ways, aluminum does behave similar to steel, but differences in elastic modulus, fatigue strength, stress-strain characteristics, and fracture properties require careful consideration of the effect of material change on the overall design.

Because all of the factors affecting structural design are interrelated, they cannot be treated in isolation. Even external hydrostatic and hydrodynamic loads are related to structural configuration because advanced analysis methods require a definition of the structure in order to interpret calculated fluid pressures and apply them to a structural model. However, for pedantic reasons, each area must be discussed by itself, although the other factors will enter into the discussion. Structural loads will be addressed first, as initial estimates of loads can be made independent of definition of the structure.

In the discussion that follows, alternative methods of analysis will be presented. This review will be nowhere near exhaustive of the many methods of analysis available. If the reader ends up slightly confused as to the best method to employ, that is understandable. In the end, the best methods are often the ones with which the designer is most familiar, as long as the limitations of those methods are known. The overall impression of this chapter should be that there are no absolutes in ship design. Probabilistic methods provide a way of dealing with uncertainty; they do not remove it. The designer should strive to avoid the contradiction of attempting to obtain exact solutions when the methods of analysis are only approximations. This is not always possible, especially when using design codes that have formulas for design, and the tendency is to express required section modulus, for example, with six significant digits, even though there may be coefficients in the formula with only two significant digits. However, hedging by 5 percent can cause a 5 percent reduction in weight and material cost, so there is a strong inducement to do so.

3.2 Structural Loads

The loads on structure can come from many sources. A listing of loads is provided in the U.S. Navy's Structural Design manual for Surface Ships (NAVSEA, 1976)

1. Basic Loads
 - a. Standard Live Loads
 - b. Dead Loads
 - c. Liquid/Tank loads
 - d. Equipment and Cargo Loads
2. Sea Environment
 - a. Hull Girder Loads
 - b. Sea Loads
 - c. Weather Loads
 - d. Ship Motion Loads
3. Operational Environment
 - a. Slamming

- b. Flooding
 - c. Aircraft Landing
 - d. Tank Overfill
 - e. Docking
 - f. Underway Replenishment
4. Combat Environment
- a. Shock
 - b. Airblast
 - c. Fragments
 - d. Gun Blast and Reaction
 - e. Missile Blast and Accidental Ignition

Not all of these loads apply to all designs, and there are other specific loads that must be considered for other designs. They will not all be discussed here, but most will be to some level of detail. Assessment of hydrodynamic loads and loads from ship motions is generally more important for the design of aluminum vessels because many of these vessels have developmental hull forms for which there is little or no experience base. Even many that have more conventional hull forms present a challenge in the determination of loads because they are operated at high speeds.

3.2.1 Hull Girder Bending

Hull girder bending moments and shear forces result from the imbalance along the length of the ship of hydrodynamic and hydrostatic forces compared to static and dynamic forces resulting from the mass of hull, cargo, fuel, and other lightweight and deadweight items. The simplest calculation is the hydrostatic balance, which is performed in conditions of still water and standard waves. The still water bending moment is a basic design moment in most structural design codes, and is almost always performed at some point during the design process.

3.2.1.1 Hydrostatic balance

Hydrostatic balance on a standard wave was once the mainstay of ship structural design, but is being replaced by more advanced methods today. One standard in use is the $1.1 \sqrt{L}$, feet, ($0.606 \sqrt{L}$, meters) standard trochoidal wave used by the U.S. Navy for hydrostatic balance. It is important to recognize that the hull girder bending moments arising from such a wave are nominal loads that seriously underestimate the maximum lifetime moments by about 80 percent (Sikora et al., 1983). When used for aluminum ships, the allowable design stress for hull girder bending is 3.5 tons per square inch (54 MPa). This is a nominal design stress to be used with the maximum combined still water bending moment and wave bending moment in order to determine a required hull girder section modulus. It is not the maximum hull girder bending stress that the hull will experience.

3.2.1.2 Model testing

The hydrostatic balance method does not address many factors such as the actual ocean environment in which the ship will operate, the effect of ship heading relative to the waves and the torsional and transverse bending moments that such orientation will create, and an ability to determine maximum lifetime loads. The first method of addressing these concerns is to

instrument actual ships or models of ships and measure hull girder bending moments in waves, either at sea or in a wave tank. There are several disadvantages with instrumentation of actual ships. The process is costly and time consuming, and several years of data are required to obtain a realistic statistical database of loads from which maxima can be predicted. Although limited trials can be run with a wave buoy nearby to determine the actual sea state, the magnitude of the waves that are creating the response in the hull can generally only be estimated. Numerous attempts have been made to develop on-board wave height meters, but these have not been successful. Most importantly, such trials are not useful for design unless testing is done on a prototype, generally not a feasible option for ship design. However, instrumented ship data do provide a good means of validating mathematical analysis methodologies, especially for advanced hull concepts used for many aluminum vessels. Many ships today have permanently installed strain gauging for the purpose of determining and reducing maximum hull girder loading. Information from those systems can become a valuable research tool.

Instrumentation of models in a wave tank is often used for design purposes, especially for new and experimental hull types. There are several types of models used. In order to measure bending moments, the hull must be able to respond to waves in a manner that can be instrumented. This is usually done by constructing the hull model in segments that are joined by a structural beam or spline. In order to measure dynamic response, the mass-stiffness characteristics of the model are made to model the first mode of vertical, and sometimes horizontal and torsional hull girder vibration modes. Models of unusual vessels, such as multi-hulled craft can be similarly constructed.

An alternative, but more expensive method of constructing instrumented models is to build with an elastomer, usually rigid vinyl. These models more closely match the actual ship structure, with actual members, including transverse bulkheads and frames and longitudinal structure incorporated into the model. The model is instrumented with strain gages, whose response is scaled to reflect the difference in stiffness between the elastomer and the actual hull material.

Because instrumented models are operated in a wave tank, the spectral density of the wave heights and wave frequencies are known. Two methods of wave tank testing are used. In the first, the model is subjected to a series of waves of different constant frequencies. In this way the transfer functions or response amplitude operators (RAO) are known. These RAOs represent the response of the hull to waves of unit height (or unit amplitude) at all potential frequencies of encounter. RAOs are determined over a range of ship headings, from head seas to following seas, generally in 30-degree or 45-degree increments. The RAOs are then mathematically integrated with the different sea spectra that the ship will encounter during its lifetime to obtain the long-term and short-term statistics of response, from which a measure of maximum bending moments can be determined.

A second method of operating an instrumented model is to generate a series of sea spectra in the wave tank that represent the most severe seas that the vessel is likely to encounter during its lifetime. In this way, the nonlinearities associated with high waves and large ship motions are accounted for. Short-term statistics of the response can then be extrapolated to determine maximum lifetime response.

The third method is to test in irregular waves over the full range of ship headings and speeds using defined sea spectra, and then through Fourier transformation obtain RAOs. With this method, the RAOs will reflect the nonlinear response that comes with higher sea states, but their use in computations will be as efficient as using RAOs generated from response to small waves.

3.2.1.3 Mathematical modeling

Because model testing is expensive and time consuming, it may not be a viable solution for design, especially if the time schedule is short. Mathematical modeling methods have been developed and are continuing to be improved for measuring response of a ship to waves. These are often referred to as seakeeping programs, because their original purpose was to determine ship motions in waves. The pressures on the hull and their integrated responses of shear forces and bending moments can be determined by the same principles. The first of these methods, which is used extensively for conventional hull types, is the strip-theory method, developed in the 1960s (Salvesen et al., 1970). The original method used a series of typical U-shaped or V-shaped forms to represent the response of the hull at various points along its length. This method has been expanded upon using finite difference methods to accurately account for the effect of hull form on response. Finite difference modeling is also used to model the response of catamarans, trimarans, and other unusual hull forms

The simplest of the seakeeping programs are linear programs. Such programs can generally only compute the response to unit wave heights, and are used to generate the RAOs, which are used in the same way as model RAOs. Linear programs can quickly generate a series of RAOs, and these programs are efficient in use in a design environment.

Linear programs do not accurately compute the response to high waves or the response of the hull at high speeds, and nonlinear seakeeping programs have been developed for computing such responses. The difficulty with the use of such programs is that the RAO method can no longer be used as the input seas that are modeled must be spectra of the highest seas that the ship will experience, similar to the method used for model testing. Unfortunately, such methods of computation are inefficient today for use in a design environment because the computer time required to simulate response is significantly greater than the real time simulated. Therefore, use of nonlinear seakeeping programs is costly for use in the ship design process, and requires more time than may be available. Fortunately, computer programs have been developed that are not fully nonlinear, yet can simulate ship response in a relatively short time with a fair degree of accuracy.

In practice, a linear seakeeping program is run to determine the conditions that will maximize response, and then a partially nonlinear program is used to further refine the conditions of maximum response. Then, if necessary, the fully nonlinear program is used to determine response during a short time period.

Although such seakeeping programs offer the means to analyze a variety of hull forms in most sea conditions and a different ship speeds, the issue of validation of the method used should be considered. Analysis should be compared to model tests or full ship data for validation of the analysis method. In comparative analysis of the same vessel in the same sea conditions

sponsored by the International Ship and Offshore Structures Congress, various authorities failed to obtain the same results, a fact that should make the designer realize that a very erudite analysis may have limited accuracy.

3.2.1.4 Design formulas

From the result of analysis of numerous vessels, formulas have been developed to estimate the maximum hull girder moments for design. For large steel vessels, agreement has been reached in the International Association of Classification Societies (IACS) of required design bending moments and minimum values of hull girder section modulus, and these requirements are contained in the rules of all the member societies. A designer may use alternative means such as those mentioned above to determine the bending moments, but these moments may not be used to reduce the rule-required section modulus.

For high-speed craft, including aluminum vessels, different classification societies have different rules for determining hull girder bending moments and shears and for determining the required midship section modulus. These requirements have been reviewed and compared in a recent Ship Structure Committee report (Stone, 2005), which should be consulted for a more complete review of the comparative requirements. There are some similarities in the requirements that Stone reviewed:

ABS HSC Guide. The required hull girder section modulus is a function of craft's length, beam, speed, block coefficient, defined service condition, and material of construction. For craft of greater length than 61 meters (200 feet) additional requirements are imposed, requiring wave bending moments to be calculated using a formula that is a function of length, beam, block coefficient, and defined service condition. These wave bending moments are added to the calculated still water moment. The section modulus requirement is then a function of this combined moment, the speed/length ratio of the craft, and the material of construction. A third requirement applies to planing craft if the speed exceeds 25 knots. The required section modulus is a function of displacement, length, vertical accelerations at the bow, center of gravity, and the stern, and the material of construction. For aluminum, the allowable stress used to determine the required section modulus is a factor of the both the welded yield strength and the welded ultimate strength. Although these formulae are provided, bending moments may be calculated using a seakeeping program as discussed above. A seakeeping analysis may be used to determine hull accelerations, and must be so used for speeds greater than 35 knots. Design equations are also provided for the bending and torsional moments of twin-hulled craft. For aluminum, the allowable stress used to determine the required section modulus of twin-hulled craft is a factor only of the unwelded yield strength.

ABS HSNC Guide. The same equation is used to determine the required hull girder section modulus as the ABS HSC Guide. For craft 24 meters (79 feet) or longer, the wave bending moments are computed using the same formula as in the ABS HSC Guide for craft of 61 m or greater length. A slam induced bending moment is computed as a function of craft displacement, length, hull acceleration at the center of gravity, and a computed slamming length, which is a function of displacement, beam, and draft. The required section modulus is now only a factor of the bending moments and the material of hull construction. For aluminum, the allowable stress used to determine the required section modulus is a factor of both the unwelded

yield strength and the welded ultimate strength. A seakeeping analysis may be used to determine the wave bending moments, but there is a requirement to use a minimum hull acceleration, which is a function of the displacement of the craft. The same formulas are given as in the ABS HSC Guide for the transverse and torsional bending moments of twin-hulled craft, except that minimum hull accelerations are imposed, independent of seakeeping analysis. The accompanying allowable stress levels are different from those for conventional craft. For aluminum, the allowable stress levels of twin-hulled vessels are a function only of the yield strength of the base metal.

DNV HSLC Rules. These rules assume that for craft of length less than 50 meters (164 feet) and with the length to depth ratio less than 12, fulfilling the scantling requirements for local loads will provide the hull girder with sufficient section modulus. For craft not meeting these guidelines, a formula is given in these rules for the slam-induced bending moments, which are a function of displacement, hull acceleration, distance between the center of gravity of the forebody and afterbody (or in the case of hogging, the distance between the forward and after centers of slamming pressures), and the length of the slamming area, which is that area divided by the beam. The slamming area is a function of the displacement, vertical acceleration, and draft. A formula is given for transverse and torsional bending moments of twin-hulled craft, but this is not a function of slam-induced bending. The required section modulus for aluminum is determined by the welded yield strength.

Load Algorithms. Sikora and Klontz (2005) developed a series of graphs relating the global forces on catamarans, trimarans and surface effect ships to speed, heading and wave frequency as a function of ship length and beam. The graphs were based on experimental data and show a great amount of scatter, implying that there may be variables that influence the response but were not considered. The loads predicted by this method were not compared to the equations in the various classification society rules, nor to any loads predicted by seakeeping programs, but do represent a step in the direction of generalized global load prediction for different hull forms.

3.2.1.5 Procedure for determining hull girder bending moments

Determining the appropriate hull girder bending moment to use in design is not straightforward, especially for a craft that will not be classed. If classification is desired, the procedure is more straightforward, except that most societies will require model tests or seakeeping analysis for loads determination, especially for different hull forms or for high-speed craft. The difficulty will be to be certain that during initial design stages the equations used to estimate bending moments predict something close to the final values.

If classification will not be required, the designer has more freedom in choosing the method for determining loads. The studies by Stone (2005), some of which are reported below, show that there can be a significant difference between societies for the required hull girder section modulus. If no model testing or seakeeping analysis is contemplated, a decision must be made as to whether or not conservatism is required in design. The formulas of the classification societies reflect anticipated service conditions, so one should not select the most conservative just because hard service is predicted for the craft. However, if a long lifetime is anticipated, the

more conservative approach should be used, especially if no fatigue analysis will be incorporated into the design process.

It is important to not mix-and-match between different design criteria. For example, if one procedure provides a lower design moment, but another has a higher allowable stress, the two should not be combined to determine a required section modulus. Consistency should be sought throughout the design process; optimistic design procedures in one area are often balanced by conservative approaches in others. More flexibility can be taken when a criteria is based on basic principles. For example, if the design bending moment is based on a probability of occurrence in a defined sea state over a certain number of years, any efforts to improve the accuracy of that prediction are acceptable. If the vessel is to operate in a different environment, redefinition of the loads in terms of that environment should be acceptable, depending on the viewpoint of the classification society if one is involved.

3.2.1.6 Comparison of Classification Society Rules

Most society rules for steel vessels combine loads and allowable stress into single equations for determining scantlings. For aluminum craft, the rules are divided into calculation of pressure loads, which are then used with equations containing allowable stresses to determine scantlings.

A discussion and examples of this procedure is provided by Stone (2005). The design loads are a function of the maximum acceleration of the hull during slamming. The accelerations are calculated at several points along the hull, including the center of gravity and the forward perpendicular. Accelerations are a function of craft length, displacement, dead rise angle, running trim angle, service condition, wave height, and speed. The service condition is one of several classifications for which the craft is designed, such as unrestricted service, passenger craft, coastal, inshore, and sheltered. The service condition definitions vary with the classification society. The required design significant wave height is generally a factor of the intended service condition.

The design pressures are generally slamming loads, although calculation of hydrostatic pressures may be required. The slamming pressures are functions of the accelerations, craft displacement, length, beam, dead rise angle, service condition, and size of the area under pressure.

The required scantlings, such as plate thickness or section modulus of stiffeners or frames, are a function of the design pressure, dimensions such as length and breadth of panel, and allowable stress. The allowable stress is a function of the material welded yield strength and the location on the hull. For example, the ABS HSC has the allowable stress for bottom longitudinals as 0.30 of the yield for hydrostatic pressure, but allows 0.55 of the yield for slamming pressure.

In comparing the design requirements of ABS and DNV for high-speed craft, Stone selected a typical 61-meter conventional hulled craft for application of the rules. Unfortunately, he made errors in the ABS calculations in the SSC report. Stone and Novak (2006) corrected those errors. A few typical design parameters from the comparative design study are shown in

Table 3-1. For ABS, the design speed is 45 knots in unrestricted service. For DNV, a cargo craft or patrol vessel of service condition R₀ is also in unrestricted service.

In many cases, the classification societies may require the accelerations to be calculated through use of a ship motion program. Whether or not required, such calculations, if performed, will permit substitution of the calculated acceleration for the rule-based acceleration. The benefits of using more detailed methods to determine hull accelerations will have a benefit in scantling reduction. The use of this refinement in loads analysis is valid for use with the classification society rules because they are intended for use with accelerations determined as accurately as possible.

In Table 3-1, the columns headed “ABS Acceleration” represent the results that would be obtained if the DNV rules were applied for all aspects of the design except for determining the hull acceleration. The values in these columns assume that numerical analysis or model testing was used to determine acceleration, which coincidentally agrees with the ABS acceleration.

Table 3-1 Comparison of Requirements of ABS HSC and DNV High Speed Light Craft

	ABS	Rule Acceleration		ABS Acceleration	
		DNV Cargo R ₀	DNV Patrol R ₀	DNV Cargo R ₀	DNV Patrol R ₀
Acceleration at CG, g's	2.42	1.69	2.95	2.42	2.42
Hull Girder Section Modulus, cm ² m	9,460	9,581	12,286	11,200	11,200
Design Pressure, Bottom Plating and Stiffeners at CG, kN/m ²	322	345.1	603.9	495	495
Thickness, Bottom Plating at CG, mm	8.56	8.11	10.73	9.71	9.71
Section Modulus, Bottom Stiffeners at CG, cm ²	48.1	35.7	62.4	51.2	51.2

This comparison shows that even there is a great difference in design acceleration, the design pressures and the resulting scantlings, are similar for the ABS High Speed Craft and the DNV Cargo R₀, but much heavier for the DNV Patrol R₀. The last two columns show that the different DNV classifications vary only through the hull accelerations.

3.2.2 Slamming Pressures

For most high-speed craft, slamming causes the controlling design pressures for shell plating and framing. Predicting these pressures is difficult for several reasons. The pressure distribution on a surface is not at all uniform, but is characterized by peak pressures distributed over a very small area. This localization of peak pressures makes them difficult to record during instrumented trials of models or full-scale vessels. The complexity of the phenomena causing slam pressures makes them difficult to mathematically model. There are some advanced

seakeeping programs that can now predict these pressures fairly accurately, but are difficult and expensive to implement in a limited design budget.

The distribution of slam pressures requires different pressures to be used for different structural items. Plating is more likely to receive the peak or near-peak pressure, but the supporting stiffeners receive lower average pressures, and a supporting grillage will receive an even lower average pressure. There are several methods of determining this reduction in pressure. The DNV HSLC Rules have the design pressure inversely proportional to the design area raised to the power 0.3. The ABS reduction comes from a figure that is based on the ratio of the design area to a reference area. This reference area, A_R , is equal to $6.95 \times 10^{-7} \times (\Delta/d)$, where A_R is the reference area in square meters, Δ is the displacement in tonnes, and d is the draft in meters at zero speed.

A comparison of the factors from the two societies is given in Figure 3-2. Two different sets of curves are given for each society. The first set is for the craft analyzed by Stone (2005), which has a length of 61 meters, and the second set is for a geometrically similar craft with a length equal to 12.35 meters. Because DNV requires that the design area be no less than $0.002 \times (\Delta/d)$, the maximum factor is cut off at 1.11 for the 61-meter craft. The DNV factor, which is inherent in pressure computation equations, becomes greater than 1.0 for smaller design areas on smaller craft. The DNV design area places a lower limit on the design area and pressure increase for small design areas, but the ABS procedure places a limit on the maximum design area and the minimum reduction in pressure.

The smaller ABS reference area for the smaller craft results in a significant reduction in the design pressure. ABS limits the reduction to 0.4, so both ABS graphs are cut off at this point. The only place where the two curves agree is for the larger craft for the range of design area sizes between 2 and 20 m², which corresponds to the area typically supported by a transverse frame.

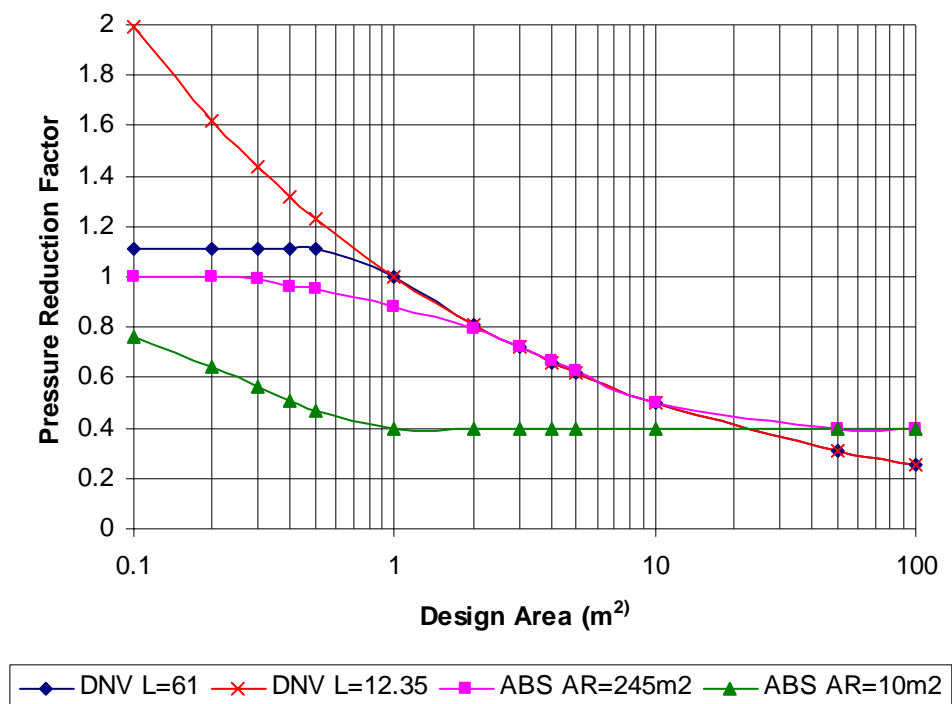


Figure 3-2 Comparison of ABS and DNV slam pressure reduction factors.

This ambiguity in design guidance for reduction of slam pressures with design area continues with the basic design equations for the slam pressures contained in various classification society rules. These pressures are based on the hull acceleration values. In the end, the most important factor is the actual scantlings required by different societies. These are the combination of acceleration values, pressure formulations, area reduction factors, structural design formulas, and allowable stress levels. The design stress levels are compared in Table 3-2, where higher stress levels are permitted by both classification societies for slam loads than for hydrostatic and wave-induced loads.

Table 3-2 Allowable Stress Levels for Bottom Plating

Location	ABS HSC	ABS HSNC	DNV HSLC
Bottom Slamming	0.90 σ_Y	0.90 σ_Y	200 $f_1 = 178$
Bottom Slamming outside 0.4L		σ_Y	
Bottom Hydrostatic Pressure	0.40 σ_Y	0.55 σ_Y	180 $f_1 = 160.2$
Side Slamming	0.90 σ_Y	0.90 σ_Y	
Side Hydrostatic Pressure	0.50 σ_Y	0.55 σ_Y	180 $f_1 = 160.2$

The classification societies all permit acceleration levels determined from trials of similar craft, model testing, or seakeeping calculations to be substituted for rule values to compute slam pressures. In many cases, such determinations are required, and rule values of acceleration are

provided only for use during initial design stages. Whether required or not, the designer will generally find it profitable to use experimental or computed accelerations instead of rule values.

Because of the complexities involved, an experimental approach using pressure gages should not be taken for determining slam loading pressures. Peak pressures will be measured only if a dense array of gages is used, but the issue of effective pressure over a design area remains. If experimental data is sought, the best approach is through strain gauging of structure or rigid vinyl modeling. A rigid vinyl panel can be inserted in a solid model to measure the structural response. In this way, the effective pressure acting on the various design areas of plating, stiffeners, and framing is directly measured. If strain gage measurements are made on the structure of a craft similar to the one being designed, then any structural dynamics associated with the slam phenomena are accounted for, and structural design can be on a static basis.

Although various means of analytically determining slam pressures exist, there is considerable variation between the results differing methodologies. In one comparison (ISSC Loads, 2000) five different methods of computing slam pressures were compared by analyzing the same vessel with the same design areas. The results of the study showed the highest calculated response to be two to three times greater than the lowest, not instilling great confidence in analytic means of obtaining pressures.

3.2.3 Hydrostatic Pressures

The pressures on the shell caused by the effective head of water are treated as static because their variation with time is much slower than the periods of response of structure. Additionally, they are generally calculated as if they are static, as they sometimes are. The general procedure is to measure the distance to the waterline from the structural member being designed, and then add some additional distance to allow for dynamic and other effects.

The U.S. Navy procedure for combatant ships is to take the design head to the waterline, and then add an additional head equal to $0.372 \sqrt{L}$ in meters ($0.675 \sqrt{L}$ in feet), where L is the length between perpendiculars. The additional head is reduced for larger noncombatant ships. The head is also measured to the waterline when the ship is heeled a specified angle, 35 degrees for smaller ships, and shell structure is additionally designed for a head up to a line between the waterline amidships and a point generally 12 feet above the weather deck at the forward perpendicular.

In the ABS HSC Guide, the design hydrostatic head is taken to the waterline plus an additional head equal to $0.0172 L + 3.653$ meters ($0.0172 L + 11.98$ feet). This additional head is multiplied by a factor ranging between 0.5 for the most restricted service to 1.0 for unrestricted service. The ABS HSNC Rules are similar, except that the factor for service conditions is 0.64.

In the DNV HSLC Rules, the additional head is equal to $(k_s - 0.15 h_0 / T) C_W$, where k_s varies from $0.5 / C_B$ at the forward perpendicular to 0.75 at midships and further aft. For a vessel with the block coefficient, C_B equal to 0.5, the additional head at the forward perpendicular is 1 meter (3.28 feet). T is the draft, h_0 is the head to the waterline, and $C_W = 0.6 + 0.002 L$ in meters ($1.96 + 0.002 L$ in feet) for vessels longer than 100 meters (320 feet).

If a designer is not constrained to follow any rules, either from a classification society or from a naval authority, the above can provide some guidance if the manner in which these design heads are intended to be used is considered. The U.S. Navy design hydrostatic loads are nominal loads, intended to be used with defined allowable stresses that include inherent factors of safety. The ABS and DNV loads are considered to be the maximum lifetime loads that the vessel will see in its defined service, and can be used for more exacting structural analysis, including finite element analysis. If there is some other basis for determining maximum loads, such as a seakeeping analysis that determines the instantaneous head during ship motions in seas, that head can be substituted with confidence for the classification society rules. Use of that analytically determined design head is overly conservative when using U.S. Navy design procedures.

Ideally, probabilistic structural design could be used if there were no constraint to follow any particular design rule. Such a methodology, if applied in a validated methodology, could permit any systematic method of determining loads to be used with the materials and structural analysis methods chosen. However, there are no validated examples of probabilistic design of ship structures available other than load and resistance factor design formulations, which are design codes in their own way.

3.3 Structural Analysis Procedures

The second leg of the design triangle is structural analysis. The analysis considers the first leg, design loads, and computes a stress or some other parameter that is consistent with the third leg, allowable stresses.

3.3.1 Frames and Stiffeners

In general, the intention of most historic rule-based structural design procedures for structure other than plating has been to calculate stresses as accurately as possible. For example, whenever a stiffener can be considered as having fixed-end conditions, the bending moment, m , at the ends is determined by some form of the equation $m = wl^2/k$, where w is the load per unit length over the span, l , of the stiffener, and k is a factor that depends on end fixity, equal to 12 for fixed ends. Factors that are based on mechanics of materials analysis are also introduced for other than full fixity at the ends of the stiffeners.

A direct example of the use of the mechanics of materials approach is found in the ABS HSC Guide, the ABS HSNV Rules and in the ABS guide for motor yachts (ABS, 2000), where the formula for required section module of stiffeners and frames is:

$$SM = \frac{144psl^2}{\sigma_a} \quad (\text{in}^3) \quad (3-1)$$

where

- p = design pressure in psi
- s = stiffener spacing in feet
- l = stiffener span in feet, and
- σ_a = allowable stress in psi.

The units of distance in equation (3-1) are in feet, but the design pressure, allowable stress and required section modulus are in powers of inches, and the force units in pressure and in allowable stress are both in pounds. Therefore, the only conversion for consistency of units is to multiply all distance measurements by 12 to convert from feet to inches. The distance units become cubed (spacing times span squared), so the factor 12^3 is introduced. Dividing by 12 in the equation $m = wl^2 / 12$ reduces 12^3 to $12^2 = 144$, and equation (3-1) results. In equation (3-1) the only factor of safety introduced is in the allowable stress.

This is an exact solution if all of the assumptions regarding end fixity and load distribution are met. Generally, those assumptions are not always met. The span is generally defined as the length to some point along an end bracket, if fitted, and loads are not always uniform, and some averaging is required. In the past, other attempts at exact solutions, including grillage analysis, ring frame analysis, and moment distribution methods were used to improve the accuracy of calculated stresses, even if the stresses were the response to arbitrary design loads. For this reason, finite element analysis has become readily accepted for analysis of structure, with as much detail used in analysis as can be practically done to model structural response to defined loads.

3.3.2 Effective Plating

When a structural shape is welded to plating, this plate-stiffener combination forms the full section that bends in accordance with beam theory. For a tee-stiffener, the flange of the tee forms one flange of the plate-stiffener, and the plate forms the other flange. In general, when there are parallel stiffeners, half of the plate between the stiffeners is credited to each stiffener in the determination of the section modulus and inertia of the plate-stiffener combination. However, shear lag and plate buckling considerations can make less than the full amount of plating effective in stiffener bending. The reduced elastic modulus of aluminum compared to steel can make less plating effective in an aluminum plate-stiffener combination.

A review of effective plating was made by Faulkner (1975), who found about 100 different methods of analysis. Shear lag arises from stiffener bending, where there are points of zero stress along the stiffener. In a simply supported member, zero stress occurs at the ends, but a fixed-end beam with a uniform has zero stress at points $0.2113 L$ from the ends. For beam bending, Timoshenko (1956) derived the equation:

$$\frac{b_e}{s} = \frac{1.1}{1 + 2\left(\frac{s}{CL}\right)^2} \quad (3-2)$$

where:

b_e = the effective breadth of plating

s = stiffener spacing

CL = the distance between points of zero stress.

Note that the plate thickness and elastic modulus do not appear in equation (3-2). For the fixed end beam, $CL = 0.577 l$, where l = the span. Note that because of the reversal of flexure

that occurs is fixed end beams, the effective breadth of plating based on shear lag is less than for simply supported beams.

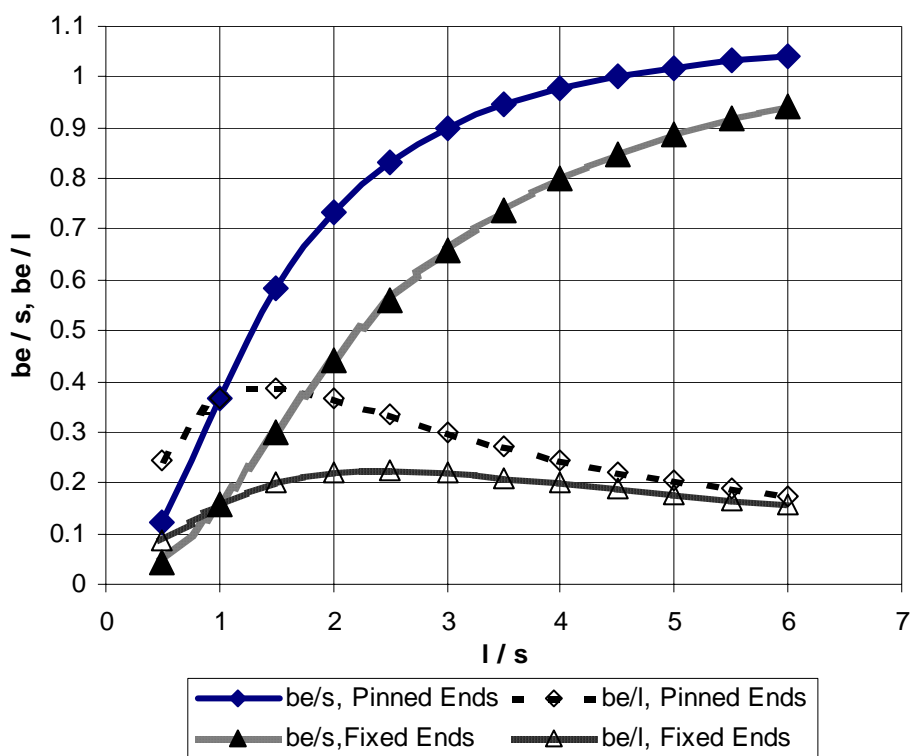


Figure 3-3 Effective breadth of plating based on shear lag.

Figure 3-3 shows the effective breadth of plating, b_e compared to the stiffener spacing, s , and to the stiffener span, l , for different ratios of stiffener span to spacing, l / s . In the simply supported case, as l/s approaches 4, the full width of plate becomes effective. When l/s is between 1 and 4 in the simply supported case, the effective breadth is approximately one-third the span. Therefore, most design codes use $b_e / l = 1/3$, and the reduced effectiveness for fixed ends is ignored.

Faulkner discusses many differing theories regarding the reduction in effective plating due to plate buckling, but states that the formula most used is attributed to von Kármán:

$$\frac{b_e}{t} = \pi \sqrt{\frac{E}{3(1-\nu^2)\sigma_y}} \tag{3-3}$$

where ν is the Poisson ratio, which if taken as 0.3 results in

$$\frac{b_e}{t} = 1.9 \sqrt{\frac{E}{\sigma_y}} \quad (3-4)$$

In equation (3-4) σ_y should be taken as the yield strength that is consistent with the value that is used for the design of the plate, either of base metal or welded. The U.S. Navy uses equation (3-4) with the coefficient rounded to 2.0, in the form:

$$\frac{b_e}{t} = 2 \sqrt{\frac{E}{\sigma_y}} \quad (3-5)$$

Table 3-3 Effective Width of Plate based on Buckling Strength

Alloy	Base Metal		Welded Properties	
	Yield Strength (MPa)	b_e/t	Yield Strength (MPa)	b_e/t
5083-H116	215	36	165	41
5086-H116	195	38	152	43
5383-H116	215	36	145	44
5456-H116	230	35	179	40

The effective width of plate calculated in accordance with equation (3-5) is shown in Table 3-3 for several aluminum alloys. The higher the yield strength, the less plate that is effective.

In the review of analyses of effective width, Faulkner cites several analyses that argue for significantly less effective width than given by equation (3-4), which is based on linear elastic analysis. As the plate begins to buckle, it is capable of carrying less of the axial load than the stiffener, and so the stress in the stiffener increases above the nominal load. Analysis with this consideration as well as test data of steel plate-stiffeners and steel box columns indicate that the coefficient in equation should be reduced from 1.9 to 1.0, which would make the effective width about half of the amount given in Table 3-3.

In the ABS HSC guide and the ABS HSNV rules, the effective width of plating is to be the smallest of the average width of plating supported, 1/3 the span, or 30 inches. For secondary structure, the effective width is also limited to $b_e / t \leq 60$. For $b_e / t = 60$ in equation (3-4), the yield strength is 80 MPa (11.6 ksi), which is 0.53 of the welded yield strength of 5086-H116. However, secondary structure, such as tank bulkheads and watertight bulkheads, have design allowable stresses of $0.60 \sigma_y$ and $0.90 \sigma_y$ respectively, which means that they are designed for a higher stress than the buckling strength of the plating.

This disregard for the buckling strength of the effective plate is justified because when subject to maximum pressure loads the plating of bulkheads becomes deformed significantly in the direction of the pressure. This deformation will be discussed below. The plate is thus

restrained by the pressure from buckling in the modes that were contemplated in the development of equation (3-4).

In the case of transverse frames, deep girders, or other members where the plating that acts in bending is supported by stiffeners, it is inappropriate to use equations (3-3) through (3-5) to compute effective plate as they are based on the buckling strength of unstiffened plate. For these situations, the effective plate should be based on shear lag alone. ABS limits the effective plate to one-third the span or 750 mm, whichever is less.

The low-pitched shell effect should be considered in buckling analysis of panels and in evaluation of effective plate width, especially when grillage is welded to the plate. In the mid-1980s an unpublished experimental study was carried out in the Structural Mechanics of Ships laboratory of the Leningrad Shipbuilding Institute on a box-like hull model made from acrylic glass (modulus of elasticity 1/70 of that of steel). The longitudinally stiffened panels of deck and bottom structures were made with plates supplied with initial deflections of about 0.25 of plate thickness fitted as in a chessboard. Strain gauging and global model stiffness indicated essentially greater effective width compared to the 0.44s conventionally accepted in national practice for longitudinally stiffened panels.

3.3.3 Analysis of Plating under Lateral Load

An exception to the effort to make an exact analysis of stress during structural design is in the response of plating to either static or dynamic pressure. With welded structure, plating is continuous over stiffeners, and this continuity permits plating subjected to continuous lateral loading on one side, such as hydrostatic pressure, to be considered fixed at the edges. The continuity also permits in-plane membrane stresses to occur as the plate is loaded laterally. These membrane stresses are important in plate that elastically deflects, especially thin plate and aluminum plate, which has an elastic modulus one-third of that of steel. Membrane stresses become even more important if any plastic deformation is permitted in the plate, including loads from emergency conditions, such as flooding. During such conditions, significant deformation in plating may be permitted, as the principal objective is survival of the vessel, not long-time serviceability. A linear elastic analysis based on classic plate theory will seriously overestimate the stresses in plating, and should not be used for design.

On the other hand, significant deformation should not be permitted in plating that is important for developing the section modulus of the hull girder. Plate that is significantly deformed cannot effectively support in-plane stress, and will not contribute to overall hull girder strength. There are few guidelines concerning the amount of deformation that can be permitted, even in steel structure, for which considerable service experience exists. Ship Structure Committee Report SSC-364 (Jennings et al., 1991) surveyed 11 classification societies for guidance on allowable deformation, and found the only explicit guidance to be given by Det Norske Veritas. The DNV guidance is to permit only 30 mm (1.18 inches) of deformation in the midbody, and deformation at the forward and after quarters not greater than $b/20$, where b is the span of the stiffeners supporting the plating. Allowable distortion in plating is less for longitudinal strength structure, as will be shown in Chapter 8, where figures for allowable distortion in aluminum plate are given.

Jennings et al. developed a method of analysis of steel plates that could be used for analysis of aluminum. Detailed nonlinear finite element analysis of plate panels was made to determine the deformations and plastic strains that occur with uniform lateral pressure. Fracture mechanics analysis was used to determine the allowable plastic strain, which was found to be 10 percent for Grade B ordinary strength hull steel. If this method is used for the analysis of aluminum, the fracture properties of the specific alloy analyzed should be used.

A beneficial side effect of membrane stresses is that a plate panel is generally not weakened by permanent deformation, unless the loads are so great as to begin to fracture the plate. Otherwise, a plate that is deformed in the same direction as the load will experience membrane stresses at even low levels of applied loads, and have considerably more strength than elastic plate bending analysis would predict.

The exception to the favorable effects of initial deformation is when a plate panel is initially deformed in the opposite direction of the applied load. Then, when the load becomes large enough, it will experience what is called snap-through buckling or oil canning, taking a deformed shape that is now in the direction of the load. In areas of the hull structure with small outward curvature, this can be a problem, leading to fatigue failure from the plate deforming inward at higher wave pressures, and then snapping outward again as the load reduces. This is a common problem in naval combatant ships, and should be considered in the design of aluminum vessels.

Plate design formulas were originally developed from experimental data on steel plates, with different factors used to reflect the amount of plastic deformation permitted in service. These factors were later modified to account for the yield strength of different steels. A correction factor computed from theory of elasticity principles was used to correct for aspect ratio in a plating panel.

The ABS HSC and the HSNC both use the following equation to determine plate thickness under lateral loading:

$$t = s \sqrt{\frac{p k}{1000 \sigma_a}} \quad (3-6)$$

where

t = required thickness in mm

s = stiffener spacing in mm

σ_a = design stress = $0.9 \sigma_0$ for bottom plating with slamming pressure

σ_0 = welded yield strength of aluminum in MPa (N/mm^2)

p = design pressure in kN/m^2

k = factor based on panel aspect ratio, varying from 0.5 for $l/s > 2.0$ to 0.308 for $l/s = 1.0$.

DNV has the following formula for design of aluminum plating:

$$t = s \sqrt{\frac{Cp}{\sigma}} \quad (3-7)$$

where:

t = required thickness in mm

s = stiffener spacing in m

p = design pressure in kN/m²

σ = allowable stress in MPa (N/mm²), and

C is a coefficient that depends on edge conditions and aspect ratio of the plate.

For a plate panel with aspect ratio $l/s \geq 2.0$ and fixed edges, $C = 500$, and for $l/s = 1.0$ and fixed edges, $C = 310$.

The ABS formulae define s in millimeters, but DNV defines s in meters, a factor of 10^3 , which becomes 10^6 when taken inside the radical, explaining the difference between the coefficients k and C. Otherwise the two equations are identical.

Consider a strip of unit width across the breadth s of a plate of infinite aspect ratio l/s and clamped edges, and loaded by a uniform pressure p. The bending moment per unit width is $M = pb^2/12$. The section modulus for that strip is $SM = t^2/6$. Therefore, the bending stress is $\sigma = M/SM = pb^2/2t^2$. Solving for t,

$$t = s \sqrt{\frac{0.5p}{\sigma}} \quad (3-8)$$

This equation is the same as the ABS and DNV formulas for fixed-edge plates of aspect ratio greater than 2, showing that their approaches to plate design are based on a linear elastic strength of materials approach.

The U.S. Navy design equation for aluminum plating is the same as is used for steel plating:

$$\frac{s}{t} \leq \frac{C}{k\sqrt{h}} \quad (3-9)$$

where

k is a factor dependant on the aspect ratio of the plate panel,

h is the design head of water in feet, and

C is a coefficient based on the material and the location on the ship, which determines the amount of permanent set that is permitted from loading.

In locations where no deformation is permitted, such as the shell plating above the waterline and weather decks, $C = 250$ for 5086-H116 plating and $C = 300$ for 5456-H116. Where a small amount of deformation is permitted, such as for tank boundaries or shell plating below the waterline, the coefficients for 5086 and 5456 are 400 and 470, respectively. Where significant deformation is permitted, such as subdivision bulkheads that are subject only to

emergency flooding loads, the respective coefficients are 500 and 600. Thus, depending on the amount of permanent deformation permitted, some plating can be half the thickness of other plating that is designed for the same hydrostatic load.

The origins of the values of k and C are not known, they have been repeated in U.S. Navy specifications for many decades. An analysis was made by Heller (1974), who considered plastic strain and work hardening of most of the materials in his analysis. Heller's analysis was based on plastic bending analysis of a strip of plating of infinite aspect ratio, but did not include in-plane membrane stresses. Heller concluded that the values of k were determined from experiments conducted in Germany in 1876 by an individual named Bach (Heller, 1974). Bach used mild steel plates, and they were loaded until they had considerable plastic deformation.

Heller determined that the values for C are equal to:

$$C = \sqrt{\frac{2\sigma_a}{\gamma}} \quad (3-10)$$

where

σ_a is the allowable stress in psi, and

γ = the specific weight of seawater = 4/9 psi/ft.

Heller concluded that the C values for no deformation were based on an allowable stress equal to the U.S. Navy design bending stress, but the values for small deformation and significant deformation were determined by allowing plastic strain of 0.005 and 0.030, respectively for the two conditions. Heller erred in his analysis because he did not consider the nominal ultimate strength of the materials used. He treated mild steel and high tensile steel as elastic-perfectly plastic materials, which ignores the increase strength that occurs in these materials after the yield point is reached. This is not surprising, because in many cases the so-called ultimate strength is an artifact of engineering stress-strain curves, where the stress is determined by dividing the load by the original cross-sectional area of the test specimen, ignoring the reduction in area that occurs because of Poisson effects and plastic strain.

Nevertheless, the ultimate strength of metals is used in many engineering calculations. For the U.S. Navy, the allowable bending stress is based on a combination of yield strength and ultimate strength, using the formula:

$$\sigma_b = 0.5 \left(\frac{\sigma_y}{1.26} + \frac{\sigma_u}{2.15} \right) \quad (3-11)$$

where:

σ_b = the allowable bending stress,

σ_y = the yield stress, which for aluminum is the welded yield stress, and

σ_u = the ultimate strength, which is for the unwelded condition of aluminum.

An analysis of the C values shows that Heller correctly identified that the values for no permanent set are based on a factor of 1.0 on the allowable bending stress. However, the values for small deformation and significant deformation come from an allowable stress in equation (3-10) equal to 1.1 σ_u and 1.8 σ_u , respectively. The appropriate values of C for several aluminum alloys are given in Table 3-4, which have been calculated from the above assumptions. Note that the C values for 5086-H116 that have been contained in U.S. Navy specifications were erroneously derived from the properties of 5086-H112 extrusions, and should be corrected.

Table 3-4 Values of Coefficient C to be used in U.S. Navy Equation for Plating

Alloy	σ_y ¹ (ksi)	σ_u ² (ksi)	σ_b ³ (ksi)	Calculated C Values			Specified C Values		
				No Set ⁴	Some Set ⁵	More Set ⁶	No Set ⁴	Some Set ⁵	More Set ⁶
5083-H116	24.0 ⁶	44.0	19.8	298	467	597			
5086-H116	22.0	40.0	18.0	285	445	569	250 ⁸	400 ⁸	500 ⁸
5383-H116	21.0 ⁷	44.2	18.6	289	468	598			
5456-H116	26.0	46.0	21.0	308	477	610	300	470	600
6005A-T61	16.7 ⁹	38.0	15.5	264	434	555			
6061-T6	15.0	38.0	14.8	258	434	555			
6063-T6	9.4 ⁹	30.0	10.7	220	385	493			
6082-T6	16.7 ⁹	45.0	17.1	277	472	604			

1. Welded yield strength
2. Ultimate strength of unwelded base metal.
3. $\sigma_b = 0.5 [(\sigma_y / 1.26) + (\sigma_u / 2.15)]$
4. For locations where no permanent deformation is permitted.
5. For locations where some deformation is permitted, including shell plating below a line 2 feet lower than the waterline, and tank boundaries.
6. For locations where considerable plastic deformation is permitted, including watertight bulkheads.
7. ABS
8. Specified values erroneously developed from properties of 5086-H112 extrusions.
9. DNV

Kihl (2003) made a more recent analysis of the U.S. Navy design equation for plating. He describes a possible derivation for the values of the C coefficients.

The U.S. Navy plate design equations have a rational basis, having been derived from very old experimental data from mild steel, and extrapolated for other grades of steel and for some aluminum alloys. They have been defended by analysis to show that the two less conservative sets of coefficients result in a consistent value of plastic strain. However, in practice, they are linear in the breadth to thickness ratio, and do not reflect nonlinearities from in-plane membrane stresses.

All of the above equations from the classification societies and the U.S. Navy are similar in that the thickness of the plating is directly proportional to the square root of the design pressure, and although allowable stress levels may reflect some allowance for deformation under load, that deformation is not explicitly involved in the calculations.

Jones and Walters (1971) gave a method of computing the load-carrying capacity and permanent set of a rectangular plate with fixed edges.

$$p = p_c \left\{ 1 + \frac{4w_0^2}{3t^2} \left[\frac{\xi_0 + (3 - 2\xi_0)^2}{3 - \xi_0} \right] \right\} \quad \text{when } \frac{w_0}{t} \leq \frac{1}{2} \quad (3-12)$$

and

$$p = p_c \frac{4w_0}{t} \left[1 + \xi_0 \frac{\xi_0 - 2}{3 - \xi_0} \left(1 - \frac{t^2}{12w_0^2} \right) \right] \quad \text{when } \frac{w_0}{t} \geq \frac{1}{2} \quad (3-13)$$

where

$$p_c = \frac{12\sigma_0 t^2}{s^2(3 - 2\xi_0)} \quad (3-14)$$

and

$$\xi_0 = \frac{s}{l} \left[\left(3 + \left(\frac{s}{l} \right)^2 \right)^{1/2} - \left(\frac{s}{l} \right) \right] \quad (3-15)$$

where

s, l = panel width and length,

t = plate thickness,

σ_0 = yield strength, and

w_0 = maximum permanent deformation.

Note that equations (3-12) and (3-13) do not compute the ultimate strength of the plating, only the pressure required to achieve a defined amount of permanent set, or the permanent set resulting from a defined pressure load. However, equation (3-4) represents the collapse pressure on the plate panel, the pressure required for the panel to completely deform plastically. Equation (3-15) was derived for analysis of steel structure, assuming that the material deforms in an elastic-perfectly plastic manner, continuing to deform plastically with no additional stress once the yield stress is exceeded. This is a conservative assumption for aluminum, which work-hardens and does not have a defined yield point.

Another method of determining plastic deformation of plating was developed by Hughes (1983), who analyzed the experimental data of Clarkson (1962). He used the factor $Q = pE/\sigma_y^2$ to analyze a plate with clamped edges that were free to slide inward.

$$Q = Q_Y + T(R_W)(\Delta Q_0 + \Delta Q_1 R_W) \quad (3-16)$$

where

Aluminum Marine Structure Guide

$$Q_Y = \frac{2}{\sqrt{(1-\nu+\nu^2)\beta^2}} \left[1 + 0.6 \left(\frac{s}{l} \right)^4 \right]$$

$$T(R_W) = \left[1 - (1 - R_W)^3 \right]^{\frac{1}{3}} \quad \text{for } R_W \leq 1, \quad \text{otherwise, } T(R_W) = 1.0$$

$$R_W = W_p / w_{p0}$$

$$w_{p0} / t = 0.7 \beta^2 / 3$$

$$\Delta Q_0 = \frac{1 + 0.5\beta \left(\frac{s}{l} \right) \left[1 + \left(\frac{s}{l} \right) \left(3.3 - \frac{1}{\beta} \right) \right]}{\sqrt{(1-\nu+\nu^2)\beta^2}}$$

$$\Delta Q_1 = 0.32 \left[\frac{\left(\frac{s}{l} \right)}{\sqrt{\beta}} \right]^{1.5}$$

and

$$\beta = \frac{s}{t} \sqrt{\frac{\sigma_y}{E}}$$

Because the method of Hughes is based on experimental data where the plates were free to slide inward, in-plane membrane stresses couldn't develop in the plate. A method for estimating plastic deformation was developed by Greenspon (1955) that used only membrane stress, ignoring plate bending stress.

$$w_m = \frac{0.164}{1 + \left(\frac{s}{l} \right)^2} \frac{P_0 s^2}{\sigma_u t} \quad (3-17)$$

where:

w_m = deformation,

P_0 = applied pressure,

S_u = ultimate strength of plate, and

s , l , and t are the width, length, and thickness of the plate.

For comparison of the above design and analysis equations, analysis will be made of the bottom plating of the 50-knot craft with a length of 61 meters and displacement of 950 tonnes that was the subject of comparative analysis by Stone (2005). The bottom plate panel at the LCG of the craft has a design pressure in accordance with the ABS HSC guide of 363 kN/m², and a

panel 800 mm long and 260 mm wide has a required thickness of 9.09 mm. For the same structure, the ABS HSNC requires a design pressure of 322 kN/m² and a required thickness of 8.56 mm. If designed to DNV patrol vessel class R0, the DNV design pressure is 604 kN/m² and the required plate thickness is 10.73 mm.

If the craft were designed in accordance with the U.S. Navy criteria, the hydrostatic design head in feet would be the draft plus $0.675 \sqrt{L}$. $L = 61 \times 3.2808 = 200$ feet, draft = $2.7 \times 3.2808 = 8.86$ feet, so the U.S. Navy design head is $8.86 + 0.675 \sqrt{200} = 18.4$ feet. An 18.4-foot head produces a static pressure of 8.18 psi, or 56.4 kN/m². (Note that the U.S. Navy criteria do not explicitly consider slam loads.) The coefficient C in equation (3-9) according to Table 3-4 is 467, and so equation (3-9) gives a required plate thickness of 0.094 in. = 2.39 mm. This seems to be too thin for any application, showing that although the U.S. Navy criteria may yield reasonable results for ships, they should not be used for smaller vessels. A summary of the various design pressures and required thickness of 5083-H116 plates for an 800 mm x 260 mm panel of bottom plating of a 61-meter, 50-knot vessel is made in Table 3-5.

Table 3-5 Comparison of Requirements for the Bottom Plating of a 61-meter, 50-Knot Craft

Design Method	Design Pressure (kN/m ²)	Required plate Thickness (mm)
ABS HSC Guide	363	9.09
ABS HSNC Rules	322	8.56
DNV HSLC Rules, Patrol Vessel R0	604	10.73
US Navy Specifications	56	2.39

A comparison of the analysis of permanent set for the bottom plating designed to the ABS HSC guide was made using the methods of Jones and Walters [equations (3-12) and (3-13)], Hughes [equation (3-16)], and Greenspon [equation (3-17)]. The results are shown in Figure 3-4, which shows the ABS design pressure and the distortion permitted by U.S. Navy specifications. The method of Hughes is based on experimental data, and should reflect actual material behavior, rather than the elastic-perfectly plastic assumption of Jones and Walters. In spite of this difference in assumption in material characteristics, the Hughes method shows near collapse after the pressure exceeds 1,000 kN/m², whereas the Jones and Walters method shows significantly less deformation. This is possibly because the edges of the plate were free to slide inward in the experimental work. The Greenspon equation is actually a linear relation between deformation and applied pressure for a defined plate geometry and material ultimate strength, and that linearity is shown in Figure 3-4.

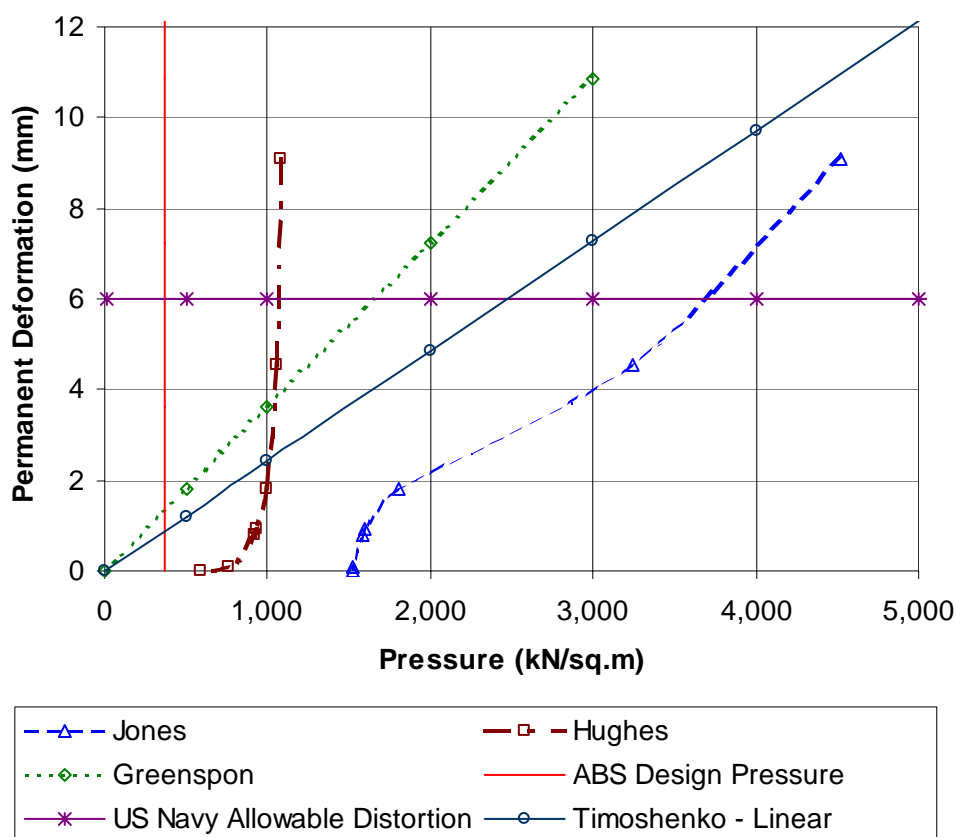


Figure 3-4 Comparison of computations of permanent set of plating as calculated using Jones and Walters (1971), Hughes (1983), and Greenspon (1955).

For comparison with the computations of plastic deformations, the elastic deflection was calculated using the formula for a clamped plate with a uniform load given by Roark (1954): $w = 0.0284 p s^4 / E t^3 (1 + 1.056 (s/l)^5)$. When plotted in Figure 3-4, the elastic deflection is greater than the permanent deformation predicted by Jones and Walters, and less than that predicted by Hughes for lower loads. This implies that the plate deforms more elastically under load than it deforms permanently.

Figure 3-4 shows that even though there is no agreement in the different methods for estimating permanent set, the ABS method selects plate thickness for a defined load that is significantly less than the collapse strength of the plating, so a significant factor of safety on ultimate strength under lateral loading exists. The comparison by Stone (2005) showed that the DNV rules for high speed craft required even greater plate thickness that ABS, except for a ferry in limited service conditions, and the ABS HSNC rules required plating only 0.5 mm thinner than the ABS HSC guide, so all of these plating design methods have large factors of safety on collapse from slam pressure. Whether or not the same factor of safety exists on fatigue strength is another issue, which will be addressed in Chapter 9.

Bruchman and Dinsbacher (1991) showed that static analysis equations are valid for computing the response of typical steel plate panels to either static pressures or dynamic slam pressures. The validity exists within 16 percent if the ratio $2\tau / T$ is greater than 1.75, where 2τ is the period of a triangular pressure pulse, approximately 0.0658 seconds for a typical recorded slam event, and T is the natural frequency of the plate panel. Bruchman and Dinsbacher used the following equation to compute the natural period of a clamped plate panel in air.

$$T = \frac{2\pi s^2}{\Psi} \left[\frac{12\rho(1-\nu^2)}{Et^2} \right]^{1/2} \quad (3-18)$$

where:

ρ = the material density (2.66 g/cm³ for aluminum)

ν = Poisson's Ratio (0.3)

E = Elastic Modulus (71 x 10³ MPa for 5083 Aluminum)

Ψ = 36, 24.6, 23.2, and 22.4 when $s/l = 1.0, 0.5, 0.333,$ and 0, respectively.

To determine the validity of using static response calculations for the slam response of aluminum plate panels, the 260 x 800 x 9.09 mm bottom panel analyzed above will be evaluated. According to equation (3-18), the natural period in air for this panel is 0.013 seconds, corresponding to a frequency of 77 Hz. The mass of the aluminum plate is 5.03 kg, and if the added mass of water is taken as equal to the mass of a half-cylinder of water with the diameter of the width of the panel, and length equal to the length of the panel, the mass of the added water would be 43.6 kg. The natural period is proportional to the square root of the mass, so that the period of the aluminum panel plus added mass is $(48.6/5.03)^{0.5} = 3.1$ times greater than the period of the panel in air. Therefore, the period of the panel in water is 0.04 seconds, and the ratio $2\tau/T = 1.62$. This is slightly less than the goal of 1.75, and so computing the response of aluminum plating panels to slam pressures is marginal if the response is treated as a static response. However, because there is such a great difference in the collapse strength and the applied load, the static evaluation should be considered valid for design.

Another view on the need for dynamic hydroelastic analysis for the response of local structure to external impacts was provided by the International Ship and Offshore Structures Congress 2003 Committee II.2, Dynamic Response. The committee drew on work of Faltinsen (1999), Faltinsen (2000), and Haugen and Faltinsen (1999). A plate strip of unit width, with moment of inertia I , modulus of elasticity E , density ρ , and length L_B was analyzed as part of a flat panel impacting the water surface at an angle α_{rel} and a relative velocity V_T . They calculated the bending stress at a distance z_{na} from the neutral axis. Their results are shown schematically in Figure 3-5. The horizontal axis is a measure of the duration of the loading on the panel compared to the longest natural period of the structure. The vertical axis is the nondimensional stress. The stresses computed using numerical hydroelastic theory during a relatively short duration of the loading vary linearly with the relative velocity and are independent of the impact angle. For a longer duration of the load, the quasi-static structural response is inversely proportional to the impact angle and is proportional to the square of the relative velocity.

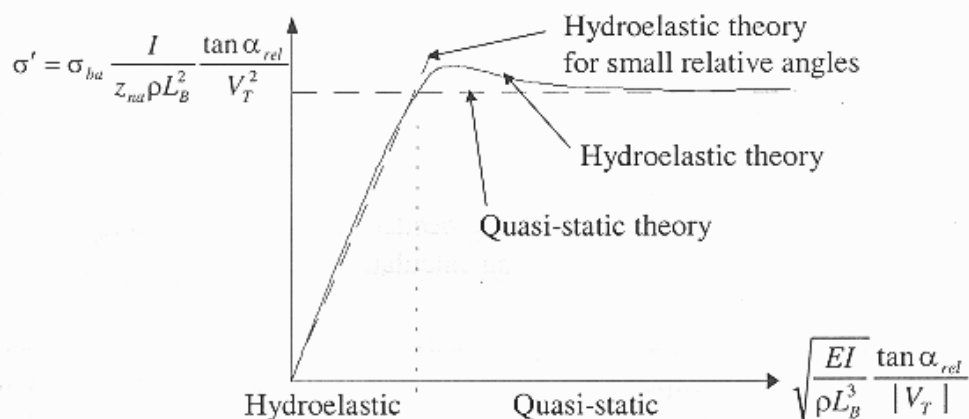


Figure 3-5 Nondimensional stress in a stiffened panel subject to impact loads. (ISSC 2003, adapted from Haugen and Faltinsen, 1999).

Aluminum has an elastic modulus 1/3 that of steel, but its density is also 1/3 that of steel. Therefore the ratio E/ρ in the horizontal axis of Figure 3-5 remains the same for aluminum as for steel. Because of the reduced elastic modulus the value of I tends to be higher for an aluminum structure than for steel, and the moment of inertia of the structure, I , is also higher because scantlings are heavier because of reduced strength of aluminum relative to steel. Therefore, the value of the quantity on the horizontal axis will be greater in an aluminum structure compared to an equivalent steel structure, meaning the need for hydroelastic analysis of slam loads is less with aluminum than for steel. Unfortunately, the above is only presented qualitatively, with computations required for specific situations.

Deflection under load is another important consideration for design of aluminum plating, especially decks. Because aluminum has a lower modulus of elasticity, it will deflect more than steel. A deck should not noticeably deflect when live loads are applied, especially foot traffic. The feel of a deck springing underfoot gives a person an uncomfortable feeling and low confidence in the structure. Excessive deflection can also have a deleterious effect on some deck coverings.

3.4 Allowable Stress Levels

In the above discussion, there are two types of loads, nominal design loads and estimates of maximum lifetime loads. An example of the former is the U.S. Navy standard design wave for longitudinal strength of height = $0.606 \sqrt{LBP}$ (meters) [$1.1 \sqrt{LBP}$ (feet)], and an example of the latter is the IACS hull girder bending moment formula, which represents a probability of exceedance of 10^{-8} .

There are also two different types of analysis methods: direct scantling determination and maximum stress analysis. Examples of direct scantling determination include the various formulae for required thickness of plating subject to lateral pressure, in which allowable stress

levels are implicitly included. Another example of direct scantling determination is in various rules for minimum thickness, which may be a function of different ship size parameters but do not follow directly from stress analysis. Direct stress analysis includes computation of bending moments in stiffeners, and finite element analysis. The objective of direct stress analysis is to obtain an accurate response to an applied load or load combination.

Because there are different types of loads and analyses, there cannot be a single type of allowable stress level. In general, it is the practice to implicitly include factors of safety within allowable stress levels. There has been a movement recently to go from a single implicit factor of safety to multiple factors, including factors on loads, to reflect more accurately uncertainties in loads, stress analysis, material strength, fabrication deficiencies, and other factors that can lead to structural failure. This method is called the Load and Resistance Factor Design (LRFD) method, and an example can be found in the Aluminum Design Manual (Aluminum Association, 2005). Alternate design codes are design codes are presented for civil engineering structures in the conventional allowable stress format and in the LRFD format. As all current design codes for aluminum marine vessels are in the allowable design format, that method will be discussed in the following material. However, there are efforts being made to develop the LRFD method for marine structures, such as those of ABS mentioned above, and the LRFD method may someday be applied to aluminum marine structures.

In general, most allowable stress levels make implicit or explicit recognition of the stresses arising from different loads. An example is the U.S. Navy interaction formula for stiffeners:

$$\frac{f_c}{0.8F_c} + \frac{f_b}{F_b} \geq 1.0 \quad (3-19)$$

where:

- f_c is the maximum compressive stress from hull girder bending,
- F_c is the column strength of the stiffener-plate combination,
- f_b is the maximum compressive bending stress in the stiffener from lateral loads, and
- F_b is the allowable bending stress, computed by equation (3-11).

This interaction formula includes several factors of safety. Using equation (3-11) for an elastic-perfectly plastic material where the yield strength and the ultimate strength are the same, the allowable stress is 0.63 of the yield strength. The factor 0.8 on column strength reflects some uncertainty in actual strength, and the factor is reduced to 0.67 if the slenderness ratio, l/r , of the column is greater than 60. Even though the elastic modulus is a factor in the calculated column strength, the ratio of $l/r = 60$ dividing the different safety factors is the same for aluminum as steel.

In equation (3-19), the hull girder bending stress includes a factor on stress, which is not described as a factor of safety, but has that function. There are specified nominal design hull girder bending stresses for various materials, to which 1.0 ton per square inch (15.4 MPa) is added when equation (3-19) is used. However, the design hull girder bending stress and the bending stress from lateral loads are based on nominal hydrostatic loads, which are about 80

percent of the maximum lifetime loads, and that percentage is implicitly considered when determining the other factors of safety in equation (3-19).

There are implicit considerations of interaction between hull girder bending stresses and stresses from lateral loads in various classification society rules. The ABS HSC guide has an allowable stress for bottom plating subject to slam loads of 0.90 of the welded yield strength for aluminum, but for hydrostatic loads, the factor is reduced to 0.40. This change in factors recognizes that that maximum local stresses from slamming occur slightly before the hull girder responds in bending, but that maximum hydrostatic loading can coincide with maximum hull girder bending.

Similarly, the ABS HSC guide has an allowable bending stress for bottom longitudinals subject to slam pressures in craft of 50 meters length or greater that is equal to 0.55 times the welded yield strength of aluminum. For sea pressures, the factor is reduced from 0.55 to 0.30. These decreases in the factor for slam pressures from 0.90 for bottom plating and 0.55 for bottom longitudinals reflects a slightly slower response time for stiffeners compared to plating.

Generally, the ABS HSC guide has the same allowable stress levels for plating and for compared to stiffeners. For example, the allowable stress for the plating of tank bulkheads and for tank stiffeners are both 0.60 times the welded yield strength.

The implicit interaction for design allowable stresses in the ABS HSC guide does not occur when finite element analysis is used. Then, all loads are to be applied simultaneously, and the von Mises equivalent stress is calculated for all points of concern. For all locations and members the allowable stress for finite element analysis is 0.833 of the welded yield strength for aluminum and for steel. In the ABS HSNC guide, the allowable stresses are 0.85 of the welded yield strength for aluminum and 0.95 of the welded yield strength for steel.

3.5 Buckling Strength

Buckling strength considerations have entered some of the preceding discussion. The effective width of plating is limited by buckling strength, and the U.S. Navy interaction formula for design allowable stress of stiffeners includes the plastic buckling strength of the plate-stiffener combination. However, a more extensive analysis of buckling should be undertaken for aluminum structure because of the low elastic modulus of aluminum. Additionally, the differences in the stress-strain behavior of aluminum compared to steel should be considered. The 5xxx-series alloys have a more rounded stress-strain curve than most steels as well as the 6xxx-series alloys, and will buckle earlier than the those materials because the more rounded stress-strain curve of the 5000-series means that the tangent modulus has been reduced before the proof stress is reached. This fact is reflected in some civil engineering design codes for aluminum.

3.5.1 Buckling Strength of Plating

A formula for the buckling strength of a plate panel in compression is given by Bleich and Ramsey (1951) as:

$$\sigma_c = \frac{\pi^2 E \eta}{12(1-\nu)} \left(\frac{t}{s}\right)^2 K \quad (3-20)$$

where:

σ_c = critical plastic buckling strength,

E = Elastic modulus,

ν = Poisson ratio,

η = a modulus factor dependant on the aspect ratio and the shape of the stress-strain curve, and

K = a factor that depends on the aspect ratio, the condition of support at the edges, and the condition of loading on the edges.

Equation (3-20) is the basis for the U.S. Navy Design Data Sheet 10-4, Strength of Structural Members, which provides charts for the solution of the design equations for all aspect ratios of plates loaded in compression and shear for all alloys and special charts are provided for 5086-H116 and 5456-H116.

A formulation similar to equation (3-20) is generally known as the Euler-Johnson method, and is used in the ABS HSC guide:

$$\begin{aligned} \sigma_c &= \sigma_E && \text{when } \sigma_E \leq \sigma_y \\ \sigma_c &= \sigma_y \left(1 - \frac{\sigma_y}{4\sigma_E}\right) && \text{otherwise.} \end{aligned} \quad (3-21)$$

where:

$$\sigma_E = 0.9 m E \left(\frac{t}{s}\right)^2 \quad (3-22)$$

where $m = 4.0$ for longitudinally stiffened shell and deck plating.

As an example of an application of the above, consider the 61-meter, 50-knot craft analyzed by Stone (2005). The bottom plating on a 260-mm x 800-mm bottom plating panel amidships is required to be 9.09 mm thick when designed of 5083-H116 in accordance with the ABS HSC guide. For comparison with the U.S. Navy DDS 100-4 and the method of Bleich and Ramsey, it will be assumed that the same scantlings were obtained for 5086-H116 plate, with $\sigma_y = 152$ MPa. Using equation (3-22), $\sigma_E = 312.4$ MPa, and equation (3-21) gives $\sigma_c = 134$ MPa. Using DDS 100-4, the corresponding value is $\sigma_c = 145$ MPa, which is slightly higher than the ABS value. However, both are much greater than the ABS HSC guide design primary stress of 98 MPa for a craft of that length and speed.

An alternative empirical expression for the ultimate strength, σ_{x0} , of plate panels was developed by Paik and Duran (2004) as:

$$\frac{\sigma_{x0}}{\sigma'_{Yp}} = \begin{cases} 1.0 & \text{for } \beta' \leq 0.46 \\ -0.215\beta' + 1.1 & \text{for } 0.46 \leq \beta' \leq 2.2 \\ -0.083\beta' + 0.81 & \text{for } \beta' > 2.2 \end{cases} \quad (3-23)$$

where

$$\beta' = \frac{s}{t} \sqrt{\frac{\sigma'_{Yp}}{E}},$$

$$\sigma'_{Yp} = \frac{P_p}{s l},$$

$$P_p = (1 - 2s'_p)(s - 2s'_p)\sigma_{Yp} + 2[ls'_p + (s - 2s'_p)s'_p]\sigma'_Y,$$

s'_p = width of the heat affected zone (HAZ) around the boundary of the plate.

σ'_Y = yield stress in the HAZ, and

σ_Y = yield stress in the unwelded base metal.

As such, this method incorporates a value of the yield strength that is weighted by the relative areas of HAZ and base metal. Equation (3-23) implicitly assumes initial deformation of the plate equal to 0.009 times the width of the plate. The validity of the equation was shown by Paik et al. (2005a) (2005b) by comparison with finite element analysis of the plate panels and by the results of tests of 13 panels in compression. The strength predicted by equation (3-23) was slightly greater than that from the finite element analysis, although both were even greater than the experimental data, which is partially accounted for by the fact that analysis was performed with the minimum specified yield strength as compared to the actual material properties of the test specimens.

3.5.2 Buckling Strength of Stiffeners

The basic formula for determining the strength of a column in compression was developed by Euler and is generally expressed in the form:

$$\sigma_{cE} = \frac{\pi^2 E}{\left(\frac{kl}{r}\right)^2} \quad (3-24)$$

where:

σ_{cE} = elastic critical buckling stress,

E = Elastic modulus,

k = the length of the column,

r = the radius of gyration of the column, equal to $\sqrt{I/A}$,

I = lowest moment of inertia of the cross section of the column,

A = cross sectional area, and

k = a factor on column length dependent on end conditions.

For fixed end columns, $k = \frac{1}{2}$, but for stiffened plate panels, k should be taken as 1.0, the value for pin ended columns because even if the stiffeners are continuous at transverse frames, they can buckle in opposite directions on opposite sides of a supporting frame, acting as pin ended. For columns fixed on one end and pinned on the other, $k = 0.7$; for a cantilever fixed on one end but constrained from rotation at the other, $k = 1.0$; and for a cantilever fixed at one end but completely free at the other, $k = 2.0$. The Euler equation is used in the ABS HSC guide and the HSNV rules with the factor $\pi^2 = 9.87$ rounded to 10.0.

Equation (3-24) is valid for long columns, but it can significantly overstate the strength of a short column (low values of kl/r) because the strength is limited by the yield strength of the material. There are several approaches for reducing the column strength computed with equation (3-24), the most common of which is the tangent modulus approach.

$$\sigma_{cp} = \sigma_t = \frac{\pi^2 E_t}{\left(\frac{kl}{r}\right)^2} \quad (3-25)$$

Equation (3-25) is the same as equation (3-24) except that the elastic modulus, E , has been replaced by the tangent modulus E_t , which is the instantaneous slope of the stress-strain curve after the proportional limit is exceeded. Equation (3-25) requires an iterative approach to solution.

The Column Research Council (Johnston, 1976) assumed that the upper limit of elastic buckling failure is defined by an average stress equal to $\frac{1}{2}$ the yield strength at a slenderness ratio:

$$C_c = \sqrt{\frac{2\pi^2 E}{\sigma_y}} \quad (3-26)$$

so that for any slenderness ratio less than C_c :

$$\sigma_{cp} = \left[1 - \frac{(kl/r)^2}{2 C_c^2} \right] \sigma_y \quad (3-27)$$

Substituting equation (3-26) into equation (3-27) results in equation (3-28), which is the same as equation (3-21).

$$\sigma_{cp} = \left[1 - \frac{\sigma_y}{4 \sigma_{cE}} \right] \sigma_y \quad (3-28)$$

Equation (3-28) is used in the ABS HSC guide and the HSNV rules to develop the elastic-plastic strength of columns. The U.S. Navy approach in DDS 100-4 is based on the same method, but with a straight-line simplification. A slenderness ratio is defined as:

$$C = \frac{kl}{r} \sqrt{\frac{\sigma_y}{E}} \quad (3-29)$$

The column strength is then calculated as the ratio σ_{cp} / σ_y , where σ_{cp} is the elastic-plastic critical buckling stress. For values of $C \geq 4.8$, the Euler equation (3-24) is used, for $C \leq 1.4$, the limiting yield strength is used, and intermediate values are determined by straight-line interpolation.

The transition point in U.S. Navy DDS-100-4 from Euler buckling to the straight-line interpolation of $C = 4.8$ represents a value of $kl/r = 144$ for mild steel with $\sigma_y = 33$ ksi (228 MPa) and $E = 207,000$ MPa (30,000 ksi). For 5086-H116 aluminum with $\sigma_y = 152$ MPa (22 ksi) and $E = 71,000$ MPa (10,300 ksi), the value of $C = 4.8$ represents a value of $kl/r = 104$, so that the linear elastic Euler buckling equation is continued into a range where plasticity effects become slightly important.

The tangent modulus approach of equation 3-25 is implemented in the Specification for Aluminum Structures in the Aluminum Design Manual (Aluminum Association, 2005). That specification includes a reduced factor of safety based on eccentricity in typical aluminum columns. The manual makes a distinction between the yield strength in compression and in tension, which is significantly different for the work-hardened 5xxx-series, particularly in unwelded extrusions.

Considering a column of 5086-H116 with a kl/r ratio of 100, DDS 100-4 gives a column strength of $\sigma_{cp} = 62$ MPa (9.0 ksi). Using the ABS procedure, $\sigma_E = 70.0$ MPa, and equation (3-28) gives $\sigma_{cp} = 69.5$ MPa (10.1 ksi), so the ABS method is slightly more optimistic than the U.S. Navy approach.

An alternative empirical expression for the ultimate strength, σ_{xu} , of stiffeners was developed by Paik and Duran (2004) as:

$$\sigma_{xu} = \frac{\sigma'_{Yseq}}{\sqrt{C_1 + C_2(\lambda')^2 + C_3(\beta')^2 + C_4(\lambda'\beta)^2 + C_5(\lambda')^4}} \leq \frac{\sigma'_{Yseq}}{(\lambda')^2} \quad (3-30)$$

where:

$$\lambda' = \left(\frac{l}{\pi r} \right) \sqrt{\frac{\sigma'_{Yseq}}{E}}$$

$$\beta' = \frac{s}{t} \sqrt{\frac{\sigma'_{Yp}}{E}},$$

$$\sigma'_{Yp} = \frac{P_p}{sI},$$

$$P_p = (1 - 2s'_p)(s - 2s'_p)\sigma_{Yp} + 2[1s'_p + (s - 2s'_p)s'_p]\sigma'_Y,$$

$$\sigma_{Yseq} = \frac{P_s}{st + h_w t_w + b_f t_f}$$

$$P_s = (s - 2s'_p)t\sigma_{Yp} + 2s'_p t\sigma'_{Yp} + (h_w - h'_w)t_w\sigma_{Ys} + h'_w t_w\sigma'_{Ys} + b_f t_f\sigma_{Ys}$$

σ_{Ys} = yield strength of the stiffener web,

σ'_{Ys} = yield strength of the HAZ of the stiffener web,

σ_{Yp} = yield strength of the plate,

σ'_{Yp} = yield strength of HAZ of the plate,

h_w, t_w = depth and thickness of the stiffener web,

h'_w = width of HAZ on the stiffener web,

s'_p = width of HAZ on the plate,

r = radius of gyration of the plate-stiffener = $\sqrt{I/A}$,

A = cross sectional area of the plate-stiffener, and

I = Moment of Inertia of the plate-stiffener, and the coefficients C1 to C5 are defined in

Table 3-6.

**Table 3-6 Coefficients for Paik-Duran Stiffener Buckling Formula
(Paik and Duran, 2004)**

Coefficient	Initial Deformation		
	Slight	Average	Severe
C ₁	0.878	1.038	1.157
C ₂	0.191	1.099	2.297
C ₃	0.106	0.093	0.152
C ₄	-0.017	-0.047	-0.138
C ₅	1.30	1.648	3.684

Equation(3-30) is similar to equation (3-23) in that incorporates a value of the yield strength that is weighted by the relative areas of HAZ and base metal. The validity of the equation was shown by Paik et al. (2005) by comparison with finite element analysis and by the results of tests of 13 panels in compression. This is the same comparative analysis that was mentioned in the discussion of the ultimate strength of plate. In the experiments and in the analyses, the panels that failed by different modes, and the Paik-Duran strength tabulated was the lower of the strength computed by equation (3-23) and equation(3-30).

3.5.3 Stiffener Tripping

Plate-stiffener combinations are subject to torsional instability of the stiffeners, where the stiffeners twist along their length between supports. This type of buckling is commonly called stiffener tripping. Asymmetric sections such as angles are more susceptible to this type of failure because the shear center is offset from the centroid of the section, causing rotation under load.

Members with little or no flange, such as bulb flats and flat bar stiffeners, are prone to tripping because they have little lateral stability.

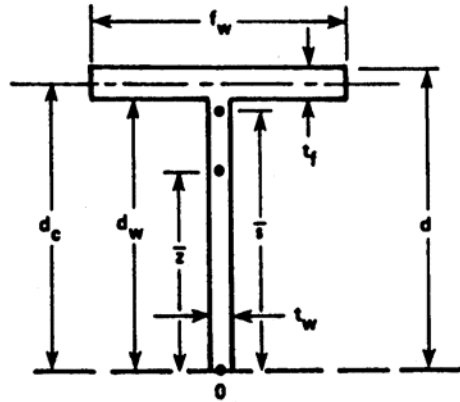
A review of various methods of analysis of stiffener tripping and design criteria to prevent tripping was made by Vara et al. (2003). The analysis methods are based on linear elastic analysis, which is then corrected for plasticity by differing methods. Most analysis methods are based on axial compression, although there are several methods developed for analyzing behavior under lateral loading, and some consider combined lateral and compressive loads. However, the solutions for lateral loads have been shown to be accurate only when the ends of the stiffeners are free to rotate, and combined loading methods have been developed only to analyze symmetric stiffeners. Therefore, only the equations for axial loads will be described below. A comparative analysis of the method of the ABS HSNC, Germanischer Lloyd, Lloyd's Register Rules for Classification of Naval Ships, the method of Adamchak (1979) and the U.S. Navy Design Data Sheet DDS 100-4 was made by Vara et al., and the results agreed within 10 percent. The method described below is that of Adamchak.

The elastic in-plane tripping stress (denoted here by σ_{cre}) for a stiffener under in-plane axial loading can be written in the form of a quadratic equation as follows:

$$(-\sigma_{cre})^2(k_2k_4 - k_6^2) + (-\sigma_{cre})(k_1k_4 + k_2k_3 - 2k_5k_6) + (k_1k_3 - k_5^2) = 0 \quad (3-31)$$

in which the k_j 's are defined as

$$\begin{aligned} k_1 &= EI_z \left(\frac{m\pi}{a} \right)^2 + 3 \frac{D_w}{d_c^3} \left(\frac{a}{m\pi} \right)^2 (1 + 3R) \\ k_2 &= -A_s + d_c t_w \left(\frac{18}{35} + \frac{18}{140} R - \frac{3}{140} R^2 \right) \\ k_3 &= GJ + E\Gamma \left(\frac{m\pi}{a} \right)^2 + \frac{3D_w}{d_c} \left(\frac{a}{m\pi} \right)^2 \left(1 + \frac{R}{3} \right) \\ k_4 &= -I_{ps} + d_c^3 t_w \left(\frac{11}{35} + \frac{1}{84} R - \frac{1}{420} R^2 \right) \\ k_5 &= -\frac{3D_w}{d_c^2} \left(\frac{a}{m\pi} \right)^2 (1 + R) \\ k_6 &= d_c^2 t_w \left(\frac{3}{35} - \frac{1}{420} R + \frac{1}{140} R^2 \right) \end{aligned} \quad (3-32)$$



I_z - MOMENT OF INERTIA ABOUT THE WEB PLANE

$$I_z = \frac{1}{12} (t_f f_w^3 + d_w t_w^3)$$

\bar{s} - HEIGHT OF SHEAR CENTER ABOVE TOE (ORIGIN)

$$\bar{s} = \frac{1}{2} \left[d_w + \frac{d_w + t_f}{1 + (d_w/t_f)(t_w/f_w)^3} \right] \approx d_c$$

Γ - LONGITUDINAL WARPING CONSTANT

$$\Gamma = \frac{1}{36} \left(t_w d_w^3 + \frac{1}{4} t_f^3 f_w \right)$$

J - ST. VENANT TORSION CONSTANT

$$J = \frac{1}{3} (d_w t_w^3 + f_w t_f^3)$$

I_t - VERTICAL MOMENT OF INERTIA ABOUT TOE (STIFFENER ALONE)

$$I_t = \frac{1}{3} t_w d_w^3 + f_w t_f \left(d_c^2 + \frac{1}{12} t_f^2 \right)$$

I_p - POLAR MOMENT OF INERTIA ABOUT TOE

$$I_p = I_t + I_z$$

\bar{z} - HEIGHT OF CENTROID ABOVE TOE

$$\bar{z} = \frac{\left[\frac{1}{2} t_w d_w^2 + f_w t_f d_c \right]}{\left[t_w d_w + f_w t_f \right]}$$

Figure 3-6 Geometrical tripping parameters for tee stiffeners (Adamchak, 1979).

Many of the parameters appearing in equation (3-32) are defined in Figure 3-6. The rest are defined below.

Aluminum Marine Structure Guide

D_w = Flexural Rigidity of Stiffener Web

$$D_w = \frac{E t_w^2}{12(1 - \nu_s^2)}$$

A_s = Stiffener Cross Section Area

$$A_s = d_w t_w + f_w t_f$$

I_{ps} = Polar Moment of Inertia About Shear Center

$$I_{ps} = I_p + A_s d_c^2 - 2A_s d_c z$$

G = Stiffener Material Shear Modulus

$$G = \frac{E}{2(1 + \mu_s)}$$

m = Tripping Mode Number

The parameter R is dimensionless and indicates the amount of rotational restraint that the plating to which the stiffener is attached provides to resist tripping. This parameter is defined as

$$R = \frac{[(Cd_c)/(4D_w)]}{1 + [(Cd_c)/(4D_w)]} \quad (3-33)$$

in which the parameter C is the rotational spring constant (in units of moment/rad/length) of the supporting plating. The formulation for C recommended in reference 5 is:

$$C = \begin{cases} C_0 \left(1 - \frac{\sigma_e}{\sigma_{pb}} \right) & \sigma_e > \sigma_{pb} \\ 0 & \sigma_e \leq \sigma_{pb} \end{cases} \quad (3-34)$$

in which σ_{pb} is the plate buckling stress

$$\sigma_{pb} = \begin{cases} \sigma_{pbe} & -\sigma_{pbe} \leq 0.5 \sigma_{yp} \\ \sigma_{yp} \left(1 - \frac{\sigma_{yp}}{4(-\sigma_{pbe})} \right) & -\sigma_{pbe} > 0.5 \sigma_{yp} \end{cases} \quad (3-35)$$

based on the classical elastic plate buckling stress

$$\sigma_{pbe} = \frac{-4\pi^2 D}{tb^2} \quad (3-36)$$

and C_0 is the unloaded rotational spring constant. The recommended relationship for C_0 is

$$C_0 = \frac{\pi^2 D}{2b} \left[1 + \left(\frac{b}{a} \right)^2 \right]^2 \quad (3-37)$$

in which the parameter D , also appearing in the expression for σ_{pbe} , refers to the flexural rigidity of the plating. Hence

$$D = \frac{Et^3}{12(1-\nu^2)} \quad (3-38)$$

The elastic tripping stress calculated according to equation (3-31) is corrected for inelastic effects in a fashion similar to that for beam-column buckling, namely

$$\frac{\sigma_{cr}}{\sigma_{ys}} = \begin{cases} \frac{\sigma_{cre}}{\sigma_{ys}} & -\sigma_{cre} \leq p_r \sigma_{ys} \\ -1 + p_r(1-p_r) \frac{\sigma_{ys}}{-\sigma_{cre}} & -\sigma_{cre} > p_r \sigma_{ys} \end{cases} \quad (3-39)$$

in which p_r is the structural proportional limit ratio (default value = 0.5).

Since the rotational resistance provided by the plating is load dependent, the solution for σ_{cr} must be carried out in an iterative fashion. Convergence is achieved when the computed value of σ_{cr} from Equation (3-39) is within an accepted tolerance of the value of σ_e assumed in Equation(3-34).

In the theoretical development of the tripping equation (3-31), the mode number m , strictly speaking, should take on only integer values. However, one may notice that, in the expressions for the coefficients k_j , the mode number always occurs in combination with the panel or stiffener length, a . Thus it is possible to define an effective length for tripping, labeled a_{ie} , which is equal to a/m , and which can be used to approximate various degrees of rotational restraint in the plane of the stiffener web provided by the connecting structure at the stiffener's ends. For example, in the current U.S. Navy design practice for determining when intermediate lateral supports are required, the effective length assumed for tripping is $a/\sqrt{2}$. This corresponds to a value of $m = \sqrt{2}$. Values for a_{ie} can be taken in the range a to $a\sqrt{2}$.

3.5.4 Stability of Stiffener and Frame Flanges and Webs

In addition to overall buckling strength and tripping strength, stiffeners and frames and other structural members must be proportioned to avoid local instability. Guidance for this is provided in the ABS HSNC Rules as:

- Flat bars, outstanding face bars, and flanges:

$$d/t \leq 0.5 (E/\sigma_y)^{1/2}$$
- Webs of built-up sections, angles, and tees;

$$d/t \leq 1.5 (E/\sigma_y)^{1/2}$$

or

$$d/t \leq 1.54 (E/\tau_y)^{1/2}$$

or

$$d/t \leq 1.15 (E/\tau_y)^{1/2} \text{ in areas subjected to slam pressures}$$
- Webs of bulb flats

$$d/t \leq 0.85 (E/\sigma_y)^{1/2}$$

where d and t are the depth and thickness of the member, and σ_y and τ_y are the yield strength of the unwelded aluminum in tension and in shear. The same equations are used for steel and aluminum. For higher strength steel with $\sigma_y = 350$ MPa and $E = 207 \times 10^3$ MPa, the limiting b/t for flanges is 12. For 5083-H116 aluminum with $\sigma_y = 215$ MPa and $E = 71 \times 10^3$ MPa, the limiting b/t for flanges is 9. Therefore, in general, the thickness of aluminum structural members should be about $12/9 = 4/3$ times thicker than an equivalent steel member.

When the in-plane (the web plane) buckling of stiffeners is considered, the shear deformation may affect buckling strength. For example, for a stiffener with the web height $h = 140$ mm and length $l = 2,000$ mm, and with the ratio of elastic modulus, E , to shear modulus, G , equal to 2.6, the shear flexibility factor is $\frac{1}{1 + (EI\pi^2/G\omega l^2)} = 0.923$, so that neglecting shear results in an 8 percent error on the non-conservative side. The usual rule to neglect shear effects in bending when $l/h \leq 10$ is not correct in assessment of buckling strength. When $l/h = 10$, the Euler stress overestimates elastic buckling stress 1.17 times. An example from testing is shown in Figure 3-7.

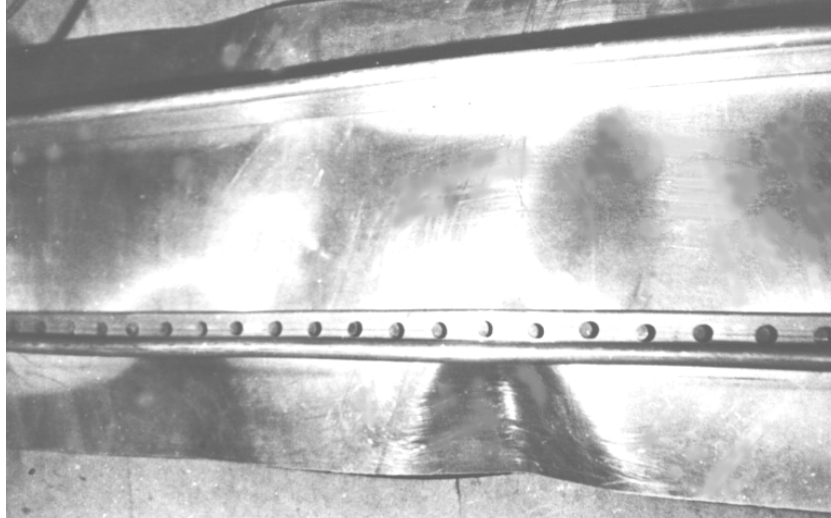


Figure 3-7 Buckling of a panel from shear in the stiffeners. (Courtesy of Sergei Petinov, St. Petersburg Polytechnic University)

3.5.5 Stability of Grillages

The above assessments of buckling strength looked at individual members and parts of individual members. However, the total strength of a structural assembly must be considered. This is particularly important when assessing the ultimate strength of the structure, the ultimate limit state. Local modes of failure may occur in stiffeners or plate panels, but other members take the load, and the failed members have a certain post-buckling strength.

An extensive testing program on stiffened aluminum plate panels for high-speed ships was undertaken by Paik et al. (2006) because there had been little such testing previously performed on aluminum structures. A total of 78 panels were tested to produce a systematic database to assess buckling collapse and the effect of initial imperfections on strength. Three collapse modes were observed: buckling of beam-columns, local buckling of stiffened webs, and lateral-torsional buckling of stiffeners.

3.6 Finite Element Analysis

For complex ship structures, analysis by the finite element method is a means of removing much uncertainty concerning load and stress distributions and boundary effects. Most classification societies and naval authorities now require such analysis for the design of all but the most routine vessels. However, finite element analysis doesn't answer all of the questions, and often poses many of its own.

With aluminum structure, the finite element modeling techniques should be essentially the same as those used for steel structure because the materials have similar Poisson ratios and the material constitutive equations behave in the same manner. Any guidance and rules of thumb learned from the analysis of steel structure is applicable to the finite element analysis of aluminum structure, including the use of substructuring techniques to analyze details of the entire ship structure.

In the analysis of stiffeners above, the concept of effective breadth of plating was discussed. However, this effect in all of its theoretical ramifications can only be modeled with a very fine mesh, large displacement elastic-plastic finite element analysis with many load steps. The same degree of refinement is necessary for buckling analysis, where a linear elastic buckling analysis that is available in many finite element analysis computer programs can seriously overestimate the strength of the structure.

Implementation of such refinement is impractical in the modeling of the entire ship, and even when analyzing small sections of the structure. The analyst is then faced with several choices. Submodeling techniques would enable modeling of the plate and offset stiffener with a very refined mesh. This detailed model of the stiffener could then be used as a super element, which in turn, can be implemented into the full structure model for a very accurate representation of the stiffener. However, a large deflection nonlinear analysis would still be required to accurately model membrane effects in plating subject to lateral loading. If stiffeners are modeled with only the plate that is considered effective in the local strength of the member, then cross-sectional area of the hull is deficient. Modeling the stiffeners with all of the plate effective, on the other hand, will overestimate their stiffness. Using the facilities of some finite element computer programs to offset the stiffeners from the plate by the height of their neutral axes is not a solution, because unless very fine mesh refinement, the effects of even linear elastic shear lag are not modeled. The essential problem is that for maximum stress effects, effective plate is limited, but for moderate loads, all of the plate is effective unless limited by shear lag. The preferred method of the author is to model all of the plating, but calculate the inertia of the stiffener as that with effective plate only.

3.7 Summary of Design

A review has been made of some of the aspects of design of aluminum ships, with the emphasis on high-speed craft. The review has not been exhaustive, but has provided some insight into various methods of design and analysis. Aluminum and steel are both metallic structures, and the mechanics of materials used for their analysis are different. There are significant differences in the material properties of the two materials, particularly in the elastic modulus, and that necessitates differences in design formulations.

Different methods of design exist, including the rules of classification societies and procedures of naval authorities. These methods give similar scantlings for the same vessel design, even though loads and allowable stress levels are different. The designer must not make the mistake of mixing the procedures by using the allowable stress levels from one procedure with the loads from another or other mixtures of procedures.

Equations exist for estimating design loads of most of the high-speed and unusual hull forms that characterize many aluminum vessels. Final design must be generally based on a more thorough analysis, either with data from at-sea tests on similar vessels, model tests, or from hydrodynamic analysis. Such methods have not been well validated and can easily lead to inconsistent results if similar vessels are designed using different methods, and even with the same method but by different persons. In the end, a very erudite analysis may have limited accuracy.

Aluminum does not have a pronounced yield point as does steel. That difference in behavior is not reflected in the various rules for design of plating under lateral pressure, particularly when the design is based on membrane action of plate and permanent set under extreme loads.

Design methods conservatively account for the reduced strength of the welds and HAZ of aluminum by using the lowest strength in design equations. A more accurate method of using an average weighted by mass of base and welded metal has been validated for compressive strength of welded panels, but not for structure in tension.

Chapter 4

Structural Details

4.1 Introduction

Structural details in aluminum are as varied as those found in steel vessel construction. A structural detail represents a solution to a structural problem, such as intersecting longitudinal stiffeners with transverse frames or bulkheads, providing access or drainage openings, or fitting a stanchion to support a deck. The same problems exist in steel and in aluminum construction, and frequently the same structural detail can be used in aluminum to solve the same structural problem that arises in steel construction, especially if the steel detail has low stress concentrations and a good fatigue life. Differences can arise because of increased sensitivity to fatigue for aluminum compared to steel, or for the need for joining dissimilar metals, such as attaching an aluminum deckhouse to a steel hull, especially if the steel detail has low stress concentrations and good fatigue life. Welding process used for aluminum generally preclude details that have little accessibility, although such details should be avoided in steel construction. Otherwise, details may be identical in steel and aluminum vessels.

The increased sensitivity of aluminum alloys to fatigue, to stress concentration [the fatigue notch factor may reach a value around 7 (Dolan, 1959)] should be a motivation for due selection of structural details. Separation of welds and shape discontinuities in structural details is recommended.

One advantage that aluminum has is greater through-thickness strength in plate because the flattened rolled-in inclusions that can occur in steel plate (other than the “Z” grades) do not occur in aluminum. Therefore, structural details in aluminum can take greater reliance on the strength of discontinuities in way of passing members, such as transverse frames or bulkheads.

There is no such thing as a poor structural detail, only poor applications of details. An example is an opening with square corners in a deck or structural member. Such a detail has high stress concentrations at the corners and should not be used in areas of even moderate stress. However, there are regions of the structure that see little stress in service, and such a structural detail is perfectly acceptable there if there are no other stresses, such as vibration.

Structural designers should be aware that not all structural details that are acceptable in smaller craft are suited for larger vessels. In craft generally less than 30 meters in length, longitudinal hull girder bending stresses are not significant, especially as far as causing fatigue problems. Also, the scantlings of smaller vessels are often dictated by minimum thickness considerations for fabrication and resistance to abuse, or for local stiffness, and stresses from local hydrodynamic loads are not always significant. Such vessels may have a very satisfactory service life, even though fabricated with poor structural details. Designers and builders should be aware that carrying forth detailing practices learned in smaller craft will not always be successful. In-service experience shows that the best details often have the fewest welds. Certainly for details such as beam brackets, rounding the change in slope where the bracket starts and removing all butt welds or chocks from this area are preferable, although more fit-up and bending of the bracket face plate are required.

Comparison of structural details can be made on several bases, such as ease of fabrication, degree of structural continuity, stress concentrations introduced, or fatigue strength. Fatigue strength ranking of details generally reflects the effect of stress concentrations, and so a ranking of different details can be made on the basis of predicted fatigue strength. In the following work, a variety of structural details were reviewed and a fatigue classification assigned in accordance with Eurocode 9. This code will be explained in greater detail in Chapter 9, but for the present, it is sufficient to note that the first number in the fatigue classification represents the stress range in MPa for a fatigue life of 2×10^6 cycles. Therefore, the higher the number, the better the detail.

4.2 Detail Classification

A comprehensive survey for the Ship Structure Committee of the structural details of 50 steel ships was completed in 1978 (Jordan and Cochran, 1978), and a follow-up survey of an additional 36 ships was completed in 1980 (Jordan and Knight, 1980), for a total of 86 ships surveyed. The following ship types and number of ships were surveyed:

- Bulk Carriers – 16
- Combination Carriers – 5
- Containerships – 24
- General Cargo Ships – 17
- Miscellaneous ships – 2
- Naval Ships – 9
- Tankers - 13

These ships are more representative of U.S.-built ships than those in the international fleet in terms of structural details. In particular, few of the ships had stiffeners that were bulb flats, a common practice in many countries except the U.S., where those steel shapes are not rolled. On these ships, a total of 607,584 details were examined, and they were classified into 12 families of details with a total of 634 distinct variations. In the SSC reports, structural failures in these details were reported. However, those evaluations are not necessarily relevant for aluminum design because the locations in which details were used and the stress levels in service were not generally reported. Jordan and Krumpfen (1990), in a later SSC report reviewed these details and assigned fatigue classifications to them. Similar classification will be done below for these details worked in aluminum.

Table 4-1 Steel Structural Detail Classifications (Jordan and Knight, 1980)

Detail Family Number	Detail Family	Number of Groups in Family	Number of Configurations in Family
1	Beam Brackets	12	145
2	Tripping Brackets	3	82
3	Non-tight Collars	3	49
4	Tight Collars	4	33
5	Gunwale Connections	2	21
6	Knife Edges	0	0
7	Miscellaneous Cutouts	8	72
8	Clearance Cutouts	5	39
9	Deck Cutouts	3	23
10	Stanchion Ends	3	94
11	Stiffener Ends	5	35
12	Panel Stiffeners	6	41
	Total	56	634

Although these details were taken from steel ships, they are nevertheless representative of the types of details that could be used design in aluminum. A factor that makes them less representative of aluminum design today is that they are taken from larger steel ships, whereas the aluminum vessels in service and being built today are smaller and generally of light-weight construction. Some of these details more typical of aluminum vessels will be discussed later. However, it is instructive to review the details used in steel ships and evaluate them for suitability of use in aluminum vessels. For that evaluation, they will be classified in accordance with the fatigue classifications of Eurocode 9. The higher the fatigue classification of a detail, the better suited it is for use in aluminum hull structure. Comments will also be made on their suitability for use in aluminum construction. There are other details that are unique to aluminum structure, and they will be discussed afterwards.

The Eurocode 9 classifications given in the following figures are generalizations based on the overall geometry. Where there is uncertainty as to the fatigue strength of a detail, and where unusual details are used, Eurocode 9 provides guidance for conducting a detailed finite element analysis using the hot-spot stress approach.

4.2.1 Beam Brackets

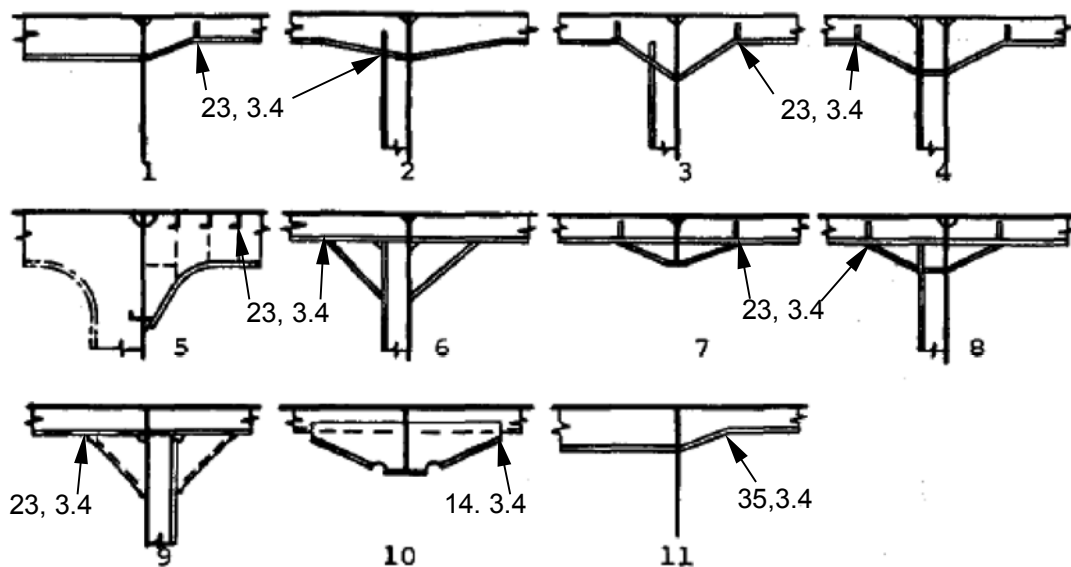
A variety of structural details are contained in this category. In general, they provide a transition from one frame or beam to another.

4.2.1.1 Longitudinal Members

The details shown can be either continuous or intercostal at the passing member, which is can be a transverse bulkhead or a deeper girder. When they are intercostal at the passing member, they form a cruciform joint, which has the classification 35, 3.4. Eurocode 9 does not have a classification for continuous members, but it should be the same or even higher than the cruciform joint. However, several of the details contain a web chock, which has a classification

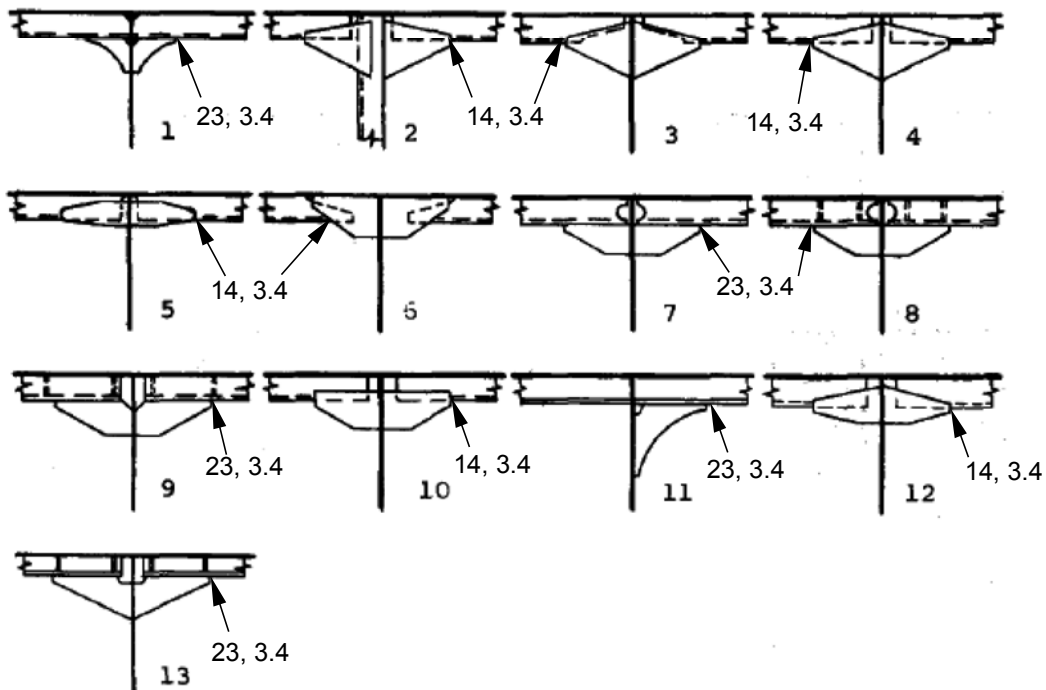
of 23, 3.4, and thus are classified for reduced fatigue strength. This demonstrates a deficiency in the Eurocode 9, because chocks generally reduce stress concentrations at hard points such as a change in direction of a flange, and therefore improve fatigue life. The difficulty comes from comparing details such as detail 1 and detail 11, where the angle formed by the butt weld in the flange caused a stress concentration. Adding the chock decreases the nominal fatigue classification, although it should be increasing it. The Eurocode 9 does not cover such a joint, which should have less fatigue strength as the angle increases. Adding a weld at a change of geometry is sometimes questionable, and must be compensated for by a reduction in stress concentration.

All of these details show good transition and may be used with confidence in aluminum structure. Detail 10 has a reduced classification because of the lap joint. However, this lap produces a local reduction in stress, which should be accounted for in determining fatigue life.



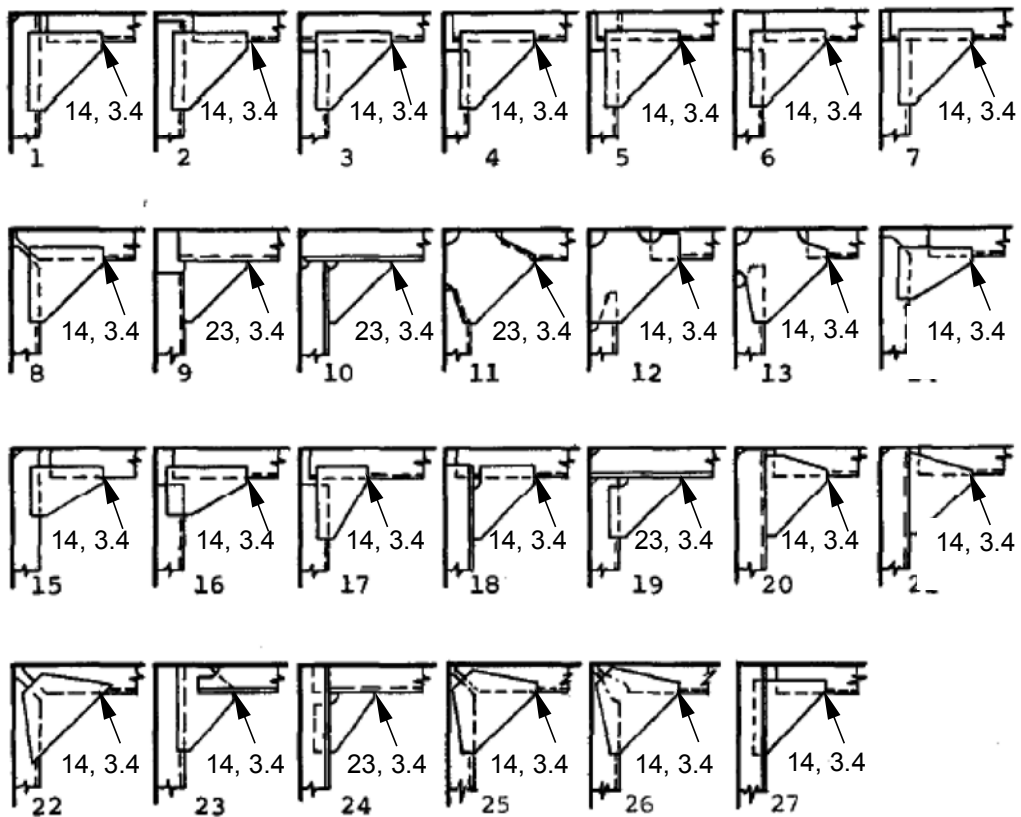
4.2.1.2 Discontinuous Longitudinal Members

These members use brackets to provide transition through passing members, a practice that is common in the design of smaller aluminum vessels to avoid the labor of watertight collars in transverse bulkheads. The brackets are generally made continuous through the bulkhead, but this is still considered as a cruciform weld with a classification of 35, 3.4. The welds to the brackets are either 23, 3.4 if the joint is a longitudinal fillet weld, or 14, 3.4 if it is a lap joint. These details may be suitable for smaller aluminum craft but should not be used in larger vessels where longitudinal hull girder bending stress is significant.



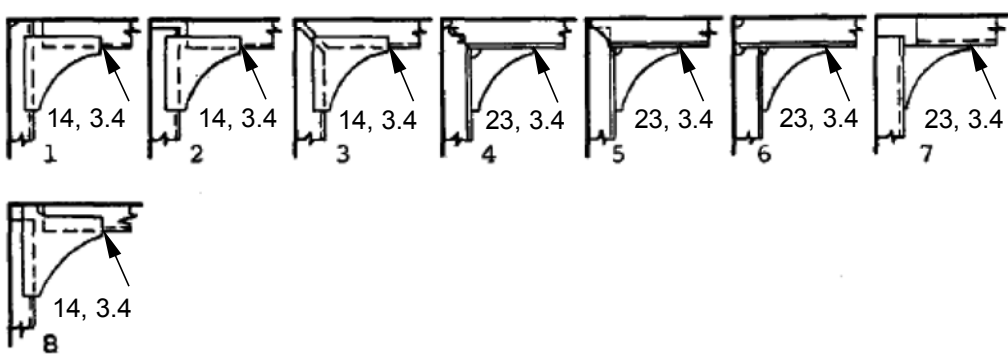
4.2.1.3 Unstiffened Corner Brackets

These brackets are used to join a transverse deck beam to a side frame. In most instances, where a lap joint is used, these can only be used where the member is an angle or a flanged plate. Details 1 through 8, 12 through 17, 22 and 23, and 25 through 27 are similar in that they join two members that are either angles, flanged plate, or possibly, bulb plate. The remainder are variations in which one or both of the members being joined are tees. None of these brackets, as shown, have stiffening on the bracket. If these were longitudinal members, they would receive the fatigue designation 14, 34 for lap joints. These details should not be used in aluminum construction where the beams or frames are subject to relatively high alternating stress. For smaller craft, they may be acceptable if the members are designed for stiffness and not for strength.



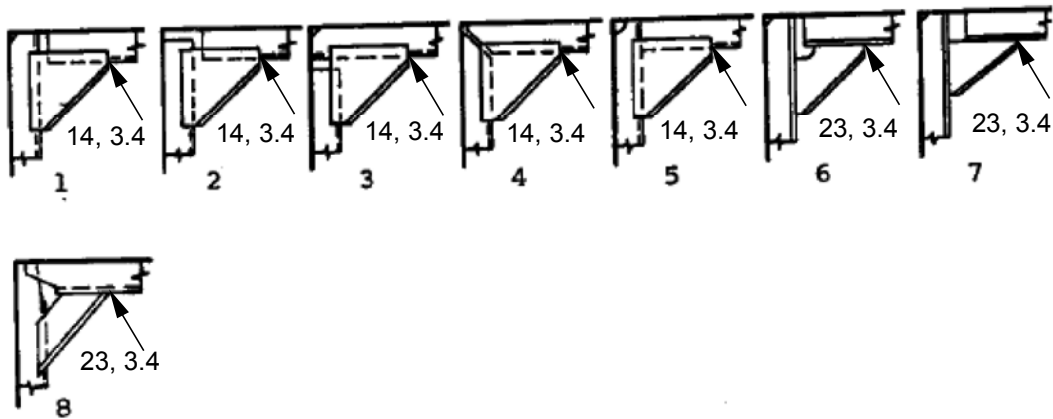
4.2.1.4 Curved corner brackets

These brackets differ from the previous only in that they have a radius, which reduces the tendency of the bracket to buckle.



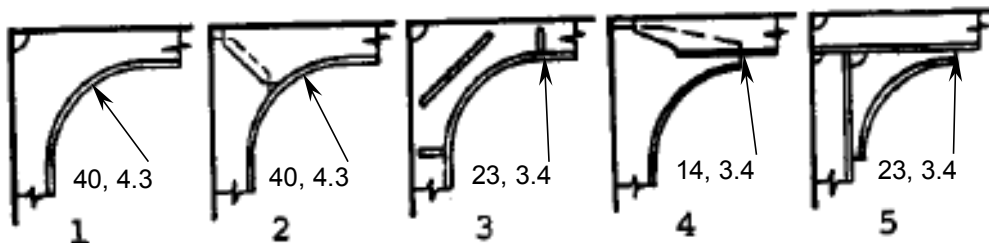
4.2.1.5 Stiffened Corner Brackets

These brackets are similar to those in the two groups above except that the bracket has been stiffened to prevent buckling. The stiffening may be done by flanging the plate or welding a flat bar on or near the edge. These details are not well suited for the structure of aluminum vessels where the frames are subject to high stress.



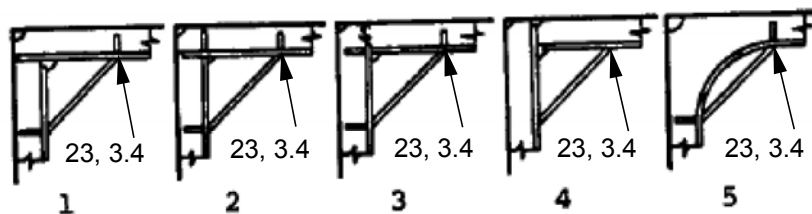
4.2.1.6 Continuous Curved Corner Brackets

Brackets 1 through 3 represent low stress concentration and high fatigue strength in the welds. Although bracket 2 incorporates a lap joint, it is in an area of lower stress and should not reduce either overall or fatigue strength. These details should be rated as 40, 4.3, continuous longitudinal fillet welds. Bracket 4 incorporates a lap joint, and is reduced to a 14, 3.4 rating, and bracket 5, with an end bracket has a 23, 3.4 rating. Detail 3 has the lower Eurocode 9 classification because of the chock.



4.2.1.6 Miscellaneous Corner Brackets

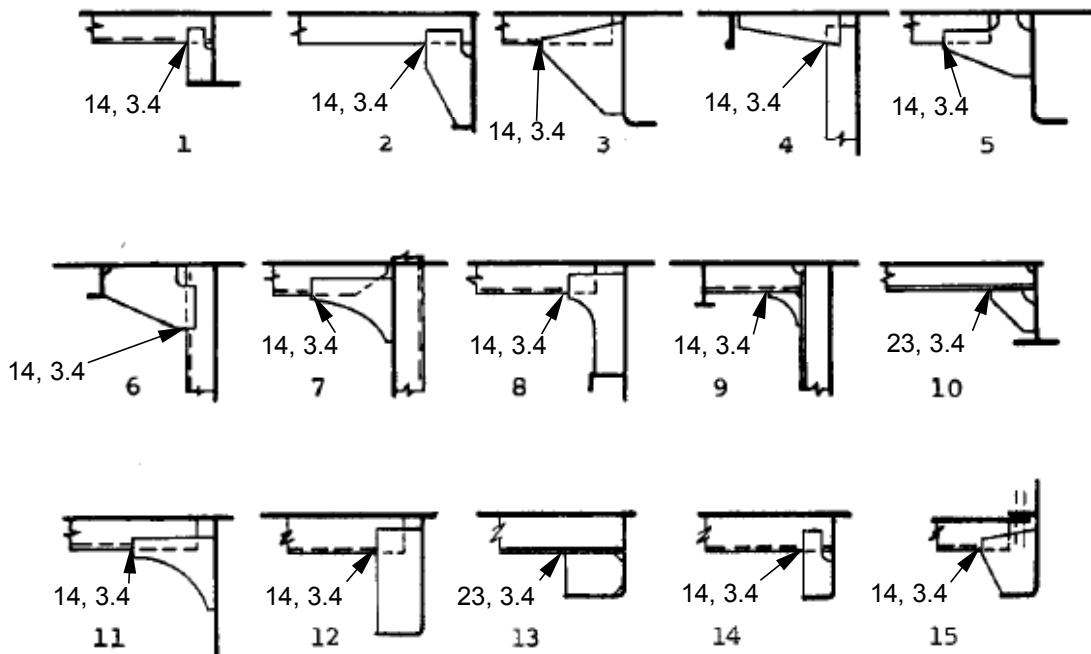
These brackets have been added to fitted intersections of members to reduce stress at the joint and are typical of aluminum warship deckhouse construction. They can be used with confidence in aluminum structure. However, they receive a Eurocode 9 classification of 23, 3.4 because of the web chocks, which, as discussed above, reduce stress at the joints.



Aluminum Marine Structure Guide

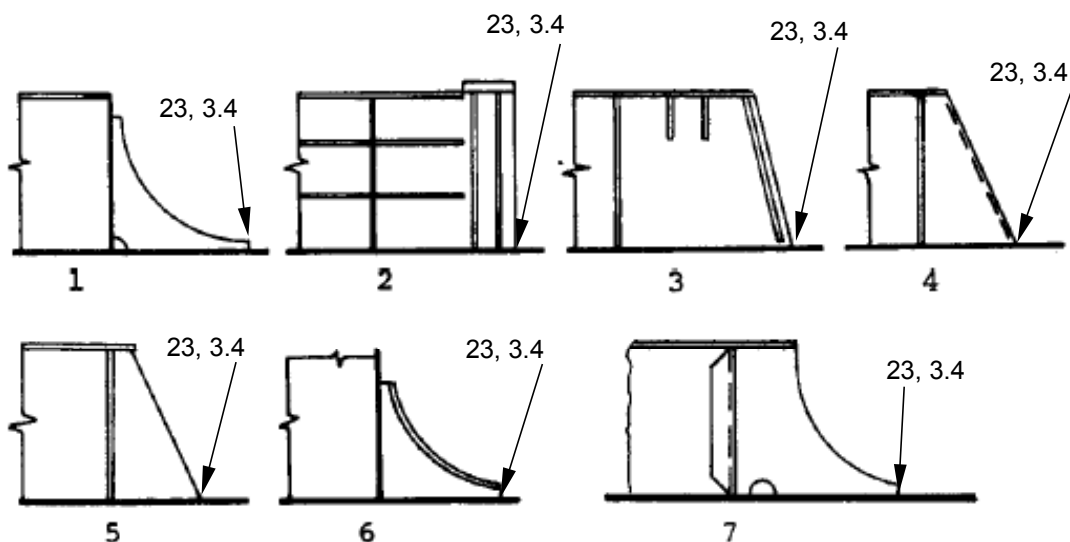
4.2.1.7 End Brackets

These brackets are used to terminate transverse and longitudinal deck girders, except for details 4 and 6, which are termination at a deck of a vertical stiffener on a longitudinal bulkhead.



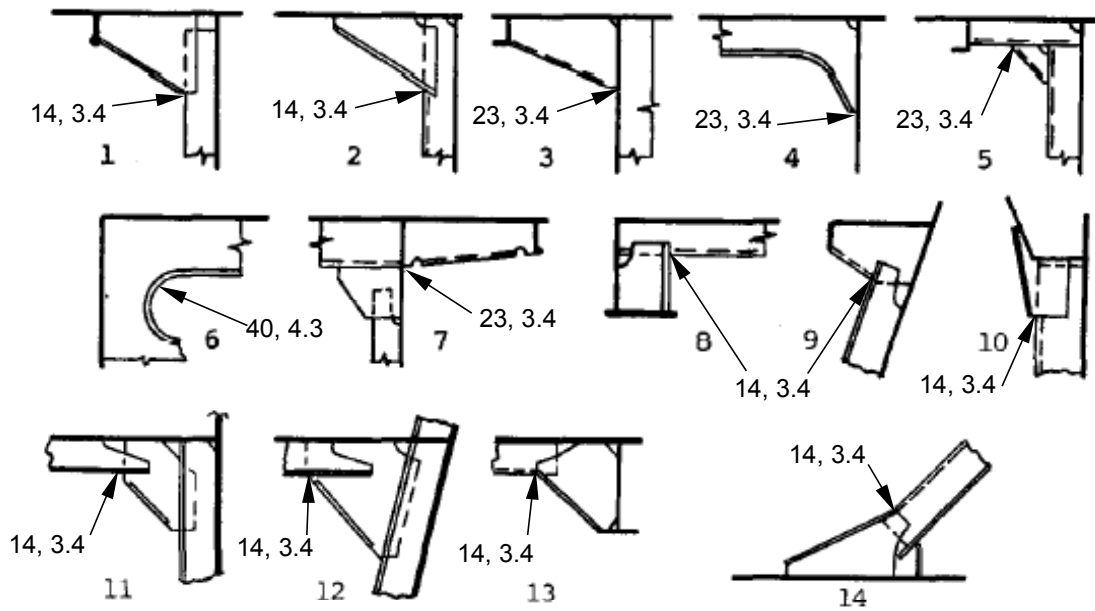
4.2.1.8 Girder End Brackets

These brackets are used to terminate heavy girders without transition into a longitudinal stiffener. This is an abrupt change in stiffness, which could be a point of fatigue crack initiation.



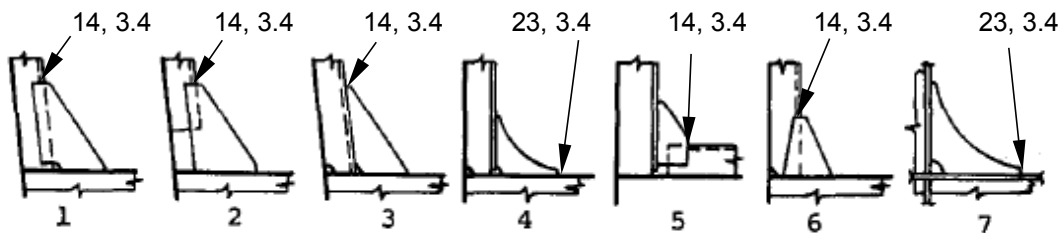
4.2.1.9 End Brackets

These brackets are similar to those in 4.2.1.7, terminating transverse and longitudinal deck girders, except for details 1, 2, and 5, which are termination at a deck of a vertical stiffener on a longitudinal bulkhead.



4.2.1.10 Side Frame Transition Brackets

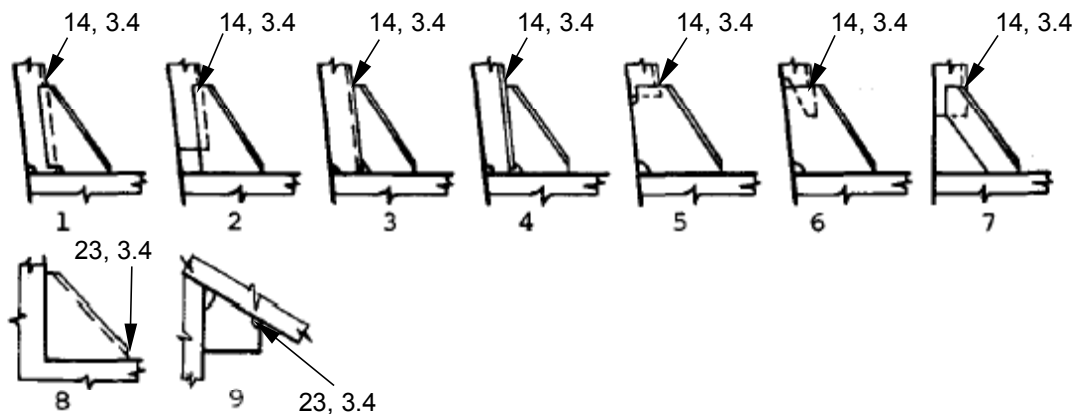
These brackets are used in transversely framed ships to end a side frame at a deck that is framed below.



4.2.1.11 Frame Transition Brackets

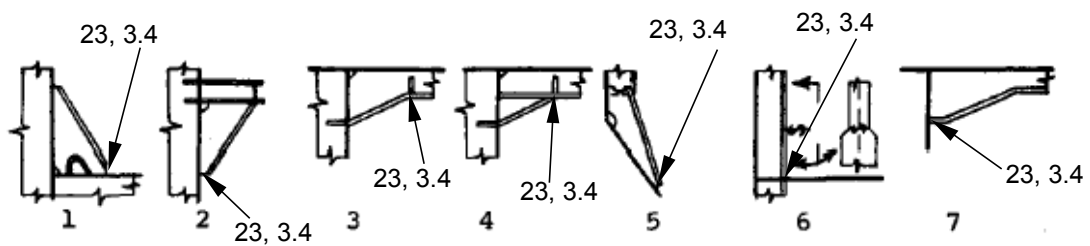
These brackets are similar to those above.

Aluminum Marine Structure Guide



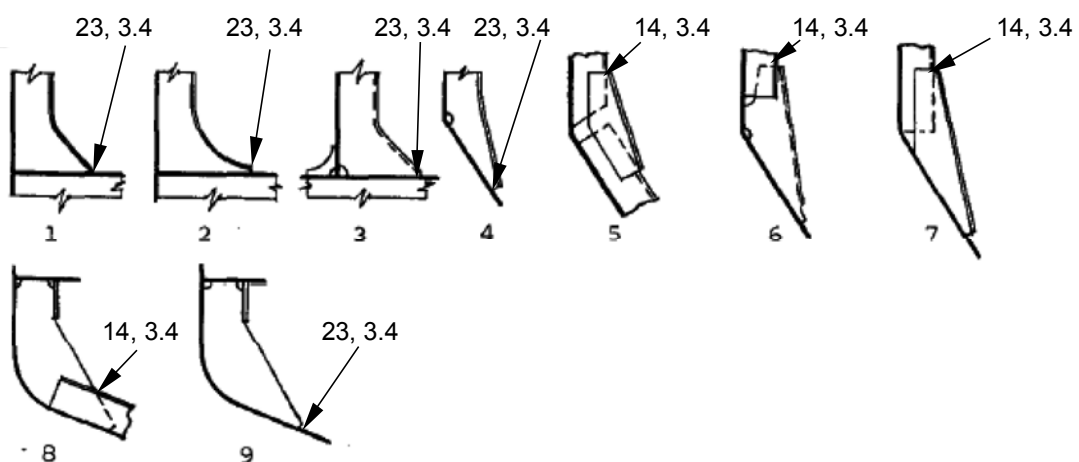
4.2.1.12 Miscellaneous Transition Brackets

These brackets form various types of transitions between members or ending a member.



4.2.1.13 Transition Brackets

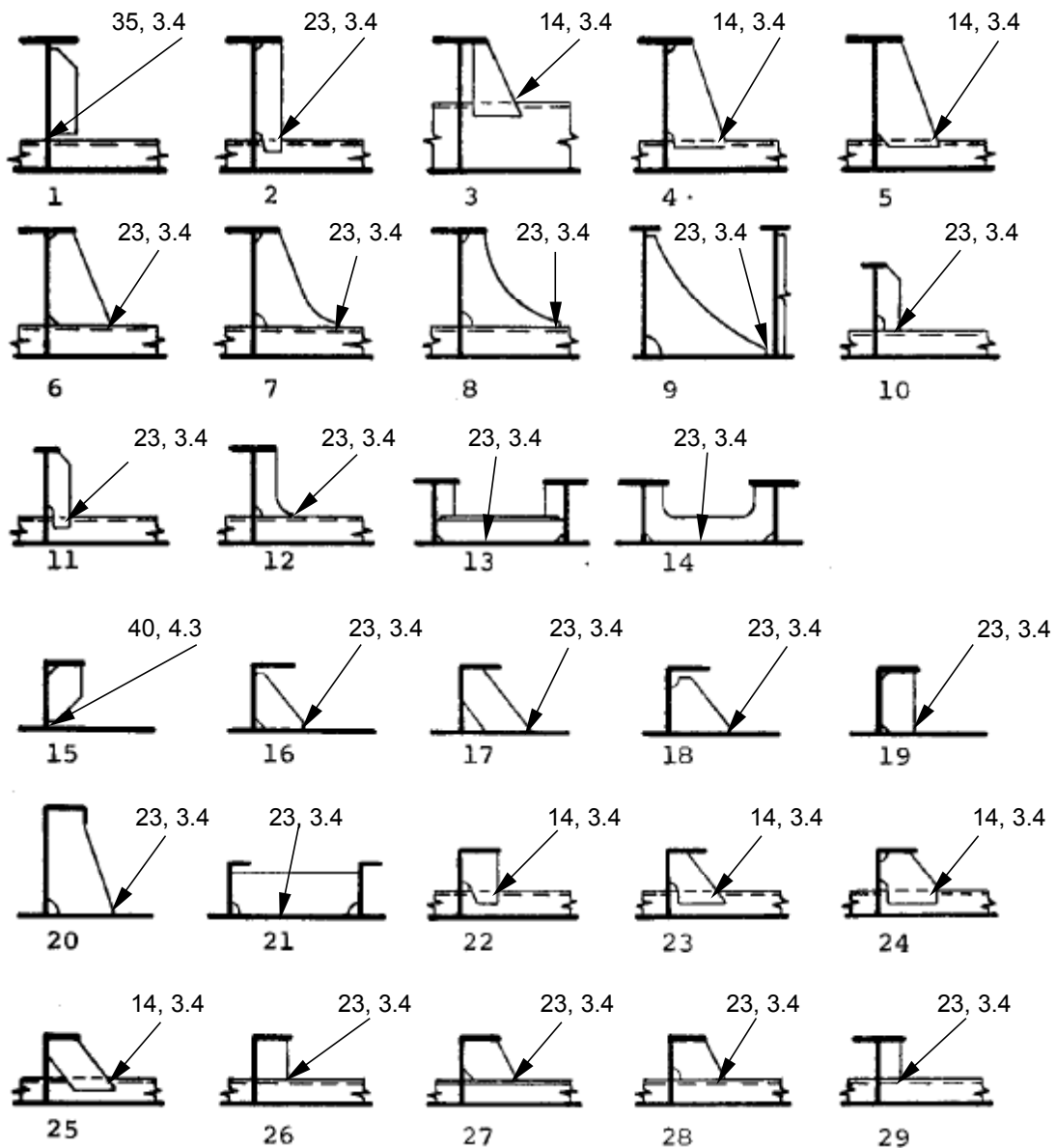
These brackets are generally used at the turn of bilge or at a chine.



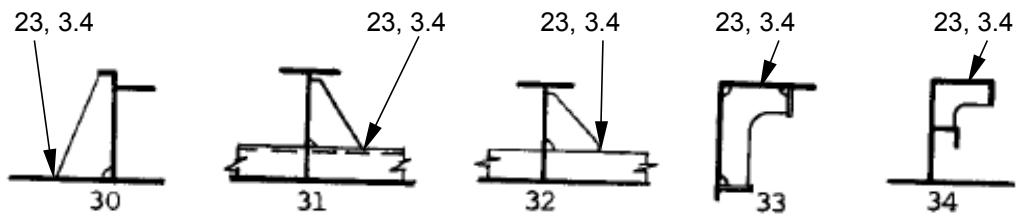
4.2.2 Tripping Brackets

This family of structural details is called tripping brackets because brackets of this type are used to provide torsional stability for longitudinal stiffeners. However, they have a greater use—providing support for a longitudinal stiffener at a transverse frame. They also serve to stiffen the web of the transverse to prevent its buckling.

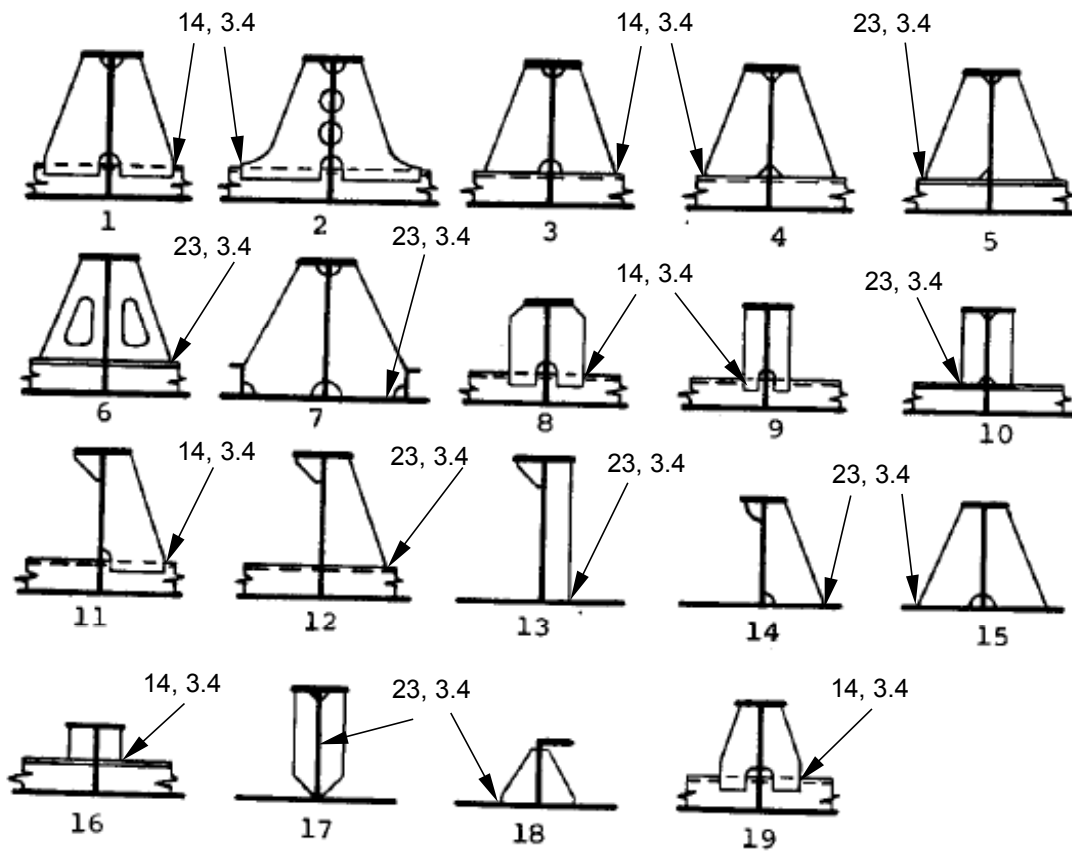
4.2.2.1 Tripping Bracket Group A



Aluminum Marine Structure Guide

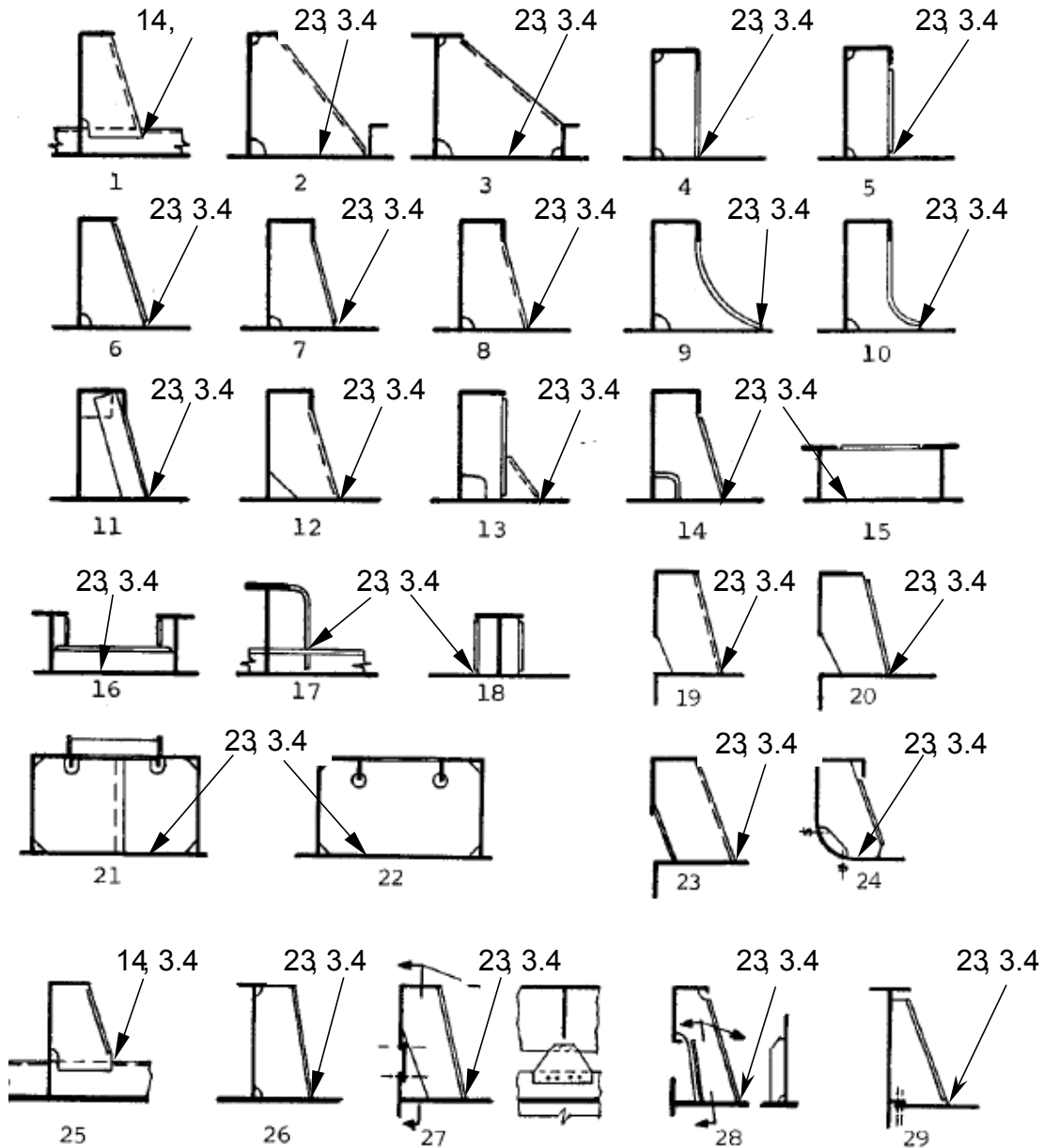


4.2.2.2 Tripping Bracket Group B



4.2.2.3 Tripping Bracket Group C

Sufficient refinement of details is not provided within the standard details of Eurocode 9 to distinguish between differences such as shown in details 10 and 11, although detail 10 should have a lower stressconcentration and better fatigue life than detail 11.

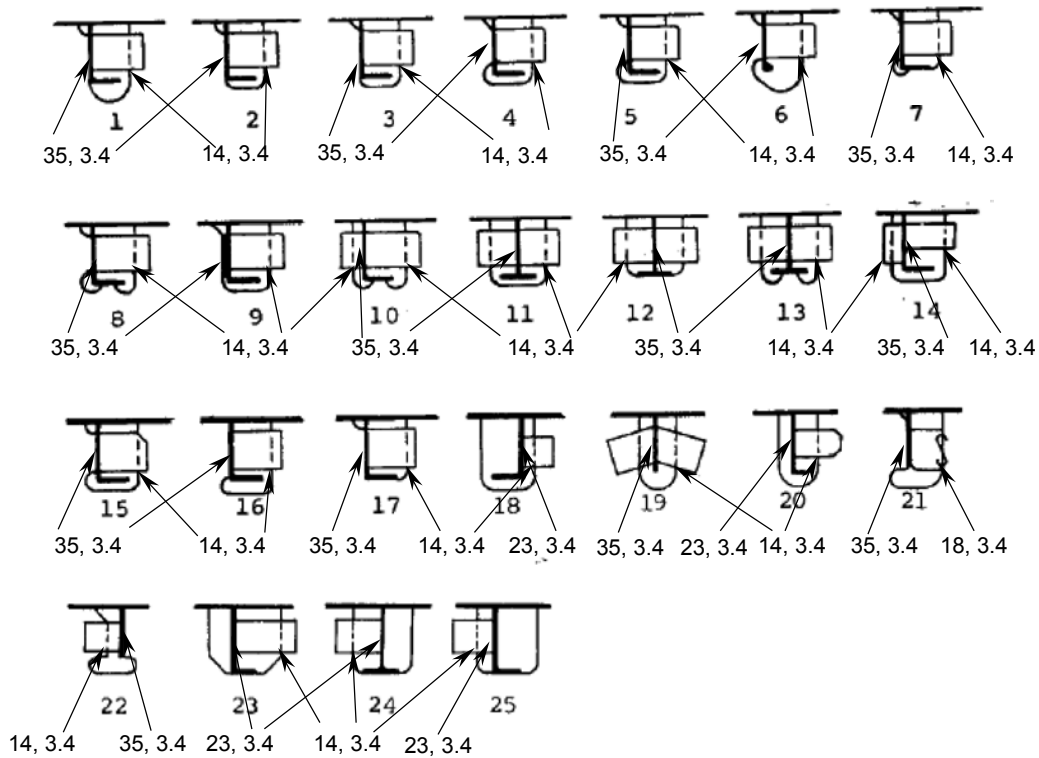


4.2.3 Nontight Collars

Collars are used where a longitudinal stiffener passes through a transverse frame of nontight bulkhead. They serve to transfer the shear force in the webs of the longitudinals into the web of the transverse. If so designed, they compensate for loss of shear strength in the transverse frame that is caused by the cutout for the longitudinal. They can also support the

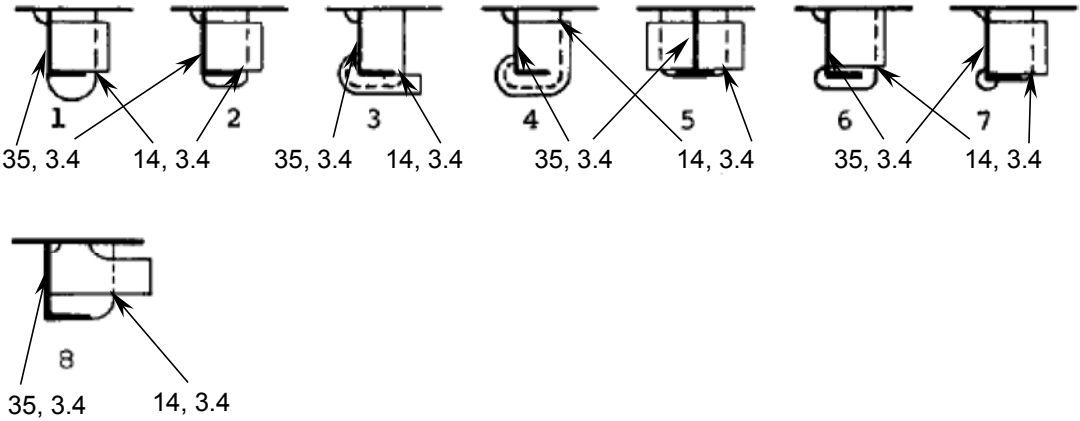
plating if high local loading in the plating could cause a local failure where the transverse frame is cut out.

4.2.3.1 Nontight Collars Group A



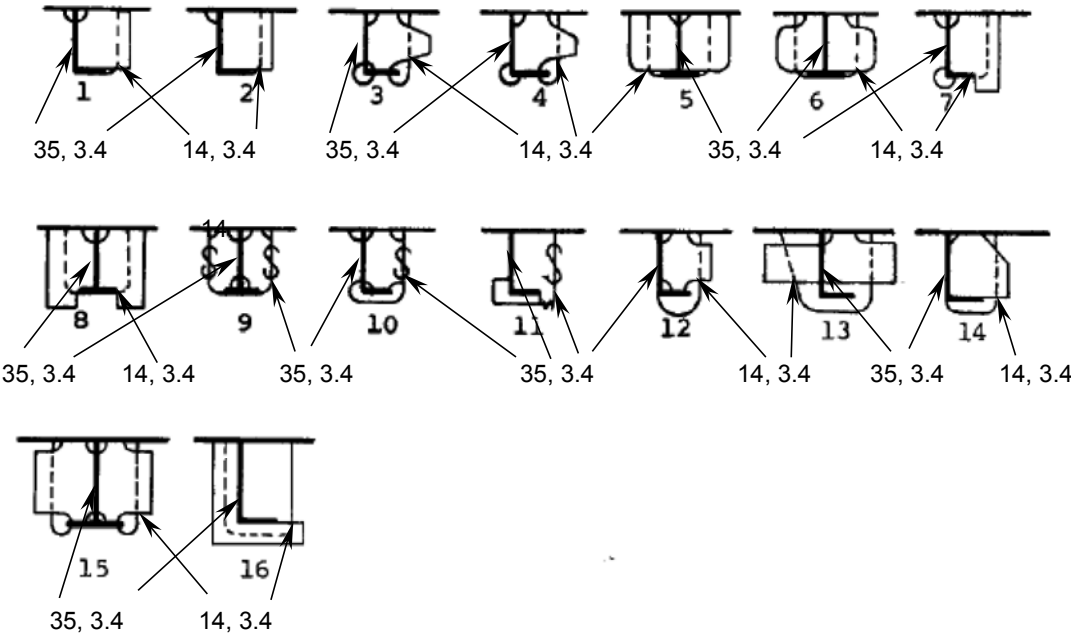
All of these collars, except for detail 21, have lap joints between the web of the transverse member and the collar plate. Therefore, for shear stress in the plane of the transverse web, they have fatigue classification 14, 3.4. Detail 21 has the classification 18, 3.4 for an attachment on edge, the standard detail that is closest to this configuration. For longitudinal hull girder bending stress in the direction of the longitudinal stiffener, they should have the classification 35, 3.4 or greater for a cruciform joint with stress in the continuous direction. However, details 18, 20, 23, 24, and 24 have the classification 23, 3.4 for a web chock. This may be too severe a downgrade, and testing of this configuration should be conducted to determine better the fatigue classification.

4.2.3.2 Nontight Collars Group B



Similar to the details in 4.3.3.1, these should have the classification 14, 3.4 in the plane of the transverse, and 35, 3.4 or greater in the longitudinal direction.

4.2.3.3 Nontight Collars Group C

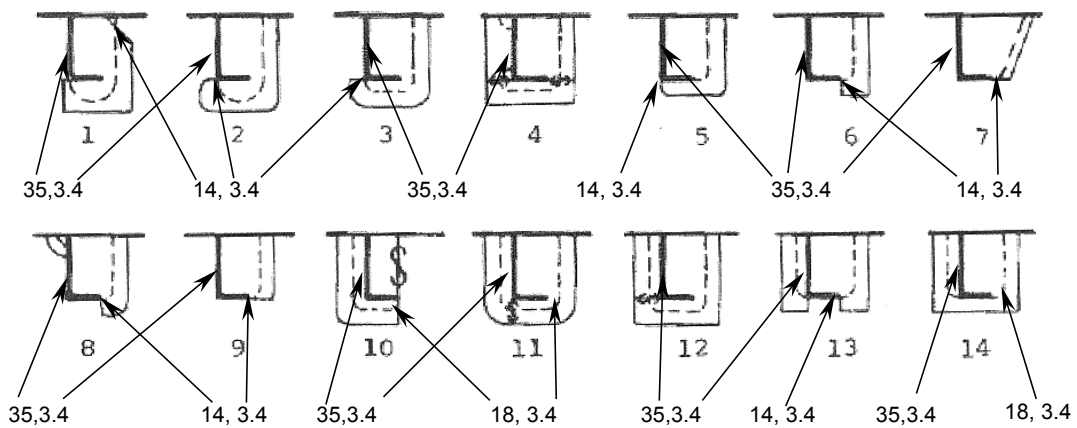


Similar to the details in 4.3.3.1, these should have the classification 14, 3.4 in the plane of the transverse because of the lap joints, and 35, 3.4 or greater in the longitudinal direction.

4.2.4 Tight Collars

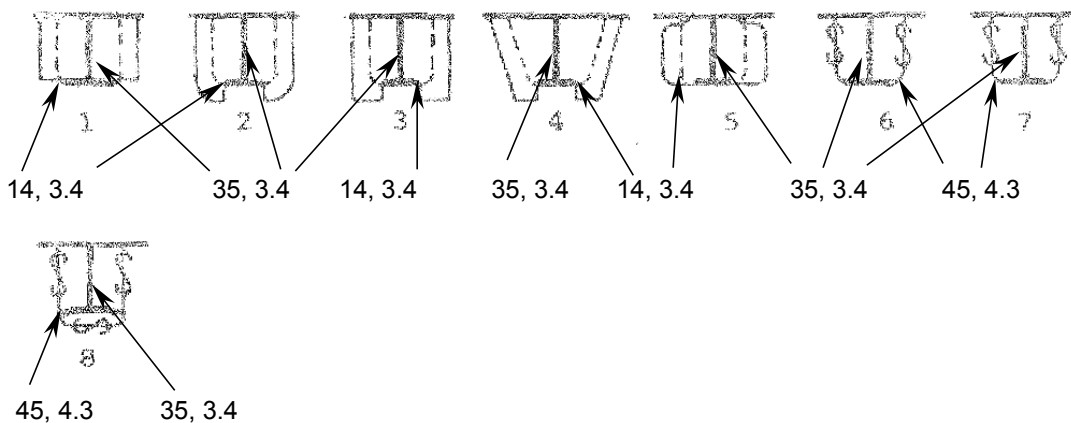
The primary purpose of tight collars is to make the transition of a stiffener through a bulkhead watertight or oiltight. They also can perform the functions of a nontight collar listed above.

4.2.4.1 Tight Collars Group A



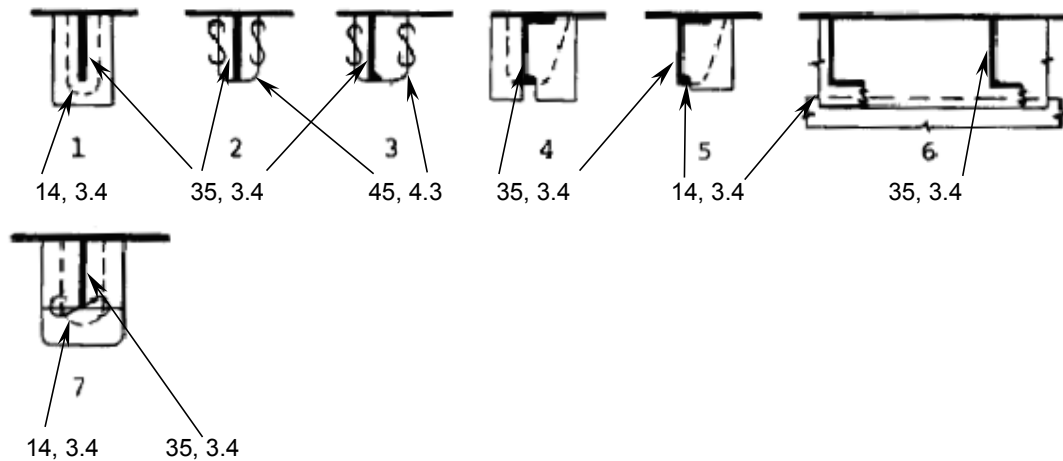
Similar to the details in 3.3.3.1, these should have the classification 14, 3.4 in the plane of the transverse because of the lap joints, and 35, 3.4 or greater in the longitudinal direction.

4.2.4.2 Tight Collars Group B



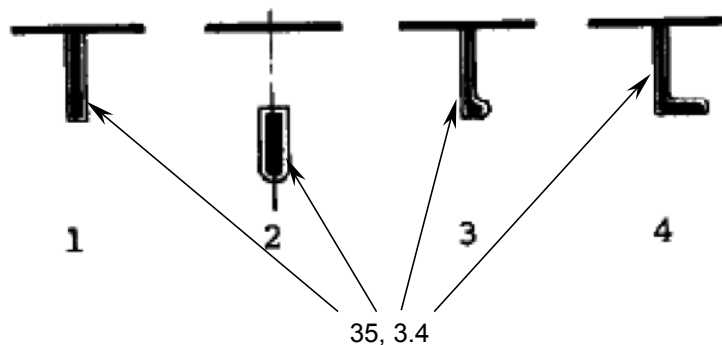
Similar to the details in 4.3.3.1, details 1 though 5 should have the classification 14, 3.4 in the plane of the transverse because of the lap joints, but details 6 through 8 should have the classification 45, 4.3 in the transverse plane. All of these should be classified as 35, 3.4 or greater in the longitudinal direction.

4.2.4.3 Tight Collars Group C



All of these details, except 2 and 3, should have the classification 14, 3.4 in the plane of the transverse because of the lap joints. Details 2 and 3 should have the classification 45, 4.3 in the transverse plane. All of these should be classified as 35, 3.4 or greater in the longitudinal direction.

4.2.4.3 Tight Collars Group D



This group are not truly collars but are a way of passing a stiffener through a bulkhead by cutting an opening in the bulkhead a little larger than the stiffener, and then threading the stiffener through the opening. Although not shown, this type of detail can be used for a tee stiffener or for any other shape. Detail 2 is a variation in which a bracket is passed through the bulkhead, providing longitudinal continuity through the bulkhead, though not in the stiffener.

This type of detail is also used at transverse frames, especially on flat panels where the stiffener can be threaded through a series of transverse frames. This works well for stick construction, where the stiffeners and frames are laid up and welded before the plate is welded

on. If the stiffeners are welded to the plating first, extremely close tolerances in locating and welding stiffeners as well as cutting out the openings is required, and for this type of construction, the transverse frames are threaded over the plate-stiffener panels.

Details 1, 3 and 4, and tee-stiffeners and other variations offer the advantage of reduced labor if dimensional tolerances can be met, because the work of fitting collars is eliminated. These details have no inherent stress concentrations and should be classified as cruciform joints, 35, 3.4. The fatigue classification of detail 2 depends on the design of the bracket to the longitudinal stiffener, as discussed in section 4.2.1.

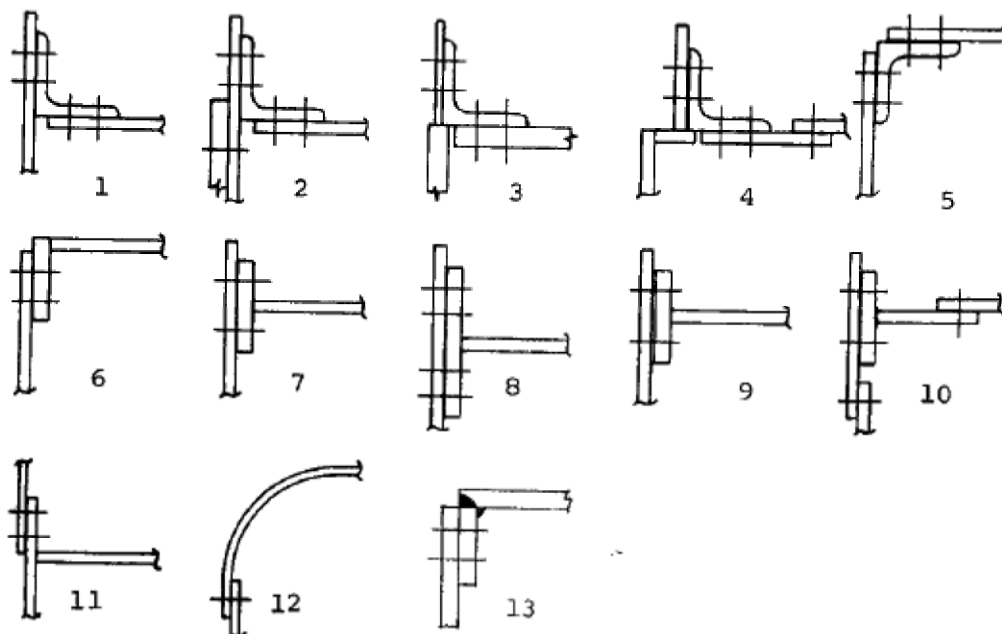
4.2.5 Gunwale Connection Details

The gunwale connection is a critical joint in a ship because it is an area of high stress from longitudinal and transverse hull girder bending, as well as high shear loads. It is often a point of crack initiation in ships that has sometimes led to hull girder failure and is therefore subject to special scrutiny in steel ships, and either riveted construction or fabrication with higher-toughness steel is required.

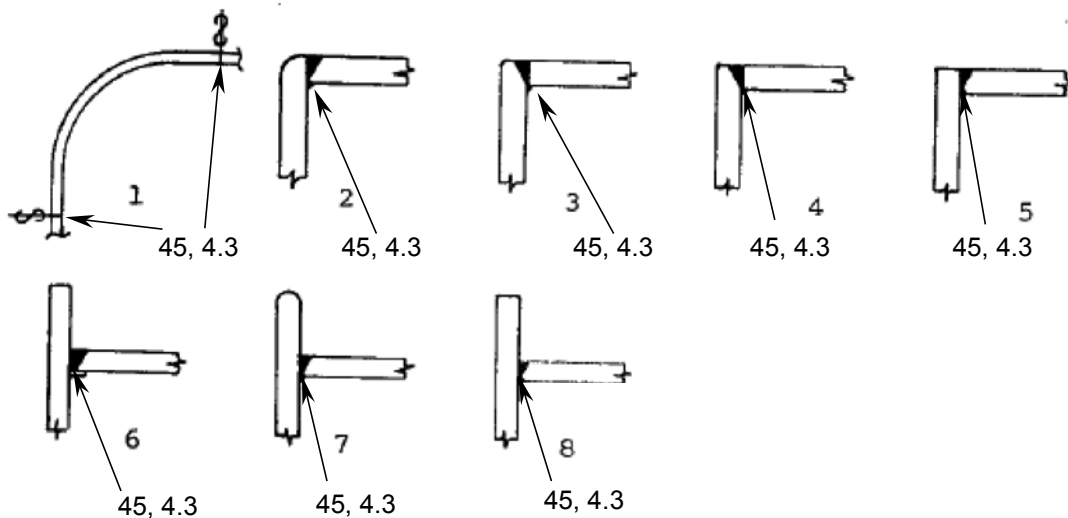
In aluminum vessels, the same historical degree of concern for crack initiation at the gunwale does not exist, primarily because aluminum plate is not subject to brittleness that can occur in some steel plate alloys. However, because the gunwale is an area of high stress, care should be shown in the design and fabrication of this area of the hull structure.

4.2.5.1 Riveted Gunwale Connection

Because of the labor involved, riveted connections are seldom used today in either steel or aluminum construction. See chapter 6 for information on fatigue of riveted joints.



4.2.5.2 Welded Gunwale Connection



These details represent some of the possible methods of forming this critical joint. They can all be classified as 45, 4.3 for a full penetration butt weld in the longitudinal direction.

4.2.6 Miscellaneous Opening Details

Openings are made in structural members for a variety of reasons, ranging from a penetration for passing electrical wires to a large hatch opening. These openings represent stress concentrations that often can be points of crack initiation. Although generally minor in nature in terms of overall structural design, their large numbers and potential for harm require that planning be given to their placement and design. This planning should include an overall plan for penetration placement, size and shape, method of cutting, and method of reinforcement.

- Penetration placement. There are certain areas of the hull that are highly stressed and in which no openings should be cut without careful engineering analysis. This can include the gunwale region, major machinery foundations, and other high-stresses areas inherent to a particular design.
- Size and shape. Several small holes placed near each other can cause as large a stress concentration as one larger opening, so consideration should be given to combining openings. Round openings have less stress concentration than square openings, and the larger dimension of an opening should be aligned with the direction of major stress.
- Method of cutting. Machine cutting by plasma arc produces a smoother edge than hand cutting with a saw, although the Eurocode 9 does not differentiate between different types of edges. If openings are planned in advance, they can be cut out when plate is being cut, saving time in fabrication.
- Method of reinforcement. Reinforcement may be required to compensate for the cross-sectional area of a strength deck that is lost by an opening. A plate panel may have its stiffening system disrupted by the opening, and a new system must be added. The opening may present too high a stress concentration, and reinforcement will be necessary to reduce stress. These are all reasons for adding reinforcement, some methods of which will be shown in the details below.

For evaluation of fatigue, cutouts and other openings fall into two categories, unreinforced and reinforced. An unreinforced opening should be regarded as the edge of a plate of base metal. Reinforcing of an opening is achieved by welding a flat bar around the inside of the opening, using a fillet weld.

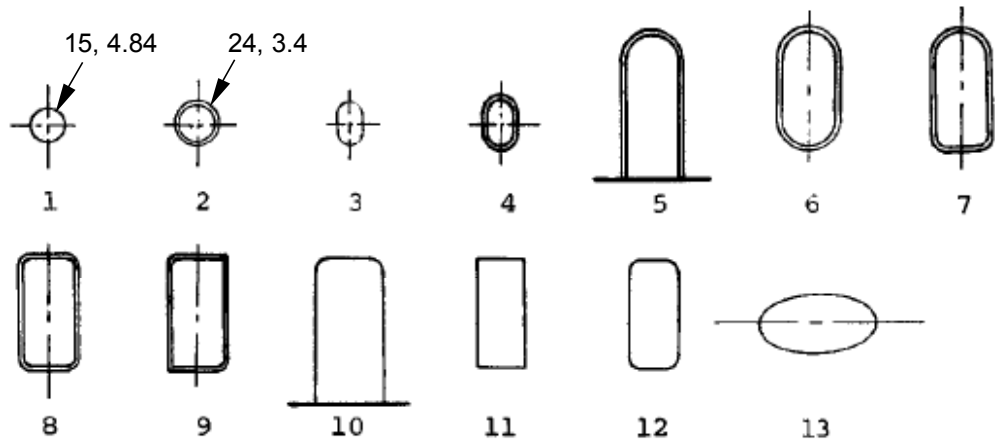
There is no classification in Eurocode 9 for edges of plate other than for machined edges or edges ground in the direction of the stress. Openings in aluminum marine structures are generally cut with either numerically controlled plasma arc cutting or cut by hand using a saw. The first method leaves a slightly better edge than the saw-cut edge, but both are rarely ground smooth. In the fatigue guidance of the Aluminum Design Manual (Aluminum Association, 2005), an edge that is not smooth can be considered as a Category B detail, with a fatigue life of 45 MPa at 2×10^6 cycles and a slope of 4.84. To use this classification with a cutout, the stress concentration of the cutout must be calculated, and the fatigue classification determined by dividing the stress range of 45 MPa by that stress concentration factor. A method for calculating stress concentration factors at openings is given in Sieve et al. (2000). If the edge of a circular hole is more than four times its diameter from the edge of the deck or any other major opening, the stress concentration factor is 3.0. The fatigue classification for such a hole would therefore be $45 / 3 = 15$, 4.84.

Eurocode 9 has no classification for a reinforcing ring around a hole. The maximum stress concentration at an opening occurs at the edges that are opposite from the direction of maximum stress, so the fillet weld for the ring is in the same direction as the stress. Therefore, the detail may be considered as the edge of a fillet weld in the direction of maximum stress, receiving the classification 40, 3.4. To apply this classification, the stress concentration for the hole should be calculated, and then the reduction in stress due to the reinforcement should be calculated. A method for doing this calculation is given in Sieve et al. (2000). A reinforcing ring the same thickness as the plate with a width seven times the plate thickness will reduce the stress by a factor of 0.55. If the hole has a stress concentration factor of 3.0, the reinforced hole would have a classification stress of $40 / (3 \times 0.55) = 24$, 3.4.

4.2.6.1 Openings

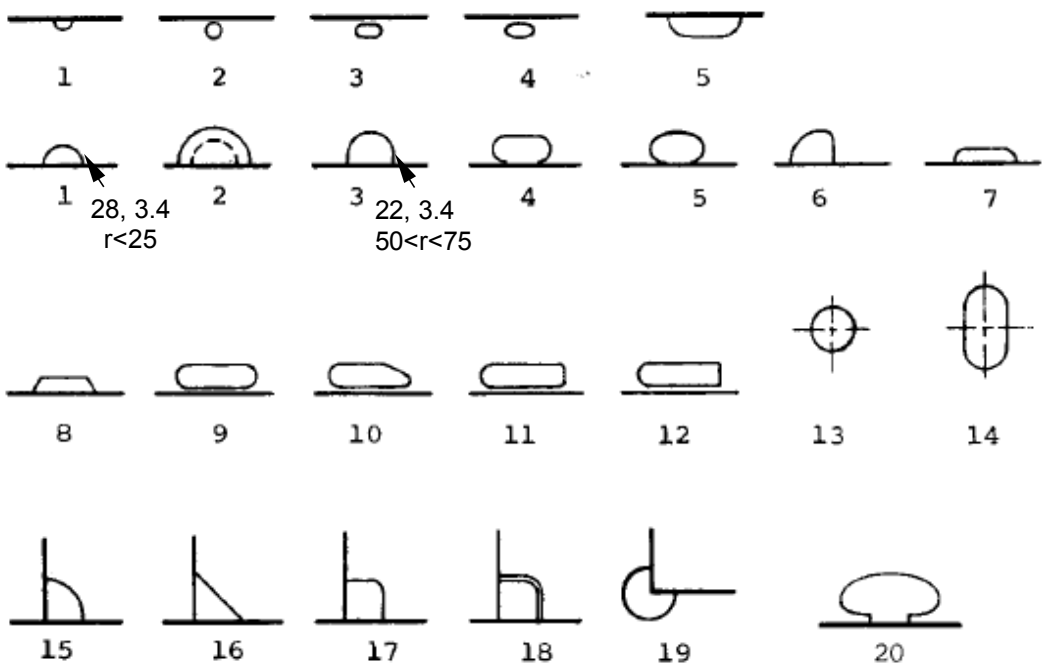
This group includes a variety of openings, reinforced and unreinforced. For example, detail 10 is an access opening in the longitudinal bulkhead of a general cargo ship, and detail 5 is a variation of that type of opening with reinforcement to reduce stress and increase stiffness. A simple opening such as detail 1, following the reasoning above, would have a Eurocode classification 15, 4.84, and a reinforced opening of detail 2 would have the classification 24, 3.4.

The remaining details in this group have not been assigned fatigue classifications, as the stress concentration factor has to be calculated for the specific geometry, using guidance such as (Sieve, et al., 2000).

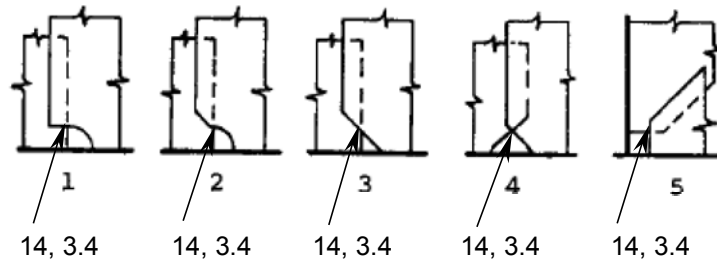


4.2.6.2 Rat Holes

Rat holes, mouse holes, or cope holes serve to provide drainage and to provide clearance over a butt weld. Eurocode 9 Classifies a circular cope hole with a radius of 25 mm or less as 28, 3.4 but provides no further guidance. Sieve, et al. (2000) classify a rat hole in steel with a radius of 2 inches (50 mm) or less as ASSHTO Class D, which has a fatigue stress range of 10.26 ksi (70.8 MPa) at 2×10^6 cycles, and if the radius is between 2 and 3 inches (75 mm) as ASSHTO Class E, with a stress range of 8.12 ksi (56.0 MPa) at 2×10^6 cycles, a reduction of 79 percent. Therefore, a rat hole with a radius between 50 and 75 mm should have a classification of $28 \times 0.79 = 22, 3.4$.

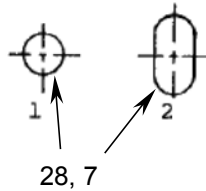


4.2.6.3 Openings at lap joints



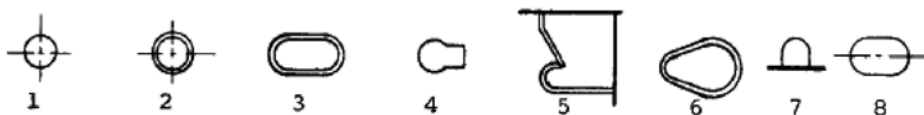
This is a convenient way to maintain an opening if a lap joint is used at a structural detail. All should be classified as 14, 3.4 for the lap joint.

4.2.6.4 Lightening holes



Aluminum vessels tend to be weight-critical, and any reduction in structural weight is helpful. Therefore, lightening holes are often seen in aluminum hull structure. These holes are generally circular, although they may also be oblong. If they are machine-cut in 5083-H116, they should have the classification of 39, 7, and 28, 7 if saw cut.

4.2.6.5 Pipeways



These are variations on the openings described in 4.2.6.1, and should be classified similarly.

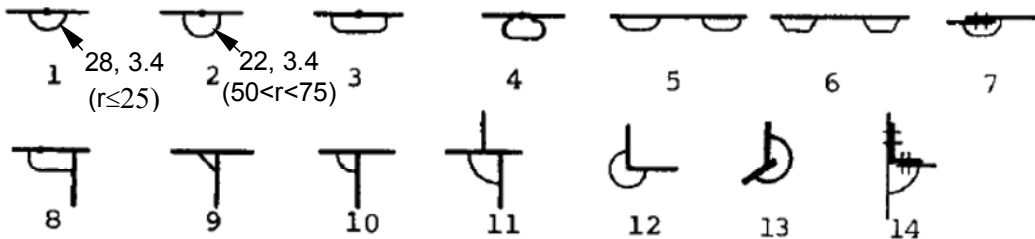
4.2.6.6 Wireways



These are also variations on the openings described in 4.2.6.1, and should be classified similarly.

4.2.6.7 Weld Clearance

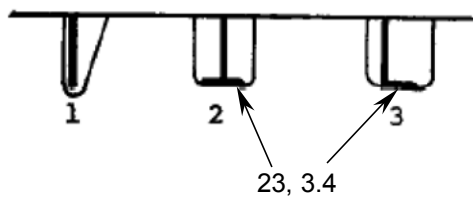
These are similar to the openings discussed in 4.2.6.2. An opening with a radius of 25 mm or less is classified as 28, 3.4, and as 22, 3.4 if the radius is between 50 and 75 mm.



4.2.7 Miscellaneous Cutout Details

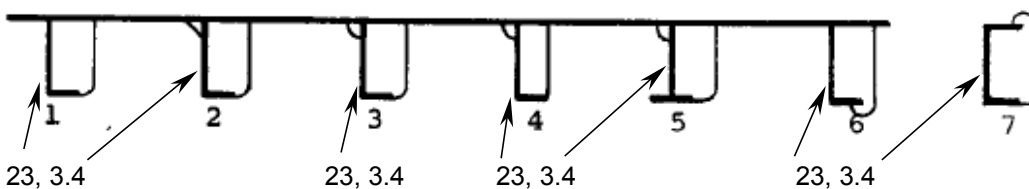
Clearance cutouts are required when a longitudinal stiffener passes through a transverse member. They may or may not have tight or nontight collars as were discussed in 4.2.4.

4.2.7.1 Flange Weld Only



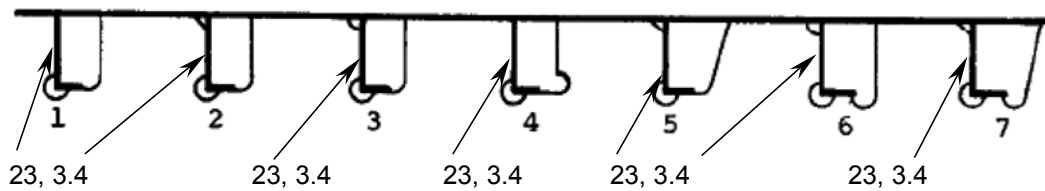
This is a common type of cutout on aluminum vessels, especially smaller craft with shallow stiffeners. The only connection between the stiffener and the web of the transverse is at the flange of the stiffener. This is an inefficient method of transferring shear stress from the web of the longitudinal to the web of the transverse, as the stress is concentrated in a short portion of the flange. This creates high stress in the fillet welds that attach the stiffener flange to the transverse web. This type of detail should not be used with deeper stiffeners or where the shear stress in the stiffener is high at the detail. Its use is restricted by classifications societies, and should not be used in areas subject to slam loads.

4.2.7.2 One-sided Cutout with Flange Weld



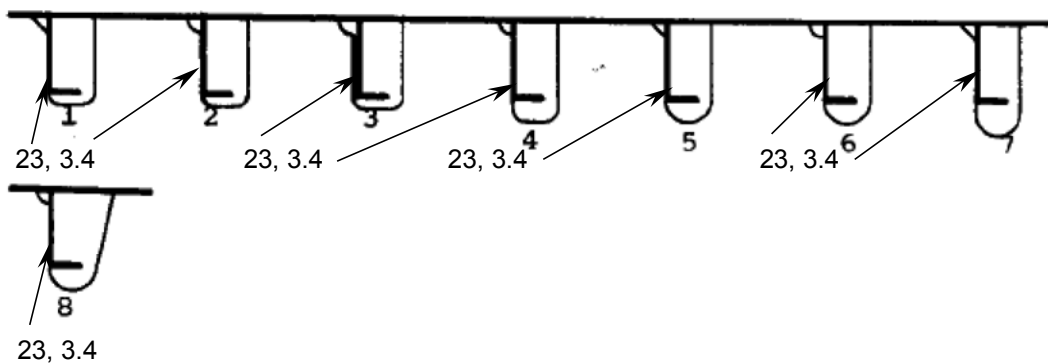
This style of cutout picks up the shear stress in the web of the stiffener and carries it through fillet welds into the web of the transverse. Additional transverse stability in the stiffener is provided by welding its flange to the web of the transverse. The shear strength of the web of the transverse is uncompensated, and the plating is not completely supported because of the opening.

4.2.7.3 One-sided with Stress Relief



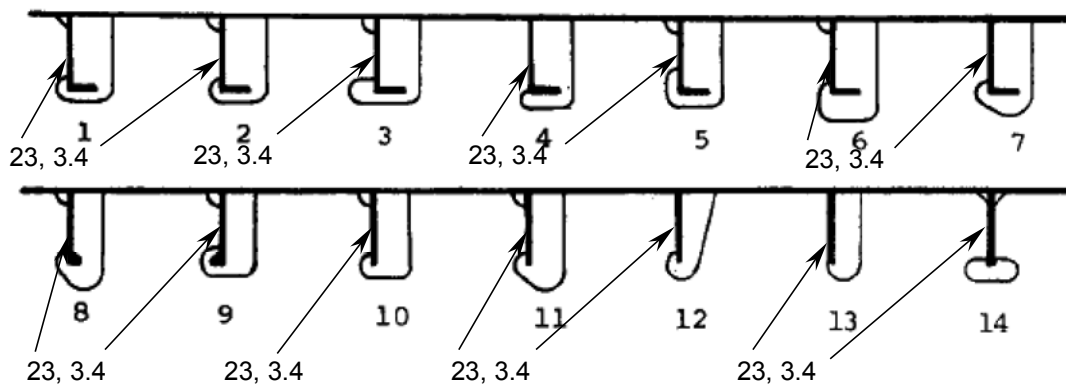
These cutouts are similar to the preceding except that a radius has been cut to reduce stress concentrations in the corners.

4.2.7.4 One-sided Cutout without Flange Weld



These cutouts are similar to those in 4.2.7.2 except that there is no attachment of the flange of the stiffener to the web of the transverse.

4.2.7.5 One-sided Cutout without Flange Weld with Stress Relief



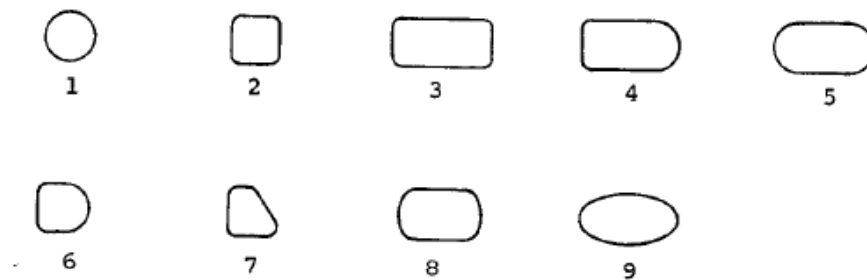
These details are similar to those above except that the corners have increased radii to reduce stress.

4.2.8 Deck Cutouts

A variety of details for openings in decks are provided, generally for passing electrical, piping, or HVAC systems.

4.2.8.1 Unreinforced Openings

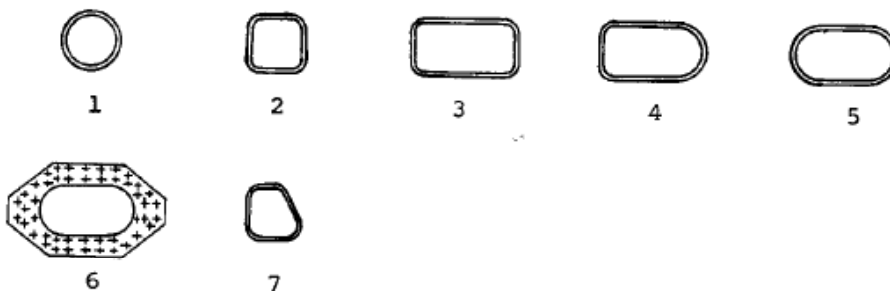
These openings do not have any reinforcement to compensate for lost deck area or to reduce stress around the opening. These larger openings should be classified as discussed in 4.2.6 as 45, 4.84, but reduced for the stress concentration factor of the opening.



4.2.8.2 Reinforced Openings

These openings are similar to those in 4.2.8.1 above except for the reinforcing ring. The reinforcing ring changes the fatigue classification from base metal to a fillet weld. As discussed in 4.2.6, the classification for a continuous fillet weld in the direction of maximum stress, 40, 4.3 should be used. This classification should be reduced for stress concentrations as in 4.2.8.1, and then increased for the presence of the ring.

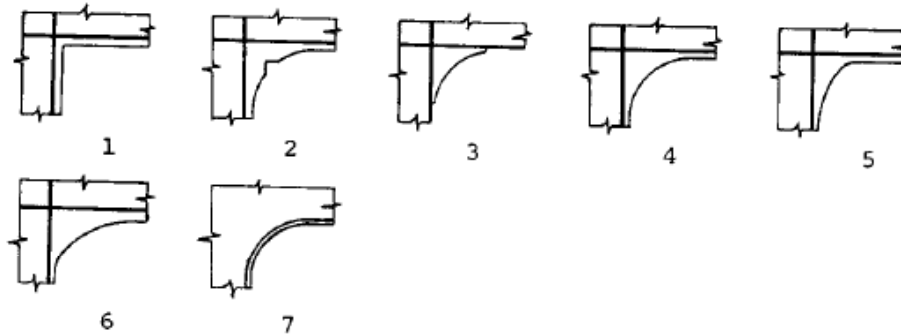
The riveted reinforcement of doubler plates shown in detail 6 is not recommended for aluminum structure. If an increase in plate thickness around an opening is required, it should be done by welding thicker insert plates, either around the entire opening or at the corners of a large opening.



4.2.8.3 Hatch Corners

The corner of a larger opening in a deck such as a hatch can have large stress concentrations that lead to fatigue cracking. There are many ways to treat the corner to reduce stress, including circular and transitional radii openings in the deck plate. The fatigue classification of the opening should be calculated as discussed in 4.2.6 above. Generally, a smoothly cut opening will have better fatigue classification than one with a welded coaming. However, if properly designed and fitted, the coaming around the edge of the opening will

reduce the stress sufficiently so that it will have greater strength than the unreinforced opening. Factors such as the smoothness of the cut will also affect the fatigue strength, with a numerically controlled plasma arc cut being better than a hand saws cut, and ground edges being better still.

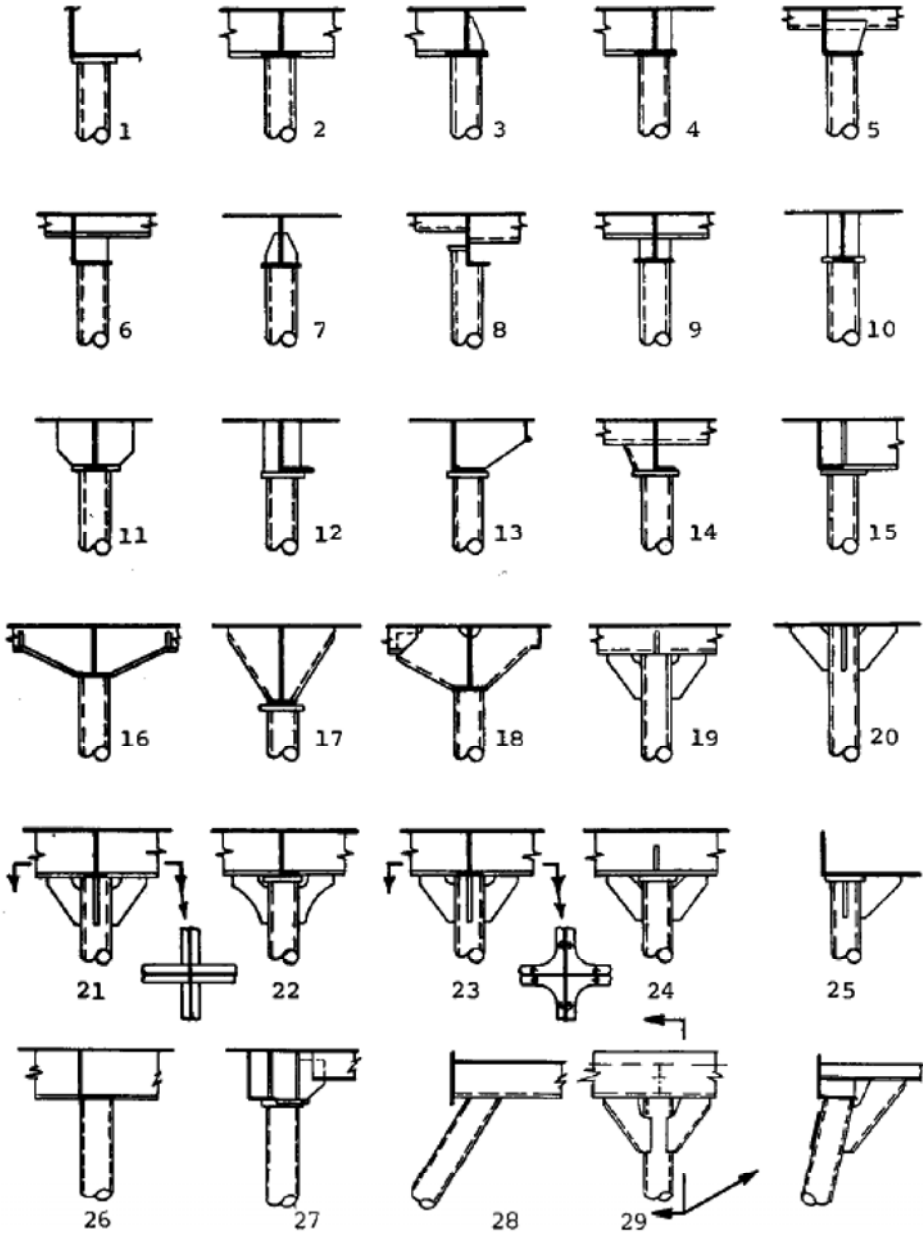


4.2.9 Stanchion Heads and Heels

A stanchion represents a concentrated load that must be transmitted from the members that it supports through the head above and to the structural members supporting it at the heel below. These details should be specially considered if there is a concern for fatigue, and have not been given a Eurocode 9 classification.

4.2.9.1 Tubular Stanchion Heads

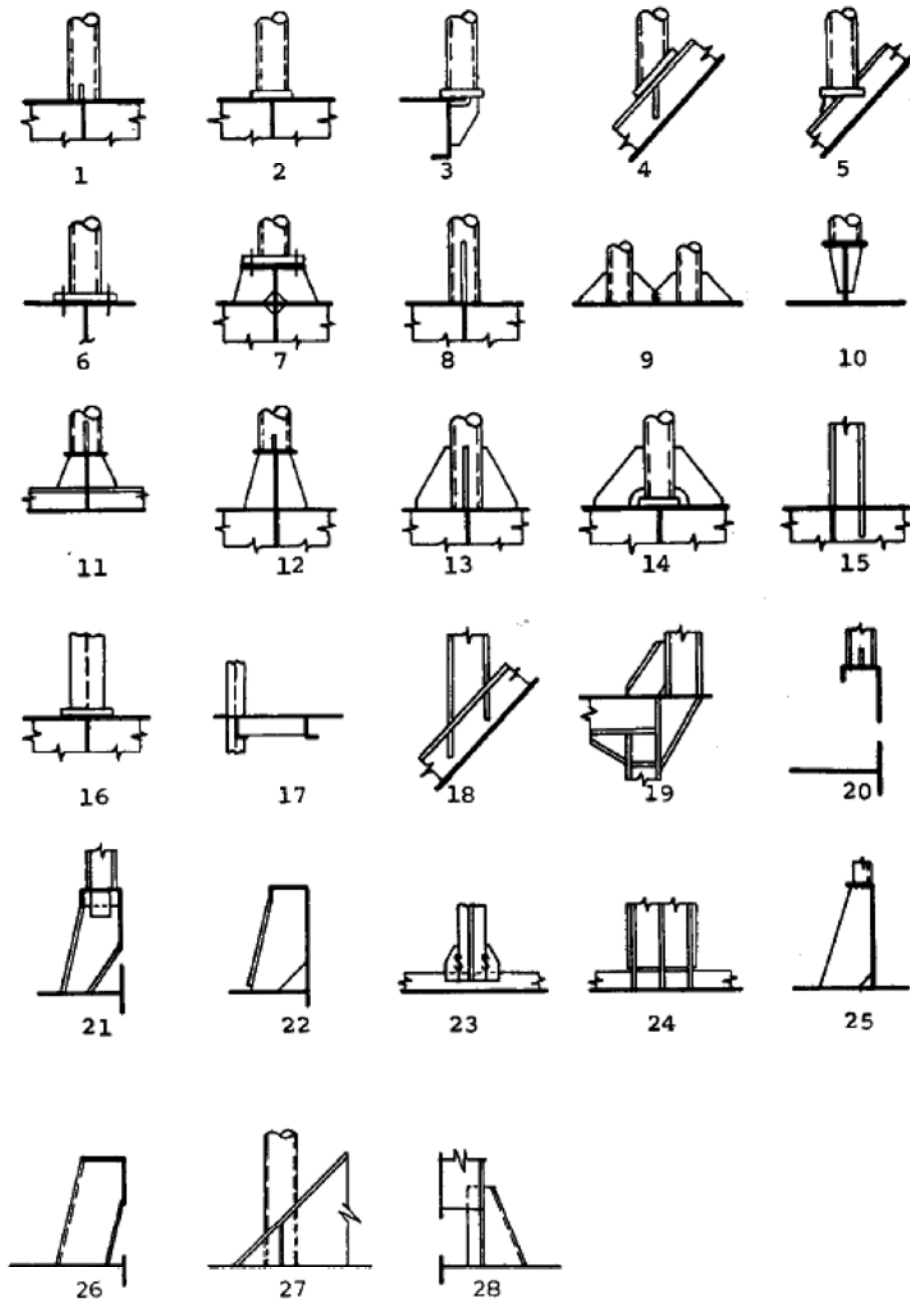
These details are for stanchions formed from circular, square, or rectangular tube. The heads of these stanchions should have a cap plate of the same or greater thickness than the tube wall thickness. The cap plate should be supported by two members crossing, as in detail 2, or if there is only one member above, chocks should be used as in details 9 and 10. Care should be shown to see that the cross-sectional area of the webs of the supporting members at least equals the cross-sectional area of the stanchion. If there is insufficient area, it should be provided by inserts in the webs, heavier chocks, or, as in details 19 through 24, with additional brackets.



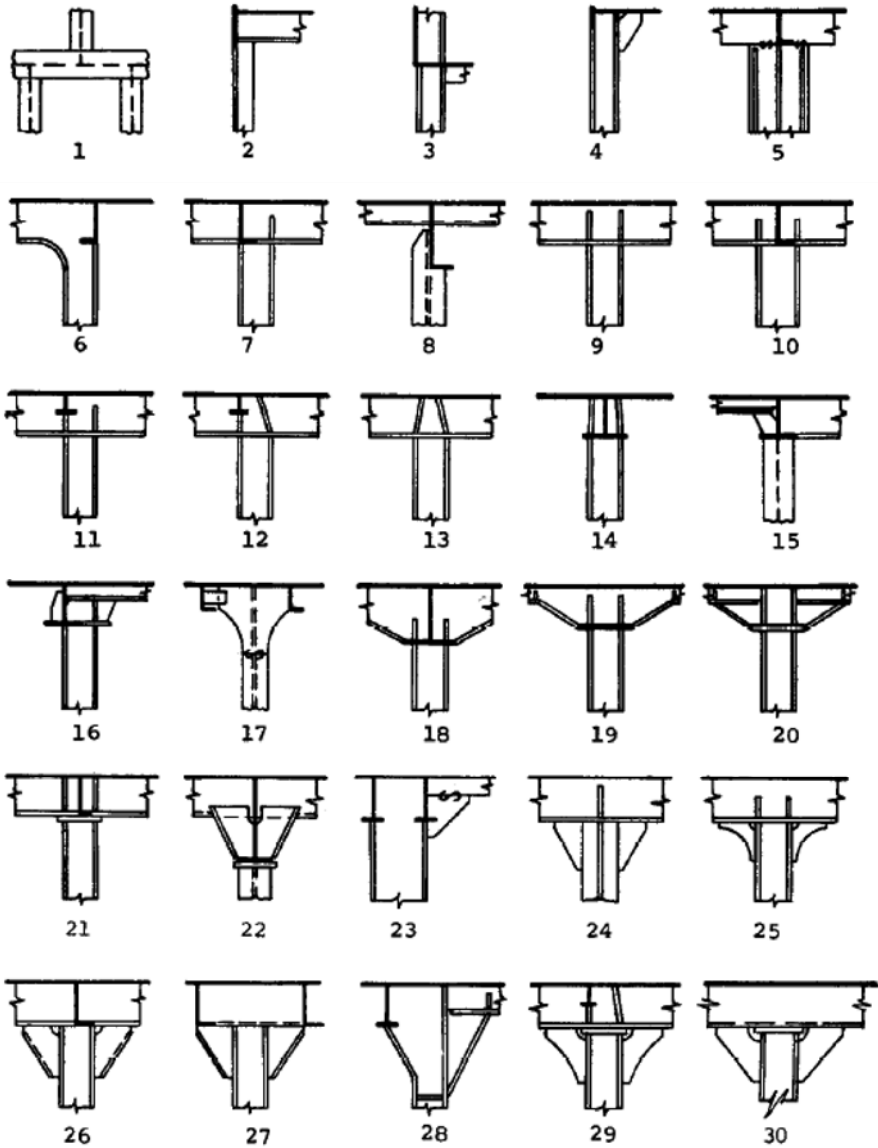
4.2.9.2 Tubular Stanchion Heels

The heels of tubular stanchions should have a sole plate of the same or greater thickness as the wall thickness of the stanchion. As with the heads of stanchions, the area of the webs of members below must equal or exceed the area of the stanchion.

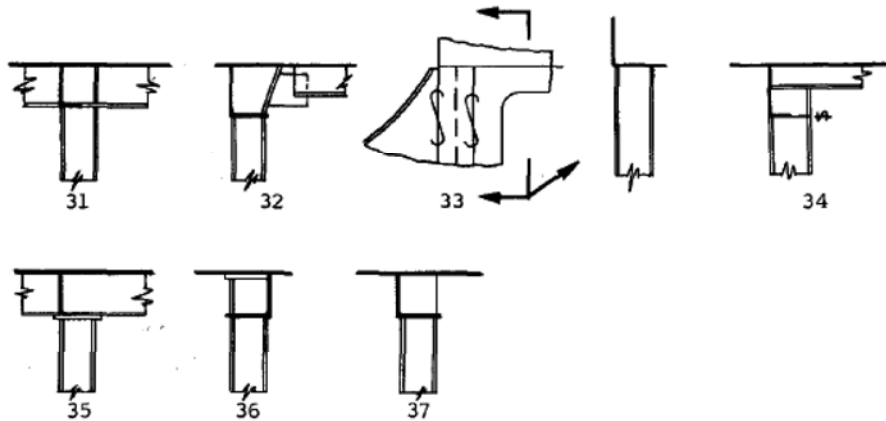
Aluminum Marine Structure Guide



4.2.9.3 Open Section Stanchions



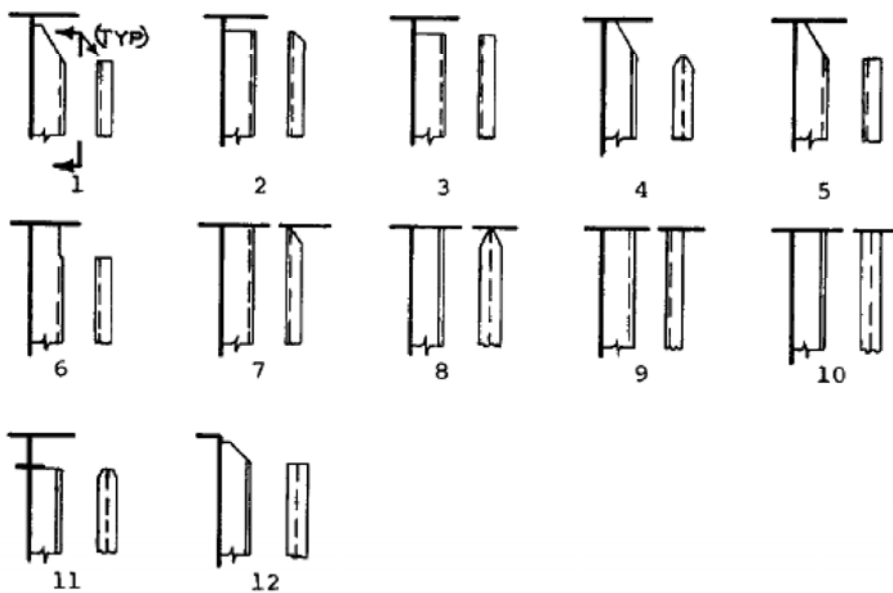
When open sections, such as H-sections are used as stanchions, the transition to other members is generally easier. However, the designer should be certain to examine the thickness of a member selected for a stanchion, because very thick flanges and webs are more difficult to transition.



4.2.10 Stiffener End Details

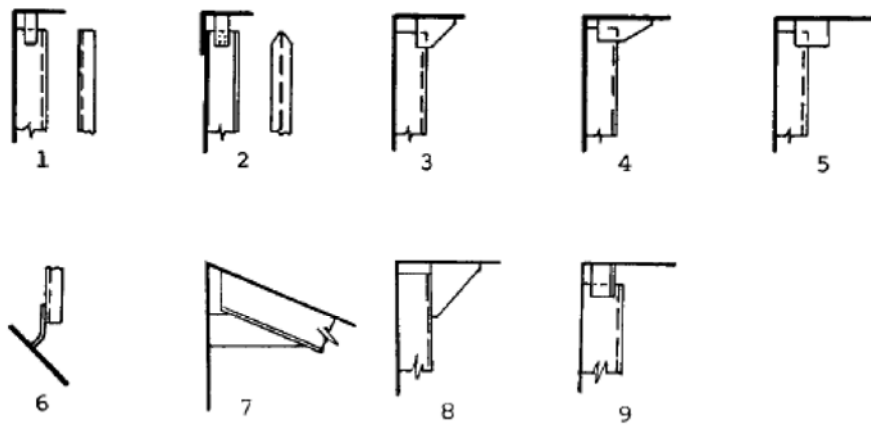
The stiffener ends included in this family are the ends of load-carrying structural angles or tees that are attached to panels of plating. Some of these are similar to details shown in 4.2.1.

4.2.10.1 Simple end details



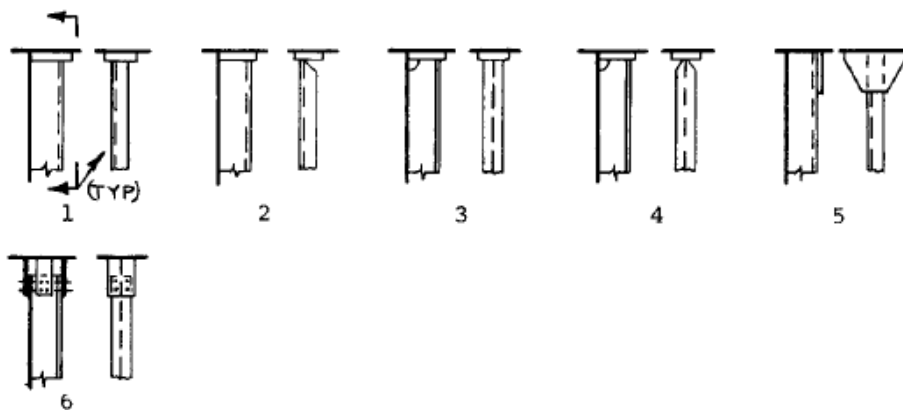
Some stiffener ends are cut straight across prior to meeting the intersecting member. Others are cut at an angle, called a snipe, to reduce stiffness more gradually, reducing the hard spot on the end. Others are welded to the intersecting member with or without the flange being sniped. Abrupt ends with hard spots such as detail 3 should be avoided unless in areas of low stress. Even then, they can cause problems if large local loads occur, such as an object dropped on a deck.

4.2.10.2 End clips



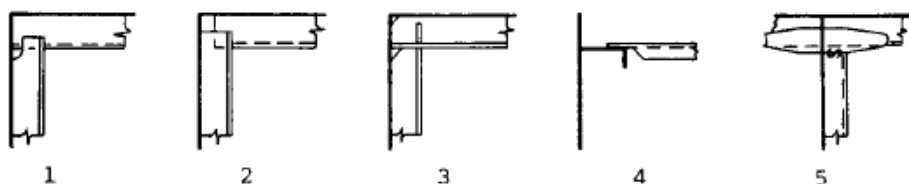
These details are a slight improvement from the previous group because a bracket or clip is added to help transmit the end load. However, lap joints have reduced fatigue strength, and should not be used where high alternating stresses occur.

4.2.10.3 End Chocks



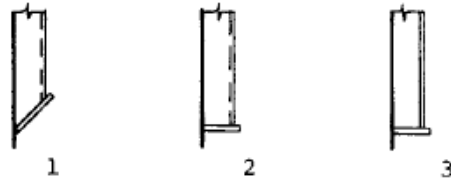
With these details, the stress concentration caused by the stiffener end is transmitted into a pad, or chock, which distributes stress around its boundary.

4.2.10.4 Corner Joints



The stiffener end is met by the end of another stiffener at right angles to it. The fitted detail 3 is preferred over lap joints.

4.2.10.5 End plates

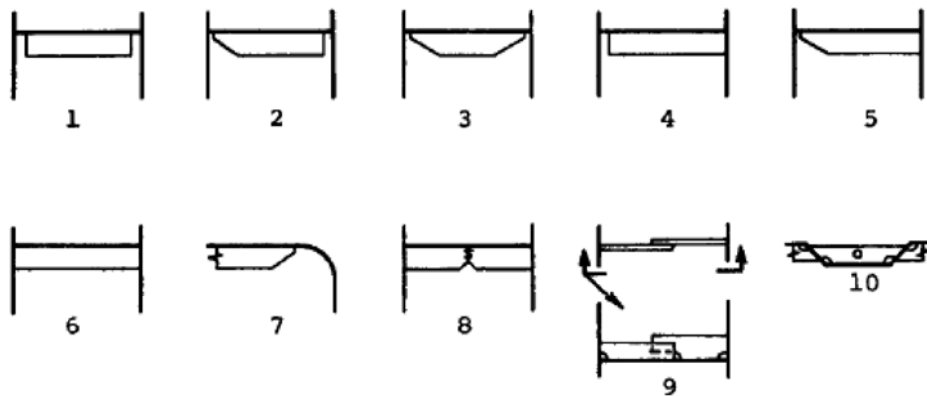


If a stiffener is to end prior to meeting an intersecting member, and end plate can distribute stress slightly, although stress concentrations still occur.

4.2.11 Panel Breakers

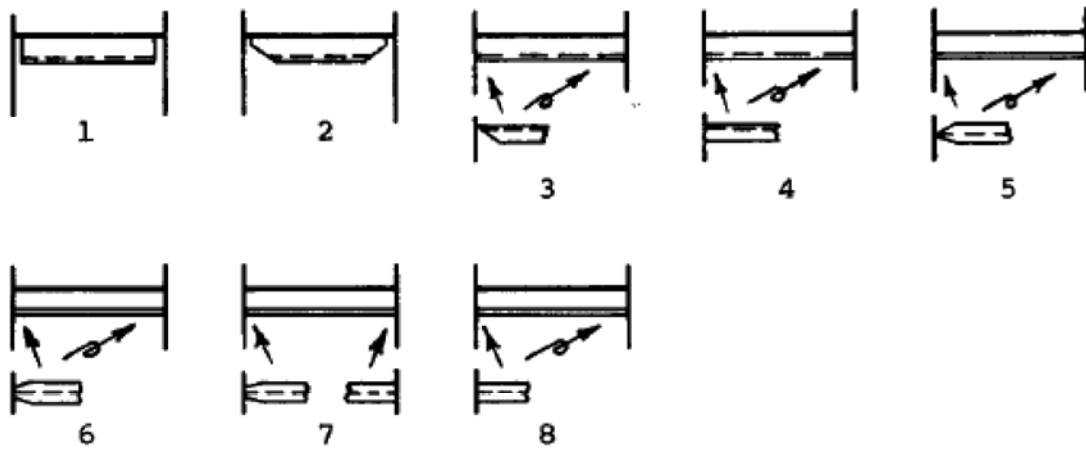
These short stiffeners are used on plate panels that require additional stiffening in addition to the regular gridwork of stiffeners. They are also used for other plating, such as the webs of built-up members and on foundations built with plate panels.

4.2.11.1 Flat Bar Stiffeners



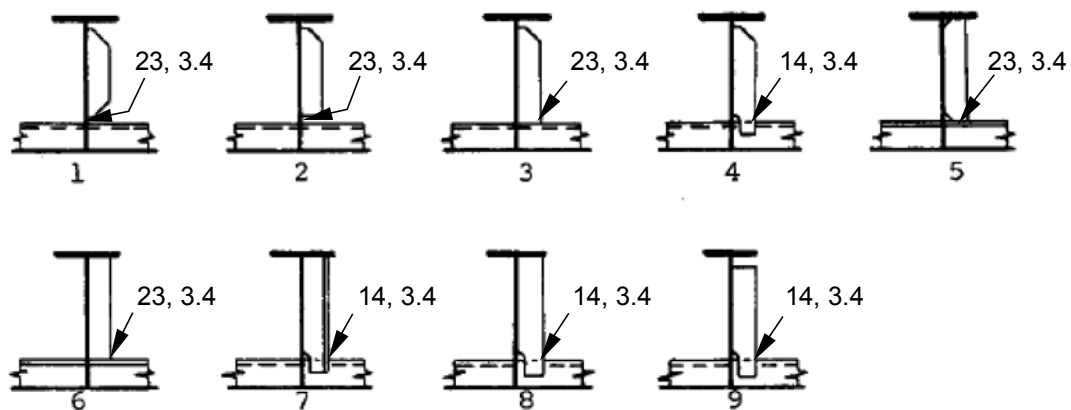
The flat bar is a simple detail, but it must be proportioned to avoid lateral instability.

4.2.11.2 Angle and Tee Stiffeners



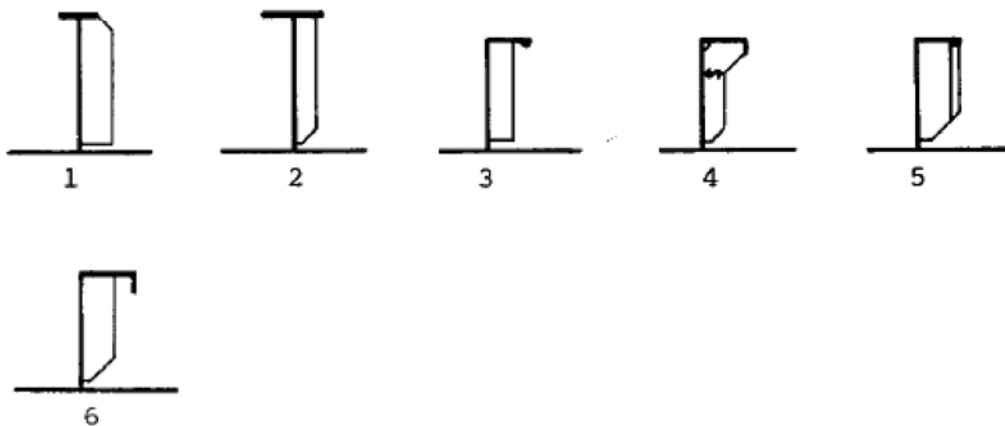
The angle has greater local stiffness than the flat bar, although its asymmetry can lead to torsional buckling. Not shown are bulb flats, which are intermediate between flat bars and angles in local stability. Because of its symmetry, the tee stiffener is the most stable. However, because it can carry a larger load, the end connections must be considered carefully, because they can have higher stress.

4.2.11.3 Girder Web Stiffeners with Longitudinal



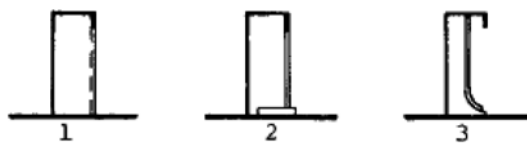
If fully fitted, as in details 5 through 8, these stiffeners provide stability for the flange of the girder. When fitted up or lapped on the intersecting stiffener, they also serve to transmit the shear load into the web of the girder. Details 1 and 2 may have a higher fatigue classification because there is no connection between the web stiffener and the intersecting stiffener, but that gap can present a high stress concentration for loads in the plane of the girder.

4.2.11.4 Girder Web Stiffeners



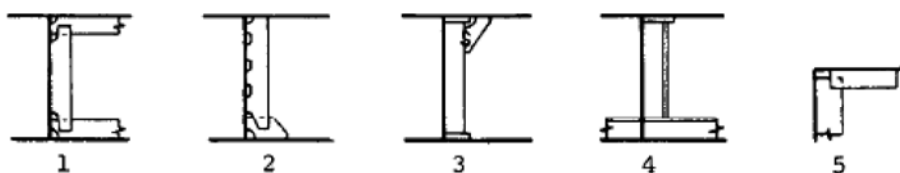
These web stiffeners occur where there are no intersecting members. They all serve as tripping brackets for the flange of the girder.

4.2.11.5 Coaming Stiffeners



These members act to support laterally the girder, which may be a hatch coaming or a bulwark. Detail 1 has a hard spot at the end, which has been eased by a pad in detail 2 and by a curved ending in detail 3.

4.2.11.6 Double Hull Bulkhead Stiffeners



These stiffeners occur within double hulls or cofferdams.

4.3 Details Specific to Aluminum Structure

The above examples were all taken from steel ships. Many of them can be used with aluminum structures because they represent the solution to similar structural problems. Aluminum has the advantage of having available a wide variety of extrusions to meet differing needs. Often these special extrusions will present different geometries than conventional stiffened structure and will call for different details.

4.3.1 Deck Panels

A variety of extruded panels that have the stiffeners extruded into them as well as sandwich panels are available, as described in Chapter 2. If these are sections such as flat bar, bulb flat, angle, or tee stiffeners, the structural detailing may be the same as if the stiffeners are welded to the plate rather than being extruded with it. However, with shallow sections, often only 25 mm (1 inch) deep, it is difficult to weld in the corners if conventional detailing is used. Often, the transverse frames in the deck will be recessed to accommodate the panel, as shown in Figure 4-1 and Figure 4-2.

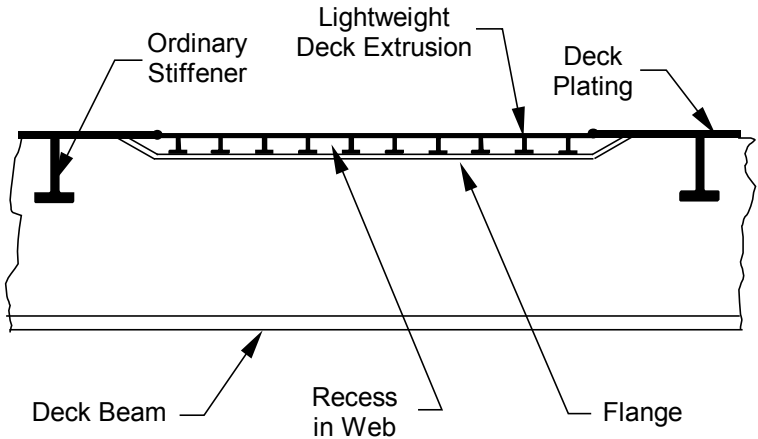


Figure 4-1 Recess in deck transverse in way of lightweight deck extrusion.



Figure 4-2 Lightweight deck extrusion on deck beam.

When these lightweight deck extrusions end at a bulkhead, the stiffeners are welded to the bulkhead plate, as in ordinary stiffened structure. It is very difficult to make the extrusion continuous through a bulkhead, and so it is generally made intercostal.



Figure 4-3 Lightweight deck extrusion at a bulkhead.

An alternate design is shown in Figure 4-4, where the deck transverse frame has a flange welded on top in line with the deck plate. A flat bar stiffener provides a watertight transition at the edge, but the plane of the deck is not maintained.

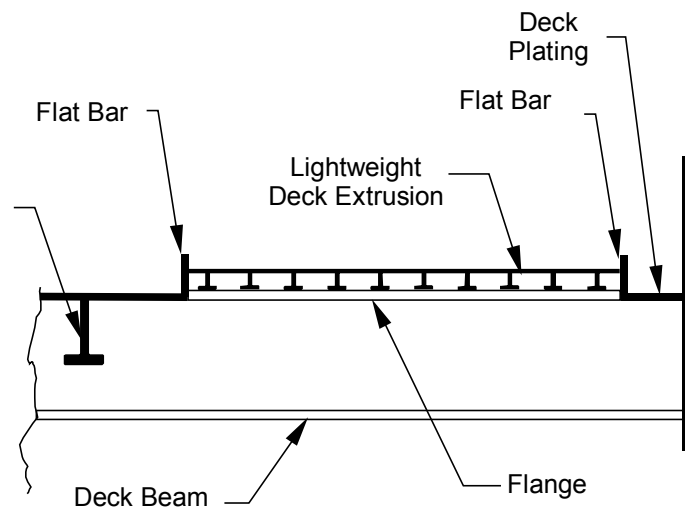


Figure 4-4 Alternate design for lightweight deck extrusions.

When lightweight corrugated or similar sandwich extrusions are used, making the transition to ordinary structure and welding joints between panels are sometimes difficult. A typical detail is shown in Figure 4-5, where flat bars are welded at the edge of the panels. Flat bars are similarly used at the ends of the extrusions to join to another extrusion. The only weld is the fillet weld of both face plates of the sandwich panel to the flat bar, with no welds between the corrugations or vertical webs within the panel. Such a joint has questionable fatigue strength.

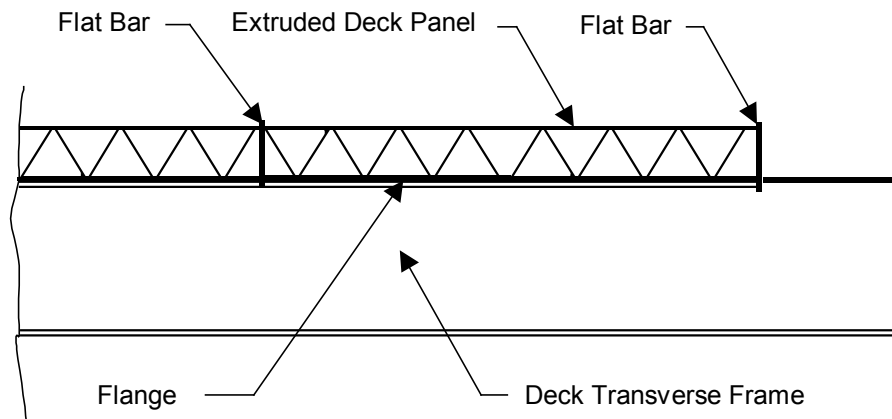


Figure 4-5 Corrugated deck extrusion.

4.3.2 Tubular Stiffeners

Although not exclusively confined to aluminum vessels, the use of rectangular and square tubing is well suited to fabrication of aluminum structure, particularly in lightweight structure such as deckhouses. Because they have good stability as stand-alone members, they are well suited to stick construction where framing and stiffeners are laid up and welded together and then the plating is welded to those members. Because aluminum is generally not prone to corrosion, the space between the tubing and the plate is not a source for corrosion as it might be with steel structure.

An example of structure under construction with tubular members is seen in Figure 4-6. The stiffeners have been butted against the frames and fillet welded all around. The plating has been welded to the stiffeners and frames with intermittent fillet welds.



Figure 4-6 Framing with tubular members.

4.3.3 Egg Crate Detailing

Because aluminum has good through-thickness properties, there is no concern for innerlaminar exclusions causing cruciform welds to fail by splitting the intervening plate apart. To take advantage of this property, increase the strength of intersections, and reduce labor, an egg crate detail such as shown in Figure 4-7 is used. The flange of the intersecting member is cut to accommodate the thickness of the member being intersected, and the web of that member is slotted to accommodate the depth and thickness of the web of the intersecting member. The two members are then slid together and welded. This type of detail is better suited for stick type construction; extremely close tolerances would be required if the stiffeners were welded to the plate first.

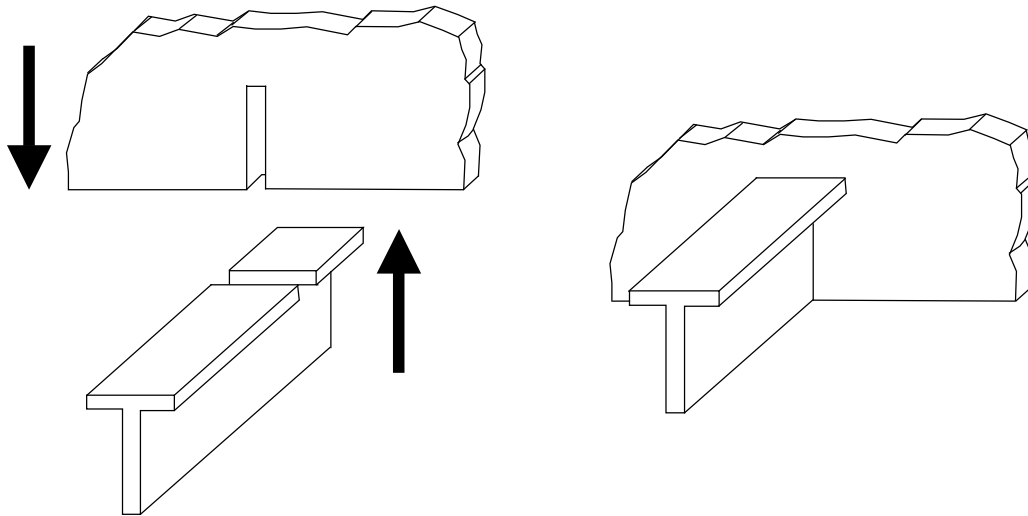


Figure 4-7 Egg crate intersection of tee with transverse.

4.3.4 Special Extrusions at the Gunwale

Section 4.2.5 showed details of gunwale connections. In aluminum hulls, special extrusions are often used at the gunwale, especially in smaller vessels, where they are shaped to act as a fender for the hull. Figure 4-8 shows several types of such extrusions used for fabrication of smaller vessels. These extrusions help form a rub rail at the gunwale. Other builders use conventional gunwale details but form the rub rail by using an extruded half-pipe section. In steel construction, a pipe or structural tube would be cut in two to form a half-round, but with aluminum, it is generally more economical to purchase the extrusion in its final form.

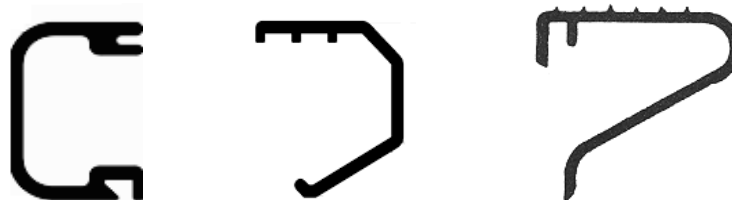


Figure 4-8 Special extrusions for gunwale.

4.4 Conclusions

A number of structural details from steel ships that could be used on aluminum vessels have been shown as well as a few details unique to aluminum construction. Evaluations have been made of the relative merits of these details when used for aluminum construction, including assignment of fatigue classification in accordance with Eurocode 9. A shipbuilder will have to determine the type of detail that best suits the construction techniques used in the yard, using higher quality details for the more critical joints. Where unproven details are used, such as for extruded deck panels, caution should be exercised until fatigue strength data is developed for these details.

Aluminum Marine Structure Guide

Chapter 5

Welding and Fabrication

5.1 Introduction

There are many similarities between fabricating ship structure with aluminum and fabricating with steel so that shipyards can make the transition from steel to aluminum without significant changes in facilities or personnel. There are many shipyards that build with both materials at the same time. However, there are some significant differences that cannot be ignored. Welding in an enclosed area is desirable for steel; it is a necessity for aluminum. Electromagnetic devices for material handling and for holding work in place are useless with aluminum. Oxyacetylene, gas or carbon arc cutting should not be used on aluminum. Workers have to be trained to understand the differences between aluminum and steel fabrication, especially workers, who need to learn new procedures. There is also a closer link between design and fabrication, and the design must often have to be changed to fit the advantages and limitations of construction capabilities.

The American Welding Society has a Committee D.3 on Welding in Marine Construction. The committee has prepared and regularly revises a Guide for Aluminum Hull Welding (AWS, 2004) that thoroughly reviews the subject of welding aluminum as it applies to marine fabrication. Much of the following material has been taken from that guide, which will be referred to as the AWS guide. The Aluminum Association published the book “Welding Aluminum: Theory and Practice” (Aluminum Association, 2002b), which provides guidance. Additional guidance is provided by the various classification societies, whose rules should be consulted when the vessel being constructed is to be classed. The American Bureau of Shipping has Part 2, Aluminum and Fiber Reinforced Plastics as part of the Rules for Materials and Welding, and it will be referred to as the ABS Rules. Military Standard MIL-STD-1689 pertains to vessels being constructed for the U.S. Navy, unless superseded by classification society rules or other contractual documents. The David W. Taylor Naval Ship Research and Development Center developed an aluminum guide (Beach et al., 1984) that has a volume on fabrication. This document may be difficult to obtain, so although reference will be made to it as the NSWCCD guide, the reader will not have to refer to it for further information.

5.2 Cutting and Forming

Aluminum is softer than steel, and therefore is easily cut with steel cutting tools. Sawing, machining, and other mechanical means of cutting can be performed in aluminum with ease. Sawing should be performed with blades that have relatively coarse teeth, and the blades should have a high speed. Saws that are commonly used include band saws and hand-held or stationary rotary saws. Jigsaws and saber saws are used for cutting curved shapes, and hole saws are used to cut circular openings. A saw-cut edge is generally suitable for welding, but they should be smoothed first by filing, planing, routing, sanding, polishing, or milling prior to solvent cleaning. Cutting with a hacksaw is not recommended except for small, thin pieces because it is time-consuming and does not present a very smooth edge.

Aluminum Marine Structure Guide

Shears are suitable for cutting plate up to 4.8 mm (0.188 in) thick, but the edge should be dressed and cleaned prior to welding. Shearing of exposed edges should not be done on alloys with a magnesium content of 3.5 percent such as 5083, 5086, or 5456 because the edge can become sensitive to stress-corrosion cracking. A nibbler is similar in action to a shear and is used for curved edges.

Cutting with numerically controlled plasma-arc cutting machines is the fastest and most accurate method of cutting aluminum. The cut edge is ready for welding, with only cleaning required. With plasma-arc cutting, intricate shapes can be easily obtained, including cut outs through which structural shapes can be passed. This process is used today in even small boatyards, who find it more economical to have an outside shop prepare plates than to have the internal work force cut the plates with saws and other mechanical means. Effective use of numerically controlled cutting requires additional advanced planning so that all openings and cutouts can be made at one time, and not when workers are fitting systems such as piping and electrical systems.

Plasma-arc cutting is done either dry or wet. In dry cutting, the plate is usually positioned above a pond of water, and in wet cutting the plate is submerged.

Another method of cutting is fluid jet cutting. A jet of water that includes abrasive particles is sent in a very high pressure stream from a nozzle. This process produces a very clean and accurate cut that leaves no heat affected zone. Plates from 1 mm to 100 mm (0.04 in to 4 inches) thick can be cut at rates between 3,500-mm/min. (140 in/min.) for the thinner sheet and 30-mm/min. (1.2 in/min.) for the thicker plate. (ALCAN, 2004).

The 5xxx-series aluminum alloys are work hardened to obtain their desired mechanical properties. Therefore, overworking these alloys in forming operations can have a deleterious effect on mechanical properties. Plates can be easily bent in a press-brake, but the minimum bend radii should be no less than those recommended by the AWS guide, which are summarized in Table 5-1.

Table 5-1 Minimum Bend Radii for Cold Bends in Aluminum Alloys as a Multiple of Plate Thickness, t (AWS, 2004)

Alloy	Base Metal Thickness (mm / in)				
	3.2 / 0.125	4.8 / 0.188	6.4 / 0.25	9.5 / 0.375	13 / 0.50
5086-H116	1.5t	2t	2.5t	3t	4t
5083-H116	1.5t	2t	2.5t	3t	4t
5454-H34	2	2t	2.5t	3t	4t
5456-H116	1.5t	2t	2.5t	3t	4t
6061-T6	2.5t	3t	3.5t	4.5t	5t

Plates can be curved with rollers, even to produce warped shapes with different curvatures at opposite ends. However, forming compound curvature is extremely difficult. If only a small amount of cross-curvature is needed, the plate can be rolled to the principal direction of curvature, and then forced into position against hull framing members. This is a

difficult operation, and if performed, the scantlings of the framing members may have to be selected to take these forming forces.

Roll forming to achieve compound curvature can be performed if a loose filler material such as sawdust or soft wood shavings is applied as the plate passes through the rolls. Curved rollers can also be used to form compound curvature. Either process to achieve compound curvature requires a great deal of skill. The best solution is to avoid compound curvature in the design of the shape of the hull.

For localized areas of compound curvature, “orange peel” sections are frequently used. Triangular plate are cut and given either single curvature, or some compound curvature using a press, and then joined together to form the desired shape, or an approximation to it.

In many cases, forming of aluminum is more difficult than steel because the 5xxx-series alloys cannot be heated to high temperatures without being changed metallurgically and becoming more susceptible to corrosion. The 6xxx-series, which are heat-treated, likewise can be heated for forming only with care. Because of the susceptibility of the high-magnesium 5xxx-series alloys to exfoliation, intergranular corrosion, and stress corrosion cracking, forming at higher temperatures must be done under controlled conditions. As mentioned above, these alloys receive their mechanical properties through cold working and are nominally considered to be non-heat treatable.

If extensive shaping of plates will be required, it may be better to select one of the annealed tempers, such as 5083-0 plate. Such tempers have less strength than the work-hardened tempers, and design calculations should reflect the reduced strength. They are not included in ASTM B 928 because they are not considered to be susceptible to sensitization. Careful control of the shaping process is required because it could lead to sensitization of material previously not sensitized.

Guidance on using heat to form 5xxx-series high-magnesium alloys was given by Hay and Holtyn (1980). The first consideration for shaping aluminum at higher temperatures is the selection of the temperature at which the operation is to be performed. Table 5-2 provides information on the change of yield strength at higher temperature for some alloys. More information is available from the Aluminum Design Manual (Aluminum Association, 2005). The lowest temperature that will result in the desired amount of softening should be selected.

The next consideration is the change in properties with plate thickness. Table 5-2 gives some indication of the reduction in strength for greater thicknesses. More information may be available from aluminum producers. Hay and Holtyn provide the information that is presented in Table 5-2 for 5456-H116 plate. The important point is that the thicker the plate, the closer the mechanical properties come to the minimum specified properties. However, it is the thicker material for which higher temperatures will generally be required for forming, and there is greater risk of not meeting the specified strength after heating and forming.

**Table 5-2 Reduction of Mechanical Properties of 5456-H116 with Increased Thickness
(Hay and Holtyn, 1980)**

Thickness Range		Yield Strength		Ultimate Strength		Elongation (%)
mm	inches	(MPa)	(ksi)	(MPa)	(ksi)	
1.60–12.69	0.063–0.449	228	33.0	317	46.0	10
12.70–31.77	0.500–1.250	228	33.0	317	46.0	12
31.78–38.12	1.251–1.500	214	31.0	303	44.0	12
38.13–76.22	1.501–3.000	200	29.0	283	41.0	12
76.23–101.60	3.001–4.000	172	25.0	276	40.0	12

If thick plates are to be heated for shaping, they must be placed in a furnace and held for several hours and “soaked” at the desired temperature. Because of the danger of loss of corrosion resistance, the maximum temperature should be less than 260 degrees Celsius (500 degrees Fahrenheit). Hay and Holtyn showed that a 70-mm (2.75-in) plate of 5456-H116 could be held at a temperature of 245 degrees Celsius (475 degrees Fahrenheit) without significantly affecting the condition of the matrix and grain boundary precipitate, although the yield strength decreased to 165 MPa (23.6 ksi), compared to the specified minimum yield strength of 200 MPa (29.0 ksi). Therefore, if forming at higher temperatures is contemplated in fabrication, the design calculations must be accordingly adjusted for the reduced mechanical properties. This is another example of the relationship between design and fabrication in aluminum.

Prior to undertaking to form an aluminum alloy at higher temperatures, a test program should be undertaken to certify that the process will result in the desired mechanical properties and corrosion resistance. Specimens of the plates to be formed should be subjected to the required heating cycle, mechanically deformed, and then tested. In addition to tensile testing, the plate should be tested in accordance with ASTM G 66 (ASSET) for exfoliation resistance and the ASTM G 67 (NAMALT) test for intergranular corrosion resistance. Both tests should be in accordance with the requirements of ASTM Specification B 928-04 for marine-grade aluminum plate. Most classification societies as well as the U.S. Navy do not generally permit forming these 5xxx-series at elevated temperatures, so the results from the test program would be used to obtain an exception to general rules.

Aluminum structural shapes are easily formed in light sections, but deeper sections are more difficult to bend without causing buckling of flanges or webs. The NSWCCD guide (Beach et al., 1984) recommends that tee stiffeners may be bent by cutting V-notches in the webs or cutting the flanges. If this method is used, holes should be drilled at the ends of the notches prior to forming to prevent cracking. This method should not be used if the design of the member is based on the unwelded strength of the shape.

Special rollers with slots to support webs can be used to bend tees and angles. For some shapes, the heating mentioned above may be necessary. However, when there is a considerable amount of curvature involved, such as for transverse frames, the best solution is to cut plate to the shape of the hull to form the web, and make the inside edge straight or slightly curved for welding a flange. This approach using numerical cutting is generally the least expensive alternative today, as the cost of numerical cutting is low, and considerable labor in the shipyard is saved.

5.3 Structural Assembly

Techniques for ship fabrication with aluminum can be almost the same as with steel. Many shipyards fabricating large aluminum vessels or aluminum deckhouses for large ships use the same type of pre-outfitted structural assemblies as with the steel structure. Aluminum suits this type of construction even better than in steel because larger subassemblies can be built of the same weight. More care in handling larger assemblies is required because of the lower stiffness of aluminum. Scantlings that are generally lighter in aluminum structure and the ineffectiveness of electromagnetic handling devices make welding temporary handling pads a necessity for aluminum subassemblies.

Unless special care is taken, distortion of aluminum subassemblies can be greater than with steel subassemblies. Concerns for alignment with other subassemblies sometimes necessitates welding additional temporary stiffening members to hold the subassembly prior to its being welded into the other structure.

Welding processes used with aluminum are not tolerant of gaps, especially uneven gaps, and so greater care must be taken with the fit-up of joints prior to welding. Punch marks or scribe marks in aluminum can become sites of fatigue crack initiation, and should be not used unless these are to be welded over.

Aluminum structure should be fabricated in enclosed conditions, either temporary shelters or permanent buildings. There are several reasons for this. Aluminum alloy 5086 has a coefficient of thermal expansion of 23.8 per degree Celsius (13.2 per degree Fahrenheit), which is about twice as great as the coefficient of steel. Therefore, dimensions will vary greatly as the temperatures change, and localized changes in temperature, such as from direct sunlight, will induce warping of structural assemblies. Aluminum must be welded with shielding gas, and protection from the wind is necessary. Moisture, even high humidity, can have a serious effect on the quality of aluminum welds, so protection from the weather is essential.

Some shipyards produce aluminum ship structure in stiffened panels, and have special aluminum panel lines for this purpose. In panel construction, plates are butt welded to form large panels prior to the welding of frames and stiffeners. Stiffeners are welded first in mechanized stations, and then the frames are fitted over the stiffeners and welded. Curved hull sections are formed by laying the plates in jigs that are curved to the shape of the hull, butt welding them, and then fitting the stiffeners and frames.

An alternative to panel construction is “stick” construction favored by boat builders. Bulkheads and frames are first laid up and tack welded together. Stiffeners are then fitted to the frames, and the entire assembly is welded. The plating is then laid over the stiffening, and welded to the frames and stiffeners. This process avoids having to construct jigs to handle curved sections, which is more advantageous for one-off designs or when only a few hulls are built to the same shape. Access to the details of stiffener-frame intersections is better prior to welding the plate, and makes these details easier to weld, especially for the small stiffeners typical of smaller craft. Alignment of intercostal members is easily accomplished when they are welded prior to welding the plate.

A picture of a vessel under construction with stick framing is shown in Figure 5-1. The hull is being constructed in the inverted position, so the welding of plating to stiffeners will be in the overhead position. When the welding is performed, temporary shelters will be put in place to keep out the weather, reduce the wind, and to minimize distortion from the sun.



Figure 5-1 Hull with stick construction of framing (Courtesy of Gulf Craft).

A disadvantage of stick construction is that light stiffeners, particularly flat bar stiffeners, have little lateral stiffness and are difficult to hold in place prior to the welding of the plate. Tee stiffeners provide greater rigidity, and the bulb tees shown in Chapter 2 are even better because they have a small flange on the faying surface, giving them greater stiffness.

5.4 Welding

The following materials will not supersede the documents of the U.S. Navy or classification societies referenced above but will mostly summarize the AWS guide. There are other new processes for welding aluminum, including laser welding and friction stir welding that will be reviewed in Chapter 14.

5.4.1 Procedures

Aluminum must be welded using a protective shielding gas. The two principal methods are Gas Tungsten Arc Welding (GTAW) (also known as TIG) and Gas Metal Arc Welding (GMAW) (also known as MIG). GTAW is generally much slower than GMAW and is generally used for welding thin materials, 1.5 mm (1/16 inch) or less. However, GMAW can also be used with material that thin if pulsed power is used. There are a number of filler metals available for welding aluminum, with advantages and disadvantages of each listed in Table 7 of the AWS guide. Selection of the filler metal will depend on the alloys being welded. Many shipyards will try to use the same filler metal for all alloys to minimize problems with inventory control and supply to the welder.

Shielding gas is either helium or argon or a combination of the two. Argon is the most effective in oxide removal when used with a direct current, electrode positive arc and is preferred for thicknesses up to 19 mm (0.75 in). Helium shielding produces a higher voltage, so for greater thicknesses and when welding out of position, mixtures of helium and argon are generally used. Protection of the weld from rain and other excessive moisture is essential for a good quality weld. It is also important that protection from the wind be provided to avoid disrupting the flow of the shielding gas.

5.4.2 Joint preparation

The fit up required for welding aluminum is more demanding than for steel. Table 11 of the AWS guide provides information on allowable root gaps, which vary depending on the weld position and joint design. A typical requirement for butt welds in 6-mm to 10-mm (1/4-inch to 3/8-inch) plate is a 0.0 to 2.4 mm (0.094 in) root gap. Butt joints must be beveled unless the thickness of the plate is 4.8 mm (0.188 in) or less.

The U.S. Navy procedures for welding are included in MIL-STD 1689, Fabrication, Welding, and Inspection of Ship's Structure, for surface ships. The specifications for joint design, including root gaps, are given in MIL-STD-22, Welded Joint Design. MIL-STD-22 makes no differentiation between steel and aluminum and permits root gaps as large as 4.8 mm (0.188 in) for butt welds in all plate thicknesses without backing. Although such large root gaps may be permitted by the U.S. Navy specifications, it is recommended that the guidance of the AWS be followed.

The AWS provides no guidance on alignment, but the ABS Rules for Materials and Welding specify that the plates should be aligned within the tolerances shown in Table 5-3, which are the same tolerances required by MIL-STD 1689 after welding.

Table 5-3 Permissible Alignment of Butt Welds (ABS)

Base Metal Thickness		Maximum Misalignment
Millimeters	Inches	
$t < 9.5$ mm	$t < 0.375$	1.5 mm (0.625 in)
$9.5 < t \leq 19.0$	$0.375 < t \leq 0.75$	3.0 mm (0.125 in)
$19.0 < t \leq 38.0$	$0.75 < t \leq 1.5$	5.0 mm (0.188 in)
$t > 38.0$	$t > 1.5$ in	6.0 mm (0.25 in)

The ABS rules require that the fit up for fillet welds be no greater than 1.5 mm (0.063 in). If the gap is greater than that, but no more than 5.0 mm (0.188 in), the gap can be accommodated by increasing the fillet weld size by the amount of the gap over 1.5 mm (0.063 in). For both butt welds and fillet welds, ABS permits excess gaps to be filled by laying weld beads on one or more of the edges to be welded (buttering). For butt welds, the buildup should not exceed 1/2 of the plate thickness or 12.7 mm (0.50 in), and for fillet welds it should not exceed the plate thickness or 12.7 mm (0.50 in).

Edge preparation prior to welding is more demanding for aluminum than for steel. A single or double bevel or a J-joint is required for all joints over 4.76 mm (0.188 in). This edge can sometimes be produced during the numerically controlled plasma arc cutting process that

shapes the pieces. Otherwise, processes to be used include high-speed milling machines, routers, planers, and saws. Sanding and grinding are not recommended for edge preparation, as they tend to leave residue that is difficult to remove.

The edges to be welded must be chemically cleaned with a solvent and then brushed with a stainless steel wire brush, which may be a hand or power brush. The surface of the plate should be cleaned with the solvent for a distance of at least 75 to 150 mm (3 to 6 inches) to avoid contaminating the weld or the shielding gas with surface residue. Chemical cleaning and brushing must be done prior to fit-up of the surfaces to be welded, so a preliminary fit-up should be made prior to cleaning to minimize the interval between cleaning and welding. AWS recommends covering the cleaned surfaces with strips of heavy paper that are taped in place if there is any length of time between cleaning and welding. ABS limits the time between cleaning and welding to 8 hours, and MIL-STD-1689 limits the time to 16 hours.

Selection of the solvent to be used is difficult because of environmental concerns and the need to have a clean surface that is free of oil, grease, oxides, and other contaminants. American National Standards Institute ANSI Z49.1, Safety in Welding, Cutting, and Allied Processes, provides guidance on solvent selection.

5.5 Tolerances

Aluminum is more prone to distortion from welding than is steel, but the tolerances for deviations from fairness in aluminum structure are not as strict as for steel. Permissible unfairness in aluminum plating is specified in two figures in the ABS Rules for Materials and Welding (Aluminum), which are very similar to figures in MIL-STD-1689. These standards will be discussed again in Chapter 8. The MIL-STD tolerance for 12.7 mm (0.50 in) strength deck plate on 610 mm (24 in) stiffener spacing is 9.5 mm (0.375 in) for aluminum, but 6.4 mm (0.25 in) for steel, showing that greater tolerances are permissible in aluminum.

MIL-STD 1689 and the ABS aluminum rules have the same tolerance for the fairness of frames and stiffeners in primary strength structure or where subject to dynamic loading, such as bottom slamming. The requirement is the unfairness be less than $C l / d_w$, where the unfairness is in millimeters when $C = 530$, and in inches when $C = 0.5$. l is the span in meters (feet) and d_w is the depth of the web in mm (inches).

These tolerances and the tolerances for plate were determined by surveys of the tolerances that can be achieved in normal shipbuilding practice. The effects of tolerances on structural strength have been studied for steel ship structure, but not as much work has been done for aluminum.

Paik (2006b) surveyed 78 welded panels, which had four stiffeners. 73 of the panels had one stiffener bay and three has 3 bays. Paik et al. considering the following types of distortion:

- Initial distortion of plating between stiffeners;
- Column type initial distortion of stiffener;
- Sideways initial distortion of stiffener;
- Residual stresses of plating between stiffeners;

- Residual stresses of stiffener web;
- Softening in the HAZ in terms of reduction of the HAZ material yield stress and breadth of softened zone.

All of the panels had 300-mm stiffener spacing, and plate thickness of 5, 6, and 8 mm. The results of the study are reported in detail, including a statistical analysis of the measured distortions. A summary of the maximum measured distortion for the initial distortion of plating between stiffeners is presented in Table 5-4, where they have been compared to the allowable distortion of ABS and MIL-STD 1689. The panels with 5-mm plate just meets the minimum MIL-STD 1689 value for longitudinal strength and similarly critical structure, but the 6-mm and 8-mm plate do not meet the longitudinal strength criteria of either ABS or the MIL-STD.

Table 5-4 Comparison of Distortion of Plate Panels Reported by Paik et al. (2006b) with ABS and MIL-STD 1689 Tolerances

Plate Thickness	Maximum Measured Distortion	ABS		MIL-STD	
		Longitudinal Strength Structure	Other Structure	Longitudinal Strength Structure	Other Structure
5	4.85	6.4	12.7	4.8	6.4
6	8.64	6.4	12.7	3.2	6.4
8	8.22	6.4	9.5	3.2	6.4

There are several comments that can be made in regard to these results. First, the welding was performed under laboratory conditions, and might be expected to be better than typical shipyard welding. Second, the initial distortion that is seen in a plate panel fabricated on a shipyard panel line generally becomes amplified when the panel is fitted into the hull structure because greater residual stresses are placed on the panel. Therefore, even greater distortion than measured is feasible. It would therefore appear that the specified tolerances are not easy to achieve, and more careful fabrication practices are required than those used by Paik et al. In this regard, stick construction with sequenced welding should produce less distortion, especially if intermittent welding is used.

Use of flame straightening to fair plate is generally not permitted in aluminum unless special permission is obtained from the classification society or the U.S. Navy. A guide for flame-straightening aluminum was provided by Hay and Holtyn (1980). The 5xxx-series aluminum should not be heated to above 288 degrees Celsius (550 degrees Fahrenheit) and should not be permitted to remain at that temperature for any length of time. Aluminum does not glow when it is heated, so a different method of determining temperature is needed. Special temperature-sensitive crayons that are manufactured for monitoring temperatures during welding are used for that purpose. Two operators are generally required for this operation. The first operator has crayons that melt at 288 °C (550 °F) and an oxy-acetylene torch to heat the plate. The second individual has a device for providing a fine spray of water and air. The individual heating the plate constantly checks the temperature with the crayon, and when it melts, the second person immediately cools the plate to 66 °C (125 °F). Extreme care must be used with

this operation because overheating can lower the mechanical strength, and it can also reduce the corrosion resistance, neither of which can be easily determined by quality control means.

An alternative method of straightening plating is to lay weld beads in a pattern on the surface of the plate. This method is not generally permitted as the ultimate strength of the unwelded plate is used in part in determination of scantlings. If an area of the hull is such that it is known in advance that appreciable distortion could occur during fabrication, the plating could be designed for the reduced properties. However, it is better if such problems are known in advance to decrease stiffener spacing or increase plating thickness to reduce distortion.

Radical distortions in plating, such as from an improper butt weld, can be corrected by cutting a slit in the plate, straightening the plate or possibly distorting it in the opposite direction, and then rewelding. Special permission may also be required for such an operation.

Avoidance of distortion is better than using the means described above for correction of excessive deformations. Most distortion occurs when plate is welded, both in the butt welds between plates and in the fillet welds to stiffeners and frames. If the plate is welded first, corrective measures can be taken to straighten welds that are bent in one direction or the other. To minimize the distortion, the plate should not be free to rotate about the axis of the weld during welding. The design of the joint should be symmetrical, as should the welding procedures. Minimum welding heat should be used, and excessive filler material should be avoided. Fillet welds should also be made with minimum heat input, and the fillets should be no greater than required for strength. To minimize weld size, the fit-up should be made as accurate as possible to minimize root gaps and irregularities in the root gaps. Small, uniform root gaps will minimize the amount of weld metal required.

The sequence of welding is very important to reduce weld distortion. Butts and seams in plating should progress outward from the center, with butts in strakes of plating welded before the longitudinal seams. Often, it is beneficial to weld only small portions at a time, welding short intermittent beads, and returning to the weld seam after structure farther away has been welded. For smaller craft and in not-critical structure, such as deckhouses, intermittent fillet welds may be used to reduce distortion.

5.6 Fabrication with Special Panels

Several varieties of special extrusions have seen increased use in lightweight vessels in recent years. These extrusions fall into two basic categories, open sections and sandwich panels. Open sections have tee, bulb flat, angle, flat bar, or other stiffener shapes extruded into a plate panel. Depending on the size and spacing of the stiffeners, as little as one stiffener and as many as four or more stiffeners are extruded into the panel. The width of these panels is limited by the size of the extrusion die, which is a maximum of about 910 mm (36 inches), depending on the extruder's capacity. These panels can be as much as 12.2 meters (40 feet) long, depending on the capability of the extruder. See Chapter 2 for more information on extrusion design and capabilities. Sandwich panels are hollow extrusions consisting of two sheets of plate connected by stiffeners that are either flat bars or in a corrugated pattern, and size availability is similar to the open stiffened panels.

The extrusions have special shapes formed into their edges so that the panels will interlock along the edges and then be welded together. A typical panel is shown in Figure 5-2, which shows one of the types of designs used to join the panels. Many shipyards have turned to advanced joining techniques for joining these panels, especially friction stir welding. The panels must be shipped to the facility that performs the welding and be joined into sections as wide as can be easily shipped back to the shipyard. For friction stir welding, the form of the panels is changed so that the weld between the panels is in the middle of the plate between the stiffeners to provide access for the friction stir welding equipment. In these cases, there is no interlocking joint, but the extrusion is made slightly thicker where the joint is to be made to compensate for the loss of metal that will occur with the welding process.

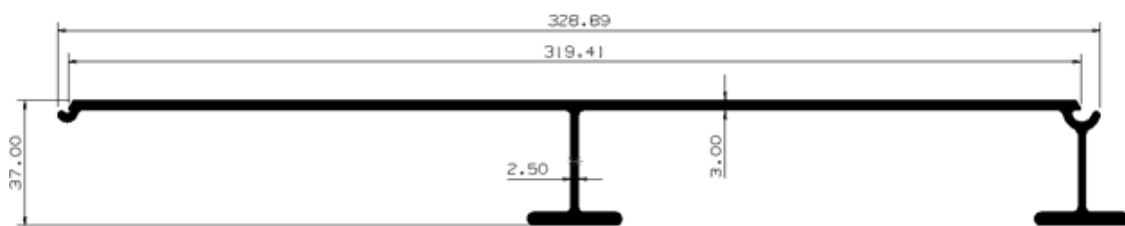


Figure 5-2 Stiffened panel extrusion (G. James Australia Pty. Ltd.).

Depending on the size of the structure, the panels that have been joined will have to be joined into even larger panels at the shipyard. The special edge shapes may be retained for making joints between individual panels, or conventional butt welds will be made. These assemblies are then joined longitudinally to make longer sections. There is no access to the inside of sandwich panels, so only the faceplates can be joined using one-sided welds. Because the internal stiffening webs in the sandwich panels cannot be welded together, the joints must occur at points of support.

Some of the design considerations for the use of integrally stiffened panels were discussed in Chapter 3, including the need to form inserts in transverse frames to support the panels. Some of the intricate details of these recesses are shown in Figure 5-3. There is a tradeoff that must be made in design between the cost savings associated with purchase of special extrusions rather than fabricating light sections from plate and stiffeners, weight reduction from very light panels, and the additional labor or the more complex geometry at the transition from conventional structure.



Figure 5-3 Recess in deck to accommodate stiffened panel extrusion (Gulf Craft).

5.7 Fabrication with Adhesives

Adhesives are becoming more widely used for joining aluminum to either aluminum or to other metals and to FRP. An adhesive that is widely used and has been tested in a marine environment is methacrylate adhesive, also known as methamethacrylate (MMA). One manufacturer, IPS Corporation states that its 300-series Weld-on adhesive has a lap shear strength at 24 °C of 17–19 MPa (2,500–2,800 psi). These bonds are resistant to intermittent exposures up to 121 °C (250 °F), but generally should not be used at temperatures above 82 °C (180° F). This adhesive is a two-component 10:1 mix ratio product that can be applied without prior application of a primer, and comes in three flavors, having open times of 5-minute, 15-minute, and 40-minute open times in which the material can be used. (IPS corporation web site).

Lloyds Register has approved weld-on 230-series methacrylate adhesive for vessels constructed under its rules for service craft. This adhesive has a lap shear strength for metal-to-metal bonding of aluminum of 9.7–10.3 MPa (1,400–1,500 psi). It is also a two-component 10:1 mix ratio product that requires application of a primer for bonding metals, and depending on the activator used can have range of working times from 30 to 120 minutes. For bonding metal the activators providing a working time of 40 minutes or less should be used. Prior to application of the adhesive in test coupons, the 6061 coupons were wiped clean with a Heptane solution and then dipped in the company's MP100 metal primer. The adhesive bond was 1 mm (0.04 in) thick, and the shear strength was tested after 28 days in air at 24 °C and in fresh water at 35 °C.

The lap bonds of the specimens tested after immersion in water were actually 25 percent stronger than those that were held in air.

Eurocode 9 fatigue strength S-N curves recognize the use of adhesives for bonding aluminum. The stress range at 2×10^6 cycles for a single-lap joint is 0.11 times the shear strength of the adhesive, and the slope of the S-N curve is -6 at that value of stress range. Therefore, for the 300-series Weld-on adhesive mentioned above with a minimum lap shear strength 17 MPa, the fatigue strength at 2×10^6 cycles is $0.11 \times 17 = 2$ MPa. By contrast, Eurocode 9 has a fatigue strength at 2×10^6 cycles of 14 MPa for a fillet-welded lap joint.

In spite of the reduced fatigue strength, use of adhesives has many advantages, including generally less labor cost. One of the great advantages for an adhesive joint is the elimination of welding-induced distortion. Therefore, it may be possible to use thinner plate if the thickness of plate selected is based on reducing welding distortion. A principle disadvantage is lack of strength in a fire. The adhesives referenced have strength only up to $121\text{ }^{\circ}\text{C}$ ($250\text{ }^{\circ}\text{F}$), but structural fire protection of aluminum is designed to prevent the aluminum from achieving a temperature of $230\text{ }^{\circ}\text{C}$ ($446\text{ }^{\circ}\text{F}$). Therefore, a significantly greater amount of fire protection insulation is required to protect adhesive joints from a fire compared to the insulation requirements for welded aluminum.

5.8 Summary

Fabricating structure with aluminum is similar to steel construction, but there are more difficulties involved. Several means of cutting aluminum are available but are generally not as efficient as steel cutting. Aluminum can be formed into different shapes, but heating is very difficult, so that compound curvature of plates should be avoided. Welding aluminum requires more joint preparation and cleanliness than is generally required for steel, and the need for shielding gas and somewhat slower welding speeds makes the process more expensive. Aluminum is more prone to distortion during welding, so more care is needed with welding procedures to reduce distortion. When distortions occur, they are more difficult to remove because of limitations on the use of heat on aluminum. The availability of extruded panels has the potential to reduce construction cost because many welds of stiffeners to plate are eliminated.

Aluminum Marine Structure Guide

Chapter 6

Riveting

Although once used as the primary method for fabricating aluminum vessels, riveting is seldom used today for fabricating primary hull structure except for very thin-hulled craft, such as canoes, and then it is used primarily for attaching secondary structure, such as thwarts. Riveting is also used for some light joiner work. Riveting was used in the early installations of aluminum deckhouses to steel hulls, where the aluminum was riveted to a steel coaming. The lack of skilled riveters in shipyards led to the adoption of swaged mechanical fasteners for that purpose.

The ABS Guide for Building and Classing High-Speed Craft (ABS, 2001) and the ABS Guide for Building and Classing High Speed Naval Craft (ABS, 2003) state that their requirements pertain to welded vessels only. The ABS Steel Vessel rules (Part 3, Chapter 1, Section 2, paragraph 1.3) state that the 1969 rules should be consulted for riveted hull construction. Those rules provided guidance for the size and spacing of rivets in heavy steel structure, not lightweight aluminum structure. The rules of Det Norske Veritas do not specifically mention riveted construction; therefore, special consideration must be made if a vessel built to those rules is to be riveted.

A principal advantage of using riveting instead of welding for joining aluminum is that there is no reduction in strength that comes from the heat of welding. Therefore, weight reduction can be made through higher design stresses. This is compensated for by the excess weight from the lap joints that are needed in riveted construction. The increase can be as much as 15 percent of the weight of the material compared to the general increase of 2.5 percent used for estimating the weight of welds.

Riveted construction can generally achieve closer tolerances because welding distortions do not exist. However, riveting is far more labor-intensive than welding, and there are few well trained riveters today for marine construction.

With steel construction, watertightness of rivet seams is obtained by mechanical upsetting of the edge of the plate using special tools with a pneumatic hammer. Because aluminum is softer, this method is not used. Instead, a sealing compound must be used between the plates being riveted to provide tightness.

6.1 Selection of Rivet Material

Anderson and Morton (1973) reported corrosion tests on riveted joints of 5456-H117 aluminum. Plates were riveted together with 1100 aluminum alloy rivets and exposed to flowing seawater and to a marine atmosphere 80 and 800 feet from the ocean for one year. Those exposed to the marine atmosphere experienced only light surface attack, with an average weight loss of 0.04 percent. Those exposed to filtered seawater flowing at 2 to 3 feet per second suffered edge corrosion and localized attack under the riveted lap joint, experiencing 1.42 percent weight loss. The 1100 alloy rivets showed poor corrosion resistance, experiencing small regions of pitting. Because the 1100 alloy has lower alloy content than the 5456-H117, the rivet

material contributed to the corrosion of the plate. The fact that the rivets were cold worked created local anodic sites that made the rivets susceptible to preferential corrosion attack.

Bieberich and Wong (1998) reported the results of another series of tests of the corrosion resistance of mechanical fasteners on aluminum. The tests were performed using bolts, not rivets, but the results should be applicable to riveted joints. The principal difference is that aluminum rivets are cold formed, which will lead to less corrosion resistance than bolts. Plates of 5083-H3 and 2519-T87 aluminum had bolts of Grade 8 carbon steel with a variety of coatings and bolts of 316 stainless steel fastened to them. The plates were exposed to a marine atmosphere 80 feet from the ocean for 2.5 years. All of the coated and uncoated carbon steel fasteners began to show significant corrosion, with the least corrosion on those coated with zinc plating, closely followed by zinc-nickel and then cadmium plated fasteners. The stainless steel bolts showed no signs of corrosion, but the plate had corroded under them, reducing the applied torque in the bolts.

These tests demonstrate that the alloy selected for rivets should have a composition that is as close to the material being joined as possible. Any difference in electrical potential between the two materials in seawater will lead to the corrosion of one or the other.

Today, mechanical fastening of aluminum is used extensively in the aerospace industry, and there are a multitude of fasteners available. Caution is needed if such fasteners are to be used for ships and craft, as the aerospace fasteners are often of an aluminum alloy unsuited for marine service. If such fasteners are used, they should be of a suitable marine aluminum alloy to avoid corrosion problems.

6.2 Guidance for Riveted Design

Guidance for riveting and mechanical fastening can be found in classification society rules and in naval specifications. That guidance will be summarized here.

6.2.1 U.S. Navy Requirements

The requirements for riveting and mechanical fastening of the U.S. Navy can be found in Military Standard 1689 (MIL-STD 1689). The material requirements for fastening aluminum to aluminum are shown in Table 6-1.

Requirements for swaged fasteners (lockpins) are contained in specification MIL-P-23469. A fastener that meets that specification is shown in Figure 6-1. The fastener is similar to a bolt, except the threads are concentric, not in a spiral. The fastener has two areas of threads, a short section close to the head that is used to hold the sleeve, and a longer section at the end that is gripped by the hydraulic device that secures the fastener. The sleeve is shown as slipped over the fastener. A special hydraulic unit draws the fastener, pressing the sleeve tightly into the material being joined and pressing the materials close together. Then the unit compresses the sleeve to hold it onto the fastener. Finally, the unit pulls on the fastener, breaking it at the notched section. This type of fastener is superior to a nut and bolt for several reasons. Once set, the fastener will not loosen from vibration. Also, the threads on aluminum bolts are weak and are easily stripped if the nut is cross-threaded or over-torqued. Commercial fasteners that are

equivalent to the military specification are readily available. The specification covers a number of alloys of corrosion resistant steel, carbon steel, and aluminum. For marine use, the 6061 alloy aluminum fasteners should be used.

Table 6-1 Materials for Mechanical Fasteners (MIL-STD 1689)

Application	Type of fastener	Material
Where required for strength and where exposed to the weather, seawater, or wet spaces.	Rivet	Aluminum
	Lockpin	CRES
	Bolt and nut	CRES
Where required for strength and where not exposed to the weather, seawater, or wet spaces.	Lockpin	MS
	Bolt and nut	MS
Where strength is not a special consideration	Rivet	Aluminum
	Lockpin	Aluminum
	Bolt and nut	Aluminum
Nonstructural applications where rivet diameter is less than 5/16 inch and material thickness does not exceed 1/8 inch.	Rivet	Aluminum



Figure 6-1 Swaged fastener (<http://www.alcoa.com/fastening>).

The rivets are specified to meet MIL-R-5674, which has now been superseded by NASM5674, which is published by the Aerospace Industries Association of America. The specification covers a number of aluminum alloys, primarily used in aerospace work. For marine use, only the 5056-H32 alloy rivets should be used.

6.2.2 Classification Society Requirements

The ABS rules (Part 2, Chapter 5, Section 11) calls for rivets to be in accordance with ASTM specification B316, Standard Specification for Aluminum and Aluminum-Alloy Rivet and Cold-Heading Wire and Rods. The specification covers aluminum in the following alloys for rivet wire and rod:

- 1100
- 2017

Aluminum Marine Structure Guide

- 2024
- 2219
- 3003
- 5005
- 5052
- 5056
- 6061
- 7050
- 7075
- 7178

The ABS rules are not otherwise specific about the alloys to be used.

6.2.3 Aluminum Design Manual

Guidance for the design of riveted aluminum structure can be found in the Aluminum Design Manual of the Aluminum Association (Aluminum Association, 2005). However, some adaptation of the guidance is needed when applied to marine structures because the design manual was formulated primarily for structures such as buildings and bridges. As such, allowable design stresses are developed considering the design loads and their probabilities of occurring, and in fabrication practices for civil engineering structures, which vary from those of ships and boats.

The Aluminum Design Manual contains the guidance for design of riveted joints in two formats, allowable stress design and load and resistance factor design (LRFD). Because the latter contains explicit consideration of the factors to be applied to loads as separate from factors to be applied to allowable stress levels, better correspondence can be made to methods of design of marine structures, even though these have not been formally cast in a LRFD format.

A riveted joint may fail in four ways. The material being joined may fail by elongation of the rivet hole, shear rupture of the material between the holes, or by fracture of the net section. The rivets may fail in shear. In the allowable stress design format, the aluminum design specifications provide a factor of safety of 2.34 for fastener shear and 1.95 for the other modes of failure. A higher factor of safety is provided for the rivets because they are more prone to errors occurring during fabrication, such as over driving or under driving.

In the LRFD format of the Aluminum Design Manual, the design stress is designated as ϕF_L . This design stress is to be equal to or greater than the stresses computed from the loads acting on the structure in accordance with the applicable building code or performance specification. Accordingly, the loads specified by a classification society or determined through testing or hydrodynamic analysis are consistent with this design formulation.

The design bearing stress on rivets and bolts is given as $\phi F_L = 2.0 \phi_U F_{TU}$, where $\phi_U = 0.85$ and F_{TU} is the ultimate tensile strength of the material that is joined by the rivet. This assumes that the center of the rivet hole is at a distance, s , from the edge that is least twice the fastener diameter, d , and in no case less than 1.5 d . For the intermediate cases where the spacing

is between 1.5 d and 2.0 d, the design stress is to be reduced by the ratio $s/2d$. This criterion ensures that for a single rivet, the block shear strength equals or exceeds the bearing strength.

The minimum spacing of rivets is 3 times the rivet diameter. This criterion was developed for compression members so that the components do not buckle between points of attachment. Holes for rivets should be no more than 1.04 times the nominal diameter of the rivet.

The design bearing load on the rivet is the design bearing stress times the effective bearing area of the rivet. The bearing area is the nominal hole diameter times the rivet's effective length. For countersunk rivets, the effective length is the thickness of the material minus one-half the depth of the countersink.

The design shear load on the rivet is the effective shear area of the rivet times the design stress for the rivet. The effective shear area of the rivet is its cross-sectional area. The design stress equals ϕF_{SU} , where $\phi = 0.65$ and F_{SU} is the minimum shear ultimate strength of the rivet, as given in Table 6-2.

Table 6-2 Ultimate Shear Strength for Rivets

Alloy Designation Before Driving	Minimum Shear Ultimate Strength, F_{SU} ¹	
	MPa	ksi
2017-T4	225	33
2024-T42	255	37
2117-T4	180	26
2219-T6	205	30
5056-H32 ²	179	26
6053-T61	135	20
6061-T6	170	25
7050-T7	270	39
7075-T6	290	42
7075-T73	280	41
7178-T6	315	46

1. Unless otherwise indicated, from Aluminum Design Manual, with reference cited to ASTM B316.
2. From Czyryca and Vassilaros (1972). The strengths cited are average strengths, which have been decreased by 15 percent to obtain the minimum shear strength.

The commentary to the aluminum LRFD specification provides the derivation of the value of $\phi = 0.65$ from computing the equivalent factor from the allowable stress design criteria. The LRFD development procedures involve adjusting the various factors so that a consistent value of the target reliability index, β_T , is reached. The value of β_T is determining the value that would be achieved in a conventional allowable stress design specification. Assuming that the average ultimate shear strength is 15 percent greater than the specified minimum strength, and the coefficient of variation in the strength as well as in the cross-sectional area is 0.10, it was found

for a ratio of dead load to live load of 0.2, the design reliability index, β , is 3.9. A value of $\phi = 0.65$ was then found to give a value of $\beta = 4.0$.

The net section area for a member in tension is the sum of the products of the thickness and the least net width of each element. The net width for a chain of holes extending across a part in a diagonal or zigzag line is the gross width minus the diameters of all of the holes plus, for each gage space in the chain, the quantity $s^2/4g$, where:

s = longitudinal center-to-center spacing (pitch) of any two consecutive holes.

g = transverse center-to-center spacing (gage) between fastener gage lines.

This is illustrated in Figure 6-2 where the net area, A_{net} is given by:

$$A_{net} = t \left(b - 2d + \frac{s^2}{4g} \right)$$

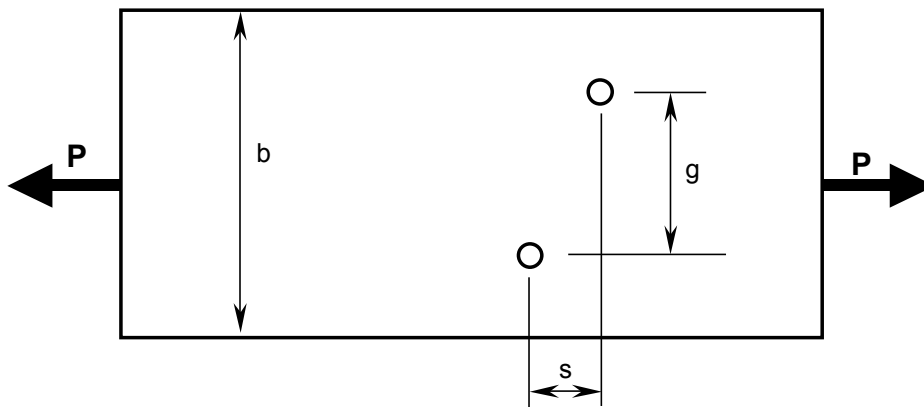


Figure 6-2 Strap in tension.

For the angle shown in Figure 6-3, the net width is found by flattening the section to find:

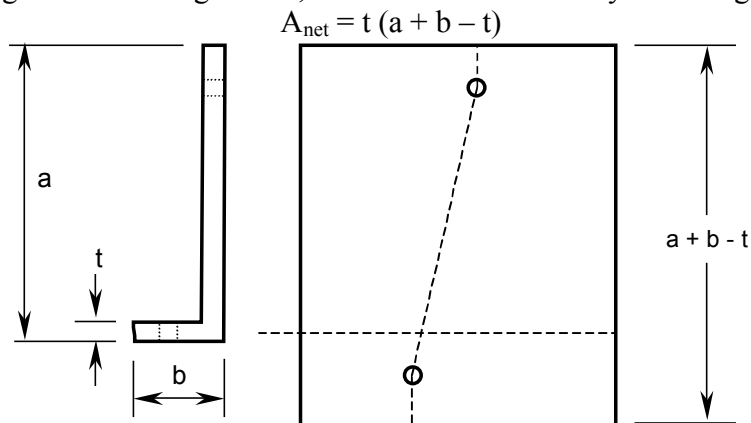


Figure 6-3 Angle in tension.

6.3 Fatigue of Riveted Joints

The Aluminum Design Manual provides guidance for the fatigue of riveted joints as shown in Figure 6-4. The fatigue classification given in Table 6-3 depends on the loading of the joint, defined by the ratio of the minimum stress to the maximum stress, where compressive stresses are considered negative. The meaning of the fatigue classification will be explained in Chapter 9. However, it is interesting to note that for the symmetric riveted joint in alternating tension and compression, the fatigue classification is Class B, which is equivalent to a butt weld in plate or in a structural member, and having a fatigue life 2×10^6 cycles at a stress range of 44.9 MPa (6.5 ksi). By contrast, a welded symmetric lapped weld is given a fatigue classification of E, which has a fatigue life 2×10^6 cycles at a stress range of 16.4 MPa (2.4 ksi).

Czyryca and Vassilaros (1972) provide guidance for the fatigue design of riveted joints in aluminum. Because fatigue failures usually occur at points of stress concentration, rivet holes are a frequent point of crack initiation. However, the complex stress distribution makes fatigue analysis by applying stress concentration factors to smooth specimen data or use of fatigue data for specimens with notches or holes does not result in reliable results. Rather, data from fatigue testing of rivet joints, such as that cited above is necessary.

90 percent of the fatigue failures in mechanical joints occur at one of the outer holes, the remainder are usually a result of fretting near one of the outer, most highly loaded holes. The following guidance results from studies of mechanical joints in aircraft structures:

- Variations in joint design are more significant than changes in the alloy used.
- Joints of high static strength do not necessarily have high fatigue strength.
- Fatigue strength of a joint increases with the number of fasteners used, but not in proportion to the static strength.
- In a multi-row lap joint, the edge rivets carry the highest load; therefore, as the number of rivets is increased, the fatigue strength is not increased proportionately.
- The greatest fatigue strength is obtained with large diameter rivets placed close together and close to the edge of the structural member, a configuration that produces lower static strength.
- Details such as poor rivet patterns, dimpling, countersinking degrade fatigue strength.

Table 6-3 Fatigue Classification of Riveted Joints (Aluminum Design Manual)

Joint Type	Load Ratio	Loading	Fatigue Classification
Symmetric (Detail 7)	$R \leq 0$	Alternating tension and compression	B
	$0 < R < 0.5$	High mean stress, little variation, either fully tensile or fully compressive.	D
	$0.5 \leq R$	Low mean stress, much variation, either fully tensile or fully compressive.	E
Asymmetric (Detail 8)	All ratios	All loading conditions.	E

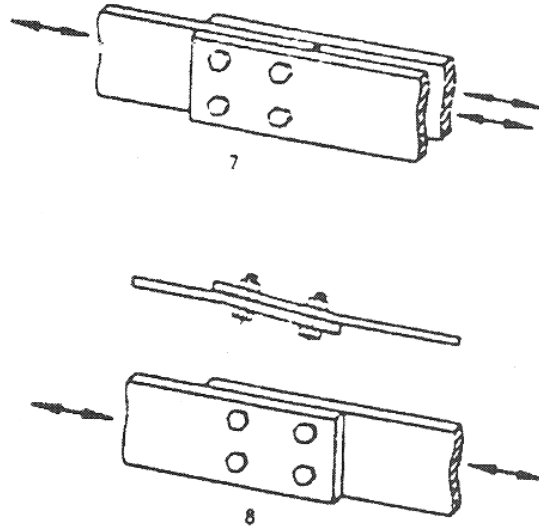


Figure 6-4 Fatigue classification of riveted joint.

6.4 Summary

Riveting can reduce weight because higher stress levels can be used. This weight reduction is partially offset by the weight of the lap joints used in riveted construction. Riveted construction has less distortion than welded construction, but the cost of fabrication is greater. Unless joints are symmetric, with an associated increase in weight, riveted joints have low fatigue strength. A sealing compound is needed in welded seams to provide watertightness. The disadvantages generally outweigh the advantages and riveting is seldom used today in marine structures.

Chapter 7

Joining Aluminum to Steel Structure

7.1 Introduction

Aluminum has been used for more than 100 years in the deckhouses and superstructures of ships, particularly combatant ships and passenger vessels in order to reduce high topside weight and improve stability. A review of that history was given by Sielski (1987). That history will be discussed here, with an emphasis on problem areas to ensure that those problems will be avoided in future construction. Many of the past problems were due to poor material selection, which can be avoided by use of approved marine aluminum alloys, but others were design problems involving poor structural details or improper mixing of metals.

7.2 Riveted Joints

The U.S. Navy began using aluminum for the deckhouses of destroyers in 1936. The structure was transversely framed with steel, and aluminum panels were riveted to the frames and to each other. In some cases, plating was mixed, with steel used in some locations, especially where a small amount of armor protection was desired. A detail of the aluminum-to-steel connection is shown in Figure 7-1.

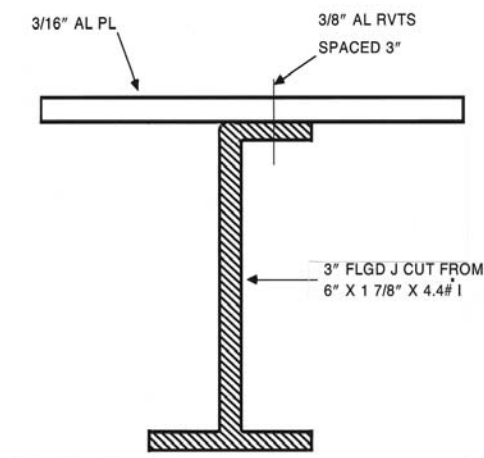


Figure 7-1 Typical mild steel frame with aluminum plate in U.S. Navy DD 693 Class destroyers.

This practice of using steel framing with aluminum and steel plate was used by the U.S. Navy for destroyer deckhouses until 1948. Following the war, the development of aluminum welding had an effect, and in 1948 the new destroyer leaders, the USS *Mitcher* (DL-2) Class had aluminum deckhouses that were entirely welded, including the transversely oriented frames. Although the *Dealy* (DE-1008) Class started with steel deckhouses, weight growth led to an aluminum deckhouse on USS *Courtney* (DE 1021) when contracted in 1953 and on subsequent ships of the class. From then until the mid-1980s, all new U.S. Navy combatant ships (destroyers, destroyer escorts, frigates and cruisers) had aluminum for the majority of their

deckhouses. In addition, aluminum was used for the deckhouse in landing ships and for the islands of aircraft carriers and amphibious assault ships.

The hulls of the ships were of steel, and the aluminum was mechanically fastened to the steel at a coaming similar to that in Figure 7-2. With this type of mechanical connection between steel and aluminum, insulating material must be placed between the two metals to avoid galvanic corrosion. Typically, rubber electrical tape was used. However, this insulation often broke down, and corrosion would occur at these joints, similar to that shown in Figure 7-3. The joint would absorb moisture, and alternate drying and wetting with seawater would build up the concentration of salt deposits, and so any breakdown of the insulation, especially at points of stress concentration, would lead to rapid corrosion. This problem was exacerbated in the earlier ships because some of the aluminum plate was prone to exfoliation. Dye and Dawson (1974) described many of the maintenance problems that occurred in these aluminum deckhouses, and they offered recommendations for repairs.

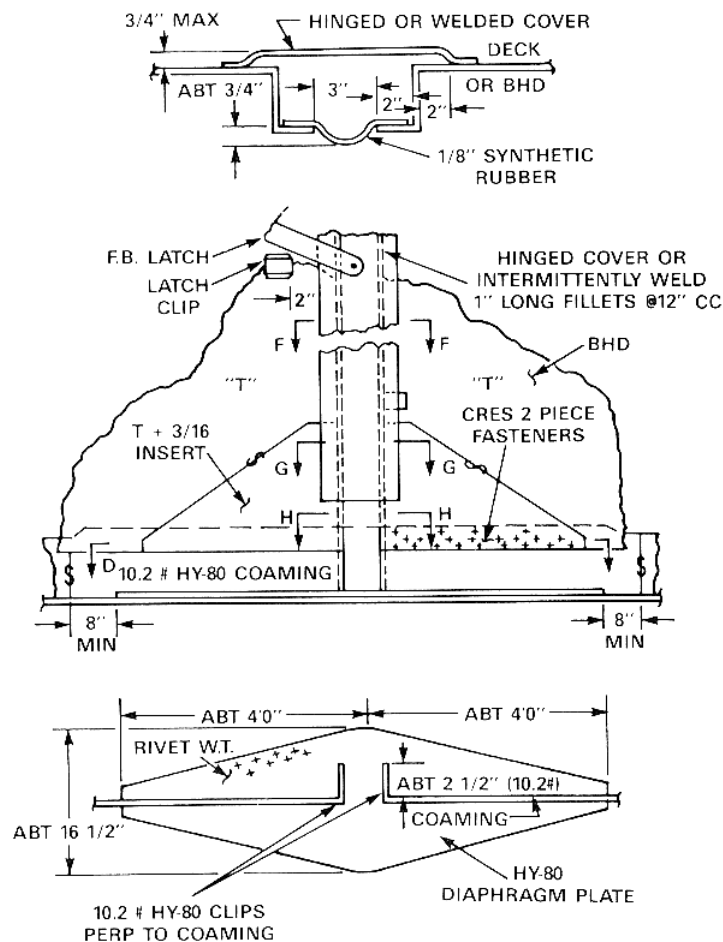


Figure 7-2 Riveted connection of an aluminum deckhouse to a steel deck at an expansion joint.

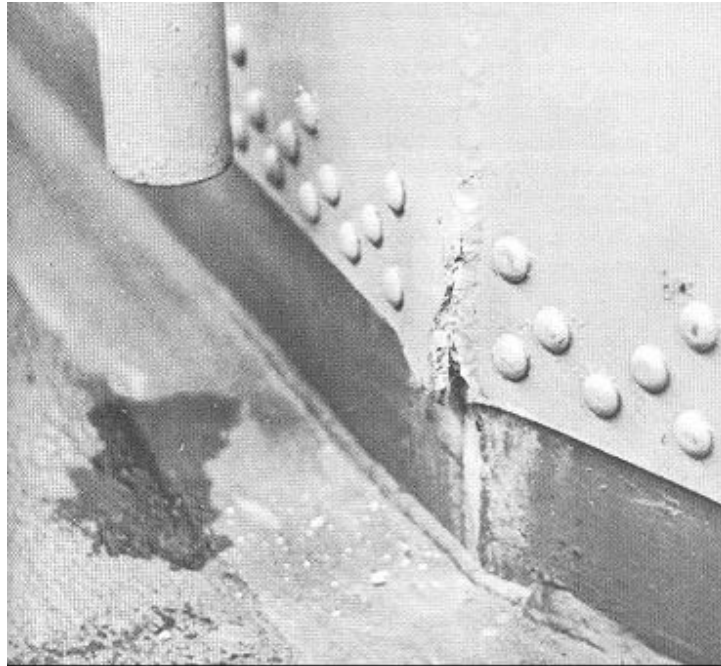


Figure 7-3 Riveted connection with corrosion in the aluminum (Dye and Dawson, 1974)

7.3 Bimetallic Joints

The problem of corrosion at the joint between the steel and aluminum was solved by the development of the bimetallic joint in the mid-1960s (McKenney and Banker, 1971). The joint is actually a trimetallic joint, as two different grades of aluminum are used. The first joints used had a 6.35-mm (0.25-inch) layer of 5456 aluminum bonded to a 9.53-mm (0.375-inch) layer of 1100 aluminum, which was bonded to a 19.05-mm (0.75-inch) layer of A516 Grade 55 steel. This initial development of the bond used explosive bonding technology, but today, several manufacturers produce this joint, and some use roll bonding. A section through a bimetallic joint is shown in Figure 7-4.

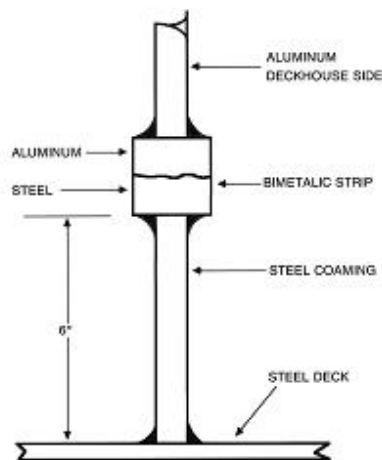


Figure 7-4 Bimetallic connection of aluminum deckhouse to a steel deck.

The bimetallic joint would seem to be a poor solution to the galvanic corrosion problem between steel and aluminum. Its success, however, comes from the clean bond that does not trap moisture and can be preserved with the proper coatings. Corrosion tests were performed in the late 1960s by E.I du Pont de Nemours Co., the developers of the bimetallic joint, as reported by McKenney and Banker. Uncoated samples were set out in the spray zone of the beach at Wrightsville Beach, North Carolina for 12 and 27 months, as shown in Figure 7-5.

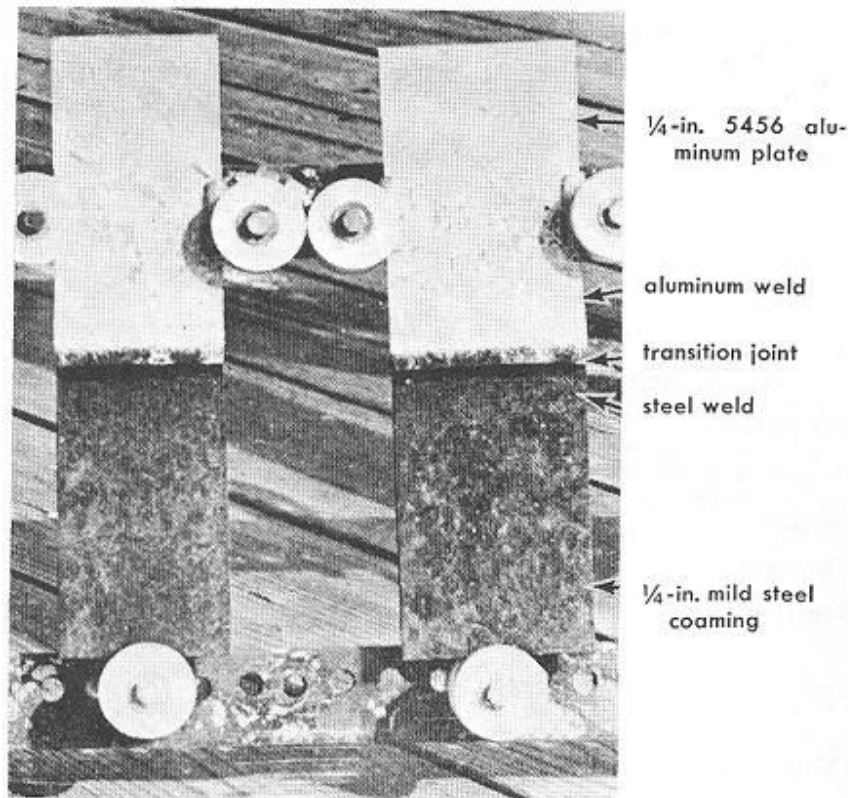


Figure 7-5 Bimetallic joints exposed to seawater spray at Wrightsville Beach, North Carolina (McKenney and Banker, 1971).

The results of these tests were very favorable. Microscopic examination of the test samples, Figure 7-6, showed that when the aluminum began to corrode at the interface, a slight penetration forms. However, rather than acting as a point of high ion concentration and accelerating corrosion, as anticipated, the area quickly filled with hydrated aluminum oxide, the corrosion product. This product occupies a larger volume than the aluminum consumed during the corrosion process, sealing the aluminum-steel interface from the corrosive environment and significantly reducing the rate of corrosion.

Although the unpainted tests showed moderately good corrosion resistance, the bimetallic joint should still be preserved when used, and should never be used in a situation where the joint is totally immersed in seawater. When used in areas where standing seawater can accumulate, such as inboard of doorways to the weather, corrosion will still occur on the aluminum, although the corrosion of the bimetallic joint will be as has been shown to be minimal.

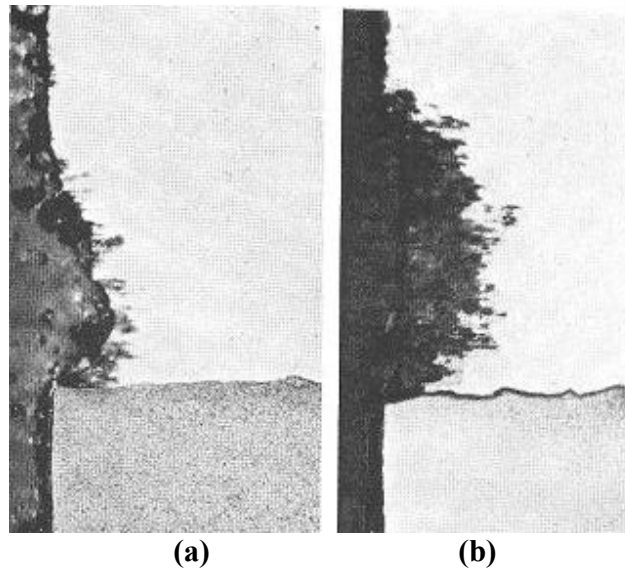


Figure 7-6 Photomicrographs illustrating corrosion penetration into uncoated bimetallic joint after (a) 12 months and (b) 27 months (McKenney and Banker, 1971).

McKenney and Banker continued the corrosion testing of the joint on painted samples that had scratches made through the paint at the bimetallic joint. After 27 months of exposure, the only indication of corrosion was a small pinpoint area beneath the scratch. There was not the general breakdown of the coating and accelerated corrosion of the aluminum as is generally seen in mechanically fastened joints between aluminum and another metal, such as seen in Figure 7-3.

The bonds in the bimetallic joint were tested for strength using a ram forced through a hole bored into the joint using a fixture and specimen similar to that shown in Figure 7-7. The weakest area of the joint occurred in the 1100 aluminum in samples that were tested after welding. This area had an ultimate tensile strength of 93 MPa (13.5 ksi). When a 25.4-mm (1-inch) wide strip of the bimetallic joint had a 6.35-mm (0.25-in) plate of 5456 aluminum welded on one side, and a plate of mild steel of the same thickness, the failure in tension was in the heat affected zone of the 5456 plate at an ultimate strength of 356 MPa (51.6 ksi). This strength is greater than the nominal 290 MPa (42 ksi) ultimate strength of welded 5456-H116, and even greater than the specified 317 MPa (46 ksi) ultimate strength of the base metal. Perhaps the restraint imposed by the thick bimetallic strip increased the strength of the joint, or the actual plate used had properties far above the specified minimum.

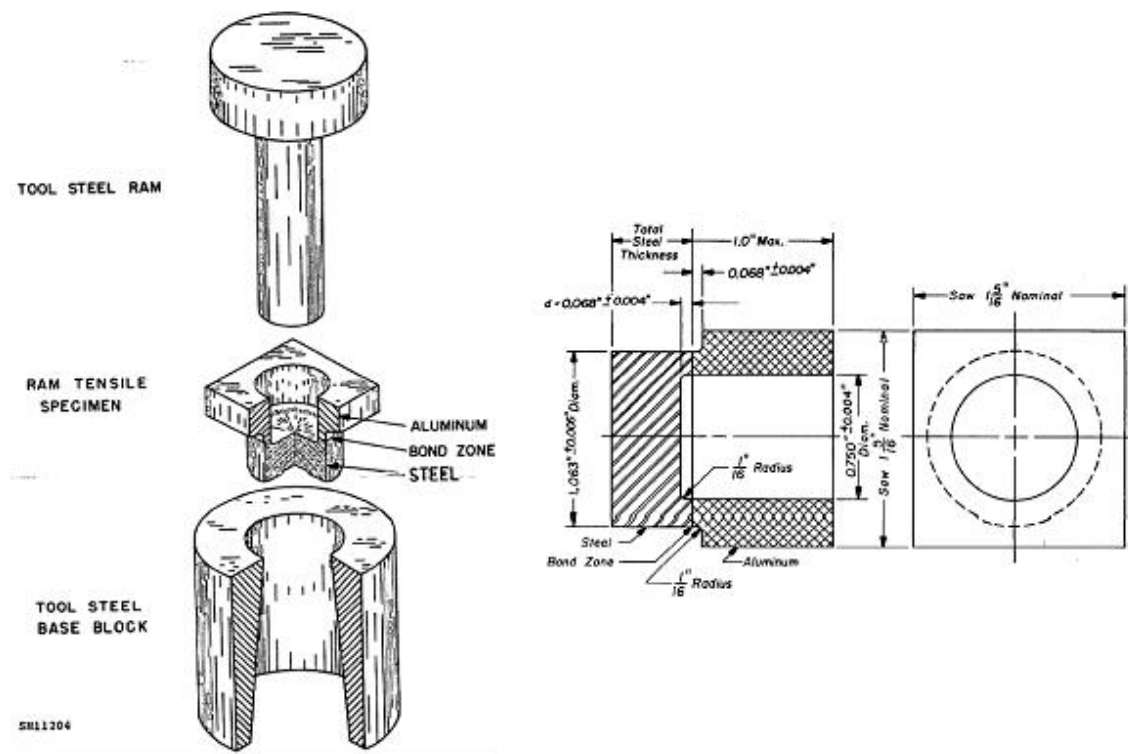


Figure 7-7 Fixture and test specimen for tensile test of bimetallic joint (MIL-J-24445A).

Based on these tests, McKenney and Banker recommended that a ratio of four-to-one be used in the design of bimetallic joints. That is, the bimetallic strip should be four times wider than the thickness of the plates being joined.

Fatigue testing was conducted by McKenney and Banker on bimetallic joints fabricated with 6.35-mm (0.25-in) thick 5456 aluminum and HY-80 steel welded to a 25.4-mm (1-inch) wide strip of the bimetallic joint. The samples tested were machined to a dog bone shape two inches wide. Fatigue failure was always in the heat affected zone of the aluminum plate. Testing was conducted at stress ranges of 138, 110, and 91 MPa (20.0, 16.0 and 13.24 ksi), with failures at 0.395×10^6 , 0.721×10^6 , and 1.267×10^6 cycles, respectively.

The U.S. Navy accepted the bimetallic joint and specification MIL-J-24445 was issued for the material in 1971, and was last revised in 1977. The specification requires fatigue testing at the following stress ranges and minimum stress cycles:

- 138 MPa (20.0 ksi) — 175,000 cycles
- 110 MPa (16.0 ksi) — 650,000 cycles
- 90 MPa (13.0 ksi) — 1,000,000 cycles

The geometry of the test specimen for the MIL-J-24445 fatigue testing is shown in Figure 7-8. Note that the geometry includes the welds of the steel and aluminum plate to the bimetallic joint.

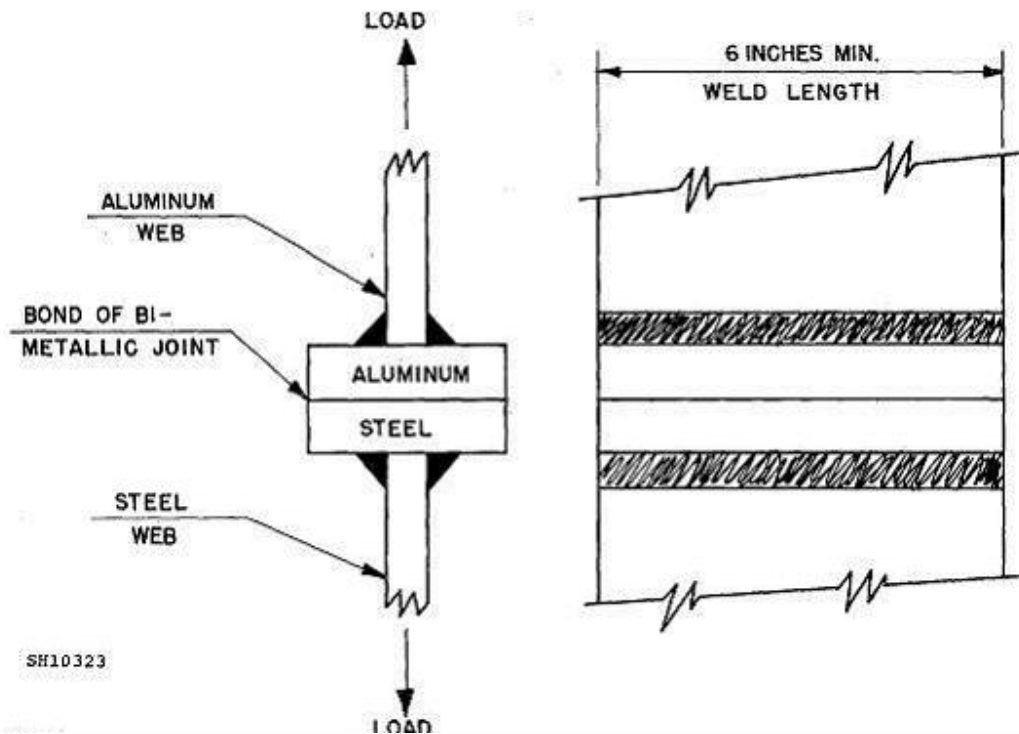


Figure 7-8 Fatigue test specimen geometry for bimetallic joint required by MIL-J 24445.

The above fatigue data are shown in Figure 7-9. Because these values are specified minima, the values can be considered as the lower limit probability values as with other design S-N curves. The class A and class B fatigue curves of the Aluminum Association fatigue curves, and fatigue curve 69-7 of Eurocode 9 are plotted on Figure 7-9. Either an Aluminum Association Class B or a Eurocode 9 class 69-7 S-N curve would be appropriate for fatigue analysis, even though those curves have significantly higher fatigue lives than would ordinarily be expected for the weld of a plate to a bar.

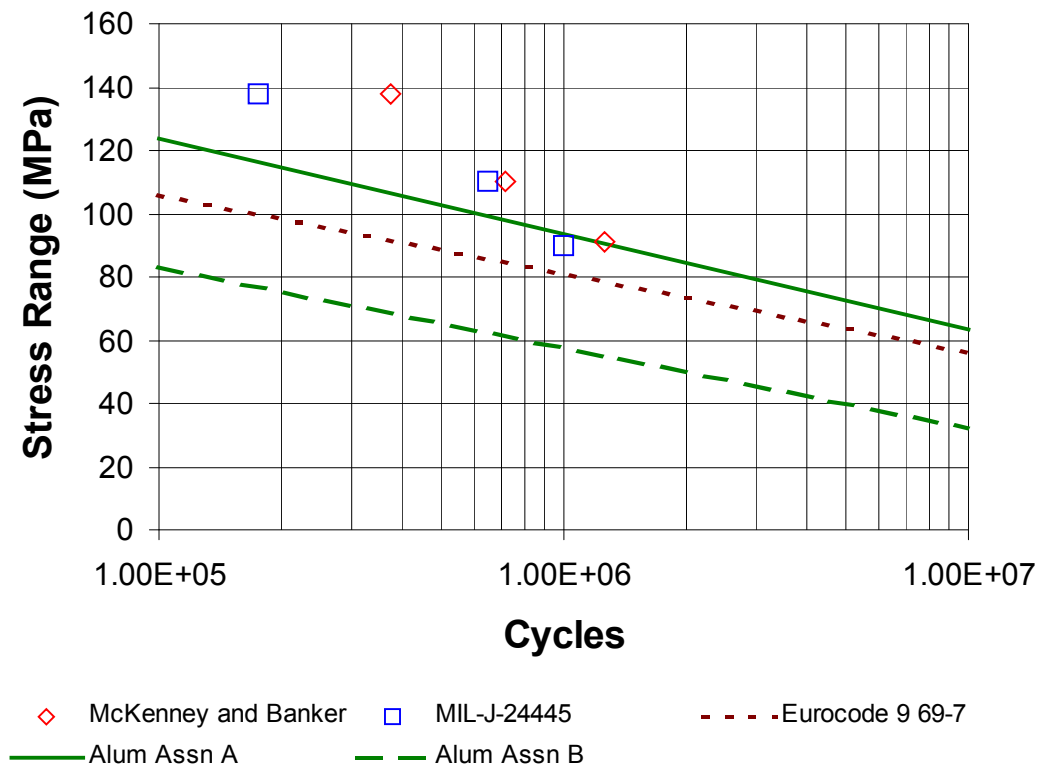


Figure 7-9 Fatigue strength of bimetallic joint.

Extrapolation of the fatigue specifications indicates a stress of about 70 MPa (10.2 ksi) at 2×10^6 cycles and slightly less than a category A detail for the Aluminum Association fatigue curves. Therefore, the fatigue strength of the joint is more than equivalent to a butt weld in aluminum plating.

In making the transition from the steel to the aluminum structure, the bimetallic strip is introduced at the base of the house sides and ends and at all bulkheads, longitudinal and transverse. Generally, the steel coaming should be between 100 and 200 mm (4 to 8 inches) high to keep the joint out of standing water. Where vertical frames on the house sides or bulkheads meet the deck, either two strips are used for the web and flange, or a pad slightly larger than the cross section of the frame is used. In no cases should the bimetallic strips or pads be welded directly to the steel deck.

Where the bimetallic strip ends at the ends of a deckhouse, curved brackets, or fashion plates, are used to provide the transition of the longitudinal hull girder bending stress from the deckhouse to the hull. There should not be an abrupt change in the bimetallic strip. Rather, the aluminum fashion plate should gradually curve to meet the bimetallic strip as shown in Figure 7-10. The bimetallic strip extends a little beyond this termination of the aluminum, and the end of the coaming is curved to the deck. If there is a faceplate on the fashion plate, it should be tapered before it meets the bimetallic strip and should not have a bimetallic strip imbedded in it, as the stress concentration from the added detailing will cancel any nominal increase in strength.

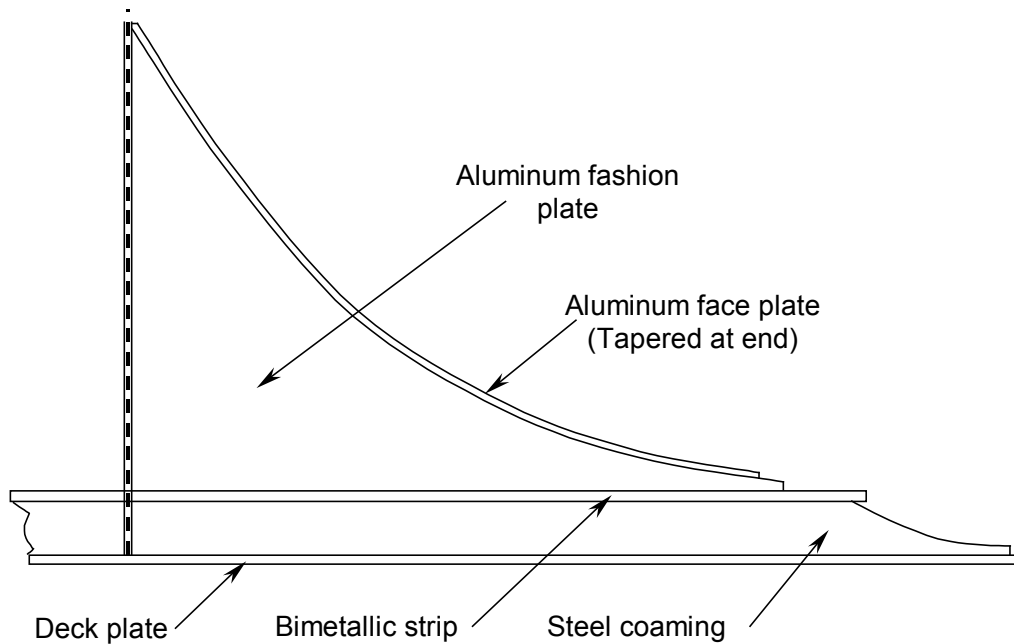


Figure 7-10 Typical fashion plate at ends of a deckhouse.

7.4 Deckhouse-Hull Interaction

7.4.1 Expansion Joints

The aluminum deckhouses of the early ships were not designed to be an integral part of the hull girder. The reduced elastic modulus of aluminum compared to steel means that at an evenly strained joint, the stress in the aluminum is one-third that of the steel. To reduce stress in the deckhouses even farther, the deckhouses were not made longitudinally continuous, but had expansion joints at several locations along their lengths such as shown in Figure 7-2. The short distance between the forward and after portions of the aluminum structure was insufficient to be able to produce a generous radius at the base of the expansion joint, and cracking at that location in both the aluminum and steel structure as shown in Figure 7-11 was common.

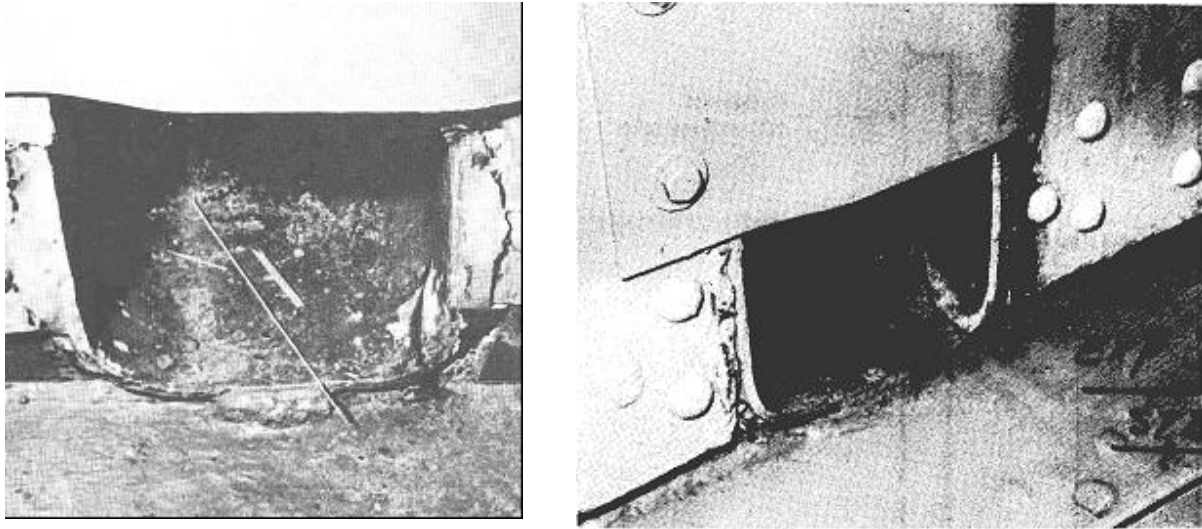


Figure 7-11 Cracking at the base of expansion joints.

Alternative designs for reduction of the stress concentration at the base of an expansion joint are shown in Figure 7-12 (Chapman's Moustache) and Figure 7-13 (attributed to Prof. N. Sivers). These designs were shown to have low stress concentrations if designed using finite element analysis but were not used in any ship construction. (Designs contributed by Professor Sergei Petinov, St. Petersburg Polytechnic University.)

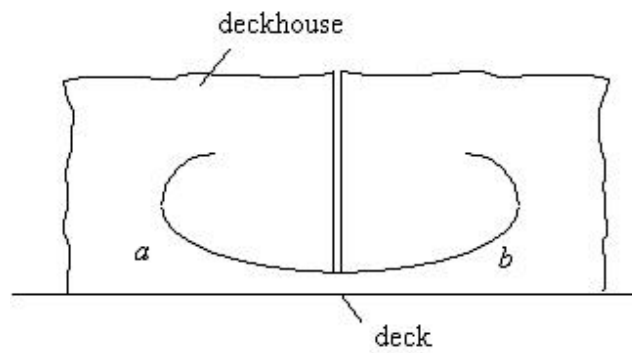


Figure 7-12 Suggested detail at the base of an expansion joint.

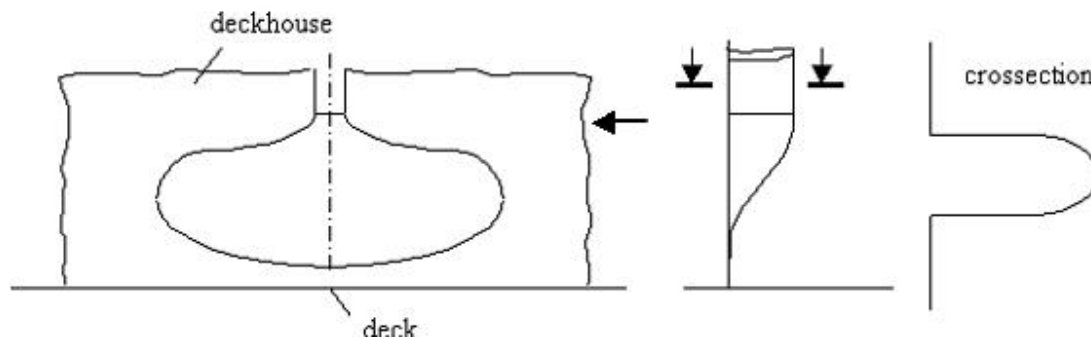


Figure 7-13 Indent at the base of an expansion joint.

7.4.2 Calculation of Stress in a Deckhouse

A review was made by deOliveira (1983) of the various methods that have been developed to estimate the stresses in a deckhouse on top of a ship's hull. Two basic methods of analysis have been used in the past to determine the stresses in the hull and in the deckhouse. The 2-beam theories consider the hull and the deckhouse to be separate beams analyzed in accordance with classic beam theory. The plane stress theories assume that the hull and deckhouse are thin flat members in which there is a state of plane stress, which can be analyzed with a stress function and the equations of the theory of elasticity. These methods generally lead to complex numerical analysis, including that of Johnson (1957), who developed a solution based on plane stress theory. That solution was simplified for use in design by Kammerer (1966), and Kammerer's method was used extensively for the analysis of naval ships until the advent of finite element methods. Kammerer was able to use computer-based analysis to make a systematic analysis of all of the basic parameters that Johnson had considered that influence deckhouse-hull interaction, the most important of which were the stress factor, modulus of elasticity factor, and shear lag factor.

The analysis of Johnson assumed that the length of the deckhouse was symmetric about midships. To overcome that limitation, Kammerer introduced a definition of effective length of deckhouse, l_e , defined as:

- If the deckhouse extends at least $0.25 L$ both forward and aft of midships, use the full length of the deckhouse.
- If the deckhouse extends no more than $0.15L$ either forward or aft of amidships, take the effective length of the deckhouse to be twice that of the shorter part.
- If the minimum longitudinal extent either forward or aft of midships is between $0.25 L$ and $0.15 L$, take the effective length as $1/2$ of its actual length plus the length of the shortest part forward or aft of midships.

Where the deckhouse is two levels high, but the lengths of the levels are unequal, l_e is the average of the effective lengths of each level.

Kammerer's method involves the computation of the combined moment of inertia of the hull with the effective area of the deckhouse amidships. The computation is carried out in a tabular manner similar to the computation of hull girder inertia and section modulus. The

effective area of each portion of the deckhouse is determined by multiplying the area of that portion by three factors. The first factor, K_1 , is a linear factor based on a trapezoidal distribution of stress in the deckhouse, with $K_1 = 1.0$ at the strength deck and $K_1 = \sigma_T / \sigma_D$ at the top of the deckhouse. σ_T / σ_D is the ratio of the stress at the top of the deckhouse, σ_T , to the stress at the strength deck, σ_D , and is found using Figure 7-14 through Figure 7-19 as will be explained below.

Factor K_3 is the ratio of the elastic modulus of the deckhouse to the elastic modulus of the hull. For an aluminum deckhouse on a steel hull, $K_3 = 10.3 \times 10^3 \text{ ksi} / 30.0 \times 10^3 \text{ ksi} = 0.434$. Factor K_4 is a reduction in effective area from shear lag based on the ratio of the width of the deckhouse to the effective length and is determined using Figure 7-20.

The ratio σ_T / σ_D can be computed for single-level and two-level deckhouses. For a single level deckhouse, the ratio of effective length to ship length, l_e/L , is computed. Using Figure 7-14, the Factor B is determined based on l_e/L and the length of the ship. With the Factor B known, Figure 7-15 is entered with the width of the deckhouse, b , to determine the ratio σ_T / σ_D . Figure 7-14 and Figure 7-15 are based on an assumption that the height of the strength deck above the neutral axis of the hull, C_H , is 15 feet. Figure 7-16 is used to determine a correction factor, K_2 , by which the ratio σ_T / σ_D from Figure 7-15 is multiplied to obtain the ratio σ_T / σ_D . For a two-level deckhouse, the same procedure is followed using Figure 7-17 through Figure 7-19.

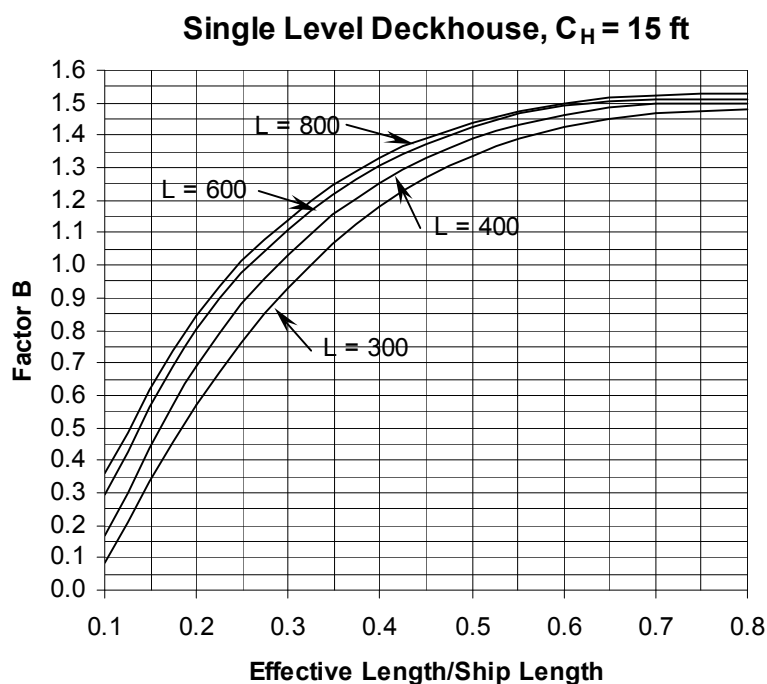


Figure 7-14 Factor B vs. effective length for single level deckhouse (Kammerer, 1966)

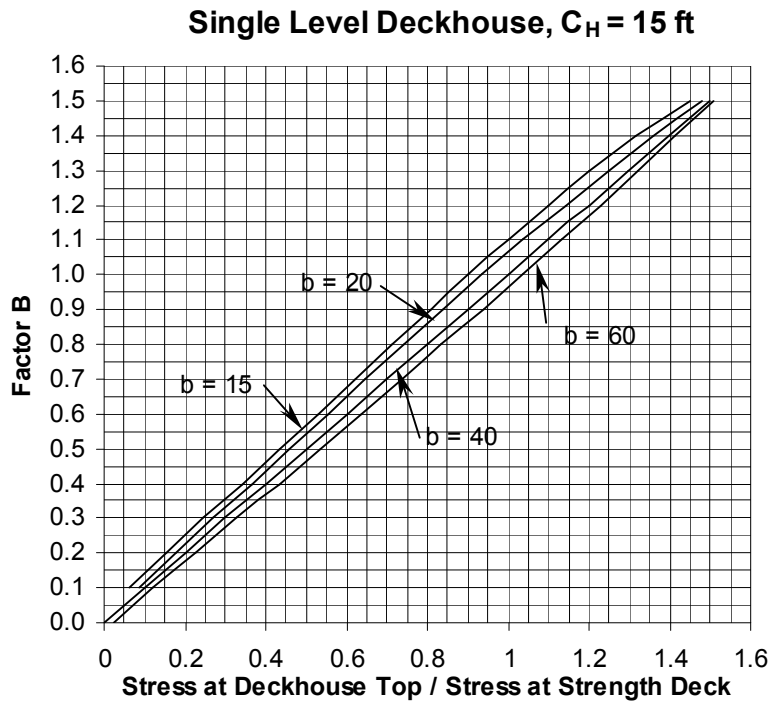


Figure 7-15 Stress ratio for a single level deckhouse, height above hull neutral axis 15 feet (Kammerer, 1966).

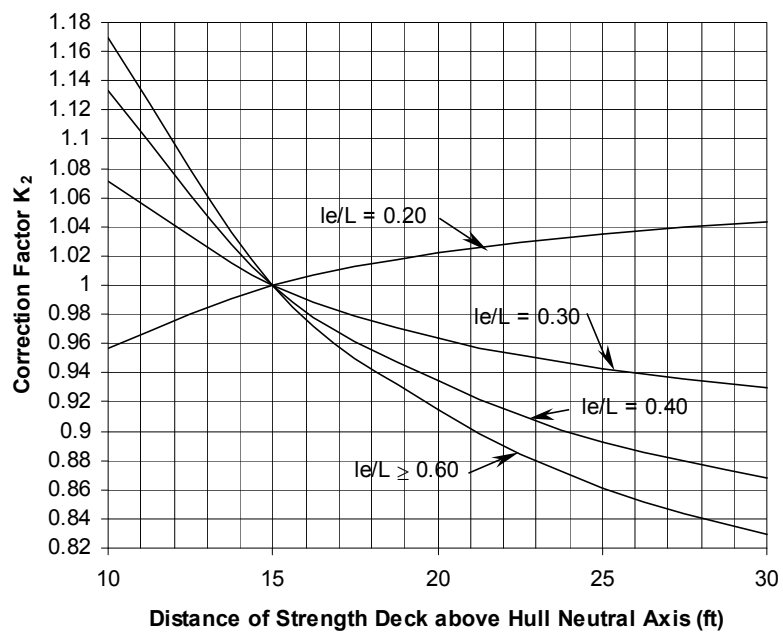


Figure 7-16 Correction factor for height of strength deck above hull neutral axis for single level deckhouse (Kammerer, 1966).

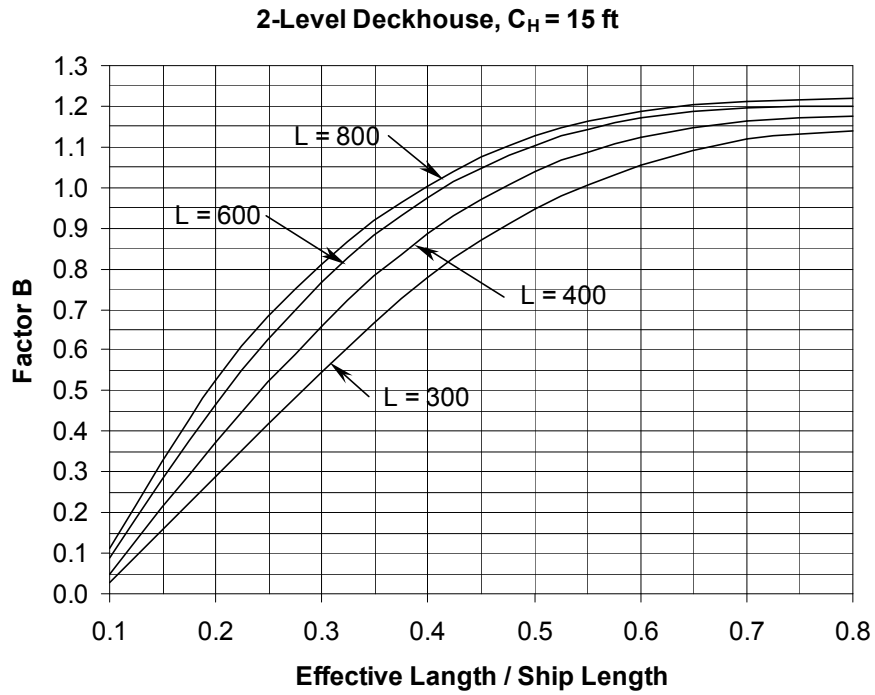


Figure 7-17 Factor B vs. effective length for 2-level deckhouse (Kammerer, 1966).

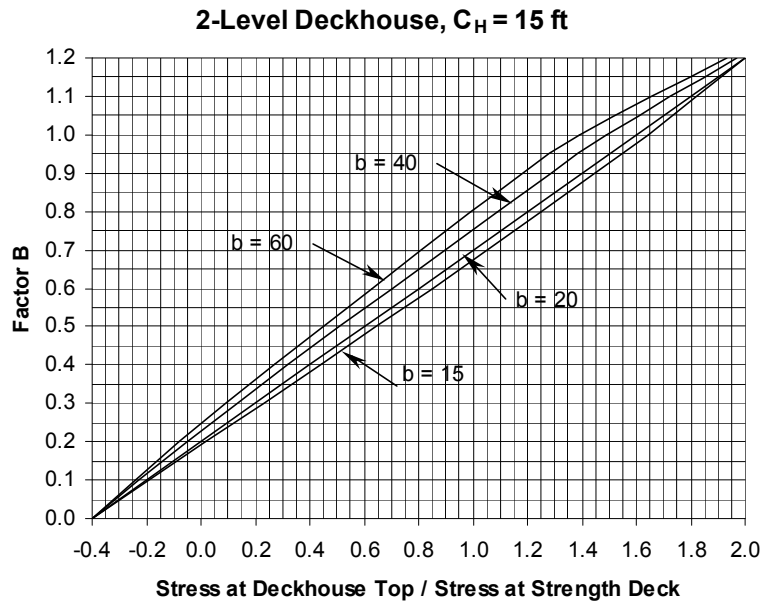


Figure 7-18 Stress ratio for a 2-level deckhouse, height above hull neutral axis 15 feet (Kammerer, 1966).

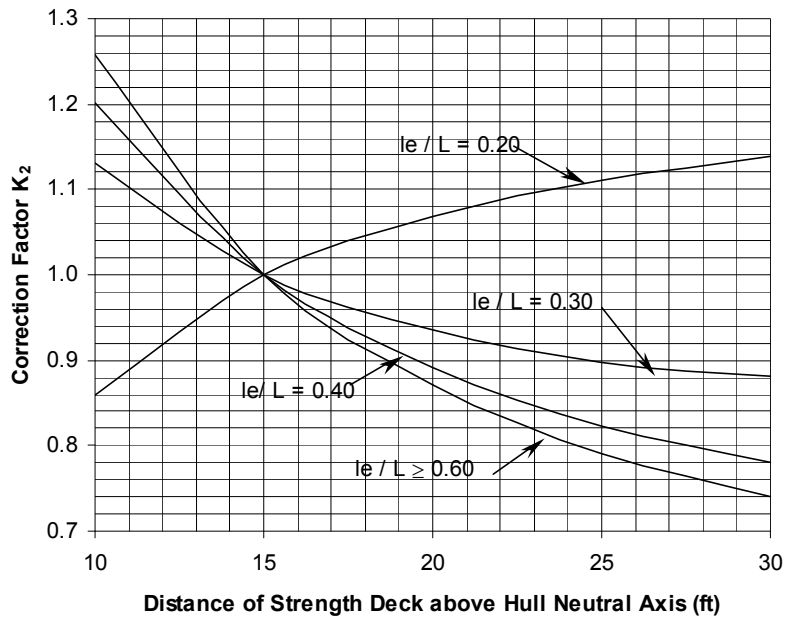


Figure 7-19 Correction factor for height of strength deck above hull neutral axis for a 2-level deckhouse (Kammerer, 1966).

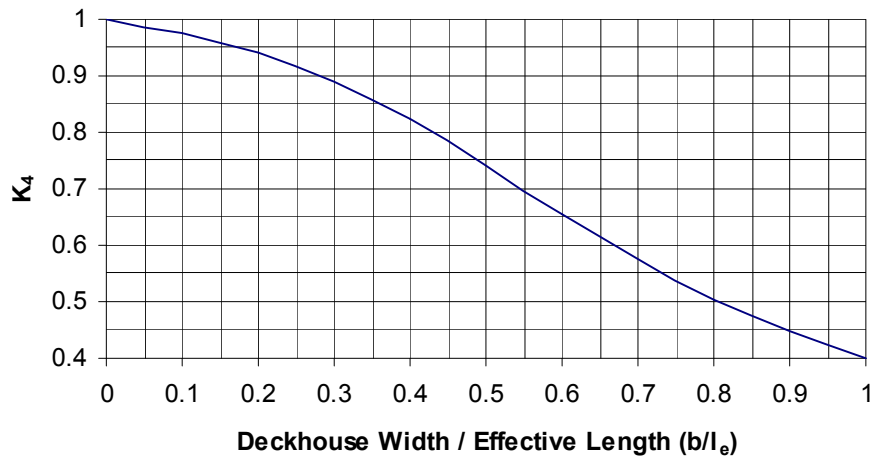


Figure 7-20 Shear lag correction factor K_4 for determining the effective area of the deckhouse (Kammerer, 1966).

With the factors σ_T / σ_D , K_3 and K_4 known, the computation is carried out and the effective cross-sectional area of the deckhouse, A_{de} is found. The height of the strength deck above the neutral axis of the combined hull and deckhouse, C_e , is determined by the equation:

$$C_e = \frac{A_H C_H}{A_H + A_{De}}$$

where:

A_H = Cross-sectional area of the hull, and

C_H = Height of strength deck above original neutral axis of the hull.

The inertia of the effective section, I_e , is then found by taking the original inertia of the hull and adding the correction for the shift of the neutral axis and the inertia of the effective deckhouse about the new neutral axis.

During the initial stages of design, Kammerer's method is an effective way to estimate the stress in the deckhouse amidships and reduction of the longitudinal hull girder bending stress amidships caused by the presence of the deckhouse. The method does not calculate stresses elsewhere in the deckhouse or hull, nor does it calculate the vertical forces at the ends of the deckhouse, which are important in determining if sufficient support for the deckhouse is being afforded by the hull. During initial design stages, these forces can be estimated by the two-beam method of computing hull-deckhouse interaction. Rather than using the complex numerical methods developed in the past, a simple plane frame computer program available in most design offices or a simplified beam input to a finite element program is easy to implement. The hull girder is modeled as a beam having the properties determined at that stage in the design process, and the deckhouse is modeled as another beam. The two beams are joined by rigid links or stiff beams at the locations of major transverse bulkheads. Then when the hull beam is subjected to hull girder bending moments, the forces between the deckhouse and hull will be computed.

During more advanced stages of the design process, a finite element model that includes the deckhouse should be constructed for any vessel having a significantly sized deckhouse. That model should be used to determine the stresses in the deckhouse and the stresses at the hull-deckhouse interface.

7.5 Isolation of the Deckhouse from the Hull

On some high-speed vessels the deckhouse is completely isolated from the hull using heavy-duty shock mounts. This serves to reduce the transmission of noise and vibration in the hull from machinery and propellers from the deckhouse and increases passenger comfort for those passenger areas that are in the deckhouse. The isolation also reduces stress in the deckhouse by eliminating hull girder bending stresses. With the reduced stress, deckhouse scantlings can be very light, although the additional weight of the isolation system and the requirement for supporting members separate from hull structure may equal or exceed the weight reduction from the light scantlings. Pictures of shock isolators are shown in Figure 7-21 and Figure 7-22. The underside of an independent deckhouse raised from the hull of a catamaran for maintenance is shown in Figure 7-23.



Figure 7-21 Shock mount supporting a corner of a deckhouse.



Figure 7-22 Close-up of deckhouse shock mount.



Figure 7-23 Catamaran with independent deckhouse raised for maintenance (Bushfield et al., 2003).

7.6 Summary

With an aluminum deckhouse on a steel hull, electrical separation of the two materials is necessary to prevent galvanic corrosion. Riveted connections with insulation between the steel and aluminum have not been effective in the past because whenever the insulation broke down, galvanic corrosion began immediately. A bonded bimetallic steel and aluminum strip welded to a steel coaming and the aluminum deckhouse provided a smooth surface that can be coated to prevent corrosion. The stresses acting in deckhouses could only be roughly estimated in the past, leading to problems in the junction between and aluminum deckhouse and a steel hull, as well as fatigue failures in the deckhouse. Finite element methods are useful today to analyze those stresses and reduce problems in service. Complete isolation of the deckhouse from the hull is another solution to the interface problem, and doing so can reduce vibration and noise in the deckhouse.

Chapter 8

Residual Stresses and Distortion

The residual stresses and distortions associated with welding aluminum structures have advantages and disadvantages compared to steel. The elastic modulus of aluminum is one-third that of steel, but the coefficient of thermal expansion is about twice as much. This means that the strains that occur from the cooling of the welds and surrounding areas will produce lower residual stress in aluminum. However, the reduced elastic modulus means that when residual stresses do occur, they will tend to produce greater distortion than in steel structure. Because aluminum conducts heat anywhere from 2.5 to 9 times faster than steel, the area heated during welding processes is greater but not as intense. In general, aluminum structure tends to distort more during welding, and tolerances for ship construction reflect this, with greater allowance for distortion being permitted in aluminum structure than in comparable steel structure.

8.1 The Nature of Distortions

Distortions can occur in welded structure for a variety of reasons, including initial distortion of plates and shapes, residual stress in plates and shapes, misalignment and mismatch of structural elements, thermal loading, straightening stresses, and welding shrinkage.

8.1.1 Distortion from Other than Welding

Rolled plates and extruded shapes are not perfect but are produced to either standard tolerances or special tolerances, if so procured. With aluminum, the standard tolerances for extrusions were discussed in Chapter 2. The standards of The Aluminum Association for structural profiles have a standard tolerance for camber and sweep in inches of 0.050 times the length in feet, or 0.0042 of the length. Therefore an 8-meter extrusion (24-foot) can have 33 millimeters of distortion (1.3 inches) (Aluminum Association, 2003). By contrast, ASTM Standard A6 calls for camber and sweep for rolled steel shapes in inches of 0.0125 times the length in feet, or 0.001 times the length for sections with a flange width of greater than 6 inches. For narrower sections, the tolerance in sweep is twice as great. Therefore, the 8-meter long steel shape with a flange width greater than 6 inches would have an allowable distortion of 8.3 mm (0.33 inches), one-fourth of the allowable for aluminum. Most aluminum extrusions have flange widths less than 150 mm (6 inches), and the allowable distortion of steel shapes in that size range is only one-half of that for comparable aluminum shapes.

The tolerances for plate are a function of thickness and width. A 6.4 mm (0.25-inch) aluminum plate that is 1.83 m (6 feet) wide will have a tolerance in flatness of 13 mm (0.5 inches). The flatness tolerance is 24 mm (0.94 inches) for the same size carbon steel plate and 35 mm (1.38 inches) for high-strength low-alloy and alloy steel plates. Therefore, a carbon steel plate has an allowable distortion that is 1.8 times greater than for an aluminum plate.

When distorted shapes are welded to uneven plate to form a stiffened panel, forces are required to bring the two together. The shapes are much stiffer than the plate, but residual stresses will remain after fabrication, and these stresses will contribute to the overall distortion of the panel.

In order to produce the shapes and plates to the required tolerances, straightening operations are used in the mill. These counteract the residual stress patterns that resulted from the initial forming and rolling of the plate or shape. The apparently straight or flat shape or plate will therefore have locked in stresses that can be released by cutting operations, and new sets of distortions will result.

When a structural assembly is fabricated, the above distortions, the distortions produced by welding, and errors and tolerances in cutting will mean that adjacent structural assemblies will not fit together precisely. Adjustments to align assemblies include forcing them together, which produces residual stresses that can lead to distortions of the combined structure, and overall distortion of the hull.

A well-aligned structure when subjected to uneven temperatures, such as heating from the sun, will distort appreciably. The higher thermal coefficient of expansion of aluminum makes it more susceptible to this type of distortion, and therefore fabrication of aluminum is generally done under cover.

When distortion of the structure occurs that is in excess of allowable tolerances, such as flatness of plate, methods of straightening need to be applied. In some carefully controlled instances, such as those described in Chapter 5, operations such as flame straightening can be performed on aluminum. These operations will reduce local distortions but can build in overall residual stresses that will lead to greater distortions of the entire structure. In one case of a steel ship, overzealous use of flame straightening on the main deck led to a curvature in the hull of about 12 inches. Therefore, it is important to control distortion at the earliest stages of fabrication, because small distortions can build up and cause later problems in the overall structure.

8.1.2 Welding Distortion

The welding process involves the formation of a molten pool of metal that is surrounded by metal that is heated to temperatures ranging from the ambient temperature to the melting temperature of the metal. The initial heating will cause yielding in compression in some areas beyond the molten area. As the weld cools and solidifies, it begins to contract. Some areas are still at a temperature where there is essentially no strength, but cooler areas beyond this will begin to yield in tension. As cooling progresses, more metal comes into tension, but there is a redistribution of stresses so that areas of residual compressive stress also exist. A very complex stress field will develop, especially in complex structural assemblies. Numerous efforts have been made to analyze the welding process using finite element analysis that include modeling of heat flow and of changes in material properties with temperature, but such modeling has been successful with only simple structures. Successful analysis usually depends on a very detailed analysis of the weld process, and development of numerical coefficients for use in the analysis of larger structural portions. Therefore, the analysis is semi-empirical in nature and has generally been restricted to steel structures. However, some insight to the residual stresses and distortion of aluminum structure can be gained from review of these analyses.

Masubuchi (1990) made a comparison between aluminum and steel of the angular distortion that occurs in a plate when a stiffener is fillet welded to it. He presented his results in

curves of plate thickness versus angular distortion, where each curve was for the amount of weld metal deposited in grams per centimeter. For comparable weld sizes then, an aluminum weld would have one-third the weight of a steel weld. Therefore the curves presented in Figure 8-1 are for 2.0 grams per centimeter in aluminum and 6 grams per centimeter in steel. On this basis, as can be seen, the steel welds produce nearly twice the angular distortion of the aluminum fillet welds.

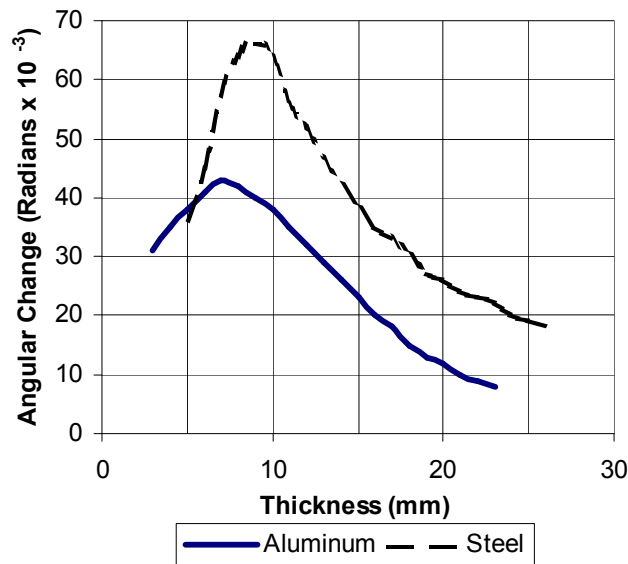


Figure 8-1 Comparison of distortion at a fillet weld (Masubuchi, 1990).

8.1.3 Patterns of Welding Distortion

When analyzing simple structures that are being welded, certain patterns of distortion will occur. Masubuchi (1990) identified six types, as shown in Figure 8-2. Conrardy and Dull (1997) analyzed the buckling and angular distortion forms in thin steel plates, using large-scale mock-up to verify their analyses, which included finite element analysis of the panels during the welding process. The predominant cause of distortion in thin panels was found to be due to buckling. The residual compressive stresses induced in plate panels were estimated by a method developed for steel panels. Distortion would occur if the compressive forces exceeded the buckling strength of the plate. This indicates that either increased plate thickness or decreased stiffener spacing can reduce buckling distortion.

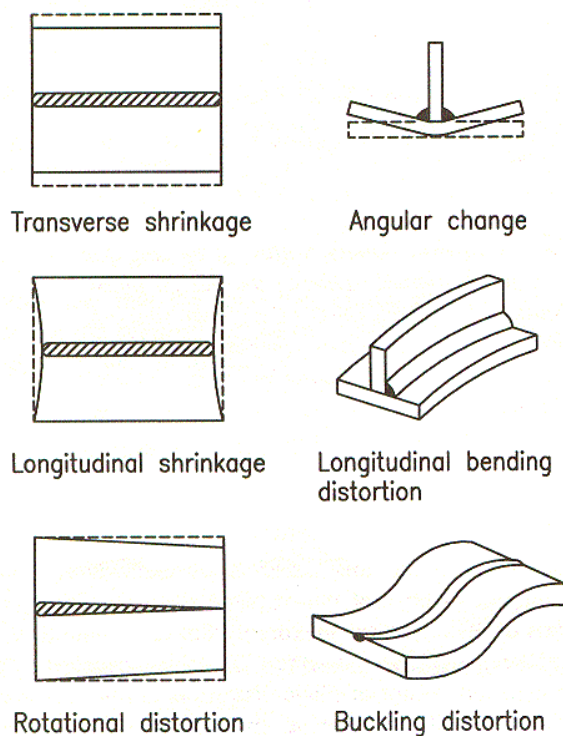


Figure 8-2 Six types of distortion identified by Masubuchi (Conrardy and Dull, 1997).

A second method for reducing buckling distortion investigated was to use “egg-crate” construction, where longitudinals and stiffeners are welded together first, and then welded to the plate. This is similar to “stick” construction commonly used in fabrication of smaller aluminum vessels. Distortion was reduced by 50 percent using this method in conjunction with pre-heating the center of the plate prior to welding.

Conrardy and Dull found that intermittent welding practically eliminated all distortion, even when high heat input welds were used. Reducing the heat input of welding can dramatically reduce distortion. However, the studies showed that the low heat required to eliminate distortion in ship-sized structural panels was less than ordinary welding processes for steel can obtain. Only alternative means, such as laser welding could achieve the low heat input welds required.

The work of Conrardy and Dull preceded the advances that have been made in recent years in the use of friction stir welding for aluminum, a process that involves relatively low heat input and has low distortion. However, the application of the process today is limited to only a few areas of ship structure.

They examined the effect of tensioning the plate prior to welding but found that it was impractical to implement with ship-sized panels. Instead, thermal tensioning of the weld zone, as shown in Figure 8-3, was used to pretension the plate. Resistance heaters were used to heat the plate while a water spray was used to cool the plate on the opposite side from the double

fillet weld, maintaining a 170 °C temperature differential. While this technique eliminated the buckling distortion, it resulted in significant angular distortion.

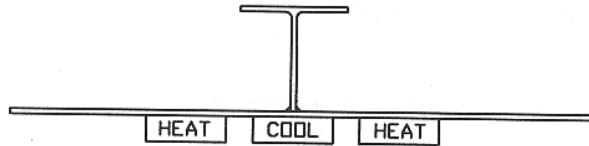


Figure 8-3 Use of heating and cooling to pretension plate (Conrardy and Dull, 1997).

Quenching of the weld by using a water spray on the back side of the fillet weld was found to be very effective in reducing both buckling distortion and angular distortion. However, this technique can have adverse effect on the metallurgical properties of the weld and needs further investigation before implementation.

Conrardy and Dull reviewed the literature but did not experiment with three methods of removing angular distortion. Applying restraint during welding will reduce the distortion because the rigidity of the restraints forces the weld to yield during cooling. Back bending of the plate prior to welding is sometimes used. This method requires experimentation to determine the amount of back bending required and is suitable only for longitudinal welds, not for transverse welds. Back side line heating of steel panels is sometimes employed to straighten them after welding. This technique is not suitable for thin panels because it tends to induce buckling distortion.

Deo and Michaleris (2002) identified three patterns of distortion in the fabrication of built-up steel tee sections, as shown in Figure 8-4. In their study, they compared detailed finite element analyses of the welding process and stiffeners to experimental results from welding steel stiffeners. The longitudinal stresses from the welding of the flange to the web can produce buckling in the web and possibly in the flange. The overall shape can bow in the plane of the web and, if the shape is asymmetric, in the plane of the flange. Similar to the welding of a stiffener to a plate, the flange can distort angularly.

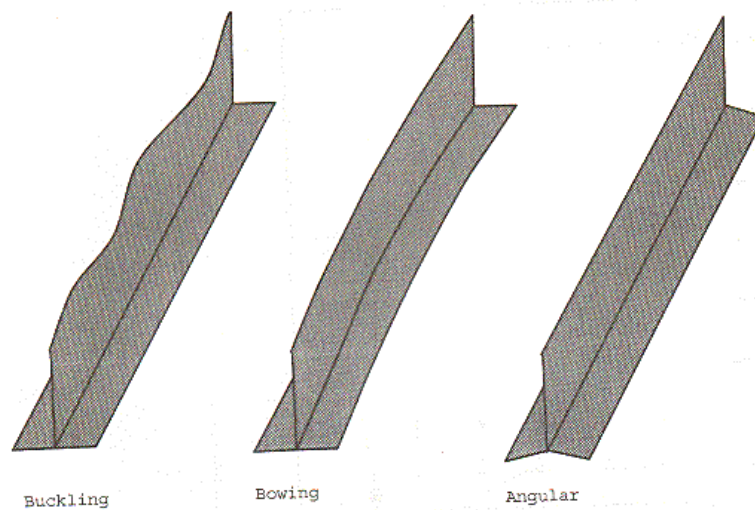


Figure 8-4 Patterns of distortion for fabricated shapes (Deo and Michaleris, 2002).

8.1.4 Analysis of a Weld Bead

Insight into the difference in residual stress and strain associated with welding aluminum and steel can be gained from use of the analysis of Seo and Jang (1999). Their analysis was for steel structure, but it will be modified somewhat here for a weld along an aluminum plate. They developed the simplified model of the welding process that is shown in Figure 8-5 and then developed the following equation for calculating the plastic strain:

$$\varepsilon_p = \varepsilon_{p1} - \varepsilon_{p2} = - \left[\alpha (T_m - T_0) + \frac{\sigma_y}{E} + \frac{\sigma_y A}{k L} \right] \quad (8-1)$$

where:

ε_p = plastic strain of inherent strain region normal to the weld line

ε_{p1} = plastic strain of welded region during temperature increasing stage

ε_{p2} = plastic strain of welded region during temperature decreasing stage

α = coefficient of thermal expansion, = $23.6 \times 10^{-6} / ^\circ\text{C}$ for 5xxx series aluminum alloys, and $11.7 \times 10^{-6} / ^\circ\text{C}$ for mild steel.

T_m = mean temperature after heat has been transferred to material softening region and base metal region

T_0 = ambient temperature

A = cross sectional area of welded region

k = spring constant of the boundary

L = Length of welded region

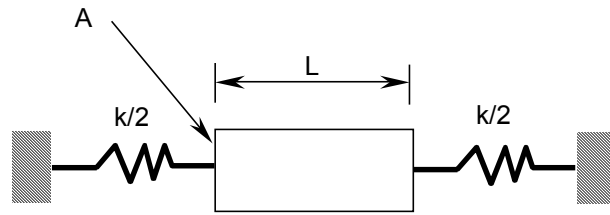


Figure 8-5 Simplified model of welding process (Seo and Jang, 1999).

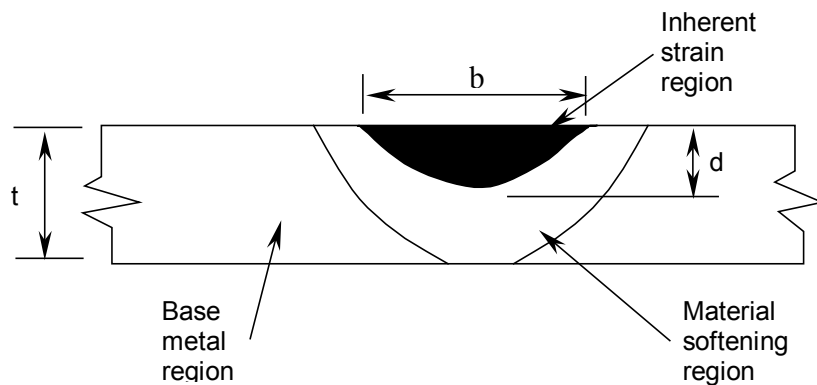


Figure 8-6 Cross section through a weld bead defining the inherent strain region (Seo and Jang, 1999).

Seo and Jang considered the weld shrinkage to occur in an inherent strain region as shown in Figure 8-6. The region has a width b , and a depth, d , which is taken as $d/2$. The width is calculated by the equation (8-2) (which has no input for thermal conductivity or specific heat).

$$b = \frac{8 f Q}{\pi (T_{\max} - T_0)} \tag{8-2}$$

where:

f = portion of the original heat input that will increase the temperature of the inherent strain region = 0.4

Q = heat input per unit length during welding in calories per centimeter

T_{\max} = maximum temperature at which the material loses the ability to resist deformation

The force per unit length, f_x , transverse to the weld bead is then:

$$f_x = E_{ix} \left[\alpha T_{c(x)} + \frac{\sigma_{yx}}{E_{ix}} + \frac{\sigma_{yx} t}{k_x b} \right] \frac{\pi}{4} d \tag{8-3}$$

where:

Aluminum Marine Structure Guide

E_{ix} = elastic modulus in the inherent strain region normal to the weld line

k_x = spring constant normal to the weld line at the boundary between the inherent strain region and the other region = $E [(t - d) / t^2]$

$T_{cx} = T_{m(x)} - T_0$, and given by the equation:

$$T_{cx} = \frac{Q \eta}{c \rho b_m} \quad (8-4)$$

where:

η = heat conduction factor, which can be taken as 1.0 for flat plate

c = specific heat of the material, which is 215 calories/kg-°C for 5083-0 and 100 calories/kg-°C for mild steel.

ρ = density, = 2.66×10^{-3} kg/cm³ for and 7.85×10^{-3} kg/cm³ for mild steel.

b_m = breadth of plate to calculate mean temperature, taken as 5 times the plate thickness for steel, based on studies by Seo and Jang. For aluminum, increase by the ratio of thermal conductivity, = $5 \times 156/54 = 14.4$ times plate thickness.

Seo and Jang used this model of the welding process in a finite element analysis of the welding process. The model will be used here for a simple geometry not to calculate the distortions from a particular welding process, but to compare aluminum and steel welding processes.

To compute the heat input, typical welding parameters for aluminum and steel will be used. The Guide for Aluminum Hull Welding (AWS, 2004) recommends that for GMAW butt welds in 6.4 mm (0.25 in) plate in the flat position, a current of 185–225 amperes at a voltage of 24–29 volts at a travel speed of 10.2–12.7 mm/second be used, an average of 5,400 watts, or 1,290 calories per second. Considering an average travel speed of 1.2 cm/second, the heat input, Q , is $1,290/1.2 = 1,075$ calories/cm.

For GMAW welding of carbon and low alloy steel, the Lincoln Electric GMAW Welding Guide (Lincoln Electric, 2006) recommends that for butt welds in 6.4 mm (0.25 in) plate in the flat position, with an electrode of 1.1 mm (0.045 in) diameter, a current of 200 amperes at a voltage of 20–22 volts at a travel speed of 5.5 mm/second be used, an average of 4,200 watts, or 1,000 calories/second. The heat input for steel, Q_s , = $1,000/0.55 = 1,820$ calories/cm.

According to the data in Chapter 2, the 5xxx series aluminum alloys lose their strength at about 400 °C, which will be taken as T_{max} in equation (8-2). If the ambient temperature, T_0 , is 25 °C, then equation (8-2) gives the width of the inherent strain region, b as 17.1 mm.

Accordingly, using equation (8-4) for 6.4 mm aluminum plate,

$$T_{cx} = \frac{Q \eta}{c \rho b_m} = \frac{1075 \times 1.0}{215 \times 2.66 \times 10^{-3} \times 14.4 \times 0.64} = 204^\circ\text{C}$$

Similarly for 6.4 mm mild steel plate, $T_{cx} = 724$ °C

Using the above in equation (8-3):

$$\begin{aligned}
 f_x &= E_{ix} \left[\alpha T_{c(x)} + \frac{\sigma_{yx}}{E_{ix}} + \frac{\sigma_{yx} t}{k_x b} \right] \frac{\pi}{4} d \\
 &= 284 \times 10^3 \left[23.6 \times 10^{-6} (204) + \frac{460}{284 \times 10^3} + \frac{460 (0.64)}{4.5 \times 10^6 (1.71)} \right] \frac{\pi}{4} (0.85) \\
 &= 123 \frac{\text{N}}{\text{mm}}
 \end{aligned}$$

Similarly $f_{x \text{ steel}} = 477 \text{ N/mm}$, and the ratio of $f_{x \text{ (aluminum)}} / f_{x \text{ (steel)}} = 123 / 477 = 0.26$. Therefore, in accordance with the model of Seo and Jang, welded aluminum structure will develop residual stress levels about one-fourth those of welded steel structures. The ratios will vary with the thickness of material, welding process, and conditions of restraint. However, the overall conclusion should remain that aluminum welding produces less residual stress than welding steel.

8.1.5 Analysis of Aluminum Welding

The above analysis was adapted from studies of steel welding and applied to aluminum welding. Although far more research has been conducted into residual stresses and distortion from steel welding, there has been some work done with aluminum. Tsai et al. (1999) investigated the effect of welding sequence on aluminum panel distortion, developing the joint rigidity method to determine the optimum welding sequence for minimum distortion.

The analysis of welding by Tsai et al. used the inherent shrinkage method that was developed and used by many researchers for analysis of welds in steel. The structure, including the welds, is modeled in a detailed finite element model. The weld metal is initially assumed to be at a temperature of 649 °C (1,200 °F) and then cools to room temperature with heat dissipating into the structure. The properties of the metal are changed incrementally with temperature changes over time until temperature equilibrium is achieved, and the resulting stresses, strains, and displacements determined. Comparison between experimental welding and numerical analysis of a butt weld between two 600 mm x 275 mm plates of 10 mm 5083 aluminum was made, with the results shown in Figure 8-7. To obtain the correlation, a calibration factor, which Tsai et al. did not further describe, was used. This same calibration factor was used by them in subsequent analyses.

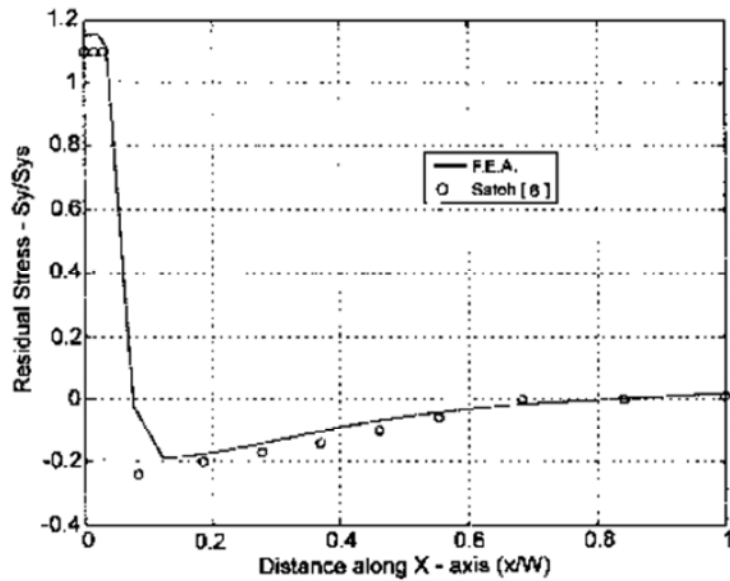


Figure 8-7 Comparison of experimental determination of residual stress with analysis with a calibration factor applied (Tsai et al., 1999)

Tsai et al. then compared the analysis of a fillet weld to experimental data for a 6.4-mm (0.25-in) plate of 5454-H34 aluminum fillet welded to another plate of the same thickness. The inherent shrinkage method was used for analysis with the correlation coefficient developed from the butt weld study described above to achieve the results shown in Figure 8-8.

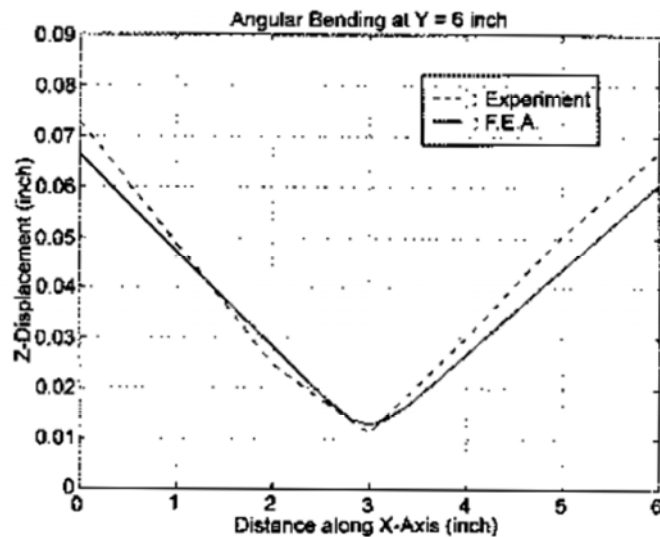


Figure 8-8 Comparison of experiment and analysis of a fillet weld of 5454-H34 aluminum (Tsai et al., 1999).

With the confidence developed from the above two studies of simple geometries, Tsai et al. then applied the inherent shrinkage method to the more complex panel shown in Figure 8-9. The analyses and experimental welding were used to validate the joint rigidity method to as a means of determining the optimum welding sequence for minimum distortion. The method is based on welding from areas that have the highest restraint to areas with the least restraint. The joint rigidity is defined as the ratio of the moment applied at a joint to the resulting rotation, as shown in Figure 8-10.

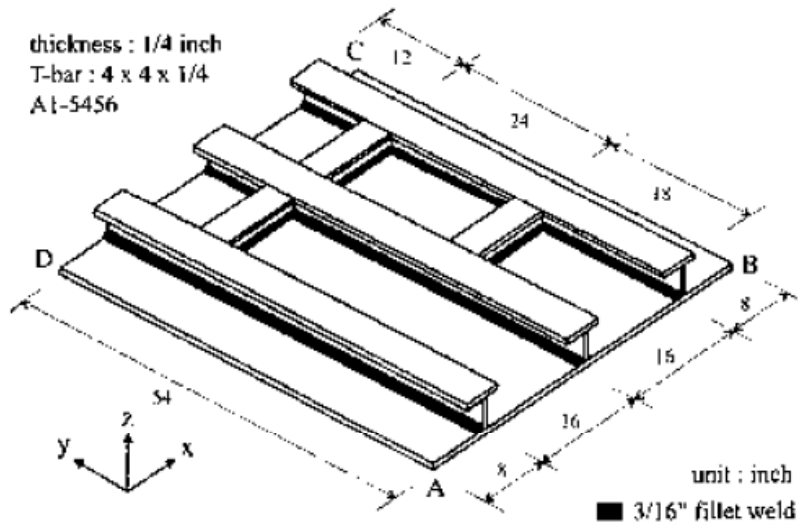


Figure 8-9 Panel analyzed for distortion (Tsai et al., 1999)

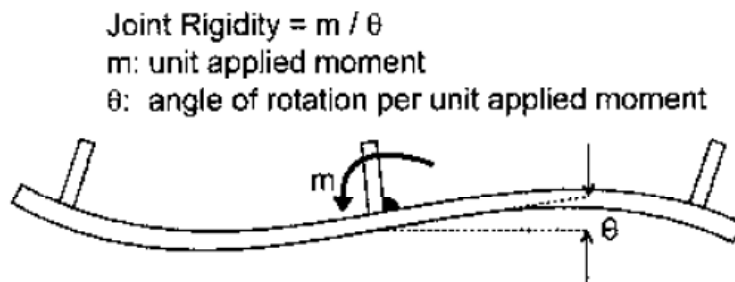


Figure 8-10 Definition of joint rigidity (Tsai et al., 1999).

The panels were welded in four different sequences, shown in Figure 8-11:

1. Welding progresses from the inner panels outward
2. Welding progresses from the from outer panels inward
3. Similar to 1 with consideration of changing structural rigidity of each joint
4. Similar to 3 with consideration of changing structural rigidity of each joint

Sequence 3 searches for the joint with highest restraint to deposit the next weld as the assembly process progresses. Sequence 4 lays the next weld at the least restrained joint.

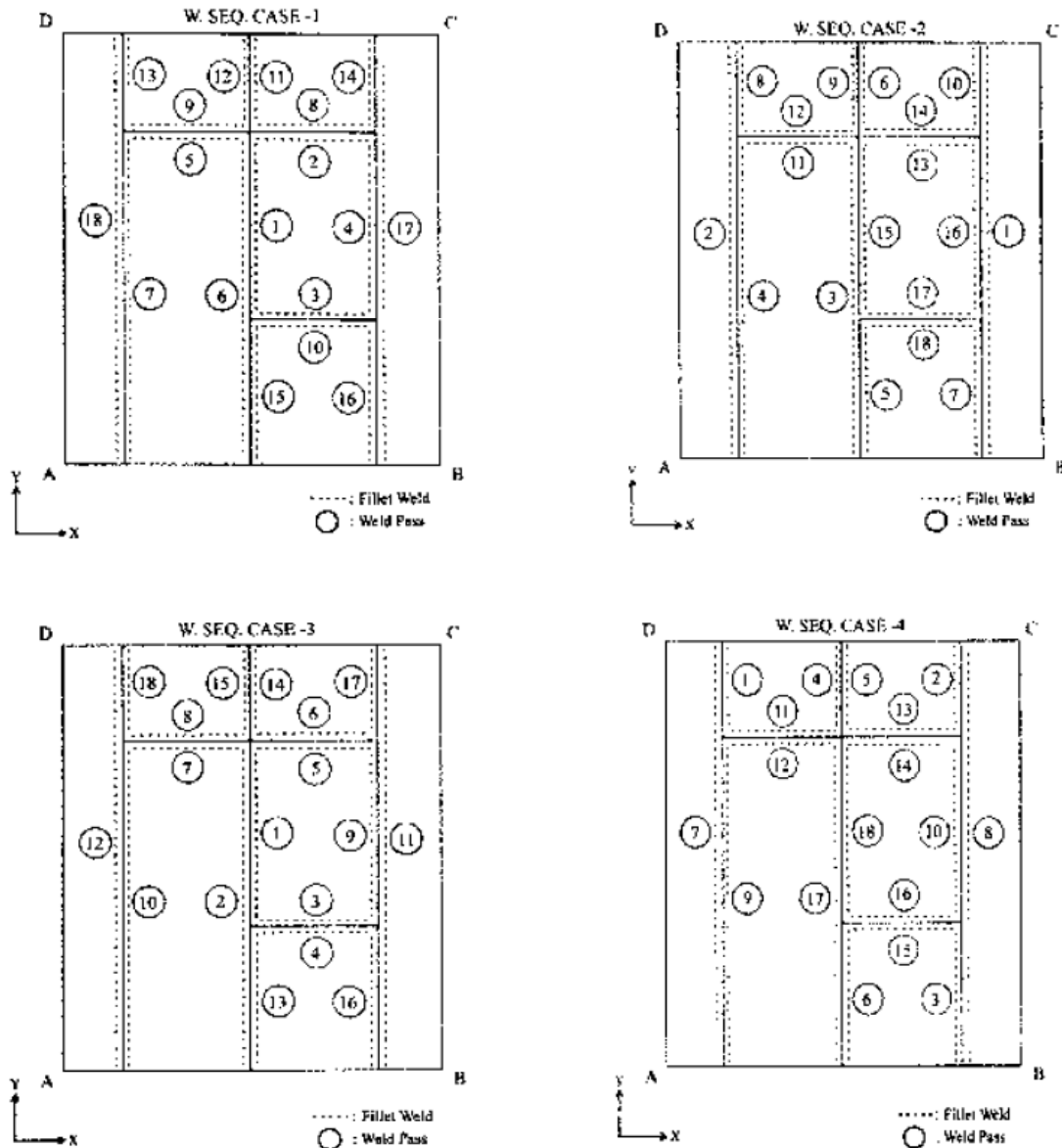


Figure 8-11 Experimental welding sequence for panels (Tsai et al., 1999)

The resulting distortions were measured, with sequences 2 and 4 showing the most distortion. A comparison of the experimental and measured distortions is shown in Figure 8-12 for welding sequence 4.

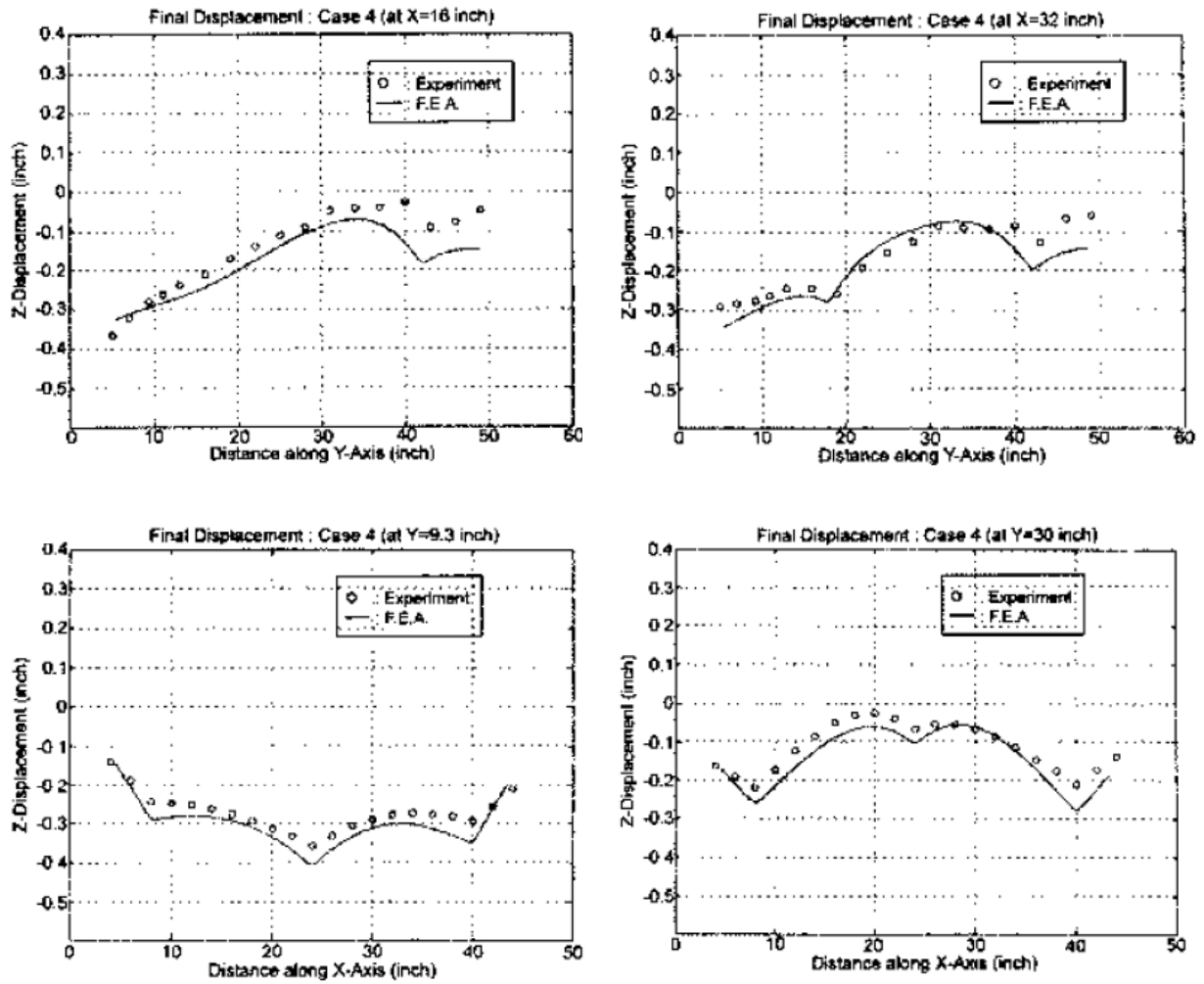


Figure 8-12 Comparison of experiment and analysis of sequence 4 of panels (Tsai et al., 1999).

The joint rigidity method was then used to analyze the panel after each welding operation and determine a weld sequence that would result in the least distortion. The resulting sequence is shown in Figure 8-13, although it was not experimentally verified. This sequence is fairly similar to sequence 3.

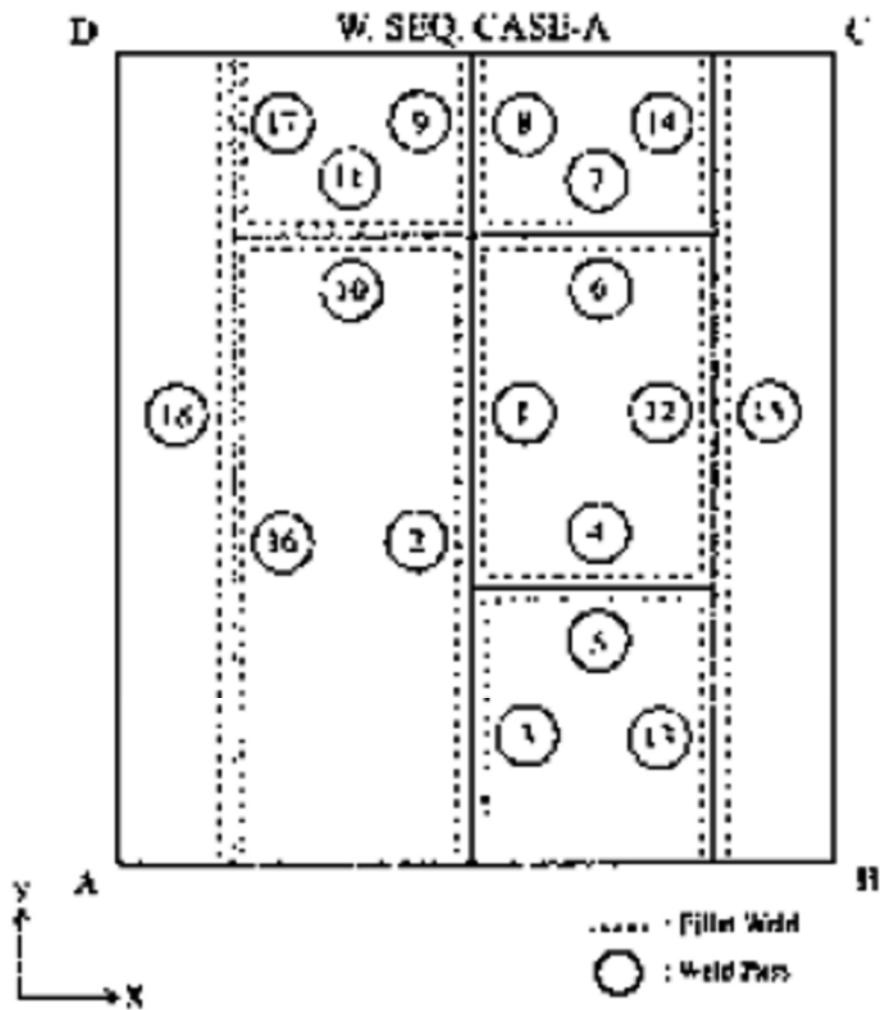


Figure 8-13 Best welding sequence determined through the joint rigidity method (Tsai et al., 1999).

A sequence that is similar to that found analytically by Tsai et al. for performing fillet welds on panels is recommended by the Guide for Aluminum Hull Welding (AWS, 2004) for the sequence of butt welds of plating, as shown in Figure 8-14.

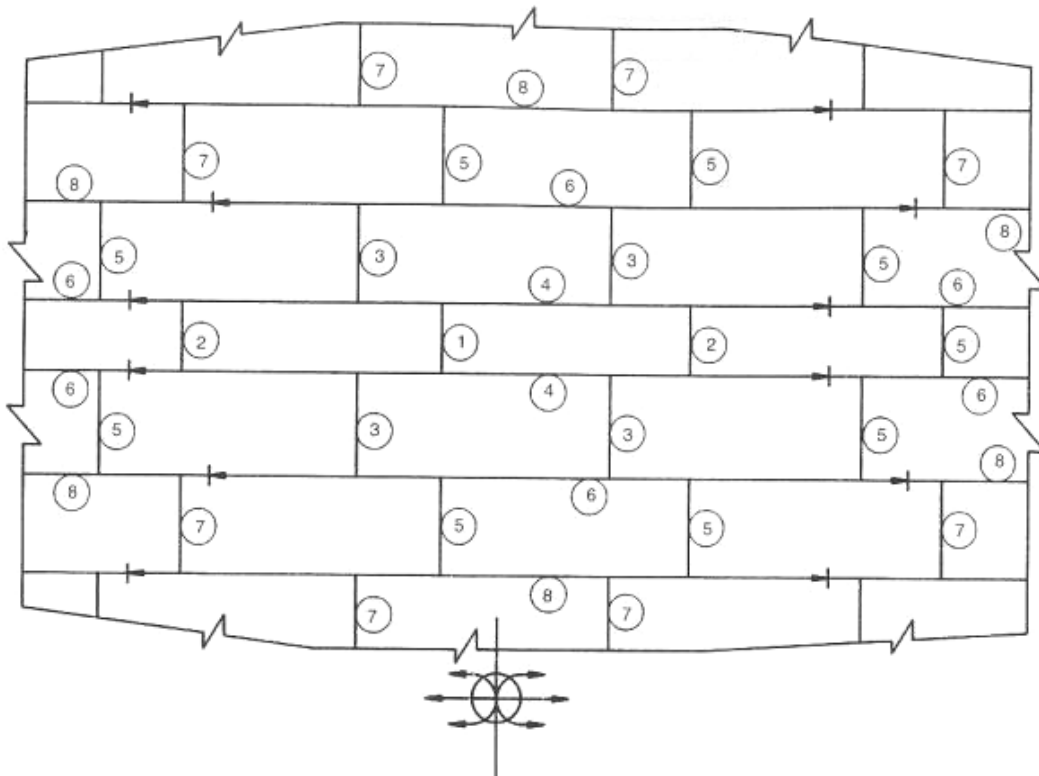


Figure 8-14 Recommended welding sequence for butt welds (AWS, 2004).

The hull welding guide makes the following recommendations:

1. In large panels consisting of a number of plates, the butt seams should be welded before the panel seams. In that way, the shrinkage caused by the many smaller joints has taken place prior to final alignment and welding of the long panel seams.
2. Welding of panels constructed of multiple plates should progress from the center toward the outer edges.
3. Starting at the center of a seam and welding outward with a backstep sequence has proven helpful in specific instances.

8.2 Distortion in Panel Fabrication

Distortion in shipbuilding is cumulative, with the distortions occurring at one stage of construction carried over to the next. If distortion and misalignment is corrected at an early stage, there will be fewer distortions in the latter stages of construction. For this reason, it is important that initial panel fabrication be as free of distortion as possible.

8.2.1 Welded Panels

One method of producing panels with minimum distortion is through specialized panel lines that produce repetitive copies of identical or similar panels in which compensation can be made for welding distortion. An example of this process as developed by one company was described at the Fifth International Forum on Aluminum Ships (Suzuki et al., 2005). In their report, Suzuki et al. also summarized a number of studies performed in Japan on the welding of aluminum but reported in Japanese-language publications.

The panels studied were produced by automatic GMAW fillet welding. The typical dimensions of the panels are 2.15 m long and 11.0 meters wide, fabricated with plate between 3 and 25 millimeters. Stiffeners range in depth from 40 to 190 mm, and the minimum stiffener spacing is 220 mm.

In the method studied, preheating was used to reduce angular distortion at the fillet welds of the stiffeners to the plate. Angular distortion in fillet welding is caused by an imbalance in the temperature between the welding side and back side of the plate. Figure 8-15 shows the result of an experimental determination of the distortion with preheating at various temperatures. The plate and stiffeners were preheated homogeneously in a furnace and then removed for welding.

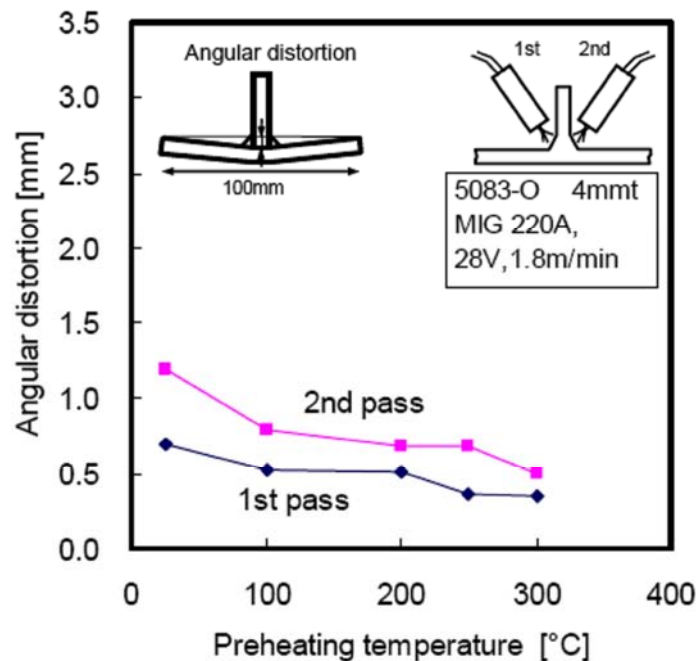


Figure 8-15 Angular distortion at a fillet weld (Suzuki et al., 2005).

Because the process of moving the panels into and out of the oven was cumbersome and failed to remove sufficiently the angular distortion, Suzuki et al. next tried a method of line preheating using in-line preheating immediately before the fillet welds as shown in Figure 8-16. The results of the in-line preheating are shown in Figure 8-17.

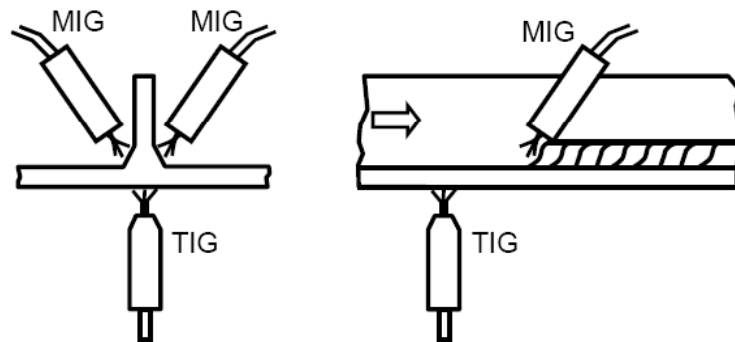


Figure 8-16 In-line preheating prior to fillet welding (Suzuki et al., 2005).

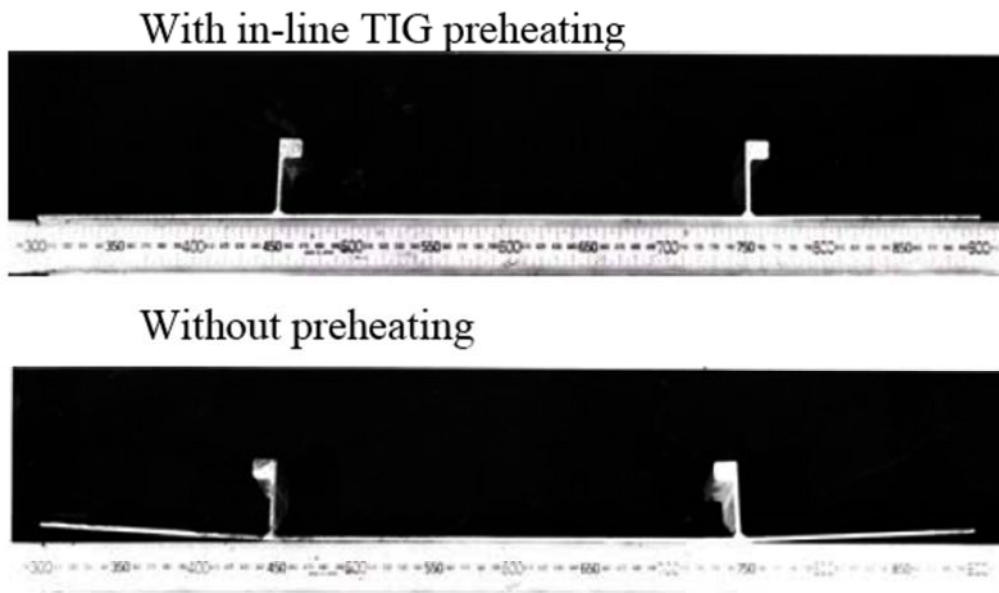


Figure 8-17 Cross-section of fillet welded stiffeners with and without in-line preheating (Suzuki et al., 2005).

In the process used in the production of the panels, the plate is preheated so that it will be 100°C at the fillet welding position, which is 150 mm and 5 seconds after the preheating torch. The in-line preheating has two benefits. Heating the plate reduces angular distortion, and having the in-line preheating on the opposite side of the plate from the fillet welds induces a reverse angular distortion.

The distance of the preheating torch from the fillet welding process affects the degree of angular distortion as shown in Figure 8-18. In this case 40-mm bulb flats with 3-mm webs were welded to a 4-mm plate. The angular distortion was reduced sufficiently if the preheating was at

a distance between 50 and 300 mm from the fillet welding position. Separate preheating or post-heating was found to be not as effective as in-line preheating.

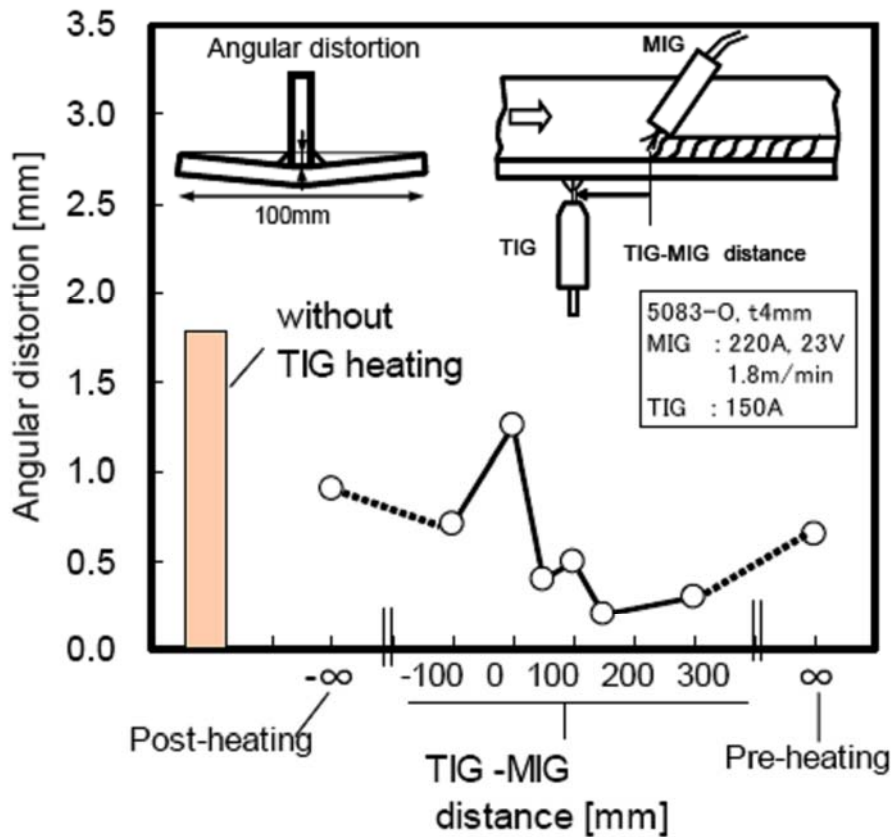


Figure 8-18 Effect of the position of the preheating torch (Suzuki et al., 2005).

Suzuki et al. reported on the effect of longitudinally stretching the panels after welding to reduce longitudinal distortion that is induced by the shrinkage along the weld lines of the panel. Figure 8-19 shows that a longitudinal stretching of 0.05 percent using an apparatus shown in Figure 8-20, effectively reduces the distortion for the panels with 4-mm and 6-mm-thick plates. This is similar to the stretching process used to straighten extrusions.

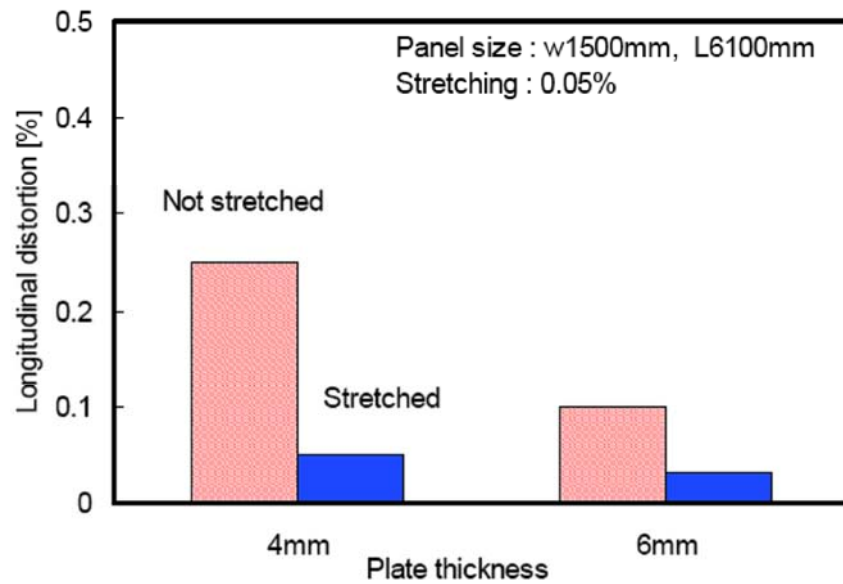


Figure 8-19 Effect of longitudinal stretching on the longitudinal distortion of welded panels (Suzuki et al., 2005).



Figure 8-20 Apparatus for stretching welded panels (Suzuki et al., 2005).

The longitudinal stretching of the panels after welding the longitudinal stiffeners helps the panel maintain its flatness even after subsequent welding operations. Figure 8-21 and Figure 8-22 show the reduction in deflection after welding of transverse frames.

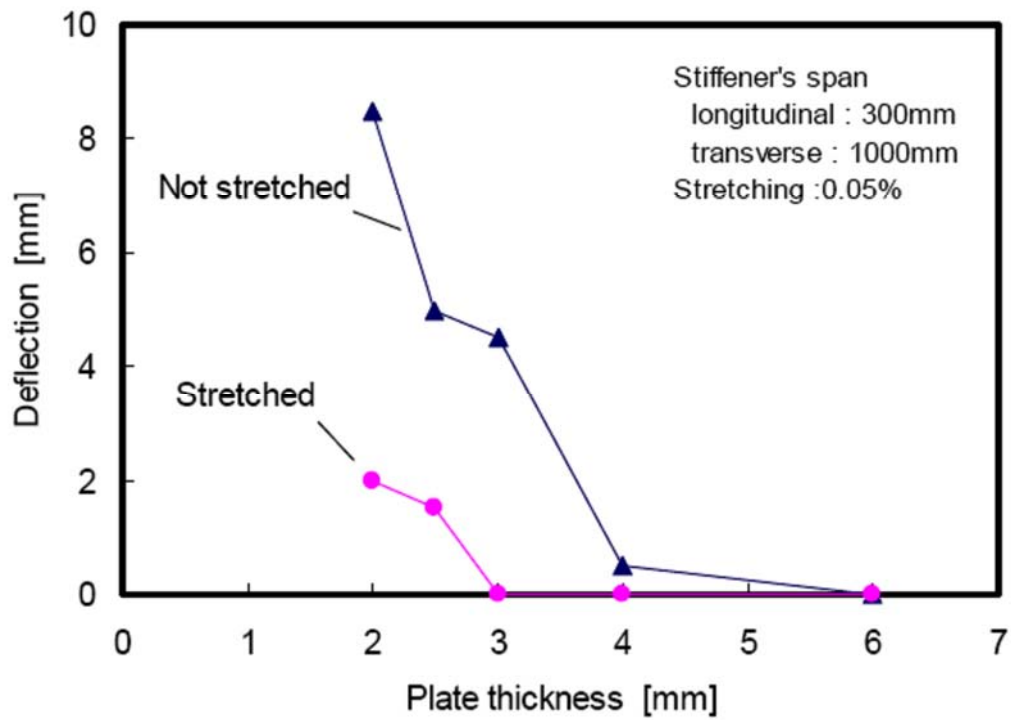


Figure 8-21 Reduction of deflection of stretched panel when welding transverse frames (Suzuki et al., 2005).

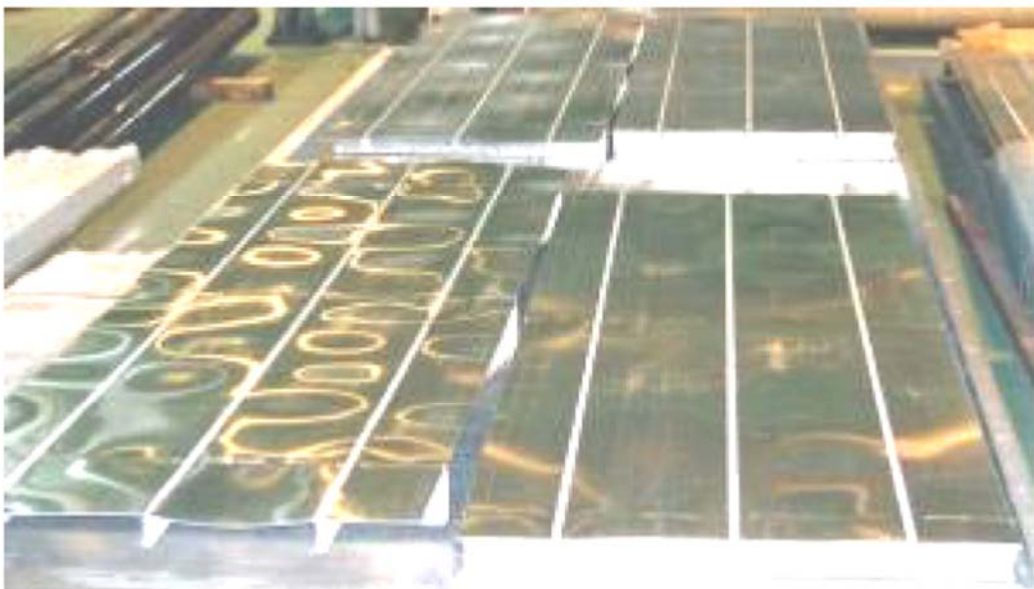


Figure 8-22 Comparison of panels with and without stretching after welding of transverse frames (Suzuki et al., 2005).

8.2.2 Extruded Panels

Another method of aluminum panel construction is to use extruded panels that integrate the stiffeners with the plate, as were described in Chapter 2. Some panels have stiffeners that are formed like conventional shapes, and others are hollow sandwich panels with either vertical or corrugated internal webs. These panels, although initially flat, are still subject to welding distortion, which was investigated by Seo et al. (1999). When two panels are butt welded together, they can experience the type of distortion shown in Figure 8-23, which is similar to that experienced when welding plates together.

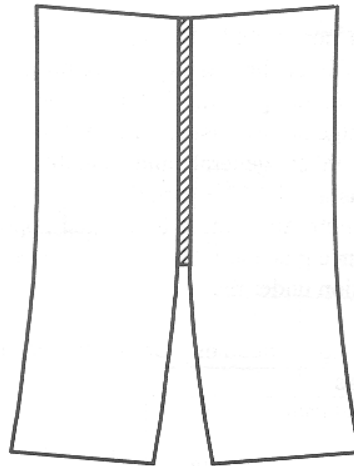


Figure 8-23 Distortion of extruded panels during welding together (Seo et al., 1999).

One way to reduce that distortion is to hold the panels in a jig such as shown in Figure 8-24. Transverse distortion of the panels can still occur from the sequence of welding on top and then on the bottom. A strongback, as shown in Figure 8-25, can reduce that distortion, although curvature can still result.

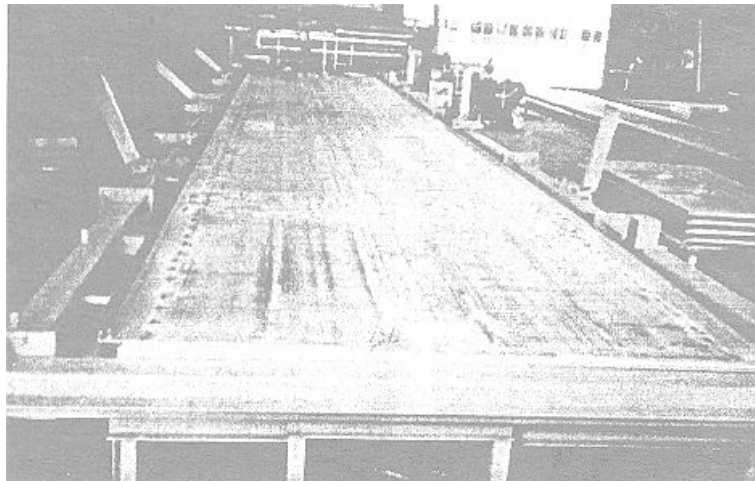


Figure 8-24 Jig used to restrain rotation of extruded panels during longitudinal welding (Seo et al., 1999).

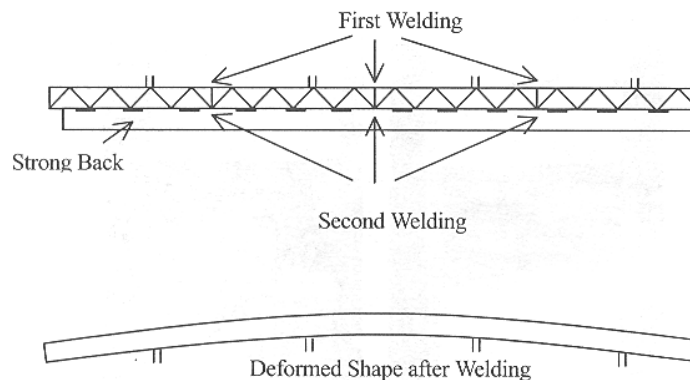


Figure 8-25 Use of strongbacks to reduce distortion when welding extruded panels (Seo et al., 1999).

8.3 Tolerances in Welded Aluminum Structures

The above studies all show that aluminum structure has residual stresses and forces producing distortion that are equal to or less than that of steel structure. However, the buckling strength of aluminum is one-third that of steel, and the residual forces from fabrication will have a somewhat greater tendency to distort the plating because of buckling. This greater tendency for distortion of aluminum plate is reflected in fabrication tolerances.

The International Association of Classification Societies has established fabrication tolerances for steel ship structure but has not yet done so for aluminum. An existing standard for aluminum ship structures is the U.S. Navy Military Standard 1689 (MIL-STD 1689). In general, the same structural tolerances apply for aluminum structure as for steel, except for the requirements for fairness of plating. Those requirements are shown in Figure 8-26 and Figure 8-27. The requirements of Figure 8-26 pertain to:

- a) Entire shell
- b) Uppermost strength deck
- c) Longitudinal strength structures within the midships $3/5$ length for displacement type ships, or as specified for other type ships, which includes innerbottom tank and the deck next below the uppermost strength deck if continuous above machinery spaces.
- d) In transversely framed ships, the permissible unfairness for structure is reduced by $1/8$ inch.
- e) Bulwarks and exterior superstructure bulkheads.

Figure 8-27 applies to:

- a) Structural bulkheads forming a boundary of a living space (stateroom, office, berthing, messing, or lounge area) and passageways contiguous to such spaces.
- b) Decks within the hull and superstructure in way of the above living spaces.
- c) Decks exposed to the weather.
- d) Tanks and main transverse bulkheads.

e) Innerbottom plate longitudinals.

For other structural bulkheads and decks, the requirements of Figure 8-27 may be increased by 1/8 inch.

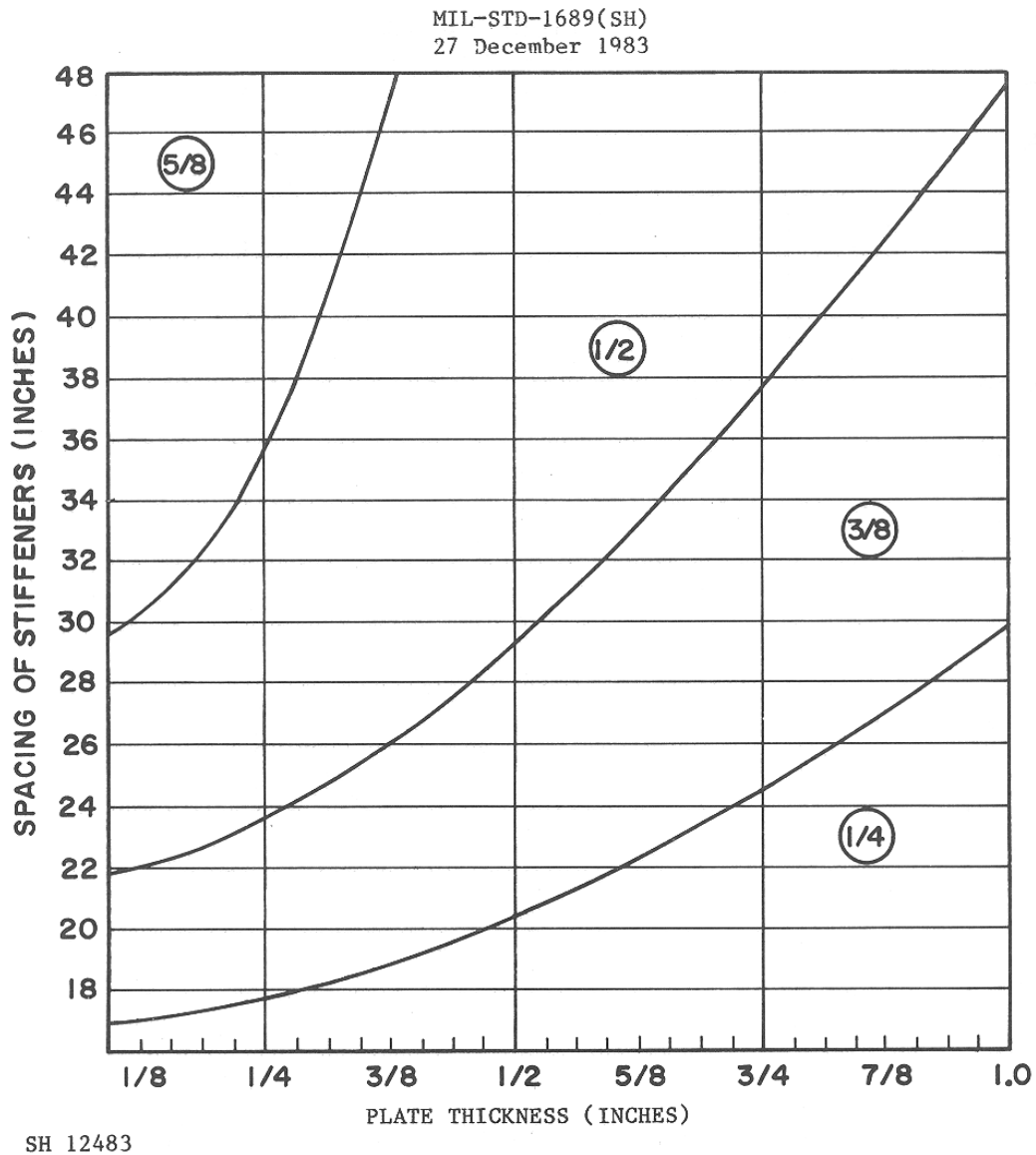


Figure 8-26 Flatness tolerances for aluminum plate in critical areas (MIL-STD 1689).

The fairness requirements for aluminum are slightly more lenient for aluminum compared to steel. For example, Figure 8-26 has the dividing line between 1/4-inch and 3/8-inch unfairness for 1/4-inch plate at 18 inch stiffener spacing, but the comparable steel requirement has the division at a 20-inch stiffener spacing. That is, for 1/4-inch plate with 19-inch stiffener spacing, the allowable unfairness for steel is 1/4 inch, but for aluminum it is 3/8 inch. The effect

of fabrication tolerances on the reliability of steel structure has been examined for steel, but similar studies remain to be conducted for aluminum.

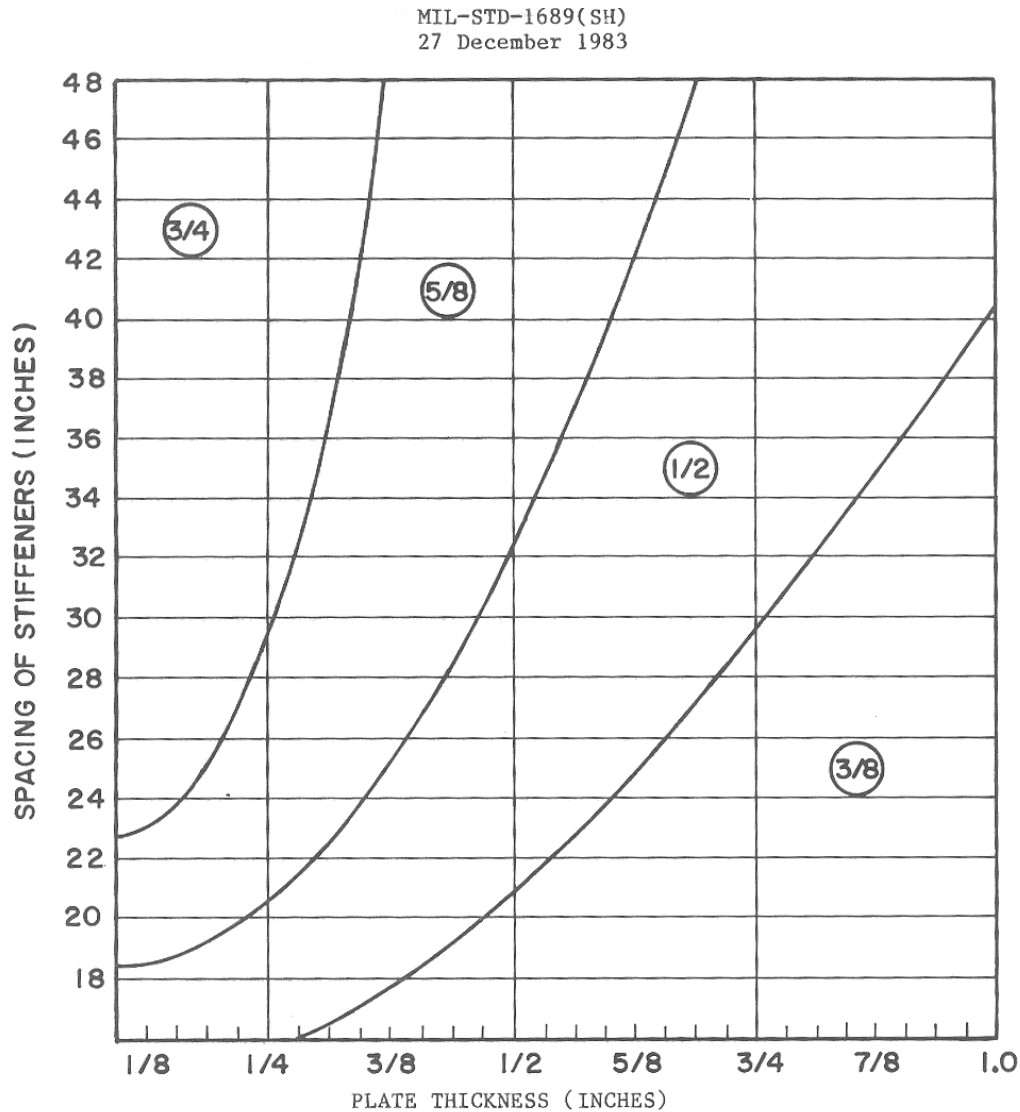


Figure 8-27 Flatness tolerances for aluminum plate in secondary structure (MIL-STD 1689).

8.4 Summary

Welded aluminum structure generally has less residual stress than comparable steel structure. However, the reduced buckling strength of aluminum means that it will tend to have greater distortion for the same level of residual stress, especially in plating. Although there has been much research done on the residual stresses and distortion of steel ship structure, much comparable work is needed for aluminum.

Chapter 9

Fatigue and Fracture Design and Analysis Procedures

9.1 Introduction

Fatigue is a failure mechanism caused by repeated cycles of increasing and decreasing stress and can occur in marine structures because they typically experience millions of load cycles during their service lives. For welded structural details, the important loading parameter is the stress range, which is the difference between the highest stress during a load cycle and the lowest stress, which may be compressive. Repeated loading, often for millions of cycles, can lead to the initiation of a crack. The consequences of cracks in structure are determined by application of the principles of fracture mechanics, the study of materials under load in the presence of a crack.

Fatigue life is determined experimentally by testing a structural detail under repeated load cycles until it fails. Many specimens of the same structural detail are tested at various stress levels to determine the relationship between the applied stress range and the number of load cycles that occur before failure. The results of the fatigue testing are commonly presented on a graph that has the stress range on a logarithmic scale as the ordinate and the number of cycles to failure on a logarithmic scale as the abscissa. This type of graph is called an S-N curve, although the relationship between stress range and cycles is generally a straight line on the graph. A typical S-N curve is shown in Figure 9-1. The relationship between S, the stress range, and N, the number of cycles to failure is expressed as:

$$N = AS^{\frac{1}{m}} \tag{9-1}$$

where A is an experimentally determined coefficient, and m is the negative slope of the S-N curve.

Experimental fatigue data typically show an extreme amount of variability, with the number of cycles to failure for a given stress range varying over as much as a full order of magnitude. Therefore, a large number of specimens must be tested to gain an accurate statistical description of the fatigue behavior of a particular structural detail. Testing can take a long time, because ship structure and many other types of structures require accurate data at a fatigue life of 10^7 cycles. This means it can take 115 days to test one specimen at a loading rate of 1 cycle per second. Because of the expense of testing, more testing is done at higher stress ranges and the results extrapolated to lower stress ranges and higher cycles.

This extrapolation is a subject of controversy, principally because of a scarcity of data at the higher stress cycles. There is a general consensus among many researchers in fatigue that the S-N curve becomes nonlinear at the higher stress cycles, with a reduced slope, sometimes assumed to become a horizontal line at some stress level. This is called the endurance limit, meaning that an infinite number of load cycles could occur below that stress range without failure.

Not all fatigue design codes acknowledge a fatigue limit, but most are bilinear, having one slope below a certain number of cycles such as 5×10^6 , and a lesser slope for the higher number of cycles. There is not universal agreement that the reduction in the slope of the S-N curves at higher cycles or the assumption of a fatigue limit is valid, especially for aluminum operating in seawater. The effect of the assumption on the predicted fatigue life can be significant. In the example discussed below and shown in Table 9-8, if the bilinear S-N curve with a reduced slope at as 5×10^6 cycles were replaced with a linear S-N curve, the predicted fatigue life would decrease by 30 percent.

Because of the variability of experimental S-N fatigue data, a lower limit is taken on fatigue strength for design. Generally this is the lower 5 percent level, meaning that if the S-N curve is used for design, a 5 percent probability of fatigue failure exists.

The design codes are developed based on experimental data from welded structural details. Several assumptions are made in the development of the S-N curves from these data.

- The effect of the aluminum alloy and its yield strength is ignored. In experimental data the discontinuities associated with welds dominate the behavior, and individual differences in the alloys are not significant.
- The effect of the mean stress level is ignored. With welded details, a local residual tensile stress develops at the base of the weld, and this overrides the effects of an average tensile or compressive stress.
- Most testing is conducted at constant amplitude. That is, a single specimen is tested at a constant stress range until failure. In service, the details are subjected to variable amplitude loading. Under variable amplitude loading, the fatigue life may be lessened because large overloads make easier transfer of the microcracks through the grain boundaries and development of macroscopic cracks. This effect is more pronounced in base metal than in welds and is ignored in the design fatigue codes.

9.2 Comparison of Aluminum and Steel

One of the principal parameters in either aluminum or steel structural design is the yield strength. The lowest strength aluminum alloy used is generally 5086-H116, which has a welded yield strength of 131 MPa. The lowest grade of steel generally used for ship construction is Ordinary Strength Steel, with a yield strength of 235 MPa, 1.8 times higher than 5086-H116 aluminum.

This ratio of strength generally carries forward into various design criteria, with the strength requirements such as cross-sectional area and section modulus being 1.8 times greater for this aluminum alloy than for steel. However, the same ratio of fatigue strength does not apply. In Figure 9-1, the fatigue strengths of two similar structural details in steel and aluminum are compared. For aluminum, the Eurocode 9 detail for the toe of a bracket is classified as 23, 3.4, meaning it has a fatigue life stress range of 23 MPa at 2×10^6 cycles, with an inverse slope of 3.4. A comparable fatigue code for welded steel details is the UK Department of Energy standard, also British Standard BS 5400, which is incorporated by ABS into their Steel Vessel Rules. Fatigue Class F is used for the toes of brackets, and has a fatigue life stress range of 68

MPa at 2×10^6 cycles, with an inverse slope of 3.0, a fatigue strength 3 times higher than aluminum.

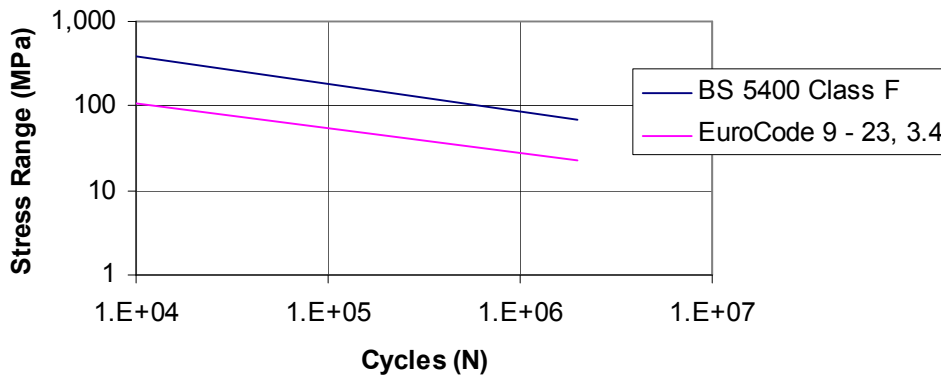


Figure 9-1 Comparison of aluminum and steel fatigue strength.

If the stress ranges of the S-N curves for steel and aluminum are divided by their respective yield strengths, Figure 9-2 results. The normalized fatigue strength of 5086-H116 aluminum is 0.6 of that of mild steel. Because of the slope of the S-N curves, if an aluminum vessel is designed to the same criteria and fabricated with the same details as a steel vessel, it will have only 13 to 20 percent of the fatigue life of the steel vessel. Of course this comparison depends on the aluminum and steel alloys being compared. If a steel with twice the yield strength of mild steel were used for comparison, the 5086-H116 would be 20 percent better than the high-strength steel.

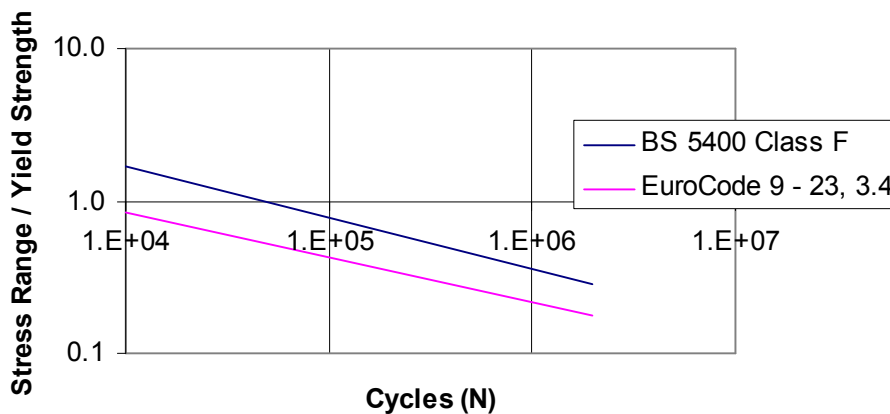


Figure 9-2 Comparison of 5086-H116 aluminum and ordinary strength steel fatigue strength normalized by yield strength.

9.3 Fatigue Design Curves

There are several design codes that provide standardized fatigue strength S-N curves for different structural details. These have been reviewed in SSC Report SSC-410 (Kramer et al.,

2000), as well as in the ongoing SSC Project SR-1434, In-Service Performance of Aluminum Structural Details.

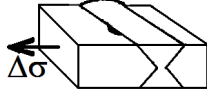
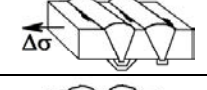
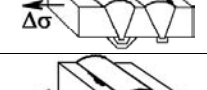
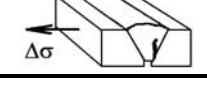
Of these design codes, the Eurocode 9 is to be preferred because it is based on large-scale testing of details at lower-stress, higher-cycle lives, which is representative of ship structure. The code is scheduled for publication in November 2006 as EN 1999-1-3, Eurocode 9. Design of Aluminium Structures, Additional Rules for Structures Susceptible to Fatigue. The information contained in this report is based on reviews of draft versions of Eurocode 9 made in the above-mentioned SSC reports. Similar to other codes, Eurocode 9 develops detail categories for the design being developed and recommends an applicable S/N curve based on a number of parameters.

The fatigue classifications of Eurocode 9 is based on the stress range of the S-N curve at 2×10^6 cycles and the negative slope of the S-N curve at that point. They are also referenced by the classification of the European Convention for Constructional Steelwork (ERAAS, 1992). Thus a full penetration transverse butt weld, which had the ERASS classification of B-10, would be classified as 35, 3.4 under Eurocode 9 because the S-N curve has a stress range at 2×10^6 cycles of 35 MPa (5.07 ksi) and a slope of -3.4 at 2×10^6 cycles. Note that like most steel fatigue design codes, the fatigue classification details assume that the fatigue lives of welded aluminum details are the same for all welded alloys. The classification also assumes that the fatigue lives depend only on the difference between the maximum and minimum stress, the stress range, and are therefore independent of average stress levels. The exception is in the fatigue strength of unwelded base metal, which does depend on the average stress level and on the aluminum alloy.

The design S-N curves are developed by taking a line two standard deviations below the mean line through the experimental data. Therefore, they represent a probability of 2.3 percent of failure after N or less loading cycles at the given stress level.

The fatigue classifications are given in Table 9-1 through Table 9-7. The details shown represent the test specimens used to develop the data at several different laboratories. Those details were related to ship-specific structural details in Chapter 4.

Table 9-1 Fatigue Classification of Aluminum Structural Details under Eurocode 9, Butt Welds

Detail Type	Internal Quality ¹	Geometric Quality ²	Type ³	Eurocode 9 Class ⁴	Sketch
Base Metal				70, 7.00	
Butt Weld, ground flush	B	B	FL	55, 7.00	
Butt Weld, ground flush	C	C	OP	45, 7.00	
Butt Weld, double sided	B	C	FL	50, 4.3	
Butt Weld, double sided	B	B	OP	40, 3.4	
Butt Weld, double sided	C	C	OP	35, 3.4	
Butt Weld, single sided with backing	C	C	FL	40, 4.3	
Butt Weld, single sided with backing	C	C	OP. HA	30, 3.4	
Butt Weld, single sided, no backing	B	B	FL	45, 4.3	
Butt Weld, single sided, no backing	C	C	FL	40, 4.3	
Butt Weld, single sided, no backing	C	C	OP. HA	30, 3.4	
Butt Weld, single sided, partial penetration	D	C		18, 3.4	

1. EN 30 042
2. EN 30 042
3. FL, flats, solids; OP, open shapes; HO, hollow, tubular
4. Stress range at 2×10^6 cycles, negative slope

Table 9-2 Fatigue Classification of Aluminum Structural Details under Eurocode 9, Cruciform Joints

Detail Type	Internal Quality ¹	Geometric Quality ²	Eurocode 9 Class ³	Sketch
Cruciform, full penetration	B	B	35, 3.4	
Cruciform, partial penetration	C	C	30, 3.4	
Cruciform, no penetration	C	C	25, 3.4	
Cruciform, one sided	C	C	12, 3.4	

1. EN 30 042
2. EN 30 042
3. FL, flats, solids; OP, open shapes; HO, hollow, tubular
4. Stress range at 2×10^6 cycles, negative slope

Table 9-3 Fatigue Classification of Aluminum Structural Details under Eurocode 9, Lap Joints

Detail Type	Internal Quality ¹	Geometric Quality ²	Eurocode 9 Class ³	Sketch
Lap Joint, Crack at Base of Weld	C	C	23, 3.4	
Lap Joint, Crack at Edge of Weld	C	C	18, 3.4	
Lap Joint, Crack at Fillet Toe	C	C	14, 3.4	

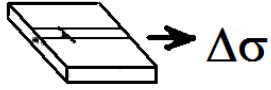
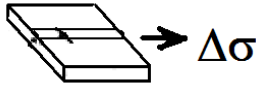
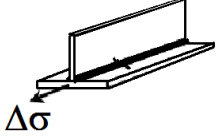
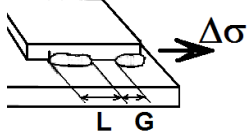
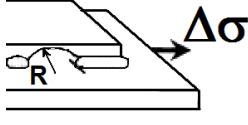
1. EN 30 042
2. EN 30 042
3. Stress range at 2×10^6 cycles, negative slope

Table 9-4 Fatigue Classification of Aluminum Structural Details under Eurocode 9, Welded Attachments, Transverse Weld Toe

Detail Type	T ¹ (mm)	L ² (mm)	Eurocode 9 Class ³	Sketch
Attachment on Surface	≤ 15	≤ 20	31, 3.4	
Attachment on Surface	≤ 4	> 20	25, 3.4	
Attachment on Surface	4 < T ≤ 10	> 20	22, 3.4	
Attachment on Surface	10 < T ≤ 15	> 20	20, 3.4	
Attachment overlapping edge	≤ 15	≤ 20	27.3, 3.4	
Attachment overlapping edge	≤ 4	> 20	22.0, 3.4	
Attachment overlapping edge	4 < T ≤ 10	> 20	19.4, 3.4	
Attachment overlapping edge	10 < T ≤ 15	> 20	17.6, 3.4	
Attachment on Edge			18, 3.4	
Attachment on Edge, Radius ≥ 50 mm, ground smooth			35, 3.4	
Attachment parallel to stress			23, 3.4	
Attachment parallel to stress, Radius ≥ 50 mm, ground smooth			35, 3.4	
Web Chock			23, 3.4	
Attachment tube			23, 3.4	

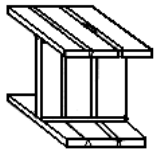
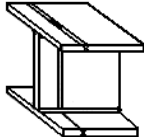
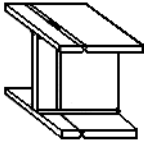
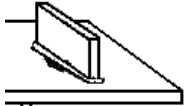
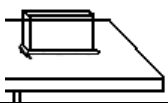
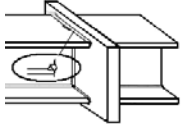
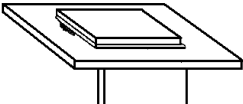
1. Thickness of base plate, mm
2. Length of attachment, mm
3. Stress range at 2×10^6 cycles, negative slope

Table 9-5 Fatigue Classification of Aluminum Structural Details under Eurocode 9, Welded Attachments, Longitudinal Welds

Detail Type	Internal Weld Quality ¹	Geometric Weld Quality ²	Eurocode 9 Class ³	Sketch
Full Penetration Butt Weld, Ground Flush	B	C	60, 4.3	
Full Penetration Butt Weld, Ground Flush	C	C	55, 4.3	
Full Penetration Butt Weld	C	D	45, 4.3	
Continuous Fillet Weld with or without stop/starts	C	D	40, 4.3	
Intermittent Fillet Weld, $G \leq 2.5 L$	C	D	35, 4.3	
Rat Hole, $R \leq 2.5 \text{ mm}$	C	D	28, 3.4	

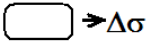
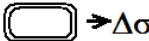
1. Weld Quality in accordance with EN 30 D42.
2. Weld Quality in accordance with EN 30 D42.
3. Stress range at 2×10^6 cycles, negative slope

Table 9-6 Fatigue Classification of Aluminum Structural Details under Eurocode 9, Welded Attachments to Built-up Beam

Detail Type	Internal Quality ¹	Geometric Quality ²	Eurocode 9 Class ³	Sketch
Butt Weld, full penetration, ground flush, single or double sided	B	B	40,3.4	
Butt Weld, full penetration, double sided	B	C	35, 3.4	
Butt Weld, full penetration, single sided	C	C	30, 3.4	
Transverse chock	C	C	18, 3.4	
Longitudinal chock	C	C	23, 3.4	
Cruciform, double sided	C	C	25, 4.3	
Attachment on Surface	C	C	20, 4.3	

1. Weld Quality in accordance with EN 30 D42.
2. Weld Quality in accordance with EN 30 D42.
3. Stress range at 2×10^6 cycles, negative slope

Table 9-7 Fatigue Classification of Aluminum Structural Details not Covered under Eurocode 9

Detail Type	Internal Quality ¹	Geometric Quality ²	Eurocode 9 Class ³	Sketch
Unreinforced Opening ⁴			45, 4.84	
Reinforced Opening ⁴			40, 3.4	

1. Weld Quality in accordance with EN 30 D42.
2. Weld Quality in accordance with EN 30 D42.
3. Stress range at 2×10^6 cycles, negative slope
4. Requires stress concentration computation.

9.4 Fatigue Data for Specific Ship Details

The above general S-N curves are based primarily on data from civil engineering structures, such as buildings and bridges. A few aluminum structural details that are used in aluminum ship and boat construction have been tested. Ye and Moan (2002) tested an extruded box stiffener in which the stiffeners were joined by lap joints, as shown in Figure 9-3. The 13 extruded sections that were fatigue tested in this study were 6082-T6, and the plates lapped on the stiffeners were 5083-H116. The stiffeners were loaded under four-point bending, so that the welds were in a region of constant bending moment, and the stress ratio, R , was 0.44. The results of the testing are shown in Figure 9-4, where the lower 5 percent confidence level nearly coincides with the Eurocode 9 fatigue classification 25-3.4. Ye and Moan chose this detail category, which is the classification for a fillet-welded attachment. These data show that for many structural details using Eurocode 9 is overly conservative. If no data were available, the classification that would be used would have been the category for a load-carrying lap joint, which is 14-3.4 and, as shown in Figure 9-4, is far below the curve that fits the data.

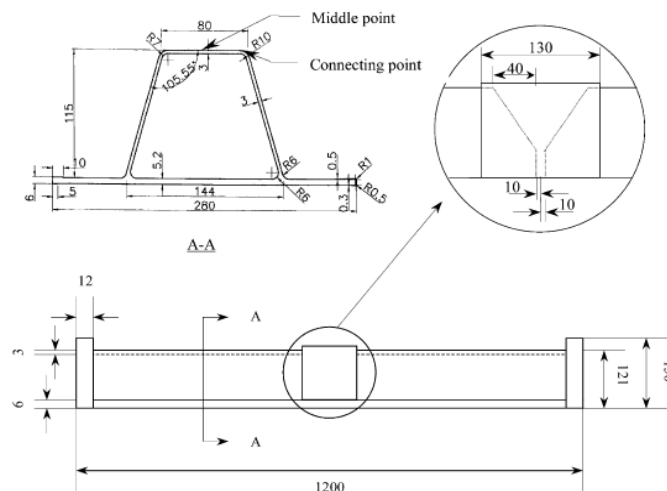


Figure 9-3 Box stiffener lap joints (Ye and Moan, 2002).

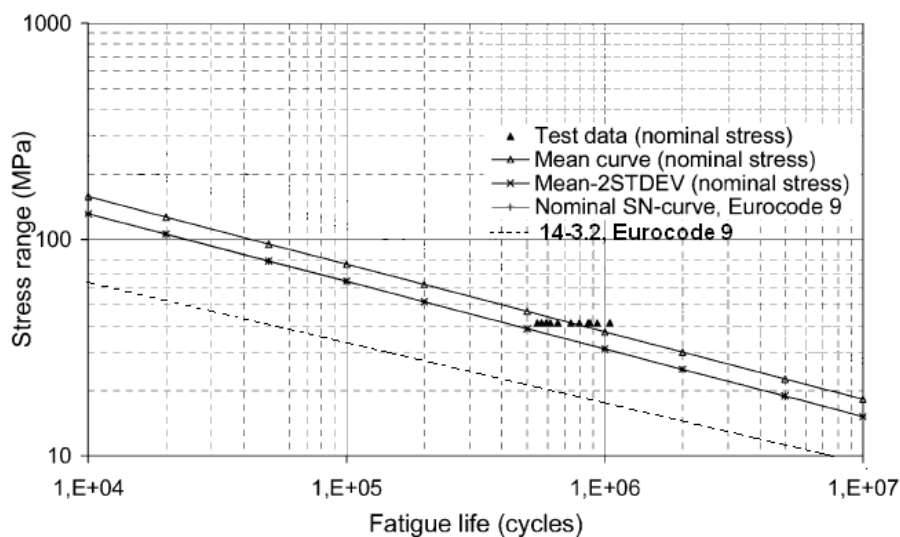


Figure 9-4 Fatigue of lapped joints of box girders (Ye and Moan, 2002).

Another ship detail was tested by Beach et al. (1981) for the intersection of a vertical bulkhead stiffener with a bottom longitudinal stiffener, such as shown in Figure 9-5. Eurocode 9 would suggest that this would be classified as 23, 3.4 as a chock. Comparison of that classification with the data is shown in Figure 9-6, where the Eurocode 9 classification seems to be conservative compared to the data, and a classification with a stress range at 2×10^6 cycles closer to 25-28MPa would be more logical.

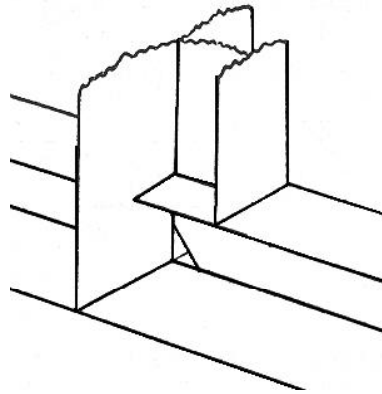


Figure 9-5 Intersection of a vertical bulkhead stiffener with a bottom longitudinal stiffener (Beach et al. 1981).

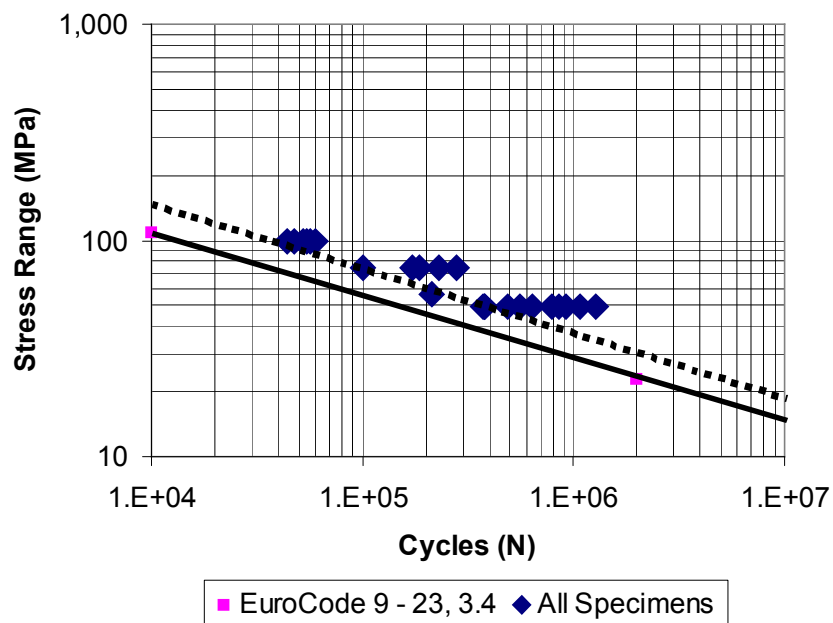


Figure 9-6 Fatigue data for stiffener intersection compared to Eurocode 9.

A very comprehensive analysis of different fatigue codes was made by Maddox (2003), who included the data of Beach et al. with other data for cruciform joints, compared to standard

curves for those configurations. All of the different codes fell below the actual data. The detail of a non-load carrying chock, on which the classification for Eurocode 9 was made, is included in a review of aluminum structural details made by Hobacher (1996). He classed the detail, shown in Figure 9-7, as having a stress range of 28 MPa at 2×10^6 cycles, which seems to fit the lower limit of the data in Figure 9-6. This illustrates that more data is needed of specific aluminum ship structural details, and that reliance should not be made on standard design codes that were developed for other types of structures.

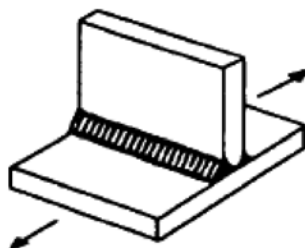


Figure 9-7 Non-load carrying chock (Hobacher, 1996).

9.5 Fatigue Analysis for Operation in a Seaway

The above discussion looked at the total number of loading cycles a specimen can endure before failure when loaded at a constant stress range. Vessels operating in a seaway do not experience such constant loading. Depending on wave height, wave period, ship speed, and ship heading relative to the waves, the bending moments to which the hull girder is subjected vary from one maximum lifetime load to very low loads that are repeated thousands of times. Over a lifetime of 20 years of operations in all types of seas, a typical ship may experience more than 10 million loading cycles. Because of higher wave encounter frequencies, high-speed ships may experience even more loading cycles, as many as 10^9 cycles. Other sources of loading than wave-induced loads, such as machinery-induced structural vibration may result in even higher numbers of loading cycles.

The summation of all the loading cycles that a ship experiences over its lifetime is called a fatigue-loading spectrum. A typical fatigue spectrum as developed by the computer program SPECTRA 8.2 (Michaelson, 2000) is shown in Figure 9-8. The fatigue spectrum is presented as an exceedance spectrum. The maximum lifetime loading ranges from a hogging moment of 17,000 meter-tonnes to a sagging moment of 19,000 meter-tonnes, a bending moment range of 36,000 meter-tonnes, a load that is not expected to be exceeded during the lifetime of the ship. However, in this example, Figure 9-8 shows that a bending moment ranging from a hogging moment of 5,000 meter-tonnes to a sagging moment of 5,050 meter-tonnes will be exceeded one million times during the ship's lifetime.



Figure 9-8 Typical fatigue loading spectrum for a 100-meter ship (SPECTRA 8.2).

To analyze fatigue life under these conditions of random loading, the theory of linear cumulative fatigue damage (Palmgren-Miner Rule) is used. According to this theory, the fatigue damage caused by repeated loading for a number of cycles at a set stress range is determined by the ratio of the number of load cycles to the fatigue strength at that stress level. For example, the Eurocode 9 detail 23, 3.4 has a fatigue life of 2,000,000 cycles at a stress range of 23 MPa. If the detail is loaded for 200,000 stress cycles at 23 MPa, then $200,000 / 2,000,000 = 0.10$ of the fatigue life of the detail will be used up.

Linear cumulative fatigue damage further assumes that fatigue damage is independent of the order of the magnitude of stress cycles of repeated loading at other stress ranges. The total fatigue damage due to repeated loading at different stress ranges is then the summation of the fatigue damage done by the number of loading cycles at each stress range. This concept is stated mathematically in equation 9.2, where D is the total cumulative fatigue damage, n_i is the number of load cycles at stress range i , and N_i is the fatigue life determined from the S-N curve of the structural detail at the stress range i . Fatigue failure is assumed to occur if D is greater than or equal to 1.0.

$$D = \sum_{i=1}^n \frac{n_i}{N_i} \tag{9-2}$$

Application of Equation (9-2) is illustrated in Table 9-8, where the calculation is carried out in a spreadsheet for a 42.67-meter 32-knot aluminum crew boat. The maximum bending moment range of 23,990 kN-meters) is divided by the section modulus to deck of 3,470 cm² m to obtain a maximum stress range of 69.1 MPa, a stress range that is exceeded only once in a lifetime of 6.3×10^7 cycles, the maximum number of cycles that a vessel of this size would encounter in a 20-year service life as shown below.

Because the fatigue-loading spectrum is expressed as an exceedance curve, the actual number of cycles for each loading block is determined by the difference between the cycles in successive load blocks. Therefore, the number of cycles in the first load block, n_1 , is 2.25 cycles – 1.00 cycles = 1.25 cycles. Because that number of cycles for that load block is intermediate

between the stress range cycles, the block stress of 66.35 MPa is the average of 67.70 MPa and 64.99 MPa. The S-N curve for the structural detail, such as the 23, 3.4 curve in Figure 9-1, is used to determine the fatigue life, N_1 , of 54,542 cycles at the stress range of 66.35 MPa. The ratio $1.25 / 54,542 = 0.000023$ is the amount of fatigue damage done by the first loading block. The sum of all of those individual block damages is 0.948, indicating that this fatigue detail, loaded by this fatigue spectrum, will not fail until after 6.2×10^7 random load cycles occur. A 20-year life was assumed, but the actual life is $20 / 0.948 = 21.1$ years. Because the S-N curve on which the calculation was based has a probability level of 2.3 percent associated with it, there is a 97.7 percent probability that the fatigue life will be greater than 21.1 years.

Table 9-8 Example of Cumulative Linear Fatigue Calculation

S/S_{max}	Stress Range (n) (Mpa)	Cycles Exceeded	No. Cycles at Stress	Block Stress (MPa)	Lower Fatigue Cycles (N_1)	Upper Fatigue Cycles (N_2)	Fatigue Cycles (N)	Fatigue Damage
1.00	67.70	1.00E+00	1.25E+00	66.35	5.4542E+04	3.8237E+03	5.4542E+04	0.000023
0.96	64.99	2.25E+00	2.78E+00	63.64	6.2845E+04	4.7886E+03	6.2845E+04	0.000044
0.92	62.28	5.03E+00	6.17E+00	60.93	7.2858E+04	6.0561E+03	7.2858E+04	0.000085
0.88	59.58	1.12E+01	1.36E+01	58.22	8.5037E+04	7.7412E+03	8.5037E+04	0.000160
0.84	56.87	2.48E+01	2.99E+01	55.51	9.9985E+04	1.0012E+04	9.9985E+04	0.000299
0.80	54.16	5.47E+01	6.54E+01	52.81	1.1852E+05	1.3116E+04	1.1852E+05	0.000552
0.76	51.45	1.20E+02	1.42E+02	50.10	1.4175E+05	1.7428E+04	1.4175E+05	0.001002
0.72	48.74	2.62E+02	3.07E+02	47.39	1.7123E+05	2.3527E+04	1.7123E+05	0.001792
0.68	46.04	5.69E+02	6.59E+02	44.68	2.0915E+05	3.2327E+04	2.0915E+05	0.003150
0.64	43.33	1.23E+03	1.40E+03	41.97	2.5869E+05	4.5309E+04	2.5869E+05	0.005431
0.60	40.62	2.63E+03	2.98E+03	39.27	3.2452E+05	6.4951E+04	3.2452E+05	0.009169
0.56	37.91	5.61E+03	6.26E+03	36.56	4.1378E+05	9.5537E+04	4.1378E+05	0.015117
0.52	35.20	1.19E+04	1.30E+04	33.85	5.3753E+05	1.4476E+05	5.3753E+05	0.024269
0.48	32.50	2.49E+04	2.70E+04	31.14	7.1372E+05	2.2709E+05	7.1372E+05	0.037793
0.44	29.79	5.19E+04	5.53E+04	28.43	9.7242E+05	3.7115E+05	9.7242E+05	0.056822
0.40	27.08	1.07E+05	1.12E+05	25.73	1.3666E+06	6.3719E+05	1.3666E+06	0.081982
0.36	24.37	2.19E+05	2.25E+05	23.02	1.9947E+06	1.1618E+06	1.9947E+06	0.112602
0.32	21.66	4.44E+05	4.45E+05	20.31	3.0527E+06	2.2837E+06	3.0527E+06	0.145638
0.28	18.96	8.88E+05	8.67E+05	17.60	4.9659E+06	4.9459E+06	4.9659E+06	0.174667
0.24	16.25	1.76E+06	1.66E+06	14.89	8.7633E+06	1.2190E+07	1.2190E+07	0.136478
0.20	13.54	3.42E+06	3.13E+06	12.19	1.7337E+07	3.6027E+07	3.6027E+07	0.086784
0.16	10.83	6.55E+06	5.73E+06	9.48	4.0744E+07	1.3996E+08	1.3996E+08	0.040906
0.12	8.12	1.23E+07	1.01E+07	6.77	1.2791E+08	8.6119E+08	8.6119E+08	0.011748
0.08	5.42	2.24E+07	1.69E+07	4.06	7.2642E+08	1.3586E+10	1.3586E+10	0.001242
0.04	2.71	3.93E+07	2.37E+07	1.35	3.0437E+10	5.1232E+12	5.1232E+12	0.000005
0.00	0.00	6.30E+07					Cumulative Total Damage =	0.947761

9.6 Development of Fatigue Loading Spectra

The fatigue-loading spectrum of Figure 9-8 was developed from the computer program SPECTRA 8.2, which is based on the measured response of ship models tested in the wave tank of the U.S. Navy's David Taylor Model Basin in Bethesda, Maryland. In particular, the ship was

assumed to be a 100-meter fine-bowed frigate operating in the North Atlantic Ocean for 20 years, of which 80 percent of the time is spent at sea. The resultant fatigue loading exceedance curve, as shown in Figure 9-8, if converted to a load range curve by adding the hog and sag moments together, becomes the fatigue spectrum in Figure 9-9. This figure is a semi-log plot, with the bending moment range on a linear scale and the fatigue cycles on a logarithmic scale. If the relationship between the load range and number of cycles followed an exponential distribution, the curve would be a straight line. However, it is slightly curved, suggesting a Weibull distribution, which is generally the distribution of fatigue loading spectra.

The Weibull distribution is given by the formula:

$$N = N_{\max} \times \exp\left(-\left(\frac{S}{S_{\max}}\right)^{\zeta} \times \ln(N_{\max})\right) \quad (9-3)$$

where:

- N is the number of loading cycles at stress range S,
- N_{\max} is total number of loading cycles,
- S_{\max} is the maximum load range,
- ζ is a Weibull parameter.

In the Weibull distribution, if $\zeta = 1.0$, the distribution is an exponential distribution. The Weibull distribution can be made to fit the distribution from SPECTRA 8.2 using regression analysis. However, to make the fit better suit the purpose, a manual trial-and error approach was used, using the maximum number of cycles from SPECTRA 8.2 for N_{\max} , and selecting the parameter ζ to ensure that the best fit between the fatigue spectrum and the Weibull distribution occurs in the region between 10^5 cycles and 10^7 cycles, which Table 9-8 shows to be the region of greatest fatigue damage. The resulting Weibull distribution with a parameter equal to 1.22 is shown in Figure 9-9 superimposed of the SPECTRA 8.2 spectrum, and the match is very close.

In order to determine the Weibull coefficients and number of load cycles for a variety of ship sizes, the procedure above was used for a family of geometrically similar ships ranging in length from 20 meters (65.5 ft) to 300 meters (984 feet). Although the frigate hull form used is not representative of the hull forms found in ships of either end of this size range, it still provides a reasonable method of determining the shape of the Weibull distributions. The actual magnitude of bending moments does not matter, only their relative values at different numbers of loading cycles.

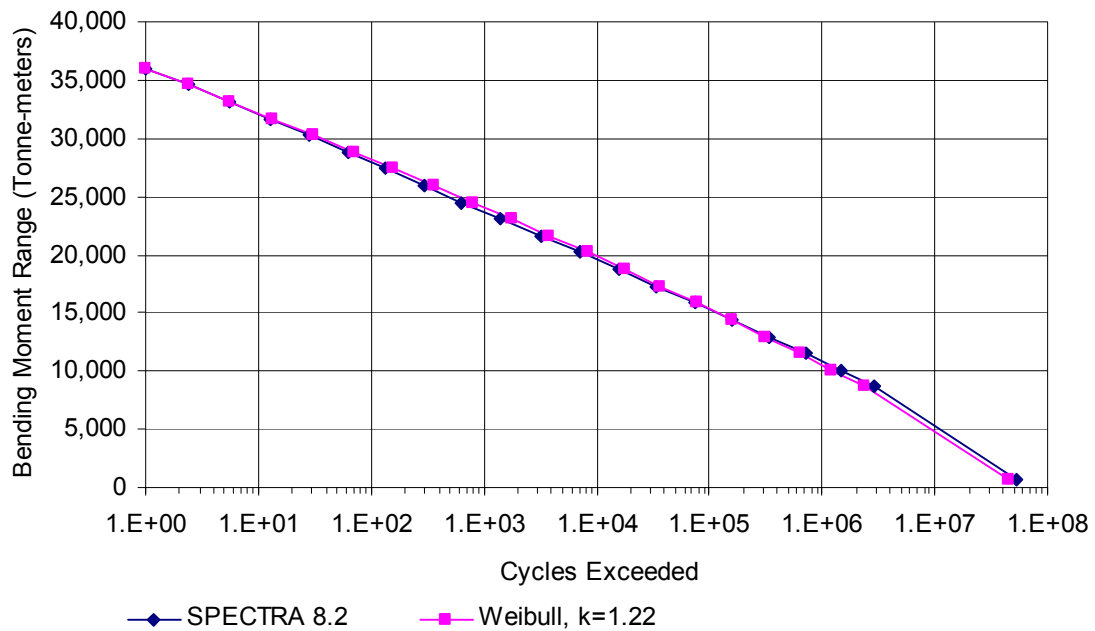


Figure 9-9 Comparison of fatigue spectrum computed by SPECTRA 8.2 with a Weibull distribution.

Figure 9-10 shows how the Weibull coefficient varies with ship length. The coefficient is rather constant for the larger ships, but becomes slightly smaller with decreasing ship length. In the analysis, the operational profile for frigates in SPECTRA was used, but that profile is not applicable to smaller craft, which will reduce speed in lower sea states than larger ships. Therefore, smaller craft may have slightly lower moments than calculated and fewer loading cycles than predicted. Therefore, the reduction in Weibull coefficient for shorter vessels shown in Figure 9-10 may be unconservative. The predicted fatigue life is very sensitive to the Weibull coefficient. For example, the calculations in Table 9-8 are based on a Weibull coefficient of 1.22. If the coefficient were changed to 1.12, the cumulative damage would change from 0.99 to 0.63, an increase in calculated fatigue life of more than 50 percent. Also shown in Figure 9-10 are the Weibull coefficients as a function of ship length developed for a proposed IACS standard for fatigue design (IACS, 1999).

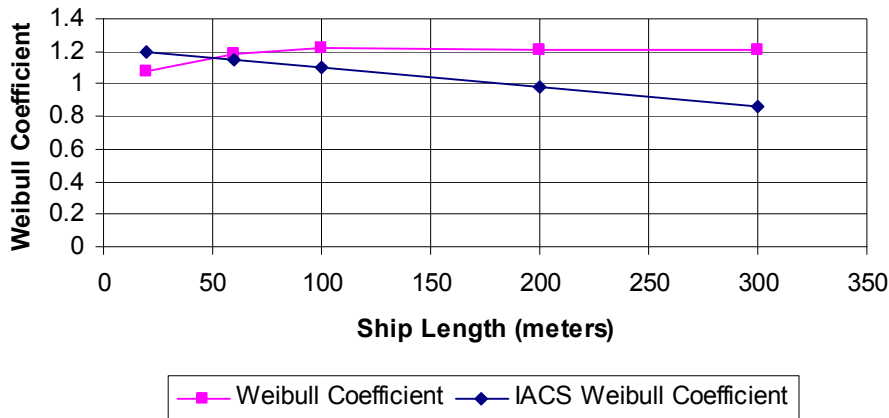


Figure 9-10 Weibull coefficient for fatigue spectra versus ship length.

The total number of loading cycles varies considerably with ship length, reflecting that the shorter ship responds more than a longer ship to the shorter waves that occur in low sea states, which are more common than high sea states. The assumption was made that the ship would be at sea for 80 percent of 20 years or $0.80 \times 20 \times 365 \times 24 \times 60 \times 60 = 5.046 \times 10^8$ seconds. Then the 20-meter ship, with 6.489×10^7 cycles, has an average encounter period of 7.78 seconds. The 100-meter ship has an average encounter period of 9.54 seconds, and the 300-meter ship has an average encounter period of 15.54 seconds. The average encounter period is related to ship length in Figure 9-12.

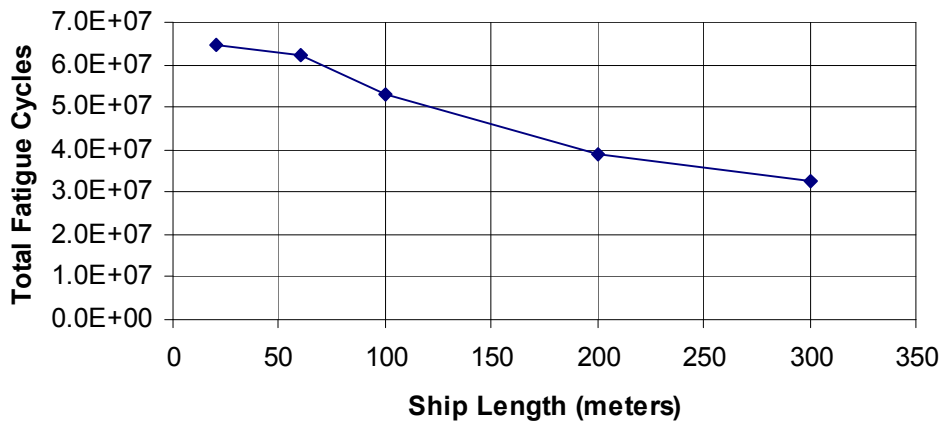


Figure 9-11 Total fatigue loading cycles for operation 80 percent over 20 years versus ship length.

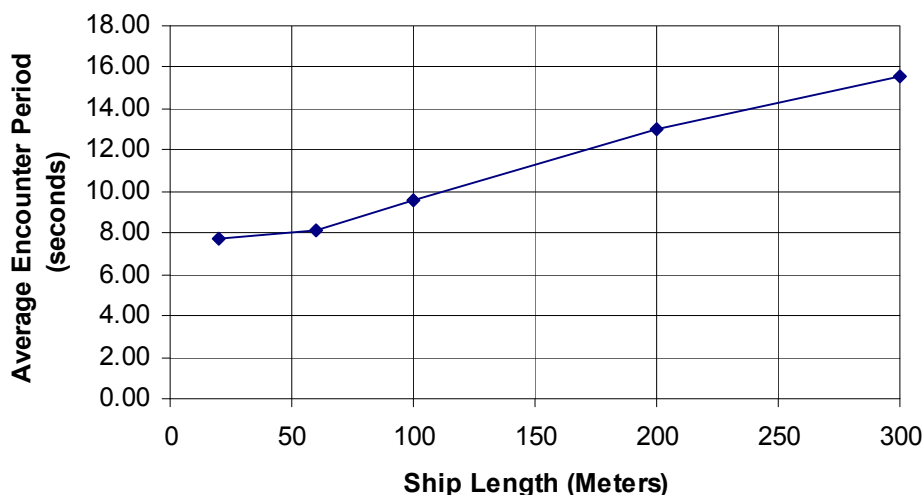


Figure 9-12 Average encounter period versus ship length.

An alternative formulation of the linear damage summation rule is the form:

$$D = \int \frac{p(S)ds}{N(S)}, \text{ or better, } D = \sum_i p_i \int \frac{p_i(S)ds}{N(S)},$$

where P_i is the probability to encounter an “i” stationary process (sea state), $p_i(S)$ is the probability density of stress distribution at a given location in a given sea state assuming a stationary process (Rayleigh distribution), and $N(S)$ is the design S-N curve for a given location expressed in terms of nominal stress and modified to consider effects of stress concentration and of mean stress. To do this, the probabilities of the loads should be assessed and considered. Mansour et al. (1996) discuss the subject of probabilistic fatigue analysis. Unfortunately, most aluminum design S-N curves are expressed in terms of the lower probability levels, and the actual probabilities are not given, which makes implementation of probabilistic fatigue difficult.

9.7 Fatigue Analysis Procedure for Preliminary Design

The above method of obtaining a fatigue loading spectrum is not necessarily accurate enough for final design, but it can be used during preliminary design stages to determine if a possible fatigue problem exists and to take steps to reduce the likelihood of fatigue damage. This approach is not necessarily applicable to multiple-hull types such as SWATH, catamarans, and trimarans, although the general approach is. Also, very high-speed craft could experience more loading cycles unless their orientation to wave direction is of a similar nature to that assumed in SPECTRA 8.2. Most loading formulations for high-speed craft as discussed in Chapter 3 are based upon an estimate of maximum lifetime loads, not nominal loads. Therefore, stress analysis using those loads should be able to determine the maximum lifetime stress at a structural detail. The stress will generally come from a combination of primary, secondary, and tertiary stresses. Depending on the type of loading producing the stresses, they may all be related in time to each other. The maximum hydrostatic head causing bending of a stiffener will

vary in intensity as a wave passes just as hull girder bending moments will vary from hog to sag with the passing wave. The challenge is to determine the phasing between maximum and minimum hull girder bending moments and maximum and minimum hydrostatic heads. If detailed calculations are performed with a ship motion program, then that phasing is determined. For preliminary design purposes, some judgment must be used to determine that phasing. The maximum lifetime stress and the minimum stress associated with the same wave cycle should be estimated to determine the maximum lifetime stress range.

With the maximum stress range known, the maximum lifetime loading cycles can be estimated from Figure 9-12, which can be used to determine the average encounter period for the vessel being designed. With the number of years that the vessel is expected to operate and the percentage of time that it will be underway, the total number of seconds the ship will be in operation during its lifetime will be known. Dividing that time by the average encounter period will provide the total lifetime fatigue cycles. Using Figure 9-10 the Weibull coefficient can be estimated. With the maximum lifetime stress range, the total lifetime fatigue cycles, and the Weibull coefficient known, the fatigue-loading spectrum can be developed using equation 9.2. Then, for the fatigue category being analyzed, the cumulative linear fatigue calculation can be performed using a spreadsheet similar to Table 9-8.

Note that the total damage calculated is inversely proportional to the fatigue life. In the example for Table 9-8, the fatigue-loading spectrum was based on 20 years of operation. The total damage was 0.998, so the actual fatigue life is $20 / 0.998 = 20.04$ years. If the total damage had been 0.50, then the fatigue life would have been 40 years, and if the damage had been 2.0, the fatigue life would have been 10 years.

9.8 Spectral Fatigue Analysis

If the preliminary fatigue analysis indicates potential fatigue problems, they should be resolved by lowering stress levels or increasing the classification of structural details. However, if the final design is marginal in that the computed fatigue lives for a significant number of structural details are near the desired fatigue life, a spectral fatigue is called for. In many cases an owner may require such an analysis, and some classification societies have special classifications for vessels that have been designed using spectral fatigue analysis.

A guide to spectral fatigue analysis is provided by ABS in their Guidance Notes on Spectral-Based Fatigue Analysis for Vessels (ABS, 2004). Although that document uses S-N curves for steel structure, the principles of fatigue analysis described are applicable to any type of hull structural material for which fatigue data is available. The procedure will work well with the Eurocode 9 fatigue guidance for aluminum structural details or any other source of S-N data for aluminum.

The ABS procedure is rather involved because it requires the calculation of a complex stress transfer function for all structural details being analyzed. This stress transfer function is generally determined by finite element analysis where the hull loading is determined by a seakeeping program that provides pressure loads on the hull plating for a range of wave headings

and frequencies. Thousands of such calculations must be performed, so an automated method of tracking stress response is needed.

For high-speed craft, the ABS procedure must be augmented to account for the anticipated operational profile. A 60-knot craft in general will not operate at that speed in all sea states, and in those sea states in which it can run at maximum speed, preferred headings relative to wave direction may be taken. This is the same as use of operational profiles used in SPECTRA 8.2 and other fatigue analysis procedures used by the U.S. Navy. Additionally, the specific wave energy spectra for the areas in which the craft will be operating should be used instead of a general ocean profile.

9.9 Fatigue Crack Growth

The above discussion concerned the process of crack initiation, where repeated alternating stress levels at a defect or discontinuity can lead to the beginning of a small crack. Fatigue crack growth analysis is used to determine the consequences of such a crack to the overall structural integrity of the structure. The rate of fatigue crack growth is related to the linear elastic stress intensity factor, K , which can be calculated by the equation:

$$K = Y \sigma \sqrt{\pi a} \quad (9-4)$$

where:

a is the length of the crack

σ is the field stress in the vicinity of the crack, and

Y is a factor depending on the geometry of the structure in which the crack exists.

Various forms for the calculation of K define the crack length as either the full length of the crack or half of its length. In some cases, the factor p is included within the radical, in others it is part of the definition of Y . Therefore, in the crack geometries defined in Table 9-9, the full equation is given for K and the crack length a is defined. Factors for other simple geometries can be found in reference textbooks on fracture mechanics, such as Broek (1978), and a more extensive compilation by Sih (1973). For more complex geometries, linear elastic finite element analysis can be used, and several finite element computer programs have modules for the computation of K . Note that the stress intensity factor, K , is a function of crack size, a , and must be recomputed for a growing crack.

Table 9-9 Stress Intensity Factors for a Few Geometries

Configuration	K	Comments
Crack normal to direction of stress in an infinite plate	$\sigma \sqrt{\pi a}$	a is one-half the crack length
Crack normal to direction of stress at the edge of a plate infinite in the direction of crack propagation.	$1.1 \sigma \sqrt{\pi a}$	a is the crack length
Crack normal to direction of stress in the center of a plate of width W	$\sigma \sqrt{\pi a} \sqrt{\secant\left(\frac{\pi a}{W}\right)}$	a is one-half the crack length

For fatigue crack growth, the alternating stress intensity factor range, ΔK , is used to determine the rate of crack growth, da/dN for each cycle, N , of stress $\Delta\sigma$. An example of crack growth rates for 5083 aluminum is shown in Figure 9-13 (Donald and Blair, 2006).

Note the typical S-shaped curve on the log-log plot in Figure 9-13. The curve is generally divided into three regions. Region I for low values of ΔK show the rates of crack growth da/dN decreasing as ΔK decreases, until ΔK reaches some threshold value below which no crack growth will occur. In the upper region III for higher values of ΔK , the crack growth rate increases rapidly to the point of unstable crack growth for high values of ΔK . The intermediate region can be approximated by a linear relationship on the log-log plot and is characterized by the equation:

$$\frac{da}{dN} = A(\Delta K)^m \tag{9-5}$$

where the coefficient A and exponent m are determined from the fatigue crack growth curve, such as Figure 9-13. When making fatigue crack growth calculations two methods of addressing the data are used. One is to adopt a single standard region II straight-line upper limit to the data. This has been done for steel but not for aluminum. Otherwise, piecewise approximation to the data is made by selecting points from curves such as Figure 9-13, using equation (9-5) as an interpolation function.

To demonstrate a fatigue crack growth computation in aluminum, a 41.39-meter 32-knot crew boat design, which was used for the comparative designs of this study, will be analyzed. The hull girder bending moments, calculated in accordance with the ABS guide for high-speed craft are 19,580 meter-tonnes sag, and 4,210 meter-tonnes hog. The section modulus of the boat, developed from scantlings selected in accordance with the requirements of the guide and a fatigue analysis, is 3,513 cm²-m to the deck. Accordingly, the maximum stresses in the main deck are 55.7 MPa compression and 12.0 MPa tension, a maximum stress range of 67.7 MPa.

This stress range was used with a Weibull exceedance curve developed in accordance with the criteria described above. In accordance with Figure 9-10 and Figure 9-11, the Weibull coefficient is 1.13, and there are 6.3×10^7 fatigue loading cycles for 20 years of service at 80 percent operability.

Aluminum Marine Structure Guide

When making fatigue crack growth calculations under random loading, load sequence effects are very important because the amount of crack growth at each loading cycle is dependent on the total crack length. Therefore, if analysis was made with all of the highest loads occurring first, the effect of lesser loads is intensified. For random loading, similar to the linear cumulative fatigue initiations described above, the most crack growth occurs at intermediate values of loadings where there are many load cycles with stress ranges high enough to cause significant crack growth.

The calculations are demonstrated in Table 9-10. The fatigue-loading histogram has been broken into 24 sub-blocks of stress levels, with the number of cycles at each stress level determined. The loading is further divided into 240 blocks to reduce the effect of load sequencing. Within each block, the stress levels remain the same, but 1/240 of the cycles are included. Thus, the 20-year loading has been broken down into one-month blocks.

Comparing Table 9-8 and Table 9-10, the values in the second column of Table 9-10 labeled “N” are 1/240 of the values in the fourth column of Table 9-8, labeled “# Cycles at Stress.” The values in the third column of Table 9-10 labeled “Stress Range (MPa)” are the same as the values in the fifth column of Table 9-8, labeled “Block Stress (MPa).”

An initial crack size of 24 millimeters was chosen (half-crack length of 12 mm), a crack size that would be fairly detectable with careful inspection. The crack was assumed to be in the center of the deck, which for the initial crack growth calculation could be considered to be an infinite plate, and in accordance with Table 9-9, $\Delta K = \sigma \sqrt{\pi a}$. The secant formula in the table could have been used, but the value of the correction would be 1.00. With ΔK determined, the slope m and coefficient A are looked up from Figure 9-13 to determine the crack growth per cycle, da/dN , which is multiplied by the number of cycles in each sub-block to determine the amount of crack growth. That growth is added to the length of the crack for the calculations in the following sub-block of loading, and the crack growth is calculated over the remainder of the loading block and for following loading blocks.

Table 9-10 Fatigue Crack Growth Calculation for a 42.7-meter Aluminum Vessel

Sub-block	Cycles (N)	Stress Range (MPa)	Half-Crack Size (a) (mm)	ΔK (MPa m ^{1/2})	m	A	da/dN (mm/cycle)	Crack growth (da) (mm)
1	5.20E-03	66.35	1.20E+01	12.88	2.73	7.44E-07	7.99E-04	4.15E-06
2	1.16E-02	63.64	1.20E+01	12.36	2.73	7.44E-07	7.13E-04	8.26E-06
3	2.57E-02	60.93	1.20E+01	11.83	2.73	7.44E-07	6.33E-04	1.63E-05
4	5.67E-02	58.22	1.20E+01	11.30	2.73	7.44E-07	5.59E-04	3.17E-05
5	1.25E-01	55.51	1.20E+01	10.78	2.73	7.44E-07	4.91E-04	6.12E-05
6	2.72E-01	52.81	1.20E+01	10.25	2.73	7.44E-07	4.28E-04	1.17E-04
7	5.92E-01	50.10	1.20E+01	9.73	2.63	9.21E-07	3.68E-04	2.18E-04
8	1.28E+00	47.39	1.20E+01	9.20	2.63	9.21E-07	3.18E-04	4.07E-04
9	2.74E+00	44.68	1.20E+01	8.68	2.38	1.54E-06	2.67E-04	7.33E-04
10	5.85E+00	41.97	1.20E+01	8.15	2.38	1.54E-06	2.30E-04	1.35E-03
11	1.24E+01	39.27	1.20E+01	7.62	3.73	1.12E-07	2.20E-04	2.73E-03
12	2.61E+01	36.56	1.20E+01	7.10	3.73	1.12E-07	1.69E-04	4.40E-03
13	5.44E+01	33.85	1.20E+01	6.58	6.03	1.84E-09	1.56E-04	8.49E-03
14	1.12E+02	31.14	1.20E+01	6.05	6.03	1.84E-09	9.47E-05	1.06E-02
15	2.30E+02	28.43	1.20E+01	5.53	5.92	2.17E-09	5.43E-05	1.25E-02
16	4.67E+02	25.73	1.20E+01	5.00	5.92	2.17E-09	3.01E-05	1.41E-02
17	9.36E+02	23.02	1.21E+01	4.48	4.82	1.00E-08	1.38E-05	1.29E-02
18	1.85E+03	20.31	1.21E+01	3.95	3.42	4.67E-08	5.14E-06	9.53E-03
19	3.61E+03	17.60	1.21E+01	3.43	3.42	4.67E-08	3.16E-06	1.14E-02
20	6.93E+03	14.89	1.21E+01	2.90	12.29	1.00E-10	4.86E-05	3.37E-01
21	1.30E+04	12.19	1.24E+01	2.41	12.29	1.00E-10	4.89E-06	6.37E-02
22	2.39E+04	9.48	1.25E+01	1.88	0.00	1.00E-10	1.00E-10	2.39E-06
23	4.22E+04	6.77	1.25E+01	1.34	0.00	1.00E-10	1.00E-10	4.22E-06
24	7.03E+04	4.06	1.25E+01	0.80	0.00	1.00E-10	1.00E-10	7.03E-06

The results of the calculation are shown in Figure 9-14, where the calculations are continued for 24 blocks, representing 24 months of operation. During this period, the 24-mm crack has grown to 50 mm in length. At this point, crack growth has increased the secant of (p / B) to 1.01, and this slight refinement on the calculations should be used for further crack growth calculations. However, as the crack continues to propagate, effective area is removed from the deck so that a revised section modulus calculation should also be made to determine the increase in stress levels for the fatigue-damaged craft. If these corrections are not used, a lower limit to the fatigue crack growth is made. If the amount of growth is determined to be unacceptable from the perspective of structural integrity, then refinement of the calculation would make the situation only more unacceptable. However, for a marginal situation, the refinement should be made, for as in Figure 9-14 shows, once crack growth begins, the rate of growth accelerates, sometimes very rapidly.

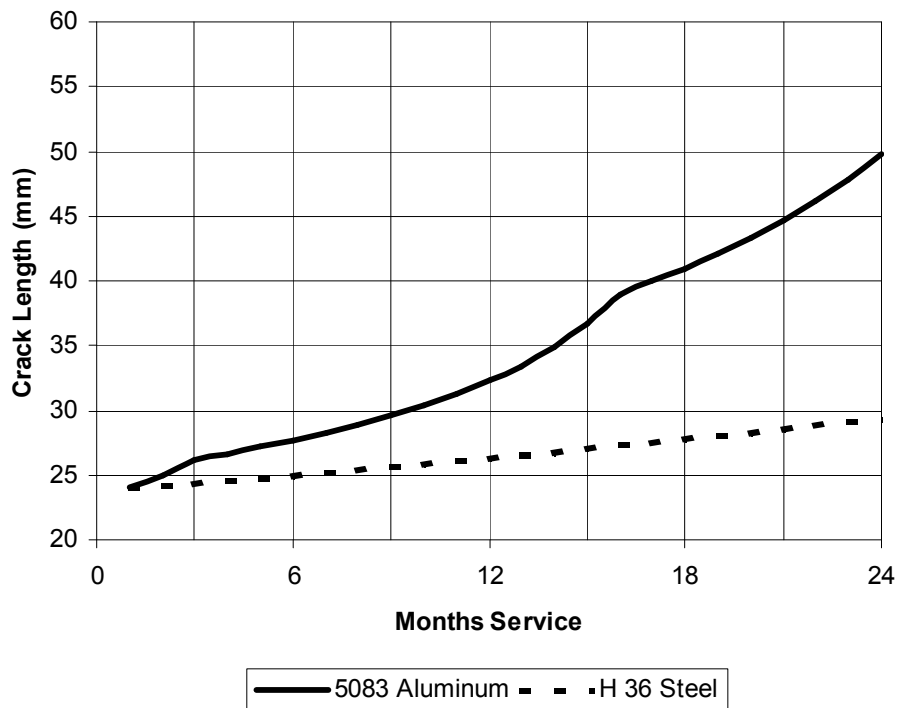


Figure 9-14 Predicted crack growth for a 43.9-m 32-knot craft.

To compare the fatigue crack growth characteristics of steel and aluminum, a typical da/dN curve for ABS Grade EH 36 steel is shown in Figure 9-15 (Leis, 1990). As with aluminum, most grades of structural steel have similar da/dN curves, with statistical variation in experimental data having more effect than the difference in alloys. Comparing the curves for steel and aluminum, the material crack growth rate in aluminum is about 30 times greater than in steel. For example, at a ΔK value of $10 \text{ MPa} \sqrt{\text{m}}$, the crack growth rate is $10 \times 10^{-6} \text{ mm/cycle}$ in steel, but $300 \times 10^{-6} \text{ mm/cycle}$ in aluminum. Although most material da/dN curves, including steel and aluminum can be normalized on a log-log plot on the basis of ΔK divided by the material elastic modulus ($\Delta K / E$), the exponential nature of the curves intensifies the difference. Although the elastic modulus of aluminum is one-third of that of steel, the coefficient of the crack growth rate makes the difference at the same value of ΔK about $3^3 = 30$ times greater.

Structural steels have a fairly constant Phase II region where the slope m is 3.0 and an upper bound to the coefficient A is $9.5 \times 10^{-9} \text{ mm/cycle}$ with ΔK in $\text{MPa} \sqrt{\text{m}}$ (Dexter and Pilarski, 2000), and that is a reasonable upper bound to the data in Figure 9-12.

For the H 36 steel version of the crew boat, the section modulus to deck is $1,659 \text{ cm}^2 \text{ m}$, so that the stresses in the deck are 118 MPa compression and 25 MPa tension, a stress range of 143 MPa. Using that information the calculations are repeated for steel, with the results shown in Figure 9-14. For the steel vessel, the 24-mm crack grew to only 30 mm, a 25 percent increase in size, compared to the doubling in size of the aluminum crack for the same operation of the

vessel over the same period of time, even though the stress level in the aluminum craft was about 50 percent less.

If the aluminum craft continued to operate for another two years without repairs made to the 50-mm crack, the crack would have grown to about 600 mm in length, after which it would become unstable and begin to propagate at an extremely rapid rate. For the steel craft, the 30-mm crack would grow to 38 mm in the same time, with continued propagation at a fairly stable rate.

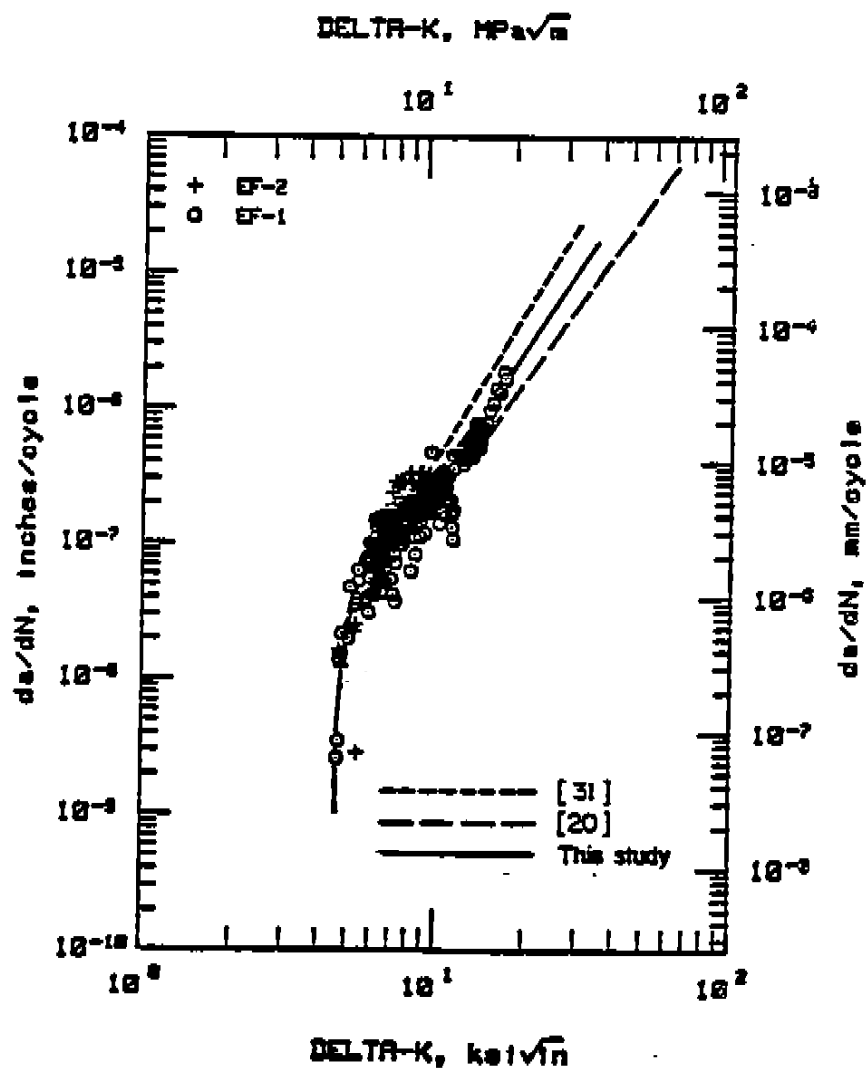


Figure 9-15 Fatigue crack growth da/dN curve for ABS Grade CH 36 steel (Leis, 1990).

These calculations demonstrate well the reason why fatigue is a concern for aluminum. With the material crack growth rate about thirty times greater for aluminum, the compounding effect of crack growth in an actual structure makes the rate of crack growth far greater. In the

situation for which the calculations were performed, a few months more of operations with the crack undetected or otherwise unrepaired would result in complete structural failure.

9.10 Fracture

Failure of material under stress in the presence of a crack is the subject of fracture mechanics. For analysis of brittle materials, such as glass, the linear elastic stress intensity factor, K , described above is used. However, for ductile materials, such as the aluminum and steel alloys, plastic flow occurs at the crack tip, and linear elastic analysis can become highly over-conservative, predicting failure where there is no danger of it occurring. For ductile materials, the J-Integral parameter, J , is used, although it can also be overly conservative for tough, ductile materials. For calculation purposes at stress levels prior to crack growth, the applied J-Integral can be determined from the stress intensity factor, K , using equations such as those in Table 9-9 using the relationship:

$$J = \frac{K^2}{E} \quad (9-6)$$

The units of J are generally Joules/mm², or kilo inch-pound/inch², with the U.S. customary units multiplied by the factor 0.1753 to obtain the SI units. For analysis of more complicated structural configurations with the finite element method, elastic plastic analysis with a computer program that computed the J-integral should be used.

For ductile material such as ship-grade aluminum and steel, the J-integral properties are characterized in different ways, one of which is the R-curve, such as Figure 9-16 (Donald and Blair, 2006). The R-curve shows the value of the J-integral, J_{mat} increasing with the applied load. The applied load is not shown on the R-curve. Instead, another result of increasing load, the amount of crack growth is shown. The R-curve illustrates that for these materials, increasing load in the presence of a crack will lead to the crack beginning to propagate by a small amount. However, the curve shows that as the crack propagates, the value of the J-integral increases rapidly, resisting further crack growth and fast fracture.

There are many ways of using the R-curve to analyze structure, but a simple method is to look at the critical value, J_{IC} , of J at which the rate of crack begins to increase initially. This is seen in Figure 9-16 as the knee of the curves, somewhat analogous to the yield point on a stress-strain curve. From Figure 9-16, the critical value of J at which crack extension begins is approximately $J_{IC} = 100 \text{ in-lb/in}^2 = 17.5 \text{ N-mm/mm}^2$. The standard value of J_{IC} is defined as the intersection of the R-curve with a line offset from the origin and with a value of $J = 2 \sigma_Y \Delta a$.

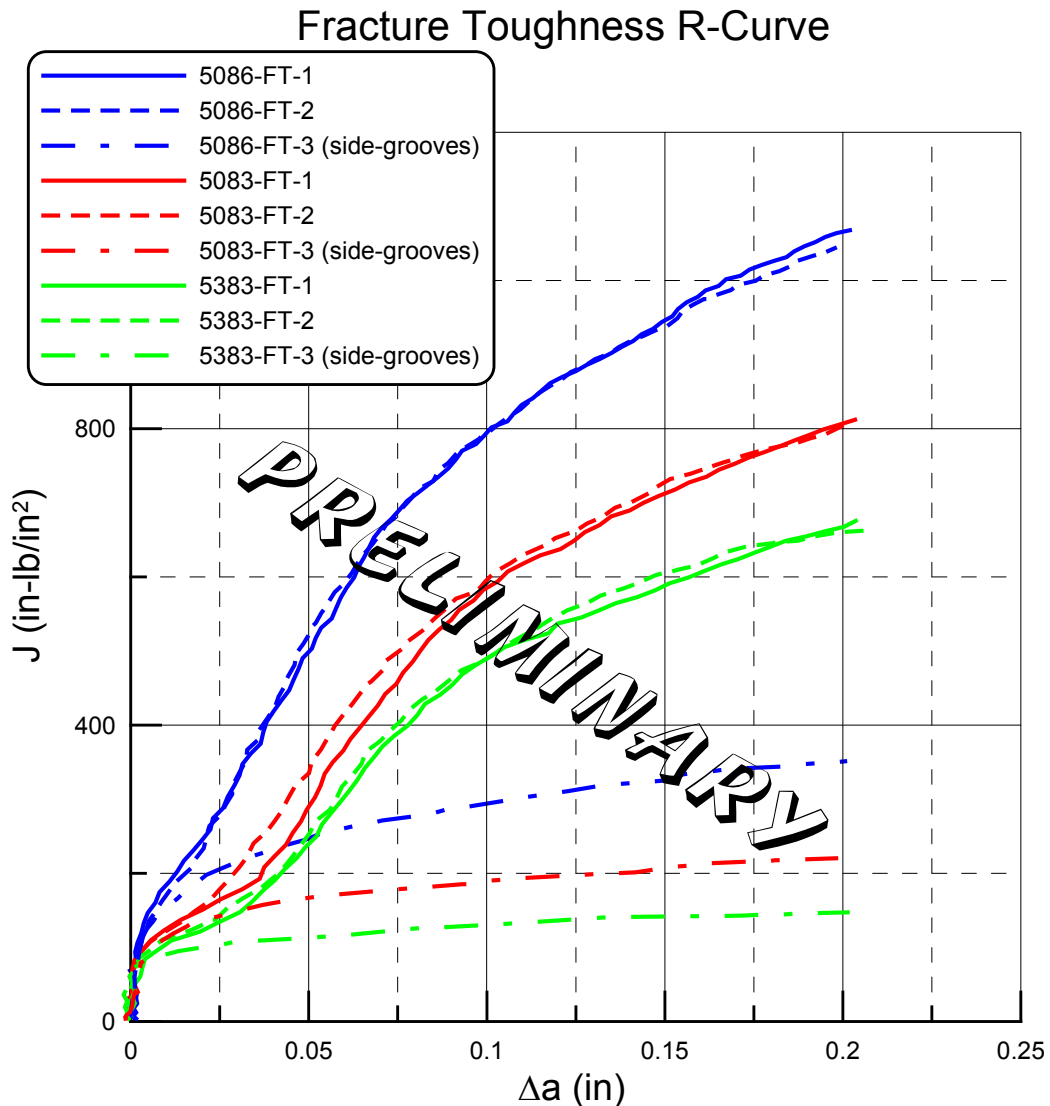


Figure 9-16 Fracture Toughness R-curves for several aluminum alloys (Donald and Blair, 2006).

For the example made above of fatigue crack growth in a 42.7 m 32-kt crew boat, the stress to the deck in the aluminum version is 91 MPa compression and 20 MPa tension. For fracture analysis in the crack opening mode, only the tensile stress is considered. The applied J-integral is then:

$$J_{\text{appl}} = \frac{\sigma^2 \pi a}{E} = \frac{(20)^2 \pi a}{71 \times 10^3} = 17.7 \times 10^{-3} a \frac{\text{N} \cdot \text{mm}}{\text{mm}^2} \quad (9-7)$$

From Figure 9-16, the critical value of J at which crack extension begins is $J_{\text{IC}} = 100 \text{ in-lb/in}^2 = 17.5 \text{ N-mm/mm}^2$. The critical crack size is then $17.5 / 17.7 \times 10^{-3} = 990 \text{ mm}$. Because of the formula by which J_{appl} is calculated, the actual critical crack length is twice this, or 1.9 m. This is a large size for a critical crack length but is a reflection of the low value of tensile stress if

the bending moments agree with the ABS formulas. If the stress level were equal to the welded yield strength of 165 MPa, then the critical crack length would be 30 mm.

For comparison with steel, an R-curve for ABS Grade EH 36 steel is shown in Figure 9-17 (Dexter and Gentilcore, 1997), where the units are in mega Joules/m². The peak value of 2.2 MJ/m² is equal to 1,000 N-mm/mm², or 5,700 in-lb/in². This is significantly greater than the maximum value of 800 in-lb/in² for 5083 shown in Figure 9-16. The critical value, J_{IC} for the EH 36 is 240 Joules/m² = 0.24 MJ/m², or 240 N-mm/mm². For the maximum deck stress of 25 MPA in hogging, the critical crack size is 50 meters! If the stress were at the yield strength of EH 36 of 355 MPa, the critical crack size would be 250 mm.

This comparison was made between several grades of aluminum and Grade EH steel. The difference would not have been great if a grade of steel with less toughness were used. ABS Grade B steel has a toughness of 360 5 N-mm/mm² (2,080 in-lbs/in²), which is still greater than the aluminum (Jennings et al., 1991).

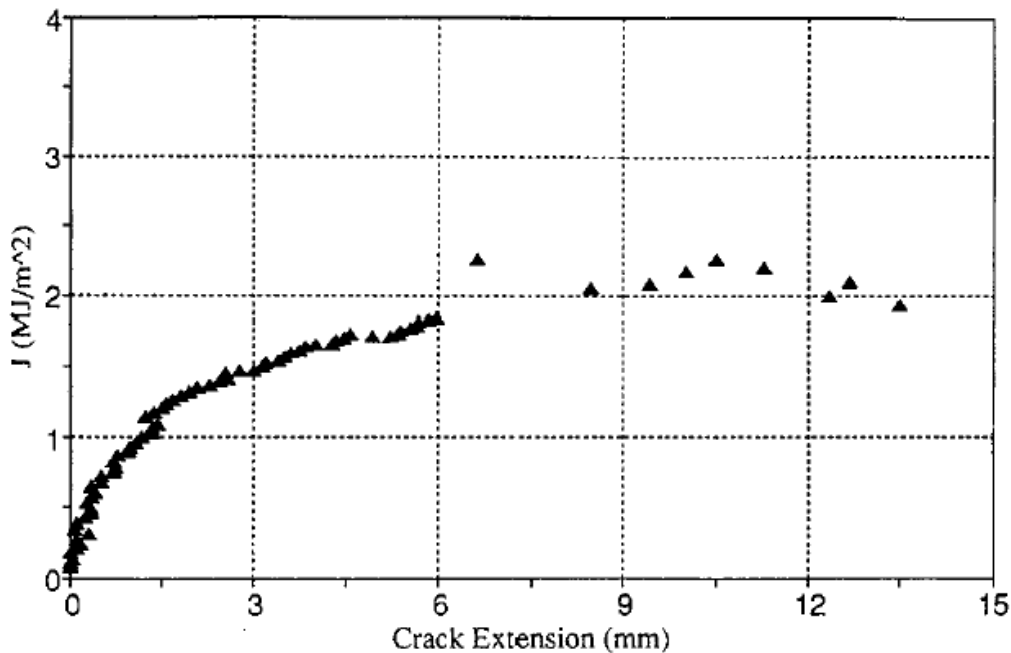


Figure 9-17 Fracture toughness R-curve for 9.5-mm ABS Grade EH 36 steel in the L-T orientation (Dexter and Gentilcore, 1997)

9.11 Summary

A generalized procedure for determining a fatigue-loading spectrum can be used during preliminary design to be assured that potential fatigue problems are addressed early in the design process. A detailed spectral fatigue analysis may be required in the final stages of design, but there must be some assurance that the vessel will have a satisfactory overall fatigue life early-on in design to avoid major changes in scantlings late in the design process.

Aluminum Marine Structure Guide

Aluminum design must be based on avoidance of crack initiation because a crack will propagate 30 times faster in aluminum than in steel. However, aluminum structure is rather tolerant of defects and will not fail by fast fracture, although it hasn't the same fracture resistance of ship-grade steels.

Chapter 10 Fire Protection

10.1 Introduction

Except for small vessels, fire protection is required on ships to prevent the spread of fire and subsequent loss of life and to safeguard the safety of the vessel. In some cases, steel structure is sufficient for this purpose, although insulation is required in many cases to prevent the spread of heat through a steel deck or bulkhead. The structural insulation requirements for aluminum are more extensive than for steel because the aluminum structure itself must be protected from the heat of the fire to prevent melting. Different authorities set out requirements, and a method for designing aluminum structural fire protection systems is published by SNAME.

Although aluminum does not burn when exposed to ordinary fires, it does melt. An example is shown in Figure 10-1, where the aluminum balconies on a steel structure were exposed to fire from plastic deck furniture and plastic partitions, and can be seen to have melted while the steel remained intact.



Figure 10-1 Result of fire aboard cruise ship *Star Princess* March 2006 (MAIB, 2006)

10.2 Regulatory Requirements

Fire and safety requirements for vessels operating in international waters are contained in the International Convention for the Safety of Life at Sea (SOLAS, 2004) and in the International Maritime Organization International Code of Safety for High Speed Craft (HSC Code). Requirements for U.S.-flag vessels are established by Section 46 of the U.S. Code of Federal

Regulations, which are in turn expanded upon in several U.S. Coast Guard Navigation and Vessel Inspection Circulars (NVIC).

10.2.1 SOLAS Requirements

The International Convention for the Safety of Life at Sea (SOLAS) has existed by international treaty in various forms since the 1910s when the first regulations were established following the *Titanic* disaster. The most recent treaty was adopted on November 1, 1974 by the convention that was convened by the International Maritime Organization (IMO), which is a body of the United Nations. Those requirements did not come into force until May 25, 1980, and SOLAS 1974 has been amended twice since then by means of protocols, the latest of which came into force on February 2, 2000. Additionally, SOLAS 1974 has been amended several times by means of resolutions adopted by the Marine Safety Committee of IMO as well as by conferences of SOLAS Contracting Governments. All of these requirements were combined into a single consolidated edition in 2004, which will be referred to as SOLAS. Enforcement of SOLAS is the responsibility of government of the state whose flag the ship is entitled to fly. That government is referred to as the Administration. In general, the SOLAS requirements apply only to ships engaged in international voyages.

The SOLAS requirements cover a number of areas affecting the safety of ships, including construction, requirements that cover structure, subdivision, stability, machinery, and electrical systems. Requirements for fire protection include fire detection, fire containment and fire extinction. Other SOLAS requirements cover lifesaving, radio communications, safety of navigation, cargos, including dangerous goods, special requirements for certain types of ships and high-speed craft, and management for safe operation of ships. Only the requirements for fire containment are summarized below.

The fire safety objectives include containing, controlling, and suppressing a fire or explosion to the compartment of origin, and to provide adequate and readily accessible means of escape for passengers and crew. To do this, the ship is divided into main horizontal and vertical thermal and structural boundaries. Accommodation spaces are separated from the remainder of the ship by such boundaries, and means of escape and access for fire fighting are provided.

There are three general classes of division, Class A, Class B, and Class C. Class A divisions are formed by bulkheads and decks and must be constructed of steel or other equivalent material, suitably stiffened, capable of preventing the passage of smoke and flame for one hour, and are insulated. The insulation is to prevent the average temperature on the unexposed side from rising more than 140 °C (252 °F) above the original temperature, and the temperature at any one point shall not be more than 180 °C (324 °F) above the original temperature. There are four Class A divisions, A-60, A-30, A-15, and A-0, which are insulated sufficiently to prevent the specified temperature rise for 60, 30, 15, and 0 minutes, respectively.

The term equivalent to steel means any non-combustible material that by itself or when properly insulated has structural integrity and is capable of maintaining that integrity until the end of the appropriate exposure period. Aluminum with appropriate insulation is specifically permitted by SOLAS.

Class B divisions are formed by bulkheads, decks, ceilings [SIC] (overhead coverings), and linings. They must be constructed of non-combustible materials and be capable of preventing the passage of smoke and flame for one half-hour. They are to be insulated to prevent the average temperature on the unexposed side from rising more than 140 °C (2252 °F) above the original temperature, and the temperature at any one point shall not be more than 225 °C (405 °F) above the original temperature. There are two Class B divisions, B-15 and B-0, which are insulated sufficiently to prevent the specified temperature rise for 15 and 0 minutes, respectively.

Class C divisions are constructed of non-combustible materials. They do not have to meet any other requirements for prevention of passage of smoke or flame, or be insulated to prevent temperature rise. Note that the maximum temperatures mentioned above for Class A and class B divisions are those to prevent fire spread. Maximum temperatures that the aluminum structure are permitted to achieve are mentioned below.

In general, the bulkheads forming stability subdivision in passenger ships carrying more than 36 passengers are to be Class A-60 in the hull, deckhouse and superstructure, including an extension of those bulkheads above the bulkhead deck. Additional requirements for containing specific spaces are set out in tables for bulkheads and decks. Separate tables are provided for the requirements for ships carrying 36 or fewer passengers. There are additional tables describing the requirements for cargo ships and tables for tankers.

Types of spaces for ships carrying more that 36 passengers are:

- (1) Control stations
- (2) Stairways
- (3) Corridors
- (4) Evacuation stations and external escape routes
- (5) Open deck spaces
- (6) Accommodation spaces of minor fire risk
- (7) Accommodation spaces of moderate fire risk
- (8) Accommodation spaces of greater fire risk
- (9) Sanitary and similar spaces
- (10) Tanks, voids, and auxiliary spaces having little r no fire risk
- (11) Auxiliary machinery spaces, cargo spaces, cargo and other oil tanks and other similar spaces of moderate fire risk
- (12) Machinery spaces and main galleys
- (13) Storerooms, workshops, pantries, etc.
- (14) Other spaces in which flammable liquids are stowed

As an example of the requirements for structural fire protection, ships carrying more than 36 passengers must have machinery spaces separated from accommodation spaces by Class A-60 bulkheads and Class A-0 decks, except for accommodation spaces of low fire risk, which need have only Class A-30 bulkheads. Ships carrying 36 passengers or less, cargo ships, and tankers must have accommodation spaces separated from machinery spaces by Class A-60 bulkheads and decks. Ships carrying more than 36 passengers must have stairways separated from accommodations of low, moderate, and high fire risk by bulkheads of Class A-0, A-15 and A-15, respectively, and by decks of Class A-0. Ships carrying 36 passengers or less, cargo ships, and

tankers must have stairways in general separated from machinery spaces by Class A-0 bulkheads and decks, although in some circumstances Class B-0 bulkheads are permitted.

SOLAS permits the use of performance-base engineering analysis to satisfy the fire safety objectives and functional requirements as an alternative to compliance with prescriptive requirements. These analyses are intended for the approval of novel or unique ship designs, and are not intended for developing alternative requirements for materials or equipment. For U.S. Flag SOLAS vessels, the U.S. Coast Guard (NVIC 6-02) recommends the use of the SFPE Engineering Guide to Performance-Based Fire Protection Analysis and Design of Buildings (SFPE, 1999) to perform these analyses.

10.2.2 IMO HSC Code

The International Code of Safety for High-Speed Craft (HSC Code 2000) was adopted by the MSC of IMO by resolution MSC 97(73) on December 5, 2000 and went into effect for vessels constructed after July 1, 2002. It was preceded by the 1994 HSC Code, which was preceded by the 1977 Code of Safety for Dynamically Supported Craft (DSC). The DSC was based on the management of risk through accommodation arrangement, active safety systems, and restricted operations. Non-traditional materials such as aluminum and composites were permitted in the DSC as long as an equivalent level of safety was achieved through additional safety measures (NVIC 6-99). The HSC Code has amplified on the requirements of the DSC for high speed craft, which are defined as capable of reaching or exceeding a speed in meters per second equal to $3.7 \nabla^{0.1667}$, where ∇ is the volume of displacement in meters cubed.

Similar to SOLAS, tables are provided for passenger vessels and cargo vessels, giving the times that bulkheads and decks must be able to provide insulation between adjacent spaces. There are six types of spaces:

- (1) Areas of major fire hazard
- (2) Areas of moderate fire hazard
- (3) Areas of minor fire hazard
- (4) Control stations
- (5) Evacuation stations and escape routes
- (6) Open spaces

Areas of major fire hazard, such as machinery spaces and flammable liquid storerooms must be separated from each other by bulkheads and decks providing 60 minutes of protection. Areas of major fire hazard must be separated from areas of moderate fire hazard, such as auxiliary machinery spaces and crew accommodation spaces, by bulkheads and decks offering 60 minutes of fire protection, but the side having moderate fire hazard need only provide protection to an aluminum bulkhead for 30 minutes.

Aluminum structures are required to be insulated so that their core temperature does not rise more than 200 °C (360 °F) above the ambient temperature during a fire test of the time specified for the type of space for which the structure forms the boundary.

10.2.3 U.S. Coast Guard Requirements

For U.S.-flagged ships operating internationally the U.S. Coast Guard has the responsibility of enforcing the SOLAS and IMO HSC Code requirements. All vessels operating in U.S. waters fall under the purview of the U.S. Coast Guard. The requirements of the U.S. Coast Guard are published in various Navigation and Vessel Inspection Circulars (NVIC). There are ten types of vessels considered under U.S. Code:

Table 10-1 Vessel Types Under U.S. Code of Federal Regulations 46

Subchapter of U.S Code CFR 46	Vessel Type	Applicable Parts of CFR 46
C	Uninspected Vessels	24 – 26
D	Tank Vessels	30 – 40
H	Passenger Vessels	70 – 89
I	Cargo and Miscellaneous Vessels	90 –106
I-A	Mobile Offshore Drilling Units	107 – 109
K	Small Passenger Vessels (Subchapter K)	114 – 122
Q	Equipment, Construction, Material	159 – 165
R	Nautical Schools	166 – 169
T	Small Passenger Vessels (Subchapter T)	175 – 187
U	Oceanographic Vessels	188 – 196

U.S Coast Guard requirements for fire protection were originally developed for Subchapter H passenger vessels. Where requirements vary, it is from this base. The fire protection requirements, where delineated in other subsections of the CFR 46 are not necessarily complete, and when so, the requirements for Subchapter H vessels pertain.

Subchapter K small passenger vessel requirements have many places where the Subchapter H requirements have been rewritten. One area is in the definition of control stations, accommodation spaces, and service spaces, so the designations are not necessarily the same in Subchapter K as in Subchapter H. For Subchapter K vessels, the U.S. Coast Guard has set out a methodology for determining equivalent fire safety (NVIC 3-01). This approach provides a formal method for incorporating novel designs that provide a level of safety equivalent to the proscriptive approach of 46 CFR Subchapter K. The approach is not to be used to approve a non-approved material, such as a system of structural fire protection. Rather, the new material should be approved from the results of standard testing procedures. The approach should not be used to justify reduced fire protection requirements based solely on short evacuation times or operational restrictions. A passenger vessel should be considered as its own best rescue platform.

Subchapter I cargo vessels do not have as extensive requirements for structural fire protection in accommodation spaces as in Subchapter H passenger vessels. Unless the bulkheads in these spaces are specifically required to be Class A or Class B, they may be Class C.

Aluminum Marine Structure Guide

Cargo vessels, either Subchapter I or Subchapter D tank vessels are assumed to be of steel construction. Should such vessels be constructed of aluminum, special consideration needs to be made of the requirements to provide equivalent protection. There are a few more requirements for tank ships than there are for cargo vessels. These additional requirements are intended to compensate for the additional hazards that are caused by carrying combustible liquids. These additional requirements include arrangement of accommodation spaces and additional structural insulation and integrity requirements for portions of the superstructure. If a vessel is designed and constructed in accordance with SOLAS requirements and meets the approval process described in 46 CFR 159, then it is considered to meet the requirements of the U.S. Code of Federal Regulations.

The specific fire protection requirements for high-speed craft are described above in SOLAS and in the IMO HSC. Those requirements are intended to provide some compensation for unusual features of vessels that meet the definition of high-speed craft. The U.S. Coast Guard does not require a vessel to be designed and constructed in accordance with these requirements; the conventional vessel requirements may be used instead. However, if the IMO HSC is used, it must be used in its entirety.

The requirements for fishing vessels are set out in 46 CFR Part 28. In general, there are no specific requirements for fishing vessels except for a few basic requirements, which depend on the number of persons living aboard.

The requirements for offshore mobile drilling units pertain mostly to accommodation spaces. For protection against fire hazards originating within the accommodation spaces, the requirements are similar to the requirements for cargo vessels. The hazard from fire or explosion originating in the drilling, processing, or other areas external to the accommodation spaces are intended to protect those spaces from the fire and effects of the explosions. The exterior of the accommodation spaces should have sufficient durability and thermal resistance to resist those hazards. Fixed offshore platforms must meet the requirements of the U.S. Minerals Management Service, not the U.S. Coast Guard.

Where passenger vessels carry automobiles and other vehicles, special requirements apply because the combustion energies generated by burning vehicles and their fuel can be twice as those from burning wood, which is the basis for the ordinary standards. Horizontal fire boundaries are required, as specified in 46 CFR table 72.05-10(f) or table 116.416(c), as applicable. If the deck is of aluminum or FRP, it must be either insulated on the top side or protected with an active system designed to protect the deck from collapse. The protection should last for at least 60 minutes and have A-0 construction. This requirement does not apply if the vessel is designed and constructed to the requirements of the IMO HSC, which assumes that passengers will be evacuated before the deck would collapse in a fire.

The basic U.S. Coast Guard requirements for structural fire protection are contained in NVIC 9-97. It is supplemented by the list of approved fire protection material in the Coast Guard Equipment Lists, COMDTINST M16714.3 series, which are published periodically by the U.S. Coast Guard Commandant G-MSE-4. The philosophy of the U.S. Coast Guard as incorporated in the U.S. Code of Federal Regulations and NVIC 9-97 is to resist or slow the

spread of fire while establishing escape routes and maintaining their integrity. The basic principles of structural fire protection are to: use materials that are resistant to ignition and flame spread and minimize the products of combustion and to arrange structures to resist fire spread and separate people from fire and the products of combustion. Structural fire protection is designed to be passive in nature, not requiring action by personnel to make the protection effective, minimizing the possibility of human error affecting the performance of the system.

Chapter 4 of NVIC 9-97 pertains specifically to providing structural fire protection for aluminum structure. In turn, the NVIC refers to SNAME T&R Bulletin 2-21 (SNAME, 1974) for specific design requirements, including acceptable materials and thicknesses to meet the various classes of fire protection. SNAME T&R Bulletin 2-21 will be discussed more fully below.

10.2.4 U.S. Navy Requirements

At one time, the fire protection insulation requirements for the U.S. Navy were far less demanding than requirements for commercial ships. In essence, U.S. Navy ships had no fire zone boundaries, only uninsulated watertight bulkheads surrounding vital spaces. Containment of a fire was done by damage control parties spraying water on the opposite side of a bulkhead to prevent flame spread. However, this has changed, and insulated fire zone bulkheads are required on U.S. Navy ships. The requirements are specified in the Part 1, Chapter 2 of the Naval Vessel Rules (NVR) of the American Bureau of Shipping.

The NVR requirements are based on the IMO A.754(18) fire test procedure, modified to provide a hydrocarbon pool fire exposure based on the UL 1709 fire curve. Three classes of barriers result from that testing, Class N-0, N-30 and N-60. The fire test includes an oil fire, whereas the commercial standards are based on a wood fire, and so higher temperatures are achieved in the U.S. Navy fire test than in the commercial testing.

The NVR require that designated bulkheads and decks be designed to protect against structural failure and prevent the passage of fire and smoke when exposed to a hydrocarbon (class B) fire for a designated test period. In addition, they should prevent excessive temperature rise on the opposite side for the time period of 60 minutes or 30 minutes for Class N-60 and N-30, respectively. Class N-0 divisions should have no flaming on the unexposed face for a minimum of 30 minutes. The average temperature of the unexposed side should not be more than 139°C (250°F) above the original temperature, and the temperature at any one point, including any joint, should not rise more than 180°C (324°F) above the original temperature. These maximum temperature increases are the same as for SOLAS Class A divisions, as mentioned above. These temperatures are for the prevention of fire spread, and are different from the maximum temperature given below that the core of aluminum structure is permitted to reach.

Ships with an overall length greater than 67 m (200 feet) are divided into main vertical fire zones of no more than 40 m or (131 feet) in length. The surface of the fire zone boundary may be stepped in either or both the horizontal or vertical planes through combinations of transverse bulkheads, longitudinal bulkheads, and decks, and are continuous from the innerbottom through the superstructure. These boundaries are currently required to meet only

the N-30 requirement. An uninsulated steel bulkhead or deck with a minimum plating thickness of 4.5 mm (0.18 inches) and 4 x 4 inch Tee stiffeners spaced 635 mm (24 inches) on center, or equivalent structure, without openings or penetrations, is considered to satisfy the requirements of N-0.

The following boundaries, if not part of a fire zone boundary are required to be Class N-0:

- Passageways and vertical accesses that are vital for egress.
- The boundary of contiguous vital spaces.
- Spaces containing flammable or combustible liquids or gases, oxidizers or other hazardous materials. Tanks shall be classification N-0 only for fire exposures outside the tank; insulation is not required inside the tank.
- Helicopter decks, flight decks and other exterior high fire risk surfaces. These N-0 boundaries shall prevent fire spread into the ship due to boundary failure.
- Weather boundaries adjoining helicopter decks, flight decks or other exterior high fire risk surfaces. These N-0 boundaries shall prevent fire spread into the ship due to boundary failure.
- Uptake and intake trunks and ventilation ducts from machinery spaces.
- Major watertight subdivisions.

Fire boundaries are not required on exterior (weather) bulkheads except for N-0 boundaries where needed to assure structural integrity of the hull girder, such as on critical stiffeners, to support fire extinguishing systems, or where the exterior is a high fire hazard such as a flight deck.

Aluminum structures must meet the structural integrity requirements under fire by testing. The average temperature of the structural core shall not rise more than 200 °C (360 °F) above its initial temperature at any time within the classification period. This requirement is the same as given in the IMO HSC code described above. Note that both specifications are for temperature rise, not for maximum temperature obtained to prevent softening and collapse of the aluminum. The requirement assumes a moderate ambient temperature, but if the ambient temperature is high, such as in an engine room, additional insulation should be considered, although the NVR does not specifically say so.

10.3 Fire Protection Insulation

One of the general principles that differentiates the structural fire protection requirements for aluminum from those of steel is that aluminum structures must be sufficiently insulated to prevent the aluminum from softening and melting in a fire. Guidance for protection of aluminum is provided by SNAME T&R Bulletin 2-21 (SNAME 1974). Structural fire protection of aluminum is designed to prevent the aluminum from achieving a temperature of 230 °C (446 °F). Note that the specifications stated above specify a temperature rise of 200 °C, so an implicit assumption of the specifications is that the ambient temperature will not be significantly greater than 30 °C (86 °F).

Insulation is not generally required to protect steel structure because it is assumed that the temperatures of ordinary shipboard fires will not be above 900 °C (1,650 °F), which is well below the melting point of steel. With proper insulation, aluminum may be used as the structural material for passenger and cargo vessels. However, because standard fire test requirements do not account for the high temperatures of oil fires, aluminum may not be used for the structure of tank vessels or tank barges. In certain vessels, such as vehicle-carrying ferries, the major supporting members for structure above the vehicle deck must be steel. In some situations, the higher thermal conductivity of aluminum might help to dissipate heat, and this is reflected in the insulation design methods discussed below, which were experimentally derived.

10.3.1 Insulation Necessary to Protect Unexposed Surfaces

The basis for the design of structural fire protection is the “S” value of the insulation. Insulation with a thickness of $1.0 \times S$ is capable of keeping the temperature on the side of the structure that is not exposed to fire (the unexposed side) from reaching a temperature that is more than 139 °C (282 °F) above ambient for 60 minutes. Different materials have different thicknesses for providing a rating of $S = 1.0$. The thickness of various materials approved by the U.S. Coast Guard to achieve an S value of 1.0 can be found in the U.S. Coast Guard Equipment Lists (COMDTINST M16714.3 series) published periodically by the Commandant of the U.S. Coast Guard G-MSE-4. The current (July 2006) approved fire insulation materials are given in Table 10-2. The lists can be obtained at the web site www.USCG.mil or <http://cgmix.uscg.mil/Equipment>.

For approval of materials not on the current U.S. Coast Guard Equipment List, approval must follow the requirements of 46 CFR 164.005 through 164.012 and Chapter 2 of NVIC 9-97. The procedure is to mount the insulation system on a steel plate and exposing the sample to the temperatures of ASTM E-119 standard fire test. The average temperature in the unexposed side of the plate must not reach an average temperature greater than 140 °C (284 °F) above ambient in 60 minutes, nor should any single point achieve a temperature greater than 180 °C (356 °F) above ambient. The SOLAS requirements are similar, except that the insulation must be placed on the unexposed side of the plate. For this reason the thickness required by SOLAS for an S rating of 1.0 may be greater than the thickness required by the U.S. Coast Guard.

**Welcome to the United States Coast Guard
Approved Equipment Listing**

This online searchable database contains approved or certified equipment by the Commandant of the U.S. Coast Guard for use on commercial vessels and recreational boats, for the reference of ship-owners, operators, builders, and other persons affected by the Marine Inspection and Navigation Laws and Regulations.

Additional listing of Coast Guard approved equipment:

The U.S. has entered into an agreement with the European Community (EC) and European Economic Area-European Free Trade Association (EEA/EFTA), whereby the Notified Bodies of the EC and EEA/EFTA will issue U.S. Coast Guard approvals for certain lifesaving, fire protection and navigation equipment. The “Agreement Between the United States of America and the European Community on Mutual Recognition of Certificates of Conformity for Marine Equipment” is generally referred to as the US-EC MRA and “Agreement Between the United States of America and the European Economic Area-European Free Trade Association Mutual Recognition of Certificates of Conformity for Marine Equipment” is generally referred to as the US-EEA/EFTA MRA. The US-EC MRA became effective on July 1st, 2004 and the US-EEA/EFTA MRA is effective on March 1, 2006.

For additional information on the US-EC MRA and US-EEA/EFTA MRA, including a list of the equipment covered by the agreement, please go to the USCG Lifesaving and Fire Safety Division website at: www.uscg.mil/hq/gm/mse4/mra.htm These agreements do not change the requirement to use USCG approved equipment on U.S. flag vessels. The Coast Guard approvals issued by EC or EEA/EFTA under the US-EC or US-EEA/EFTA MRA are available to the public on the MarED website at: <http://www.mared.org/>. The MarED website contains general approval information similar to what can be found on CGMIX as well as information about the MarED Group, Notified Bodies and the MED.

**Table 10-2 U.S. Coast Guard Approved Fire Protection
(U.S. Coast Guard Equipment List, July 2006)**

Approval Number	Manufacturer	Item Description	Usage	S (mm)
164.107/001/0	THERMAL CERAMICS	"FireMaster Marine Blanket", Calcium Magnesium-Silicate fiber insulation, 96 kg/m ³ (6.0 lb/ft ³) nominal density. Tested and approved to the IMO FTP Code, annex 1, part 3.	Aluminum Decks, 2 mm min. thickness Aluminum Bulkheads, 2 mm min. thickness	A-60: 50 A-30: 38 A-60: 50 A-30: 38
164.107/002/0	THERMAL CERAMICS	"FireMaster Marine Blanket", Calcium Magnesium-Silicate fiber insulation, 96 kg/m ³ (6.0 lb/ft ³) nominal density, 63 mm thick.	Aluminum Bulkheads, 5 mm min. thickness	A-60: 63
164.107/003/0	AMERICAN SPRAYED FIBERS, INC.	Type "Dendamix" sprayed fiber approved as meeting Parts 1 and 3 of Annex I of the IMO FTP Code in nominal density of 112 kg/m ³ (7 lb/cu. ft ³)	Bulkhead Insulation	A-60: 45 Stiffeners, 18
164.107/004/0	AMERICAN SPRAYED FIBERS, INC.	Type "Dendamix" sprayed fiber approved as meeting Parts 1 and 3 of Annex I of the IMO FTP Code in nominal. density of 112 kg/m ³ (7 lb/ft ³)	Deck (horizontal application below the deck)	A-60: 17.5
164.107/005/0	ROCK WOOL MANUFACTURING CO	Type "Delta Marine Board" mineral wool approved as meeting Parts 1 and 3 of Annex I of the IMO FTP Code in nominal density of 112 to 128 kg/m ³ (7 to 8 lb/ ft ³)	Bulkhead Insulation (vertical application)	A-60: 76 Stiffeners: 38
164.107/006/0	ROCK WOOL MANUFACTURING CO	"Delta Marine Board" mineral wool approved as meeting Parts 1 and 3 of Annex 1 of the IMO FTP Code in nominal density of 112 to 128 kg/m ³ (7 to 8 lb/ ft ³)	Deck Insulation (horizontal applications)	A-60: 50 Stiffeners: 25
164.107/007/0	AMERICAN SPRAYED FIBERS, INC.	Type "Dendamix Marine" sprayed fiber insulation approved as meeting Parts 1 and 3 of Annex 1 of the IMO FTP Code in nominal density of 156 kg/m ³ (9.7 lb/ft ³)	Underneath Aluminum Decks (horizontal application)	A-60: 25.4 A-30: 1.3 Stiffeners: same thickness

Approval Number	Manufacturer	Item Description	Usage	S (mm)
164.107/008/0	AMERICAN SPRAYED FIBERS, INC.	Type "Dendamix Marine" sprayed fiber insulation approved as meeting Parts 1 and 3 of Annex 1 of the IMO FTP Code in nominal density of 156 kg/m ³ (9.7 lb/ft ³)	Aluminum Bulkheads (vertical application)	A-60: 50.8 Stiffeners: same thickness

As an example of S values in Table 10-2, the Thermal Ceramics Firemaster Marine Blanket has an S value of 50 mm on an aluminum bulkhead because that thickness provides 60 minutes of protection (A-60). The American Sprayed Fibers Dendamix has an S value of 45 mm.

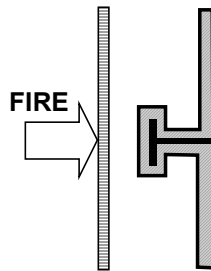
In general, the time that a layer of insulation can prevent the rise of temperature is proportional to the square of the thickness. If the insulating value of the side of the structure exposed to the fire is F_E , and the value of the unexposed side is F_U , the total value of the insulation, $F_T = F_E + F_U$. The S values that provide less than 60 minutes of protection are given in Table 10-3. For example, the S value of Firemaster is 55 mm, which provides 60 minutes of protection. If only 30 minutes of protection are required, Table 10-3 indicates that $0.70 S = 0.70 \times 55 = 38$ mm will provide that protection. Notice that Table 10-2 shows that 38 mm is approved for A-30 protection with this product. If testing shows that lesser values of thickness than called for in Table 10-3 will provide the required protection, those approved values should be used, because the table is only an approximation.

Table 10-3 Minimum F_T Values Required to the Limit the Temperature Rise on the Unexposed Face (SNAME, 1974)

Insulating Period (minutes)	Minimum F_T as a Fraction of S
0	0.00
15	0.50
30	0.70
45	0.86
60	1.00

If there is an air space of at least 25 mm (1 inch) between the structure and a joiner bulkhead material or other fireproof sheathing, a contribution to the insulation value is given by the air space. Depending on the orientation, the type of sheathing, and the type of insulation on the structure (if any), the insulation value according to SNAME T&R Bulletin 2-21 can range between 0.0S and 0.15S, as shown in Figure 10-2 through Figure 10-5. In these figures, a vertical orientation implies a bulkhead, and a horizontal orientation means a deck.

In these figures two types of sheathing are shown. The first type is steel, which may be perforated, as long as the perforations do not exceed 25 percent of the surface area. The steel



Notes:

- Air space must be at least 25 mm
- Structural fire protection approved iaw 64 CFR 164.007
- Joiner bulkhead panels approved iaw 64 CFR 164.008

Figure 10-5 Air spaces with insulating value of 0.15 S (SNAME 1974)

10.3.2 Insulation to Protect the Aluminum Structure

The above discussion pertains to the structure and insulation forming a barrier to the spread of the heat of a fire. However, the aluminum structure itself must also be protected. The goal is that the temperature rise of the aluminum be no greater than 200 °C (360 °F) above the ambient. The assumption is that the ambient temperature is 30 °C (86 °F), so that the temperature of the aluminum is no greater than 230 °C (446 °F). If the ambient temperature is anticipated to be significantly greater than 30 °C (86 °F), special consideration should be made, although there is no rule requirement to that effect.

Insulation with a value of 1.0 S is intended to prevent a temperature rise of 260 °C, and so the requirements for protection of aluminum are more demanding. Because insulation prevents the transmission of heat, insulation on the unexposed side of the structure will reduce the effectiveness of the insulation on the exposed side. The minimum insulation requirements for the exposed side are for installations where there is no insulation on the unexposed side. These are tabulated in Table 10-1, which provides the required value of the insulation on the side exposed to the fire, F_E , in terms of fraction of S. For example, if 60 minutes of protection is desired, F_E is 0.72 S. If insulation with an S value of 55 mm is used, the required thickness is $0.72 \times 55 = 40$ mm.

Table 10-4 F_E Values to Limit Temperature Rise of Aluminum Structure to 200 °C (360 °F) (SNAME, 1974)

Insulating Period (minutes)	Minimum F_E Values (Fraction of S)
0	0.00
15	0.25
30	0.45
45	0.61
60	0.72

If the unexposed side is insulated to a value F_U , then the value of the insulation on the exposed side, F_E is reduced to the value protecting the core, F_C , by the equation:

$$F_C = F_E - f F_U^2$$

where f is an experimentally determined factor depending on the extent of the insulation on the unexposed side. If 25 mm or more of fire protection insulation is on the unexposed side, $f = 0.1$, otherwise, $f = 0.5$. In the above calculation, the value of F_E and F_U should include the effect of any air gap, if present, especially on the unexposed side of the structure.

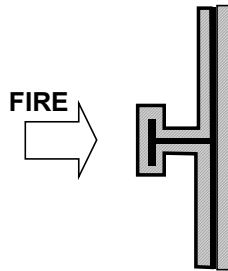


Figure 10-6 Example of fire protection insulation.

As an example, consider the insulated structure in Figure 10-6, with insulation on both sides with a value of 1.0 S, and of a thickness greater than 25mm. Then:

$$F_E = 1.0 \text{ S}$$

$$F_U = 1.0 \text{ S}$$

$$f = 0.1, \text{ and}$$

$$F_C = 1.0 - 0.1 (1.0)^2 = 0.9 \text{ S}$$

According to Table 10-1, protection of the aluminum for 60 minutes requires F_C to be 0.70 S, and so sufficient protection is provided for the aluminum structure. The total insulation value of the system is $F_T = F_E + F_U = 1.0 + 1.0 = 2.0 \text{ S}$. Therefore, lesser amounts of insulation can be used to provide protection for the aluminum and prevent the spread of heat.

These requirements are based on aluminum structure with a minimum thickness of 4.8 mm (0.18 in), partially because of the heat capacity of the aluminum. Thinner material will require special consideration.

Generally stiffeners will have insulation surrounding them of the same thickness required for the deck or bulkhead that they support. Consideration should be made for exceptionally deep members for which heat cannot be conducted back to the plate that is supported, although no data exists to indicate how deep a member must be before additional insulation is required. Such members should be insulated using the F_C values below. The stiffening members need have only one-half the thickness of the insulation on the plate that they support if they are located behind an insulating panel with an insulating value of at least $2/3 \text{ S}$.

10.3.3 Aluminum Surrounded by Fire

The insulation requirements for stanchions, pillars and other structure that are surrounded by fire are greater than for structure with a fire on one side only. The SNAME T&R bulletin provides values of the required insulation, F_C , for such structure, and those values are given in

Table 10-5. The bulletin cautions that those values are not based on experimental data, but on judgment. When determining the value of insulation provided, air space may be included.

Generally, the rules for fire protection do not require any decks or bulkheads to be designed using the values of Table 10-5. However, consideration should be given to the particularities of a design to determine if a structural bulkhead is critical to the support of structure above and could conceivably become engulfed by a fire. In that case, prudence dictates that it be insulated as if it were a stanchion.

Table 10-5 F_C Values to Limit Temperature Rise of Aluminum Structure Surrounded by Fire to 200 °C (360 °F) (SNAME, 1974)

Insulating Period (minutes)	Minimum F_C Values (Fraction of S)
0	0.00
15	0.50
30	0.90
45	1.20
60	1.40

10.3.4 Insulation to Meet U.S. Navy Requirements

The U.S. Navy has approved Thermal Ceramics Structo-Guard, which is made from a calcium-magnesium-silicate fiber. The manufacturer states that its FB material meet 46 CFR 164.007/70 structural fire protection testing for A-30, and the FC material for A-60. According to the manufacturer, this product has a NAVSEA rating of N-30 if a bulkhead is insulated with two 38-mm (1.5-inch) thick layers on one the fire side. The insulation weighs 96 kg / m³ (6 lb / ft³), but it is installed with an adhesive layer, so a barrier meeting N-30 on one side would weigh 9.45 kg/ m² (1.94 lb / ft²). If both side of a bulkhead need to be insulated, a total of 152 mm (6 inches) of insulation is required and a barrier meeting N-30 would weigh 18.9 kg/ m² (3.88 lb / ft²). Part of the approval process is that the insulated aluminum panel has to pass U.S. Navy shock testing with the insulation installed prior to the fire test.

10.4 Alternative Design Approach

Instead of following the rules described above to determine insulation requirements, fire load calculations may be made to determine the needed fire protection insulation. This approach is described in SNAME T&R Bulletin 2-21, and endorsed in U.S. Coast Guard NVIC 9-97. The approach can be advantageous for compartments that have a very small fire load, such as passenger seating areas that have simple furniture and little other flammable materials. The design approach does not change the assumed temperatures and intensity of the fire; it only changes the duration.

The first step is to determine which compartments are to be separated by effective fire boundaries. The following general guidelines apply:

1. Normally, spaces of unlike character, such as a stateroom and a corridor, must be separated by effective fire boundaries. Exceptions to this include spaces directly

Aluminum Marine Structure Guide

associated with each other, such as a head associated with a stateroom or pantry next to a galley.

2. On passenger ships, like compartments, such as adjacent staterooms, must be separated from each other.
3. On cargo ships, several like compartments, such as adjacent staterooms, may be combined with each other as long as the combined area of each combined space does not exceed 50 m^2 (538 ft^2).

The next step is to calculate the total deck area of each compartment. Afterwards the fire load of each compartment is calculated. In general, items may be considered as having the same heat of combustion of wood, which is $4,450 \text{ k cal/kg}$ ($8,000 \text{ BTU/lb}$) unless they have unusually high or low heat of combustion. The following items should be included:

1. Fixed Items. Wall and overhead linings, deck coverings, electrical wiring insulation, light diffusers, moldings, and similar items should be included.
2. Furnishings. Include all furniture, mattresses, curtains, decorations, and similar items.
3. Contents. Clothing and personal effects are included in staterooms as 7.32 kg/m^2 (1.5 lb.ft^2) and for public spaces, 0.732 kg/m^2 (0.15 lb.ft^2). Include life jackets, cargo, stores, paper and books in offices, and similar items.

The weight of all combustibles in each compartment is divided by the area to find the fire loading of the compartment. In general, in order to simplify requirements, all similar compartments, such as staterooms of a similar nature, should be considered as having the same fire load. For guidance, typical values of fire loading for typical compartments are given in Table 10-6. For certain spaces shown in the table, minimum values are given.

To find the required time of an equivalent standard fire, Table 10-7 is used, with only 15-minute increments considered. The table includes a margin of safety for additional items that are not included in the determination of fire load. This is a sliding scale, which is greater for lower fire loadings, and is 10 percent for 24.41 kg/m^2 (5.0 lbs/ft^2).

**Table 10-6 Typical Fire Loading of Various Spaces
(SNAME, 1974)**

Space	Fire Load (kg/m ² / lbs/ft ²)
Control Spaces: Wheelhouse/ Chartroom Fire Control Stations	7.32 / 1.5 7.32 / 1.5
Escape Routes Corridors Stairway Enclosures	7.32 / 1.5 4.88 / 1.0
Accommodation Spaces ¹ Staterooms: Fire resistant furnishings Combustible furnishings Public Spaces: Fire resistant furnishings in lounges, restaurants, etc. Ferry vessels Combustible furnishings Restrooms not part of staterooms	14.65 / 3.0 24.41 / 5.0 14.65 / 3.0 7.32 / 1.5 24.41 / 5.0 1.95 / 0.4
Service Spaces Galleys Pantries with no food heating appliances Food concessions on ferry vessels with no combustible storage Workshops Storerooms Combustible Cleaning gear only Laundries Ship's laundry Private use	48.82 / 10.0 19.53 / 4.0* 7.32 / 1.5 48.82 / 10.0* 48.82 / 10.0* 14.65 / 3.0 48.82 / 10.0* 7.32 / 1.5
Main Machinery and Cargo Spaces	48.82 / 10.0
Auxiliary Machinery Rooms (Fan Rooms, etc.)	24.41 / 5.0
Tanks and Voids	0.0

‡ Allowance is made for personal effects as follows:

1. Staterooms: 7.32 kg/m² (1.5 lb/ft²)
2. Public spaces: 0.732 kg/m² (0.15 lb/ft²)

* Fire loading for typical compartments so marked may not differ from typical values shown.

Table 10-7 Equivalent of Fire Loading to Duration of the Standard Fire Test (SNAME, 1974)

Fire Load (kg/m ² / lbs/ft ²)	Time of Equivalent Standard Fire (minutes)
Less than 2.44 (0.5)	0
2.44 to 9.75 (0.5 to 1.99)	15
9.76 to 21.96 (2.0 to 4.59)	30
21.97 to 34.16 (4.5 to 6.99)	45
34.17 (7.0) and greater	60

With the duration of fire determined, the required insulation values are determined using Table 10-8. In general, insulation sufficient to protect the structure in accordance with these calculations will be sufficient unless known flammable items exist on the opposite side of the structure. If that is the case, total insulation should be provided to meet the requirements of Table 10-3 based on the calculated time of an equivalent fire.

Table 10-8 F_C Values Required for Structure (SNAME, 1974)

Fire Load (lbs/ft ²)	F _C Required as a fraction of S
Less than 0.5	0
0.5 to 1.99	0.25
2.0 to 4.99	0.45
4.5 to 6.99	0.61
7.0 and greater	0.72

10.5 Support of Insulation

Support of insulation and panels that provide insulation must be such that the supporting members are able to withstand the heat of the fire to which they will be exposed. If pins are used that are welded to the aluminum structure, they must be bimetallic steel pins with an aluminum base, using steel speed clips to hold the insulation. If the insulation is located entirely behind insulating panels, then all-aluminum pins and speed clips may be use.

Insulating panels must be supported with steel supports or the equivalent that can withstand the intensity of a fire. Bulkhead panels can be supported by steel members attached to the deck, from which they should be separated by a dielectric material to minimize the possibility of corrosion. Supports at the top of bulkhead panels must be protected by overhead sheathing or other insulation to be certain they will not be exposed to the fire.

10.6 Research in Fire Protection Materials

Research has been conducted by different organizations to improve the fire protection insulation that is required for aluminum structure. The materials mentioned below show promise, but have not been approved by regulatory bodies, and some of the test methods used are not standard.

A sprayed fire protection material was studied by Green (2005). Following a concern that materials that can be directly sprayed to the structure, a low-cost test was developed to simulate the dynamic forces that act on ship structural panels. The following materials were evaluated on aluminum structure:

- Isolatek International Cafco Blaze Shield II
- Span-World Distribution Temp-Coat 101 and Fyre Sheild
- Superior Products SP2001F Fire Retardant
- Carboline Intumastic 285

None of these materials tested is listed on the current U.S. Coast Guard approved material list. To test the durability of the materials, composite and aluminum panels were made measuring 6 inches x 72 inches. The panels were fatigue tested by flexing the panels to a deflection of 1/50 of the length for 100,000 cycles and then subjected to impact loading by a dropped weight that produced 50 foot-pounds of energy.

After the fatigue testing, all of the aluminum panels had retained their protective coating except for the SP2001F. The drop weight testing dislodged most of the coatings except for the Intumastic 285. Although this coating has promise because of its durability, it will require fire testing to demonstrate its acceptability for fire protection of aluminum structures.

A product that meets European Directives 97/69, 80/1107, 89/391, and 98/24 is Fibrofax, made from synthetic vitreous fibers (of silicates) of random orientation, whose percentage by weight of alkaline oxides and alkaline-earth oxides ($\text{Na}_2\text{O} + \text{K}_2\text{O} + \text{MgO} + \text{BaO}$) exceeds 18% (ALCAN, 2004). Fibrofax is 38 mm thick and weighs $3.65 \text{ kg} / \text{m}^2$ ($0.228 \text{ lb} / \text{ft}^2$) for A-30 protection and 50 mm thick and $4.80 \text{ kg} / \text{m}^2$ ($0.30 \text{ lb} / \text{ft}^2$) for A-60 protection.

The National Shipbuilding Research Program has conducted a study of improved fire protection insulation for aluminum structure aimed particularly at the vehicle deck of ferries (NSRP, 2001). The product studied under project was estimated to weigh about 0.2 to 0.4 pounds per square foot (1.0 to $2.0 \text{ kg} / \text{m}^2$), and have an installed cost ranging from \$0.07 to \$1.00 per square foot.

10.7 Summary

Aluminum structure requires more fire protection insulation than does steel because the aluminum must be protected from the heat of a fire. Requirements for fire protection are set out by the SOLAS requirements of IMO, the IMO High Speed Craft Code, the U.S. Coast Guard, and by classification societies. A methodology for designing structural fire protection systems is provided by SNAME T&R Bulletin 2-21. However, that bulletin was issued more than 30 years ago and should be updated, and recommended testing should be conducted, including structure that is surrounded by fire.

Aluminum Marine Structure Guide

Chapter 11

Vibration

11.1 Introduction

Structural vibration can occur in ships and boats because there are a number of sources of harmonic energy that can excite the structure into vibratory motion. These sources include the propulsion train, other machinery, and hull slamming loads. Hull structure is an efficient transmitter of energy, so a source of vibration energy at one end of the ship can excite vibration at the other end if the natural frequency of vibration of the structure is close to the frequency of the forcing function, a condition known as resonance.

The most important way to avoid vibration problems is to avoid resonance between the natural frequency of vibration of the structure and the frequency of system that produces the energy. In most cases, this means having a higher frequency of the structure than the forcing function. It will be shown below that for equivalent structures with little weight other than the structure itself, aluminum will have a slightly higher natural frequency than the equivalent steel structure. If a modest amount of dead weight is added, the frequencies for the two materials will come close to being equal.

If resonance cannot be avoided and vibration levels are unacceptable, the amplitude of vibration can be reduced by applying damping materials to the structure. Damping materials will absorb some of the energy of vibration, reducing the amplitude. A better method, which reduces the weight impact of damping materials, is to provide vibration isolation mounts for machinery.

Vibration problems can be more acute in aluminum structure than in steel because aluminum has greater potential for fatigue damage. Structural details located in areas not normally subjected to significant stresses can develop fatigue cracks if the structure vibrates significantly. Vibration in structure can also cause unpleasant and sometimes excessive noise, especially in accommodation areas. Vibration can also be unpleasant for passengers and crew, and even if not causing structural harm, can reduce confidence in the seaworthiness of the vessel.

11.2 Computing Vibration Frequencies

As mentioned above, a goal in vibration reduction is the avoidance of resonance, which requires calculating the natural frequency of vibration of the structure. There are many textbooks, handbooks, and other sources of information for computing the frequency of vibration of structure. One such source is (Hurty and Rubinstein, 1964) and another is a manual developed by the David Taylor Model Basin (McGoldrick, 1957). Much of the material below was taken from those sources.

11.2.1 Single Degree of Freedom System

For a simple one degree of freedom system such as shown in Figure 11-1, the natural frequency of vibration in cycles per second (Hertz) is given by the equation:

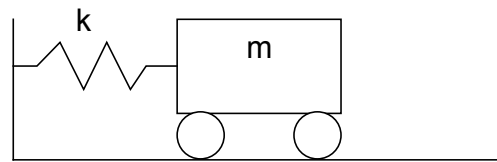


Figure 11-1 Single degree of freedom system.

$$f = \frac{1}{2\pi} \sqrt{\frac{k}{m}} \quad (11-1)$$

where

m = the mass that is vibrating, and

k = the stiffness of the massless spring connected to the mass.

The frequency of a structure can be computed if the mass and stiffness can be determined, and then used in equation (11-1). This is generally not trivial because of the complex nature of ship structure, which can have thousands of degrees of freedom, and for which the mass is distributed throughout the system. However, closed-form solutions do exist for several simple systems, and analysis of these will provide some insight into the response of more complex systems.

11.2.2 Beam Vibrations

For a uniform beam with differing conditions of end restraint, the natural frequency of vibration is given by the equation:

$$f = \frac{C}{2\pi L^2} \sqrt{\frac{EI}{\mu}} \quad (11-2)$$

where for aluminum:

f = natural frequency of vibration in Hertz

L = length of the beam in mm (inches)

E = modulus of elasticity = 71×10^6 kg / mm sec² (10.3×10^6 psi)

I = moment of inertia of the beam in mm⁴ (in⁴)

μ = mass per unit length in kg/mm (lb-sec²/in²)

C = coefficient dependent on end conditions, given in Table 11-1.

The elastic modulus, E_a , of aluminum = 71×10^3 MPa, or 71×10^3 Newtons / millimeter². However, the Newton is the force required to accelerate one kilogram at one meter per second squared, so 10^{-3} Newtons are required to accelerate one kilogram at one millimeter per second squared, or $1 \text{ N} = 10^3 \text{ kg mm / sec}^2$. Therefore, $E_a = 71 \times 10^6 \text{ kg / mm sec}^2$. Likewise for steel, $E_s = 206 \times 10^3 \text{ MPa} = 206 \times 10^6 \text{ kg / mm sec}^2$.

Table 11-1 Coefficients for Natural Frequencies of Beams (McGoldrick, 1957) and (Hurty and Rubinstein, 1964)

End Fixity	Coefficient (C)				Sketch of first mode
	Mode (n)				
	1	2	3	n>3	
Fixed-fixed	22.4	61.7	121	$\left(\frac{(2n+1)\pi}{2}\right)^2$	
Pinned-pinned	π^2	$(\frac{2\pi}{2})$	$(\frac{3\pi}{2})$	$(n\pi)^2$	
Fixed-pinned	15.4	50.0	104	$\left(\frac{(4n+1)\pi}{4}\right)^2$	
Canti-lever	$0.36 \pi^2$	22.0	61.7	$\left(\frac{(2n-1)\pi}{2}\right)^2$	
Free-free	22.4	61.7	121	$\left(\frac{(2n+1)\pi}{2}\right)^2$	

When determining the inertia of a plate-beam combination for vibration calculations, the effective plate should be computed using only shear lag considerations. Because vibrations occur with relatively small displacements compared to the load capacity of the structure, plasticity or buckling considerations should not be made in determining the width of effective plate. The amount of effective plate should be either the stiffener spacing or one-third the span, whichever is less. For computing the mass per unit length, the full width of the plate should be used, as well as any dead weight, including paint and insulation, deck coverings, and stores and cargo that will move with the structure. Additionally, equipment or machinery that is attached to the structure should be included in mass calculation. If the mass of such items can be reasonably

distributed, the average mass per length should be used. If the mass is concentrated in a small area, either one of the equations below for lumped mass should be used, or more detailed finite element calculations, as described below, should be used.

For stiffeners that are continuous through supporting frames, the assumption of simply supported ends should be used unless the supporting structure at the detail of the intersection is heavy enough to justify the assumption of fixity. Otherwise, as the stiffener on one side of the support moves up, the stiffener on the other side will move in the opposite direction, acting as if there were no restraint on rotation at the supports.

If the structure is part of the hull adjacent to the water or is part of a tank boundary, the added mass of fluids should also be added to the mass. A convenient method is to take the added mass of liquids as equal to the mass of a half-cylinder of the liquid with the diameter equal to the width of the panel and length equal to the length of the panel. If the structure is part of a bulkhead with fluid on both sides, a full cylinder of the liquids should be used.

11.2.3 Uniform Beams with a Lumped Mass

The above equations are applicable when the stiffness of the beam and associated mass that is participating in the motion are uniformly distributed. McGoldrick covers two cases when there is an additional lumped mass supported by the beam.

For a simply supported beam with a concentrated mass, m , in the center, the frequency is given by:

$$f = 1.1 \sqrt{\frac{EI}{\left(m + \frac{17}{35} \mu L\right) L^3}} \quad (11-3)$$

For a cantilevered beam with a concentrated mass, m , at the end, the frequency is given by:

$$f = 0.28 \sqrt{\frac{EI}{\left(m + \frac{33}{140} \mu L\right) L^3}} \quad (11-4)$$

For other cases, where there is a single lumped mass that is significantly greater than the mass of the structure, an approximation to the natural frequency can be made by treating it as a single degree of freedom system and applying equation (11-1). The stiffness of the system can be found by applying a unit force in the assumed direction of motion and solving for the deflection. Otherwise, finite element analysis, as described below, should be used.

11.2.4 Uniform Plate with Simply Supported Edges

A solution for a uniform plate with simply supported edges is given by the first mode of vibration by McGoldrick. A similar solution for the first mode and for higher modes is given by Hurty and Rubinstein (1964) as:

$$f = \frac{\pi}{2} \left(\frac{p^2}{a^2} + \frac{n^2}{b^2} \right) \sqrt{\frac{E t^3}{12 m (1 - \nu^2)}} \quad (11-5)$$

where:

a, b, and t are the length, width, and thickness of the plate, respectively,
 m = the mass per unit area of the plate, and
 p and n are 1 less than the number of nodes in the direction of length and width,
 respectively. For the first mode of vibration, p = n = 1.

A simply supported plate vibrating with two nodes in the direction of length and with three nodes in the direction of width is shown in Figure 11-2. Plates are capable of vibrating in many higher modes, although these generally do not show significant amplitude. As with stiffeners, simple supports are a reasonable assumption as adjacent plates of the same size and thickness will vibrate with the same pattern in opposite directions. More complex geometries and changes in plate thickness can be analyzed using finite element analysis, as described below.

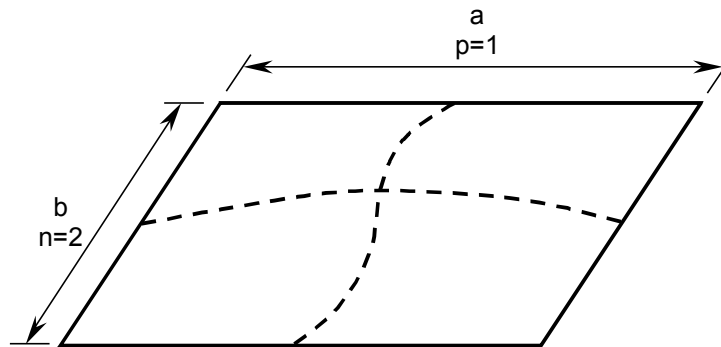


Figure 11-2 Simply supported plate vibrating.

11.2.5 Continuous Structural Systems

The above methods for estimating frequencies of vibration apply to simple structural systems. For larger portions of the structure, finite element modeling may be used. Most finite element computer programs include routines for computing the natural frequencies of vibration of the structure, often called eigenvalues. In addition, the programs will determine the shapes of the different modes of vibration, also called eigenvectors, which are important for understanding the portion of the structure that is moving the most during a particular mode of vibration and for determining points that do not move at all, called nodes.

In some cases, the dynamic characteristics of cargo or other systems must be modeled, rather than treating them as masses rigidly attached to the structure. This was demonstrated by Jia and Ulfvarson (2006) who analyzed the aluminum deck structure of an automobile carrier. The mass of the individual vehicles was modeled to include rotary inertia, and the attachment of the vehicle to the structure was through a system that emulated the dynamics of the vehicles' suspension systems and the stiffness of tires. Good correspondence was found between calculated frequencies and frequencies measured with an instrumented impact hammer.

11.3 Determining the Forcing Function

If vibration reduction is to be achieved through resonance avoidance, two things need to be known, the natural frequencies of vibration of the structure and the frequencies of the forcing functions. The estimation of the first was described above. Determining the frequencies of forcing functions requires knowledge of the various systems aboard the vessel.

The greatest forces that can cause vibration often come from the propeller or propellers on vessels with conventional propulsion. As a propeller turns, any unbalance in the weight of the propeller, lack of straightness of the propeller shaft, or hydrodynamic unbalance between the blades of the propeller will cause uneven forces on the hull at the frequency of shaft rotation. A propeller shaft rotating at 300 rpm will have a shaft-rate frequency of 5 Hz. Most structural systems, such as stiffeners and plate panels will have natural frequencies greater than this, and resonance avoidance is not an issue. However, large massive items of the structure, such as a mast or a deckhouse, can often have natural frequencies of 5 Hz or less. The greatest structure having such low frequencies is the hull itself. The first mode of hull girder vibration is generally in the 1 to 2 Hz range. It is extremely difficult to significantly change the natural frequencies of such systems without a significant increase in weight. Because fixed-pitch propellers operate at a variety of shaft rates at speeds other than full speed, resonance with the hull girder or with massive portions of the structure over some range of shaft speeds generally cannot be avoided. The most effective way to reduce shaft-rate vibrations is to ensure that the propeller shaft is straight and well aligned and that the propeller itself is well balanced both statically and dynamically. Resonances will occur, but the forces may not be high enough to cause a vibration problem.

The next source of vibration from propellers is blade-rate excitation. As the propeller usually operates in an uneven flow field, the forces on individual blades will vary as the shaft rotates. Additionally, the clearance between blade tips and the hull and nearby appendages can cause uneven forces at the blade rate. A cavitating or semi-cavitating propeller will also have uneven forces at blade rate as the degree of cavitation increases and decreases in the flow field and with changes in the depth the blade is immersed in the water as the shaft rotates. The frequency of blade-rate excitation is equal to the shaft speed times the number of propeller blades. A 3-bladed propeller operating at 300 rpm will have a blade-rate frequency of $300 \times 3 / 60 = 15$ Hz. If the propeller has five blades, the frequency would be 25 Hz. Making structure stiff enough so that the frequency is greater than 15 Hz is far simpler than making it stiffer than 25 Hz. The contradiction is that the blade-rate forces on the 5-bladed propeller are less than on a 3-bladed propeller of the same size and speed, so that strict resonance avoidance doesn't always result in the lowest levels of vibration.

Resonance avoidance is possible with slow to medium shaft speeds. However, high-speed shafts with supercavitating propellers operate with speeds as high as 9,000 rpm, and avoidance of shaft-rate and blade-rate resonance is unavoidable. For such craft, vibration reduction can only come from a well-supported and aligned propulsion system with excellent balance in the system.

Other forms of propulsion, such as waterjets or ducted propellers do not result in the same exciting forces as do conventional propellers. However, they often have high energy levels, especially for high-speed vessels, and they can be a significant source of vibratory energy.

11.4 Hull Girder Whipping

Slamming and sometimes ordinary wave encounter will excite the various modes of hull girder vibration. The hull will vibrate as a free-free beam in vertical, lateral, and torsional modes. Such vibration is generally not a problem in itself except for the additional fatigue cycles imposed on the hull structure. The frequency of the significant modes of hull vibration ranges from about 1 Hz to about 10 Hz for most vessels. If a significant portion of the vessel, such as a deckhouse or a mast has a natural frequency that resonates with one of these hull modes, then significant amplitudes of vibration can occur.

McGoldrick gives two empirical methods for estimating the first vertical frequency for conventional steel hulls. The first of these is Schlick's empirical formula:

$$N = C \sqrt{\frac{I_H}{\Delta L^3}} \quad (11-6)$$

where:

- N = frequency in cycles per minute,
- C = empirical constant, varying between 1.28×10^5 to 1.57×10^5 ,
- I_H = Inertia of the hull girder in feet² inches²,
- Δ = displacement in long tons, and
- L = length between perpendiculars in feet.

A second method is Burrill's empirical formula:

$$N = \frac{\phi \sqrt{\frac{I_H}{\Delta L^3}}}{\sqrt{\left(1 + \frac{B}{2d}\right)(1+r)}} \quad (11-7)$$

where the symbols are the same as in Schlick's formula and:

- ϕ = empirical constant = 24×10^5 ,
- B = beam of ship in feet,
- D = draft in feet, and
- R = Lockwood Taylor's shear correction factor:

$$r = \frac{3.5 D^2 (3 a^3 + 9 a^2 + 6 a + 1.2)}{L^2 (3 a + 1)} \quad (11-8)$$

where:

a = B / D, and
 D = depth of hull in feet.

As both of the formulae were developed for steel hulls, the inertia of the hull girder, I_H , should be divided by 3 for aluminum. These formulae were developed for larger ships and are not necessarily applicable to smaller craft. For such vessels, especially multi-hulled craft, where the transverse bending (flapping) modes are important, analyses using finite element modeling may be required.

Friis Hansen et al. (1995) developed an approximate relationship for aluminum similar to the above:

$$\Omega_2 \approx 14.45 \sqrt{\frac{EI}{\Delta L^3}} \quad (11-9)$$

11.5 Energy and Damping

Computation of structural vibratory response to a forcing function is beyond the scope of this guide. However, an important aspect of such calculations is determining the structural damping. In one study of a 70-meter aluminum surface effects ship (ISSC V.2, 2000) the damping ratio for vertical bending was found to be 0.014 in both the on-cushion and off-cushion conditions. The damping ratio reported is the ratio between the damping coefficient and the critical damping.

During free vibration, energy is continuously transferred between the strain energy of the structure and the kinematic energy of the mass. For complex systems, the transformation from one state to another is never complete; there is always some portion of the structure in motion while other portions have stored strain energy. However, with simple undamped systems vibrating in a single mode, the harmonic motion oscillates from a time of zero strain and maximum system velocity to a time of zero velocity and maximum strain energy. In such systems, the strain energy and the kinematic energy are equal (Hurty and Rubinstein, 1964). The strain energy, U, and the kinematic energy, T, for a beam are given by:

$$U = \frac{1}{2} \int_0^L EI \left(\frac{d^2w}{dx^2} \right)^2 dx \quad (11-10)$$

and

$$T = \frac{1}{2} \int_0^L \mu \left(\frac{dw}{dt} \right)^2 dx \quad (11-11)$$

where w is the displacement of the beam along its length, x, and μ is the mass per unit length.

For a simply supported beam of length L and frequency of vibration f , the displacement, w , is given by:

$$w = W \sin\left(\frac{\pi x}{L}\right) \sin(2\pi f t) \quad (11-12)$$

where W is the maximum displacement.

Substituting equation (11-12) into equations (11-10) and (11-11):

$$U_{\max} = \frac{EI W^2 \pi^4}{4L^3} \quad (11-13)$$

$$T_{\max} = \mu W^2 \pi^2 f^2 L \quad (11-14)$$

where U_{\max} and T_{\max} are the maximum strain and kinematic energies. If U_{\max} and T_{\max} are equated and solved for f , equation (11-2) results, with the coefficient $C = \pi^2$, which agrees with Table 11-1 for the first mode of vibration. This is an application of Rayleigh's principle, that in a conservative system the frequency of vibration is stationary. This principle can be used to estimate the frequency of the first mode of vibration of a system by assuming a displacement function and determining the strain and kinematic energy by using forms of equations (11-10) and (11-11).

If a simply supported beam is vibrating in its second mode, the displacement is similar to Figure 11-3. The motion is anti-symmetric about the center of the beam, and so it vibrates as if it were two separate simply supported beams of length $L/2$. The strain energy for the second mode of vibration, $U_{2\max}$, of the beam is found using equation (11-9) as:

$$U_{2\max} = \frac{4EI W_2^2 \pi^4}{L^3} \quad (11-15)$$

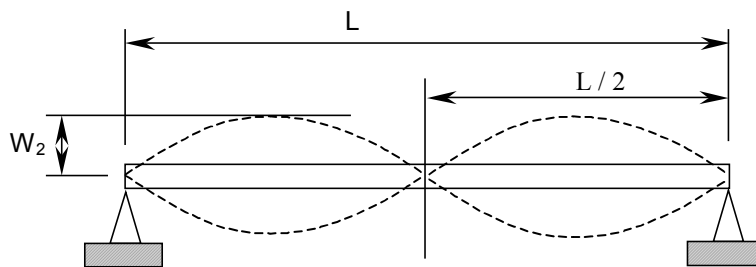


Figure 11-3 Simply supported beam vibrating in its second mode.

Comparing equations (11-12) and (11-14), if the strain energy for the first mode, U_{\max} , is equal to the strain energy of the second mode, $U_{2\max}$, then $W_2 = W/4$. For the same amount of energy exciting resonance, the response of the first mode will be four times greater than the

response of the second mode. Alternatively, sixteen times as much energy is required to excite the second mode to the same amplitude of response as the first mode. The ratios will differ for other structural systems, but the principle remains the same, higher modes require greater energy for excitation. This doesn't mean that a system won't vibrate in higher modes; the response depends on the frequency of the exciting energy.

11.6 Comparison of Aluminum and Steel

11.6.1 Plates

If the ratio for the frequencies of two plates of the same dimensions but of different thicknesses in aluminum and steel is compared using equation (11-5), the ratio is:

$$\frac{f_a}{f_s} = \sqrt{\frac{E_a t_a^3 m_s}{E_s t_s^3 m_a}} \quad (11-16)$$

If $m_s = \rho_s t_s$, and $m_a = \rho_a t_a$, where ρ_s and ρ_a are the density of steel and aluminum, respectively:

$$\frac{f_a}{f_s} = \sqrt{\frac{E_a t_a^3 \rho_s t_s}{E_s t_s^3 \rho_a t_a}} \quad (11-17)$$

Because $E_a / E_s = 1/3$, and $\rho_s / \rho_a = 3$, equation (11-16) becomes:

$$\frac{f_a}{f_s} = \frac{t_a}{t_s} \quad (11-18)$$

and so the ratios of the frequencies of the plates are proportional to the thickness of the plates.

Comparing two similar designs in aluminum and steel, a bottom plate panel in the bow of the 60-meter 50-knot craft examined by Stone (2005) had the following characteristics:

$$s = 0.26 \text{ m}$$

$$L = 0.80 \text{ m}$$

$$p = \text{design pressure by ABS HSV guide} = 222 \text{ kN/mm}^2$$

$$\sigma_a = \text{allowable stress} = 0.90 \sigma_y \text{ for both steel and aluminum.}$$

$$k = \text{factor for aspect ratio} = 0.50$$

Using 5083-H116 plate with $\sigma_y = 165 \text{ MPa}$, and HS 36 steel plate with $\sigma_y = 355 \text{ MPa}$,

$$t_a = s \sqrt{\frac{p k}{1000 \sigma_a}} = 260 \sqrt{\frac{222 \times 0.5}{1000 \times 0.90 \times 165}} = 7.1 \text{ mm}$$

and

$$t_a = s \sqrt{\frac{p k}{1000 \sigma_a}} = 260 \sqrt{\frac{222 \times 0.5}{1000 \times 0.90 \times 355}} = 4.85 \text{ mm}$$

If these thicknesses are rounded to 7.0 mm and 5.0 mm, and are used in equation (11-5) with $m_a = 2.66 \times 10^3 \text{ kg/m}^3 \times 0.007 \text{ m} = 18.6 \text{ kg/m}^2$.

$$f_a = \frac{\pi}{2} \left(\frac{1}{a^2} + \frac{1}{b^2} \right) \sqrt{\frac{E_a t_a^3}{12 m_a (1 - \nu^2)}} = \frac{\pi}{2} \left(\frac{1}{0.80^2} + \frac{1}{0.26^2} \right) \sqrt{\frac{71 \times 10^9 \times (7 \times 10^{-3})^3}{12 \times 18.6 (1 - 0.3^2)}} = 281 \text{ Hz}$$

Similarly for steel, $f_s = 200 \text{ Hz}$, and $f_a / f_s = 281 / 200 = 1.4 = t_a / t_s$. Thus, in this comparative design case, the aluminum plate panel has a natural frequency that is 40 percent greater than the frequency of the equivalent steel plate.

Consider now the case of a dead load on the plate. In the same comparative design example, all of the dimensions will remain the same, and the thickness of the aluminum and steel plates will remain 7.0 mm and 5.0 mm, respectively. Then if a dead load of 200 kg/m^2 (40 lb/ft^2) is added, the masses per unit area become $m_a = 218.6 \text{ kg/m}^2$, and $m_s = 239.2 \text{ kg/m}^2$. Then $f_a = 82.0 \text{ Hz}$ and $f_s = 80.8 \text{ Hz}$. The mass of the dead load dominates, and the increased thickness of the aluminum just compensates for its reduced elastic modulus in determining the natural frequency.

11.6.2 Stiffeners

The natural frequency for simply supported stiffeners is given by equation (11-2) and Table 11-1 as:

$$f = \frac{\pi}{2L^2} \sqrt{\frac{EI}{\mu}} \quad (11-19)$$

If two structures of aluminum and steel are compared, this becomes:

$$\frac{f_a}{f_s} = \sqrt{\frac{E_a I_a \mu_s}{E_s I_s \mu_a}} \quad (11-20)$$

Because $\mu = A_x \times \rho$, where A_x is the cross-sectional area of the plate-beam combination, and ρ is the density of the material, and $E_a / E_s = 1/3$, and $\rho_s / \rho_a = 3$, equation (11-19) becomes:

$$\frac{f_a}{f_s} = \sqrt{\frac{I_a A_{x_s}}{3 I_s A_{x_a}}} \quad (11-21)$$

The difference in frequencies will be explored further using the example structure compared above for plates. For stiffeners, the design pressure is 222.4 kN/m^2 , and the allowable

Aluminum Marine Structure Guide

stress for both aluminum and steel, σ_a , is $0.55 \sigma_y$. For 6061-T6 aluminum extrusions, $\sigma_y = 138$ MPa, so $\sigma_a = 0.55 \times 138 = 75.9$ MPa. For HS-36 steel, $\sigma_y = 355$ MPa, so $\sigma_a = 0.55 \times 355 = 195$ MPa. The proportions of the structure are:

$$L = 800 \text{ mm}$$

$$s = 260 \text{ mm}$$

The ABS HSC requires the section modulus to be $SM = 83.3 \rho s L^2 / \sigma_a$, so:

$$SM_a = 83.3 \times 222.4 \times 0.260 \times (0.800)^2 / 75.9 = 40.6 \text{ cm}^3, \text{ and}$$

$$SM_s = 83.3 \times 222.4 \times 0.260 \times (0.800)^2 / 195 = 15.8 \text{ cm}^3.$$

For the aluminum 7 mm plate, $s / t = 260 / 7 = 37 t$, and $L / 3 = 800 / 3 = 266$ mm, so effective plate for strength should be limited to $35t = 145$ mm. On 245 mm of 7 mm plate, a 3" x 3" x 1.5 T has a section modulus to flange of 41.6 cm^3 . The cross-sectional area of the shape is 830 mm^2 , and the area of the plate is $260 \times 7 = 1,820 \text{ mm}^2$, so the entire cross sectional area $A_x = 830 + 1,820 = 2,650 \text{ mm}^2$. The density of aluminum, $\rho = 2.66 \times 10^{-6} \text{ kg/mm}^3$, so the mass per unit length $\mu = 2,650 \times 2.66 \times 10^{-6} = 2.57 \times 10^{-3} \text{ kg/mm}$. The natural frequency of vibration of the plate-beam is then:

$$f_a = \frac{\pi}{2(800)^2} \sqrt{\frac{71 \times 10^6 \times 2.56 \times 10^6}{2.57 \times 10^{-3}}} = 395 \text{ Hz}.$$

Similarly, for the steel, a 2.5" x 2" x 3/16" x 2.75# L has a section modulus to flange on 260 mm of 5 mm plate of 19.7 cm^3 , and has an inertia of $1.0 \times 10^6 \text{ mm}^4$. The natural frequency for the steel section is 295 Hz, so the equivalent aluminum has a frequency that is 30 percent greater.

If, as was done for the steel and aluminum plates, a dead weight of 200 kg/m^2 is added, the frequencies become 136 Hz for aluminum and 148 Hz for steel, nearly equal.

Using equation (11-12) to find the maximum strain energy of the aluminum stiffener vibrating in its first mode with amplitude $W = 1 \text{ mm}$:

$$U_{Al} = \frac{W^2 (71 \times 10^6) (2.56 \times 10^6) \pi^4}{4(800)^2} = 8.64 \frac{\text{kg mm}^2}{\text{sec}^2} = 8.64 \text{ Joules}$$

Similarly, the energy of the first mode for the equivalent steel stiffener $U_{st} = 9.80$ Joules. Therefore, almost the same energy is required to excite the steel and aluminum structures to the same amplitude in the absence of significant damping. Because the energy is proportional to the square of the amplitude, the amplitude of vibration of the aluminum stiffener is only 6 percent greater than the amplitude of the steel stiffener for the same energy of excitation.

If in the calculation of energies, the 200 kg/m^2 were added as a dead load, the results would be the same, as mass or frequency do not enter equation (11-12). If equation (11-13) were used instead, one would find that the increased mass is compensated for by the lower frequency, and the kinematic energy would remain the same as the strain energy. The only difference in response would occur if the forcing frequency were closer to the natural frequency of the more massive system. Only then would the response be greater. The above examples are summarized in Table 11-2.

**Table 11-2 Comparison of Vibration Frequencies of
Equivalent Aluminum and Steel Panels**

Characteristic	Aluminum	Steel
Alloy	plate 5083-H116 stiffeners 6061-T6	HS 36
Yield Strength	plate 165 MPa stiffeners 138 MPa	355 MPa
Allowable stress	plate 148 MPa stiffeners 76 MPa	plate 320 MPa stiffeners 195 MPa
Panel size	800 mm x 260 mm	800 mm x 260 mm
Design pressure	222 kN/m ²	222 kN/m ²
Scantlings Selected	3" x 3" x 1.5# T 7 mm plate	2.5" x 2v x 3/16" L 5 mm plate
Plate Frequency (Hz)	281	200
Plate Frequency with 200 kg/m ² dead load (Hz)	82	81
Stiffener Frequency (Hz)	395	295
Stiffener Frequency with 200 kg/m ² dead load (Hz)	136	148
Energy for 1 mm amplitude vibration in first mode (Joules)	8.64	9.80

11.7 Summary

Similar steel and aluminum structures will have natural frequencies of vibration that are similar and will require about the same amount of energy for excitation. Therefore, an aluminum hull is no more prone to either local vibration problems or hull girder vibration problems than a steel hull, particularly if classification society requirements for inertia of structural members and the hull girder are met. Although not significantly more prone to vibration problems than steel structure, aluminum structure can have more fatigue cracking problems from vibration. Structure should be proportioned to avoid resonance with various forcing functions aboard ship. If that cannot be avoided, then damping materials must be added. Hull girder vibration can be a problem, and simple methods for estimating the hull girder frequencies are needed for the advanced design stages of aluminum vessels.

Aluminum Marine Structure Guide

Chapter 12

Maintenance and Repair

Properly designed and maintained, aluminum marine structures can see many years of service with minimal problems. There are many aluminum workboats that have seen 30 and more years of satisfactory service with little evidence of corrosion or cracking of the structure. Nevertheless, because aluminum can be very prone to fatigue crack growth, cracking of structure does occur, such as in the aluminum deckhouses of steel-hulled ships. Many of the sources of corrosion in aluminum, particularly galvanic corrosion, tend to be rapid and concentrated, generally requiring immediate action to restore structural integrity. Although the 5xxx-series aluminum alloys do not generally require painting to avoid corrosion, improper painting procedures can lead to corrosion problems. Contact with most other metals, which are cathodic to aluminum, can lead to rapid wastage of aluminum. Use of improper alloys, especially those containing copper, will also lead to rapid corrosion, against which coating systems offer little protection if the aluminum is constantly exposed to seawater.

12.1 Painting and Preservation

Marine-grade alloys of the 5xxx series, particularly those procured under ASTM B 928, do not have to be painted for service in a marine environment. These alloys have inherent corrosion protection because they form an oxide film on their surface, which protects the aluminum from further corrosion. However, when that oxide film is constantly removed or disturbed, progressive corrosion can take place. Local corrosion can take place in regions subject to extreme scrubbing action, such as that caused by turbulent flow adjacent to projections from underwater hulls, over rudders, and similar surfaces. In such cases, special coatings are required (Beach et al., 1984).

The 6xxx-series aluminum alloys are being used more extensively today, especially for lightweight extruded panels. Where they are used in a situation likely to be exposed to seawater, they are required to be coated with an effective system to prevent corrosion. However, most 6xxx-series stiffeners within the hull are usually bare. Although not required for preservation, marine-grade aluminum is often painted for appearance. Additionally, the bottom is generally coated so that an anti-fouling paint may be applied.

12.1.1 Preparation for Painting

Guidance on preparation of aluminum for painting is provided in “Aluminum and the SEA” (ALCAN, 2004). Much of the following guidance is taken from that document. Additional guidance comes from the booklet, Care of Aluminum, 2002, available from the Aluminum Association (2002a), and from the NSW Carderock aluminum guide (Beach, 1984).

The natural or heat-treat oxide film that covers uncoated aluminum must be removed because it prevents the adhesion of paints to the surface. This removal procedure is referred to as deoxidation. While an oxide layer will form instantaneously on the aluminum surface as soon as deoxidized material comes into contact with air, the newly formed oxide will be much more homogeneous and amenable to subsequent treating and painting. Degreasing should be

Aluminum Marine Structure Guide

performed prior to deoxidation to prevent grease and oils from becoming imbedded into the surface of the aluminum. The purpose of degreasing is to remove all foreign bodies, including solid particles and fatty products (oils, greases), which have infiltrated the metal's natural or heat-treat oxide film. Degreasing with detergents is preferable to the use of organic solvents. Solvents that are too "light" such as acetone are not recommended as they are tricky to handle and highly flammable. Degreasing should be done by treating small areas at a time, using clean lint-free cloths that are frequently replaced to ensure that impurities are removed rather than just spread around.

There are four accepted options for deoxidizing the surface of aluminum: etching, blasting, disk grinding, and wire brushing.

Etching involves chemically removing the surface layer of aluminum so that it will accept the wash primer. This will result in both oxide removal and some removal of base metal. The etching medium is a phosphoric acid solution that is applied liberally to all the surfaces to be treated. It is applied with a brush, cloth, or sometimes a mop, taking care to protect the operator from splashes. After application, the medium must be left to act as directed by the manufacturer, usually for 20 to 30 minutes. The surfaces are then washed off with fresh water until the wash water returns to a neutral pH level.

Blasting is done with an abrasive suitable for use on aluminum alloys, such as aluminum oxide, or any other inert abrasive. Abrasives that will contaminate the surface of the aluminum, such as copper slag or iron oxide, must be avoided. Abrasives should not be used if they were previously used for blasting steel. Blasting must always be done on surfaces that are clean and dry and be followed by thorough dust removal. Preparation of aluminum should include blasting or grinding to a clean silver color. Steel shot must not be used because it can cause pitting corrosion.

Disk grinding is used on surfaces that cannot be treated by etching or abrasive cleaning. It must be carried out with coarse grit aluminum oxide wheels to achieve a well-keyed adhesive substrate. However, coatings do not adhere to surfaces treated in this way as well as after etching or blasting.

Wire brushing should be done only after the surface is thoroughly degreased and is completely free of grease, oil, paint, water, or other fluids or contaminants. Either hand or power-driven wire brushes can be used. If the surface is not properly cleaned beforehand, these contaminants can be worked into the surface by the brushes. The brushes must be stainless steel, and the bristles should be about 0.25 mm (0.01 in) in diameter.

Blasting with high-pressure water has been experimented with for preparation of aluminum for coating. This method should only be used if an established procedure is followed.

12.1.2 Painting

Surfaces should be primed as soon as possible following preparation to prevent the oxide film from absorbing moisture or the treated surfaces from attracting impurities. Generally, this is a maximum period of four hours. Effective protection against an aggressive marine environment

is obtained by multi-layer coatings in which each coat contributes to the efficiency of the system. The types of paint most widely used at present are based on polyurethane or epoxy resins.

The preferred primer for aluminum is an epoxy system, of which there are a number available from paint manufacturers, including systems produced specifically for aluminum. An alternative primer is a reactive primer, usually with a vinyl resin base and containing a certain amount of phosphoric acid. Application of these coatings should follow the manufacturers' recommendations but must always be preceded by proper preparation of the aluminum as reviewed above. The primer ensures that the coatings adhere to the aluminum and provides a seal to prevent corrosion.

Formerly, zinc chromate primers were used for protection of marine aluminum structures. Zinc chromate is one of the anticorrosive pigments most frequently used in the formulation of primers and is still used extensively today, particularly in the aircraft industry. It is also offered as a primer for steel in consumer applications. However, it has been identified as a carcinogen and has been banned for many applications. Different alternatives for an anticorrosive pigment that are environmentally acceptable have been proposed in order to replace zinc chromate, including zinc phosphate. Various modifications have been made to this family of pigments to improve its properties, and a second generation of phosphate pigments, incorporating elements such as molybdenum, aluminum, or iron have been produced. These were reviewed by Bethencourta et al. (2003) to demonstrate their effectiveness for protecting steel. With time, similar progress might be made for the protection of aluminum.

Special fillers are used to achieve a smooth surface, especially on yachts and other vessels where appearance is important and a slight increase in weight is acceptable. Preference should be given to solvent-free epoxy fillers as these are suited to immersion and will not shrink as they harden. Fillers should never be applied directly onto the metal but instead between successive coats of epoxy primer. Application is by spatula or more often using a float. Once it has dried, the filler should be sanded using wet or dry abrasive paper. Some fillers may require washing with fresh water after curing, especially if this occurs at low temperature. All dust should be carefully removed from the surface before the next coat of primer is applied.

Finish coats are used to reinforce the water tightness of the paint system and enhance its appearance. A variety of coatings are available, including polyurethane, which provides a very smooth appearance. The type of finish coat applied must be compatible with the primer used. The manufacturer should be consulted for this information.

Antifouling paints are required on the bottom of an aluminum vessel to prevent fouling by marine growth. Aluminum and its mineral compounds such as alumina (Al_2O_3), the corrosion product of aluminum, are non-toxic to marine growth, and offer no protection to a bare bottom. Antifouling paints based on copper oxide must be avoided as they can severely corrode the underlying metal. Since the early 1970s, the biocide used in most commercial antifouling paints has been based on a salt of tin, tributyl tin (TBT), which is compatible with aluminum. Because this biocide is toxic to the marine environment, the International Maritime Organization banned TBT based antifouling paints in 2003. A number of paint manufacturers have developed antifouling paints that are compatible with aluminum. These coatings are not strictly antifouling

because they do not contain toxins that kill marine life. Rather, the coatings release when marine growth develop on them, keeping the hull clean.

Potable water tanks do not have to be coated because the chemical composition of the 5xxx and 6xxx-series alloys are considered “food-grade” materials, and they can therefore be used uncoated to make drinking water tanks. Before use however, it is essential to thoroughly clean the insides of the tanks and rinse them several times, preferably with hot drinking water. Potable water tanks may also be painted if desired, in which case the protection products must be supported by a manufacturer’s certificate of safety (ALCAN, 2004).

Coatings may be required on other tanks, such as sewage tanks and gray water tanks that include acids and fats from the galley. Sewage and these chemicals can cause corrosion of aluminum, and such tanks should be coated for protection.

The U.S. Navy provides guidance for painting aluminum in Chapter 631 of the Naval Ships Technical Manual. It recommends grit blast, epoxy primer (MIL-DTL-24441 or MIL-PRF-23236) and silicone alkyd topcoat (MIL-PRF-24635). However, this system is currently being reviewed for improvement in performance.

12.2 Corrosion Problems

An error that is sometimes made in priming aluminum has diminished in recent years because of environmental bans on lead-based paint. However, even if no such bans exist, lead paint should never be used on aluminum, as it will promote corrosion. In the same way, iron oxide primers should not be used, as they also promote corrosion. Examples of corrosion caused by these primers are shown in Figure 12-1 and Figure 12-2. In Figure 12-1, a steel door frame was primed before the aluminum, and the primer, which was either red lead or red iron oxide, spilled over onto the aluminum. In this situation, the aluminum should be sanded or blasted down to bare metal at least 150 mm (6 in) from the edge to ensure that all of the primer is removed. In Figure 12-2, there is paint blistering, corrosion, and some star cracking on the aluminum paint that was primed with iron oxide. The entire area must be blasted or sanded to bare metal, and the areas of corrosion ground out before repriming the surface.

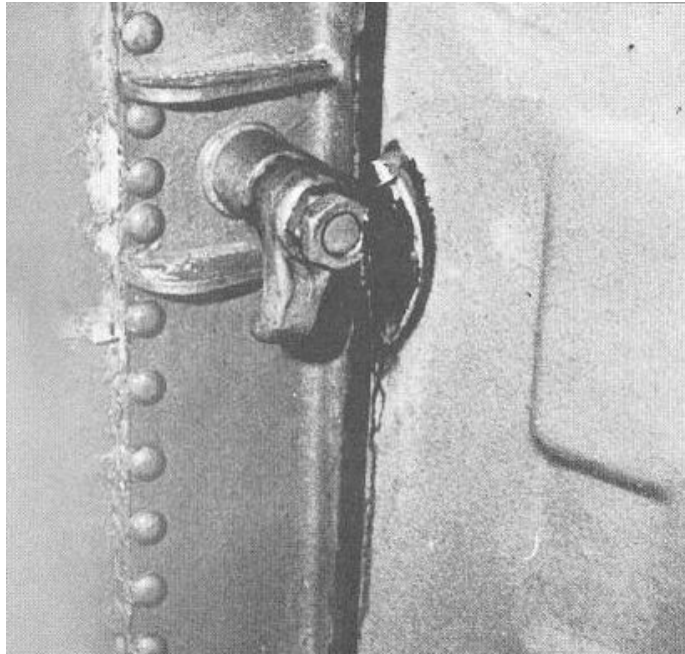


Figure 12-1 Corrosion of aluminum where lead or iron oxide primer spilled over from priming a steel door frame (Dye and Dawson, 1973).

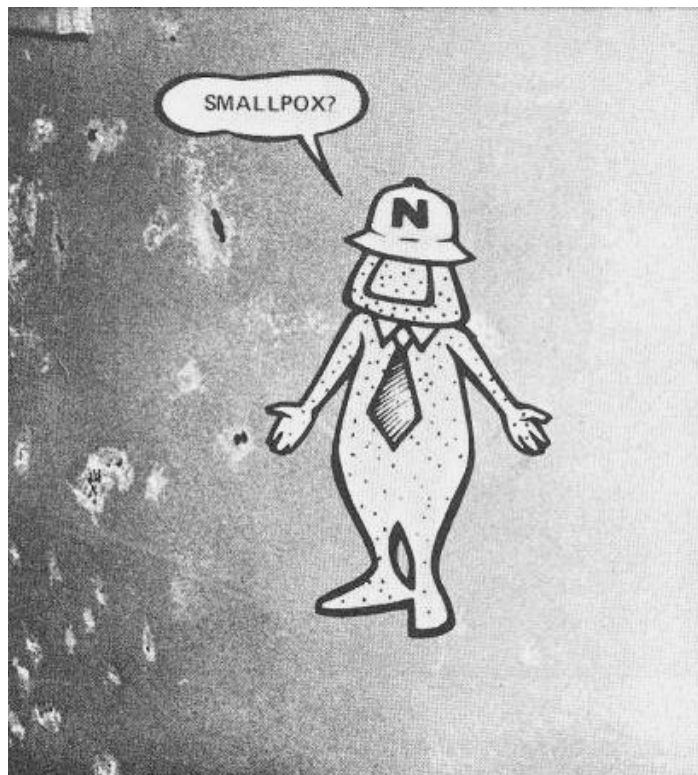


Figure 12-2 Corrosion of aluminum primed with iron oxide (Dye and Dawson, 1973).

The corrosion resistance of aluminum, even with effective coatings, may be insufficient in cases where entrapment of seawater can cause a high buildup of salt concentration from repeated wetting and drying. Even a good coating system may not protect such areas, and the best solution is to provide drainage. An example is shown in Figure 12-3, where an internal stiffener within a fan room accumulated a high salt concentration from spray entering through the intake. In this case, the plate had been painted with zinc chromate primer before the use of that coating had been banned for environmental reasons.



Figure 12-3 Corrosion where standing water at an internal stiffener permitted buildup of salt concentrations (Dye and Dawson, 1973).

Some craft have been constructed with alloys that do not belong in a marine environment, such as the 2xxx and 7xxx series. These craft, such as air cushion vehicles, are intended to operate in the water for only a short time, and then be stored in a dry environment. These craft should be rinsed with fresh water after removal from seawater, with special attention paid to crevices and pockets where water can accumulate. They should then be thoroughly inspected for any signs of breakdown of coatings.

12.3 Repair of Cracking

There are generally three causes of cracking in aluminum structure; cracking at improper welds, fatigue cracking from stress concentrations or poor structural details, and stress-corrosion cracking. Most times, the difference can only be determined through detailed analysis of loads, stresses, and metallurgical examination, which are generally impractical in a repair situation that is characterized by little available time.

The procedure used in repair situations is generally trial-and error. If a crack is found, it is generally in a weld or initiated in a weld. The repairs undertaken consist of safe-ending the

crack, grinding out the crack, and rewelding. However, if time permits, a thorough engineering evaluation should be made prior to repair. This is especially important if the same area cracks in a fleet of similar vessels and should always be done if a failure recurs shortly after repairs are made.

An investigation of cracking should include an estimate of the fatigue load spectrum that the vessel has encountered during its lifetime, the stress spectrum resulting from those loads, and a linear cumulative fatigue damage calculation using the assumed S-N curve for the structure or structural detail that has cracked. If this is not possible, then a stress concentration analysis can be made under an assumed loading. A redesign should significantly reduce the stress at the area of cracking, usually by 50 percent if possible. If that cannot be done, weld fatigue strength improvement techniques, as will be discussed below, should be employed.

12.3.1 Safe-ending Cracks

The tip of a crack represents a very high stress concentration. Because aluminum has a high coefficient of thermal expansion, high strains develop during welding, which can cause the crack to continue to propagate during a repair weld. The crack surface often has a 45-degree angle through a plate, so a distance equal to the thickness of the plate can separate the crack tip on opposite sides of the plate. Therefore, the tip of the crack should be drilled out with a hole equal to at least three times the plate thickness. Prior to drilling a hole to safe-end a crack, the plate surface should be ground clean, and dye penetrant should be used to be certain that the crack tip has been located. After safe-ending the crack, dye penetrant should be used again to ensure that the crack does not extend beyond the hole. If the crack has propagated in two or more directions from the point of crack initiation, all of the crack tips must be found and safe-ended.

If time does not permit rewelding of a crack after the ends have been drilled out, reaming or grinding the surface of the holes smooth can slow further re-cracking. Then insert a high strength stainless steel bolt with heavy washers into the opening and tighten to near the breaking strength of the bolt. The compressive stresses from the bolt will slow the process of crack reinitiation. Temporary watertightness can be provided by using a polysulfide sealant.

12.3.2 Welding a Doubler Plate

A longer lasting temporary repair can be made by welding a doubler plate over the crack. However, the crack must be safe-ended as described above before welding the doubler plate. The corners of the doubler should have a minimum radius of 75 mm (3 in), and the edges of the doubler should be at least 150 mm (6 in) from the crack. If the doubler crosses a weld in the plate, the weld should be ground flush and the doubler extended at least 150 mm (6 in) beyond the weld. A drawing of a doubler plate over a crack is shown in Figure 12-4. Note that in this figure, the crack has crossed the web of a stiffener. Therefore, the web must be examined carefully to see if the crack has propagated into it, and if so, the crack tip must be safe-ended. In this case, a cope hole can be ground in the web of the stiffener to clear it from the crack.

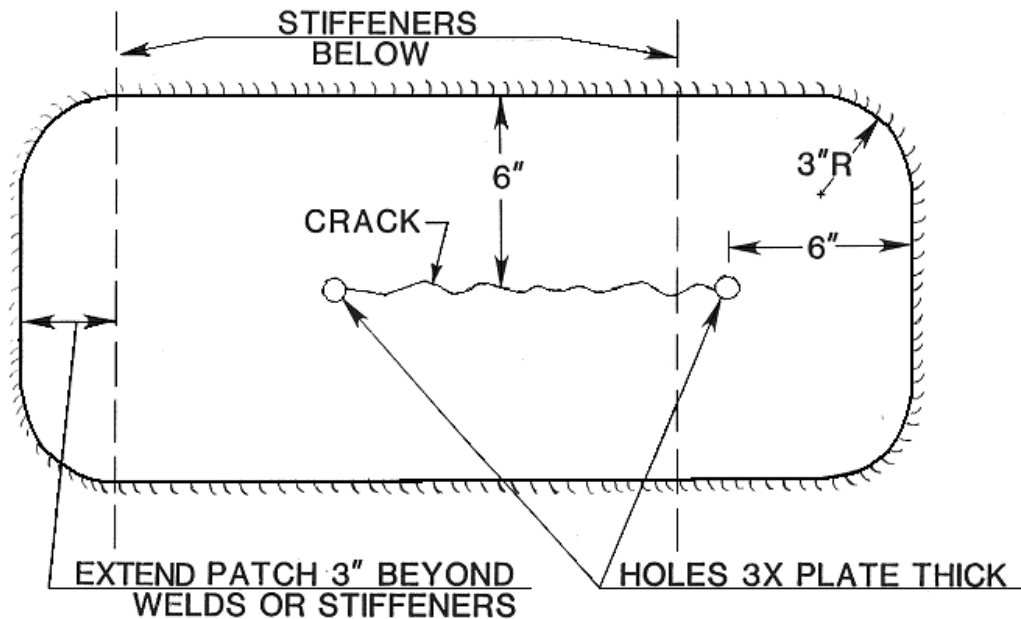


Figure 12-4 Doubler plate welded over a crack.

Even though the doubler plate may be intended as only a temporary repair, every effort should be made to use proper welding procedures and achieve as high a quality weld as possible. To achieve additional resistance from crack initiation, the edges of the fillet welds of the doubler can be ground smooth. Guidance on weld profiles and grinding to improve them is shown in Figure 12-5. The grooming of the weld profile should not reduce the thickness of the plate by 10 percent or 0.8 mm (0.03 in), whichever is less. Grinding should be perpendicular to the edge of the weld, not parallel to it, as that will place grooves in the weld that can be points of crack initiation and reduce the fatigue life, rather than improving it.

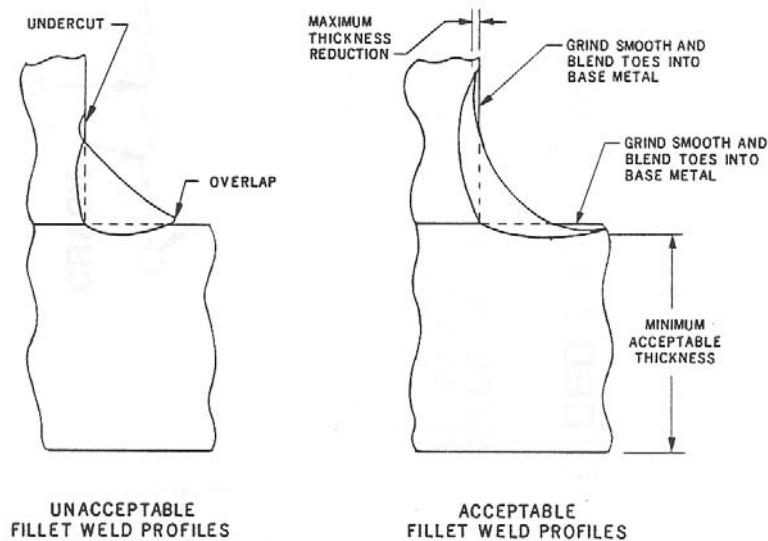


Figure 12-5 Improving weld profiles in fillet welds.

12.3.3 Grinding out the Crack and Welding

In aluminum, cracks do not usually follow a straight line. Therefore, it is important, if at all possible, to inspect both sides of a crack and determine its path and if it has propagated in different directions. An example is where the crack has crossed a stiffener in Figure 12-4. The web of the stiffener should be ground clean and inspected with dye penetrant for cracks. The crack should be ground out for its entire length in preparation for welding. The surface should be thoroughly cleaned with a solvent prior to welding to remove any traces of the dye penetrant, oil, grease, oxide film, and imbedded particles of any kind.

Rewelding should begin at the hole and then progress towards the center of the crack. If the crack has propagated in two or more directions, each crack tip should be safe-ended before rewelding, and all repair welds progressed towards the center of the crack, using back-stepping for larger cracks. The last weld should be thoroughly fused with the first and the crater filled. The weld should be made from both sides, back chipping or grinding the back side prior to welding. The surface should be carefully inspected after back chipping or grinding, but dye penetrant should not be used for this purpose as it can contaminate the joint.

If a two-sided weld cannot be made, a permanent or removable backing strip should be used for all butt welds. An example of how a backing strip can be fit for repair of a tubular member is shown in Figure 12-6. To temporarily hold the backing strip, a weld wire is short-circuited to the strip in one or more locations that will permit the strip to be inserted through the opening. Tack welds are then used to hold the strip in place prior to final welding.

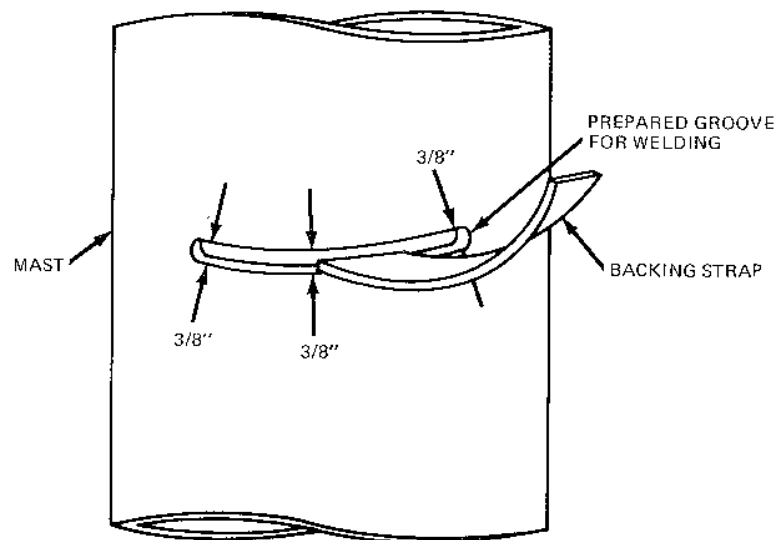


Figure 12-6 Inserting a backing strip in a tubular member.

Again, every effort should be made to ensure the quality of the repair weld is as good as or better than original construction welds. Radiographic inspection should be used to ensure that there are no imbedded defects in the welds. If this is done, then the weld surface should be

ground flush to maximize fatigue life. If it is not possible to radiograph the weld, then the weld bead should not be ground off, as this may be contributing to the strength of a defective weld. Instead, contouring similar to that shown in Figure 12-7 should be used. Grinding should be perpendicular to the direction of the weld, not parallel to it.

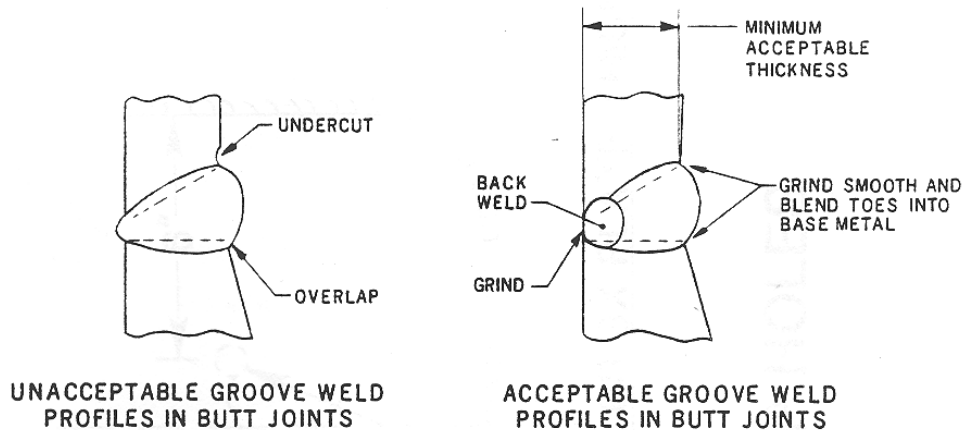


Figure 12-7 Improving the profile of a butt weld.

The value of flush grinding a butt weld is seen in the S-N curves of Eurocode 9. A butt weld made from both sides has a fatigue classification of 35, 3.4, meaning that the detail has a fatigue life of 35 MPa at 2×10^6 cycles, with a negative slope on a log-log graph of 3.4. For a butt weld that has been ground flush, the classification becomes 45, 7.0. The difference in slopes means that for less than 5×10^5 cycles, the weld with reinforcement has a greater fatigue life, but at higher cycles, the flush ground weld is superior. This is shown in Figure 12-8.

Other data on the fatigue strength of butt welds does not agree with the S-N curves of Eurocode 9. For example, data developed at the Naval Surface Warfare Center, Carderock Division (Hay et al., 1995) would have a classification of 34, 2.64 for as-welded butt welds and 127, 5.45 for flush ground butt welds. These S-N curves are also shown on Figure 12-8. This data provides even greater confidence in the value of grinding welds flush to improve fatigue life, assuming that the weld is first inspected using radiographic inspection. The Eurocode 9 S-N curves possibly do not reflect such inspection.

Cracks should never be repaired by simply welding over the crack without the preparation mentioned above. Such repairs will allow the crack to quickly reinitiate, and the crack will propagate at a faster rate than if no repairs had been attempted. An example of such an unsuccessful weld repair is shown in Figure 12-9.

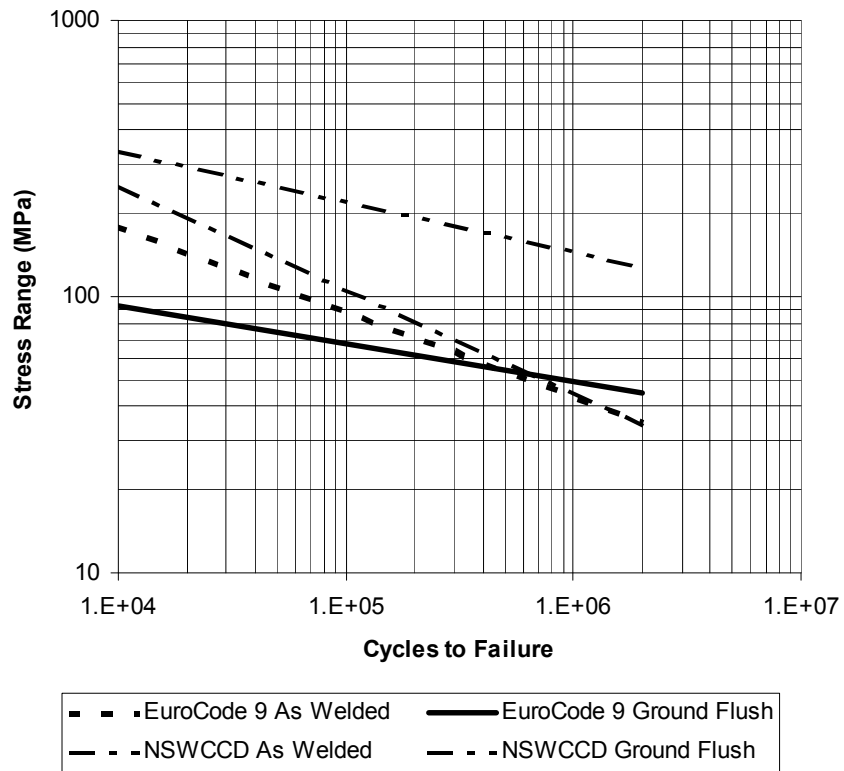


Figure 12-8 Comparison of Eurocode 9 and NSWCCD fatigue S-N curves for butt welds.

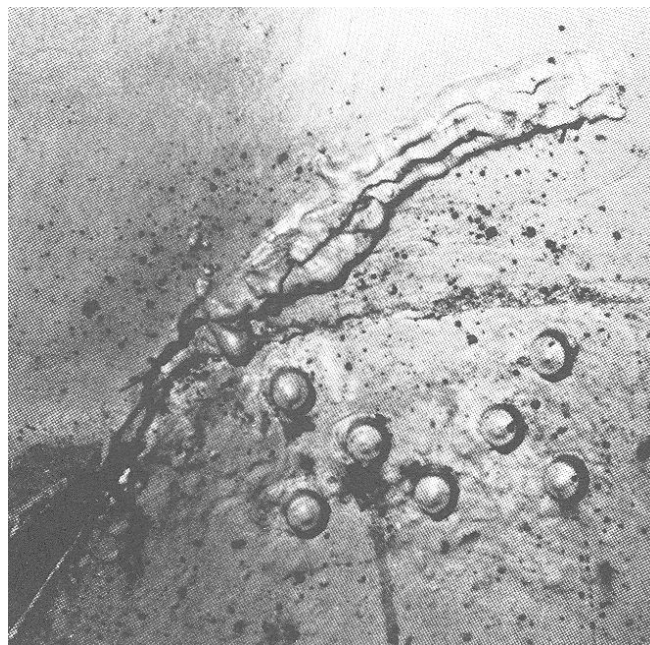


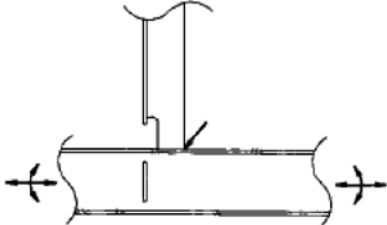
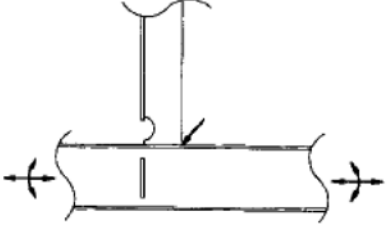
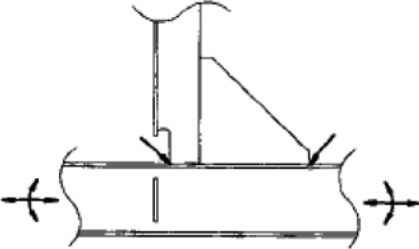
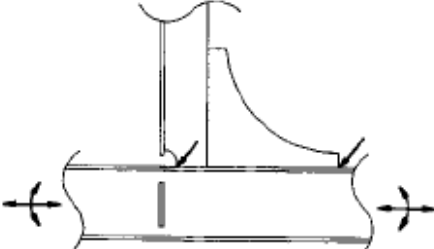
Figure 12-9 Recracking of one-sided repair weld where the original crack was not removed (Dye and Dawson, 1974).

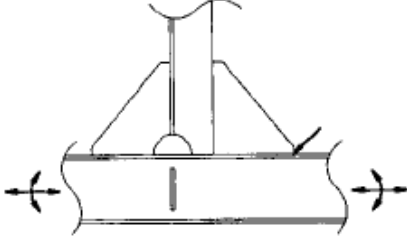
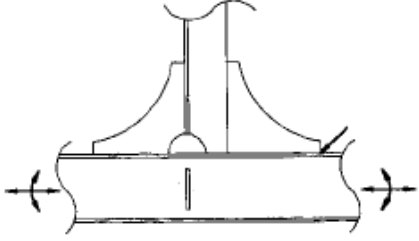
12.4 Repairs of Overstressed or Improperly Designed Details

Because aluminum is more susceptible to fatigue cracking than steel, many structural details that are acceptable in steel are unacceptable in aluminum structure. Structural details are discussed more fully in Chapter 4, which should be consulted for improvement in details. A structural detail may have to be completely redesigned and large sections of the structure replaced in order to solve a persistent cracking problem. In other cases, the situation can be improved by adding brackets, radiused transition plates, or insert plates.

Means of improving the fatigue life of structural details for steel ships are shown in the Ship Structure Committee Report “Improved Ship Hull Structural Details Relative to Fatigue” (Stambaugh et al., 1994). Although the report was written for steel ships, the principles involved for reducing stress concentration factors at structural details are equally applicable to aluminum structural details. An example is given in Table 12-1 for the intersection of two members. Six different configurations of the same detail have stress concentration factors ranging from 3.3 to 2.0. Reduction of the stress concentration factor by this amount can extend the life of an aluminum detail by about five times. Further examples are given in Stambaugh et al. of changes in details to improve fatigue life. In addition, examination of the structural details in Chapter 4 will show similar details with different fatigue classifications and provide guidance on the improvement of a detail that cracks in service.

Table 12-1 Improvement in Fatigue Life of Structural Detail by Adding Brackets

Detail	Stress Concentration Factor	Detail	Stress Concentration Factor
	3.3		2.8
	2.7		2.3

Detail	Stress Concentration Factor	Detail	Stress Concentration Factor
	2.7		2.0

Fatigue cracking from poor structural details is often a problem with vessels in the 30 to 60-meter size range. Designers of smaller vessels try to extend their knowledge of ship design and fabrication into the larger sized vessels without a full appreciation of the effect of increased longitudinal hull girder bending moments on fatigue. Structural detailing and fabrication practices that were acceptable for the smaller craft will not succeed in the larger vessels unless the scantlings are sufficient to reduce the stresses significantly.

One area of concern is at the corners of openings, such as hatch openings. Doubler plates should not be used for repairs of cracks if they occur in such areas of high stress concentration. Instead, thicker insert plates should be used in the corners, as shown in Figure 12-10. The insert plate should be at least 3 mm (0.125 in) thicker than the original plate. If the insert is thicker than that, the edges should be chamfered at a slope of at least 4 to 1. The radius of the corner should preferably be equal to one-fourth the width of the opening, but no less than one-eighth the width. The length, L of the insert should be at least 300 mm (12 in) greater than the radius. The corners of insert plates should have a radius of at least 75 mm (3 in) or twice the thickness of the plate, whichever is greater.

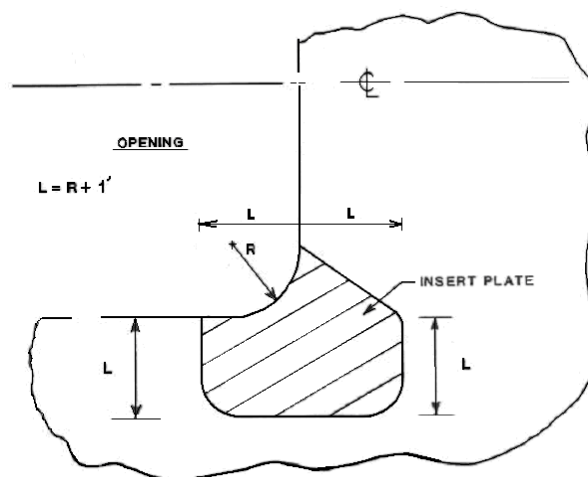


Figure 12-10 Reinforcement of a hatch opening.

12.5 Repairs for Corrosion or Stress Corrosion

Although aluminum is very resistant to corrosion, there are instances where it will occur. Where seawater is permitted to collect and then evaporate, as was shown in Figure 12-3, high concentrations of salt will accumulate and may eventually corrode through the aluminum structure because there will always be minute gaps in the coating. Although marine alloys are tested for exfoliation and intergranular corrosion, there are instances where the wrong material is used and corrosion results. Both exfoliation and intergranular corrosion are caused by the magnesium migrating to the grain boundaries, and this generally occurs only in alloys with 3.0 percent or more magnesium content.

Exfoliation occurs at the exposed edges of plate and is characterized a leafy or flaky appearance, such as in Figure 12-11 and Figure 12-12. Another example of exfoliating is shown in Chapter 2. When the exfoliation is extensive, the unsound area of the plate should be replaced, preferably with plate procured to ASTM Specification B 928 because 5xxx-series alloys produced in the H116 and H321 tempers in accordance with that specification are resistant to exfoliation and stress corrosion cracking. If that is not possible, the free edges of replacement plate should be clad welded to seal the exfoliation-prone edges. No special precautions are necessary when welding new plate to exfoliated plate except to be certain that all areas of corrosion on the existing plate have been removed and that welding is to solid metal. If the extent of exfoliation is not extensive, the plate should be ground back to solid metal and the free edges seal welded at least 150 mm (6 in) on each side of the damaged edge. Once exfoliation has been detected, all free edges should be seal welded as a precaution against further exfoliation. Exfoliation-prone plate can only be detected by removing samples and using microphotographs for metallurgical examination.

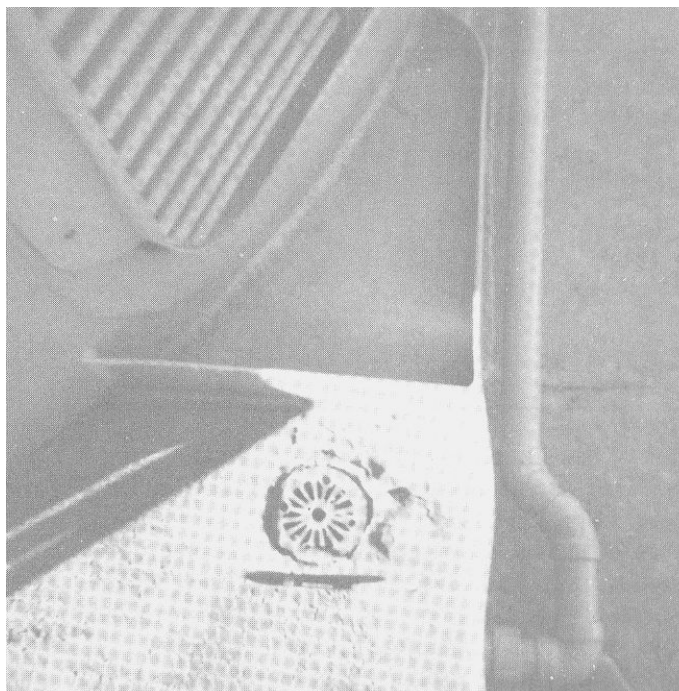


Figure 12-11 Exfoliation of 5454-H321 plate at a deck drain (Dye and Dawson, 1974).



Figure 12-12 Exfoliation at a joint between a 5456-H321 deckhouse and a steel coaming (Dye and Dawson, 1974).

Bushfield et al. (2003) described a recent example of extensive intergranular corrosion when a number of vessels were constructed of 5083-H321 prior to the development of ASTM B 928 in 2004. The corrosion damage is shown in Figure 12-13 through Figure 12-15. In such cases, the remedy is complete replacement of all of the corroded plate. In such a situation, samples should be cut from plate that has not yet shown signs of corrosion and the plate tested for intergranular corrosion susceptibility in accordance with ASTM G67. The sample plate should also be tested for exfoliation susceptibility in accordance with ASTM G66.

5xxx-series aluminum alloys with magnesium contents greater than 3 percent can become susceptible to stress corrosion cracking if exposed to temperatures greater than 67 °C (150 °F) for extended periods. For elevated temperature applications, such as uptake spaces and stacks, alloy 5454 should be used. However, this alloy has not generally been used for topside structures, such as decks. Prolonged exposure of exposed topside structure to sunlight, especially in a hot climate, can lead to sensitization of the aluminum to stress corrosion cracking because the deck temperature can easily exceed 67 °C in such circumstances. Stress corrosion cracking is sometimes difficult to distinguish from cracking resulting from other causes, such as high stress. The example shown in Figure 12-15 demonstrates one characteristic, which is cracking in the heat-affected zone of the weld, rather than in the toe of the weld or in the weld itself.



Figure 12-13 Intergranular corrosion with plate beginning to pop out (Bushfield et al., 2003).



Figure 12-14 Pitting corrosion on a plate susceptible to intergranular corrosion (Bushfield et al., 2003).



Figure 12-15 Stress corrosion cracking and pitting on shell plating (Bushfield et al., 2003).

In a situation where stress corrosion cracking occurs, repair welding the cracks is not effective, as the plate beyond the heat affected zone is very likely to be as sensitized as the area that cracked. Replacement of the plate is necessary in this case, although samples can be removed for metallurgical examination prior to replacement. Note that procurement of plate to the specifications of ASTM B 928 does not provide resistance to stress corrosion cracking if the plate is exposed to service at elevated temperatures. If stress levels do not permit the lower strength 5454-H32 or H34 plate to be substituted, efforts should be made to protect the replacement plate from higher temperatures, such as providing insulation or protection from the sun when operating in hot climates.

12.6 Summary

Aluminum has the potential for excellent corrosion resistance. However, poor preservation methods, improper alloys, or bimetallic coupling can lead to rapid corrosion. Rapid crack propagation rates make aluminum susceptible to fatigue cracking, and an improperly designed aluminum vessel can become a maintenance headache. Redesign of areas prone to fatigue cracking is necessary to promote the safe life of the vessel.

Aluminum Marine Structure Guide

Chapter 13

Mitigating Slam Loads

The pressures from bottom slamming are often the cause of damage in all forms of vessels. Even large bulk carriers are not immune, and many such ship have instrumentation in the bow to indicated conditions that can produce damage because operators at the bridge at the stern do not always perceive the impact of wave. With smaller craft, the operators generally feel the impact of slam loads but cannot often correlate the feeling in the back of their teeth to the magnitude of loading on the structure or the structural response. For this reason, methods of limiting of mitigating the effects of slam loads are needed.

An example of the difference between accelerations at the bow and at the operator's station in small craft was reported after an individual was locked in the forepeak of a torpedo boat that operated at 55 knots for several hours in sea state 3. The individual died from injuries, while the operators aft of midships were somewhat uncomfortable but able to endure the pounding.

13.1 Structural Design

Aluminum vessels have the capacity to react to an overload situation through plastic deformation of the structure, although not to the same extent as steel structures. Depending on the alloy, aluminum can deform from 8 to 14 percent, whereas the marine steel alloys can deform 25 percent or more. Because the energy absorbed through plastic strain is significantly greater than the energy of elastic strain, this is an effective means of absorbing energy. Slam loads are of a short duration, and energy absorption is important for reaction to slam loads. If plastic deformation occurs without structural collapse or fracture, the vessel can then safely return to port, at which time a decision can be made as to whether repairs are needed.

For plastic deformation to occur without structural failure, there are several principles of design that should be followed. The first principle is avoidance of stress concentrations. Structural details should have continuity and be continuously welded so that stress can flow smoothly from one member to another. Any cutouts in the webs of members adjacent to the shell in areas subjected to slam loads should have collar plates fitted to continuously support plating. The second principle is proportioning of members. Stiffeners and frames should be symmetric tee sections and their webs and flanges proportioned so that they do not buckle and overloads can be absorbed by plastic deformation. In calculating the buckling strength using the methods referred to in Chapter 3, the yield strength of the unwelded aluminum should be used as the strength goal. Finally, plating should be continuously welded at stiffeners and frames.

Such provisions for plastic deformation should not be an explicit part of the design criteria, which should be for elastic response to specified loads. The provision for plasticity provides an implicit increase in load capability that will accommodate overloads that can come from slam loading. There can be many sources of overloads in high speed craft, such as surface effect craft falling off of cushion.

13.2 Preferred Course and Speed

One of the most important methods to limit ship motions and slam loads in a seaway is to make the operator aware of the effects of heading and speed on those motions. An effective way of accomplishing this is shown in the polar plot of pitch angle versus heading in Figure 13-1. This figure provides the pitch response for three different speeds. Figure 13-1 is taken from Chiu et al. (2005), which was intended to demonstrate a technique of angular measuring ship motions with a system of accelerometers. Perhaps that explains why there are apparent anomalies in Figure 13-1 that the authors did not mention. The response of a vessel in a seaway is generally symmetric port and starboard with respect to ship motions. The data of Chiu et al. is asymmetric, but in Figure 13-1 only the data from 0 to 180 degrees is plotted, with the data from 180 to 360 degrees taken symmetrically.

The unusual feature of the data of Chiu et al. is that greater pitch response occurs in beam seas than in head seas or stern seas, which is not usually the case for large vessels. However the 100-ton patrol boat on which the data was measured is a planing craft in moderate seas, sea state 3, and that is typical behavior for that type of craft. More meaningful information could come from a polar plot of bow accelerations at different headings and speeds, but the data in Figure 13-1 will help the operator of this craft take the most favorable heading and speed if motions and slam loads start becoming excessive.

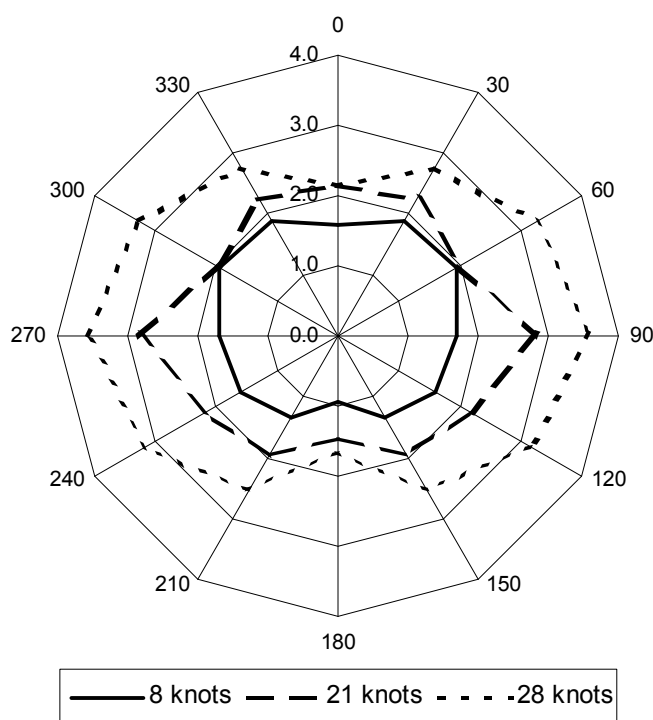


Figure 13-1 Polar plot of pitch angle for a patrol vessel in Sea State 3 (Chiu et al., 2005).

13.3 Weather Routing

With vessels designed for limited service and operating on a short fixed route, the answer to load reduction will often be avoidance or delay of service. If predicted sea states on the vessel's route exceed design maxima, the vessel must remain in port until the weather abates.

For vessels operating on a longer route, the weather patterns that cause high loads can sometimes be avoided by taking alternative courses. To do this, many weather routing services are available. Effective use of such services includes knowledge of the response of the vessel to different sea states so that a route can be selected that avoids sea conditions that will cause damage, yet deviate less from the route that results in the shortest transit. In many cases, a route that has a greater distance traveled will result in a shorter transit time because speed will not have to be reduced as much, if at all.

13.4 Hull Instrumentation

Classification societies determine many of the loads applied to the structure of high-speed vessels from the accelerations that the craft experience when operating at high speeds. This basic relationship between slam loads and accelerations was first established by Heller and Jasper (1961) and further developed by Allen and Jones (1978). Whether determined by empirical formulae or by numerical analysis or model tests, all high-speed craft have design values of acceleration incorporated into the process for determining scantlings. Furthermore, these design values represent the maximum allowable value for craft in limited service conditions, and for craft with unlimited service conditions, the design acceleration represents the value of acceleration with a probability of exceedance of 10^{-8} . Therefore, to avoid damage from slamming, it is incumbent on the operator to avoid exceeding the design acceleration value.

To aid in this process, many classification societies either require or else provide special classification for vessels having hull-monitoring systems. As an example, the ABS Guide for Building and Classing High Speed Naval Craft (HSNC) has three notations for installations made in accordance with the ABS Guide for Hull Condition Monitoring Systems (ABS, 2003A).

HM1: This notation and the appropriate description of "Green Seas Warning" are assigned to a vessel having hull condition monitoring systems for the purpose of motion monitoring.

HM2: This notation and the appropriate description of "Hull Girder Stress" will be assigned to a vessel having a stress monitoring system. The system may include local stress and fatigue monitoring system.

HM3: This notation and the appropriate description of "Full VDM" will be assigned to a vessel having a Voyage Data Monitoring system.

However, the Specialist Committee V.2 of the International Ship and Offshore Structures Congress in 2000 cautioned that acceleration values might not be a reliable indicator of slam loads for large high-speed craft. These craft have identifiable vertical acceleration peaks, but such forces and accelerations have short duration and are in many cases only a minor part of the total forces and accelerations experienced by the vessel. Then the slamming forces have little effect on the craft's motions, and slamming can be neglected when the motions are calculated. Thus, for large high speed craft the vertical acceleration is not as relevant a parameter as for

smaller craft. Relative velocities and angles between the structural part and the water surface at the point of impact are more important parameters (ISSC V2, 2000).

For such vessels, either pressure gauges mounted at strategic points or strain gauges on critical structure are a more reliable indicator of slamming. Pressure gauges may not be accurate indicators of the possibility of damage from slam pressures because the peak pressures tend to be localized. If the peak does not occur at the pressure transducer, the effect on slamming may be underestimated, but if the peak occurs right at the transducer, the effect may be overestimated. Strain gauges placed on a plate panel will indicate the averaged effect of the slam loads, and will indicate if structural damage is being done. However, if a plate panel is significantly dished in from a slam load, subsequent slams will indicate lesser stress because of greater membrane stress on a deformed plate panel. Either a number of plate panels should be strain gauged, or gauges should be placed on stiffeners, which are more linear in their behavior, even if slightly deformed plastically.

Hull monitoring systems have been used for some time on tankers because slam pressures can cause damage at the bow but not induce sufficient ship motions for the operators to sense that particularly severe waves are being encountered. Slaughter et al. (1997) reviewed those installations, of which there were over 200 HRMS installed at that time, with at least 11 active manufacturers. Most systems measured basic hull girder response with deck-mounted strain gauges. Most manufacturers offer additional sensors and capabilities, including position (GPS), motions (accelerometers, gyros), hull hydrostatic pressure (external and in-tank), weather and motion prediction, and linkage to other ship instruments such as speed, power, and cargo loading. Typical system costs at that time were about \$50,000 for the equipment and an additional \$50,000 for installation. Four different types of instrumentation were used for measuring strain:

- Short baseline, measuring strain in material samples less than 1-inch long with foil gauges that are either bonded to the structure with epoxy or welded to the structure.
- Long baseline, typically 2 meters long, oriented along stress axis of interest, either with a linear potentiometer, linear variable differential transformer, or a linear displacement transducer.
- Derived systems in which the hull girder bending moment and stress are estimated using motion sensors.
- Developmental systems, including fiber optics, acoustic, and laser/radar ranging, all of which were considered to be proven technology but not yet commercial state of the art.

Pressure gauges were most frequently used to measure slamming pressures. Underwater gauges should be replaceable without entering drydock and should not be overly damped if slam pressure accuracy is desired. Failure of pressure sensors were the most frequent equipment failure in hull monitoring systems.

Signals from gauges to the central processing unit were either hard-wired, using grounded cable, or by radio link. Preprocessors were generally required near the sensors in hard-wired installations to reduce transmission loss, and the radio systems required transmitters near

the sensors. Several manufacturers were experimenting with fiber optic systems for transmission of data, but they were not in commercial operation.

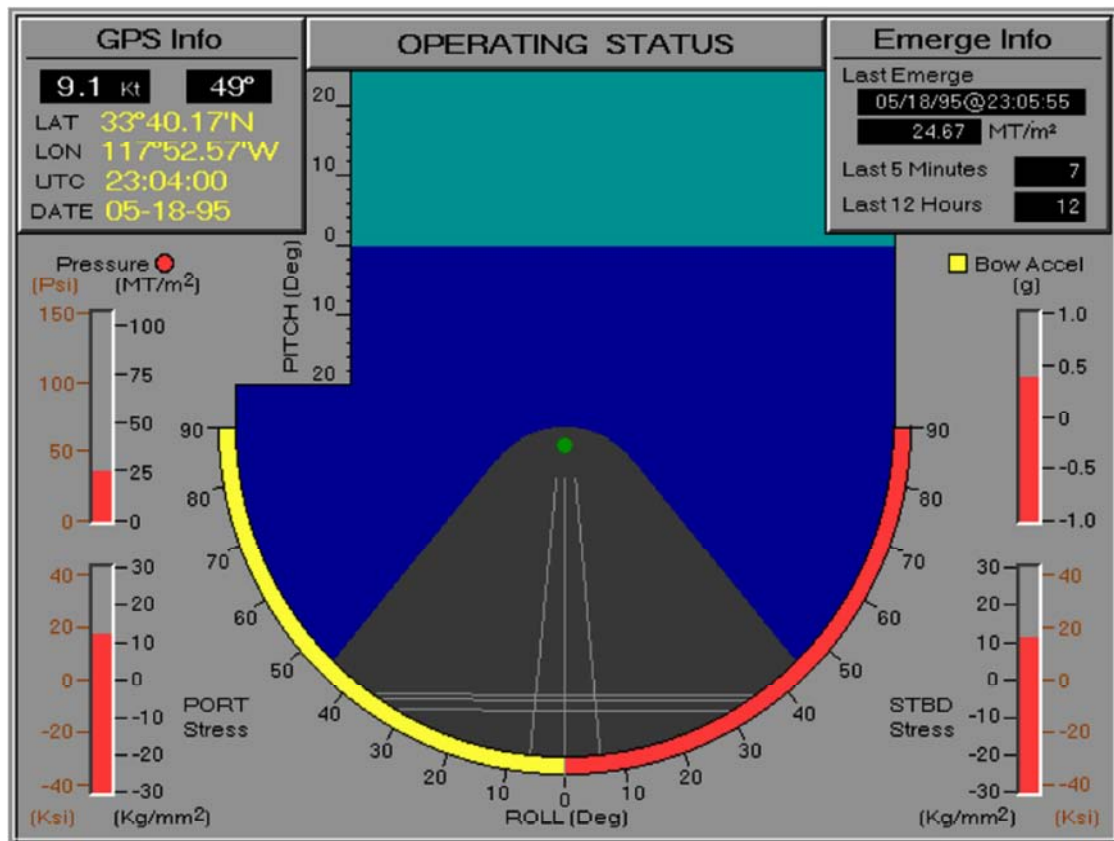


Figure 13-2 Example of the bridge display from a hull monitoring system for a tanker (Slaughter et al., 1997).

An example of the display available on the bridge for such a system is shown in Figure 13-2. This system continuously informs watch personnel of deck stresses, bow pressure and accelerations. The system sounds alarms as critical limits are approached and even shows the effectiveness of the ship's latest maneuvers. A large amount of data can be displayed on the display unit, and most systems feature several different screens that the user can select for the desired information. However, adding another display to a crowded bridge can present difficulties.

Steen and Kauczynski (2002) made a more recent review of hull monitoring systems, including various systems for measuring ship motions and for providing operational guidance to the ship's operators. A new method to measure the local stress on the ship hull is to apply fiber optic sensors (Bragg grids).

Systems are available that use ordinary ship radar for measurements of wave height. These systems measure not only the wave height but also the directional wave spectrum, determining the distribution of the wave energy as a function of the wave direction and frequency. The systems analyze reflections of the radar signals caused by waves to determine the sea condition, using the sea clutter, which is usually filtered out of the display on the radar screen. Wave height and periods of waves are determined from the modulation of the radar signals (echoes) from water surface roughness. The systems require radar having the X-band, and in addition the radar rotation speed and the applied frequencies must fulfill some requirements. In many cases it is therefore more convenient to add dedicated radar for this system.

Systems are available that measure ship motion based on a collection of high-precision accelerometers and inclinometers or gyroscopes. In combination with on-line computations performed by integrated circuitry, the system can make accurate measurement of acceleration and motion in six degrees of freedom. The motion or acceleration on any point on the ship can then be found by means of this small unit, making costly and complex cabling of accelerometers placed around the ship no longer necessary.

Measurements of the ship position and speed over ground can presently be made using global positioning satellites (GPS). Three classes of GPS systems are available:

- GPS - tolerance of the vessel location in a range of 1-20 m
- DGPS - tolerance of the vessel location in a range of 1 m
- CDGPS - tolerance of the vessel location in a range of 1 cm

Modern GPS receivers allow determination of the location and speed of ships in surge, sway and heave with a quite high accuracy. With the installation of two or more antennas on the hull, separated at a minimum distance of 3–5 m, it is also possible to determine the ship rotations in roll, pitch and yaw.

Koshio et al. (2005) provide an example of a hull monitoring system that is integrated with a ship remote monitoring system for the Japanese Super Liner Ogasawara, a 140-meter, 39-knot surface effects ship. The system includes a data communication & management system, navigation support system, and four remote monitoring systems, consisting of systems for the propulsion and lift engines, seals, and a remote monitoring system for hull structure. In the hull monitoring system, about 60 sensors are monitored on board, including accelerations, pressures and strains. Fiber optic sensors are applied to monitor the hull girder longitudinal bending strains. All monitored, time-history data are analyzed statistically on board, along with wave data, ship motions and accelerations, and the results are displayed on the screen as shown in Figure 13-3. If an emergency occurs or the monitored data exceeds designated values, the system alerts the crew and sends an alarm signal with monitored data to the central station via a satellite communication system. Cumulative fatigue damage of important members of the ship structure is calculated from monitored strains for use in structural maintenance.



Figure 13-3 Display of monitoring system of super liner Ogasawara (Koshio et al., 2005).

An alternative, less expensive system is an “off-line” system. Such a system operates with non-instrumented input, i.e. with visually estimated sea state, ship speed, and heading angle. Software based on application of the Wiener-Khinchin theorem using a wave frequency spectrum, a hull response frequency spectrum, a response function variance, and characteristic response parameters (ship motion parameters, stress in a particular location, etc.) provides output in the form of indications of limiting operational conditions or in the form of recommended changes of ship speed, heading angle, to avoid excessive slams, or excessive damage accumulation in a particular location. An off-line system is capable of providing approximate guidance, but at a far reduced cost compared to a system that requires gauging, installation, and maintenance, which may be important for relatively small craft (Petinov, 2006).

13.5 Summary

Because the magnitude of slam loads can be uncertain, structure in areas subject to such loads should be designed to withstand overloads that exceed the specified design pressures. Information on the effect of changes of course and speed on slam loads should be made available to the operators of vessels that could incur slam damage so that slamming can be reduced if it occurs. Sea conditions that would possible produce slam damage should be avoided, but routing systems need to have information as to the possibility of slamming occurring in different sea states and at different speeds and headings. Because the operator often cannot perceive the severity of a slam in terms of structural damage, instrumentation systems should be used to make operators aware of current conditions.

Aluminum Marine Structure Guide

Chapter 14

Emerging Technologies

Aluminum is being increasingly used for high-speed vessels and other high-value craft. Aluminum construction is more expensive than steel, so there are incentives to reduce cost, both through lighter weight structure and through improved fabrication methods. However, the high value of the vessels constructed means that there are generally funds available for investing in new technologies. One of these is friction stir welding, which has rapidly gone from being a laboratory curiosity to being an accepted method of production. Laser welding and electron beam welding are more mature technologies, having been around for several decades, and research is underway to apply these methods to join aluminum for marine structures.

14.1 Stir Welding

There are many processes used to join aluminum, the most commonly used being described in Chapter 5. Stir welding, which has several forms, is has had increased use in fabricating marine structures, especially friction stir welding. There are other forms of stir welding, including laser stir welding, thermal stir welding, and electrospark fusion, which are still in the research stage, but show promise for the future.

14.1.1 Friction Stir Welding

Friction stir welding is a solid state joining process developed by The Welding Institute in 1991. The process will be described in detail in the Ship Structure Committee report In-Service Performance of Aluminum Structural Details, project SR 1434, and will be only briefly described here. The process was initially investigated by a number of industries and has found great usage in the marine industry for joining lightweight panels. The process has been used for corner sections, T-sections and different lap-joint configurations, but it is most suited for butt welds. It is an essentially solid-state process in which the metal never reaches the melting temperature, and a high quality weld can generally be made with fewer weld defects, low residual stresses, absence of solidification cracking, porosity and oxidation. Because the metal never reaches the melting point, shielding gas is not necessary.

14.1.1.1 Friction Stir Welding Process. The process is shown in Figure 14-1 where the plates to be joined are clamped on a backing plate to resist the vertical, longitudinal and lateral forces, trying to lift and push them apart. A cylindrical shoulder tool with a specially designed and profiled probe, similar to that shown in Figure 14-2, made from a hard, wear resistant material relative to the material being welded, is rotated at a high speed and slowly plunged into the abutting edges of the parts to be joined.

The rotating tip of the friction stir welding tool produces the heating action in the material along the bond line and produces the required thermo-mechanical deformation. During welding, the probe first makes contact as it is plunged into the joint region. This initial plunging friction heats a cylindrical column of metal underneath the probe: the material softens and plasticizes without reaching the melting point and allows traversing of the tool along the welding line. The depth of penetration is controlled by the length of the probe below the shoulder of the

tool. The contacting shoulder applies additional frictional heat to the weld region and prevents the highly plasticized material from being expelled during the welding operation. Once the shoulder makes contact the adjacent thermally softened region takes up a frustum shape corresponding to that of the overall tool geometry.

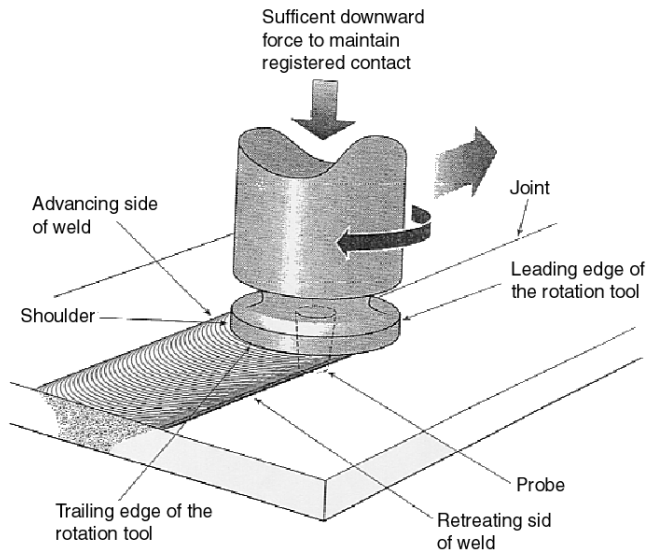


Figure 14-1 Schematic illustration of friction stir welding (TWT).

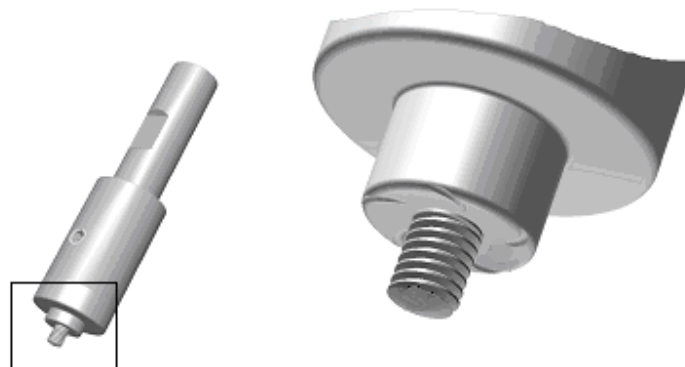


Figure 14-2 Tip of the friction stir welding tool (TWT).

The design of the rotating tip varies with the thickness and composition of the parts being joined, and various tip designs are proprietary to different organizations conducting friction stir welding. Other variables of the process include rotational speed, speed of advancement, downward force of the tool, and fixturing for holding the parts.

The process produces a solid-state weld without addition of a filler wire. Therefore, the parts to be joined must have a minimum gap between them because as the metal reforms and consolidates as the tool moves on; any difference in the volume is compensated for by a reduction in thickness. If the gap is uneven, the thickness of the resulting weld will also be uneven. Because there is a reduction in thickness, some designers have special extrusions made

that have slightly increased thickness at the edges to be joined so that the resulting weld is the same thickness as the base plate.

Friction stir welds are not symmetric about the weld centerline due to the tool rotation. The side of the weld on which the rotational velocity of the tool has the same direction as the welding velocity is called the advancing side of the weld; the side of the weld on which the two velocities have opposite direction is the retreating side of the weld. Notice a slight buildup on the advancing side in the section through a weld shown in Figure 14-3. This flush is not always present, but is generally removed by grinding or machining to maintain a smooth surface.

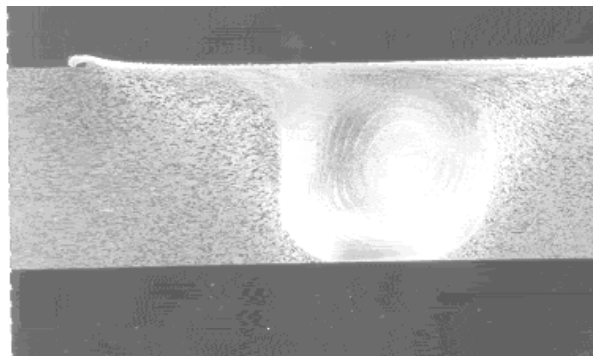


Figure 14-3 Section through friction stir weld (Advanced Joining Technologies web site).

The profile of completed welds showing the characteristic cycloidal pattern of ripples that are produced by the final sweep of the trailing circumferential edge of the shoulder is shown in Figure 14-4.

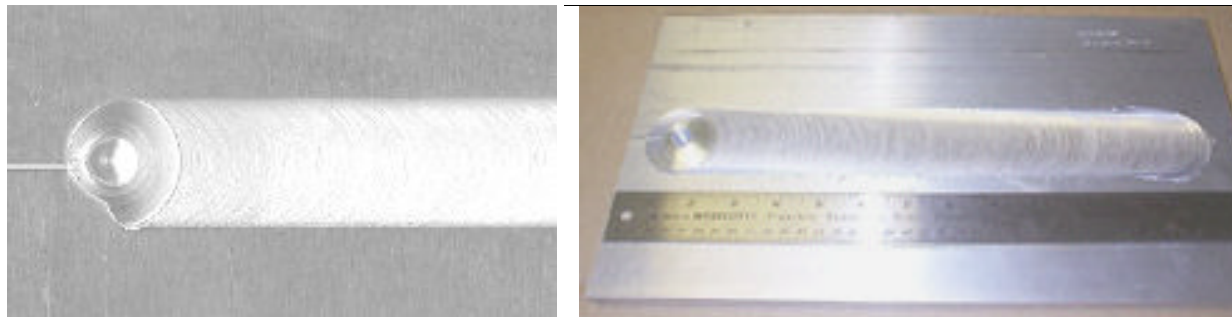


Figure 14-4 Completed friction stir welds.

14.1.1.2 Facilities for Friction Stir Welding. Typical facilities for joining extrusions to form a panel are shown in Figure 14-5. A flat table holds the completed portion of the panel in place while the sections being joined are clamped and the moving friction stir welding head moves over the joint. Tables such as this are available for making welds as long as 15 meters (50 feet) (Halverson and Hinrichs, 2006). For shorter welds, a milling machine can be used.

Koshio et al. (2005) provide an example of friction stir welding at the Tamano works of Mitsui Engineering and Shipbuilding Company in Japan. Friction stir welding was used for low distortion welding of aluminum hull structure, including the very thin plates of the

superstructure. Extruded panels of A6N01S-T5 alloy were joined using the process, as were some plates of A5083-H32 alloy. The facilities in the shipyard are shown in Figure 14-6, and the fabricated panels are shown in Figure 14-7.

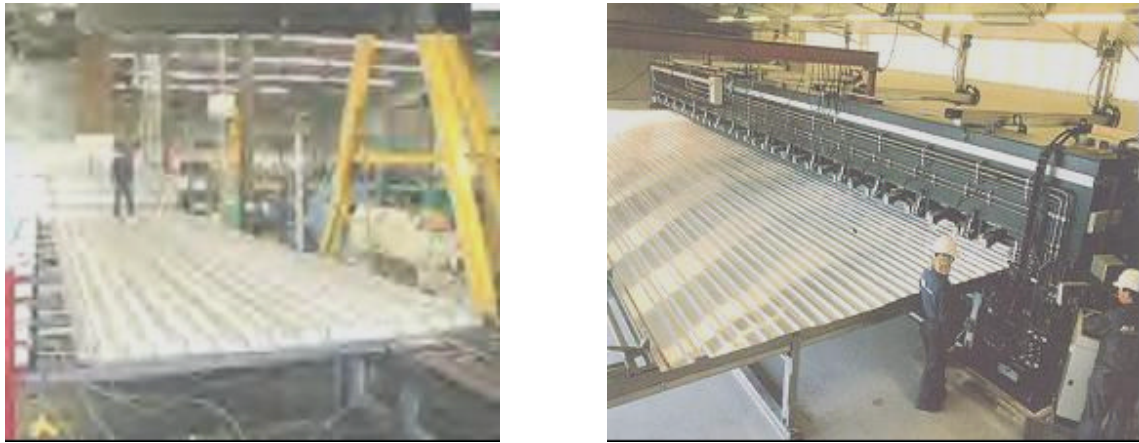


Figure 14-5 Friction stir welding panels together (Advanced Joining Technologies web site and The Welding Institute).



Figure 14-6 Friction stir welding facilities at the Tamano works of Mitsui Engineering and Shipbuilding Company (Koshio et al., 2005).

14.1.1.3 Advantages of Friction Stir Welding. Friction stir welding takes place in the solid phase, below the melting point of the material to be joined. This permits joining similar and dissimilar aluminium (e.g. 2xxx-series to 7xxx-series) alloys and in some cases dissimilar metals, using highly specialized techniques for forming such things as bimetallic transition joints. The principal advantage for lightweight aluminium construction is the low distortion that results from the process. No shielding gas is required during the process. Although a flash as mentioned above can form, there are no fumes, sparks, or spatter to clean up. As long as the root gaps in the joints are consistent, a consistent quality weld will be made.



Figure 14-7 Panels fabricated using friction stir welding at the Tamano works of Mitsui Engineering and Shipbuilding Company (Koshio et al., 2005).

The American Welding Society has developed inspection requirements (Halverson and Hinrichs, 2006). Each friction stir welding procedure specification must be documented in accordance with the latest AWS ANSI/AWS D1.2-XX Structural Welding code — Aluminum. Procedure qualification records for each welding procedure must be recorded as well. The American Bureau of Shipping is one of the certifying agencies. A typical production quality-sampling plan might call for ultrasonic, radiographic, or dye penetrant inspection of the weld root. In a recent ship design reported by Halverson and Hinrichs, initial sampling was done of a test specimen that was removed from the end of a weld on every third panel. As the process became stable, the frequency was reduced to every fifth panel welded. The test specimen provided for a joint tensile and a root bend test with the specimen containing the friction stir welding tool hole at end of the weld being discarded.

One of the main limitations of the friction stir welding process are at present is the need for heavy equipment to provide the high axial and transverse loads applied and for stable backing and clamping elements with a high degree of stiffness. This gives limited flexibility compared to fusion welding processes, so the process is too complex for shipboard production or repair welds. The process leaves a hole at the end of each weld, and in some cases, produces discrepant weld quality at the start and termination ends of the welds. The termination hole can be dealt with by use of a retractable pin, locating it in a structurally benign area of assemblies, use of run-off tabs, or repair with a conventional arc welding process. The discrepant portions of the welds typically are cut off the weldments. Typical welding speeds are about 750mm/min for welding 5mm thick 6000 series aluminum alloy on commercially available machines, which is slower than welding using GMAW.

14.1.1.4 Materials and Thickness. Friction stir welding can be used for joining all aluminum alloys, including those that cannot normally be joined by conventional fusion techniques. A major group sponsored project undertaken by The Welding Institute demonstrated that the aluminum alloys of the 2xxx, 5xxx, 6xxx, 7xxx, and 8xxx-series could be successfully welded to yield reproducible, high integrity welds within defined parametric tolerances:

Single pass butt joints with aluminum alloys have been made in thicknesses ranging from 1.2 to 50 mm without the need for edge preparation. Parameters for butt welding of most

aluminum alloys have been optimised in a thickness range from 1.6 to 10 mm. Special lap joining tools have been developed for aluminum with thicknesses of 1.2 - 6.4 mm. Thicknesses of up to 100 mm in 6082 alloy can be welded using two passes.

Kimapong and Watanabe (2004) successfully used friction stir welding to join 2-mm 5083 plate to mild steel of the same thickness. In the process, shown in Figure 14-8, the 2-mm diameter pin of the friction stir welding head is offset 0.2 mm from the edge of the steel plate, so that it rotates entirely within the aluminum. The best welds were made with a rotational speed of 250 rpm, a 25 mm/min welding speed with the maximum tensile strength of about 240 MPa, compared to the 276 MPa tensile strength of GMAW welds in 5083 (AWS, 2004). This strength may be sufficient for this type of a weld to replace the bimetallic joint currently used between steel and aluminum. The joint will present a smooth surface and will therefore be sightlier and will be easier to maintain and present a lower radar cross section.

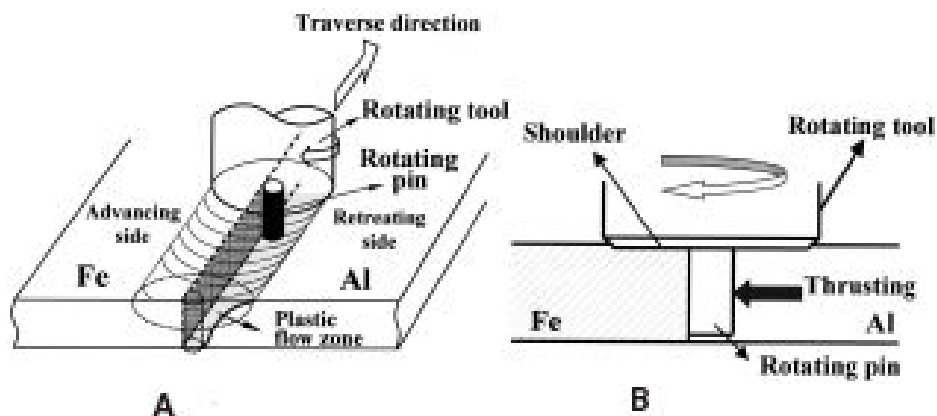


Figure 14-8 Friction stir welding aluminum to steel (Kimapong and Watanabe, 2004).

A section through the completed weld is shown in Figure 14-9. Judging from the SEM photograph and EDS analysis, no intermetallic compounds were observed at the central and bottom regions of the interface between Fe and Al. However, the EDS line analysis of Fe and Al suggests that intermetallic compounds of are FeAl and FeAl₃ were formed at the upper region of the interface.

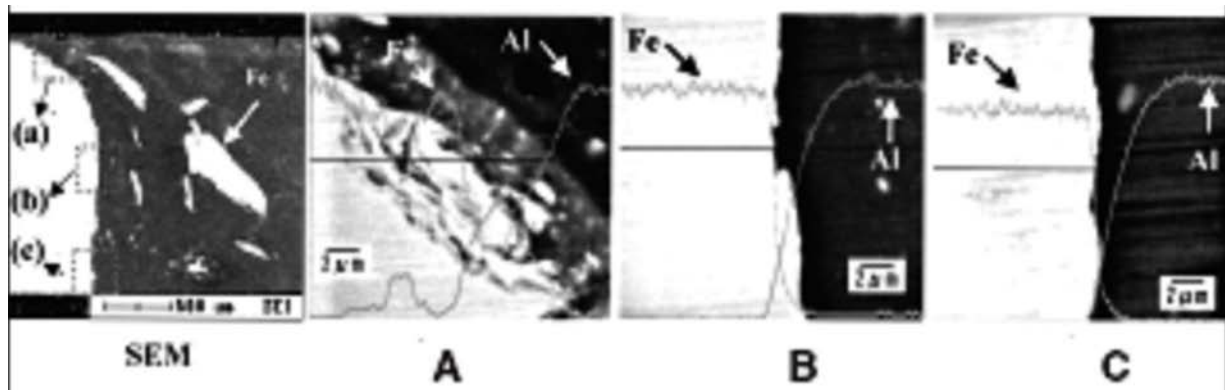


Figure 14-9 Scanning electron microscope image and EDS line analysis of friction stir welding joint between aluminum and steel. A — upper position; B — middle position; C — bottom position. (Kimapong and Watanabe, 2004).

Figure 14-10 shows an optical micrograph of a cross-section of a fractured tensile specimen near the Fe/Al interface. This photograph shows that the fracture occurred along the interface between the Fe fragments and the Al matrix and that the incipient cracking (indicated by an arrow in the photograph) occurred at the interface between the Fe fragment and the Al matrix. This suggests that cracking and fracture tend to occur at the interface between the Fe fragment and Al matrix.

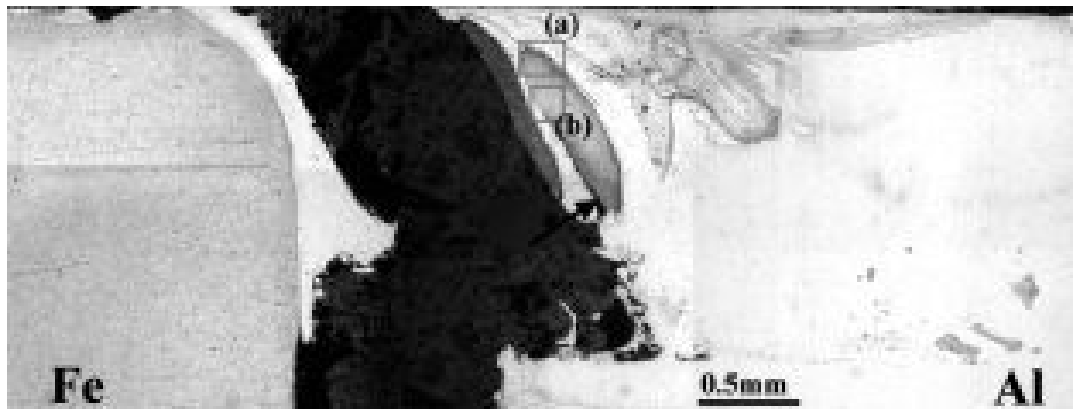


Figure 14-10 Cross-sectional view aluminum to steel friction stir welded joint after tension test. Fracture occurred along the interface between the steel fragment and the aluminum matrix. (Kimapong and Watanabe, 2004).

14.1.1.5 Joint Design. A number of different joint geometries, such as those shown in Figure 14-11, are possible with friction stir welding (Halverson and Hinrichs, 2006).

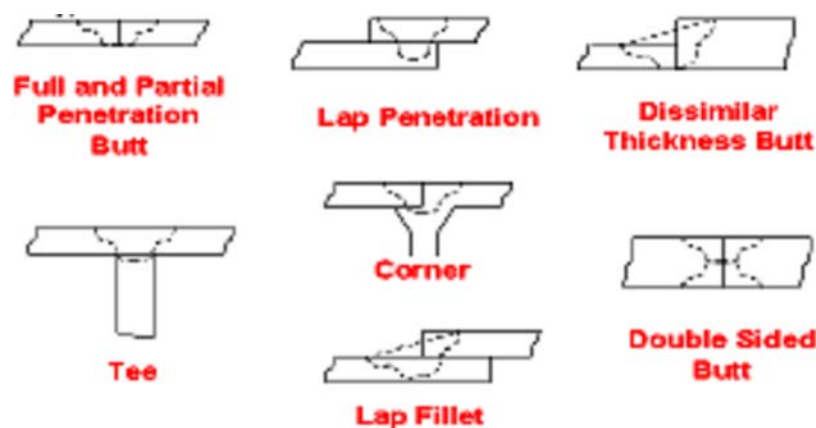


Figure 14-11 Friction stir weld joint geometries (Halverson and Hinrichs, 2006).

An example of lap joints is in a study by Cederqvist and Reynolds (2001) in which sheets of 2.29 mm Alclad 2024-T3 and bare 7075-T6 sheet were joined in lap welds that had an overlap of 50.8 mm. Joint efficiencies of 86 percent were reported, similar to the efficiencies of friction stir butt welds in the same materials.

In some cases, friction stir welding has been found to be a more economical method of producing wide plates. There is a greater cost per pound of the widest plates, which can be rolled up to 210 inches wide. Narrower plates can be joined using friction stir welding for a net cost savings.

14.1.1.6 Strength of Friction Stir Welded Joints. Typical tensile properties of friction stir welded 5xxx, 6xxx and 7xxx series alloys are given in Table 14-1. The data comes from studies conducted by Dawes and Thomas (1995), Backlund et al. (1998), and Midling et al. (1998). For the 5083-0, the strength of the friction stir weld is the same as the base metal because the alloy is essentially annealed. For the stronger 5083-H321 alloy, the yield strength of 153 MPa is 61 percent of the strength of the base metal but comparable to the 159 MPa yield strength of GMAW in the same material (AWS, 2004).

Fatigue tests on friction stir welds made from 6 mm thick 5083-0 and 2014-T6 have been conducted by Dawes and Thomas (1995). The fatigue performance of friction stir butt welds in alloy 5083-0 was comparable to that of the parent material when tested using a stress ratio of $R=0.1$. Analysis of the available fatigue data has shown that the performance of friction stir welds is comparable with that of fusion welds, and in most cases substantially better. Data on the fatigue strength of alloy 6082 were compiled for Ship Structure Committee project SR 1434, In-Service Performance of Aluminum Structural Details and are presented in Figure 14-12. The data are compared to the European Standard S-N curves for butt welds in aluminum, and as can be seen, the friction stir welds all exceed the standard.

Table 14-1 Typical Mechanical Properties of Friction Stir Welded Aluminum Specimens

Material	0.2% Proof strength Mpa	Tensile strength Mpa	Elongation %	Welding factor UTS _{FSW} /UTS _{PARENT}
5083-0 Parent	148	298	23,5	N/A
5083-0 FSWed	141	298	23	(1.00)
5083-H321 Parent	249	336	16,5	N/A
5083-H321FSWed	153	305	22,5	0.91
6082-T6 Parent	286	301	10,4	N/A
6082-T6 FSWed	160	254	4,85	0.83
6082-T6 FSWed and aged	274	300	6,4	(1.00)
6082-T4 Parent	149	260	22,9	N/A
6082-T4 FSWed	138	244	18,8	(0.93)
6082-T4 FSWed and aged	285	310	9,9	(1.19)
7108-T79 Parent	295	370	14	N/A
7108-T79 FSWed	210	320	12	(0.86)
7108-T79 FSWed naturally aged	245	350	11	(0.95)

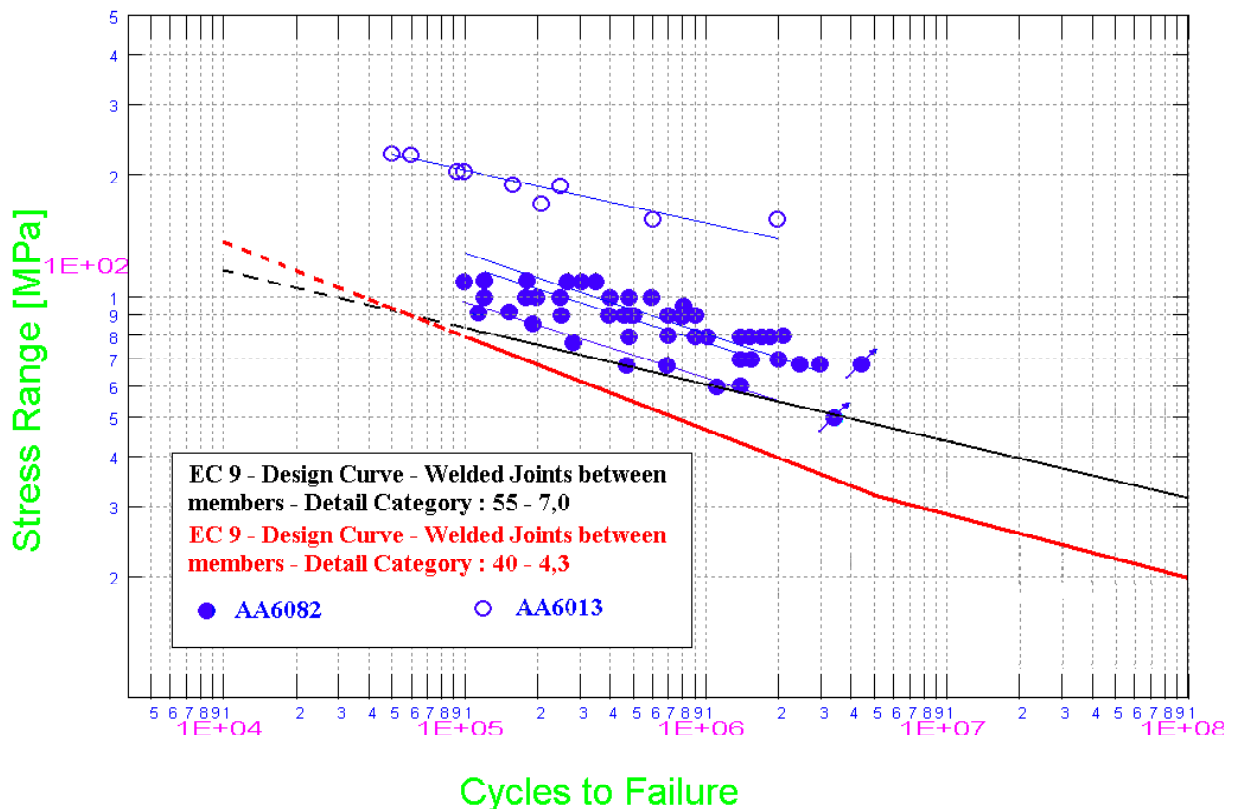


Figure 14-12 Transverse friction stir welds on aluminum alloys 6013 and 6082 compared with EC-9 curves.

The Ship Structure Committee will study the effects of the reduced residual stresses and distortions on the buckling strength of aluminum panels in project SR-1454, Buckling Collapse Testing on Friction Stir Welded Aluminum Stiffened Plate Structures. The objective of the study

is to develop a mechanical buckling collapse test database on full-scale prototypes of 5xxx-series aluminum stiffened plate structures fabricated by friction stir welding.

14.1.2 Laser Stir Welding

Laser stir welding is a developing technology that combines the energy of a laser beam with the oscillating motion of the beam to stir the molten pool. Alcoa, Inc. and Pennsylvania State University have developed this process, and the two organizations have patented the process. The following material is taken from information furnished by Alcoa and from a published report by two of the developers (Martukanitz and Tressler, 2006).

Laser beam welding a fusion joining process that employs concentrated laser beams to melt the parts together. The welding is achieved upon solidification of the fused weld-regions. The process is commonly used to join lap-penetration, square- butt, edge- butt and tee- fillet type joints. The process is illustrated in Figure 14-13 and Figure 14-14.

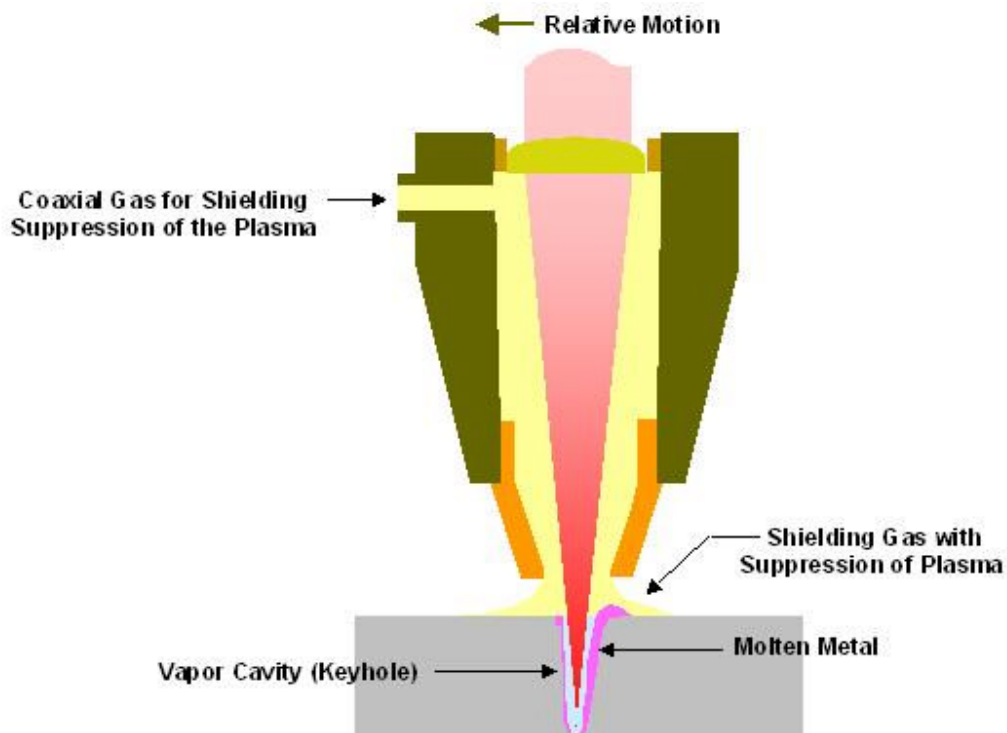


Figure 14-13 Laser beam welding process (Alcoa, Inc.)

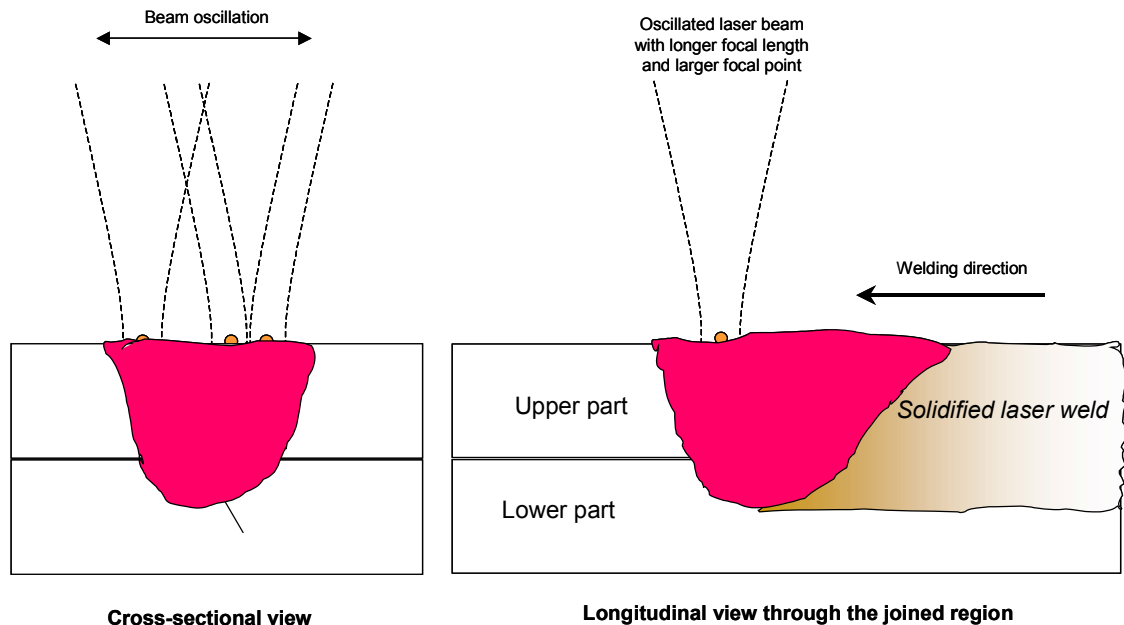


Figure 14-14 Laser beam welding of a lap-penetration joint with the conduction mode.
Note: due to limited optical coupling and reflectivity of the beam, this mode is problematic for welding aluminum. (Alcoa, Inc.)

Unlike the conventional laser beam process, which is based on welding with a keyhole that moves into and melts the solid parts ahead of it, laser stir welding establishes a molten pool and moves the keyhole in it while continuously re-filling the pool with the adjoining molten metal. The welding is accomplished by translating a self-healing keyhole through a molten pool. This process is illustrated in Figure 14-15, and the apparatus for performing the welds shown in Figure 14-16.

The process manipulates the laser beam in a circular pattern that provides a stirring action, resulting in improved weld soundness for laser beam welding of aluminum alloys, which has been verified through high-speed imaging of the weld pool. Implementation of this technique using rotating transmissive optics is relatively straightforward and offers the potential for scaling of powers up to 10 kW.

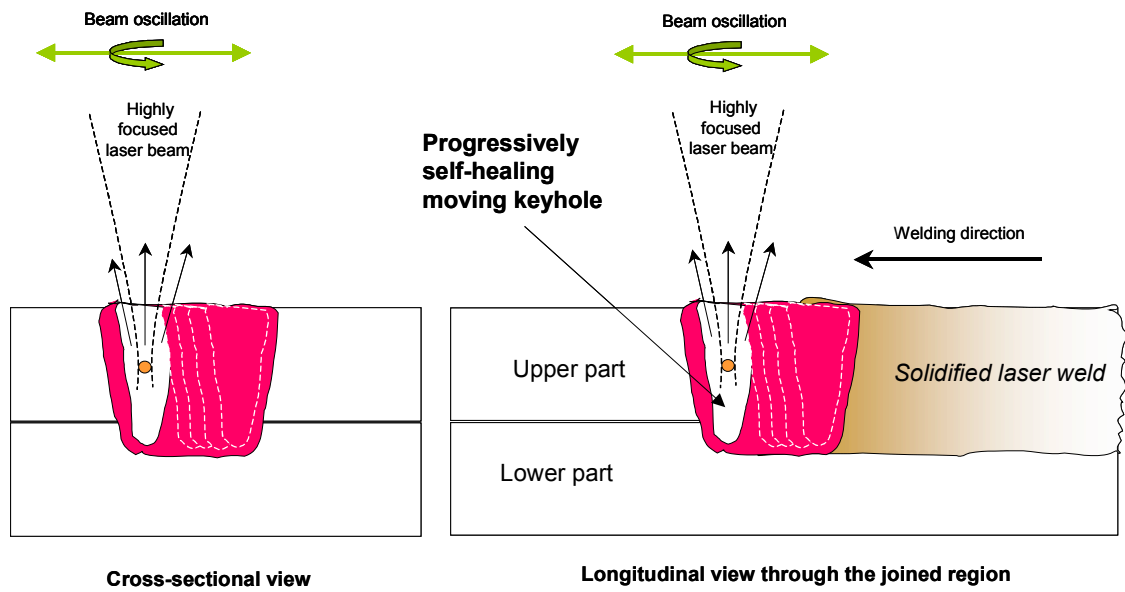


Figure 14-15 Concept for simultaneously welding with the laser beam process in the keyhole and conduction modes by translating a self-healing keyhole through the molten pool (Israel Stol & R. P. Martukanitz, Alcoa, Inc.).



Figure 14-16 Experimental apparatus for laser stir welding (Martukanitz and Tressler, 2006).

The initial investigations of laser stir welding involved aluminum alloy 6013-T4 having a thickness of 3.0 mm. Laser beam welds were produced using a TRUMPF 4.5kW diode-pumped Nd:YAG laser with fiber optic beam delivery through a 600 μ m diameter fiber. Various weld configurations were evaluated for the 6013-T4 alloy and included butt, lap, and fillet welds, using filler alloy 4047. A rotating transmissive optical system supplied by Laser Mechanisms Inc. (Farmington Hills, MI) was integrated into the laser welding cell. The rotating optics was utilized during laser stir welding to manipulate the beam in a circular motion, and involves the addition of two process parameters, circle size and rotational velocity. The optical system was moved along the part using a linear positioning system. During this investigation, for the purpose of comparison, welds were also produced using the conventional laser beam welding technique, deactivating the rotating optics to produce a stationary beam for conventional laser beam welding.

The results of the process are shown in Figure 14-17, Figure 14- 19, Figure 14-21 for a laser stir lap weld, laser stir lap fillet weld, and a laser stir fillet weld. Comparable welds performed by the laser beam process are shown in Figure 14-18, Figure 14-20, and Figure 14-22.

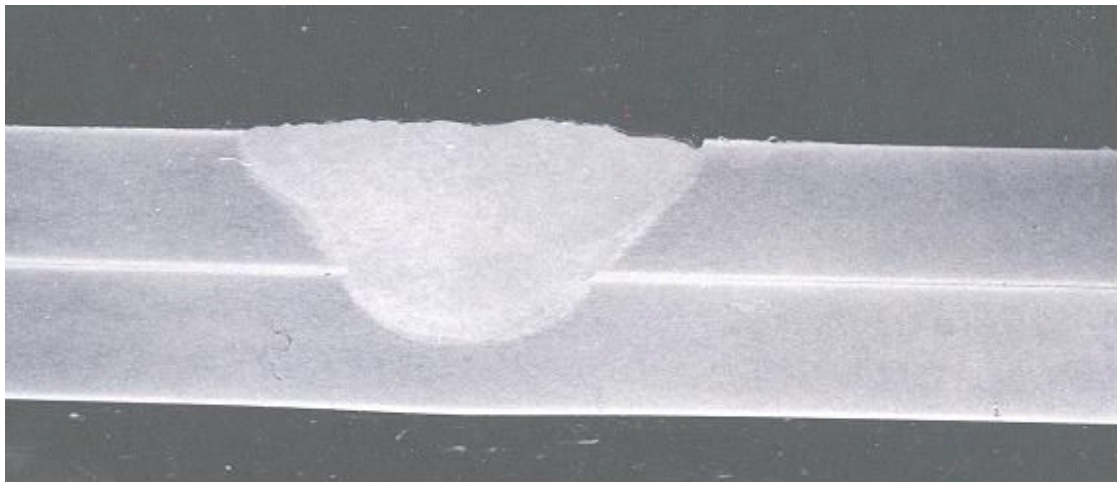


Figure 14-17 Laser stir lap weld (Alcoa, Inc.).

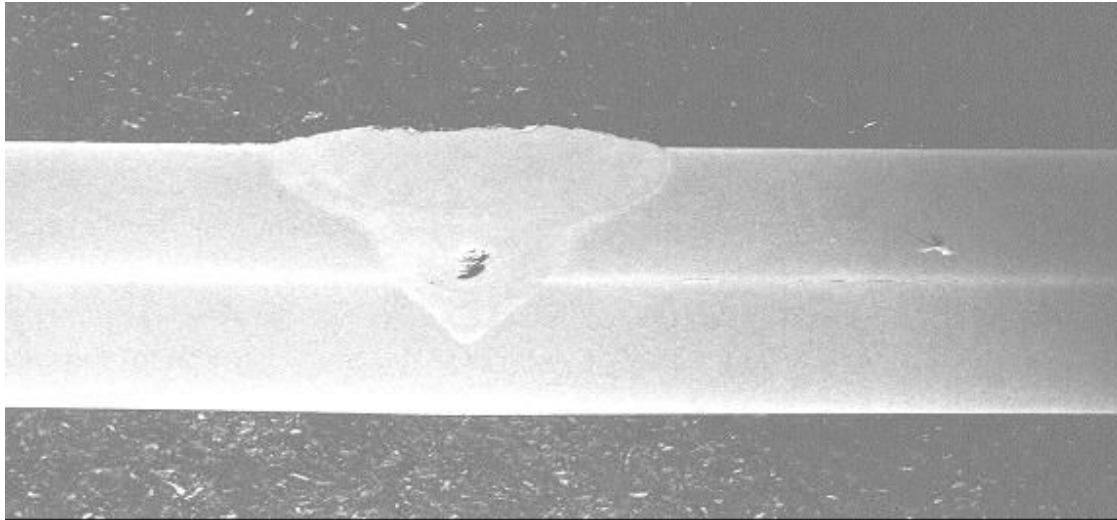


Figure 14-18 Laser beam lap weld (Alcoa, Inc.).

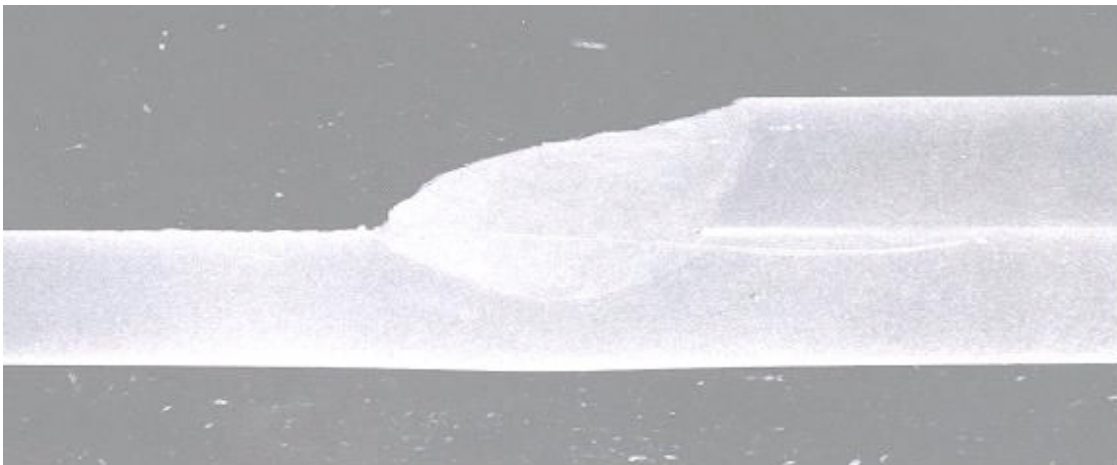


Figure 14- 19 Laser stir lap fillet weld (Alcoa).



Figure 14-20 Laser beam lap fillet weld, which is impractical to control in production (Alcoa, Inc.).

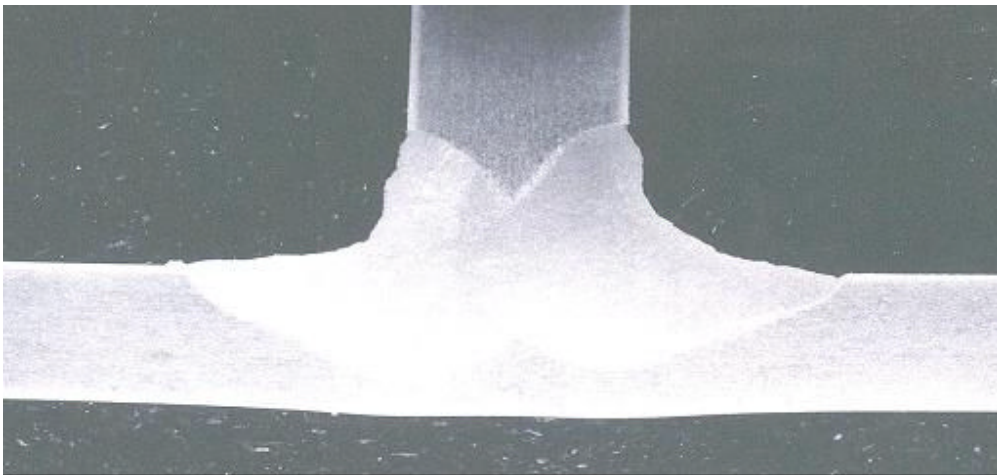


Figure 14-21 Laser stir fillet weld (Alcoa, Inc.).

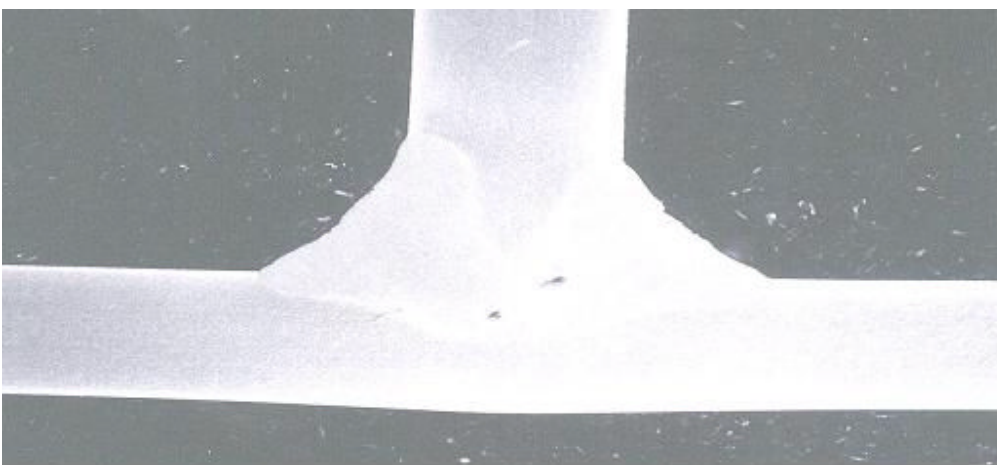


Figure 14-22 Laser beam fillet weld (Alcoa, Inc.).

The results of initial fatigue testing of laser stir welds between 6013-T4 and 6061-T6 plate 3 mm (0.118 in. thick is shown in Figure 14-23. The fatigue strengths of the laser stir welds are significantly greater than the fatigue strengths of the laser beam welds.

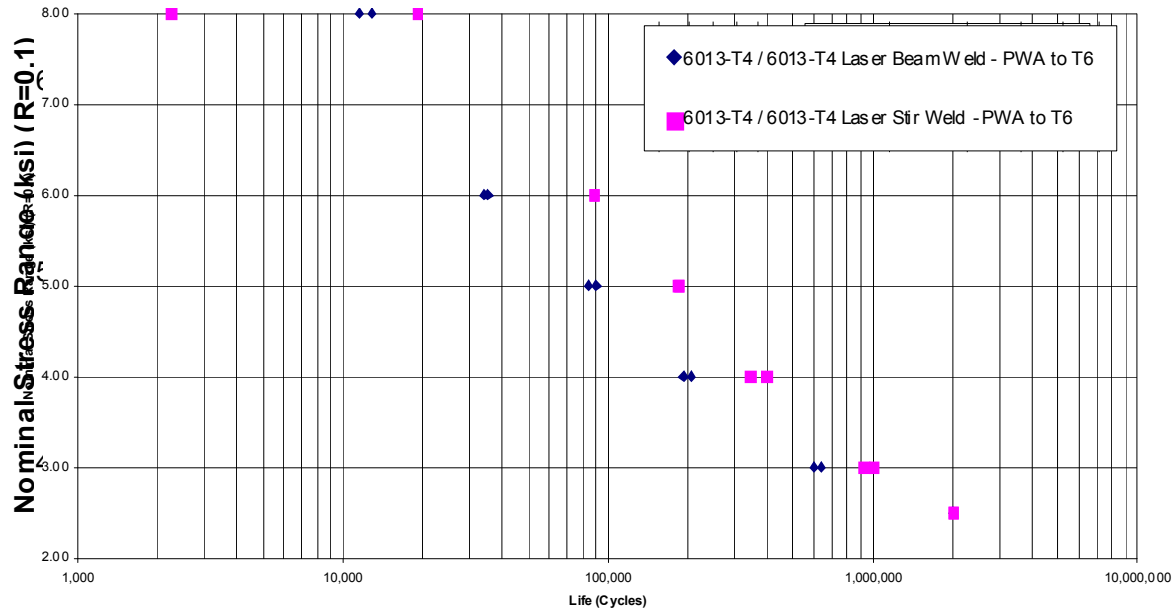


Figure 14-23 Fatigue testing of laser stir welded and laser welded lap penetration joints between 0.118 in. (3 mm) thick 6013-T4 Sheet PWA to T6 (Alcoa, Inc.).

Some of the advantages cited for the laser stir welding process include:

1. Capability to weld lap fillet joints, which is presently very difficult with conventional laser beam welding
2. Capability to weld lap-penetration, square butt, single and double fillet tee joints.
3. Capability to weld lap penetration joints with interfacial widths that are equal or wider than the thinnest part of a stack-up, which is nearly impossible to achieve with thicker stack-ups (e.g. 1mm-4.5mm) using the conventional Laser Beam process.
4. Lap-penetration joints with improved fatigue performance and strength, due to wider interfacial weld widths.
5. Sounder welds with reduced porosity and more consistent quality.
6. Improved control over and extra forgiveness to placement of filler-wire to the welding region (keyhole).
7. Improved control over the weld geometry and weld convexity at the back sides of fully penetrated
8. Capability to deposit single and lap fillet welds with nearly perfect triangle shaped cross-sections and without undercuts, which afford significant reduction in the stress-rising geometry associated with convex welds deposited with the conventional Laser Beam welding process and subjected to fatigue type cyclic loading.
9. Near total elimination of uncontrolled localized “expulsions” of molten metal from the weld region (keyhole), which commonly occurs when welding certain alloys with the conventional Laser Beam welding process. These can lead to gross variations in

- the geometry (e.g. weld skips, open craters, excessive weld spatter and quality (e.g. missed welds, open and bulk voids) of the weld deposits.
10. Significant increase in welding speeds of travel when welding thin (e.g. 1mm) and highly reflective (e.g. 3003) parts.
 11. Increased tolerance to variations in joint gap and placement of the laser beam and filler wire.
 12. Capability to weld a broader range of part thickness (e.g. 1-mm to 5-mm).
 13. Can be readily adapted and used with standard YAG, CO₂ and fiber optics type lasers, thus affording maximized system percentage use of these systems by switching between the laser welding modes (i.e. conventional versus laser stir welding) at different stations.

Possible applications of the process as envisioned by the developers are illustrated in Figure 14-24. Note that the developers have not demonstrated the possibility of using laser stir welding to perform butt joints, for which the friction stir welding process has been applied extensively in the marine industry. The laser stir welding process could conceivably reduce the amount of expensive equipment and fixturing needed for friction stir welding and even result in a process that could be used to perform laser stir welding on the ways, and not just in a specialized shop.

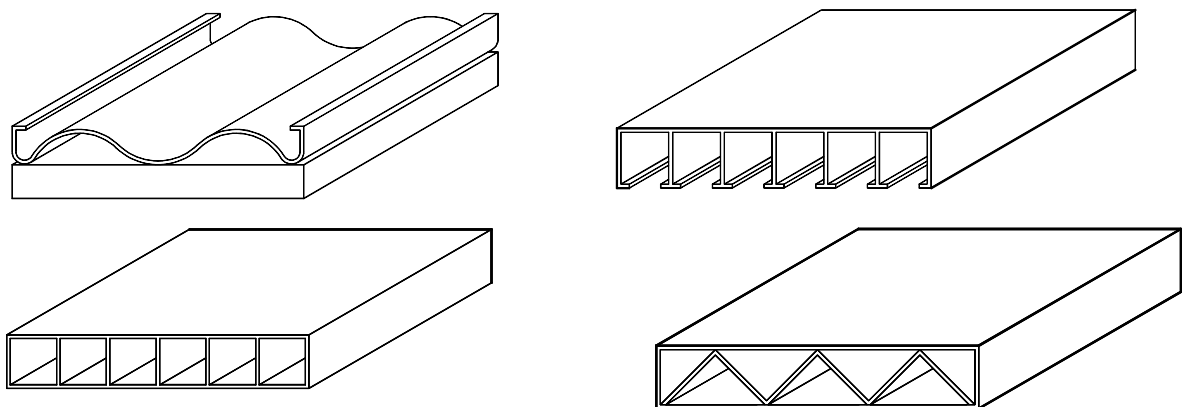


Figure 14-24 Possible applications of laser stir welding (Alcoa, Inc.).

14.1.3 Thermal Stir Welding

National Aeronautics and Space Administration's Marshall Space Flight Center is developing a joining technology called thermal stir welding that improves upon fusion welding and friction stir welding (www.nasasolutions.com). Thermal stir welding is capable of joining dissimilar materials at high welding speeds. In the process, heating and stirring functions are independent of each other, providing more degrees of freedom for process control and optimization. Having a separate heating function makes it easier to weld alloys with higher melting temperatures, such as steel and Inconel alloys. Thermal stir welding has many similarities and attributes typical of friction stir and fusion welding processes. It enables the

joining of dissimilar metals with keyhole closeout and elimination of the backing anvil requirement of friction stir welding.

The thermal stir process separates the characteristic heating and matrix transformation processes of the friction stir welding process using a fusion welding apparatus (laser, plasma torch, etc.) to initially melt the material. It may also use a solid state heating process such as induction resistance heating. If a fusion heating apparatus is employed to heat the material, a separate grinding/extrusion feature recrystallizes the resulting dendritic matrix structure as it transforms from the melted temperature state through the plastic temperature state. The apparatus used for the weld process is enclosed in a main housing, which allows for the possibility of an inert environment in the melting compartment if needed.

14.1.4 Electrospark Fusion

The Rolls-Royce Company has developed and patented a process called electrospark fusion. The following information is taken from the U.S. patent for the process. An electrospark alloying apparatus includes a main body member; a collet coupled to the main body member, and a heat sink adjacent the collet. The collet is adapted to receive and hold a consumable electrode. The apparatus can also include a drive for rotating the electrode. Further, the apparatus can include an inert gas supply and a discharge opening in the main body member for facilitating lamellar gas flow of inert gas from the inert gas supply around the electrode. A method of electrospark alloying includes electrospark alloying a workpiece with a consumable electrode and cooling the electrode during the electrospark welding. The present invention relates generally to a method and apparatus for electrospark alloying. More particularly, in one embodiment of the present invention, the electrospark alloying defines a micro-welding process for depositing a portion of the rotating electrode onto the work piece to form a fully dense metallurgical bond there between. Although the invention was developed for the repair of metallic gas turbine engine components, certain applications may be outside of this field.

Electrospark alloying refers to a micro-welding process that uses a short duration electrical pulse to melt and deposit a portion of a consumable metallic electrode onto a metallic base material. The deposited material alloys with the base material to form a metallurgical bond. The short duration of the electrical pulse allows for the extremely rapid solidification of the deposited material and results in a fine-grained homogeneous weld deposit. In an electrospark alloying process, the electrode and the work piece are conductive and form the terminal points of a direct current power source. When a surge of energy is applied to the electrode, a spark is generated between the electrode and the work piece. A portion of the metal electrode is melted due to the high temperature of the spark, which is then transferred from the electrode to the substrate surface by short circuit transfer.

Reynolds et al., 2003) provide additional information on the electrospark deposition process. The basic equipment for the process is shown schematically in Figure 14-25. A direct current power source is connected to the electrode holder, which consists of an inner metallic lining to provide mechanical stability and an outer nonconductive material. The electrode holder may also provide shielding gas. The moving electrode deposits small amounts of material when a momentary short circuit is created and then broken away by the movement of the electrode, which is generally circular. The process has low deposition rates, with deposits limited to about

250 μm thick at rates of about one gram per hour, and so has been used mostly for the refurbishment of small parts or for depositing material of different properties on the substrate. The process has very little heat input to the substrate and dilutes the substrate by a very small amount, permitting dissimilar metals to be deposited. The process has the potential for deposition of various metals on aluminum, especially for localized wear resistance, although such use has not been demonstrated to date.

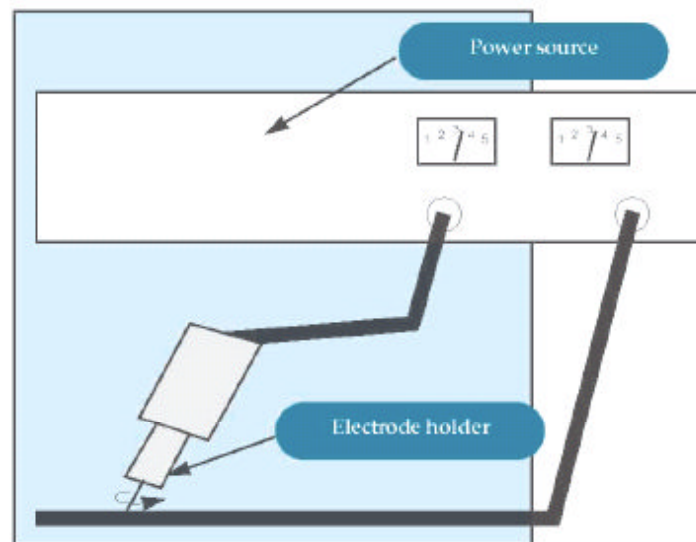


Figure 14-25 Electrospark welding apparatus (Reynolds et al., 2003).

14.2 Laser Welding

Although friction stir welding has found a useful niche in the fabrication of lightweight aluminum panels, it is limited in usefulness for other portions of the structure because of the equipment involved. Welding with a high-energy laser has the potential for greater flexibility and greater use. After the development of the laser in the late 1950s, the laser welding process was developed as a use of this new technology, and The Laser Institute of America was started in 1968 to promote the process. The following summary of the laser welding process was obtained from Wikipedia, the free encyclopedia (www.wikipedia.com) and in turn is based on Cary and Helzer (2005) and on Weman (2003).

The two types of lasers commonly used in metalworking are solid-state lasers and gas lasers (especially carbon dioxide lasers). The first uses one of several solid media, including synthetic ruby and chromium in aluminum oxide, neodymium in glass (Nd:glass), and the most common type, crystal composed of yttrium, aluminum, and garnet doped with neodymium (Nd:YAG). Gas lasers use mixtures of gases such as helium, nitrogen, and carbon dioxide as a medium.

Solid-state lasers operate at wavelengths on the order of 1 micrometer, much shorter than gas lasers, and as a result require that operators wear special eyewear to prevent cornea damage. Nd:YAG lasers can operate in both pulsed and continuous mode, but the other types are limited to pulsed mode. All use a single crystal shaped as a rod approximately 20 mm in diameter and

200 mm long, and the ends are ground flat. This rod is surrounded by a flash tube containing xenon or krypton. When flashed, the laser emits a pulse of light lasting about two milliseconds. Typical power output for ruby lasers is 10–20 W, while the Nd:YAG laser outputs between 0.04–600 W. To deliver the laser beam to the weld area, fiber optics are usually employed.

Gas lasers use high-voltage, low-current power sources to supply the energy needed to excite the gas mixture used as a lasing medium. These lasers can operate in both continuous and pulsed mode, and the wavelength of the laser beam is 10.6 μm . As a result of the higher wavelength, a lens and mirror delivery system is used. Power outputs for gas lasers can be much higher than solid-state lasers, reaching 25 kW.

Because Nd:YAG lasers can deliver the beam through a fiber optic cable, they have the potential for a great deal of flexibility in their use. The fiber optic cables can be 100 meters long, bringing the laser beam to the workpiece. The process can include shielding gas as well as filler wire. Welding of 2024/5052/6061 aluminum is reported to require filler metal of 4047 aluminum to make hermetic, crack-free welds (Miller, 2005).

Pastor et al. (1999) made a study of laser welding on 5182 and 5754 alloys for automotive applications. Previous studies had shown that porosity, loss of alloying elements and, for some heat treatable aluminum alloys, solidification cracking occurred during laser welding of aluminum alloys. Part of the difficulty came from the poor coupling between aluminum alloys and the laser beam. Aluminum alloys absorb the laser more efficiently as the laser wavelength decreases. For this study, a Nd:YAG laser with a characteristic wavelength of 1.06 μm was used because other studies showed that it had provided better coupling with aluminum than the CO₂ laser, which has a characteristic wavelength of 10.6 μm .

In the study, bead-on-plate autogenous welds (no filler metal) were produced using a 3.0-kW continuous-wave Nd:YAG laser on thin sheets of 5182 and 5754 aluminum alloys with thicknesses of 1.0 mm and 1.45 mm, respectively. Both alloys were in the annealed condition prior to welding. A schematic of the setup is shown in Figure 14-26.

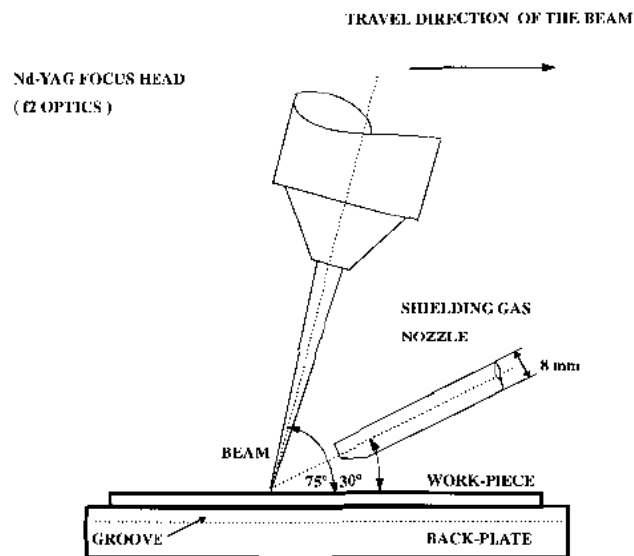


Figure 14-26 Laser welding schematic (Pastor et al. 1999).

The beam was delivered using a 600- μm diameter fiber of fused silica to an f2 focus optics manipulated through a micropositioning stage mounted on a linear translation device. The focal length of the f2 optics for Nd:YAG laser is 77.7 mm. The beam radius at the focal point is 300 μm . The beam was provided at a 75-deg forward angle relative to the workpiece to prevent damage to the optics due to back reflection. An ancillary copper nozzle having an 8.0-mm inside diameter was used to provide shielding gas. This gas nozzle was directed opposite to the direction of travel at an angle of 30 deg with the workpiece. During welding, the aluminum sheets were placed horizontally on a copper back plate. The back plate had a U-shaped groove of 2.0-mm width and 1.5-mm depth under the weld region. Therefore, the liquid metal was not supported by the back plate. Helium was used as the shielding gas. Because of its high thermal conductivity, helium can easily conduct heat away from the plasma plume and keep the plasma volume small.

The study found that the laser beam had to be focused within a range of 1.5 mm to prevent porosity from forming in the weld. Chemical studies of the weld metal found that the magnesium content decreased. No testing of tensile properties was made of the welds, although with the proper welding parameters, the welds shown in Figure 14-27 appear to be of good quality.

Laser stir and laser stir hybrid welding processes recently developed by Alcoa Inc. and Pennsylvania State University offer significant advantages over the conventional laser beam and laser/GMA welding processes.

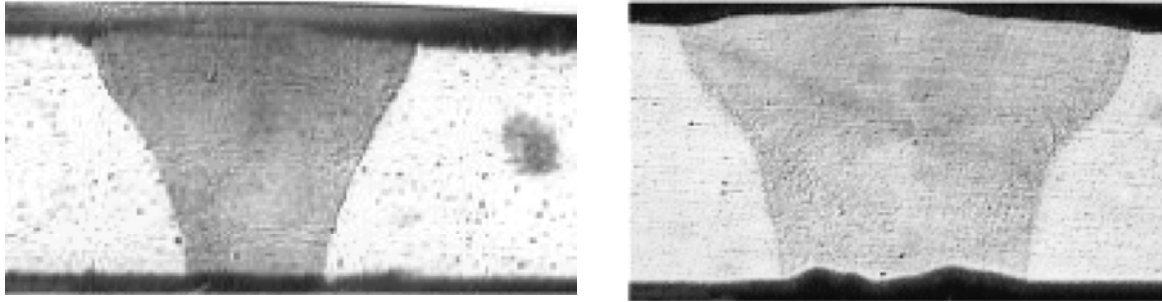


Figure 14-27 Section through laser welds in of 5182 and 5754 alloys (Pastor et al., 1999).

Zhao and Debroy (2001) made further studies of magnesium loss in welding of 5xxx-series alloys using alloy 5182. An experimental and theoretical study was carried out to seek a quantitative understanding of the influences of various welding variables on vaporization and composition change during conduction mode laser welding of aluminum, and a model for the calculation of vaporization rate and weld metal composition change was developed. The model showed that the vaporization was concentrated in a small high-temperature region under the laser beam where the local vapor pressure exceeded the ambient pressure. The model can serve as a basis for the quantitative understanding of the influences of various welding variables on the heat transfer, fluid flow, and vaporization occurring during conduction mode laser welding of aluminum alloys, but it does not solve the problem. Therefore, further development of the laser welding process will be necessary before it can be applied to marine aluminum alloys. The 6xxx-series have a significantly lower magnesium content than the 5xxx-series and may be more suited for the laser welding process.

14.3 Electron Beam Welding

The following summary of the electron beam welding process was obtained from Wikipedia, the free encyclopedia (www.wikipedia.com) and in turn is based on Cary and Helzer (2005). Electron beam welding is a fusion welding process in which a beam of high-velocity electrons is applied to the materials being joined. The workpieces melt as the kinetic energy of the electrons is transformed into heat upon impact, and the filler metal, if used, also melts to form part of the weld. Pressure is not applied, and a shielding gas is not used, though the welding is often done in conditions of a vacuum to prevent dispersion of the electron beam. The process was developed in France and released on November 23, 1957 in Paris by J. A. Stohr.

As the electrons strike the workpiece, their energy is converted into heat, instantly vaporizing the metal under temperatures near 25,000 °C. The heat penetrates deeply, making it possible to weld much thicker workpieces than is possible with most other welding processes. However, because the electron beam is tightly focused, the total heat input is actually much lower than that of any arc welding process. As a result, the effect of welding on the surrounding material is minimal, and the heat-affected zone is small. Distortion is slight, and the workpiece cools rapidly.

The three primary methods of electron beam welding are each applied in different welding environments. The method first developed requires that the welding chamber be at a hard vacuum. Material as thick as 15 cm (6 in) can be welded, and the distance between the welding gun and workpiece (the stand-off distance) can be as great as 0.7 m (30 in). As electron beam gun technology advanced, it became possible to perform electron beam welding in a soft vacuum. This allows for larger welding chambers and reduces the time and equipment required to attain evacuate the chamber, but reduces the maximum stand-off distance by half and decreases the maximum material thickness to 5 cm (2 in). The third electron beam welding mode is called nonvacuum or out-of-vacuum electron beam welding, since it is performed at atmospheric pressure. The standoff distance must be diminished to 4 cm (1.5 in), and the maximum material thickness is about 5 cm (2 in). However, it allows for workpieces of any size to be welded, since the size of the welding chamber is no longer a factor.

The process became widely used beginning in the 1960s, initially for welding small, thin materials, but with the development of nonvacuum processes, was used for thick materials. One of the biggest uses in the marine industry was for welding the thick aluminum spheres for liquid natural gas carriers in the 1960s.

Although 6xxx-series alloys can be extruded in corrugated sandwich panels with thickness as little as 2 mm, the 5xxx series are limited to about 3.3 mm in 5086 alloy and to about 4.6 mm in 5083 alloy. However, research is being done to produce such panels using electron beam welding (Kryzhevich et al., 2005) as shown in Figure 14-28.

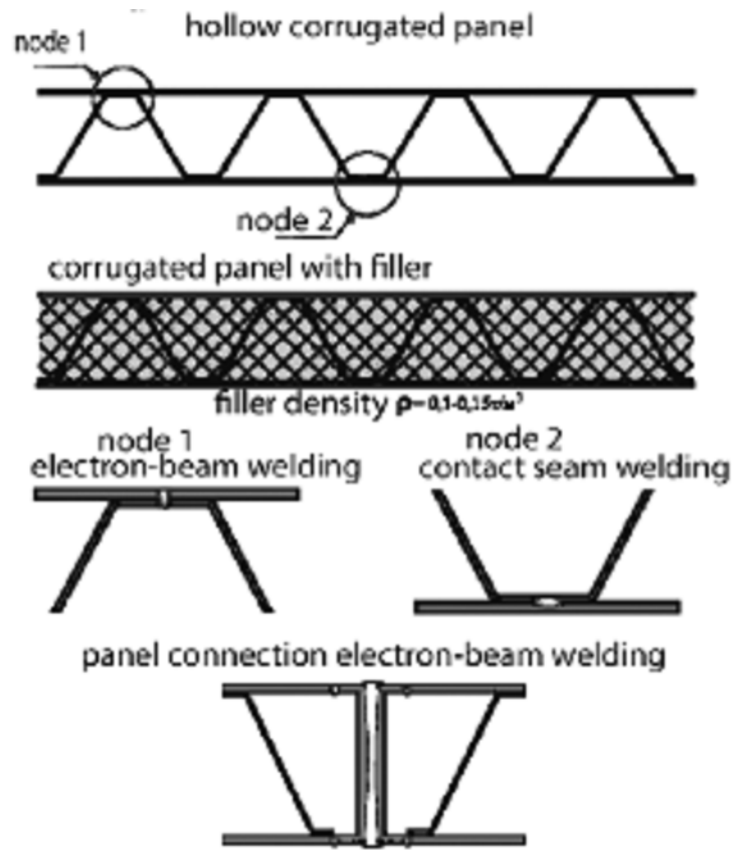


Figure 14-28 Electron beam welding of panels (Kryzhevich et al., 2005).

Although electron beam welding is used in this reported project, the same low distortion welds could in principle be made with laser welding and possibly friction stir welding, although the latter would be difficult because of the need for a backup fixture beneath the weld.

14.4 Summary

Although friction stir welding is a relatively new technology, it has found rapid application in the fabrication of lightweight marine structures, primarily for joining integrally stiffened extrusions to make structural panels. Studies are being made on the use of laser welding and electron beam welding, but they are not used today for fabrication of aluminum marine structures. The processes of laser welding and stir welding are being combined as laser stir welding, a process that holds promise for use in fabrication of aluminum marine vessels.

Chapter 15

Research Needs

In reviewing current knowledge in design and construction of aluminum ships and craft, a number of deficiencies have been revealed. These deficiencies do not prevent vessels from being designed and constructed, but they do limit their efficiency. The following projects are proposed:

1. Design Strength of Welded Aluminum
2. Fatigue of Aluminum Structural Details
3. Corrosion Properties of Marine Alloys
4. Structural Loads on High Performance Aluminum Marine Vehicles
5. Fatigue Loading Spectrum for High Performance Aluminum Marine Vehicles
6. Fatigue Strength Under Multi-Axial Loading
7. Elevated-Temperature Resistance Aluminum Alloys
8. Reliability of Aluminum High Speed Vessels
9. Fire Protection of Aluminum Structure
10. Friction Stir Welded Bimetallic Strip
11. Mitigation of Loads on High-Speed Vessels
12. Line-heating of Aluminum Plates
13. Development of Improved Welding Processes

15.1 Design Strength of Welded Aluminum

There is currently no agreement between different classification authorities and U.S. Navy references on the design strength to be used for welded aluminum alloys. The strength of the weld metal and heat affected zone of the weld are significantly less than that of the base metal, so strength cannot be specified as a material property but must be experimentally derived. For example, the specified yield strength for 5456-H116 plate is 230 MPa (33.0 ksi), but the welded yield strength can vary between 125 MPa (19 ksi) and 179 MPa (26 ksi), depending on the reference used to determine welded yield strength.

The majority of current design criteria are based on the welded yield strength of aluminum alloys. However, the yield strength cited by different authorities can vary by as much as 70 percent. The rule requirements of the classification societies generally determine the thickness of plating to be inversely proportional to the square root of the yield strength; therefore, the required thickness of plating can vary by 30 percent just because of the value of yield strength used.

There is no clear indication that the welded yield strength should be used for design. Because it can be 70 percent or less than the strength of the base metal, a considerable penalty in design strength is incurred by designing to the welded yield strength. Alternate methods have been proposed, such as a weighted average strength level, but these methods lack experimental verification.

Tasks:

1. Fabricate large-scale articles of welded aluminum structure. The articles should represent typical welded high-speed craft structures and should be designed to fail under tensile loading.
2. Characterize the mechanical properties of the materials used, both base metal and welded properties.
3. Test the articles to failure under tensile loading. Determine if the actual failure load is predicted best by analysis using strength data from small gauge length welded tensile specimens, large gauge length welded tensile specimens, base metal properties, or some combination of the above.
4. Fabricate a series of tensile specimens of the type that best meet the needs determined from Task 3. Specimens should be made of all aluminum alloys contemplated for use in construction of high performance marine vehicles.
5. Conduct testing and present the results in a form useful to designers.
6. Propose appropriate new standards for determining the material properties of welded aluminum alloys used in fabrication of high performance marine vehicles.

15.2 Fatigue of Aluminum Structural Details

There are many issues related to the fatigue strength of high-speed aluminum vehicles. Several organizations have compiled databases relating to the fatigue strength of aluminum structural details and have published design codes. The most recent of these codes is Eurocode 9, which was developed by merging data from most of the other sources and developing new data from testing of medium-scale specimens typical of the details used in civil engineering structures. These codes all assume that the fatigue strength of welded details is the same for all aluminum alloys and that mean stress effects are not significant. The data from which these design codes were developed does not reflect many of the structural details currently used or proposed for use in construction of high performance aluminum marine vehicles. A testing program is needed to address these deficiencies.

Tasks:

1. Survey current high performance marine vehicles to determine the types of details in current use, noting if any have had fatigue or other failures in service. Survey designers of future vehicles to determine emerging needs.
2. Attempt to classify these structural details in accordance with existing fatigue design codes, including those of The Aluminum Association and Eurocode 9.
3. Identify specific deficiencies of details that do not fit existing fatigue classifications. Develop a test program to determine the fatigue lives of those details.
4. Fabricate specimens of structural details for fatigue testing. Details should be full scale to replicate residual stress patterns associated with marine structures. Replication of full-scale conditions for a large number of specimens can be best simulated by construction a large aluminum box beam that will have details included in the upper and lower flanges. This will permit many details to be loaded at the same time and without the requirement for a high-capacity testing machine.
5. Conduct constant-amplitude fatigue testing at stress ranges that will provide data at 10^6 fatigue cycles or more.

6. Use the data to either confirm classification of the details within existing fatigue classifications or propose a separate fatigue classification for specific details that do not fit existing classifications.

15.3 Corrosion Properties of Marine Alloys

There exists no consistent data to compare the corrosion resistance of different aluminum alloys. This problem has become more acute with the introduction of 6xxx-series extruded aluminum alloys in forms that include plate and stiffening. These alloys have less corrosion resistance than the 5xxx-series alloys formerly used exclusively for marine structures, but the difference in corrosion resistance has not been quantified. The 6xxx extrusions are currently being used only topside and in dry locations, but some builders want to use them more extensively throughout the hull. Consistent data comparing the various alloys is needed, as well as a basis for relating that data to service experience. Corrosion resistance of 5xxx alloys has not been assured in the past, although a new ASTM specification has been developed to address intergranular corrosion. That specification is being applied to 5xxx-series aluminum plate, but perhaps it or some other criterion should be used for 6xxx series plate and extrusions. In addition, some designers are proposing to use 7xxx-series alloys for high performance marine vehicles, but these alloys are purported to have even poorer corrosion resistance than the 6xxx-series, although that difference has not been quantified.

Tasks:

1. Survey literature worldwide to find any existing data on corrosion of aluminum in a marine environment.
2. Develop a test program that will include both short-term accelerated testing and long-term testing of base metal and welded alloys. Specimens should be bare metal as well as coated, but with scratches in the coating.
3. Conduct testing, using existing test specifications to the maximum extent possible.
4. Report short-term results, and continue long term testing with annual reports of results.

15.4 Structural Loads on High Performance Aluminum Marine Vehicles

Estimation of structural loads during the early design stages is particularly critical for the design of high performance aluminum marine vehicles. These vehicles typically have very light scantlings, sometimes only a few millimeters thick. Loads are not accurately known until the latter stages of design when detailed hydrodynamic analysis and model testing is completed. A change of only one millimeter in thickness made in the latter stages of design can increase the weight significantly and radically change the overall performance of the vehicle. Current methods for estimating the hydrodynamic loads for the design of high performance marine vehicles are based on hull accelerations in a seaway. Methods are used to estimate hull accelerations based on factors such as vessel size and speed, and these accelerations are used to estimate load parameters including hull bending moments and design pressures. A systematic analysis of a variety of hull forms is needed to determine if the correlation between hull accelerations and hydrodynamic loads is valid, or if other means are necessary to predict loads.

Tasks:

1. Assemble existing data from model tests and seakeeping analyses of high performance marine vehicles.
2. Identify gaps in the knowledge base concerning size and types of vessels tested and analyzed. Develop a series of hull forms appropriate for analysis to fill those gaps.
3. Analyze the hull forms using a nonlinear seakeeping program to determine hull motion, bending moments, and local pressure distributions, including slam events and the resulting accelerations, bending moments, and pressure distributions.
4. Develop empirical relations between motions and loads and vessel parameters, including dimensions, speed and heading, and operational profiles. Determine if the loads are best predicted using motion data such as hull accelerations, or if they are better determined from vessel dimension and operational profile.
5. Develop a methodology for predicting hydrodynamic loads during the early design stages of high performance marine vehicles.

15.5 Fatigue Loading Spectrum for High Performance Aluminum Marine Vehicles

Fatigue is an important design parameter for high performance aluminum marine vehicles compared to vessels constructed of steel. Fatigue strengths of aluminum structural details are a lower fraction of the yield strength, making fatigue strength control scantlings in many cases. Fatigue crack growth rates are thirty times faster in aluminum than in steel at the same stress level, so analysis of fatigue crack growth is important in making some design decisions and in assessing failures in service. Accurate fatigue-loading spectra are needed during early design stages in order to perform fatigue analysis, and these fatigue-loading spectra are also needed to assess problems in existing vessels. Methods exist for developing fatigue loading spectra for conventional surface ships, such as the NSWCCD computer program SPECRA, but not for high performance marine vehicles. Universal response amplitude operators (RAOs) need to be developed for a variety of hull forms, including multi-hulled vessels. Sea spectra that are typical of the operational areas in which high performance naval vessels are expected to operate need to be developed. The RAOs and sea spectra should be integrated into a design tool for predicting fatigue spectra for fatigue analysis.

Tasks:

1. Assemble existing RAO data from model tests and seakeeping analyses of high performance marine vehicles.
2. Identify gaps in the knowledge base concerning size and types of vessels tested and analyzed. Develop a series of hull forms appropriate for analysis to fill those gaps.
3. Analyze the hull forms using a linear seakeeping program to determine RAOs for hull bending moments and for hydrodynamic loads. Generalize the RAOs on the basis of vessel parameters, including dimensions and speed.
4. From the operational profiles and specifications of existing and pending high performance marine vehicle designs, identify the ocean and littoral areas in which the vessels will operate, and obtain sea spectra for those areas. Develop a typical or a series of typical operating profiles of vessel speed and heading in differing sea states.
5. Develop a methodology or modify an existing methodology to use this information to develop fatigue-loading spectra.

15.6 Fatigue Strength Under Multi-Axial Loading

Many high performance marine vehicles are of multi-hull form where longitudinal, transverse, and torsional bending interact to produce fatigue stresses. Therefore, structural details are subject to multi-axial loading. There is no established methodology for determining the effect of this loading on the fatigue life of specimens for which single-axis fatigue data is available. Fatigue analysis is particularly important for aluminum vessels because fatigue life is often the governing parameter for these vessels. The different multi-axial loadings occur at different phases during a loading cycle, and a means of combining all of the different loads to assess the fatigue strength of structural details is needed. There is currently no universal parameter for correlating cyclic multiaxial stress/strain with fatigue life for marine structures, although the Ship Structure Committee has investigated the subject for steel ships (Stambaugh et al., 1990). Very few methods have been investigated for welded joints as a group, particularly in aluminum, and additional validation efforts are required before they can be recommended for application to marine structures. Potentially useful tools for extrapolating the responses of aluminum structural details from one stress state to another and for life correlation in high cycle multiaxial regimes include the use of maximum shear stress for crack initiation and maximum principal stress for crack growth.

Tasks:

1. Define spatial and temporal characteristics of principal stresses in the welded aluminum details of high performance marine vehicles. The characteristics of principal stresses include magnitudes, phase relationships, gradients, and mean stress components, and the random nature of each. Develop typical fatigue loading spectra for a variety of high performance marine vehicles.
2. Design and fabricate test specimens that will represent typical structural details that are subject to multi-axial fatigue.
3. Conduct multiaxial fatigue tests on marine structural details. Multiaxial fatigue testing should be conducted to validate approaches using representative stresses and strains identified in the previous task.
4. Analyze structural details. Analyze the details tested using the various multi-axial analysis methods using the loadings developed during task 1 and the loading applied during task 2.
5. Correlation of analysis and definition of methodology. Conduct analytical correlation to validate the various multiaxial fatigue techniques. Develop a methodology for use in design and analysis of failures of existing craft.

15.7 Elevated-Temperature Resistance Aluminum Alloys

The 5xxx-series magnesium-strengthened alloys are used for the structure of aluminum ships and high-speed craft because of their higher welded strength and good corrosion resistance. However, most alloys in the 5xxx-series should not be used at temperatures above 66 °C (150 °F) because the metal becomes sensitized to stress corrosion at these temperatures. For higher temperature applications, alloy 5454 must be used, which has a yield strength 60 to 70 percent of that of the higher strength marine structural alloys. The use of 5454 alloy can result in a proportional increase in structural weight, although the entire vessel will not be affected, only the exposed topside areas.

Until extended operations began in Persian Gulf, sensitization of aluminum has not been a problem for the U.S. Navy. Under these extreme conditions, deck temperatures become extremely hot, and at least one instance of sensitization of 5456-H116 plate has been documented. Until aluminum manufacturers develop new high-strength weldable marine alloys that are not sensitive to prolonged exposure at higher temperatures, means must be found to mitigate the effects of high temperatures and strong sunlight. Avoidance of dark paints may be sufficient, or perhaps more extensive use of insulation will be necessary.

Tasks:

1. Obtain aluminum plate in the alloys used for the structure of high-speed craft, and prepare specimens for long-term exposure to higher temperatures. Plate panels will be welded, and then coated with different paints of differing reflectivity.
2. Characterize the materials prior to exposure at elevated temperatures.
3. Expose the panels to a sunlight-induced high-temperature environment for an extended period of time, at least 6 months. Use thermocouples to measure the temperature of the plate.
4. For control purposes, expose samples of each welded alloy to elevated temperatures in the laboratory for extended periods of time.
5. Conduct metallurgical examination of the plates after extended periods of exposure. Continue testing for at least two years.
6. Develop standards for thermal protection of plating.

15.8 Reliability of Aluminum High Speed Vessels

The uncertainty in design of aluminum vessels is evidenced in the ABS Rules for Building and Classing High Speed Naval Craft. Section 3.1.3 requires that the final design be based on finite element analysis where the allowable stress for steel is 0.95 of the yield strength, but for the same vessel constructed of aluminum, the stresses are limited to 85 percent of the welded yield strength. This is an 11 percent penalty paid for aluminum, reflecting greater uncertainty in the strength of aluminum structure. The design standards for aluminum vessels need to be made consistent with those for steel vessels, and reliability analysis provides a means of doing so.

Tasks:

1. Develop a series of structural designs in both steel and aluminum structure, using the current ABS Rules for Building and Classing High Speed Naval Craft. Two distinctly different hull forms should be considered, and three variations in length for each made. The designs should include all ship systems to a conceptual design stage, but the structural design should be advanced, including numerical prediction of loads and finite element modeling of structure.
2. Using a consistent methodology, perform a reliability analysis of the steel and aluminum vessels.
3. Identify the major sources of uncertainty in the analysis, and develop a plan for reducing that uncertainty.
4. Recommend changes to the design procedure that will put both designs at an equivalent level of reliability.

15.9 Fire Protection of Aluminum Structure

Aluminum structure requires more fire protection insulation than does steel because the aluminum must be protected from the heat of a fire. SNAME T&R Bulletin 2-21 (SNAME 1974) provides current guidance for protection of aluminum. This document was developed from extensive testing done in the 1970s, and is still relevant for use today. However, there were several areas not adequately covered by the testing at that time, and should be investigated today because of the increased use of aluminum for high-speed vessels. The greatest deficiency occurs in the insulation requirements for stanchions, pillars and other structure that are surrounded by fire are greater than for structure with a fire on one side only. The SNAME T&R bulletin provides values of the required insulation, but the bulletin cautions that those values are not based on experimental data, but on judgment. In some instances, the lack of well defined standards for fire protection of aluminum results in such structure being fabricated of steel to provide safety of the vessel.

Tasks:

1. Review current design standards for fire protection of aluminum structure, determining their experimental basis.
2. Perform thermal analysis of structural configurations for which data is lacking and determine thermal insulation requirements.
3. Conduct small-scale testing to confirm the results of calculations.
4. Perform large-scale testing to validate insulation design standards.
5. Develop new design standards, including a revision of SNAME T&R Bulletin 2-21.

15.10 Friction Stir Welded Bimetallic Strip

The current method of joining aluminum structured to steel structure uses the bimetallic (actually trimetallic) joint where a 6.35-mm (0.25-inch) layer of 5456 aluminum is bonded to a 9.53-mm (0.375-inch) layer of 1100 aluminum, which is bonded to a 19.05-mm (0.75-inch) layer of A516 Grade 55 steel. The bond is either explosively formed or roll bonded. The bond has a minimum ultimate tensile strength is 76 MPa (11.0 ksi), which means in application a strip of the material is required that is four times wider than the thickness of the plate to be joined. The resulting joint is unsightly, requires more maintenance, and presents a reflective corner that increases radar cross section. Recent research in Japan has developed the technology for using friction stir welding to join 2-mm (0.08-in) 5083 aluminum plate to mild steel of the same thickness. A tensile strength of about 240 MPa (35 ksi) was produced, compared to the 276 MPa (40 ksi) tensile strength of GMAW welds in 5083. Further development of this process can lead to a product useful for marine use.

Tasks:

1. Use friction stir welding to join marine-grade aluminum to various grades of steel, including ordinary strength steel and HSLA-80. Vary the welding parameters to determine the range that will produce good bonds.
2. Conduct mechanical testing of the joint, including tensile, shear, fracture toughness, and fatigue testing to determine the design strength of the bond.
3. Conduct testing for exfoliation and intergranular corrosion of the aluminum.

4. Conduct long-term corrosion testing of the bond, including immersion and marine environmental testing for general corrosion and stress-corrosion cracking. Test both unpainted and painted specimens, the latter including specimens with scratches in the paint.
5. Report the results of the studies, including recommended standards for production.

15.11 Mitigation of Loads on High-Speed Vessels

Uncertainty of the loads and possible damage to structure can severely limit the speed and direction taken by high-speed vessels, especially ones designed for limited sea conditions but used in open ocean service. Many such commercial vessels have hull-monitoring systems installed to provide operators information as to possible hull damage from operations at high speed in greater sea states. Based on the information from these hull-monitoring systems, operators will reduce speed, change course, or both, when heavier weather is encountered.

Such information relies on real-time information such as hull accelerations, slam pressures, and stress measurements. Although hull accelerations are a key parameter for determining the design loads for high-speed vessels, uncertainties inherent in the design process make the design value of hull acceleration conservative as a guide to limiting speeds and headings. Slam pressures on the bow or wet deck are not reliable indicators of maximum loads because peak pressures are very localized, and a sensor may underestimate the severity of loads if the peak does not occur at the point being measured. Strain gauging can be overly conservative in aluminum structure, for although the design of aluminum structure is based on the welded yield strength, failure is more related to the strength of the base metal, which will tend to be greater than minimum specified values.

A survey of actual installations made to date and their efficiency in mitigating damage is needed, along with input from operators as to whether the use of monitoring systems unduly hampers operations. A reliability-based approach to the type and placement of sensors and establishment of limiting values is needed to ensure that damage does not occur during operations, but that the hull monitoring system does not create false alarms that require operations to be hindered when there is no danger of structural damage.

If these hull-monitoring systems are equipped with means of recording data over extended periods of time, a basis will exist for comparing predicted motions and loads to actual values seen in service. Analysis of this data can reduce uncertainty in loads prediction and therefore decrease scantlings of future high-speed vessels.

Tasks:

1. Survey current requirements of classification societies for hull monitoring systems of high-speed vessels. Review the installations made on different vessels, including the type of sensors, basis for limits, and method of presentation of data to operators. Survey operators to determine the effectiveness of the systems and their drawbacks.
2. For an actual high-speed vessel either currently in service or in design and construction, perform a reliability analysis of the hull structure, relating probability of

damage to indicators that be placed onboard to monitor the motions, loads, and structural response.

3. Based on the reliability analysis, recommend a suite of onboard sensors and their values that should be used to limit ship operations. Install the system on the vessel.
4. Periodically review the operation of the hull monitoring system with vessel operators. Collect data for analysis and comparison with the reliability analysis.
5. Develop recommendations for future hull monitoring systems on high-speed vessels. Develop revised design criteria from the analysis of returned data from operations.

15.12 Line-heating of Aluminum Plates

Because of the possibility of degrading the physical and corrosion-resisting properties when exposed to higher temperatures for extended periods, aluminum plates are not generally formed using furnacing or other high-temperature methods, which limits the degree to which shipyards can shape the plates. In particular, compound curvature is avoided in aluminum hull design because of the difficulties of forming the plate.

Past studies, such as Hay and Holton (1980) have provided guidance on the use of flame-straightening to remove distortions from aluminum panels. This methodology of heating followed by immediate quenching can be adapted to provide a means of forming aluminum plates using line heating, such as is routinely done with steel. This technology will decrease the cost of forming aluminum plate and will increase the possibilities for hull forms of aluminum vessels.

Tasks:

1. Review the literature for methods of heat application to aluminum plate, including determination of metallurgical damage from excessive or prolonged heat application.
2. Develop a methodology for application of line heating to aluminum plates of various alloys and thicknesses.
3. Perform testing on aluminum plates of various alloys and thicknesses to determine the amount of angular distortion per heating pass.
4. Perform metallurgical and mechanical properties testing of the line-heated plates to determine that no degradation of properties has occurred.
5. Using existing guidelines for forming steel plate by line heating, develop similar guidelines for aluminum plates.
6. Provide a demonstration of the methodology developed by forming a large plate with compound curvature such as might be used in the hull of an aluminum vessel.

15.13 Development of Improved Welding Processes

There are several emerging technologies for the improvement of welding aluminum. These include:

- Gas metal buried arc welding of thick sections
- Gas metal buried arc welding of lap penetration joints
- Laser stir welding
- Advanced friction stir welding processes (i.e., 45-mm long tools)

Aluminum Marine Structure Guide

These technologies have promise, and exploratory research should be conducted to determine their applicability to boat- and ship-building.

Tasks:

1. Survey emerging welding technologies, determining their advantages and limitations for use in fabricating marine aluminum structures.
2. Develop research proposals for development of the technologies and application to boat- and ship-building.

Chapter 16 Summary

Aluminum is the material of choice for many ships and craft because of low weight, ease of fabrication, and reasonable cost. Aluminum is versatile in the many product forms in which it can be obtained. There are a variety of alloys that are produced for the marine market, and the designer must determine the particular alloy or combinations of alloys best suited for a particular design. Often, that decision will be tempered by other considerations, such as the availability from suppliers as well as familiarity of shipyard fabricators and customers with the different alloys.

Aluminum and steel are both metallic structures, but the mechanics of materials used for their analysis are sometimes different because of their behavior at higher stress levels. Whereas most structural steels have a definite yield point, aluminum alloys lose stiffness in a more gradual manner, which calls for a slightly different approach to limit state analysis. The difference in behavior is not reflected in the various rules for design of plating under lateral pressure, particularly when the design is based on membrane action of plate and permanent set under extreme loads. There are significant differences in the material properties of the two materials, particularly in the elastic modulus, and those necessitate differences in design criteria, especially when historical empirical design criteria are used that were developed for steel structures.

Despite differences in the mechanics of materials, aluminum hull structures are generally designed using the same methods that are used for steel. Different methods of design exist, including the rules of classification societies and procedures of naval authorities. These methods give similar scantlings for the same vessel design, even though loads and allowable stress levels are different. The designer must not make the mistake of mixing the procedures by using the allowable stress levels from one procedure with the loads from another or other mixtures of procedures.

Equations exist for estimating design loads of most of the high-speed and unusual hull forms that characterize many aluminum vessels. Final design must be generally based on a more thorough analysis, either with data from at-sea tests on similar vessels, model tests, or from hydrodynamic analysis. Such methods have not been well validated and can easily lead to inconsistent results if similar vessels are designed using different methods, and even with the same method but by different persons. In the end, a very erudite analysis may have limited accuracy.

Design methods conservatively account for the reduced strength of the welds and HAZ of aluminum by using the lowest strength in design equations. A more accurate method of using an average yield strength weighted by mass of base and welded metal has been validated for compressive strength of welded panels, but not for structure in tension.

Many structural details that are used on steel ships can also be used on aluminum vessels, although greater consideration is needed for fatigue strength with aluminum design. There are

also structural details that are unique to aluminum construction, especially because of the ease with which special extrusions can be made. Evaluations have been made of the relative merits of these details when used for aluminum construction, including assignment of fatigue classification in accordance with Eurocode 9. A shipbuilder will have to determine the type of detail that best suits the construction techniques used in the yard, using higher quality details for the more critical joints. Where unproven details are used, such as for extruded deck panels, caution should be exercised until fatigue strength data is developed for these details.

The relative ease with which new extrusion dies can be designed and manufactured presents both an opportunity and a challenge to the designer. The advantages of generally quicker procurement time and reduced cost for standard extrusions must be compared to the possible advantages of reduced weight, reduced total fabrication cost, and special functionality that a custom-designed extrusion can provide.

Long-term corrosion tests are needed for all of the alloys currently being used or considered for use in the structure of high-speed aluminum vessels, including 6xxx-series alloys. Testing should include partial immersion in seawater, immersion in flowing seawater, and exposure to a marine environment near the surf. The specimens should be in the base metal and welded condition and should have one-half of their number sensitized by holding for four weeks at 100 °C. The same alloys should be tested using standardized accelerated corrosion tests, and the results of the long-term testing compared to the results of the accelerated testing to develop standards for accelerated corrosion tests.

The service temperature of deck structures for aluminum ships operating in very hot climates should be determined, and the degree of sensitization that occurs under those conditions to 5xxx-series alloys determined. A process for rapid sensitization of these alloys should be developed and applied to a series of alloys that will then be tested for stress-corrosion testing in the welded and unwelded condition, both sensitized and unsensitized. For comparison, 6xxx-series alloys should be included in the stress-corrosion testing. Friction stir welds in 5xxx-series alloys and 6xxx-series alloys should also be tested.

Fabricating structure with aluminum is similar to steel construction, but there are more difficulties involved. Several means of cutting aluminum are available but are generally not as efficient as steel cutting. Aluminum can be formed into different shapes, but heating is very difficult, so compound curvature of plates should be avoided. Welding aluminum requires more joint preparation and cleanliness than is generally required for steel, and the need for shielding gas and somewhat slower welding speeds makes the process more expensive. Aluminum is more prone to distortion during welding, so more care is needed with welding procedures to reduce distortion. When distortions occur, they are more difficult to remove because of limitations on the use of heat on aluminum. The availability of extruded panels has the potential to reduce construction cost because many welds of stiffeners to plate are eliminated.

Riveting can reduce weight because higher stress levels can be used. This weight reduction is partially offset by the weight of the lap joints used in riveted construction. Riveted construction has less distortion than welded construction, but the cost of fabrication is greater. Unless joints are symmetric, with an associated increase in weight, riveted joints have low

fatigue strength. A sealing compound is needed in welded seams to provide watertightness. The disadvantages generally outweigh the advantages, and riveting is seldom used today in marine structures.

With an aluminum deckhouse on a steel hull, electrical separation of the two materials is necessary to prevent galvanic corrosion. Riveted connections with insulation between the steel and aluminum have not been effective in the past because whenever the insulation broke down, galvanic corrosion began immediately. A bonded bimetallic steel and aluminum strip welded to a steel coaming and the aluminum deckhouse provided a smooth surface that can be coated to prevent corrosion. The stresses acting in deckhouses could only be roughly estimated in the past, leading to problems in the junction between and aluminum deckhouse and a steel hull, as well as fatigue failures in the deckhouse. Finite element methods are useful today to analyze those stresses and reduce problems in service. Complete isolation of the deckhouse from the hull is another solution to the interface problem, and doing so can reduce vibration and noise in the deckhouse.

Welded aluminum structure generally has less residual stress than comparable steel structure. However, the reduced buckling strength of aluminum means that it will tend to have greater distortion for the same level of residual stress, especially in plating. Although there has been much research done on the residual stresses and distortion of steel ship structure, much comparable work is needed for aluminum.

A generalized procedure for determining a fatigue-loading spectrum can be used during preliminary design to be assured that potential fatigue problems are addressed early in the design process. A detailed spectral fatigue analysis may be required in the final stages of design, but there must be some assurance that the vessel will have a satisfactory overall fatigue life early-on in design to avoid major changes in scantlings late in the design process.

Aluminum design must be based on avoidance of crack initiation because a fatigue crack can propagate as much as 30 times faster in aluminum than in steel. However, aluminum structure is rather tolerant of defects and will not fail by fast fracture, although it hasn't the same fracture resistance of ship-grade steels.

Aluminum structure requires more fire protection insulation than does steel because the aluminum loses strength at a lower temperature and must be protected from the heat of a fire. Requirements for fire protection are set out by the SOLAS requirements of IMO, the IMO High Speed Craft Code, the U.S. Coast Guard, and by classification societies. For naval vessels there are additional requirements specified by naval authorities. A methodology for designing structural fire protection systems is provided by SNAME T&R Bulletin 2-21. However, that bulletin was issued more than 30 years ago and should be updated, and recommended testing should be conducted, including structure that is surrounded by fire.

Similar steel and aluminum structures will have natural frequencies of vibration that are similar and will require about the same amount of energy for the same amplitude of excitation. Therefore, an aluminum hull is no more prone to vibration problems than a steel hull. Although not significantly more prone to vibration problems than steel structure, aluminum structure can

Aluminum Marine Structure Guide

have more fatigue cracking problems from vibration. Structure should be proportioned to avoid resonance with various forcing functions aboard ship. If that cannot be avoided, then damping materials must be added. Hull girder vibration can be a problem, and simple methods for estimating the hull girder frequencies are needed for the advanced design stages of aluminum vessels.

Aluminum has the potential for excellent corrosion resistance. However, poor preservation methods, improper alloys, or bimetallic coupling can lead to rapid corrosion. Rapid crack propagation rates make aluminum susceptible to fatigue cracking, and an improperly designed aluminum vessel can become a maintenance headache. Redesign of areas prone to fatigue cracking is necessary to promote the safe life of the vessel.

Because the magnitude of slam loads can be uncertain, structure in areas subject to such loads should be designed to withstand overloads that exceed the specified design pressures. Information on the effect of changes of course and speed on slam loads should be made available to the operators of vessels that could incur slam damage so that slamming can be reduced if it occurs. Sea conditions that would possibly produce slam damage should be avoided, but routing systems need to have information as to the possibility of slamming occurring in different sea states and at different speeds and headings. Because the operator often cannot perceive the severity of a slam in terms of structural damage, instrumentation systems should be used to make operators aware of current conditions.

Although friction stir welding is a relatively new technology, it has found rapid application in the fabrication of lightweight marine structures, primarily for joining integrally stiffened extrusions to make structural panels. Studies are being made on the use of laser welding and electron beam welding, but they are not used to any extent today for fabrication of aluminum marine structures.

Although aluminum vessels have been designed and built for decades, many new applications are occurring today, and the methods for design and construction continue to evolve. This report has reviewed many of these methods, but the designer and fabricator should always be alert to new developments in the technology.

Chapter 17

References

- ABS, Rules for Materials and Welding, Part 2, Aluminum and Fiber Reinforced Plastics, Chapter 5, Appendix 1, Table 2, American Bureau of Shipping, 2006.
- ABS, Guidance Notes on Spectral-Based Fatigue Analysis for Vessels, American Bureau of Shipping, January 2004.
- ABS, Guide for Building and Classing High Speed Naval Craft, American Bureau of Shipping, 2003.
- ABS, 2003A. Guide for Hull Condition Monitoring Systems, 2003.
- ABS, Guide for Building and Classing High-Speed Craft, American Bureau of Shipping, October 2001.
- ABS, Guide for Building and Classing Motor Pleasure Yachts, American Bureau of Shipping, February, 2000.
- Adamchak, John C., Design Equations for Tripping of Stiffeners under Inplane and Lateral Loads, David Taylor Naval Ship Research and Development Center report DTNSRDC 79/064, October 1979.
- AEC, 2002. Aluminum Extrusion Manual, Aluminum Extruders Council, Wauconda, Illinois.
- Ailor, W.H., Aluminum Alloys After Five Years in Seawater, contained in Materials Performance and the Deep Sea, American Society of Testing and Materials STP-445, 1969, pp. 115-130.
- ALCAN, 2004, Aluminum and the Sea, ALCAN Aerospace Transportation and Industry, Pechiney Rhenalu ALCAN Group, www.alcan-marine.com, Paris, December, 2004.
- Allen, Raymond G., and R.R. Jones. A Simplified Method for Determining Structural Design Limit Pressures on High Performance Marine Vehicles. Proceedings of the AIAA/SNAME Advance Marine Vehicle Conference, San Diego, 1978.
- Aluminum Association, 2006, International Alloy Designations and Chemical Composition Limits for Wrought Aluminum and Wrought Aluminum Alloys, The Aluminum Association, Arlington, Virginia, April 2006..
- Aluminum Association, 2006a, Aluminum Standards and Data, 2006, The Aluminum Association, Arlington, Virginia.
- Aluminum Association, 2005, Aluminum Design Manual, The Aluminum Association, Arlington, Virginia.
- Aluminum Association, 2005a, Tempers for Aluminum and Aluminum Alloy Products, The Aluminum Association, Arlington, Virginia, November 2005.
- Aluminum Association, 2003, Aluminum Standards and Data, The Aluminum Association, Arlington, Virginia.
- Aluminum Association, 2002a. Care of Aluminum, The Aluminum Association, Arlington, Virginia.
- Aluminum Association, 2002b. Welding Aluminum, Theory and Practice, The Aluminum Association, Arlington, Virginia.
- Aluminum Association. The Aluminum Association Alloy Designation System for Wrought Aluminum, The Aluminum Association, Arlington, Virginia, October, 1954.

Aluminum Marine Structure Guide

- Anderson, D.R. and A.G. S. Morton. Low Temperature Mechanical Properties of 316 Stainless Steel and 5000 Series Aluminum Alloys and Comments on Arctic Surface Effects Vehicle Repairability, Naval Ship Research and Development Center report 28-778, November 1973.
- ASTM B928. High Magnesium Aluminum-Alloy Sheet & Plate for Marine Service, 2004 Annual Book of ASTM Standards, American Society for Testing and Materials, Philadelphia, Pennsylvania, 2004.
- ASTM G15-93. Designation G15-93, Standard Terminology Relating to Corrosion and Corrosion Testing, 1995 Annual Book of ASTM Standards – Metal Test Methods and Analytical Procedures, American Society for Testing and Materials, Philadelphia, Pennsylvania, 1995.
- ASTM G66, Designation G 66, Standard Test Method for Visual Assessment of Exfoliation Corrosion Susceptibility of 5XXX Series Aluminum Alloys (ASSET Test), 1995 Annual Book of ASTM Standards – Metals Test Methods and Analytical Procedures, American Society for Testing and Materials, Philadelphia, Pennsylvania, 1995.
- ASTM G67, Designation G 67, Standard Test Method for Determining the Susceptibility to Intergranular Corrosion of 5XXX Series Aluminum Alloys by Mass Loss After Exposure to Nitric Acid (NAMLT Test), 1995 Annual Book of ASTM Standards – Metals Test Methods and Analytical Procedures, American Society for Testing and Materials, Philadelphia, Pennsylvania, 1995.
- AWS, 2004, Guide for Aluminum Hull Welding, AWS D3.7, American Welding Society, 2004.
- Backlund, J., A. Norlin, and A. Andersson. Friction stir welding – weld properties and manufacturing techniques, 7th Inalco Conference, Cambridge, April 15–17, 1998, ISBN 1 85573 417 6.
- Basil, J.L. The Resistance to Corrosion of Cast and Wrought Aluminum Alloys in Sea Water, United States Naval Engineering Experiment Station, Annapolis, Maryland Research and Development Report 4H(4) 066918, October 3, 1952.
- Basil, J.L. Resistance to Corrosion of Several Wrought Aluminum Alloys in Natural Sea Water, United States Naval Engineering Experiment Station, Annapolis, Maryland Research and Development Report 040037A(4), March 24, 1954.
- Basil, J.L. Sea Water Corrosion Test of Aluminum 6061 Alloy with XB605 Anodes, United States Naval Engineering Experiment Station, Annapolis, Maryland Research and Development Report 040039K(4), March 22, 1957.
- Beach, Jeffrey E., Lloyd C. Dye, Joseph A Hauser, Robert E. Johnson, Robert R. Jones, and Jerome P. Sikora. Fatigue Life Assessment of PGG-511-Class Bottom Longitudinals. David W. Taylor Naval Ship Research and Development Center, June, 1981.
- Beach, Jeffrey E., Robert E. Johnson, Natale S. Nappi, SR., Robert A. Sielski, William A. Palko, Thomas W. Montemarano, and William E. Lukens. A Guide for the Use of Aluminum Alloys in Naval Ship Construction and Design, David W. Taylor Naval Ship Research and Development Center, DTNSRDC 84/015, 1984.
- Bethencourta, M., F. J. Botana, M. Marcos, R. M. Osunaa and J. M. Sánchez-Amayaa. Inhibitor Properties of Green Pigments for Paints, Progress in Organic Coatings, Vol. 46, Issue 4, June 2003, Pp. 280-287.
- Bieberich, E. Bradley and Catherine Wong. Marine Atmosphere Corrosion of Fasteners and Aluminum Armor for USMC Amphibious Vehicles. Naval Surface Warfare Center, Carderock Division report CARDIVNSWC-TR-61-98-01 February 1998.

- Bleich, Friedrich, and Lyle B. Ramsey. A Design Manual on the Buckling Strength of Metal Structures, The Society of Naval Architects and Marine Engineers Technical and Research Bulletin Number 2-2, 1951.
- Boykin, C.V. and M.L. Sellers. Practical Problems Relating to the Use of Aluminum Alloys in Ship Construction, Transactions of the Society of Naval Architects and Marine Engineers, 1953, pp. 358–409.
- Broek, David. Elementary Engineering Fracture Mechanics, Sijthoff and Noordhoff, 1978.
- Bruchman, Daniel, and Alfred Dinsbacher. Permanent Set of Laterally Loaded Plating: New and Previous Methods, David Taylor Research Center report SSPD-91-173-58, May 1991.
- Bushfield, Harold Sr., Marc Cruder, Rendall Farley, and Jim Towers, Marine Aluminum Plate - ASTM Standard Specification B 928 And The Events Leading To Its Adoption. Presented at the October, 2003 Meeting of the Society of Naval Architects and Marine Engineers, San Francisco, California.
- C&R, 1938. Detail Specifications for Building Destroyers, Numbers 423, 424, 429 to 436, Navy Department, Bureau of Construction and Repair; Washington, D.C., 1938.
- C&R, 1936. Detail Specifications for Building Destroyers, Numbers 409 to 420, Navy Department, Bureau of Construction and Repair; Washington, D.C., 1936.
- C&R, 1936A. Bureau of Construction and Repair Newsletter, No. 18, 15 February 1936, pp. 5-6.
- C&R, 1935. Detail Specifications for Building Destroyers, Numbers 394 to 396, Navy Department, Bureau of Construction and Repair; Washington, D.C., 1935.
- C&R, 1934. Detail Specifications for Building Destroyers, Numbers 384 to 393, Navy Department, Bureau of Construction and Repair; Washington, D.C., 1934.
- Cary, Howard B. and Scott C. Helzer (2005). Modern Welding Technology. Upper Saddle River, New Jersey: Pearson Education. ISBN 0-13-113029-3. pp. 202-06.
- Cederqvist, L. and A. P. Reynolds. Factors Affecting the Properties of Friction Stir Welded Aluminum Lap Joints, Welding Journal, December 2001.
- Chiu, Forng-Chen, Sao-Wei Liu, Wen-Chuan Tiao, and Jenhwa Guo. Development of a Simple System to Measure 5 DOF Ship Motions in a Seaway, presented at International conference of Fast Sea Transportation (FAST 2005). St. Petersburg, Russia, June 27-30, 2005.
- Clarkson, J. Uniform Pressure Tests of Plates with Edges Free to Slide Inwards, Transactions of the RINA, Vol. 104, 1962.
- Collette, Matthew, Strength and Reliability of Aluminium Stiffened Panels, submitted for the degree of Doctor of Philosophy, School of Marine Science and Technology, Faculty of Science, Agriculture and Engineering, University of Newcastle, Newcastle upon Tyne, 2005.
- Conrardy, Chris and Randy Dull. Control of Distortion in Thin Ship Panels, Journal of Ship Production, Vol. 13, No. 2, May 1997, pp. 83–92.
- Czyryca, Ernest J. and H.P Hack. Corrosion of Aluminum Alloys in Exfoliation-Resistant Tempers Exposed to Marine Environments for Two Years, David W. Taylor Naval Ship Research and Development Center report 4432, November 1974.
- Czyryca, Earnest J. and Michael G. Vassilaros. Engineering Properties of Structural Aluminum Alloys: A Handbook, Naval Ship Research and Development Center Report 3571, June 1972.
- Dawes C. J., Thomas W. M. Friction Stir Joining of Aluminum Alloys, TWI Bulletin Nov/Dec 1995.

Aluminum Marine Structure Guide

- Deo, M.V. and P Michaeleris. Experimental Verification of Distortion Analysis of Welded Stiffeners, *Journal of Ship Production*, Vol. 18, No. 4, November 2002, pp. 216–225.
- DeOliveira, Joao G. Hull-Deckhouse Interaction, Chapter 3 in *Ship Structural Design Concepts*, Second Cycle, J. Harvey Evans, ed., Cornell Maritime Press, 1983.
- Dexter, Robert J. and Michael L. Gentilcore. Evaluation of Ductile Fracture Models for Ship Structural Details, Ship Structure Committee report SSC-393, 1997.
- Dexter, Robert J. and Paul J Pilarski, Effect of Welded Stiffeners on Crack Growth Rate, Ship Structure Committee report SSC-413, 2000.
- Dix, E. H. et al., Influence of Service Temperature on Resistance of Wrought Aluminum-Magnesium Alloy to Corrosion, *Corrosion*, Vol. 15, pp. 55T-61T (1959).
- DNV, Rules for Classification of High Speed, Light Craft and Naval Surface Craft, Det Norske Veritas, July, 2000.
- Dolan, T.J. Basic Concepts of Fatigue Damage in Metals. *Metal Fatigue*, N.Y.1959.
- Donald, J. Keith and Amy Blair. Fracture Mechanics Characterization of Aluminum Alloys for Marine Structural Applications, Ship Structure Committee report SSC-448, 2007.
- Dye, Lloyd C. and Thomas Dawson, Ship Hull Structure Maintenance and Repair, Naval Sea Systems Command, NAVSEA 0900-LP-082-3010, March 1974.
- Engh, B., O. Solli, S. Aabo, and A.J. Paauw. The Influence of the Corrosive Environment on the Fatigue Life of Aluminum Alloys, presented at the Third International Conference on Aluminum Weldments, Munich, April 15-17, 1985.
- ERAAS, 1992. European Recommendations for Aluminum Alloy Structures Fatigue Design, European Convention for Constructional Steelwork, Doc No. 68, First Edition, Brussels, 1992.
- EuroCode 9: Design of Aluminium Structures, Part 2: Structures Susceptible to Fatigue, CEN/TC250/SC 9, Draft for Eurocode 9 Part 2, December 1996,
- Faltinsen, O. Water entry of a Wedge by Hydroelastic Orthotropic Plate Theory. *Journal of Ship Research*, Vol. 3, No. 3, pp. 25-36, 1999.
- Faltinsen, O. Hydroelastic Slamming. *Journal of Marine Science and Technology*, Vol. 5, pp. 49-65, 2000.
- Faulkner, Douglas. A Review of Effective Plating for Use in the Analysis of Stiffened Plating in Bending and Compression, *Journal of Ship Research*, Vol. 19, No. 1, pp. 1–17, March 1975.
- Forrest, Matthew G. Applications and Uses of Aluminum Alloys in Ship Construction, *Transactions of the Society of Naval Architects and Marine Engineers*, 1947, pp. 305–331.
- Friedman, N., U.S. Destroyers, an Illustrated Design History, Annapolis, Maryland, United States Naval Institute, 1982.
- Friis Hansen, P. et al. (1995). Long Term Springing and Whipping Stresses in High Speed Vessels, *Proceeding of the FAST 1995 Conference*, pp 473-485.
- Fujii, C.T, C.D. Beachem, D.A. Meyn, and B.F. Brown (1972). Study of the Fracture Mechanism of 5456-H321 Aluminum Alloy, NRL Memorandum Report 2422, Naval Research Laboratory, April 1972.
- Goddard, H.P, et al., *The Corrosion of Light Metals*, John Wiley and Sons, New York, 1967.
- Greene, Eric. Labor-saving Passive Fire Protection Systems for Aluminum and Composite Construction. Ship Structure Committee Report 44, 2005.
- Greenspon, J.E. An Approximation to the Plastic Deformation of a Rectangular Plate Under Static Load with Design Implications, David W. Taylor Model Basin Report 940, June 1955.

- Gross, M.R., Low-Cycle Fatigue of Materials for Submarine Construction, *Naval Engineers Journal*, Vol.75, No. 5, pp.783–797, October 1963.
- Halverson, Bruce and John F. Hinrichs. Friction Stir Welding (FSW) of Littoral Combat Ship Deckhouse, presented at the Society of Naval Architects and Marine Engineers Maritime Technology Conference and Exposition, Ft. Lauderdale, Florida, October 11–13, 2006.
- Haugen, E.M., O Faltinsen. Theoretical studies of Wetdeck Slamming and Comparisons with Full-scale Measurements. Fifth International Conference on Fast Sea Transportation (FAST 99), Seattle. 1999.
- Hay, Robert A. and Chester H. Holtyn. The Effect of Thermal Fabrication Practices on Aluminum, *Naval Engineers Journal*, pp. 37–43, 1980.
- Hay, William, James Kuny, Ann Fajardo, Dave Kihl, and Jerome Sikora. Lifetime loads and Fatigue Analysis of CG-47 Class Based on Full Scale Trials of USS Monterey CG-61), Model Tests, and Finite Element Analysis, Volume II—Lifetime Stress and Fatigue Analysis. CARDEROCKDIV-U-SSM-65-95/27 March 1995, Naval Surface Warfare Center, Carderock Division.
- Heller, S. Reese Jr. and Norman H. Jasper. On the Structural Design of Planing Craft. *Transactions of the Royal Institution of Naval Architects*, Volume 103, 1961.
- Heller, S. Reese Jr., *Structural Design of Ship Plating Subjected to Uniform Lateral Load*, *International Shipbuilding Progress*, Vol. 21, No. 244, December 1974.
- Hobbacher, A., *Fatigue Design of Welded Joints and Components: Recommendations of IIW Joint Working Group XIII-XV*. 1996, Cambridge: Abington.
- Hobson, R.P., "Notes on the Yacht Defender and the Use of Aluminum in Marine Construction," *U.S. Naval Institute Proceedings*, Vol. 23, No. 82, 1897, pp. 249-282; Vol. 23, No. 83, 1897, pp. 523-562.
- HSC Code 2000. *International Code of Safety for High-Speed Craft*, International Maritime Organization, London.
- Hughes, Owen. *Ship Structural Design: A Rationally-Based, Computer Aided, Optimum Approach*, John Wiley & Sons, 1983.
- Hurty, Walter C. and Moshe F. Rubenstein. *Dynamics of Structures*, Prentice-Hall, 1964.
- Hval, M. and V. Sande. A New High Strength Aluminium Alloy for Marine Application, Presented at Aluitech 1997.
- IAI, 2006. International Aluminium Institute website, <http://www.world-aluminium.org>.
- IACS, 2005. Requirements Concerning Materials and Welding, International Association of Classification Societies, 2005.
- IACS, 1999. Fatigue Assessment of the Ship Structures, Report No. 56, , International Association of Classification Societies, 1999.
- ISSC Loads. Report of Technical Committee I.2, Loads, 14th International Ship and Offshore Structures Congress, Elsevier, Vol. 1, pp 132, 2000.
- ISSC V.2. Reply by Committee to discussion of the report of Specialist Committee V.2, Structural Design of High Speed Vessels, 14th International Ship and Offshore Structures Congress, Elsevier, Vol. 3, pp 217–218, 2000.
- Jennings, Eric, Kim Grubbs, Charles Zanis, and Louis Raymond. Inelastic Deformation of Plate Panels, Ship Structure Committee Report SSC 364, 1991.
- Jia, Junbo and Anders Ulfvarson. Modal Testing and Finite Element Calculations for Lightweight Aluminum Panels in Car Carriers, *Marine Technology*, Vol/ 43, No.1, January, 2006, pp. 11–21.

Aluminum Marine Structure Guide

- Johnson, A. Stresses in Deckhouses and Superstructures, Transactions of the Royal Institution of Naval Architects, March, 1957.
- Johnston, Bruce G. Structural Stability Research Council Guide to Stability Design Criteria for Metal Structures, Third Edition, John Wiley & Sons, 1976.
- Jones, Norman, and R.M Walters. Large Deflections of Rectangular Plates, Journal of Ship Research, Society of Naval Architects and Marine Engineers, Vol. 15, 1971, pp. 164–171 and 288.
- Jordan, C.R., and C.S. Cochran, 1978. In-service Performance of Structural Details, Ship Structure Committee Report SSC-272.
- Jordan, C.R., and L.T. Knight, 1980. Further Survey of In-service Performance of Structural Details, Ship Structure Committee Report SSC-294.
- Jordan, C.R., and R.P. Krumpfen, Jr., 1990. Design Guide for Ship Structural Details, Ship Structure Committee Report SSC-331.
- Kammerer, J.T. A Design Procedure for Determining the Contribution of Deckhouses to the Longitudinal Strength of Ships, Presented at the Third Annual meeting of the Association of Senior Engineers of the Bureau of Ships, Washington, D.C., March 25, 1966.
- Kihl, David. Strength and Permanent Set of HSLA-65 Plates Subjected to Lateral Pressure, Naval Surface Warfare Center report NSWCCD-65-TR-2003/12, May 2003.
- Kimapong, K. and T. Watanabe. Friction Stir Welding of Aluminum Alloy to Steel, Welding Journal, October 2004, pp. 277-S–282-s.
- Koshio, Keisuke, Shigeru Tanaka, Masahiro Takemura, and Katsuyoshi Nishimura. Structural Design of Super Liner Ogasawara, Fifth International Forum on Aluminum Ships, Tokyo, October 11–13, 2005, pp. 61–67.
- Kramer, R.K., B. Rampolla, and A. Magnusson, 2000, Fatigue of Structural Weldments. Ship Structure Committee Report SSC-410.
- Kryzhevich, Gennadij B., Semion D. Knoring, and Valerij M. Shaposhnikov. Experience and Prospect of Using Aluminum Alloys for Construction of Fast Ships, International Conference on Fast Sea Transportation (FAST 2005), St. Petersburg, Russia, June 27–30 2005.
- Leis, Brian N. Structural Behavior after Fatigue, Ship Structure Committee Report SSC-358, 1990.
- Leveau, C.W., Aluminum and Its Use in Naval Craft, Parts I and II, Naval Engineers Journal, pp. 13-27, Feb. 1965 and pp. 205-219, Apr. 1965.
- Lincoln Electric. GMAW Welding Guide, available at web site <http://www.lincolnelectric.com>, 2006.
- MacNaught, D.F. Design of Typical Tanker Shell Longitudinals and Bottom Plating, Society of Naval Architects and Marine Engineers T&R Bulletin Number 2-9, 1964.
- Maddox, Stephen J. Review of Fatigue Assessment Procedures for Welded Aluminum Structures, International Journal of Fatigue, Vol. XX, 2003.
- MAIB, 2006. Report on the Investigation of the Fire Onboard Star Princess off Jamaica 23 March 2006, Marine Accident Investigation Branch, Report No 28/2006, October 2006, Southampton, United Kingdom.
- Mansour, A.E., P.H. Wirsching, G. White, and B. Ayyub. Probability-Based Ship Design, Implementation of Design Guidelines for Ships: A Demonstration. Ship Structure Committee Report SSC 392, 1996.

- Martukanitz, Richard and J.F. Tressler, *Mixing it Up: Laser Stir Welding Shows Promise for the Joining of Aluminum Alloys*, Industrial Laser Solutions March, 2006
- Masubuchi, Koichi. *Analysis of Welded Structures*. Pergamon Press, 1990.
- MATLAB, September 1968. Annapolis Laboratory of Naval Research and Development Center letter NP10310 (A813 DCV) Assigt 1-813-844-10, MATLAB 254 to commander, Naval Ship Engineering Center, dated September 24, 1968.
- MATLAB, October 1968. Annapolis Laboratory of Naval Research and Development Center letter NP10310 (A813 DCV) Assigt 1-813-844, MATLAB 253 to Commander, Naval Ship Engineering Center, dated October 2, 1968.
- McGoldrick, R.T. *A Vibration Manual for Engineers*, David Taylor Model Basin report R-189, second edition, December 1957. Naval Surface Warfare Center, Carderock Division, West Bethesda, Maryland.
- McGuire, S.C., *Aluminum: Its Alloys and Their Use in Ship Construction*, Transactions of the Society of Naval Architects and Marine Engineers, 1895, pp. 69-97.
- McKenney, Charles R. and John G. Banker. *Explosion-bonded Metals of Marine Structural Applications*, Marine Technology, pp. 285-292, July 1971.
- Mears, R.B. and R.H. Brown. *Resistance of Marine Alloys to Marine Exposure*, Transactions of the Society of Naval Architects and Marine Engineers, 1944, pp. 91-113.
- Michaelson, Robert W., *User's Guide for SPECTRA: Version 8.3*. Naval Surface Warfare Center, Carderock Division Report NSWCCD-65-TR-2000/07, 2000.
- Midling, O.T., L.D. Oosterkamp, and J. Bersaas. 15-17 April 1998, *Friction Stir Welding Aluminum – Process and Applications*, 7th Inalco Conference, Cambridge, April 15-17, 1998, ISBN 1 85573.
- Miller, Carl B. *Laser Welding*, U.S. Laser Corporation, 2005.
- Muckle, W. *Aluminium Alloys and Their Application to Shipbuilding*, The British Shipbuilding Association, Research Item S.7, 1948.
- Munse, William H., Thomas W. Wilbur, Martin L. Tellalian, Kim Nicoll, and Kevin Wilson. *Fatigue Characterization of Fabricated Ship Details for Design*. Ship Structure Committee Report SSC-318, 1983.
- NAVSHIPS 0900-029-9010, *A Guide for Selection and Use of Aluminum Alloys for Structures of Ships of the United States Navy*, 1971.
- NAVSEA 0900-LP-097-4010. *Structural Design Manual for Surface Ships*, 1976.
- Niederberger, R.B., J.L. Basil, and G.T. Bedford. *Corrosion and Stress-Corrosion of 5000-Series Aluminum Alloys in Marine Environments*, United States Navy Marine Engineering Laboratory, Annapolis, Maryland Research and Development Report 86 101A, Sub Project S-R007 01 02, Task 0701, April 27, 1964.
- NSRP, 2001. *Results of Enhanced Fire Protective Material Systems*, National Shipbuilding Research Program report ASE_932006, 2001.
- NVIC 9-97. *Guide to Structural Fire Protection*. Navigation and Vessel Inspection Circular No. 9-97, US Coast Guard COMDTPUB P16700.4, October .31, 1997
- NVIC 6-99. *Plan Review, Inspection, and Certification Guidance for Vessels Built to the International Code of Safety for High Speed Craft and Additional Information Regarding Non-code High Speed Vessels*. Navigation and Vessel Inspection Circular No. 6-99, US Coast Guard COMDTPUB P16700.4, June 8, 1999.
- NVIC 6-02. *2000 Amendments to SOLAS Chapter II-2*. Navigation and Vessel Inspection Circular No. 6-02, US Coast Guard COMDTPUB P16700.4, May 20, 2002.

Aluminum Marine Structure Guide

- NVIC 3-01. Guide to Establish Equivalency to Fire Safety Regulations for Small Passenger Vessels (46 CFR Subchapter K). Navigation and Vessel Inspection Circular No. 3-01, US Coast Guard COMDTPUB P16700.4, April 24, 2001.
- Paik, Jeom Kee, Jae Myung Lee, Jung Yong Ryu, Jun Ho Jang, Celine Renaud, and Paul E. Hess III (2006a). Mechanical Buckling Collapse Testing on Aluminum Stiffened Plate Structures for Marine Applications, Presented at the World Maritime Technology Conference, March 6–10, 2006, London.
- Paik, Jeom Kee, Anil K. Thayamballi, Jung Yong Ryu, Joon Ho Jang, Jung Kwan Seo, Sang Wook Park, Sun Kee Seo, Celine Renaud, H. Paul Cojeen, and Nam In Kim (2006b). The Statistics of Weld Induced Initial Imperfections in Aluminum Stiffened Plate Structures for Marine Applications, *International Journal of Maritime Engineering*, Dated June 2006.
- Paik, Jeom Kee, Owen F. Hughes, Paul E. Hess III, and Celine Renaud, (2005b). Ultimate Limit State Design Technology for Aluminum Multi-Hull Ship Structures, *Transactions of the Society of Naval Architects and Marine Engineers*, Vol. 113, 2005, pp. 270–305.
- Paik, Jeom Kee, Sjoerd van der Veen, Alexandre Duran, Matthew Collette, (2005a). Ultimate Compressive Strength Design Methods of Aluminum Welded Stiffened Panel Structures for Aerospace, Marine and Land-Based Applications: A Benchmark Study. *Thin-Walled Structures* 43 (2005) pp. 1550–1566.
- Paik, Jeom Kee and Alexandre Duran. Ultimate Strength of Aluminum Plates and Stiffened Panels for Marine Applications, *Marine Technology*, Vol. 41, No. 3, July 2004.
- Palko, William A. Phase I Structural and Environmental Testing of Alforge Aluminum Panels, David Taylor Naval Research and Development Center report TM-28-81-259, October 1981.
- Pastor, M., H. Zhao, R. P. Martukanitz and T. Debroy. Porosity, Underfill and Magnesium Loss during Continuous Wave Nd:YAG Laser Welding of Thin Plates of Aluminum Alloys 5182 and 5754. *Welding Journal, Welding Research Supplement*, June 1999, pp. 207s–216s.
- Petinov, Sergei. St. Petersburg Polytechnic University, private correspondence to the author, 2006.
- Pyne, S.N., P.W. Snyder, and H.D. McKinnon, "The Use of Aluminum Alloys in Vessels of the United States Navy," *BuShips Technical Bulletin No. I*, U.S. Navy Department, Washington, D.C., September, 1940.
- Rausch, M.W. Sea Water Corrosion Resistance and Tensile Properties of Aluminum Alloy 6066-T6, United States Naval Engineering Experiment Station, Annapolis, Maryland Evaluation Report 910037AZ, NS-013-118, February 17, 1958.
- Reynolds, James L. Jr., Richard L Holden, and Lawrence E. Brown. Electro-spark Deposition, *Advanced Materials and Processes*, pp. 33–37, March 2003.
- Roark, Raymond J. *Formulas for Stress and Strain*, McGraw-Hill, 1954.
- Salvesen, N., E.O. Tuck, and O. Faltinsen. Ship Motions and Sea Loads, *Transactions of the Society of Naval Architects and Marine Engineers*, vol. 78, 1970.
- Seo, Seung Il and Chang Doo Jang. A Study on the Prediction of Deformations of Welded Ship Structures, *Journal of Ship Production*, Vol. 15, No. 2, May 1999, pp. 73–81.
- Seo, Seung Il, Chan Suk Lee, and Sang Rok Lee. Basic Studies on the Production Technology for Application of Large Extrusion Profiles of Aluminum A605A Alloy to Ship Structures, *Journal of Ship Production*, Vol. 15, No. 3, August 1999, pp. 156–163.
- SFPE, 1999. *SFPE Engineering Guide to Performance-Based Fire Protection Analysis and Design of Buildings*, Society of Fire Protection Engineers and National Fire Association.

- Shumaker, M.B. Method of Eliminating Stress Corrosion Susceptibility of Alforge Welded Aluminum Alloy 5456 Panels, David Taylor Naval Research and Development Center report SME-79-94, September 1979.
- Sielski, Robert A. The History of Aluminum as a Deckhouse Material, Naval Engineers Journal, Vol. 99, No. 3, pp. 165–172, May 1987.
- Sieve, Michael W., David P. Kihl, and Bilal M. Ayyub. Fatigue Design Guidance for Surface Ships. NSWCCD-65-TR-2000/25, Naval Surface Warfare Systems, Carderock Division, 2000.
- Sih, George C., Handbook of Stress Intensity Factors, Lehigh University, Bethlehem, Pennsylvania, 1973.
- Sikora, Jerome P. and Nathan B. Klontz. Seaway Load Prediction Algorithms for High Speed Hull Forms, Transactions of the Society of Naval Architects and Marine engineers, Vol 113, 2005, pp. 501–510.
- Sikora, Jerome P., Alfred Dinsenbacher, and Jeffrey E. Beach. A Method for Estimating Lifetime Loads and Fatigue Lives for SWATH and Conventional Monohull Ships, Naval Engineers Journal, May, 1983.
- Skillingberg, Michael, The Aluminum Industry Continues Support for the Marine Market--New Temper Definitions Published, The Aluminum Association, Inc., Washington, DC, www.aluminum.org, 2006.
- Slaughter, Stephen B., Maxwell C. Cheung, David Sucharski, & B. Cowper. State of the Art in Hull Monitoring Systems, Ship Structure Committee Report SSC-401, 1997.
- SNAME, 1974. Aluminum Fire Protection Guidelines, Society of Naval Architects and Marine Engineers, Technical and Research Bulletin 2-21.
- Spencer, J.S., P.H. Wirsching, X Wang, and A.E. Mansour. Development of Reliability Based Classification Rules for Tankers. Transactions of the Society of Naval Architects and Marine Engineers, Vol. 111, pp. 409–436, 2003.
- SOLAS 2004. International Convention for the Safety of Life at Sea, 1974. Consolidated Edition 2004, International Maritime Organization, London.
- Stambaugh, Karl A., Paul R. Van Mater Jr., and William H. Munse. Fatigue Performance Under Multiaxial Loading, SSC-356, Ship Structure Committee, 1990.
- Stambaugh, Karl A., Frederick Lawrence, and Stimati Dimitriakis. Improved Ship Hull Structural Details Relative to Fatigue, Ship Structure Committee Report SSC 379, 1994.
- Steen, Sverre and Wojciech Kauczynski. Integrated Systems for Ship Handling and Monitoring of Hull Loads, 2002.
- Stone, Kevin F., Comparative Structural Requirements for High Speed Craft, Ship Structure Committee Report SSC-439, 2005.
- Stone, Kevin F. and Derek S. Novak. Comparative Structural Requirements for High Speed Craft, presented at the 2006 annual meeting of the Society of Naval Architects and Marine Engineers, Ft. Lauderdale, Florida, October 12–13, 2006.
- Sutton, Frank. Corrosion and Stress-Corrosion Properties of Nonheat-Treatable Aluminum Alloys in Marine Environments, United States Naval Engineering Experiment Station, Annapolis, Maryland Research and Development Report 910037L, Sub-project S-R 007 01 02, Task 0701, June 12, 1961.

Aluminum Marine Structure Guide

- Sutton, Frank. Corrosion and Stress-Corrosion Properties of Nonheat-Treatable Aluminum Alloys in Marine Environments, United States Naval Engineering Experiment Station, Annapolis, Maryland Research and Development Report 910037M, Sub-project S-R 007 01 02, Task 0701, September 5, 1961.
- Suzuki Yoshikazu, Shinji Takeno and Shoutarou Takemura. Distortion Control in Fillet Welding for Stiffened 5083 Alloy Panels, The Fifth International Forum on Aluminum Ships Tokyo, Japan 11-13, October, 2005.
- Taylor, S.R., G.L. Cahen Jr., G.E. Stoner, P.J. Moran, and M.W. Ferralli. Implantation of Ionized Monomer into Aluminum Alloy 6061 for Marine Corrosion Protection, David W. Taylor Naval Ship Research and Development Center report DTNSRDC 84/046, July 1984.
- Timoshenko, S. Theory of Materials, Part II, Van Nostrand, 1956.
- Timoshenko, S. Theory of Plates and Shells, McGraw-Hill, 1959.
- Tower Extrusions, Mechanical Property Comparison, 6005A VS 6061, Tower Extrusions, Olney, Texas, www.towerextrusion.com.
- Tsai, C. L., S. C. Park And W. T. Cheng. Welding Distortion of a Thin-Plate Panel Structure, Welding Journal, Welding Research Supplement, May 1999. pp. 156–165.
- Vara, Roger, Christopher M. Potter, Robert A. Sielski, Jerome P. Sikora, L.Robert Hill, John C. Adamchak, David P. Kihl, Jay. Herbert, Roger I. Basu, Larrie Ferreiro, Joan Watts, Paul D. Herrington. Adaptation of Commercial Structural Criteria to Military Needs, Gulf Coast Region Maritime Technology Center, University of New Orleans, GCRMTC Project No. AMTC 00-5161, May 2003. NTIS No. PB2004-101323.
- Vassilaros, Michael G. and Earnest J. Czyryca. Mechanical Properties of 5XXX-Series Aluminum Alloys with Exfoliation-Resistant Tempers, Naval Research and Development Center Report NSRDC 28-293, August 1972,
- Vassilaros, Michael G. and Ernest J. Czyryca. Natural Aging and Sensitizing of 5000-Series Marine Aluminum Alloys, David W. Taylor Naval Ship Research and Development Center report DTNSRDC/SME-78/106, June 1979.
- Vreeland, D. C. and R. J. Ferrara, Field investigation of the Corrosion of Aluminum-Hulled Naval Vessels, Naval Ship Research and Development Center Report C2846, February 1969.
- Wacker, George A. Stress-Corrosion Studies of Aluminum Alloy 5456-H321 in Seawater, Naval Ship Research and Development Center Annapolis Division report 2436, July 1967.
- Wacker, George A. and H.P. Chu. Selection of Aluminum Alloys for Submarine Hydraulic Systems, Naval Ship Research and Development Center Report 3210, February 1970.
- Wang, Suqin, Balji Menon, Derek Novak. On the Assessment of Motions and Structural Loads of a High-Speed Catamaran, presented at International conference of Fast Sea Transportation (FAST 2005). St. Petersburg, Russia, June 27-30, 2005.
- Weman, Klas (2003). Welding Processes Handbook. New York: CRC Press LLC. ISBN 0-8493-1773-8.
- Ye, Naiquan and Torgeir Moan. Fatigue and Static Behaviour of Aluminum Box-stiffener Lap Joints, International Journal of Fatigue, Vol. 24, 2002, pp. 581–589.
- Zhao, H. and T. Debroy. Metallurgical and Materials Transactions B Volume 32b, February 2001, p.163.

SHIP STRUCTURE COMMITTEE LIAISON MEMBERS

LIAISON MEMBERS

American Society of Naval Engineers	Captain Dennis K. Kruse (USN Ret.)
Bath Iron Works	Mr. Steve Tarpay
Colorado School of Mines	Dr. Stephen Liu
Edison Welding Institute	Mr. Rich Green
International Maritime Organization	Mr. Igor Ponomarev
Int'l Ship and Offshore Structure Congress	Dr. Alaa Mansour
INTERTANKO	Mr. Dragos Rauta
Massachusetts Institute of Technology	
Memorial University of Newfoundland	Dr. M. R. Haddara
National Cargo Bureau	Captain Jim McNamara
National Transportation Safety Board - OMS	Dr. Jack Spencer
Office of Naval Research	Dr. Yapa Rajapaksie
Oil Companies International Maritime Forum	Mr. Phillip Murphy
Samsung Heavy Industries, Inc.	Dr. Satish Kumar
United States Coast Guard Academy	Commander Kurt Colella
United States Merchant Marine Academy	William Caliendo / Peter Web
United States Naval Academy	Dr. Ramswar Bhattacharyya
University of British Columbia	Dr. S. Calisal
University of California Berkeley	Dr. Robert Bea
Univ. of Houston - Composites Eng & Appl.	
University of Maryland	Dr. Bilal Ayyub
University of Michigan	Dr. Michael Bernitsas
Virginia Polytechnic and State Institute	Dr. Alan Brown
Webb Institute	Prof. Roger Compton

RECENT SHIP STRUCTURE COMMITTEE PUBLICATIONS

Ship Structure Committee Publications on the Web - All reports from SSC 1 to current are available to be downloaded from the Ship Structure Committee Web Site at URL:

<http://www.shipstructure.org>

SSC 445 – SSC 393 are available on the SSC CD-ROM Library. Visit the National Technical Information Service (NTIS) Web Site for ordering hard copies of all SSC research reports at

URL: <http://www.ntis.gov>

SSC Report Number	Report Bibliography
SSC 451	Mechanical Collapse Testing On Aluminum Stiffened Panels For Marine Applications, Paik J.K. 2007
SSC 450	Ship Structure Committee: Effectiveness Survey, Buck R. Phillips, M.L., Jones L.M, Jr. 2007
SSC 449	Hydrodynamic Pressures and Impact Loads for High Speed Catamaran/SES, Vorus. W 2007
SSC 448	Fracture Mechanics Characterization of Aluminum Alloys for Marine Structural Applications, Donald J.K., Blair A. 2007
SSC 447	Fatigue and Fracture Behavior of Fusion and Friction Stir Welded Aluminum Components, Kramer R. 2007
SSC 446	Comparative Study of Naval and Commercial Ship Structure Design Standards, Kendrick, A., Daley C. 2007
SSC 450	Ship Structure Committee: Effectiveness Survey
SSC 449	Hydrodynamic Pressures and Impact Loads for High Speed Catamaran / SES
SSC 448	Fracture Mechanics Characterization of Aluminum Alloys for Marine Structural Applications
SSC 447	Fatigue and Fracture Behavior of Fusion and Friction Stir Welded Aluminum Components
SSC 446	Comparative Study of Naval and Commercial Ship Structure Design Standards
SSC 445	Structural Survivability of Modern Liners, Iversen R. 2005
SSC 444	In-Service Non-Destructive Estimation of the Remaining Fatigue Life of Welded Joints, Dexter R.J., Swanson K.M., Shield C.K. 2005
SSC 443	Design Guidelines for Doubler Plate Repairs on Ship Structures Sensharma P.K., Dinovitzer A., Traynham Y. 2005